AGARD-LS-178

AGARD-LS-178

AGARD

ADVISORY GROUP FOR AEROSPACE RESEARCH & DEVELOPMENT
7 RUE ANCELLE 92200 NEUILLY SUR SEINE FRANCE

AGARD LECTURE SERIES 178

Rotorcraft System Identification

(Identification des Systèmes de Voilures Tournantes)

This material in this publication was assembled to support a Lecture Series under the sponsorship of the Flight Mechanics Panel of AGARD and the Consultant and Exchange Programme of AGARD presented on 4th—5th November 1991 in Ottobrunn, Germany, 7th—8th November 1991 in Rome, Italy and 13th—14th November 1991 in College Park, Maryland, United States.

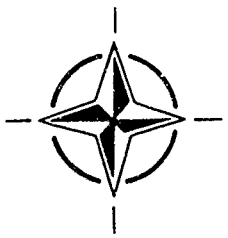

NORTH ATLANTIC TREATY ORGANIZATION

Published October 1991

Distribution and Availability on Back Cover

AGARD
ADVISORY GROUP FOR AEROSPACE RESEARCH & DEVELOPMENT
7 RUE ANCELLE 92200 NEUILLY SUR SEINE FRANCE

AGARD LECTURE SERIES 178

Rotorcraft System Identification

(Identification des Systèmes de Voilures Tournantes)

This material in this publication was assembled to support a Lecture Series under the sponsorship of the Flight Mechanics Panel of AGARD and the Consultant and Exchange Programme of AGARD presented on 4th—5th November 1991 in Ottobrunn, Germany, 7th—8th November 1991 in Rome, Italy and 13th—14th November 1991 in College Park, Maryland, United States

North Atlantic Treaty Organization
Organisation du Traité de l'Atlantique Nord

The Mission of AGARD

According to its Charter, the mission of AGARD is to bring together the leading personalities of the NATO nations in the fields of science and technology relating to aerospace for the following purposes:

- Recommending effective ways for the member nations to use their research and development capabilities for the common benefit of the NATO community;
- Providing scientific and technical advice and assistance to the Military Committee in the field of aerospace research and development (with particular regard to its military application);
- Continuously stimulating advances in the aerospace sciences relevant to strengthening the common defence posture,
- Improving the co-operation among member nations in aerospace research and development,
- Exchange of scientific and technical information;
- Providing assistance to member nations for the purpose of increasing their scientific and technical potential,
- Rendering scientific and technical assistance, as requested, to other NATO bodies and to member nations in connection with research and development problems in the aerospace field

The highest authority within AGARD is the National Delegates Board consisting of officially appointed senior representatives from each member nation. The mission of AGARD is carried out through the Panels which are composed of experts appointed by the National Delegates, the Consultant and Exchange Programme and the Aerospace Applications Studies Programme The results of AGARD work are reported to the member nations and the NATO Authorities through the AGARD series of publications of which this is one.

Participation in AGARD activities is by invitation only and is normally limited to citizens of the NATO nations

Published October 1991

ISBN 92-835-0640-5

Printed by Specialised Printing Services Limited
40 Chigwell Lane, Loughton, Essex IG10 3TZ

Abstract

Owing to the highly coupled flight dynamic behaviour of rotorcraft configurations, long term interdisciplinary scientific knowledge combined with practical flight test experience is required to use system identification and mathematical modelling tools in the most efficient way.

This Lecture Series is intended to establish an improved dialogue between government organisations, research institutions and industry in order to apply these tools more routinely in rotorcraft system design, development and evaluation

The Lecture Series is supported by an unique flight test data set which was specially generated and analysed within a recent Working Group in the Flight Mechanics Panel of AGARD on Rotorcraft System Identification (WG 18).

This Lecture Series, sponsored by the Flight Mechanics Panel of AGARD, has been implemented by the Consultant and Exchange Programme.

Abrégé

Considerant les interactions complexes du comportement dynamique en vol des voilures tournantes, l'emploi optimal de outils de modélisation mathématique et d'identification de systèmes demande des connaissances scientifiques interdisciplinaires approfondies, avec une expérience pratique des essais en vol

L'objet de ce cycle de conférences est: d'instaurer un dialogue plus étroit entre les organismes gouvernamentaux, les etablissements de recherche et l'industrie pour promouvoir l'emploi systematique de ces modélisations pour l'etude, le développement et l'évaluation des systèmes de voilures tournantes

Le support de ce cycle de conferences comprend un ensemble de données unique relatif aux essais en vol, qui a été specialement elabore et analysé par le groupe de travail No.18 du Panel FMP de l'AGARD sur l'Identification des systèmes de voilures tournantes

Ce cycle de conférences est présente dans le cadre du programme des Consultants et des Echanges, sous l'egide du Panel AGARD de la Mécanique du Vol

List of Speakers

Lecture Series Director: Dr Peter Hamel
DLR
Institut fur Flugmechanik
Postfach 3267
3300 Braunschweig
Germany

SPEAKERS

Dr Dev Banerjee
Building 530, MS 325
McDonnell Douglas Helicopter Comp.
5000 East McDowell Road
Mesa, Arizona 85205-9797
United States

Mr Ronald W DuVal
Advanced Rotorcraft Technology Inc.
Mountain View, California
United States

Mr Jurgen Kaletka
DLR
Institut fur Flugmechanik
Postfach 3267
3300 Braunschweig
Germany

Prof. David Murray-Smith
Department of Electronics and
Electrical Engineering
The University
Glasgow, G12 8QQ
United Kingdom

Dr Mark B. Tischler
Aeroflightdynamics Directorate
US Army Aviation R&T Activity
Ames Research Center MS 211-2
Moffet Field, Ca. 94035-1000
United States

Mr Jan H. Breeman
NLR
Department Flight Testing and Helicopters
PO Box 90502
1059 BM Amsterdam
The Netherlands

Mr K.W. Harding
McDonnell Douglas Helicopter Comp.
5000 East McDowell Road
Mesa, Arizona 85205-9797
United States

Prof Jaap H de Leeuw
Institute for Aerospace Studies
University of Toronto
4925 Dufferin Street
Downview, Ontario
Canada M3H 5T6

Dr Gareth D Padfield
Flight Systems (Bedford) Department
Building 109
Ministry of Defence (PE)
Royal Aerospace Establishment
Bedford, MK41 6AE
United Kingdom

Contents

INTRODUCTION AND OVERVIEW

by

Peter G.Hamel
Institut für Flugmechanik
Deutsche Forschungsanstalt für Luft- und Raumfahrt e V. (DLR)
Flughafen
DW-3300 Braunschweig, Germany

"It is evident that some of these (stability and control) derivatives are strongly affected by the main rotor's wake in ways that are difficult to predict This difficulty is what makes the parameter identification process so valuable as the helicopter's development matures beyound its first flight."

Raymond W.Prouty (R&W International, July 1990)

1. Background

The rotorcraft dynamic response behaviour (output) due o pilot control or gust disturbance effects (input) is described by the interaction of inertial and aerodynamic forces as well as elastomechanic and control forces. It is evident that the rotorcraft performance, stability, controllability and sensitivity is principally influenced by all four kinds of forces acting on the airframe and rotor system. The relative interactions and interferences between these forces and its effects on the rotorcraft dynamic response is varying between different rotorcraft flight states and configurations.

Whereas static and dynamic structural parameters can be adequately modeled without airloads by analytical, numerical, and ground-test tools, the prediction of aeromechanical forces and loads of the rotor system and its wake interactions with the empennage and tail rotor require windtunnel and flight test validation experiments [1].

Due to aerodynamic scale effects, windtunnel model deficiencies and constrained "free-flight" capabilities certain limitations in the quality and applicability of rotorcraft windtunnel model data have always to be envisaged

Therefore, flight tests are important and necessary to isolate limits and assess uncertainties from the prediction techniques of rotorcraft aeromechanics. Perhaps more than any other technique system identification provides the best basis for rotorcraft flight/ground test data correlation by extracting as much information as possible from free flight tests.

2. Methodology of System Identification

Precisely defined, system identification is the determination of a system, on the basis of input and output measurements, within a specified class of systems to which the system under test is equivalent. More directly, rotorcraft system identification is related to flight test validation of a predicted mathematical model describing specific qualitative (model structure) and quantitative (model parameters) flight mechanical characteristics.

The system identification framework can be divided into three major parts [2]:

- **Instrumentation and Filters** which cover the entire flight data acquisition process including adequate instrumentation and airborne or ground-based digital recording equipment. Effects of all kinds of data quality have to be accounted for.
- **Flight Test Techniques** which are related to selected rotorcraft maneuvering procedures in order to optimize control inputs. The input signals have to be optimized in their spectral composition in order to excite all rotorcraft response modes from which parameters are to be estimated
- **Analysis of Flight Test Data** which includes the mathematical model of the rotorcraft and an estimation criterion which devises some iterative computational algorithm to adjust some kind of starting value or a priori estimate of the unknown parameters until a set of best parameter estimates is obtained which minimizes the response error

Corresponding to these strongly interdependent topics four important aspects of the art and science of system identification have to be carefully treated (Figure 1):

- Importance of the control input shape in order to excite all modes of the vehicle dynamic **motions**.
- Type of rotorcraft under investigation in order to define the structure of possible mathematical **models**.
- Selection of instrumentation and filters for high accuracy **measurements**.
- Quality of data analysis by selecting most suitable time or frequency domain identification **methods**.

These "**Quad-M**"-requirements must be carefully investigated from a physical standpoint in order to define and execute a successful experiment for system identification [3].

3. Benefits of System Identification

The objective to validate mathematical models from the knowledge of control inputs and system responses via flight test data collection and analysis will improve the confidence and reduce the uncertainty of important aerodynamic stability and control parameters describing rotorcraft flight mechanics.

Seen from the aspect of cost effectiveness important benefits of rotorcraft system identification are related to the potential to reduce the amount of costly and time-consuming rotorcraft flight testing with respect to specification and certification requirements. Improved assessment and evaluation of flying qualities becomes possible (Figure 2).

An additional important factor is emerging from the area of implementation of active-control-technology (ACT) concepts offering the promise of significantly increased rotorcraft performance and operational capabilities. It is well-known, that this approach extends the traditional trade-offs between aerodynamics, structures and propulsion to include the capabilities of a fulltime, full-authority digital fly-by-wire/light flight control system. It is imperative that the actual aerodynamic stability and control parameters have to turn out as predicted, since the inherent stability margins may be lower and the flight control system must compensate these deficiencies to provide required handling qualities. In cases of high bandwidth model-following flight control system designs accurate mathematical models improve feedforward control and, consequently, lower feedback gains for model deficiency compensation (Figure 3)

Still more important, system identification techniques become in the future mandatory for model validation purposes of ground-based rotorcraft simulators. Such simulators require extremely accurate mathematical models in order to be accepted by pilots and government organizations for realistic complementary rotorcraft mission training (Figure 4).

4. Requirement for Multidisciplinary Collaboration

Due to the highly complex aeromechanical and coupled flight dynamic behaviour of helicopter and other rotorcraft configurations, long term interdisciplinary scientific knowledge combined with practical research expertise is required in order to use identification and mathematical modeling tools in a most efficient way. It is also important to establish an improved dialogue between research institutions and industry.

One efficient way of developing this knowledge and providing the research expertise is by using the combined strengths and complementary facilities of the relevant NATO nations in a collaborative programme. This is an area ideally suited to the mission of ADARD [4].

5. AGARD FMP Working Group 18

The Flight Mechanics Panel of the Advisory Group for Aerospace Research and Development (AGARD) which for the last twenty years has sponsored activities in the field of flight vehicle parameter and system identification [2, 5, 6] decided in 1987 that the optimum way in which AGARD could contribute to this area was to set up a Working Group (FMP WG 18) comprising a wide range of research specialists and industry representatives, tasked with exploring and reporting on the topic of Rotorcraft System Identification.

The two principal objectives of the Working Group were

1. to evaluate the strength and weakness of the different approaches and to develop guidelines for the application of identification techniques to be used more routinely in design and development.
2. to define an integrated and coordinated methodology for application of system identification based on the strengths of each method.

These objectives have been pursued in a time frame of about three years (1988-1990), through the exercising of the full range of available individual system identification methods on three common data sets (AH-64 of MDHC, BO-105 of DLR, and SA-330 of RAE) and a critical review of accomplishments

The objective of this Working Group was to provide an overview and expertise to industry for

- **better understanding** the underlying scientific, technical and operational methodologies involved in rotorcraft system identification and
- **increased utilization** of this modern flight test tool

in cooperation with research centers of excellence in this field.

To be as effective as possible in achieving the declared objectives and making sensible recommendations, the Group has requested industry to provide information with respect to any experience of using system identification tools in the rotorcraft system design and validation process [7].

For the Working Group, a common flight test data base was provided for three significantly different helicopter types:

- The attack helicopter MDHC AH-64 (Apache):
  MDHC provided data from flight tests at 130 knots. These data were selected from different flight tests. They included manoeuvres with doublet, frequency sweep, and pulse-type inputs for all controls.
- The small transport helicopter MBB BO-105:
  DLR provided data from flight tests at 80 knots, specifically generated for identification purposes. They included three types of input signals, 3211 multistep [1]), frequency sweeps, and doublets for all controls.
- The medium size transport helicopter Aerospatiale SA-330 (PUMA):
  RAE provided two sets of flight test data: (a) for the 80 knots flight condition, manoeuvres with 3211 multistep inputs for all controls, and (b) for the 60, 80, and 100 knots flight conditions, 3211 multistep, and frequency sweeps for the longitudinal cyclic control.

The flight test data quality was extensively investigated to detect and correct data errors and to make sure that reliable data were used for the identification. Results obtained from data channel consistency checks were generated by various WG Members. Comparisons of the results and conclusions were in good agreement.

As the evaluation of all data files would have caused too high a workload for the WG, each data provider (DLR, MDHC, RAE) suggested minimum data subsets to be used as data for the identification and verification. In general, it was tried to use flight test data with multistep 3211 input signals or frequency sweeps for the identification. Then other test data, e.g. with doublet inputs, were chosen for the verification to evaluate the reliability of the identified mathematical models. Results provided by the WG Members were compared in various formats: time histories; frequency responses; tables of derivatives; and eigenvalues.

6. Objective of the Lecture Series

The outcome of the Working Group and the final AGARD Advisory Report (AR 280) form the basis of this Lecture Series which has the objectives of

- bringing together a number of experts from research organisations and industry who identified a strong requirement for application of system identification tools,
- providing WG-18 members as the kernel of lecturers who should share and cross-fertilise their experience, and
- utilizing benchmark flight test data from recent helicopter flight test programmes to demonstrate the art and science of rotorcraft system identification.

7. Structure of the Lecture Series

Coming back to the "Quad-M"-requirements of rotorcraft system identification (Figure 1) the papers to be presented by the lecturers are organized in an equivalent way. The upper part of Figure 5 indicates the relationship of papers 2 to 7 among the four major areas of rotorcraft stability and control estimation: **motions** (maneuvers and input design), **measurements** (instrumentation and data aquisition), **methods** (time and frequency domain identification) and **models** (model structure and robustness).

In the lower part of Figure 5 unique identification results of the three significantly different helicopter types evaluated by the Working Group 18 are presented in papers 8 to 10

In the final papers 11 to 14 various application areas are discussed, like rotorcraft development risk reduction, data gathering for helicopter simulators, acceptance testing of helicopter flying qualities and model provision for flight control optimisation

8. Bibliography

[1] Hamel, P.G. et al.
Rotorcraft Model Testing at DNW - Experience and Perspectives
Ten Years of Testing at DNW (1980-1990) Colloquium, 16 October 1990, Nordostpolder (1990), pp. 6.1-6.12

[2] Hamel, P.G.
Aircraft Parameter Identification Methods and their Application - Survey and Future Aspects
AGARD LS 104, Paper 1, November 1979

[3] Hamel, P.G.
Flight Vehicle System Identification - Status and Prospects
DLR-Mitt.87-22(1987), pp 52-90

[4] Hamel, P.G.
The Collaborative Role of AGARD in Recent Advances in Rotorcraft System Identification
AGARD Highlights 90/1, pp. 36-41, 1990

[5] Anon.
Methods fo Aircraft State and Parameter Identification
AGARD CP-172, May 1975

[1]) The 3211 multistep input is a series of four contiguous steps with alternating signs, lasting for 3, 2, 1 and 1 time units. The length of the time unit is adjustable to centre the frequency band of the input around the rotorcraft natural frequencies. This DLR-designed input signal is relatively easy for a pilot to fly and accepted by the international flight test community [6].

[6] R.Maine and K.Iliff
Identification of Dynamic Systems with Applications to Aircraft
AGARD AG 300, Vol.3, Part 1, December 1986

[7] Anon.
Rotorcraft System Identification
AGARD AR 280, 1991

Acknowledgements
The author wishes to record his appreciation of the members of the Working Group 18 of the AGARD Flight Mechanics Panel who have contributed to the unique and excellent work and accomplishments of this group and, consequently, provided the "nutrient" of this Lecture Series.

9. Figures

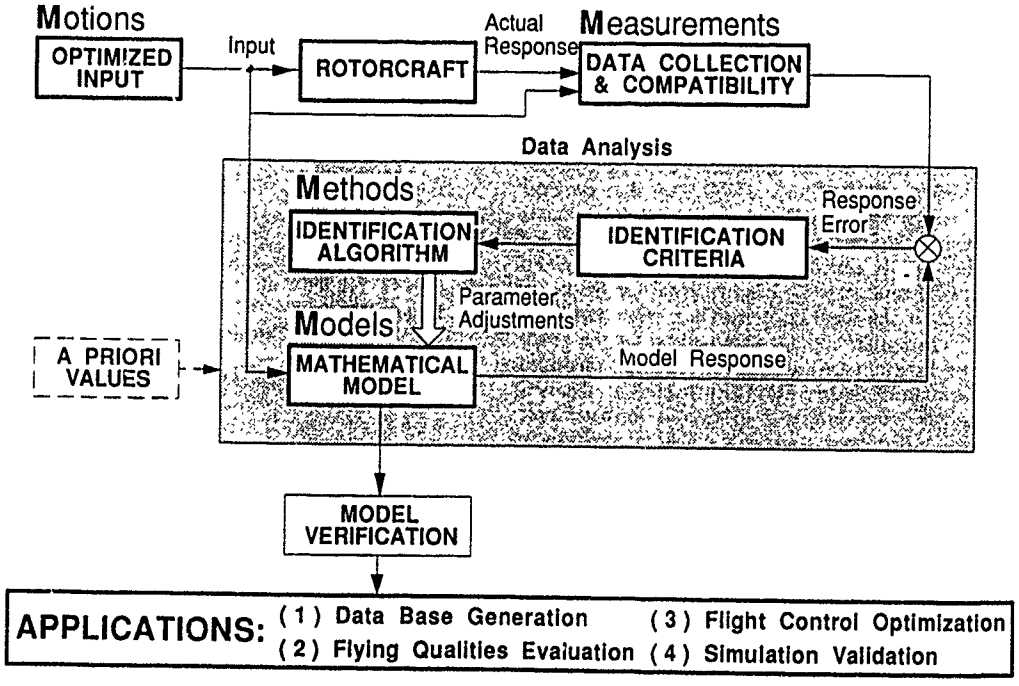

Figure 1. "Quad-M" Requirements for System Identification

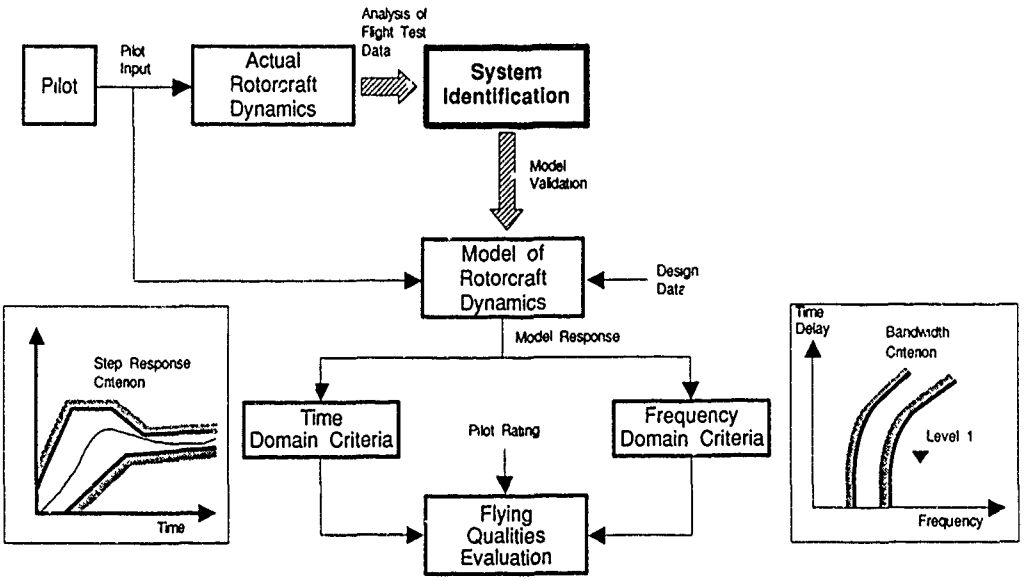

Figure 2. System Identification for Rotorcraft Flying Qualities Evaluation

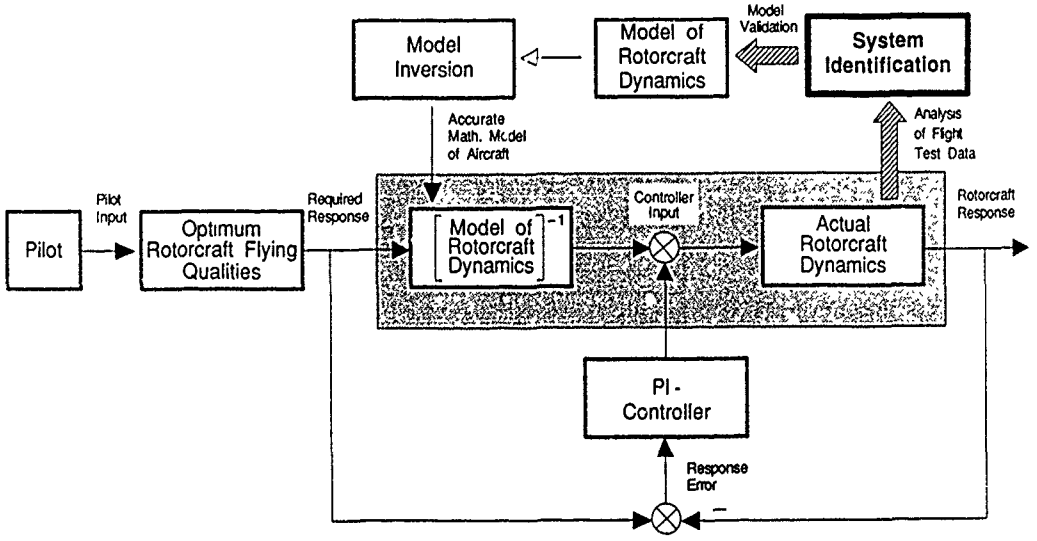

Figure 3. System Identification for Rotorcraft Flight Control Optimization

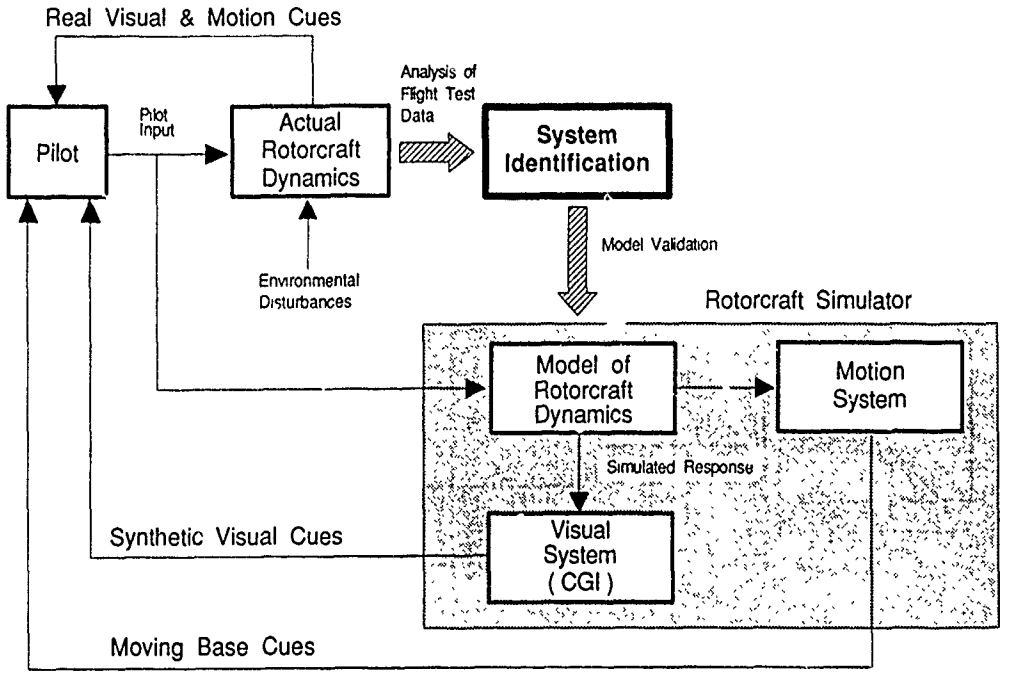

Figure 4. System Identification for Rotorcraft Simulation Validation

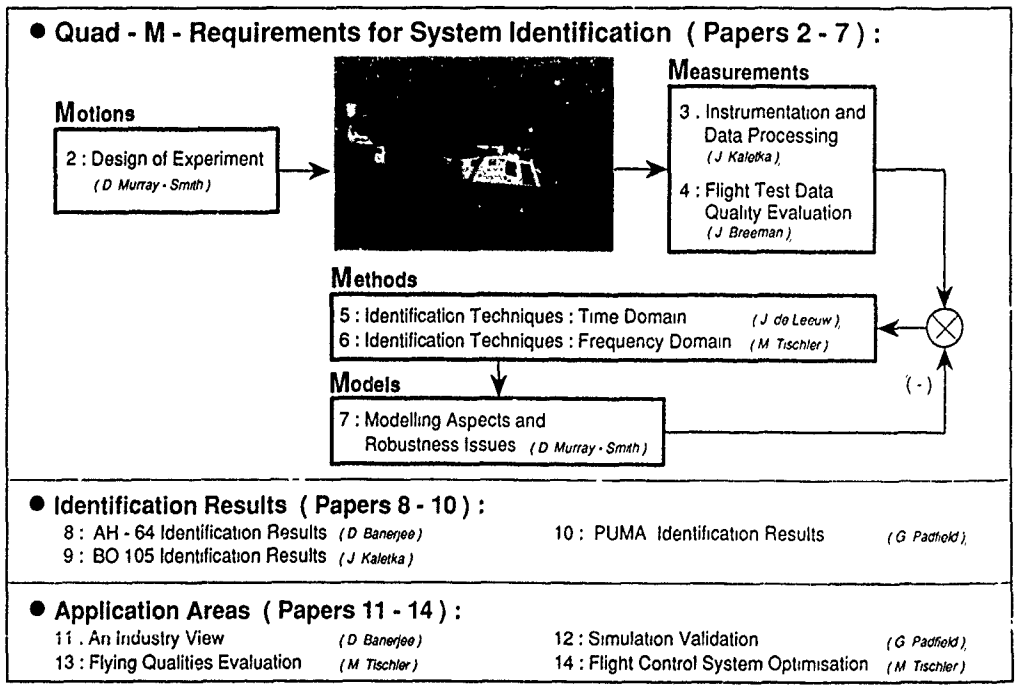

Figure 5. AGARD LS 178 Concept

DESIGN OF EXPERIMENTS

by

David J. Murray-Smith
Department of Electronics and Electrical Engineering
The University
Glasgow, Scotland

and

Gareth D. Padfield
Defence Research Agency
Aerospace Division
RAE Bedford, England

Summary

The planning and conduct of flight experiments is a critically important part of the system identification process. Factors such as the choice of test input signal and the duration of the experiment can have a major influence on the quality of the identification results. Other factors such as the quality of flightcrew and groundcrew briefings and the availability of on-line monitoring facilities also greatly influence the effectiveness of any flight testing programme. Inevitably there is a trade-off between performance and flight safety which must be taken fully into account at all stages of identification flight trials and influences the experiment design process and test matrix in a very significant way. Other important practical constraints arise in experiment design, especially when test input signals have to be applied manually by the pilot. The paper includes an outline of the forms of test input most commonly used for identification and provides an account of methods of experimental design in which the value of a frequency-domain approach is emphasised.

1 Introduction

The success of helicopter system identification methods depends, to a considerable extent, on the quality of the associated flight experiments. Any inadequacies and inconsistencies which appear in the identification results can usually be eliminated only through additional flight testing. It is important, therefore, to maximise the information content of experimental response data by good planning and experiment design.

This paper is concerned with the planning and conduct of flight experiments designed specifically for the purposes of system identification. Flight experiments designed primarily for other purposes seldom provide a reliable basis for system identification work.

Special emphasis is given to the trade-offs which are involved in flight experiments for system identification, especially those associated with performance and flight safety. More detailed questions of test input design are also considered, although the extent to which detailed design is appropriate depends on how much is known in advance about the dynamics of the vehicle under test. However, preliminary characterisation of the rotorcraft dynamics through the use of a broad-band test signal can often provide a basis for more detailed design work to maximise the information content of the measured response data. This necessitates careful consideration of factors such as system bandwidth and frequency content of the test signal, sampling rates, signal amplitudes and signal-to-noise ratios.

2 The Planning and Conduct of Flight Experiments

During the planning and conduct phases of system identification flight trials it is crucial to take account of the trade-offs between performance and flight safety. In this context, performance relates to both the effectiveness and the efficiency of the experiments; there are further trade- offs involved here, related to the need to monitor the data quality, while maximising the productivity, during the available flight time. This section addresses these trade-offs under a number of key headings.

2.1 Defining the test matrix

Parameters that make up the test matrix dimensions include aircraft configuration (mass, inertias, cg location) and AFCS status, initial trim conditions (airspeed, climb angle, sideslip and turn rate), pressure altitude, outside air temperature (oat), control input (axis, shape, size, direction) together with any constraints that need to apply, *eg* in/out of-ground effect (i/oge), light turbulence, within telemetry coverage etc. To support a comprehensive simulation model validation exercise, the test matrix will contain hundreds of individual events. For example, a single input shape applied on each control, with two repeats and two amplitudes, would amount to 48 events at each trim condition. The requirement for several input shapes and a range of trim points magnifies the task to the extent that an efficient test plan is essential to avoid wasted flight and ground time. In general, a single flight should last about one hour at the most; fuel burn causes the configuration to change and crew fatigue can set in. The ideal test plan will define a sequence that takes account of fuel burn and the need to combine events in the post-flight analysis, hence flying these close together. Weather changes over the period of the trial can upset well prepared plans and dictate a need for flexibility, particularly in the temperate climates of Northern Europe. The passage of a front can change the altitude at which calm air is found from, say, 2000 to 6000 ft. While the rotor can be made to work at similar thrust and torque conditions through mass changes, the fuselage aerodynamics will be markedly different at the two densities.

The test plan can be assembled with the aid of a simulation model of the vehicle to be flown. In particular, input shapes, timings and amplitudes can be defined and expected response amplitudes established. Regions of potential instability or high stresses can be identified and estimates of flight time requirements made. Identification runs with nonlinear simulation test data can support the flight trials and provide initial estimates of required model structures and parameters. Above all, to take account of uncertainties in the initial modelling, the test plan needs to be flexible with respect to control input shape. The quality of the data and potential for successful identification hinge on having appropriate designs which can only be validated in flight. This topic is further developed in section 3, but the requirements for on-line analysis are covered below.

2.2 Flightcrew/groundcrew briefings and the test plan.

The test matrix will need to be developed with the support of the flightcrew. The flight test plan will then need to be developed in a series of briefings that commence well in advance of the trials. Aspects that need to be covered include;

(a) the need for specialised cockpit instrumentation to assist the aircrew with performance and safety monitoring, *eg* displays showing desired and actual test input, or margins between current flight state and the flight envelope boundary.

(b) the need for piloted ground simulation to enable practice and refinement of test procedures.

(c) the need to assess every potential risk carefully and to establish an incremental approach (from a known condition) to each new test point to minimise such risk, *eg* in-ground-effect (ige) hover manoeuvres are best approached from out-of-ground-effect (oge) states in a series of well defined steps; high bank manoeuvres need to be approached from lower bank conditions.

(d) the need to establish recovery procedures depending on the type of response, *eg* stable modes will eventually decay leaving the aircraft close to the original trim point, while unstable modes can cause rapid departures. The recovery technique used in the two situations will be very different; it is important that the pilot understands that dangerous conditions can sometimes more easily be encroached during recovery than the test manoeuvre itself, particularly close to the flight limits.

2.3 On-line monitoring; performance and safety aspects

During the course of a flight, data quality and flight safety will be paramount in the minds of the aircrew. In most cases it is important, if not essential, that support is provided from a ground station, where key data are available in real time from the aircraft via a telemetry link. It is obviously crucial that a good, uninterrupted radio link is available between the aircraft and the ground, and that all personnel are trained in using this communication medium. Aspects covered by the groundcrew include,

(a) monitoring of critical stresses from the rotors and fuselage/transmission, particularly during frequency sweeping and recovery from step inputs, when large transients can occur; visual display of outputs should be scaled to give a wide range between the no-damage and never-exceed levels.

(b) monitoring of response amplitude to establish whether linearity assumptions can be invoked.

(c) monitoring of control input quality if applied manually.

(d) limited inter-event analysis can be performed to determine key data characteristics, *eg* response spectra, input/output coherence, kinematic consistency. This is a vital stage in the validation of the experimental design; while much more inter-flight and post-trial analysis can, and will need to be carried out, the inter-event work can serve to refine the input shapes and timings to achieve the optimum for each test point.

(e) monitor data quality to establish levels of measurement noise (*eg* dropouts, emc effects) and process noise (*eg* turbulence, vibration)

(f) generally to assist the aircrew in approaching a new condition or test point incrementally.

(g) in all the above, an agreed acceptance/rejection criteria needs to be established during the ground briefings. In the case of disagreement, the aircraft captain will always be the final arbiter.

2.4 Flying the test points

Calm air is essential for accurate rotorcraft system identification, unless turbulence itself is the subject of interest; to date however, to the authors' knowledge, no flight research has addressed this topic for rotorcraft operating conditions. Ideally, the atmospheric conditions should be calm; this will ease the trim point flying, enable repeatable manoeuvres to be flown and simplify the identification considerably. There are several trade-offs relating to the question of whether the controls should be input manually or automatically through the stabilisation system. For simple input shapes, the pilot is very capable of applying and refining the test inputs to improve the response content. Pilots have additional flight safety concerns with auto - inputs, and validation can be time consuming. On the other hand, complex input shapes can be applied more efficiently, in a regular/repeatable fashion, through the automatic system. A practical method for manual application has been developed at the DLR.

(i) main pilot trims aircraft;

(ii) copilot inputs required signal, with hands off other controls;

(iii) main pilot monitors flight safety and may apply corrective control in secondary axes;

(iv) at event completion the main pilot retrims aircraft.

Such an approach ensures that unwanted, correlated control inputs by the copilot are avoided.

Flight time in close to ideal conditions is a premium during a trials programme and should be exploited fully. This may often be at the expense of conducting enough analysis to judge the data value. Without a comprehensive on-line capability, this dilemma will always prevail; the pressure to capitalise on good conditions/serviceability is hard to resist.

3 Test Inputs for Parameter Identification

3.1 Forms of input commonly used

One form of test input which has been used widely for the identification of fixed-wing aircraft is the doublet. Fig 1 shows an ideal doublet and the corresponding autospectrum which has a well defined peak at a frequency which depends upon the time duration of the positive and negative phases of the signal. Since these phases are of equal duration in the ideal doublet the signal has a mean value of zero. This is a desirable feature of test inputs for most identification applications since a non-zero mean value, as in a step input, produces a change of operating condition away from the initial trimmed state.

Doublet signals can be used by pilots to search for natural frequencies of the aircraft and can be applied very effectively to excite the short-period mode in longitudinal motion and also the Dutch roll. However, as has been pointed-out by Plaetschke *et al* (1979), some derivatives can only be found as ratios in the vicinity of the natural frequencies although others may be

identifiable individually. In the case of the helicopter the highly coupled form of model structure presents significant difficulties in this respect. Doublet inputs and other similar test signals are therefore generally regarded as having limited value for helicopter identification due to their relatively small bandwidth. These inputs are, however, capable of exciting modes in either axis and can be of value when used in conjunction with other forms of test input.

A second type of simple multi-step test signal, which has been used widely for rotorcraft system identification is the so-called '3-2-1-1' pseudo-stochastic signal (Plaetschke *et al*, 1979; Kaletka, 1979). The numbers used in the designation of this type of input refer to the relative time intervals between control reversals. Fig 2 shows the form of this signal in the time domain together with the corresponding representation in the frequency-domain in terms of the auto- spectrum. It can be seen that this form of input provides more energy than the doublet, especially at the lower frequencies, and can in principle provide broader band excitation. Difficulties can arise, however, for cases in which stability margins are small since the use of a 3-2-1-1 test signal may not allow an adequate length of data record during the unforced part of the response (Kaletka, 1979; Leith *et al*, 1989). It should be noted that a modified form of 3-2-1-1 test signal, involving a reduced amplitude of the initial step, has been used by de Leeuw and Hui (1989) to reduce the magnitude of the initial part of the response and to balance the total perturbation about the trimmed flight condition. This may permit a larger overall amplitude of the input without violating constraints associated with nonlinear effects.

Sinusoidal control inputs at high enough frequencies can result in an aircraft response that is dominated by the control derivatives and this fact has been used by de Leeuw and Hui (1989) for estimation of such quantities.

One form of test signal which has been used increasingly in recent years to provide broadband excitation is the 'frequency sweep' (Tischler *et al*,1985). Such signals generally involve an initial phase during which two sinusoidal cycles of input are applied having a frequency equal to the lower bound of the required frequency range. The second phase also involves sinusoidal excitation, but in this case the signal period is gradually decreased until the control is being driven at a relatively high frequency and usually with a significantly smaller amplitude of motion. The control is then returned to the trim condition. The overall period of a frequency sweep test input is normally chosen from available information concerning the dynamics of the vehicle in order to provide good identification of the low frequency modes and to give an even excitation of the vehicle dynamics over the frequency range of interest (Tischler, 1987).

The coherence function is a very useful measure of the degree to which a given test signal provides satisfactory excitation, as a function of frequency (Tischler, 1987). This quantity may be interpreted as the fraction of the output autospectrum which may be accounted for by means of a linear relationship with the input autospectrum (Otnes *et al*, 1978). Ideally the coherence function should have a value of unity and smaller values may be associated with the presence of nonlinearities in the system being identified, process noise (*ie* turbulence and gusts) and lack of input power and/or lack of response power (Bendat *et al*, 1980, 1986).

3.2 Constraints associated with manual input of test signals

As described in section 2.4 inputs applied through the stabilisation system provide clear advantages over the manual application of test signals for cases where complicated signal shapes are required. However, in cases where signal shapes are relatively simple, there can be advantages in pilot involvement. It has been found that, after appropriate training, pilots are capable of applying such signals with the required level of accuracy and repeatability.

When test signals are to be applied by the pilot using the normal controls a number of important issues arise. Limits imposed by the neuromuscular system affect the maximum rate of change of input and this influences the achievable bandwidth of the excitation. Similarly, any departures from the ideal timing of control input changes will also have a direct effect on the autospectrum of the test signal applied to the vehicle.

In addition to the problems associated with the spectral characteristics of the resulting test inputs, difficulties can be encountered in generating repeatable signals having exactly the required amplitudes in each direction. Test inputs which are too small are ineffective in terms of the resulting signal-to-noise ratios, while test inputs which are too large produce nonlinear behaviour. For signals which involve a long sequence of control movements it may be

necessary for the pilot to take corrective action during the experiment in order to ensure that the aircraft response remains within specified limits. Such intervention by the pilot is generally undesirable. It should be avoided, wherever possible, by careful preliminary design of the flight experiments. Where tests are carried out in flight conditions involving small margins of stability some additional control may be essential and this is best accomplished by the pilot using pulse inputs. The use of a stability augmentation system is undesirable in system identification tests because the continuous feedback can introduce unwanted correlations between input and output.

4 Methods for Experimental Design

In any consideration of experimental design for parameter identification testing it is important to emphasise that designs based on any available mathematical model of the vehicle are unlikely to be optimal in practice due to uncertainties in the model. It is important to be able to characterise some flight data prior to any any detailed experimental design. Such preliminary flight data must, of course, be chosen to be representative of the flight condition for which the proposed identification tests are to be performed.

4.1 A quantitative basis for comparison of test inputs

Before attempting to carry out a flight test experiment design it is important to establish a quantitative basis upon which comparisons can be made. One well-established approach for comparing identification experiments is based on the use of the Cramer-Rao bound (Plaetschke and Schulz, 1979). In that approach the variance of parameter estimates is related to elements of the dispersion matrix, which can be calculated from the measured responses. Inputs giving a dispersion matrix with small elements are preferred in comparison with inputs producing much larger elements. This has led to the development of algorithms for designing inputs which minimise some appropriate function of the dispersion matrix.

Care must be exercised in the application of algorithms based upon the dispersion matrix since this matrix only provides a lower bound on the covariance of parameter estimates. The elements of the dispersion matrix are equal to the covariance values only for the special case of an efficient estimator. It should be noted that in situations where relatively long test records are available maximum likelihood estimators (which are asymptotically efficient) can be used reliably with inputs designed using the dispersion matrix.

4.2 A frequency-domain approach to design

In general, in designing a test signal for identification a three-stage process may be adopted. The first stage involves initial simulation and analysis, based on the best currently available mathematical model, to obtain a first estimate of the dynamic range for testing. This provides a basis for the second stage which involves the design of a preliminary experiment using broad-band test signals such as frequency sweeps. Analysis of the results from this initial characterisation is of considerable value for the design of the flight experiments from which parameter estimates are to be obtained. For example, assumptions of the overall linearity can be checked by examining the coherence of selected pairs of input and output variables and the tests can also provide opportunities to characterize the linear and nonlinear dynamic characteristics of the actuation system.

Requirements in terms of test signal frequency range are determined by the most demanding application of the identified model. Examples of demanding applications include flight control system design, the development of research flight simulators and their application in handling-qualities studies at the limit of of the flight envelope. Typical requirements involve upper frequency limits of at least 20 rad/s in order to capture regressing lead-lag and flap modes in helicopters such as the BO105. With lower-order models and less demanding applications it is appropriate to use test inputs conditioned to avoid high frequencies which could excite higher order rotor and engine modes. It should be noted that since the response following the application of the test input is dominated by the natural modes, the run length required for estimation of stability derivatives is generally greater than that needed if only the control derivatives are to be estimated.

Practical broad-band multi-step test inputs can be designed to avoid excitation at resonant frequencies while giving a satisfactory dispersion matrix. Leith and Murray-Smith (1989) have applied a frequency-domain approach to this design problem involving a cost function of the form

$$I = \sum_{k=1}^{m} a_k |F(\omega_k)|^2 ,$$

where $F(\omega_k)$ is the Fourier transform of a general multi-step signal for n steps, ω_k are frequencies (rad/s) and a_k are constants (k = 1,2, ... m). The values of the weightings a and the frequencies ω in this cost function are chosen to meet the requirements in terms of frequencies which should or should not be excited by the input. For a given number of steps, n, in the multi-step input the cost function is maximised in terms of the timing of these steps. Specifying a large positive coefficient a results in an input with a large auto-spectrum component at the frequency ω_k. Conversely, specifying a large negative a results in an input signal with a small auto-spectrum component at ω_k. This allows inputs to be synthesised which satisfy the general guidelines for test signals outlined above.

The weightings chosen for the different parts of the frequency range in this form of approach can have considerable significance in terms of robustness. Since the model of the vehicle is not known exactly the frequencies of the natural modes are not known exactly. In order to allow for uncertainties inputs should avoid exciting a range of frequencies around the predicted position of each resonance. This should also tend to reduce the overall sensitivity to errors introduced by the pilot in applying the test inputs since errors in the auto-spectrum are then less significant in their effects.

In the case of a flight tests on the Lynx helicopter a double-doublet form of input, designed using this frequency-domain approach, was found to provide useful test records, without stability augmentation, of more than 30 seconds duration before pilot intervention became necessary. Using 3-2-1-1 inputs with the same helicopter useful test records could not be obtained since corrective pilot actions were required very early in each test and the resulting records were of very short duration (Leith and Murray-Smith, (1989)).

It is important to note that the application of any form of test input design process depends upon the availability of initial estimates for the parameters to be identified. The design of truly optimal inputs is thus impossible and the process of selecting the most appropriate form of input is an iterative one. An experienced test pilot can provide valuable assistance in the process of searching for the best input for a particular application.

5 Conclusions

The success or otherwise of system identification work in any field of application depends very largely upon the availability of high quality experimental response data and thus upon the planning and conduct of the associated experiments. In the case of rotorcraft identification it is essential to recognise that there are trade-offs in terms of performance and flight safety. Careful planning and experimental design are therefore of critical importance in order to maximise the information content of the measured response data while maintaining adequate safety margins.

The design of experiments for identification purposes is influenced very much by the information available about the system under test. The optimisation of experiments for system identification is therefore an iterative process with repeated phases of experimentation, model refinement, experimental design and further experimentation. Cost and time constraints in the case of rotorcraft flight testing mean that the experiment design process is, in reality, often only a three stage process involving initial simulation studies, a preliminary experiment based on a broad-band test signal followed by a further stage of analysis and refinement of the design.

Within this overall design process the selection of test input signals presents special problems. One requires an input which will excite the system over the full range of frequencies of interest and give an adequate signal-to-noise ratio for all the measured response variables. On the other hand the excursions from the initial trim condition must not be so large that assumptions of linearity, upon which most identification algorithms depend, are invalidated. Frequency-domain methods have been shown to have some advantages in handling this design problem since they allow multi-step test signals to be tailored to avoid excitation of the system at resonant frequencies while maximising an appropriate measure of the information content of the response data.

References

Bendat, J.S. and Piersol, A.G.,
"Engineering Applications of Correlation and Spectral Analysis"
John Wiley and Sons Inc., New York, 1980.

Bendat, J.S. and Piersol, A.G.,
"Random Data: Analysis and Measurement Procedures", Second Edition,
John Wiley and Sons Inc., New York, 1986.

de Leeuw, J.H. and Hui, K.,
The application of linear maximum likelihood estimation of aerodynamic derivatives for the Bell 205 and Bell 206.
Vertica, Vol.13, No.3, pp. 369-392, 1989.

Kaletka, J.,
Rotorcraft identification experience.
AGARD-LS-104, Paper No.7, 1979.

Leith, D. and Murray-Smith, D.J.,
Experience with multi-step test inputs for helicopter parameter identification.
Vertica, Vol.13, No.3, pp. 403-412, 1989.

Otnes, R.K. and Enochson, L.,
"Applied Time Series Analysis",
John Wiley and Sons Inc., New York, 1978.

Plaetschke, E. and Schulz, G.,
Practical input signal design.
AGARD-LS-104, Paper No.3, 1979.

Tischler, M.B., Leung, J.G.M. and
Dugan, D.C.,
Frequency domain identification of XV-15 tilt-rotor aircraft dynamics in hovering flight.
J. American Helicopter Society, Vol.30, No.2,
pp. 38-48, 1985.

Tischler, M.B.,
"Frequency Response Identification of XV-15 Tilt-Rotor Aircraft Dynamics",
NASA TM-89428, 1987.

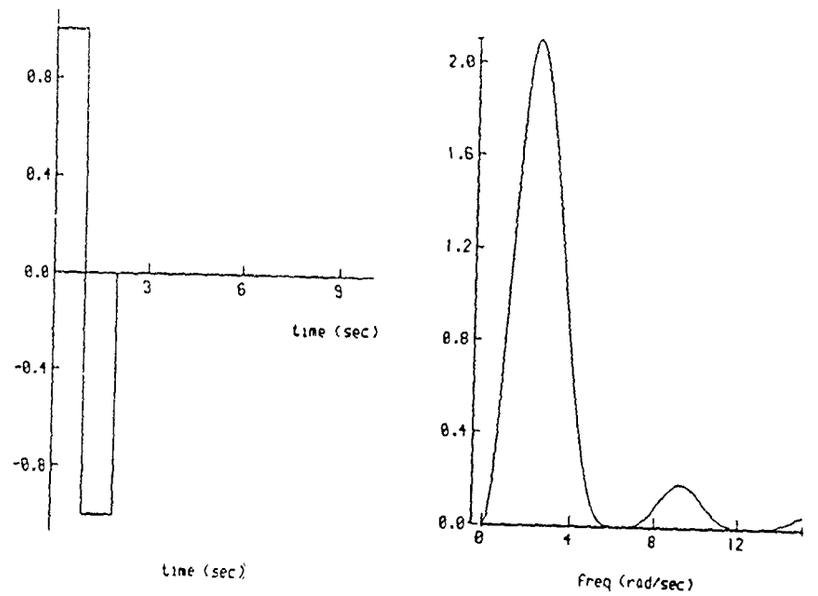

Fig 1 Doublet Time and Frequency Profile

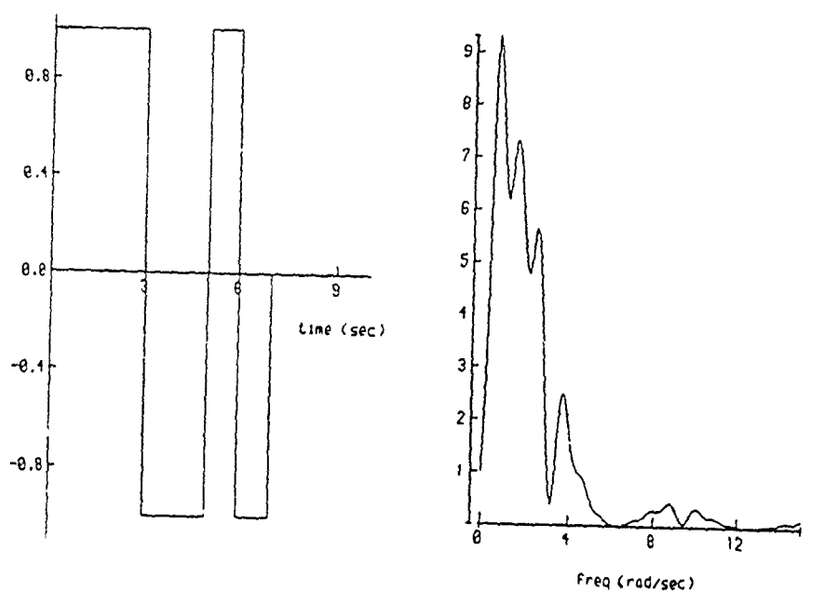

Fig 2 3211 multistep time and frequency profile

INSTRUMENTATION AND DATA PROCESSING

by

Jürgen Kaletka
Deutsche Forschungsanstalt für Luft- und Raumfahrt e.V. (DLR)
Institut für Flugmechanik
DW-3300 Braunschweig, Flughafen, Germany

1. Summary

The quality of measured flight test data is critically important to system identification. Inaccurate or kinematically inconsistent data can lead to identification of an incorrect model or inability to obtain convergence of the estimation solution. Therefore, this Lecture concentrates on instrumentation and data processing aspects from a system identification point of view. It is mainly based on the work of the AGARD Working Group WG-18 on *Rotorcraft System Identification* who concentrated on the identification of 6 degrees of freedom models. In addition, rotor blade instrumentation needed for the determination of extended models with explicit rotor degrees of freedom is addressed

2. Introduction

Independent from the actually applied method, the general system identification approach is always based on the same principle: the measured inputs and outputs of a system are used to extract the unknown system characteristics. There are many differences in the complexity of identification techniques and their requirements: 'parametric' methods need an a priori knowledge of the model structure and often parameter starting values, whereas 'nonparametric' methods (e g. spectra analysis) work without model structure. But all methods rely on the information provided by the amplitude and phase relationship between

- the measured control inputs and
- the measured system response.

Consequently, errors in the measurements must also cause errors in the identification and it is evident that an appropriate instrumentation is necessary. Although methods to detect errors and to correct or even completely reconstruct unreliable measurements have been developed and are successfully applied, they cannot avoid that information is lost that could have been provided by accurately measured data.

This Lecture first gives a brief introduction to the basic identification procedure to illustrate the importance of accurate flight test data. Then, the measurements required for the determination of 6 degrees of freedom models (DOF) are summarized and the data provided to the Working Group are reviewed. The measurement of rotor data needed for the identification of models with rotor degrees of freedom is addressed. Some typical problem areas and sensor characteristics are discussed in more detail, and finally, the main data processing steps and the associated equations are summarized

3. Principle of System Identification Approach

Specifications for the required measured variables, the selection of appropriate sensors, and the conditioning of the measurements highly depend on the flight test objectives and the data evaluation approaches Therefore, before concentrating on instrumentation subjects, the basic approach for system identification is first characterized (a more detailed presentation will be given in the lecture on *Identification Techniques* [1].): The helicopter characteristics are described by a system of coupled linear differential equations in the form of

$$\dot{\mathbf{x}} = \mathbf{A}\mathbf{x} + \mathbf{B}\mathbf{u} \qquad (1)$$

with $\mathbf{x}$ as state vector and $\mathbf{u}$ as control vector. The objective of system identification is to determine the unknown coefficients in the state and control matrices $\mathbf{A}$ and $\mathbf{B}$ by matching the calculated model response to the measured flight test data. As the system characteristics are deducted form measurements it is obvious that data errors will degrade the results and that major emphasis should be placed on measurement accuracy. Depending on the applied identification techniques there is also a different sensitivity to data errors as will be demonstrated for two of the most commonly used identification approaches: the equation-error method and the output-error technique.

3.1 Equation error method

The basic approach is depicted in Figure 1. The control inputs $\mathbf{u}$, the aircraft state response $\mathbf{x}$, and the acceleration response $\mathbf{x}$ are measured. As seen in the Figure, both the measured state and control time history data are used as known values in the mathematical model formulation. The identification algorithm then minimizes the difference between the

model and the measured acceleration response $\dot{x}$ by adjusting the model coefficients.

As the state and control variables are taken from measurements and are treated as known, each equation in the mathematical model is decoupled and can be identified separately and independently from the remaining equations, giving the approach the name *equation error technique*. As usually the squared differences of the calculated and measured acceleration response are minimized it is also often called *Least Squares equation error method*. As the determination of the unknowns has a closed solution (no iterations are needed), the approach is computationally very efficient with low storage and CPU requirements. It can easily be implemented and is in particular suited for smaller computers.

When the obtained model is used for any applications, usually the control inputs are given and the model response is calculated by integrating the differential system. When this is done, the obtained model response can be significantly different from the measured variables (even with the same data set that was used for the identification) for two main reasons:

- The **A** and **B** matrices were not identified accurately for reasons related to the identification procedure itself.
- The quality of the measurements of the control variables and, in particular, of the state variables was not appropriate.

The second reason leads to the main disadvantage of the equation error method:

1. Absolutely accurate control **and** state measurements are required and only low noise levels in the measured accelerations can be tolerated.
2. Measurements for all control, state, **and** acceleration variables of the mathematical model are needed.

In consequence, there are very high accuracy requirements for the instrumentation system, which can often not be met. This is particularly true for helicopters, where vibration noise deteriorates all measurements and air speed data are usually of lower quality and, in low speed conditions, are often not available at all. To some extend, the application advantages of equation error methods are 'payed' by high efforts in both the improvement of sensor accuracy and instrumentation hardware and the development of complex data processing software like state estimation and reconstruction methods.

3.2 Output error method

The general approach for an output error identification techniques is shown in Figure 2. The control inputs and the aircraft response are measured. Similar to the above described equation error approach the aircraft is modeled by a set of linear differential equations as given in equation (1). In addition, an observation- or measurement vector y is defined. It allows combinations of model states and control variables to generate model responses that can be compared to the measured aircraft response:

$$\mathbf{y} = \mathbf{C}\mathbf{x} + \mathbf{D}\mathbf{u} \qquad (2)$$

Using the measured control inputs, the model response y is calculated. The identification algorithm then minimizes the differences between the calculated and measured time histories by adjusting the unknown parameters in the state and control matrices **A** and **B** and the observation matrices **C** and **D**. As the model and aircraft outputs are compared, this approach is called an *output error technique*. There are some distinct differences in comparison to equation error methods:

- based on control measurements, the model states are calculated by integrating the differential equations. The identification of the unknown parameters is an iterative process as an update of the model yields a new model response to be compared to the flight test data.
- The use of the observation equations gives a higher flexibility in the selection of the outputs to be compared.
- As calculated (and not measured) model states are used, the method is less sensitive to model structure errors and errors or noise in the states.
- It is not absolutely necessary to measure all accelerations and states.

The application of output error methods certainly should not justify a decrease in instrumentation accuracy requirements. However, such techniques can better cope with errors in the response measurements than equation error techniques. In particular the fact that various output measurements, and probably also redundant data, can be used in the observation vector makes it easier to adapt the data evaluation to an existing instrumentation system. However, two main requirements for the instrumentation are:

- control inputs must be measured accurately,
- phase shift errors in the measurements must be avoided.

System identification can only be successful when reliable flight test data are available. This is generally true for both identification approaches but particularly for equation error techniques. Analyst working in the field of system identification should be aware that measurement errors will cause (more or less) errors in the identification results. Therefore it is essential to establish a close contact to instrumentation engineers, to make them familiar with the evaluation of the measured data and the high accuracy requirements.

4. Measurements for the Identification of Models with 6 Degrees of Freedom

Measurements needed for the identification primarily depend on the structure of the mathematical model. In the Working Group it was decided to concentrate on the identification of a linear rigid body helicopter model with six degrees of freedom. The identification of such models represents the present standard of rotorcraft identification. In the following, the required measurements are summarized. Then the data provided to the Working Group are reviewed.

4.1 Required measurements

A linear rigid body helicopter model with 6 degrees of freedom is given by a system of eight coupled first order differential equations:

$$\dot{\mathbf{x}} = \mathbf{A}\mathbf{x} + \mathbf{B}\mathbf{u} \tag{3}$$

with the state vector

$$\mathbf{x}^T = (u, v, w, p, q, r, \Phi, \Theta)$$

and the control vector

$$\mathbf{u}^T = (\delta_{lon}, \delta_{lat}, \delta_{col}, \delta_{ped})$$

As previously described, an equation error technique needs the measurements of all components of the control vector **u**, the state vector **x**, and the acceleration vector $\dot{\mathbf{x}}$. When an output error method is applied, the variables to be included in the measurement vector can to a certain extent be chosen by the analyst. In general, the measured state variables are used or equivalent data like dynamic pressure, angle of attack, and sideslip angle instead of the speed components. In addition (or eventually in replacement) however, measurements like linear and rotational accelerations, or helicopter position data, etc. can also be included. There are close relationships between instrumentation and parameter identification:

1. In any case, the measurement vector and the helicopter instrumentation are directly dependent from each other. Usually, the instrumentation is given and the observation variables can only be selected from the available measurements. The request for additional measurements requires an extension of the instrumentation
2. The selection of the considered measurements can have a significant effect on the identified parameters and the model validity. When only measurements dominated by the low frequency helicopter characteristics are chosen, like speed components and attitude angles, the model will give a good representation of the lower frequency range but it can be less accurate for higher frequencies. The opposite result will be obtained by the use of mainly higher frequency data like accelerations and rates. Although it depends on the intended application of the model, it is in general advisable to use both data groups in the measurement equations

For the six degrees of freedom models like they were used in the Working Group, a 'standard' set of suitable variables to be measured can be recommended:

1. controls,
2. airspeed data,
   - speed components in longitudinal, lateral, and normal direction (u, v, w),
     or
   - airspeed, angle of attack, and angle of sideslip (V, α, β),
3. linear accelerations,
   - linear accelerations (a_x, a_y, a_z),
4. angular information,
   - rates (p, q, r),
   - roll and pitch attitude (Φ, Θ),

   and optionally

   - rotational accelerations ($\dot{p}, \dot{q}, \dot{r}$).
     The measurement of helicopter rotational accelerations is difficult and often not available. Therefore, differentiation of the measured rates is probably more appropriate.

4.2 Measurements provided to the Working Group

Three different data bases were made available to the Working Group: AH-64 (Apache) of MDHC, BO 105 of DLR, and SA 330 (PUMA) of RAE. Table 1 to Table 3 summarize the provided measurements. They demonstrate that the instrumentation systems of each of the three helicopters could easily provide the measurements that were recommended for the identification.

- controls,
- speed variables and linear accelerations,
- rates and attitude angles.

In the following sections the individual measurement variables and their sources are reviewed for the three data bases.

4.2.1 Measurement of control variables

System identification methods assume that control inputs are measured without any errors. In practice, the control movements can quite accurately be obtained from carefully calibrated synchros or potentiometers. The main problems arise from unsufficient signal resolutions and, in particular, from the sensor locations. As it is seen from Table 1 both the BO 105 and the SA-330 control inputs were measured at the pilot's controls whereas the AH-64 data were obtained from the actuator output.

4.2.2 Measurement of speed variables and linear accelerations

The speed and linear acceleration measurements are summarized in Table 2.

The standard source for airspeed data is a noseboom system with a pressure sensor and two vanes (angle of attack and sideslip). Such systems have been developed for fixed wing aircraft and were then also used for helicopters although they do not work in the low speed and hover flight regime. Specific helicopter airspeed systems are still rare. From the three considered helicopters only the BO 105 is equipped with a Helicopter Air Data System HADS (swivelling probe installed under the rotor). The AH-64 and the SA-330 provided data from a noseboom system. In addition, the AH-64 data base included ground speed data. As the mathematical models are based on airspeed components, it is preferred to work with measured air data As the airspeed information from the AH-64 turned out to be suitable, the ground speed data were not used in the Working Group. (The interesting aspect however of having both, ground and air speed data with an acceptable accuracy is the determination of wind and gust disturbances, which can allow the identification of the helicopter's gust disturbances characteristics).

All three helicopters were equipped with linear accelerometers installed close to the Center of Gravity. In addition, the AH-64 and the SA-330 had a second unit with linear accelerometers For the AH-64 it was installed close to the pilot's seat, and in the SA-330 it was integrated within a transportable sensor package, the so-called agility package.

4.2.3 Measurement of angular variables

The measurements for the angular information (rates, attitude angles, heading, rotational accelerations) are listed in Table 3. All three helicopters provided rate data obtained from individual rate gyros. (for the AH-64, the gyros are integrated in a Heading Attitude Reference System (HARS)). The AH-64 data also gave differentiated attitude angles and the SA-330 provided additionally the signals obtained from the agility package rate gyros.

For the attitude angles and heading, vertical and directional gyros were used. Again, the SA-330 data base gave in addition the agility package data.

Rotational accelerations were only provided in the AH-64 data base. They were obtained from angular accelerometers. Such measurements are needed for equation error methods and can be very helpful as part of the measurement vector in output error techniques, to emphasise the higher frequency range of the model validity. As angular acceleration measurements are seldom available, the rotational accelerations are often derived by differentiating the measured rates.

4.3 Comments

Comparing the above data measurement requirements and the provided measurements from the three helicopters, it can be seen that helicopter instrumentation systems in general can easily provide the data needed for the identification of 6 DOF models. Although the three helicopters were mainly equipped with individual sensor systems, there is no specific preference for such an instrumentation system compared to an inertia system package. However, it is absolutely necessary to know the sensor characteristics and, probably even more important, the data processing like filtering and sampling rates, that is done along the data flow from the sensor to the data recording. For commercially available instrumentation packages it is often difficult to obtain more detailed information. From this point of view some advantages are seen in the use of individually installed sensors. They can also provide more redundancies in the measurements which can be used for data quality investigations

A high measurement accuracy is the dominant requirement for system identification. The transducers used for the measurements of control positions, linear accelerations, rates, and attitudes are usually potentiometers or synchros, linear accelerometers, and gyros. The today available sensors generally provide high accuracies and are appropriate for identification purposes. However, when transducers are selected and installed, emphasis should be placed on three aspects:

- the measuring range has be chosen to, on one hand, provide a high signal resolution and accuracy and, on the other hand, avoid signal saturation for the planned flight test experiments.
- cross axis sensitivities can generate significant problems and must be kept as small as possible. They can be caused by both, sensor characteristics and installation misalignments.
- a careful calibration with clearly defined signs is absolutely necessary. In addition to a sensor calibration in the laboratory, it is advisable to run an additional calibration (or at least use a few test points) with the complete instrumentation equipment engaged. Here the data flow from the sensor to the recording system can be checked.

From the review of the provided data bases it can be concluded that modern instrumentation systems do meet system identification requirements so far as the availability of measurements is concerned. The fact that analysts still sometimes have to state that data were not appropriate for system identification purposes is often related to the way how the instrumentation system was used or it is a lack of more detailed information about the sensors and the on-board data processing. Again, a close contact to the instrumentation engineers and a detailed information exchange

is strongly recommended. However, there are several detailed problem areas, both instrumentation and helicopter related, that can cause significant difficulties. Some of them will be addressed in the section on *Problem Areas*

5. Measurements for the Identification of Models with Rotor Degrees of Freedom

Helicopter models with 6 degrees of freedom are useful for applications that require an appropriate representation of the helicopter dynamics in the low- and mid-frequency range (up to about 10 rad/s for the BO 105), like handling qualities evaluations or piloted simulations. However, when models with a more reliable representation of the higher frequency dynamics are needed, for instance for high-bandwidth control-system design, it is necessary to extend the model formulations by equations for the rotor dynamics. Consequently, the identification of such extended models requires measurements for the rotor degrees of freedom.

The identification of models with rotor degrees of freedom were beyond the scope of detailed study by the Working Group. It is still a major research task and presently there are only few attempts with good results. This is certainly also due to the fact that quite often rotor measurements are either not available at all or they are of lower quality. This is particularly true for hingeless rotors as, in contrast to articulated rotors, blade motions can no longer be measured at physical hinges but have to be derived from blade bending measurements.

To approach the identification of helicopter models with rotor degrees of freedom, DLR concentrated on a model formulation with 3 additional degrees of freedom representing the rotor coning, longitudinal and lateral flapping. Consequently, the required rotor measurement were flapping for all four blades and rotor azimuth. The DLR BO 105 rotor was instrumented with a pair of strain gauges at the location of the equivalent hinge offset. The obtained signals were fed to a specially developed rotor signal module mounted on top of the rotor (Figure 3). The module was equipped with analogue amplifiers and a digital processor that is used for A/D conversion, the data transfer via slipring to the on-board data recording system, the sychronization of the rotor data with the data stream from the sensors installed in the helicopter body, and, optionally, any real time rotor data processing [3]. The rotor azimuth was measured by a saw-tooth potentiometer.

For the calibration of the flapping motion, first the usually used static technique was applied by bending the (non-rotating) blade. When the obtained results turned out to be not satisfactory, the signal calibration was done at the rotating blade under conditions of airloads and centrifugal forces [3]. As schematically shown in Figure 4, the blade tip deflections and the corresponding strain gauge signals were measured on the ground for different collective control positions (maximum: almost take-off). The calibration was done for each of the four blades and, for redundancy, for two different azimuth locations.

As an representative example for the obtained flight test data Figure 5 presents for a collective input signal the measured flapping angles for each blade (rotating system) and the azimuth angle. It can be seen that the data have practically the same response characteristics for mean values, amplitude changes, and higher order effects. The obtained data accuracy also allowed the calculation of a reliable tip path plane motion by a multiblade coordinate transformation to obtain longitudinal and lateral flapping and coning. These variables that are defined in a body fixed non-rotating axis system, are shown in Figure 6 for longitudinal, lateral, and collective control inputs. Higher frequency noise is small proving that the calibrations and measurements of the individual blades are consistent to each other. The primary axis responses can clearly be recognized. The time histories of longitudinal flapping due to longitudinal stick and coning due to collective indicate that the rotor response has at least a 2nd order system characteristic. The lateral flapping response due to a lateral stick input shows a significantly different characteristic as both, the roll moment of inertia and the fuselage aerodynamic moments in the roll axis are small.

Results obtained from the identification of the extended model are given in the lecture on *BO 105 Identification Results* [4].

6. On-board Data Processing

Extensive on-board data processing is needed for all processes that are based on the immediate availability of measurements. Such on-line data processing is for example a prerequisite for control systems, ranging from mode stabilization up to in-flight simulation. As rotorcraft system identification still is an off-line procedure, no specific on-board data processing is required except for the standard signal conditioning steps converting sensor signals to the appropriate format for data recording. They include all modifying operations applied to signals like the adaption of transducer outputs to the input requirements of the data handling system (e.g. synchro to analogue conversion), signal amplification, filtering, multiplexing, digitization, and data recording (often on board of the aircraft to avoid disturbances from the telemetry). The data conditioning is certainly necessary and helps to maintain the data quality. However, some of the procedures can significantly modify the original sensor output data.

For system identification, care must be taken with analogue (anti-aliasing) filters, causing phase shifts, and with data sampling when data are scanned

sequentially with time delays between the individual channels These effects can be corrected during the further data processing. However, it is evident, that the analyst must know exactly what has 'happened' to the data. Only then, appropriate corrections can be made. In practise, here is quite often the main gap: the instrumentation engineers are not informed of the data requirements for a specific evaluation and the analysts are not aware of the data conditioning steps that can already have deteriorated the data for their applications. Therefore, a close cooperation and a detailed information exchange between these two groups is absolute necessary. It can be more important than increasing a sensor accuracy by another tenth of a percent in order to generate more reliable data.

7. Problem Areas

Some of the typical problem areas in helicopter flight data measurement were also seen in the data provided to the Working Group. They are mainly due to helicopter and sensor characteristics but also can occur during the signal conditioning. Some examples are illustrated in more detail:

7.1 Airspeed measurement

The conventional sources for air data measurement are vanes and pressure probes. They were originally developed for fixed wing aircraft and are also used for helicopters. Rotorcraft, however pose special problems in accurate sensing of air data: The sensors have to be installed on a relatively long boom to keep them away from main rotor wakes. The boom must be quite stiff to avoid oscillations excited by the helicopter vibration. With decreasing speed, pressure measurements become more and more inaccurate and near hover both, pressure tubes and vanes cannot be used at all. Although these deficiencies are obvious and well known, only a few air data systems are available that were designed to also operate in the low speed regime of helicopters.

The AH-64 and the SA-330 use a boom to provide air data. For the flight conditions considered in the Working Group (120 kn for the AH-64 and 80 kn for the SA-330) the systems gave good measurements. (The AH-64 is additionally equipped with a low range airspeed system. These data however were not provided to the Working Group).

The BO 105 uses a helicopter air data system. It consists of a swivelling pitot static probe installed at the fuselage close to the rotor. For low speed it is designed to work within the rotor downwash. Measurements are dynamic pressure and probe angle of attack and sideslip. For the flight condition considered in the Working Group (80 kn) the sensor is out of the rotor downwash and aligns with the total flow. The measurements however show that rotor wake interferences cannot be avoided in dynamic flight manoeuvres. Figure 7 shows the helicopter response due to a longitudinal stick doublet input. In the speed data, and particularly in the lateral speed, significant disturbances are seen They are caused by rotor wakes that 'hit' the sensor when the helicopter pitches nose-down. Then, the sensor rotates to the left and indicates a high sideslip angle and consequently a high sideward speed In the signals this effect is seen like a data drop-out It can last for even a few seconds until the sensor is in undisturbed flow again

7.2 Measurement of linear accelerations and rates

All measurements of the helicopter motion are influenced by a high vibration level. This is particularly true for the linear accelerations and the rates. For BO 105 data obtained from a longitudinal stick control input Figure 8 first presents the actually measured unfiltered data. Then, on the same scale, it shows the data after being filtered by a digital low-pass filter with a cut-off frequency of 12.5 Hz. From the comparison it can be seen

- the high frequency noise (mainly blade harmonics) can easily be removed by low-pass filters. As system identification results are very sensitive to phase errors, zero-phase shift digital filters should used.
- for the linear accelerations (and in particular the forward and sideward accelerations) there is a very low signal-to-noise ratio. In this test, the helicopter forward and sideward accelerations are less than 0.5 m/s^2. (In general, helicopters cannot produce large linear accelerations, except for the vertical axis). The vibration level on the data is more than 5 m/s^2 and reaches even higher values in other flight conditions (flare and hover). Consequently, the measuring range of the accelerometers is practically defined by the vibration levels. Therefore, the BO 105 was equipped with sensors of a ± 12 m/s^2 range for a_x and a_y. Although the 'useful' part of the signal is less than 5 % of the total sensor range a high accuracy is required for system identification.

  Fortunately, linear accelerometers belong to the best sensors in an aircraft instrumentation. They have a high linearity and resolution with only small hysteresis and work in a wide bandwidth without significant phase errors. Nevertheless, the sensor range should carefully be selected to avoid saturation and still to provide a high signal resolution.

  Helicopter responses due to control inputs are primarily rates (not linear accelerations). Therefore, the 'useful' signal in the rate measurements is still dominant although it is also highly deteriorated by the helicopter vibration. Together with linear accelerometers, rate gyros have reached a high quality and, for the identification,

rates certainly belong to the most accurate and important measurements.

7.3 Measurement of rotational accelerations

Rotational accelerations where only measured in the AH-64. For the identification they are useful as they provide more high frequency information for the determination of the moment equations. Figure 9 first shows the measured roll and pitch accelerations due to a longitudinal control input. The high vibration level is obvious. Then, the filtered data (digital filter, 12.5 Hz cut-off frequency) are plotted together with data that were obtained by differentiating the measured rates. The agreement is very good and proves a high consistency although the measurements still show a higher noise level. It cannot yet finally be answered how helpful measured rotational accelerations can be for the identification in comparison to differentiated signals obtained from accurately measured rates.

7.4 Measurement of the control inputs

The influence of data errors on the identification results also depends on the applied identification technique. Least Squares equation error methods assume that all variables are accurate whereas more complex output error techniques allow measurement errors on the response variables. All techniques, however, fully rely on accurately measured control inputs and, at best, can compensate for noise on the measurements. Although it is relatively easy to measure the control positions, there are two main error sources: signal resolution and sensor position.

The control inputs for system identification purposes are usually small to allow a linearised model formulation, whereas the sensors, e.g. potentiometers, normally measure the full range of the controls. For the identification data, it must be made sure that the range of interest is sufficiently resolved.

Control positions are often measured at the pilot controls. When they are used in the identification the characteristics of the (mechanical) linkage and of the hydraulic system have often to be neglected. Attempts to model and identify effects like backlash, flexibility, hydraulic characteristics lead to highly non-linear models and significantly complicate the identification. Therefore, it should be tried to measured the control inputs as close to the rotor as possible. In any case, the measurement must be related to the control input at the blades. When feedback systems are engaged, the sum of both, the pilot inputs and the control system activity, must be measured unless both inputs are provided separately.

For the AH-64, measurements of the hydraulic actuator positions at the main rotor (or tail rotor) swashplate were given These locations have the advantage of being close to the rotor but still in the non-rotating system.

For the BO 105, stick deflections, collective lever, and pedal positions were used. Control linkage effects were assumed to be negligible and the hydraulic system was supposed to be represented by a time delay or time constant on the control measurements. Specific measurements have shown that these assumptions can be justified

The SA-330 data base gave control positions obtained from three different locations. However, except from pilot controls (similar to the BO 105) the other data were obtained in the rotating system at only one control rod and one blade root. A transformation into the fixed axis system was not given. For dynamic tests, it also seems to be necessary to include at least three blade control angles to derive three controls in the non-rotating system. Therefore, the inputs measured at the pilot position were used for the identification.

7.5 Measurement of rotor data

In the Working Group, emphasis was placed on the identification of 6 DOF rigid models. Rotor degrees of freedom were not considered and no rotor measurements were provided to the Group. Presently there is only minor experience in the identification of helicopter models with rotor degrees of freedom and any related measurement problems. However, from the recent DLR work where blade flapping was measured at one position (equivalent hinge) for each blade, a few general statements can be made:

- Blade motions for hingeless and bearingless rotors have to be measured by pairs of strain gauges glued on the blades. One of the positions should be at the equivalent hinge offset. The installation must be done very precisely and identical for all blades. It has to be checked that coupling influences due to blade lagging or torsion are small and can be neglected.
- As strain gauge signals have a low voltage level, they should be amplified before they are transferred from the rotor to the body.
- A main problem is the calibration of the strain gauge signals. It should be considered if a static calibration is adequate or if a calibration on the rotating rotor is necessary. Strain gauge temperature sensitivities and signal drifts must be taken into account and compensated.
- The measurement of the rotor azimuth is often done by a short impulse (blip) generated by the passage of a selected blade per revolution. In particular with lower sampling rates this approach can be quite inaccurate and a continuous measurement of the azimuth angle using for instance a saw-tooth potentiometer is recommended.

7.6 Signal filtering

As some measurements of the helicopter motion are very noisy, low-pass filtering is usually applied before the data are used for system identification. It must be taken into account that analogue filters not only reduce the high frequency amplitudes but also influence the phase characteristics of the measured signal. In particular with higher order filters, the phase shifts can already be significant at frequencies far below the filter cut-off frequency. Considering that the identification is based on the amplitude and phase relationship between the individual measurements it is quite obvious that filters can strongly deteriorate identification results and even render them unusable. Therefore, it is absolutely necessary that all measurements are passed through identical filters. This requirement is often neglected as it is not so important for most data evaluation other than system identification. Only when zero-phase shift filters with a constant gain of 1.0 in the frequency range of interest are applied, it is possible to filter selected measurements. Here, digital off-line filters are applied.

When sensors with integrated (analogue) filters or sensor packages (e.g. inertial systems) are used, it is essential to know the built-in signal processing. As an example Figure 10 compares linear acceleration measurements obtained from an 'agility' sensor package and from individual accelerometers. The package signals do not follow the more dynamic manoeuvre part in the data when the control input is given. A closer view also showed that there is a phase lag between the accelerometer and the package data. It indicates that some strong damping or filtering was done in the agility package although the data are still very noisy.

For the identification it was decided to use the individually measured linear accelerations.

7.7 Signal resolution

For system identification usually only small amplitude control inputs are applied to keep the helicopter response so small that linear models can be used. When the amplification or scaling of the data is based on the maximum helicopter response capability, the small amplitudes can probably not be resolved satisfactorily by the data recording system. For the pitch and roll attitude response due to lateral and collective control inputs Figure 11 demonstrates that the digitization of the vertical gyro signal could only resolve about 0.3 degrees per bit. As the tests with controls other than collective (e.g. the shown lateral control input) produced attitude angles between 20° and 30° the resolution errors probably do not affect the identification results significantly. However, such problems can usually be avoided when signal amplification is based on the expected maximum amplitudes of the specific tests.

7.8 Control input generation

It is widely agreed that for system identification specific control inputs should be used to properly excite the aircraft modes. Some of the designed input signals are quite complex so that they cannot be generated by the pilot but require electronic devices. Only the AH-64 was equipped with a specially designed Gold Oscillator Box (GOB) unit. It commanded sinusoidal frequency sweeps in two ranges from 0.1 Hz to 3 Hz and 0.3 Hz to 13 Hz. For the BO 105 and the SA-330 only pilot generated inputs were used. (In the BO 105 a relatively simple display was installed. It showed the prescribed signal and the actual control position.) The input signals used in the Working Group, doublet, multistep, and frequency sweep could be generated by the pilot without any real difficulties. It proved that system identification does not require an electronic control input device when rigid body models have to be identified. It is only needed when frequencies exceeding the human capability (more than 2 Hz to 5 Hz) are required.

8. Off-line Data Processing

The off-line data processing for system identification purposes mainly includes:

- conversion to a consistent unit system,
- detection and removal of data drop outs,
- low-pass filtering,
- corrections for the centre of gravity, and
- the calculation of additional variables.

These procedures are standard for flight testing and therefore this section will briefly document the off-line data processing conducted within the Working Group and, for completeness, give the applied equations.

A more detailed data analysis for detecting and correcting data deficiencies is considered as a first essential task in data evaluation and system identification. It will be described in the lecture on *Flight Test Data Quality Evaluation* ([2]).

8.1 Unit system

The measurements needed for system identification were converted to the International Unit System (SI) based on meter, second, kilogram and radian. Control displacements were given in percent with 100 percent as full travel.

8.2 Data drop outs

When data drop outs are restricted to only a few samples it can be justified to eliminate these samples and reconstruct a new value by interpolation between the neighbouring data. Of course, this technique

cannot reproduce the lost data. However, it gives a more realistic value for the sample instead of keeping the drop out data. It is also the only possibility to avoid even more data distortion which occurs when the uncorrected measurement is filtered. For the data in the Working Group only minor work had to be done to eliminate drop-outs.

8.3 Digital low-pass filtering

Problems associated with analogue filtering have already been addressed. Analogue filters significantly influence the phase where this effect increases with higher filter order. As identification results are very sensitive to phase errors it should be tried to reduce analogue filtering as much as possible. Here, high sampling rates make it possible to use anti-aliasing filters with a high cut-off frequency. When, in addition, these filters have the same characteristics, their influence in the frequency range of interest is small and similar. Then, zero-phase shift digital filtering can be applied to

1. eliminate the unwanted higher frequency effects and noise, and
2. to reduce the sampling rate.

This approach was consequently used for the measurement of the BO 105 data, where almost all analogue filters where removed. Comparisons of the obtained data to previous flight test measurements with strong analogue low-pass filtering clearly showed the data quality improvements.

The efficiency of digital filters has already been show in Figure 8.

8.4 Calculation of speed components at the sensor position

Using the measured airspeed, angle of attack and angle of sideslip (V, α, β), the longitudinal, lateral, and normal speed components at the sensor position (boom) were calculated by

$$u_b = V \cdot \cos\alpha \cdot \cos\beta \tag{4}$$

$$v_b = V \cdot \sin\beta \tag{5}$$

$$w_b = V \cdot \sin\alpha \cdot \cos\beta \tag{6}$$

8.5 Correction for CG Position

In contrast to data obtained from rate and attitude gyros, the measurements of linear accelerations and aerodynamic data are influenced by the distance between the sensor position and the helicopter centre of gravity (CG) Ideally, these sensors should be installed at the CG. Linear accelerometer locations can at least be close to the CG. Air data sensors, however, are usually installed far in front of the aircraft. During dynamic flight tests the measured signals also contain acceleration or speed components due to the helicopter angular motion. Mathematical models as used for system identification always describe the forces and moments with respect to the CG. There are two different approaches to handle the influence of the CG location on the measurements:

1. the measurements are corrected for CG position, or
2. in the measurement equations the model response is transformed to the individual sensor location.

In the Working Group the first approach was chosen.

With the sensor locations in

x-direction (positive forward):	x_m
y-direction (positive to the right):	y_m
z-direction (positive downward):	z_m

the speed components at the CG (u_{cg}, v_{cg}, w_{cg}) are obtained as

$$u_{cg} = u_b - z_m \cdot q + y_m \cdot r \tag{7}$$

$$v_{cg} = v_b - x_m \cdot r + z_m \cdot p \tag{8}$$

$$w_{cg} = w_b - y_m \cdot p + x_m \cdot q \tag{9}$$

where u_b, v_b, and w_b are the speed components measured at the sensor position (see equations (4) to (6)).

For the corrections of the linear acceleration measurements the rotational accelerations ($\dot{p}$, $\dot{q}$, $\dot{r}$) are needed. When no measurements are available, differentiated rates are used. Then, the linear accelerations at the CG are:

$$\begin{aligned} a_{xcg} = a_x &- z_m \cdot \dot{q} + y_m \cdot \dot{r} \\ &- (y_m \cdot p - x_m \cdot q) \cdot q \\ &+ (x_m \cdot r - z_m \cdot p) \cdot r \end{aligned} \tag{10}$$

$$\begin{aligned} a_{ycg} = a_y &- x_m \cdot \dot{r} + z_m \cdot \dot{p} \\ &- (z_m \cdot q - y_m \cdot r) \cdot r \\ &+ (y_m \cdot p - x_m \cdot q) \cdot p \end{aligned} \tag{11}$$

$$\begin{aligned} a_{zcg} = a_z &- y_m \cdot \dot{p} + x_m \cdot \dot{q} \\ &- (x_m \cdot r - z_m \cdot p) \cdot p \\ &+ (z_m \cdot q - y_m \cdot r) \cdot q \end{aligned} \tag{12}$$

For the helicopters studied by the Working Group, the linear accelerometers were located close to the CG. The AH-64, however, was equipped with a second accelerometer package installed at the pilot seat position with a distance of about 1.50 meters from the CG. To demonstrate the influence of the (still relatively small) off-CG location, Figure 12 shows for a tail rotor input

1. the uncorrected and the CG corrected longitudinal accelerations obtained from the pilot seat sensor,
2. the uncorrected and the CG corrected lateral accelerations obtained from the pilot seat sensor,

3. the CG corrected lateral acceleration obtained from the pilot seat sensor and the lateral acceleration obtained from the CG accelerometer package.

Considering that the helicopter response to a pedal input is primarily a yaw motion, it makes sense that the longitudinal acceleration is not much influenced by the CG distance. The lateral acceleration however clearly shows differences. The improvement obtained from the signal correction becomes evident in the last part of the figure where the sinals obtained from the different sensors are in good agreement.

8.6 Calculation of the tip path plane motion from flapping measurements

For the identification of extended models with rotor degrees of freedom, the rotor tip path plane motion is modeled in a body-fixed axis system. As the rotor data are measured in the rotating system, they first have to be transformed. For the flapping measurements the corresponding equations to derive rotor coning, longitudinal flapping, and lateral flapping are given below. In practice, the blades are usually marked by coloured tape. Therefore, the following notations for the flapping angles β of the individual blades will refer to the blade colours blue, green, yellow, and red.

Coning β_0:

$$\beta_0 = 0.25 \cdot (\beta_{blue} + \beta_{green} + \beta_{yellow} + \beta_{red}) \qquad (13)$$

Longitudinal flapping β_c:

$$\beta_c = 0.5 \cdot \begin{bmatrix} \beta_{blue} \cdot \cos(\psi + 0.0 \cdot \pi) + \\ \beta_{green} \cdot \cos(\psi + 0.5 \cdot \pi) + \\ \beta_{yellow} \cdot \cos(\psi + 1.0 \cdot \pi) + \\ \beta_{red} \cdot \cos(\psi + 1.5 \cdot \pi) \end{bmatrix} \qquad (14)$$

Lateral flapping β_s:

$$\beta_s = 0.5 \cdot \begin{bmatrix} \beta_{blue} \cdot \sin(\psi + 0.0 \cdot \pi) + \\ \beta_{green} \cdot \sin(\psi + 0.5 \cdot \pi) + \\ \beta_{yellow} \cdot \sin(\psi + 1.0 \cdot \pi) + \\ \beta_{red} \cdot \sin(\psi + 1.5 \cdot \pi) \end{bmatrix} \qquad (15)$$

with

β_{blue}	Flapping angle, blue blade	$\psi = 0$
β_{green}	Flapping angle, green blade	$\psi = 0.5\pi$
β_{yellow}	Flapping angle, yellow blade	$\psi = 1.0\pi$
β_{red}	Flapping angle, red blade	$\psi = 1.5\pi$
ψ	rotor azimuth angle	

(the rotor azimuth angle $\psi$is defined to be zero when the blue blade aligns with the tail boom).

9. Conclusions

So far as the availability of measurements is concerned it was seen that the instrumentation systems of the three helicopters provided more signals than usually needed for system identification. The flight tests have also shown that no specific instrumentation, like electronic control input boxes, is required To generate reliable and useful data seems to be more a task of properly defined measurement ranges, careful data processing, and of course the flight testing itself. In conclusion some main guidelines can be given:

1. Control inputs can be generated by the pilot. Some training and if possible a display type device are helpful. Electronically generated inputs with a direct link to the control are not necessary unless high frequencies are needed,
2. If possible, the sensors should have a measuring range that is suitable for the expected signal amplitudes,
3. If analogue filtering of signals is applied it is important that all signals used for the identification are filtered and the filters have identical characteristics,
4. The signal digitization range should be defined by the maximum signal amplitudes in the tests to obtain a good signal resolution,
5. Standard data processing steps, like removal of drop outs, digital low-pass filtering, CG correction, etc., are applicable and adequate.

The measurement of rotor data was addressed. The presently available data from the hingeless BO 105 rotor seemed to be reliable and indicated that such measurements can be generated in a quality suitable for system identification purposes.

10. Bibliography

[1] de Leeuw, J.H.
Identification Techniques
AGARD LS178, Paper 5, 1991

[2] Breeman, J.H.
Flight Test Data Quality Evaluation
AGARD LS178, Paper 4, 1991

[3] Holland, R.
The Rotor-Signal Module of MFI90
International Telemetering Conference, San Diego, US, Nov 1989

[4] Kaletka, J.
BO 105 Identification Results
AGARD LS178, Paper 9, 1991

Measured Variable	AH-64	BO 105	SA-330
Main rotor longitudinal cyclic	actuator	stick	stick
Main rotor lateral cyclic	actuator	stick	stick
Main rotor collective	actuator	collective lever	collective lever
Tail rotor collective	actuator	pedal	pedal

Table 1. Measurement of control variables

Measured Variable	AH-64	BO 105	SA-330
Airspeed			
Longitudinal airspeed		HADS**	
Lateral airspeed		HADS**	
Vertical airspeed		HADS**	
Total airspeed	pressure sensor at noseboom		pressure sensor at noseboom
Angle of attack	vane at noseboom		vane at noseboom
Angle of sideslip	vane at noseboom		vane at noseboom
Groundspeed			
Longitudinal groundspeed	doppler radar		
Lateral groundspeed	doppler radar		
Vertical groundspeed	HARS*		
Linear accelerations			
Longitudinal acceleration	accelerometers at CG and pilot's seat	accelerometer at CG	accelerometer at CG, agility package
Lateral acceleration	accelerometers at CG and pilot's seat	accelerometer at CG	accelerometer at CG, agility package
Vertical acccleration	accelerometers at CG and pilot's seat	accelerometer at CG	accelerometer at CG, agility package

* HARS : Heading Attitude Reference System
** HADS : Helicopter Air Data System

Table 2. Measurement of speed variables and linear accelerations

Measured Variable	AH-64	BO 105	SA-330
Rates			
Roll rate	HARS* and derived from roll angle (Euler)	rate gyro	rate gyro and agility package
Pitch rate	HARS* and derived from roll angle (Euler)	rate gyro	rate gyro and agility package
Yaw rate	HARS* and derived from yaw angle (Euler)	rate gyro	rate gyro and agility package
Attitude angles			
Roll angle	HARS*	vertical gyro	vertical gyro and agility package
Pitch angle	HARS*	vertical gyro	vertical gyro and agility package
Yaw angle (heading)	HARS*	directional gyro	directional gyro and agility package
Angular accelerations			
Roll acceleration	angular accelerometer		
Pitch acceleration	angular accelerometer		
Yaw acceleration	angular accelerometer		

* HARS : Heading Attitude Reference System

Table 3. Measurement of rates, attitude angles, and rotational accelerations

11. Figures

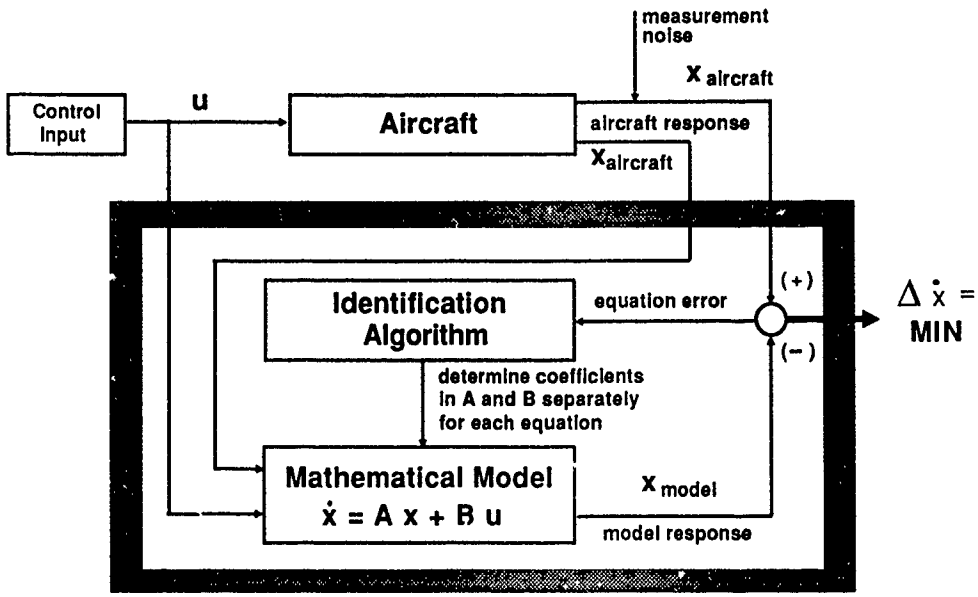

Figure 1. Principle of equation-error identification technique

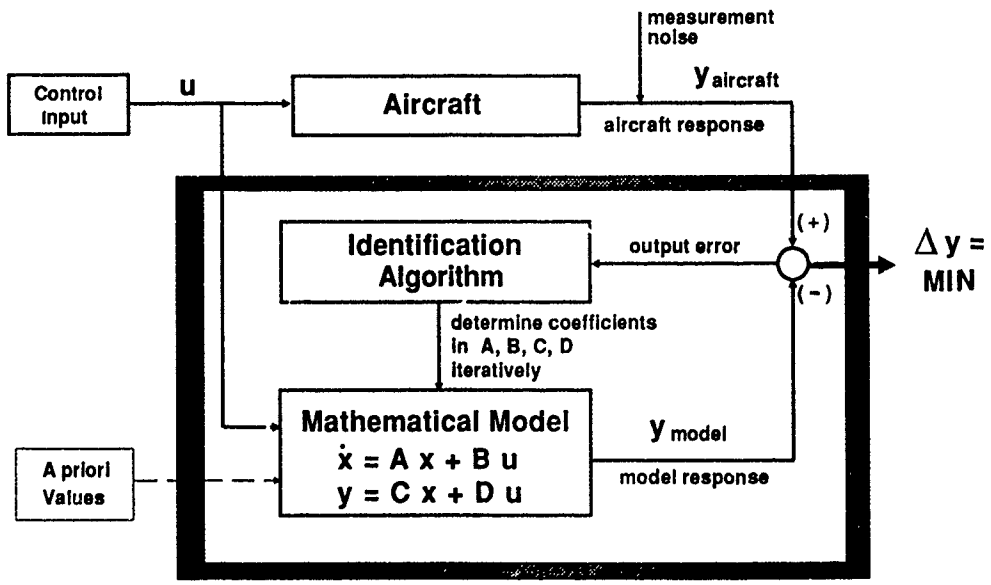

Figure 2. Principle of output-error identification technique

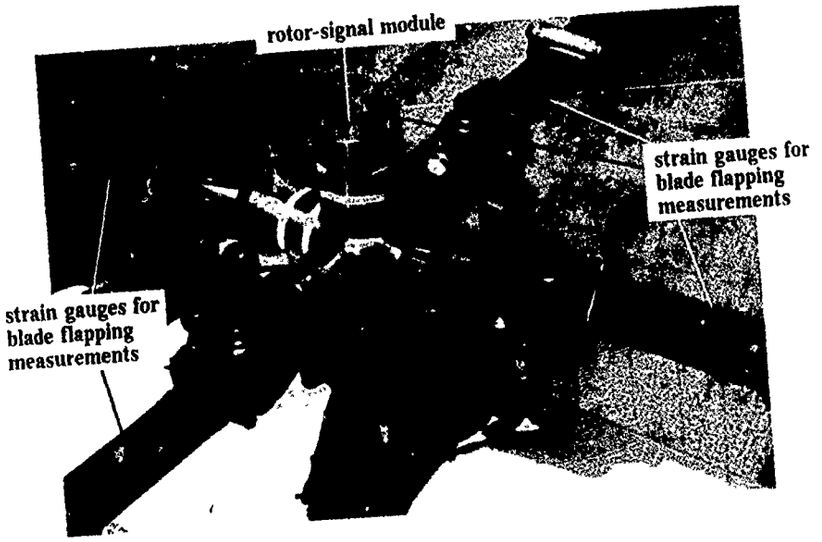

Figure 3. Measurement of blade flapping angle

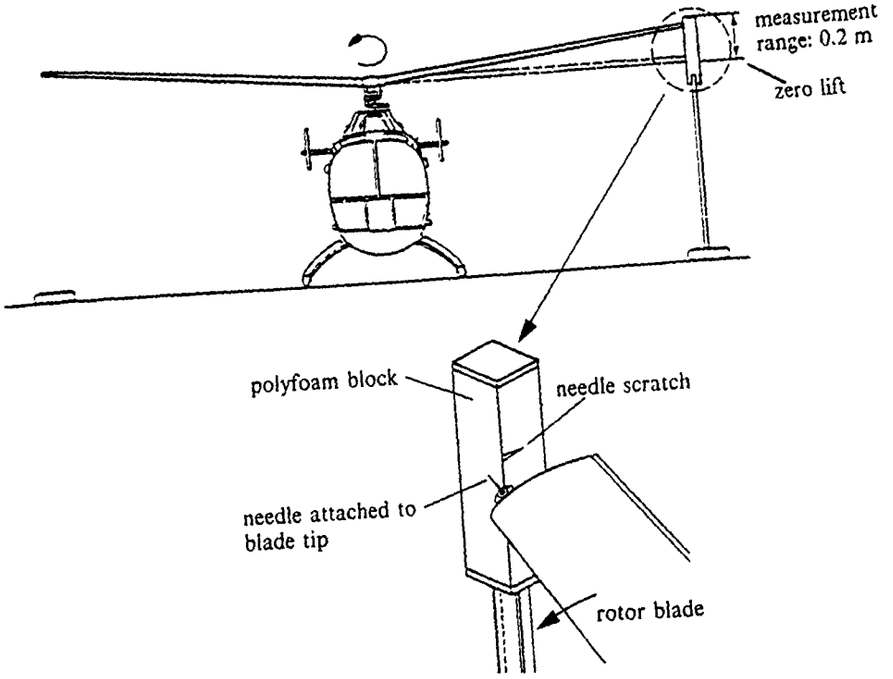

Figure 4. Calibration of blade flapping angle

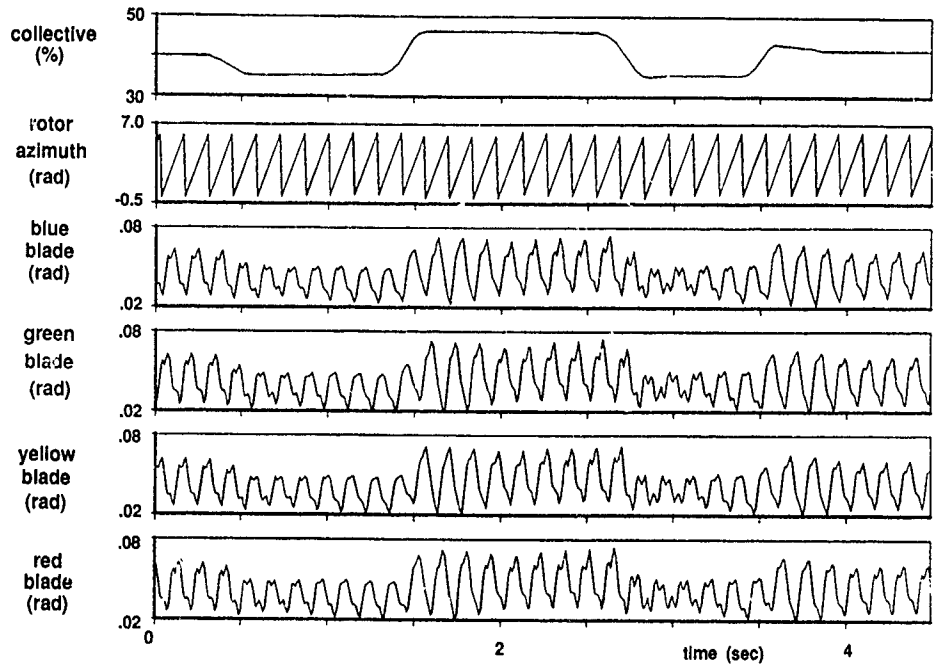

Figure 5. Measured rotor azimuth and blade flapping for a collective input

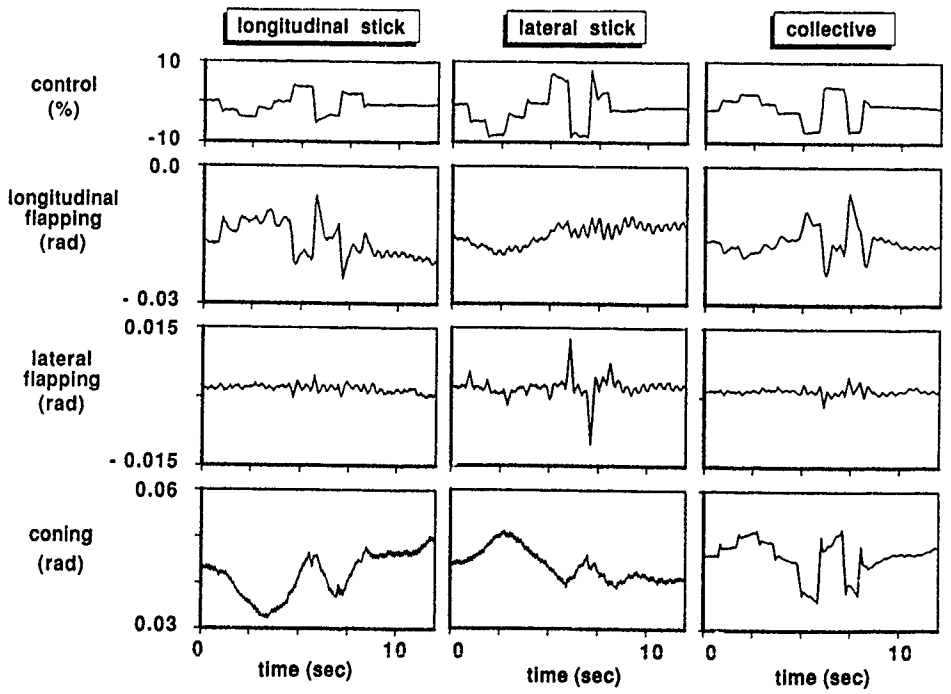

Figure 6. Tip path plane response, derived from blade flapping measurements

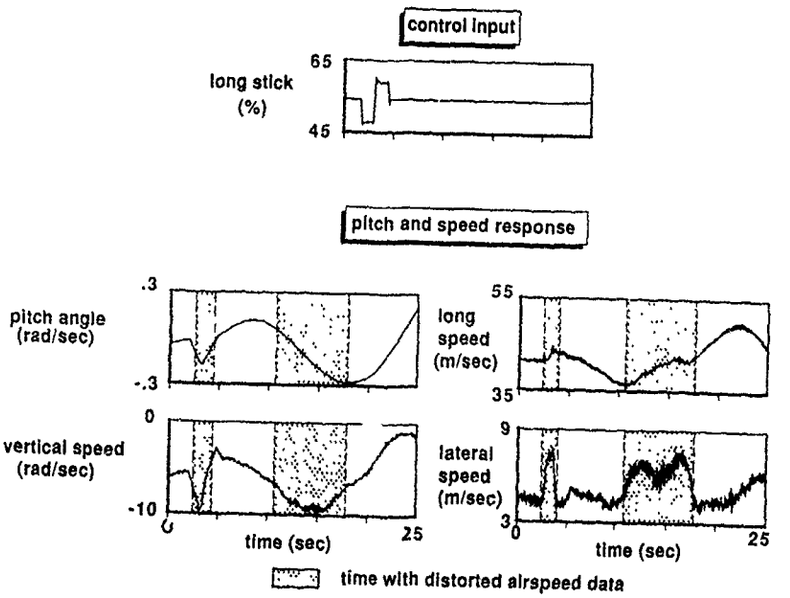

Figure 7. Distortions in airspeed measurement

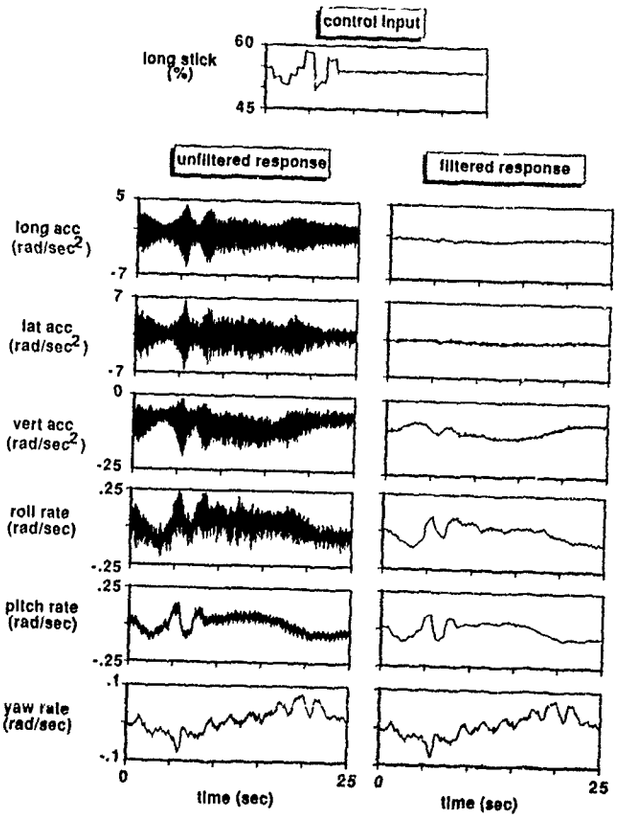

Figure 8. BO 105 data: comparison of unfiltered and filtered linear accelerations and rates

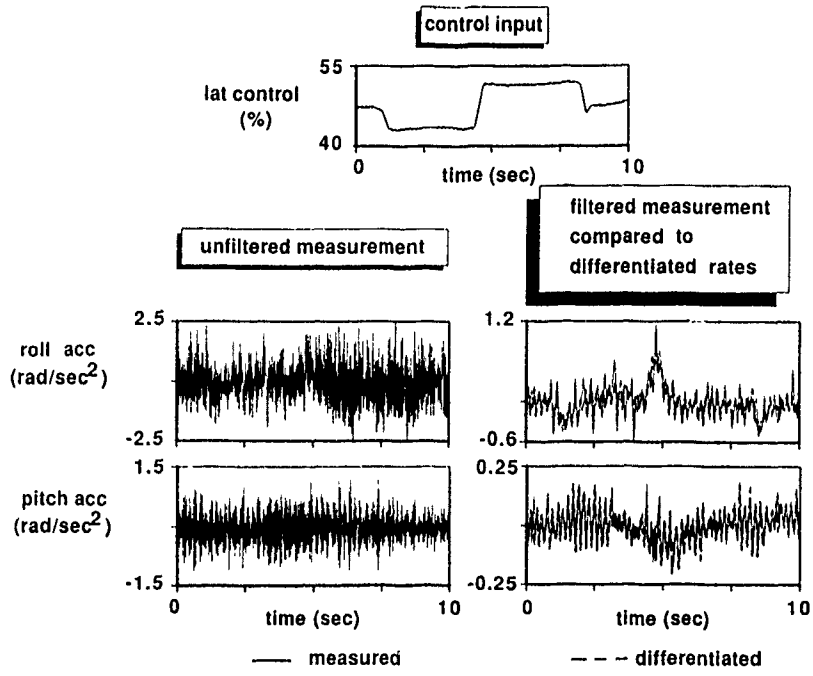

Figure 9. Measured AH-64 unfiltered and filtered rotational accelerations and comparison with differentiated rates

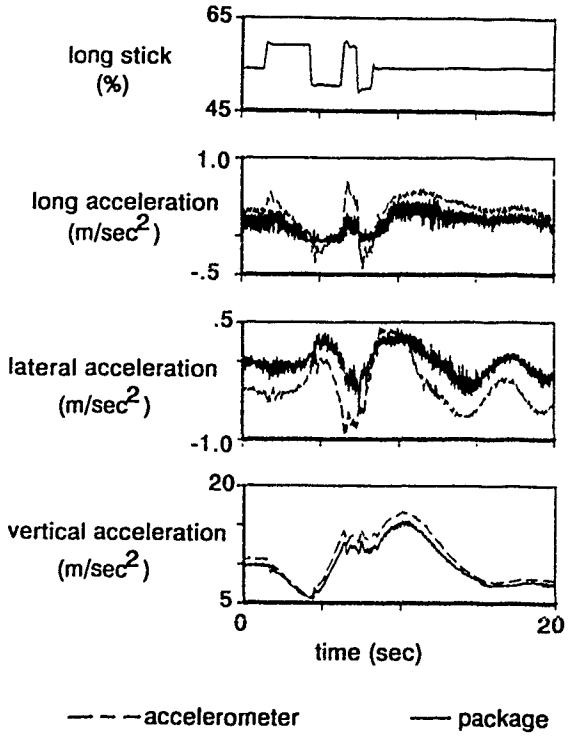

Figure 10. Comparison of linear acceleration measurements obtained from an 'agility' package and individual accelerometers

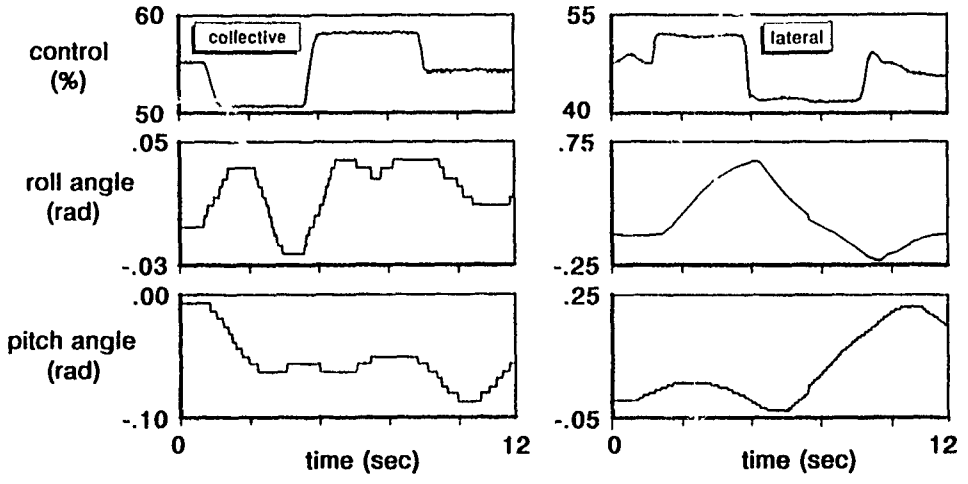

Figure 11. Resolution of the pitch and roll attitude measurements (AH-64)

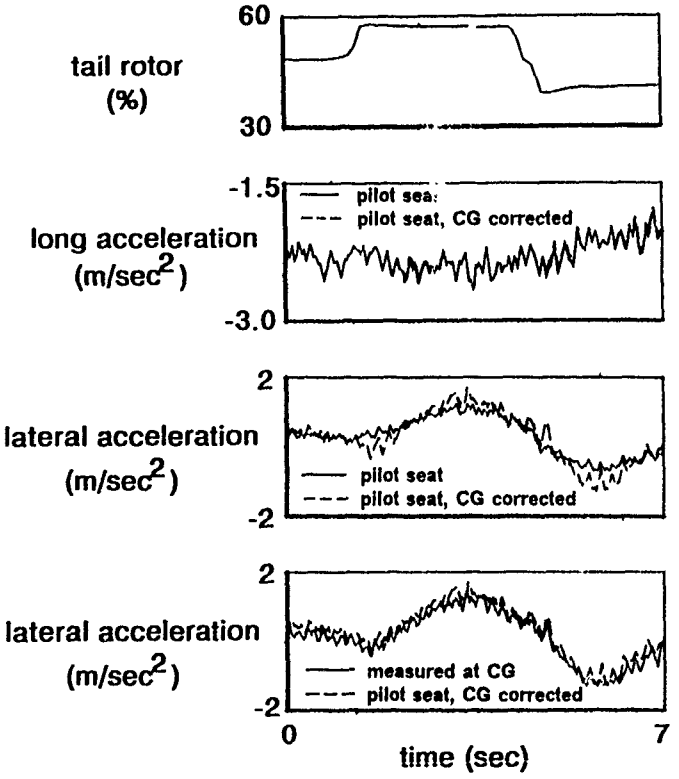

Figure 12. CG correction of linear accelerometer measurements (AH-64)

Flight Test Data Quality Evaluation

J. H. Breeman

National Aerospace Laboratory (NLR)
Anthony Fokkerweg 2
Amsterdam
The Netherlands

1 Introduction

The quality of the measurement data determines the quality of the parameter identification results. Therefore it is of the utmost importance to insure the data quality before any attempt at identification is made. In principle the best time to perform data quality checks is in dedicated tests before or during the actual flight tests: in the instrumentation laboratory, on the flight line and during instrumentation check-out flights. Accurate determination of each individual error effect can also be done best in a dedicated test. These tests are ideally performed with a computer online in the aircraft to reduce the loss of time and the cost of flight tests with inaccurate measurements.

The evaluation of the data quality from existing flight test data, as was the case for the Working Group, is generally much more difficult. But it is still very important to do this evaluation for the following reasons:

1. A particular measurement channel may deteriorate or fail during the course of a flight test program.

2. A specific error effect may only be present during actual flight tests, such as static pressure distortions in dynamic flight conditions. These effects can only be determined from the flight tests.

For the members of the Working Group there were two extra reasons to spend a considerable amount of time on the data quality. The first reason is that the data recordings were made by another institute. Within one institute, one is familiar with the verification procedures in use by the instrumentation department and one knows how far they can be relied on and when caution is needed.

A more important reason is the fact that the evaluation of the data quality also gives a good feel for the data contents. It gives a first indication of the actual accuracy of the measurements and it can clear up misunderstandings in the definition of measured variables (e.g. sign conventions).

Apart from complete failure, which is often (but not always!) easy to spot there are a number of errors that can occur:

1. Sensing: the transducer may not sense the desired quantity directly, for example a static pressure may be distorted by the flow around the aircraft.

2. Transducer: change in bias, sensitivity, range, change in sensitive axis (misalignment), hysteresis, output noise, spikes. Sensitivity to temperature, vibration or electromagnetic radiation.

3. Data aquisition system: changes in offset, gain and range in the analog components, such as amplifiers, pre-sample filters and A/D converters. Change in filter characteristics of the pre-sample filters. Bit errors in the recording chain (dropouts). Time shifts and other phase errors.

Because of the large number of possible error sources, an intimate knowledge with the characteristics of the instrumentation system is absolutely necessary for succesful correction of data errors.

2 Techniques

2.1 Data inspection

Visual inspection of dataplots is an important first step in the evaluation of data quality. The measurements can be scrutinized for obvious errors such as wrong signs, excessive measurement noise, data dropouts, spikes and missing (or even exchanged!) data channels.

In addition frequency domain techniques can be very useful for data quality evaluation. Examples are:

1. Time shift of a signal can be determined by examining the slope of the phase response of the signal with respect to a reference. This method is very sensitive, but it is most useful in ground checks, because it may be difficult to find a suitable reference measurement in flight. Time domain modelling can also be used to determine time shift.

2. Initial checks of compatibility between variables may be quickly performed in the frequency domain. For instance it can be verified that that q/θ has a $1/s$ frequency response characteristic. Sign errors are also easily detected by inspecting the phase response.

3. The coherence function can be used to ensure that both input and output signals have low noise contents and are well correlated with each other.

4. The noise spectrum can give an indication of the correct functioning of a transducer (channel). Excessive noise (perhaps in part of the frequency spectrum) can give an indication of malfunction in sensing, transducer or data acquisition. For example discrete frequencies in a gyroscope signal could indicate a bearing failure, noise spikes could be a vibration problem or faulty wiring or connectors. Noise analysis also gives vital information for the design of data processing filters, which remove the measurement noise and allow the sampling rate to be reduced.

This may also be a good place to warn for the effect of pre-sample filtering. If a failing transducer has high-frequency noise or sudden steps in its output, the pre-sample filters will transform the signals in smooth signals, thus masking the problem. In normal operation pre-sample filters are essential to prevent aliasing errors, but it may be a good idea to record the unfiltered signals as an instrumentation test. Another important point is the negative effect of phase errors in the analogue filters on the parameter identification. Some authors even recommend dispensing with anti-aliasing filters altogether.

If recording techniques permit it, it is therefore recommended to use the highest possible sampling rates (and pre-sample filter bandwidths) and to reduce the sample rate in the analysis by linear-phase digital filtering in the ground processing. This has the added advantage of allowing a more considered choice of sampling rate in the data analysis.

2.2 Compatibility checking

2.2.1 Introduction

Any redundancy in the measured variables can be exploited to verify the data quality. There are a large number of techniques in use for the purpose of data quality evaluation. In fact everyone has his own private tricks.

The measurement of a single variable by two different transducers is a simple example:

1. If the transducers are of the same type, the outputs of the two measurement channels can be compared to find discrepancies in sensing, transducer or data acquisition.

2. If the two transducers are of a different type, the characteristic errors will be different. This difference can be used to determine if one of the signals is wrong.

3. Even if one transducer is much better than the other, a comparison is still very useful, if only to show that the "better" transducer has failed completely.

In practice it is rare that two redundant transducers are used, but it is not uncommon to have a standard aircraft instrument as well as a flight test instrumentation sensor. In this case it is strongly recommended to record the aircraft instrument output as well. The disadvantage is not so much the extra data channel to be wired in the aircraft, but rather the extra effort needed to calibrate and evaluate the aircraft instrument, which is necessary to allow its use for data quality checks.

Redundant information can also be used in a complementary filter approach, e.g. rate gyro data is used for the low frequency range and angular accelerometer data is used for the higher frequency range (this is just a special case of the state estimation techniques described below). It is very important that undesirable error characteristics, such as hysteresis, nonlinearities or spurious responses, do not destroy the quality of the overall result. In the example given, rate accelerometers tend to have these undesirable error characteristics.

2.2.2 Kinematic compatibility checking

A special case of compatibility checking is Kinematic Compatibility checking. Here the kinematic relationships that exist between the different measured variables are used. The procedure can be applied in many forms: from the simple comparison between two signals to the complete six-degree-of-freedom flight path reconstruction. The procedure is also called Kinematic Consistency checking or Flight Path Reconstruction. The chosen name reflects whether the procedure is seen as an independent check or as an integral part of the processing (see Section 3). Descriptions can be found in Gerlach [1] and Wingrove [2]. Klein [3] seems to have introduced the term compatibility checking. The following set of equations describe the six-degree-of-freedom kinematic equations:

$$
\begin{aligned}
\dot{u} &= (a_x - g\sin\theta) - qw + rv \\
\dot{v} &= (a_y + g\cos\theta\sin\phi) - ru + pw \\
\dot{w} &= (a_z + g\cos\theta\cos\phi) - pv + qu \\
\dot{\phi} &= p + (q\sin\phi + r\cos\phi)\tan\theta \\
\dot{\theta} &= (q\cos\phi - r\sin\phi) \\
\dot{\psi} &= (q\sin\phi + r\cos\phi)/\cos\theta \\
\dot{x}_g &= u\cos\theta\cos\psi + v(\sin\phi\sin\theta\cos\psi - \cos\phi\sin\psi) \\
&\quad + w(\cos\phi\sin\theta\cos\psi + \sin\phi\sin\psi) + u_w \\
\dot{y}_g &= u\cos\theta\sin\psi + v(\sin\phi\sin\theta\sin\psi + \cos\phi\cos\psi) \\
&\quad + w(\cos\phi\sin\theta\sin\psi - \sin\phi\cos\psi) + v_w \\
\dot{h} &= u\sin\theta - v\sin\phi\cos\theta - w\cos\phi\cos\theta - w_w
\end{aligned}
$$

Inputs:

$$a_x, a_y, a_z, p, q, r$$

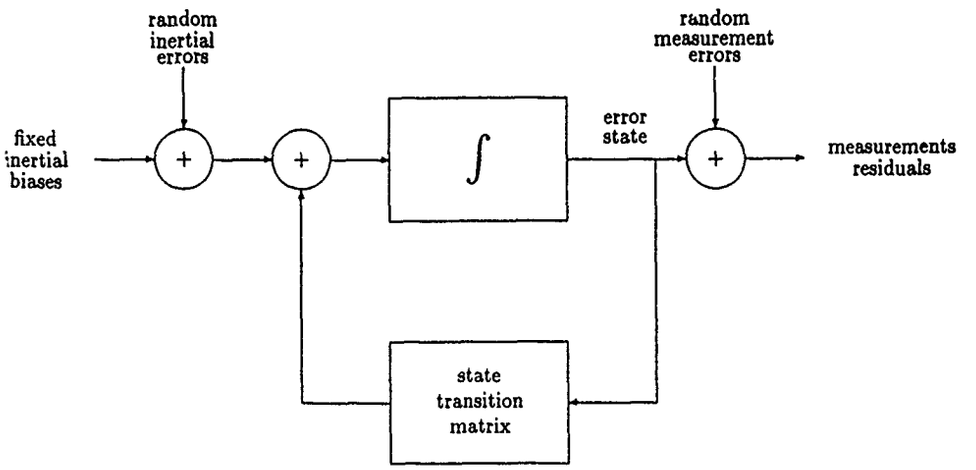

Figure 1. Basic instrumentation error model

Error Model for Inputs:

$$a_x = (1.0 + \lambda_{a_x})\, a_{x_{true}} + b_{a_x} + n_{a_x} - \tau_{a_x}\dot{a}_x$$

etc.

Outputs:

$$\phi, \theta, \psi, V, \alpha, \beta, h, x_g, y_g$$

Error Model for Outputs:

$$\phi_{out} = (1.0 + \lambda_\phi)\,\phi + b_\phi + n_\phi - \tau_\phi\dot{\phi}$$

etc.

In practice these equations must be extended with terms describing the navigation over a spherical and rotating earth. Linearizing these equations leads to the basic block diagram as shown in Figure 1. The errors in the velocities u, v, w, the attitude angles ϕ, θ, ψ and the position in earth axes are the components of the state. The errors in the inertial measurements a_x, a_y, a_z, p, q, r are treated not as *observations*, but as *inputs* to the error model. In addition the wind speed components u_w, v_w and w_w are included as inputs to the model. The idea is that the errors in the input signals drive the error state.

In principle any measurement which depends on the state vector can appear in the observation equation, for example air speed or doppler velocity, pressure or radio altitude, angle of attack or angle of sideslip, latitude and longitude from Inertial Navigation Systems, VOR/DME or the Global Positioning System. The error in the measurements, whether in the input or in the observation vector, can be modelled as bias (b), scale factor error (λ), time shift (τ) and white, gaussian random noise (n). If this random noise is not white and gaussian it may be necessary to extend the state with a model of the noise characteristics.

With modern inertial sensors the measurement errors are very small. As a consequence the variations in the wind components during a recording become the dominant error source. This makes it possible as well as desirable to estimate these wind variations. The estimation of the absolute wind components requires the presence of absolute position or velocity references of reasonable accuracy, e.g. from an INS, VOR/DME or GPS. However, it should be noted that in general only the variations in the wind speed components are of interest for flight mechanics, because constant wind components only affect the error in the absolute velocities in earth-fixed coordinates. This means that absolute position references are not strictly required, although they can be of great use.

One simple way of modelling the wind variations that works very well in practice describes the wind variation as a linear trend in time and as proportional to altitude. A more sophisticated description may use a colored gaussian noise model, but such a wind model will have to depend on the weather conditions.

The estimation of wind components is an example of the use of estimation procedures to reconstruct an unmeasured state component. Another practical example is the estimation of the angle of attack in the case that no direct measurement is available or the direct measurement is unusable. See Section 3 for further discussion on how the reconstructed state should be used.

It is in general not possible to identify the large number of parameters in the described error models, because the basic observability and identifiability the-

ory is applicable here. If too many error components are included the standard deviations of the estimates increase rapidly and the correlation coefficients approach one. The degree of correlation is also dependent on the type of and shape of the manoeuvre, so it is feasible to perform specially designed manoeuvres for the purpose of identifying the error components, but these manoeuvres will not necessarily be optimal for parameter identification. It may be more fruitful to combine several different manoeuvres in a multi-manoeuvre analysis and then estimate an error model which is valid for all the recordings (again see Section 3).

A simple example of compatibility checking is the comparison of a rate gyroscope and an attitude gyroscope. The rate signal can be integrated and compared with the attitude signal. Error models for each of the two types of gyroscopes can be defined, e.g. bias and time shift for the rate gyroscope and linear drift and time shift for the attitude gyroscope. The difference between the signals can then be attributed to various errors sources and the parameters of the error model can be estimated using parameter identification.

Even this simple example already points out a common problem, i.e. the bias of the rate gyroscope has exactly the same effect as the linear drift of the attitude gyroscope and the same is true for time shifts. This means that the errors in the different measurements must have different characteristics in order to be useful for compatibility checking. If it could be assumed that the attitude gyroscope has negligible drift and the rate gyroscope has a negligible (or perhaps known) time shift, then rate gyro bias and the time shift of the attitude gyro can be put in the error model and values for these parameters can be found. But in general these assumptions are difficult to make and need the advice of the instrumentation department.

The bias in the rate gyro will always have the same effect, a linear increase of the error with time. But a scale factor error, e.g. in the attitude measurement, will only be noticeable if larger excursions are present. Even in the case of large excursions, the estimate of bias and scale factor may be highly correlated, e.g. when the attitude angle happens to increases linearly with time. This demonstrates the dependence of identifiability on the manoeuvre shape.

As a final example in manoeuvres that do not deviate too much from level flight the following simplified equation is valid:

$$\dot{w} = q.u + a_z$$

This shows that the effect of a bias in the normal acceleration a_z on w (angle of attack) is almost equivalent to the effect of a bias in the pitch rate signal q. In the estimation procedure this will show up as a high correlation between the estimates of the two error parameters. An independent measurement of the attitude angle would of course solve this simple problem.

In the actual practice of flight testing all these problems are present at the same time and are consequently much more difficult to detect.

2.2.3 Solution techniques

The formulated problem can be solved by a number of different methods. For more detailed descriptions see Maine [4] or Mulder [5]. In principle no one method is theoretically superior, because all estimators can be shown to be Maximum Likelihood estimators for a specific choice of error model. In other words the assumed error model determines which solution method applies. The techniques used by the Working Group are:

Weighted Least-Squares (WLS): This method solves the case where the random error is in the inputs (so-called state noise). It is a very simple and efficient procedure.

Extended Kalman Filter/Smoother (EKSF): A standard Kalman filter estimates the state of a linear system with an error model which allows noise in the inputs (state noise) as well noise in the observations. The Kalman algorithm is a recursive formula, which proceeds sequentially (filters) through the data. For a fixed time interval a substantial improvement in accuracy can be obtained by adding a smoothing step in the reverse time direction. Nonlinear kinematic equations are handled by linearizing around a nominal trajectory (usually the current best estimate of the trajectory is used) and bias and scale factors can be estimated by including them as undriven states with unknown initial condition, see Jonkers [6]. The EKSF is more expensive than the WLS method, but cheaper than the OE or FE methods. Because of the recursive formulation the computer memory requirements are also modest. The disadvantage is that is is not easy to include arbitrary error components into the error model.

Output Error (OE): This method applies in the case where all errors are in the observations, i.e. there is no state noise. In principle the method compares a simulation of the actual system with the measurements, while integrating the sensitivity functions, which describe the influence of the model parameters on the state. After one simulation run, a Gauss-Newton optimization is used to find new estimates of the model parameters. In practice this process has to be repeated for several iterations, which makes this method expensive in computer time. In addition the sensitivity matrix can be of large dimension, which adds to the computer memory requirements. The advantage of the OE method is that it is very easy to incorporate parameters in the error model. The incorporation of nonlinear models in the OE method

can be handled by deriving the sensitivity equations analytically by hand, but this makes it cumbersome to change the error models. Numerical calculation of the sensitivities is a better solution here and results in very flexible software programs.

Filter Error (FE): This method solves the most general problem formulation, i.e. with state noise and observation noise. In principle it is a combination of a Kalman Filter in an Output Error parameter identification iteration. The FE method is the most expensive in computer time and the most complex to use and therefore is seldomly used for compatibilty checking.

Of course it is not always possible or even necessary to use the complete error model. Omitting error components or observations which are not important can reduce the problem formulation considerably, but the same solution techniques still apply. For example it could be assumed that the air data measurements do not give useful information on the estimation of the attitude errors. This might be true if very accurate attitude angle measurements are available. In this case the estimation of attitude and velocity error components can be performed seperately, saving much computer time.

3 Use of error corrections

After all error corrections have been determined as far as possible, the question remains what to do with this information. There are two extreme philosophies:

1. The identified error components are put in an error model, which is added to the aerodynamic model. The parameter identification procedure is then performed on the combined model, using the original measured variables as observations. The values of the errors components determined by compatibility checking are sometimes used as initial conditions.

2. All error corrections are applied to the measured variables and the parameter identification procedure is performed on the corrected variables.

The first procedure has the advantage that the parameter identification results are a true Maximum Likelihood estimate of the complete problem, in other words the solution is theoretically optimal. In the second procedure is the parameter identification is much simpler due to the smaller model. In fact if all measurement errors are corrected (and the complete state can be reconstructed), the Maximum Likelihood estimator reduces to a simple Equation Error estimator.

In practice a compromise between the two approaches is always made: for some error components it cannot be expected that better values can be found by including these in the PI model and the corrected instead of the original measurements are used. For other error components it can be expected that the combined PI will yield the best values. It is not possible to give a clearcut recommendation which error component should be included and which should not be, the final choice must always depend on the judgement of the analyst.

Finally the instrumentation department should always be asked to verify the estimated instrument errors. It may turn out that an error which seems to have been succesfully modelled in one way, should be actually attributed to an entirely different error source which happens to have the same effect.

When a large number of manoeuvres are conducted in a particular flight and in one flight condition, the error model identified for each of the manoeuvres should ideally be the same. This makes good physical sense since the calibration of the instrumentation will change very little during one particular flight. Failure of a sensor or other instrumentation components during the flight would, of course, be an exception.

This suggests that when a sufficient number of recordings are available, mean values of the biases and scale factors should be used as corrections for the whole flight. Simple statistical analysis can be performed to establish if the sample is large enough so that statistically significant values can be determined. If only some of the estimated error components are significant, it may be necessary to reduce the size of the error model until only significant parameters remain.

4 Data compatibility tools in use at the institutes

4.1 ARL

Compatibility checking of helicopter flight data at ARL is based on the full nonlinear six-degrees of freedom kinematic equations, supplemented if necessary by the three equations describing the aircraft position in earth axes. The accelerometer and gyro measurements are regarded as inputs and are assumed to be subject to systematic bias and scale factor errors. For more details see Evans [7] and Feik [8]. Two solution methods are in use. The first method is a Maximum Likelihood estimator (ML), which is a very flexible program that easily allows different combinations of observed outputs, alternative problem formulations and error models. The sensitivity matrix is calculated numerically, which makes the estimation of parameters in general non-linear systems possible, including systems with discontinuities and time shifts, see Blackwell [9]. The second method is an Extended Kalman Filter (EKF) which models random errors in the inertial instruments, but allows a more restricted set of outputs.

4.2 US Army

The US Army uses the program Smoothing for Aircraft Kinematics (SMACK) for consistency analysis, see Bach [10] [11]. This program solves the full nonlinear, six-degree-of-freedom aircraft kinematic equations and estimates time-varying winds, states and measurements. In the process measurement biases and scale factors are identified.

The very general problem formulation of SMACK is presented in a block diagram form in Figure 2. Here, the position in earth axes x, y, z and their first and second derivatives, the euler angles ϕ, θ and ψ and their first and second derivatives and (optionally) the wind velocities in earth coordinates w_x, w_y and w_z are components of the state. In the measurement model the state components are transformed to radio range, bearing and elevation ($\mathcal{P}$), airspeed and flow angles ($\mathcal{A}$), body accelerations ($\mathcal{L}$), windspeed and direction ($\mathcal{W}$), body angular rates ($\mathcal{R}$) and angular accelerations ($\mathcal{Z}$). All these variables can be treated as measurements, estimates or both. The higher derivative forcing functions δx, δy, δh, δl, δm, δn, g_x, g_y, g_h are calculated during the estimation procedure so as to minimize the chosen performance measure.

The program is based on a zero phase-shift backward information filter and forward smoother algorithm which produces a zero phase shifted output estimates with a cutoff frequency which is one tenth of the sample rate. The solution is iterative, providing improved state and measurement estimates until a minimum squared-error is achieved.

In the US Army procedure a 3-DOF check of the attitude angles is conducted first. Then, the identified angular error parameters and their covariances are used as start-up values in an overall 6-DOF check. The error model is then refined by iteration until only statistically significant biases and scale factors remain (see Kaletka [12].

4.3 DLR

DLR uses a Maximum Likelihood program for the purpose of flight path reconstruction. The full nonlinear six-degrees of freedom kinematic equations are used. The sensitivity matrix is also calculated numerically, see Plaetschke [13] and Jategaonkar [14].

4.4 Georgia Institute of Technology

The integrated rate signals were compared with the attitude angles to identify the inertial errors.

4.5 MDHC

The bias and scale factor of the angular accelerations were determined using a least-squares procedure which minimized the difference between the integrated angular accelerations and the body rates. A Kalman filter/smoother was also applied to insure data consistency, to reduce the effect of measurement noise on the state estimates and to estimate unmeasured states.

4.6 NLR

In the past the standard identification procedure at NLR used an extended Kalman filer/smoother to reconstruct the complete state of the aircraft based on an optimal combination of inertial and air data measurements. The accelerometer and gyro errors were modelled as state noise, the bias in these instruments were modelled as extra states, and pressure altitude, airspeed and sideslip angle errors were modelled as observation noise, see Breeman [15]. In recent years NLR employed highly accurate inertial systems for all its flight tests. Therefore the current flight path reconstruction program is based on a model that includes a variations in the wind components with time and altitude and errors in the air data sensors, but no errors at all in the inertial sensors. In the parameter identification phase the smoothed time histories are then used in a linear regression program. Because the helicopter data provided did not include either of the above combinations of accurate measurements, NLR used its output error program for compatibility checking. This program uses nonlinear kinematic equations and allows estimating biases in accelerometers and gyros.

4.7 University of Glasgow

The frequency domain parameter identification techniques used were not sensitive to bias errors, so that compatibilty checking before parameter identification was not necessary. However, bias estimation was performed for the verification runs.

4.8 NAE/University of Toronto

The compatibility checking procedure uses the full set of kinematic equations of motion. As a first step a least-square fit procedure is used to determine gyro and attitude biases and then the reconstructed attitudes and rates are used to determine accelerometer and velocity biases. The reconstructed state is normally used in the following parameter identification.

4.9 RAE

Data compatibility checking is a standard procedure at RAE, where it is a part of the Parameter Estimation Package (PEP). In the preliminary data interpretation phase the KINECON program performs this task. The aim is to find likely calibration errors, such as bias errors. Bias estimates can be derived using a weighted least squares output-error algorithm. In a later stage of the processing filtered or smoothed estimates from the measurements and reconstructions of unmeasured states are computed using an extended Kalman filter algorithm. The program DEKFIS (Discrete Extended Kalman Filter/Smoother typically uses measurements

from rate and attitude gyros, accelerometers and airspeed probe and incidence vanes and has the option to revise calibration factors.

4.10 CERT

For flight path reconstruction CERT applies the same Output Error program as used for identification, see Gimonet [16]. The full six-degree-of-freedom nonlinear kinematic equations are used and the locations of the sensors are taken into account. Nonlinear kinematic terms are dealt with in the calculation of the sensitivities. Inertial sensors are treated as inputs and air data and attitude angles are the observations. Bias and scale factor of all measurements are included in the error model, but time delays are estimated manually after the first identification results.

5 Conclusions

It can be concluded that data quality evaluation is a necessary step in the process leading to succesful parameter identification. However, the final test of the validity of this procedure lies in the quality of the parameter identification results.

References

[1] Gerlach, O.H. *Determination of performance and stability parameters from non-steady flight test manoeuvres.* SAE paper 700236, Kansas, 1970.

[2] Wingrove, R.C. *Applications of a technique for estimating aircraft states from recorded flight test data.* AIAA 72-965, 1972.

[3] Klein, V. et al *Compatibility check of measured aircraft responses using kinematic equations and extended kalman filter.* NASA TN D-8514, 1977.

[4] Maine, R.E. et al *Identification of dynamic systems.* AGARD AG-300-Vol.2, 1985.

[5] Mulder, J.A. et al *Analysis of aircraft performance, stability and control measurements.* AGARD LS-104, 1979.

[6] Jonkers, H.L. *Application of the Kalman filter to flight path reconstruction from flight test data including estimation of instrumental bias error corrections.* TUD Report VTH-162, Delft, 1976.

[7] Evans, R.J. et al *Aircraft flight data compatibility checking using Maximum Likelihood and Extended Kalman Filter estimation.* 7th IFAC Symposium on Identification and System Parameter Identification, York, 1985.

[8] Feik, R.A. *On the application of compatibility checking techniques to dynamic flight test data.* AR-003-931, Melbourne, 1984.

[9] Blackwell, J.A *Maximum Likelihood parameter estimation program for general non-linear systems.* ARL Aero Tech Memo 392, 1988.

[10] Bach, R.E. et al *Applications of state estimation in aircraft flight data analysis.* AIAA 83-2087, 1983.

[11] Bach, R.E. Jr. *State estimation applications in aircraft flight-data analysis (A user's manual for SMACK).* 1984.

[12] Kaletka, J. et al *Time and frequency-domain identification and verification of BO 105 dynamic models.* 15th European Rotorcraft Forum, Amsterdam, 1989.

[13] Plaetschke, E. et al *Maximum-Likelihood schätzung von Parametern linearer Systeme aus Flugversuchsdaten - Ein FORTRAN-Programm.* DFVLR-Mitt. 84-10, 1984.

[14] Jategaonkar, R. et al *Maximum likelihood parameter estimation from flight test data for general non-linear systems.* DFVLR-FB 83-14, 1983.

[15] Breeman, J.H. et al *Evaluation of a method to extract performance data from dynamic manoeuvres for a jet transport aircraft.* 11th ICAS Congress, Lisbon, 1978.

[16] Gimonet, B. *Flight path reconstruction at ONERA.* private communication, 1988.

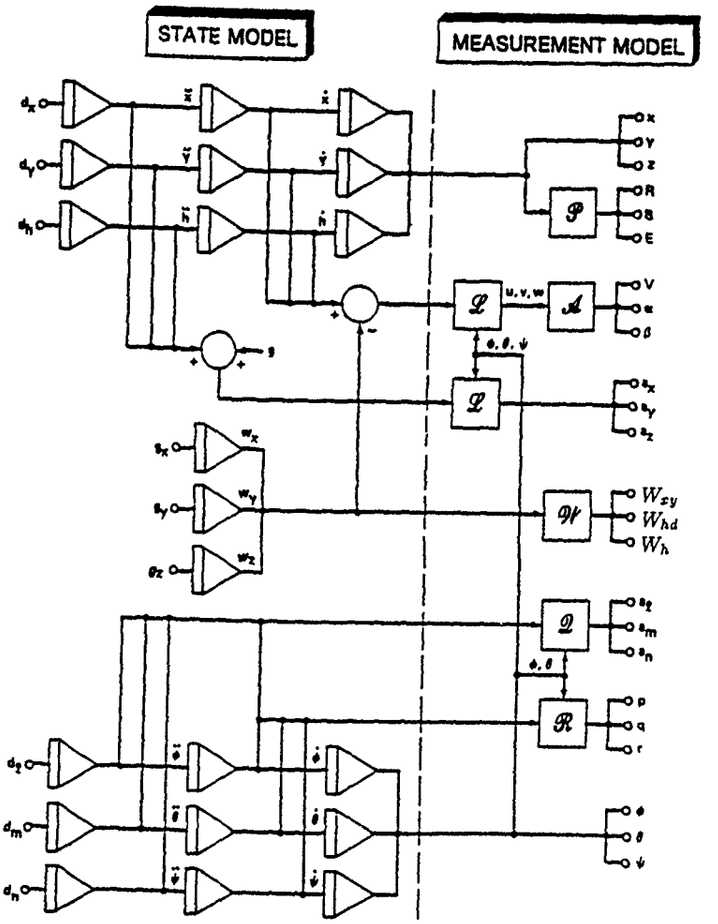

Figure 2: General structure for state estimation [SMACK]

IDENTIFICATION TECHNIQUES

MODEL STRUCTURE AND TIME DOMAIN METHODS*

J. H. de Leeuw
Institute for Aerospace Studies
University of Toronto
Toronto, Ontario, Canada

5.1 Introduction

This section presents an overview of rotorcraft system identification techniques used by WG 18. More thorough coverage of the general system identification field, including extensive treatment of the theoretical basis of the various techniques, is found in a number of excellent textbooks (Ljung, 1987 [5.1]); Soderstrom et al, 1989 [5.2], Bendat et al., 1986 [5.3]) and reference publications (Maine et al, 1986 [5.4]; Klein, 1980 [5.5]; Tischler, 1987 [5.6].

This section first considers the selection of model structure. Here, special emphasis is given to ensuring that the model structure is appropriate to the intended model application. For example, simple decoupled first-order models that characterize the helicopter dynamics over a limited frequency range may be suitable for handling-qualities applications, while coupled 6-DoF models suitable for a broader range are needed for piloted simulation. At the other end of the complexity spectrum are models needed for use in advanced high-bandwidth rotorcraft flight control system design that must consider the coupled fuselage/rotor/airmass dynamics. Both non-parametric model structures (frequency-responses) and parametric model structures (transfer functions and state-space equations) are considered in the two sections dealing with Identification Techniques.

The next step in the identification problem definition is the formulation of the criterion or "cost" function. The simplest formulation, referred to as "equation-error" is valid when the measurement noise is small relative to process noise. This assumption, while often not suitable for the high measurement noise environment of the rotorcraft, has the advantage of resulting in a cost function that is linear in the unknown parameters. This leads to the simple and rapidly-implemented least-squares (step-wise) regression techniques for identification. A more complex formulation, referred to as "output-error" is valid when process noise is small relative to measurement noise — a better assumption for rotorcraft data. Output-error techniques are more mathematically complex than equation-error techniques, and also require more sophisticated nonlinear search algorithms to determine the unknown parameters. A third approach to the cost function formulation is based on the use of frequency-responses. This approach requires much more preprocessing of the flight data, but has the advantage of being valid in the presence of both measurement and process noise. Also, the frequency-response formulation allows for the consideration of the differing frequency content of the state variables. It is discussed in the next section of this report.

Once the model structure and cost function have been defined, the model is identified from the input/output time-history data using either time-domain or frequency-domain methods. Each method contains at its core a sophisticated search method to find the set of parameter values that provides the best fit according to the adopted cost function. Again, the choice of methods depends on the application, the formulation of the cost function (frequency-response methods are completed in the frequency-domain), the familiarity of the analyst with the methods, and finally the availability of computational tools. For example, the extraction of nonlinear models or identification from flight data with distinctly non-symmetric wave forms is best completed in the time-domain. On the other hand, when the model structure includes widely separated dynamic modes (such as low-frequency rigid body dynamics and high frequency rotor dynamics) or when highly unstable modes are present, the identification in the frequency-domain has some distinct advantages. Both time-domain and frequency-domain methods were extensively used by WG 18.

The final step in system identification is referred to as "model verification." Here the extracted model is driven with flight data not used in the identification process to ensure the correctness of the identification procedure, and the utility of the model in predicting control responses rather than simply matching them. Model verification is completed in the time-domain in the WG 18 study, although frequency-domain verification techniques have also been used (Kaletka et al., 1989 [5.7]).

5.2 Model Structure

5.2.1 General

Selection of model structure is a critical step in system identification, which will greatly affect both the degree of difficulty in extracting the unknown parameters, and the utility of the identified model in its intended application. For example, while a 1-DoF roll response model containing 3 unknown parameters (gain, roll mode, time delay) is fairly easy to obtain and is often quite sufficient to evaluate on-axis handling qualities, it is obviously unsuitable for investigations of cross-coupling effects. On the other hand, a flight control design model that

*Based on the text prepared for the WG 18 report which benefitted from inputs from M. B. Tischler and the editor.

considers coupled fuselage/rotor/airmass dynamics may contain nearly 100 parameters and will require rotor state measurements and significant computational capability. The simplest model structure that serves the intended application is the best choice.

Model structures can be broadly divided into two groups: nonparametric and parametric. A nonparametric model is one in which no model order or form of the differential equations-of-motion are assumed. Generally, nonparametric models are expressed as frequency-responses between key input/output variable pairs (e.g., pitch-rate response to longitudinal stick), that are calculated using Fast Fourier Transform techniques. Nonparametric models are presented in Bode plot format of Log-magnitude and phase of the input-to-output ratio versus frequency. Typical applications of nonparametric identification results are handling-qualities analyses based on bandwidth and phase delay and simulation model validation. Non-parametric identification is a relatively fast and easy process, and has even been implemented in real time for control system performance validation.

A parametric model requires the assumption of both system order and the structure of the system's dynamical equations. The simplest parametric model structure is a transfer-function, which is a (lumped) pole-zero representation of the input-to-output process. These models have relatively few unknown parameters. On the other end of the scale is a full 6-DoF (or higher) set of coupled linear differential multi-input/multi-output (MIMO) state-space equations, derived from Newton's Laws applied to the helicopter system. Such a rotorcraft model may contain as many as 50-100 unknown parameters — a formidable identification problem. Common applications of parametric models include control system design, wind-tunnel validation, and math model derivation and validation. Key aspects of model structure selection for transfer-function and MIMO state-space model formulation are discussed in the following paragraphs.

Transfer-Function Model Structure Selection. Transfer-function models are generally identified by direct fitting of the nonparametric frequency responses. Specific aspects of the model structure that must be considered are:

- Selection of input/output variable pairs,
- Frequency-range of model applicability,
- Physically meaningful order of the numerator and denominator polynomials,
- Inclusion of equivalent time delay, and
- Fixing, freeing, or constraining coefficients in the fitting process.

In order to illustrate some of these aspects, consider the selection of transfer function model structure for handling-qualities analyses. Such analyses are generally concerned with lumped low-order (equivalent systems) characterizations of on-axis input-to-output responses in terms of gain, natural frequency, damping ratio, and time delay that are representative of the helicopter's response in the pilot's "crossover frequency range" (e.g., 0.1-10 rad/sec). Results for the AH-64 show that the short-term pitch dynamics are very well characterized by such a simple model. However, transfer-function models for high-bandwidth flight control system design need to be of fairly high order (8th order for the BO-105) to adequately predict achievable gain levels.

MIMO State-Space Model Structure Selection. The MIMO state-space model structure problem is much more complicated than the transfer-function model problem. The analyst must make a host of *a priori* decisions that will profoundly effect the difficulty in extracting parameters, and the validity of the extracted parameters. As in transfer-function model structure selection, the overall goal is to select a model structure that is consistent with the frequency range of interest. Some of the many important aspects of state-space model structure formulation for rotorcraft are:

- Degree of coupling between the longitudinal and lateral/directional motions
- Order of model needed to characterize the frequency range of interest
- Identifiability of the parameters as a function of the available measurements
- What parameters are known and should be fixed (e.g., gearing, gravity, filter dynamics)
- Physical constraints between the parameters (e.g., common actuators, aerodynamic symmetry, geometry).

Since most of the WG 18 effort involved identification of 6-DoF MIMO state-space models, this model structure is presented in detail below.

5.2.2 6 DoF State-Space Model Structure

In the study undertaken by WG 18 the area of application was chosen to be that of helicopter flying qualities, i.e., the dynamic performance of the helicopter in response to its flight controls and as evidenced by the traditional flight mechanical variables. As a consequence, the basic dynamic equations selected for the aircraft model are the usual equations of flight mechanics as given in Equations (5.5.1) through (5.5.4).

Force equations

$$\begin{aligned} m\dot{u} + m(qw - rv) &= X - mg\sin\theta \\ m\dot{v} + m(ru - pw) &= Y + mg\cos\theta\sin\phi \\ m\dot{w} + m(pv - qu) &= Z + mg\cos\theta\cos\phi \end{aligned} \qquad (5.1)$$

Moment equations

$$\begin{aligned} I_x\dot{p} - I_{zx}\dot{r} + (I_z - I_y)qr - I_{zx}pq &= L \\ I_y\dot{q} + (I_x - I_z)rp + I_{zx}(p^2 - r^2) &= M \\ I_z\dot{r} - I_{zx}\dot{p} + (I_y - I_x)pq + I_{zx}qr &= N \end{aligned} \qquad (5.2)$$

Kinematic equations for Euler rates

$$\begin{aligned} \dot{\phi} &= p + \sin\phi \tan\theta\, q + \cos\phi \tan\theta\, r \\ \dot{\theta} &= \cos\phi\, q - \sin\phi\, r \\ \dot{\psi} &= \frac{\sin\phi}{\cos\theta} q + \frac{\cos\phi}{\cos\theta} r \end{aligned} \qquad (5.3)$$

Assumptions

$$I_{xy} = 0, \quad I_{yz} = 0 \qquad (5.4)$$

Gyroscopic reactions due to rotating elements of the helicopter are neglected.

These equations are non-linear in structure because of the gravitational and rotation related terms in the force equations and the appearance of products of angular rates in the moment equations. The model also has to adopt expressions for the aerodynamic forces (X, Y and Z) and moments (L, M and N) that are central in the equations.

In this regard a judgement has to be made which state variables are significant for the particular application. For conventional, fixed-wing aircraft 6 degrees-of-freedom models involving only the rigid body states u, v, w, p, q and r, and even the simpler longitudinal or lateral subsystems, have been remarkably successful. For dynamically more complex aircraft, and this certainly includes helicopters, additional states and auxiliary dynamic equations may be required to provide a satisfactory representation. In the case of the helicopter, the dynamics of the main rotor represents such a complication, introducing the potential need of adding state variables associated with blade flapping, flexible blade mode, airmass motion or combinations of these. Another source of complexity is that the rotor drive is governed to maintain constant rotational speed by a control system which may add states and equations to the model.

Fortunately, in many current helicopters, the eigenvalues associated with these additional states are sufficiently higher than those of the rigid body modes, such that by constraining the flight control inputs to relatively gradual excitations, the rotor modes approximately are not excited and a model based on the rigid body states can still give useful results. It should be pointed out, however, that especially in the highly manoeuvreable modern helicopter, this approximation to the model structure is likely to be marginal.

The model that has been adopted as the basis for the WG 18 study is the fully coupled, 6 degrees-of-freedom rigid body system of equations given in (5.1) through (5.4).

A simplified set of equations results under the assumption that products of angular rates are small and can be neglected in the moment equations.

Furthermore, by dividing the force equations by the mass and multiplying the simplified moment equations by the inverse inertia matrix, forces and moments are presented as "specific" quantities (equations (5.5) through (5.7)). This substitution, however, implies

- that for calculating the full values of the aerodynamic parameters the knowledge of these mass and inertia properties of the aircraft is required and
- that these properties are constants.

Specific forces

$$\tilde{X} = X/m, \quad \tilde{Y} = Y/m, \quad \tilde{Z} = Z/m \qquad (5.5)$$

Specific moments

$$\begin{pmatrix} \tilde{L} \\ \tilde{M} \\ \tilde{N} \end{pmatrix} = \begin{pmatrix} I_x & 0 & -I_{zx} \\ 0 & I_y & 0 \\ -I_{zx} & 0 & I_z \end{pmatrix}^{-1} \begin{pmatrix} L \\ M \\ N \end{pmatrix} \qquad (5.6)$$

$$\begin{aligned} \tilde{L} &= \frac{I_z L + I_{zx} N}{I_x I_z - I_{zx}^2} \\ \tilde{M} &= \frac{M}{I_y} \\ \tilde{N} &= \frac{I_{zx} L + I_x N}{I_x I_z - I_{zx}^2} \end{aligned} \qquad (5.7)$$

This gives the following sets of equations for the accelerations (5.8) and (5.9), in which the mass and the moments of inertia no longer appear explicitly.

Equations for linear accelerations

$$\begin{aligned} \dot{u} &= \tilde{X} - g \sin\theta - qw + rv \\ \dot{v} &= \tilde{Y} + g \cos\theta \sin\phi - ru + pw \\ \dot{w} &= \tilde{Z} + g \cos\theta \cos\phi - pv + qu \end{aligned} \qquad (5.8)$$

Equations for angular accelerations

$$\dot{p} = \tilde{L}, \quad \dot{q} = \tilde{M}, \quad \dot{r} = \tilde{N} \qquad (5.9)$$

The linear form that is assumed for the specific aerodynamic forces and moments is given in (5.10) and (5.11).

Equations for the specific aerodynamic forces

$$\begin{pmatrix} \tilde{X} \\ \tilde{Y} \\ \tilde{Z} \end{pmatrix} = \begin{pmatrix} \tilde{X}_o \\ \tilde{Y}_o \\ \tilde{Z}_o \end{pmatrix} + \begin{pmatrix} \Delta\tilde{X} \\ \Delta\tilde{Y} \\ \Delta\tilde{Z} \end{pmatrix} \qquad (5.10)$$

with

$$\begin{pmatrix} \Delta\tilde{X} \\ \Delta\tilde{Y} \\ \Delta\tilde{Z} \end{pmatrix} = \begin{pmatrix} X_u & X_v & X_w \\ Y_u & Y_v & Y_w \\ Z_u & Z_v & Z_w \end{pmatrix} \begin{pmatrix} \Delta u \\ \Delta v \\ \Delta w \end{pmatrix} + \begin{pmatrix} X_p & X_q & X_r \\ Y_p & Y_q & Y_r \\ Z_p & Z_q & Z_r \end{pmatrix} \begin{pmatrix} \Delta p \\ \Delta q \\ \Delta r \end{pmatrix} + \begin{pmatrix} X_{\delta lon} & X_{\delta lat} & X_{\delta ped} & X_{\delta col} \\ Y_{\delta lon} & Y_{\delta lat} & Y_{\delta ped} & Y_{\delta col} \\ Z_{\delta lon} & Z_{\delta lat} & Z_{\delta ped} & Z_{\delta col} \end{pmatrix} \begin{pmatrix} \Delta\delta_{lon} \\ \Delta\delta_{lat} \\ \Delta\delta_{ped} \\ \Delta\delta_{col} \end{pmatrix} \quad (5.11)$$

Equations for the specific aerodynamic forces

$$\begin{pmatrix} \tilde{L} \\ \tilde{M} \\ \tilde{N} \end{pmatrix} = \begin{pmatrix} \tilde{L}_o \\ \tilde{M}_o \\ \tilde{N}_o \end{pmatrix} + \begin{pmatrix} \Delta\tilde{L} \\ \Delta\tilde{M} \\ \Delta\tilde{N} \end{pmatrix} \quad (5.12)$$

with

$$\begin{pmatrix} \Delta\tilde{L} \\ \Delta\tilde{M} \\ \Delta\tilde{N} \end{pmatrix} = \begin{pmatrix} L_u & L_v & L_w \\ M_u & M_v & M_w \\ N_u & N_v & N_w \end{pmatrix} \begin{pmatrix} \Delta u \\ \Delta v \\ \Delta w \end{pmatrix} + \begin{pmatrix} L_p & L_q & L_r \\ M_p & M_q & M_r \\ N_p & N_q & N_r \end{pmatrix} \begin{pmatrix} \Delta p \\ \Delta q \\ \Delta r \end{pmatrix} + \begin{pmatrix} L_{\delta lon} & L_{\delta lat} & L_{\delta ped} & L_{\delta col} \\ M_{\delta lon} & M_{\delta lat} & M_{\delta ped} & M_{\delta col} \\ N_{\delta lon} & N_{\delta lat} & N_{\delta ped} & N_{\delta col} \end{pmatrix} \begin{pmatrix} \Delta\delta_{lon} \\ \Delta\delta_{lat} \\ \Delta\delta_{ped} \\ \Delta\delta_{col} \end{pmatrix} \quad (5.13)$$

The derivatives used are the *specific derivatives* of the ISO-Standards [5.8].

As the aerodynamic forces are the only external forces in the equations (5.10), it is their effect that will be measured by accelerometers. We, therefore, write

$$\begin{pmatrix} \tilde{X} \\ \tilde{Y} \\ \tilde{Z} \end{pmatrix} = \begin{pmatrix} a_x \\ a_y \\ a_z \end{pmatrix} \quad (5.14)$$

According to (5.10) this is decomposed to give

$$\begin{pmatrix} \tilde{X} \\ \tilde{Y} \\ \tilde{Z} \end{pmatrix} = \begin{pmatrix} \tilde{X}_0 \\ \tilde{Y}_0 \\ \tilde{Z}_0 \end{pmatrix} + \begin{pmatrix} \Delta\tilde{X} \\ \Delta\tilde{Y} \\ \Delta\tilde{Z} \end{pmatrix} = \begin{pmatrix} a_{x0} \\ a_{y0} \\ a_{z0} \end{pmatrix} + \begin{pmatrix} \Delta a_x \\ \Delta a_y \\ \Delta a_z \end{pmatrix} \quad (5.15)$$

The remaining nonlinear terms (products) in equation (5.15) can be approximated assuming

- small values of the angular speeds (p, q and r),
- small variations of the Euler angles ϕ and θ,
- small variations of the translational speeds (u, v and w).

This leads to the fully linearized equations of the translational accelerations.

$$\begin{pmatrix} \dot{u} \\ \dot{v} \\ \dot{w} \end{pmatrix} = \begin{pmatrix} a_{x0} \\ a_{y0} \\ a_{z0} \end{pmatrix} + \begin{pmatrix} \Delta a_x \\ \Delta a_y \\ \Delta a_z \end{pmatrix} + g \begin{pmatrix} -\sin\theta_0 - \Delta\theta\cos\theta_0 \\ \Delta\phi\cos\theta_0 \\ \cos\theta_0 - \Delta\theta\sin\theta_0 \end{pmatrix} + \begin{pmatrix} -w_0 q + v_0 r \\ -u_0 r + w_0 p \\ -v_0 p + u_0 q \end{pmatrix} \quad (5.16)$$

In the estimation analysis the control inputs are assumed to be known accurately. In the helicopters for this study, the flight controls are actuated by hydraulic systems. The control deflection that is measured may represent the position of a control actuator rather than the immediate aerodynamic control input. In lieu of modelling this power control system, an effective time delay between the measured control motion and the actual rotor control input is assumed. In addition, although rotor state variables have been omitted explicitly, the rotor dynamics can be coarsely modelled as time delay between rotor control applications and the aerodynamic response. Although this delay has to be small, it may still affect the behaviour of the faster rigid body modes. To acknowledge these effects, the model formulation allows, as a compromise, the introduction of a single time delay for each of the four flight controls.

To complete the information necessary for the parameter estimation algorithms, the relationship between the observed variables and the state variables has to be specified. This requires detailed calibration knowledge of the various sensors and their locations, so that corrected values to the centre of gravity of the aircraft can be determined. The data supplied by the experimental groups were largely preprocessed to supply data relative to the centre of gravity. It was further assumed that the calibration relationships were linear with unity scale factors, but allowing for unknown bias values.

In each experiment the available measured variables were assessed by several different data compatibility checks. It is noteworthy that incompatibilities were found that perhaps reflect the difficulty of interpreting helicopter air data measurements with certainty. In principle these air data sensors are to be calibrated in steady, rectilinear flight over a representative range of speeds and climb rates. This is a difficult task and still only defines the performance of the air data system under static conditions, leaving the dynamic response characteristics unknown to all intents and purposes. The measurements provided by the 'inertial instruments, such as the accelerometers and angular rate gyros, also contain offsets which (although they should be small in good quality sensors) will vary between experiments. The model for the observation equation is shown in (5.17).

$$
\begin{aligned}
u_m &= u + b_u \\
v_m &= v + b_v \\
w_m &= w + b_w \\
p_m &= p + b_p \\
q_m &= q + b_q \\
r_m &= r + b_r \\
\phi_m &= \phi + b_\phi \\
\theta_m &= \theta + b_\theta \\
a_{xm} &= a_x + b_x \\
a_{ym} &= a_y + b_y \\
a_{zm} &= a_z + b_z
\end{aligned}
\qquad (5.17)
$$

5.2.3 General State and Observation Equations

The general state and observation equations are described in (5.18).

$$
\begin{aligned}
\dot{x}(t) &= f[x(t), u(t), \xi_{true}] + F\, n(t) \\
\dot{y}(t_i) &= g[x(t_i), u(t_i), \xi] + G\, \eta(t_i) \\
x(0) &= x_0
\end{aligned}
\qquad (5.18)
$$

where

x = state vector = $(u, v, w, p, q, r, \phi, \theta)^T$

y = measurement vector = $(u_m, v_m, w_m, p_m, q_m, r_m, \phi_m, \theta_m, a_{xm}, a_{ym}, a_{zm})^T$ (It may also include the angular acceleration $\dot{p}_m, \dot{q}_m, \dot{r}_m$, if available.)

ξ = vector of unknown parameters, such as X_u, $L_{\delta lon}$, etc.

$Fn(t)$ = state noise — ideally zero in output error method

$\eta(t_i)$ = Gaussian, white random identity sequence

$G\eta(t_i)$ = measurement noise

u = control input vector = $(\delta_{lon}, \delta_{lat}, \delta_{col}, \delta_{ped})^T$

For our linear case, they take the special form of equation (5.19).

$$
\begin{aligned}
\dot{x}(t) &= A\, x(t) + B\, u(t) + S + V + F\, n(t) \\
\dot{y}(t_i) &= C\, x(t_i) + D\, u(t_i) + H + G\, \eta(t_i) \\
x(0) &= x_0
\end{aligned}
\qquad (5.19)
$$

In these equations

A and **B** are the matrices containing the stability and control derivatives.

S represents vector of aerodynamic biases, which represent the reference state about which the manoeuvre is performed plus the effects of any deviations from perfect trim in the initial state for each manoeuvre.

The vector **V** contains the gravity and rotation related terms in the force equation.

n(t) is the noise in the state equation.

The observation equation is in time discrete form, representing the sampled nature of the experiments and contains the matrices **C** and **D** which relate the observed variables to the state and control variables. No new unknown parameters appear in these matrices if the calibrations contain accurate scale factors.

The vector **H** contains any measurement bias.

$\eta(t_i)$ represents the noise sequence in the measurements.

With the system structure now laid down, the problem becomes primarily one of estimating the parameter values that describe the aerodynamic response to changes in the state variables (the stability derivatives) and the controls (the control derivatives). An important element of system identification remains in the deselection of those parameters that do not or only marginally contribute to the fidelity of the model response, a procedure referred to as *model structure determination*.

5.3 Time-Domain Identification Methods

There is a vast body of theoretical literature on the properties of time-domain optimal estimation methods, when special forms are assumed for the noise that appears in equation (5.19).

One set of assumptions defines the so-called output error method, another leads to regression methods or the so-called equation error method. These will now be discussed in general terms.

5.3.1 Output Error Method

The idealized situation underlying this method is based on the absence of noise in the state equation and the assumption that the noise in the observation equation consists of a zero-mean sequence of independent random variables with a Gaussian distribution identity covariance. The objective is to adjust the values for the unknown

parameters in the model to obtain the best possible fit between the measured data y_m and the calculated model response y_c. For aircraft identification the Maximum Likelihood Technique is mostly used: For each set of parameter values in the model, the probability of the response time histories taking values near the observed values can be defined and a maximum likelihood solution is obtained for that set of parametric values that maximizes this probability. With all unknown parameters collected in a vector ξ, the Maximum Likelihood estimate of ξ is obtained by minimizing the negative log likelihood function given in (5.20).

$$J(\xi) = \frac{1}{2}\sum_{i=1}^{N}\left[y_m(t_i) - y_{c\xi}(t_i)\right]^T \left(GG^T\right)^{-1}\left[y_m(t_i) - y_{c\xi}(t_i)\right] + \ln\left|G(\xi)G^T(\xi)\right| \tag{5.20}$$

with
y_m = measured

and
$y_{c\xi}$ = model output based on parameter vector ξ

The difference between the measured and model response time histories that appears in the cost function is the 'output' error of the model, so explaining the name of the method.

Both terms of the sum in this equation include the matrix G which describes the magnitude information of the measurement noise. (The product GG^T is the measurement noise covariance matrix). When the noise is known, the second term in equation (5.20) is constant and can be neglected for the minimum search. The cost function then reduces to

$$J(\xi) = \frac{1}{2}\sum_{i=1}^{N}\left[y_m(t_i) - y_{c\xi}(t_i)\right]^T \left(GG^T\right)^{-1}\left[y_m(t_i) - y_{c\xi}(t_i)\right] \tag{5.21}$$

In this case, the criterion is quadratic, weighted by the measurement covariance matrix. So in principle, the technique is a weighted least squares output error method. In general, the Maximum Likelihood method also estimates noise statistics, but this is often omitted and weighting matrices are selected based on the experience of the analyst.

If the matrix G is not known, the measurement noise covariance matrix must also be determined. It is obtained from.

$$GG^T = \frac{1}{N}\sum_{i=1}^{N}\left[y_m(t_i) - y_{c\xi}(t_i)\right]^T\left[y_m(t_i) - y_{c\xi}(t_i)\right]^T \tag{5.22}$$

The off-diagonal terms in this matrix are in practice usually omitted.

The set of parameter values that minimizes the Maximum Likelihood cost function has to be found by a search procedure. Several types of such procedures exist and depending on the circumstances one or another may prove to be more effective. However, the most widespread method is the Gauss-Newton or Newton-Raphson algorithm, which starts from a set of initial estimates for the parameters and then refines these estimates by an iterative method that stops when a desired level of convergence has been reached. The updating algorithm is

$$\xi_{k+1} = \xi_k - \left[\nabla_\xi^2 J(\xi_k)\right]^{-1}\left[\nabla_\xi^2 J(\xi_k)\right] \tag{5.23}$$

with

$$\nabla_\xi J(\xi_k) = -\sum_{i=1}^{N}\left(\left[y_m(t_i) - y_{c\xi_k}(t_i)\right]^T \cdot \left(GG^T\right)^{-1}\left[\nabla_\xi\, y_{c\xi_k}(t_i)\right]\right) \tag{5.24}$$

$$\begin{aligned}\nabla_\xi^2 J(\xi_k) = &-\sum_{i=1}^{N}\left(\left[\nabla_\xi\, y_{c\xi_k}(t_i)\right]^T \cdot \left(GG^T\right)^{-1}\left[\nabla_\xi\, y_{c\xi_k}(t_i)\right]\right) \\ &+\sum_{i=1}^{N}\left(\left[y_m(t_i) - y_{c\xi_k}(t_i)\right]^T \cdot \left(GG^T\right)^{-1}\left[\nabla_\xi^2\, y_{c\xi_k}(t_i)\right]\right)\end{aligned} \tag{5.25}$$

In the last equation, (5.25), the second gradient $\nabla_\xi^2\, y_{c\xi_k}(t_i)$ is needed. Its computation requires a large effort. As this expression becomes zero when the optimum set of estimated parameters is reached, it can be justified to neglect this term when the initial starting values for the unknown parameters are not too far away from the final 'true' values so that convergence to the desired state is assured. This approach, known as the Gauss-Newton or modified Newton-Raphson approximation, is computationally very efficient and sometimes results in superior convergence performance of the iterative search. Neglecting the second gradient does not affect the final optimal values of the parameters.

In brief, the Maximum Likelihood Technique is an iterative procedure. It minimizes the differences between measured data and the calculated response of the identified model by modifying the model parameters. The main steps in the procedure are:

1. calculation of the cost function value; (5.20),
2. determination of the measurement noise covariance matrix; (5.22),
3. update of the values of the unknown parameters; (5.23),

4. calculation of the time history response of the updated model,

5. calculation of the new value of the cost function.

This procedure is repeated until the change in the cost function is smaller than a prescribed value. The magnitude of the change in the cost function thus indicates convergence of the estimation. To start the technique, a first guess for the unknowns, the *a priori* values, is needed. They should be as close as possible to the 'true' values to improve the convergence and to avoid that the estimation ends up in a spurious local minimum. To obtain starting values, a least squares equation error technique is often applied.

The core of the computational effort lies in the calculation of the gradient of the cost function with respect to the parameter vector. This gradient can be computed by finite difference techniques or by analytic differentiation. In the finite difference technique the elements of the gradient are determined by perturbing each of the elements of the parameter vector in turn, reintegrating the model equations to determine the perturbed model response and then using these perturbations to form the approximate finite difference form of the desired partial derivative. The choice of the magnitude of the parameter perturbation has to be made with care when the model equations are nonlinear. In the latter case the alternative of analytic differentiation is not attractive, but for the case of linear systems, the application of analytic differentiation often turns out to be much more efficient.

The Maximum Likelihood estimator also provides a measure of the reliability of each estimate. From (5.25) the Gauss-Newton Approximation (neglection of the second gradient) yields

$$I(\xi) = \sum_{i=1}^{N} \left(\left[\nabla_{\xi} y_{c\xi}(t_i) \right]^T (GG^T)^{-1} \left[\nabla_{\xi} y_{c\xi}(t_i) \right] \right) \qquad (5.26)$$

This is the so-called information matrix. For the idealized case of no state noise and 'simple' measurement error properties the Maximum Likelihood estimation leads to asymptotically efficient unbiased parameter estimates. Then, the inverse of the information matrix given in (5.5.27)

$$\text{covar}(\xi) = [I(\xi)]^{-1} \qquad (5.27)$$

is the covariance matrix of the estimation errors, which is a measure for the accuracy of the estimated unknowns. This uncertainty level, called the Cramer-Rao bound, for the individual parameters is obtained from the diagonal terms by

$$CR(\xi_m) = [\text{covar}(m, m)]^{1/2} \qquad (5.28)$$

The obtained values are often referred to as standard deviations of the identified parameters. It should be mentioned, that these values indicate the lowest obtainable bound. They are very useful for the comparison to each other to develop a feeling about the reliability of the estimation. For a practical interpretation they are usually too small and it is often suggested to multiply these values by a factor of 5 to 10 to make the standard deviation physically more meaningful.

The covariance matrix (5.27) also provides information about the correlation between the parameters determined as the above procedure. The correlation coefficients are obtained from

$$\rho(\xi_m, \xi_m) = \frac{\text{covar}(m, n)}{[\text{covar}(nn)\text{cova}(mm)]^{1/2}} \qquad (5.29)$$

Both the standard deviations and the correlation coefficients are extremely helpful in the search for an appropriate model structure. Output error techniques make this information readily available as it is obtained from the inverse of the information matrix, which has to be calculated anyhow for the estimation procedure.

It should be pointed out that the reality of the working model obviously represents a considerably more complex situation than that of the ideal assumptions in the observation equation of no state noise and random measurement noise of a simple statistical type. In the first place, the measurement errors are likely to contain modelling errors of their own, largely because of the limited knowledge of the dynamic behaviour of the air data system. The magnitude of these modelling errors may be appreciated from the data compatibility studies. To the extent that such modelling errors exist, the measurement error will contain contributions that reflect the particulars of the manoeuvre. Secondly, the assumption of no-state-noise is equally, or perhaps even more strongly, violated. The flight tests may have experienced some residual turbulence which would then represent a random contribution to the state noise. More importantly, the model we have adopted for the helicopter is only an approximation to its real characteristics and will therefore contribute modelling error to the state noise. Under these non-ideal real circumstances it is not possible to state that the use of the output error algorithms will lead to unbiased estimated parameters. Nevertheless, use of the algorithm to estimate parameter values remains a powerful and useful tool. Also the indicators of the "quality" of the parameter estimates embodied in the Cramer-Rao bounds and correlation matrix are still expected to indicate in a relative sense which parameters are firmly determined and which parameters play a less important role in the model. This information provides then a guide to removing the marginal parameters from the parameter set to be used.

In practice several different computer programs based on the output error method are in use. Some of these are confined to linear model equations, others deal with the full non-linear equations. The use of linear algorithms

requires either the use of the linearized forms of the gravity and rotation related terms in the force equations or, as an alternative, the treatment of these nonlinear terms as known functions calculated from measured values. If the model with its optimally estimated parameters provides small differences between the calculated model responses and measured variables, then the latter approach will be reasonable and computationally effective.

5.3.2 Equation Error Method

The theoretical ideal case leading to the output error method is based on no-state-noise so that only measurement noise is present and it is furthermore assumed to be of a simple random type. A converse ideal situation would occur when the measurements are without error and the state-noise present is assumed to be random with simple statistical properties. In this case the unknown parameters can be estimated with non-iterative methods in which the system model equations do not have to be integrated. As shown, the application of this method uses the methodology of regression analysis.

If we assume that a sufficient number of observed variables are available to determine the state variables from the observation equations, then, if the measured variables are measured without error, the state variables can also be determined without error. These are then completely deterministic. Now, the linear parametric representation of the specific aerodynamic forces and moments in terms of the perfectly known state variables can be confronted with the time histories of these forces and moments as determined from the accelerometer measurements and the angular accelerations provided by numerical differentiation of the angular rate measurements (or from angular accelerometers, if available):

$$y(t_i) = \xi_o + \xi_1 x(t_i) + \ldots + \xi_{n-1} x(t_i) + \varepsilon(t_i)$$

or

$$y + x\,\xi \qquad (5.30)$$

The functions $x_1(t_i)$ through $x_{n-1}(t_i)$ represent the perfectly known static variables and control inputs and y(ti) represents one of the observed components of the specific force or angular acceleration. The function $\varepsilon(t_i)$ is called the equation error. The following assumptions are made:

- The equation error ε is stationary with zero mean.
- ε is uncorrelated with the state variables.
- The state variables x_j are without error.
- ε is identically distributed, uncorrelated and has the variance σ^2.

In vector form, the observation vector y represents the variables measured at N time intervals, one at a time. Similarly, the state variables and control inputs are each perfectly known at N intervals. The vector y is then Nx1 and the matrix X is Nxn. Under these circumstances the parameter vector ξ associated with the particular observed variable is estimated to be

$$\xi_{est} = (x^T x)^{-1} x^T y \qquad (5.31)$$

The covariance of the estimated parameter vector is given by (5.32).

$$E\left\{(\xi_{est} - \xi)(\xi_{est} - \xi)^T\right\} = \sigma^2 (x^T x)^{-1} \qquad (5.32)$$

with σ^2 estimated by

$$s^2 = \frac{1}{N - n} \sum_{i=1}^{N} \varepsilon_{est}(t_i)$$

and

$$\varepsilon_{est}(t_i) = y(t_i) - y_{est}(t_i)$$

$$y_{est}(t_i) = (\xi_{est})_0 + (\xi_{est})_1\, x_1(t_i) + \ldots + (\xi_{est})_{n-1}\, x_{n-1}(t_i)$$

When in addition, the state noise is assumed to be normal, i.e., to have a Gaussian distribution, then the classical measures of significance of the regression, the F number, the partial F numbers and the squared multiple correlation coefficient, can be expressed as in (5.33).

$$F = \frac{\xi_{est} x^T y - N\bar{y}^2}{(n-1)s^2}$$

$$\bar{y} = \frac{1}{N} \sum_{i=1}^{N} y(t_1)$$

$$F_p = \frac{(\xi_{est})_j^2}{s^2 (\xi_{est})_j} \qquad (5.33)$$

$$R^2 = \frac{\xi_{est}^T x^T y - N\bar{y}^2}{y^T y - N\bar{y}^2}$$

A deliberate selection of the significant parameters can be made by using a stepwise regression procedure. In such a procedure, the (regression) model increases its complexity by adding one new term at a time from the group of available state variables and control inputs to the model. The selection can be guided subjectively by the analyst or be under the control of a computer algorithm. Typically, the first regression variable selected is the one that exhibits the largest correlation with the dependent variable, y. Subsequent decisions are made on the basis of new, modified regression problems in which modified dependent variables are represented at each step by their residuals that result when the prediction by the model determined in the previous step; is subtracted, e.g., after two steps

$$y'(t_i) = y(t_i) - (\xi_{est})_0 - (\xi_{est})_1\, x_1(t_i) - (\xi_{est})_2\, x_2(t_i) \qquad (5.34)$$

The next regressor to be added to the model will be that variable from amongst the remaining candidate regressor functions that shows the highest correlation with the modified dependent variable. At each step the partial F numbers are determined for each of the parameters that have been entered into the problem and only those that exceed a threshold for their partial F values stipulated by the analyst will be retained. The procedure will terminate when no further additions to the model can meet the threshold criterion.

Several implementations of the stepwise regression procedure are available in commercial statistics software packages, and a number of laboratories have developed their own programmes. The actual matrix arithmetic in these programmes is finely tuned to be as efficient as possible and to minimize the effects of poorly conditioned problems.

As mentioned previously, the rigorous theory for this method is based on the assumptions of perfectly known state variables and random noise. For the F values to be statistically meaningful this random noise has to be a white, Gaussian sequence. In reality these assumptions are violated. Even when state reconstructed values are used for the state variables, hopefully improving their accuracy, these will still not be perfectly known. Under such conditions, the estimates will no longer be unbiased. Also the noise statistics do not satisfy the assumed characteristics, partly because of modelling errors, and the information carried by the partial F values as determined by the application of the regression method is no longer closely related to the actual variance of the parameter estimates. This is clearly illustrated when the parameter variances calculated on the basis of applying the method to a number of different experimental time histories are analyzed. These turn out to be significantly larger than the variances inferred from the partial F values. As is the case in the application of the output error method under non-ideal circumstances, the use of the equation error method and the information about the relative importance of the various parameters, especially where augmented by practical judgement, nevertheless provides usable information.

5.3.3 Closing Comments

On theoretical grounds the application of both output-error and equation-error methods is flawed in that neither promises to deliver unbiased estimates of the parameters. Since in the analysis of flight test data of aircraft for which the model is not accurately known *a priori*, the preference for a particular method or combination of methods will depend on the ability of the identified model to predict aircraft performance in some sense. This ability is assessed via considerations of model verification and model robustness studies.

References

[5.1] Ljung, L., *System Identification; Theory for the User*, Prentice-Hall Inc. Englewood Cliffs, New Jersey, 1987.

[5.2] Soderstrom, T., Stoica, P., *System Identification*, Prentice-Hall Inc., Englewood Cliffs, New Jersey, 1989.

[5.3] Bendat, J. S., Piersol, A. G., *Random Data; Analysis and Measurement Procedures*, Second Edition, John Wiley & Sons, Inc., New York, 1986.

[5.4] Maine, R., Iliff, K. W., *Identification of Dynamic Systems; Application to Aircraft*, AGARD AG-300, 1986.

[5.5] Klein, V., *Maximum Likelihood Method for Estimating Airplane Stability and Control Parameters from Flight Data in the Frequency-Domain*, NASA TP-1637, 1980.

[5.6] Tischler, M. B., *Frequency-Response Identification of XV-15 Tiltrotor Aircraft Dynamics*, NASA TM-89428, ARMY TM-87-A-2, 1987.

[5.7] Kaletka, J., von Grünhagen, W., *Identification of Mathematical Derivative Models for the Design of a Model Following Control System*, 45th Annual National Forum of the American Helicopter Society, Boston, MA, 1989.

[5.8] Anon., *Flight Dynamics — Concepts, Quantities and Symbols — Part 3: Derivatives of Forces, Moments and Their Coefficients*, International Standard ISO 1151-3, 1989.

IDENTIFICATION TECHNIQUES

FREQUENCY DOMAIN METHODS

Mark B. Tischler
Aeroflightdynamics Directorate
U.S. Army Aviation Research & Technology Activity
Ames Research Center
Moffet Field, California, U.S.A.

The starting point in frequency-domain identification methods is the conversion of time-based data to frequency-based data. This conversion, which is a batch and non-iterative process, involves a considerable amount of data conditioning not required for time-domain methods. However, once the frequency-domain data base is completed, the computational burden of the parameter nonlinear search is considerably reduced. Also, there are some important benefits of formulating the cost function in the frequency-domain. This section presents an overview of frequency-domain methods used by WG 18 members.

Overview of Frequency-Domain Methods. Discrete data are converted from time sequences to frequency sequences using the Fast Fourier Transform (FFT), in conjunction with data windowing and digital filtering. These resulting frequency sequences are estimates of the Fourier Series coefficients for continuous time-history signals. These Fourier coefficients are used to calculate the signal power spectral density (PSD) functions, which provide important information on the frequency content of excitation and response signals, as needed in test input design. The frequency-response function and associated accuracy metric, the coherence function, are determined directly from the PSD results; these are the "non-parametric" identification results that are very useful for handling-qualities analyses, simulation validation, and flight control. Frequency-response data obtained from flight responses containing multiple control inputs are post-processed to remove the effects of partially-correlated control inputs.

Parametric identification equations based on output-error and equation-error cost function formulations presented earlier for the time-domain techniques are essentially unchanged for the frequency-domain solution, once the time index is replaced by the frequency index. Transfer-function identification is completed by direct fitting of single-input/single-output (SISO) frequency-responses using an assumed transfer-function model structure. State-space model identification based on frequency-response cost functions is achieved by simultaneously fitting the MIMO set of frequency-responses.

Conversion to the Frequency-Domain. Continuous time-history signals are converted to the frequency-domain via the Fourier Transform. For example, the time-based signal x(t) is converted to the frequency-based signal X(f) by:

$$X(f) = \int_{-\infty}^{\infty} x(t)\, e^{-j\omega t}\, dt \qquad (6.1)$$

The condition for existence of the Fourier Transform X(f) is:

$$\int_{-\infty}^{\infty} |x(t)|\, dt < \infty \qquad (6.2)$$

This condition for existence is satisfied provided that the time-history signal x(t) is bounded (i.e., does not blow up). The piloted frequency-sweep technique requires that the test starts and ends in trim ($x(0) = x(t_f) = 0$), thereby ensuring that this condition is satisfied. It is important to emphasize here that the Fourier Transform is valid and can be determined without modification for flight data obtained from helicopters that exhibit either stable or unstable (most common) dynamic characteristics. Furthermore, the frequency-response function H(f) which relates the input and output Fourier Transforms (X(f) and Y(f), respectively) will also exist and be completely valid for either stable or unstable systems:

$$Y(f) = H(f)\, X(f) \qquad (6.3)$$

Flight test techniques and numerical examples of extracting unstable responses are presented by Tischler [5.5.7].

Real time-history data is of finite time duration (T, secs), so the Fourier Transform of equation (5.5.35) becomes the Finite Fourier Transform:

$$X(f, T) = \int_0^T x(t)\, e^{-j2\pi ft}\, dt \qquad (6.4)$$

The record length T is the fundamental period of the signal, and defines the minimum frequency of identification:

$$\omega_{min} = 2\pi/T \qquad (6.5)$$

Frequencies $\omega < \omega_{min}$ DO NOT EXIST in the data and, so cannot be identified ["padding with zeroes" simply produces interpolation, and does not allow lower frequencies to be identified].

When the data is in digital form, as is the case here, the Finite Fourier Transform is calculated digitally via the Discrete Fourier Transform (DFT):

$$X(f_k) = X(k\,\Delta f) = \Delta t \sum_{n=0}^{N-1} x_n \exp[-j2\pi(kn)/N]; \quad k = 0, 1, 2, ..., N-1 \qquad (6.6)$$

where:

$X(f_k)$	=	Fourier coefficients
x_n	=	$x(n\,\Delta t)$ = data points
Δt	=	time increment
N	=	number of discrete frequency points

Finally, the Fast Fourier Transform ("FFT") is a numerically efficient algorithm for calculating the DFT. The quality (accuracy, resolution, random error content) of the achievable frequency-domain data and resulting model identification results are significantly enhanced by a number of relatively easy, but important data processing procedures (Bendat and Piersol, 1986 [6.1]; Tischler, 1987 [6.2]; Tischler and Cauffman, 1990 [6.3]):

- Digital prefiltering
- Overlapped/tapered windowing
- Chirp z-transform
- Composite window averaging

When the time-history does not end in trim (e.g., 3211 test inputs), a correction term can be applied to the FFT to account for the conversion error introduced by the truncation effects in equation (6.4) (Fu et al., 1983 [6.4]). However, this correction term is not significant if tapered, overlapped windows are used, as is recommended.

Spectral Functions. The Fourier coefficients can be manipulated to determine the spectral distribution of the input, output, and cross-correlated signals — the power spectral density ("PSD") functions:

Input autospectrum:

$$\tilde{G}_{xx}(f_k) = \frac{2}{TU}|X(f_k)|^2; \quad U = 1.63 \text{ for Hanning window} \qquad (6.7)$$

= distribution of xx as a function of frequency

Output autospectrum:

$$\tilde{G}_{yy}(f_k) = \frac{2}{TU}|Y(f_k)|^2 \qquad (6.8)$$

= distribution of yy as a function of frequency

Cross spectrum:

$$\tilde{G}_{xy}(f_k) = \frac{2}{TU}[X \cdot (f_k)Y(f_k)] \qquad (6.9)$$

= distribution of xy as a function of frequency

Examination of the input autospectrum provides the bandwidth of the excitation signal, the key characteristic for input signal design. Test inputs for system identification must have excitation bandwidths that cover the frequency range of the intended application.

Frequency-Response Calculation. The SISO frequency-response H(f) is determined from the PSD functions:

$$H(f) = \frac{G_{xy}(f)}{G_{xx}(f)} \qquad (6.10)$$

The frequency-response as determined from equation (6.10) is unbiased in the presence of both output measurement noise (aircraft response sensors), and process noise (e.g., turbulence). This is a key benefit of frequency-response based identification methods as compared to equation-error or output-error approaches.

The coherence function Y^2_{xy} calculated at each frequency point indicates the accuracy of the identified frequency-response:

$$Y^2_{xy} = \frac{|G_{xy}(f)|^2}{G_{xx}(f)G_{yy}(f)} \qquad (6.11)$$

Coherence function values less than unity are due to nonlinearities in the input-to-output process, or the presence of measurement noise or process noise. A coherence function of greater than 0.6 generally indicates acceptable identification accuracy for that frequency point.

Frequency-Response Identification When Multiple Partially-Correlated Inputs are Present. Most test data generated by a pilot or with computer generated signals involve inputs to multiple controls. For example, in the frequency-sweep test technique, the pilot may apply inputs in the secondary channels to maintain aircraft motion near the reference flight condition. If dynamic coupling exists in the system being identified, the presence of correlated secondary inputs, if ignored, will bias frequency-responses obtained from the SISO relationship of equation (6.10) (Tischler, 1987 [6.2]). The correct responses are obtained from the multi-input/single-output MISO solution of the matrix frequency-response equation at each frequency point (Otnes et al., 1978 [6.5]):

$$T(f_k) = G_{xx}^{-1}(f_k)\, G_{xy}(f_k) \qquad (6.12)$$

where

$G_{xx}(f_k)$ = n_c x n_c matrix of auto and cross-spectra between the n_c inputs,

$G_{xy}(f_k)$ = n_c x 1 matrix of SISO cross-spectra between each control input and the single input.

The associated coherence function obtained from the MISO solution is referred to as the "partial coherence":

$$\gamma^2_{x_i y\, n_c\text{-}1)!} = \frac{\left|G^2_{x_i y\, n_c\text{-}1)!}\right|}{G_{x_i x_i\, n_c\text{-}1)!}\; G_{yy\, n_c\text{-}1)!}} \qquad (6.13)$$

This solution is repeated for each of the (n_0) outputs to obtain the (n_c x n_0) MIMO set of "conditioned" *frequency-responses.*

Output-Error and Equation-Error Formulations in the Frequency-Domain. The time-domain state equations (5.19) are converted to the frequency-domain by taking the Fourier Transform and dropping the initial conditions *and bias terms:*

$$\begin{aligned} j\omega\, X(\omega) &= A\, X(\omega) + B\, u(\omega) + G_{nn}(\omega) \\ Y(\omega) &= C\, X(\omega) + D\, u(\omega) + G_{\eta\eta}(\omega) \end{aligned} \qquad (6.14)$$

where:

$u(\omega)$ and $Y(\omega)$ are the control (input) and output Fourier coefficients obtained from equation (6.6) with $\omega = 2\pi f$,

$G_{nn}(\omega)$ is the PSD of the process noise,

$G_{\eta\eta}(\omega)$ is the PSD of the measurement noise.

Including both process and measurement noise sources leads to the general frequency-domain Maximum-Likelihood problem (Klein, 1980 [5.5]). The frequency-domain output-error and equation-error solutions follow directly from the earlier time-domain solutions:

$G_{nn}(\omega) = 0 \Rightarrow$ Output-error

$G_{\eta\eta}(\omega) = 0 \Rightarrow$ Equation-error

At first look, it may appear that a great deal of computational effort has been expended to arrive right back at the same equation-error and output-error solutions obtainable in the time domain. But, there are some important benefits of using the frequency-domain formulation, especially for identifying higher-order models of helicopter dynamics that include widely spaced dynamic modes (e.g., fuselage and rotor modes). This problem is discussed in detail by Fu et al (1990, [6.6]). In the current application to the identification of 6-DoF handling-qualities models, the most significant benefits of the frequency-domain methods are:

- Direct estimation of time-delays. This is very important for achieving a representative model. Time delays are directly and very accuracy determined with frequency-domain methods, since such delays have a linear effect on the cost function. In contrast, time-domain methods can estimate these delays only in an indirect fashion.

- Band-limiting data and frequency weighting. In the frequency-domain formulation, the cost function is calculated only in the frequency range selected by the user. This allows the analyst to closely match the data with the model structure. For example, the 6-DoF identification is conducted in the frequency range up to the first rotor regressing flapping mode. Within the identification range, the frequency-domain fitting errors are equally weighed at all frequencies. Unless specific explicit weighting is applied, the time-domain formulation provides higher weighting of the lower frequencies which can degrade the identification of the higher-frequency modes. Also, the data must be digitally filtered to achieve time-domain band-limiting for consistency with the model structure.

Frequency-Response Cost Function Formulation. The frequency-response cost function is formulated by taking the Laplace Transform of equation (6.7) on page 94 and solving for the state-space model transfer-function T_m:

$$T_m(s) = C[sI - A]^{-1} B + D \qquad (6.15)$$

A matrix of time delays r is included in the model by noting that:

$$T_d(s) = e^{-rs} \qquad (6.16)$$

$$T_m(j\omega) = \left(C[j\omega I - A]^{-1} B + D\right) e^{-j\omega r} \qquad (6.17)$$

The unknown state-space model parameters (θ) in the matrices A, B, and r are determined by minimizing J, a weighted cost function of the error ε between the identified frequency responses $T(j\omega)$ [of equation (6.12) and the model responses $T_m(j\omega)$ [of equation (6.17)] over a selected frequency range:

$$J(\theta) \approx \sum_{n=1}^{n_\omega} \varepsilon^T(\omega_n, \theta) W \varepsilon(\omega_n, \theta) \qquad (6.18)$$

The frequency ranges for the identification criterion (ω_1, ω_2, ..., ω_n) are selected individually for each input/output pair according to their individual ranges of good coherence. In this way, only valid data are used in the fitting process. Within these frequency ranges, the

points are selected linearly across the logarithmic frequency range. The weighting matrix (W) is based on the values of coherence at each frequency point to emphasize the most accurate data. These features are key benefits of the frequency-response approach.

As in the time-domain methods, the Cramer-Rao bounds and parameter correlation information are obtained from the numerical estimate of the Hessian matrix H. For the frequency response method:

$$H = \nabla^2_{\theta} J = \frac{\partial^2 J}{\partial \theta^2} \cong 2D^T W D \qquad (6.19)$$

where $D \equiv \partial \varepsilon_i / \partial \theta_j$ is obtained numerically from first differences.

The Cramer-Rao lower bound for each parameter (CR_i) is obtained as before:

$$CR_i = \sqrt{(H^{-1})_{ii}} \qquad (6.20)$$

A reasonable estimate of the parameter standard deviation usually requires a scale factor of 5-10 on the Cramer-Rao bound to account for modelling errors and non-Gaussian noise. The frequency-response ratio of equation (6.20) eliminates the noise effects, which from experience lowers the appropriate scale factor to about 2.

Concluding Remarks Regarding Frequency-Domain Methods. Frequency-domain methods provide some important benefits in rotorcraft system identification, especially in the identification of higher-order models with widely spaced dynamic modes. The tradeoff is in the considerable amount of data conditioning involved in the conversion of the time-domain data base to the frequency-domain data base. The proliferation of data in this conversion process makes a data-basing capability very important. Also, since frequency-domain methods tend to be graphics intensive (spectral curves, frequency-response, coherence, etc), user-friendly graphics-oriented software is important. The growing availability of frequency-domain identification software is a key factor in recent growth of interest in these techniques. Sophisticated software for output-error and equation-error formulations has been developed by DLR and University of Glasgow. The AFDD has developed an integrated package for the frequency-response based approach.

References

[6.1] Bendat, J. S., Piersol, A. G., *Random Data; Analysis and Measurement Procedures*, Second Edition, John Wiley & Sons; Inc., New York, 1986.

[6.2] Tischler, M. B., *Frequency-Response Identification of XV-15 Tiltrotor Aircraft Dynamics*, NASA TM-89428, ARMY TM-87-A-2, 1987.

[6.3] Tischler, M. B., Cauffman, M. G., *Frequency-Response Method for Rotorcraft System Identification with Applications to the BO 105 Helicopter*, 46th Forum, American Helicopter Society, Dynamics I-Session, Washington, DC, 1990.

[6.4] Fu, K. H., Marchand, M., *Helicopter System Identification in the Frequency-Domain*, 9th European Rotorcraft Forum, Stresa, Italy, 1989.

[6.5] Otnes, R. K., Enochson, L., *Applied Time Series Analysis*, John Wiley & Sons, Inc., New York, 1978.

[6.6] Fu, K. H., Kaletka, J., *Frequency-Domain Identification of BO 105; Derivative Models with Rotor Degrees of Freedom*, 16th European Rotorcraft Forum, Glasgow, UK, 1990.

MODELLING ASPECTS AND ROBUSTNESS ISSUES IN ROTORCRAFT SYSTEM IDENTIFICATION

by

D. J. Murray-Smith
Department of Electronics and Electrical Engineering
University of Glasgow
Glasgow, G12 8QQ
Scotland, United Kingdom

Summary

The concept of robustness is examined and discussed in the context of rotorcraft system identification and modelling. A classification of robustness issues is proposed involving experimental design aspects, identification techniques, model structure estimation, parameter estimation and the robustness of the complete mathematical model resulting from the application of identification processes. Associated tests of robustness are proposed and a set of special recommendations is presented for each of the aspects considered. Within these recommendations particular emphasis is placed on the need for a good user interface which fully exploits the use of computer graphics and for reliable tools for the assessment of model structure.The need for preliminary flight tests to characterise the dynamics of the system and thus guide the design of identification experiments is also emphasised. A further recommendation is that design criteria should be established for verification inputs.

1 Introduction

Deficiencies in mathematical models used for piloted simulations and for flight control law design can impose important limitations and constraints in research and development programmes for new aircraft. These, in turn, can lead to significant additional costs.

System identification methods can contribute significantly to the processes of model development and validation provided due account is taken of the issues of identifiability and robustness. Identifiability relates to the potential for successful derivation of a mathematical model of a given structure from given experimental response data. Robustness, on the other hand, concerns the degree to which an identified model is altered when factors such as the test data record length, test input signal magnitude or identification algorithm are changed. Successful adoption of system identification methods by the rotorcraft industry hinges on the formulation of guidelines to ensure robustness and a comprehensive demonstration of robustness through the application of such guidelines.

Robustness issues in rotorcraft system identification may be classified conveniently as follows:

(a) robustness and reliability of *a priori* information required for successful system identification.

(b) robustness of the identification technique used for establishing the structure of the model and estimating parameters of the model.

(c) robustness (consistency and accuracy) of the identified model structure.

(d) robustness (consistency and accuracy) of the estimated parameters.

(e) overall robustness of the resulting mathematical model.

This discussion paper puts forward proposals for the robustness conditions and tests required for all aspects of the problem. In some cases the proposals are tentative and the need for more substantiation work is identified. While it is clearly attractive to maximise robustness at all stages, it must also be recognised that valuable work has been done with the techniques of system identification in cases where success has been limited because of lack of robustness but where the fragility of results has provided important new insight in terms of the mathematical model.

It must be admitted that lack of robustness has been an important factor which has limited the use of identification techniques by industry in the past. However, it must be pointed out that the industrial organisations that will benefit

the most and the earliest from this enabling technology are those that commit resources to it during its development.

2 *A priori* Information: Experimental Design and Data Consistency

Successful initial design of an identification experiment depends critically upon the level of uncertainty within the information available at the outset, including the accuracy of any available mathematical models of the vehicle. Accurate experimental design requires prior knowledge of the characteristics of the vehicle and such information is, of course, never fully available. A second concern is the accuracy and consistency of the measurements themselves: both of these issues can be discussed under the heading of a priori information.

2.1 Experimental Design

As has been pointed out by Murray-Smith and Padfield (1991), experimental designs based on available mathematical models are unlikely to be optimal due to model uncertainties. It is important, therefore, to be able to characterise some flight test data, if available, prior to any detailed experimental design. Such preliminary data must, of course, be representative of the flight condition for which the proposed identification tests are to be performed. Characterisation of these data sets may be carried out in terms of spectral content, amplitude probability density, maximum excursions and noise content. Measures such as these, taken together with a mathematical model of the vehicle and any other available information, provide useful insight which can have considerable influence on the design and conduct of flight experiments for system identification purposes.

Closely associated with the analysis of any preliminary flight data is a requirement for careful assessment of the instrumentation available on the aircraft to ensure that it is adequate for system identification purposes. Questions of robustness of estimates and robustness of identification methods are closely associated with the quality of the flight test data which, of course, depends ultimately on the quality of the instrumentation.

Careful attention to detail in the design and conduct of flight experiments can greatly enhance the effectiveness and value of a flight test programme. Initial conditions must be defined for each test and these conditions must be repeatable. This is possible only when there is a low turbulence level which would of course apply unless turbulence modelling is a specific objective of the flight test programme. At the analysis stage it is therefore necessary to determine the means and standard deviations of the records from all the channels prior to the application of the control input. This process allows one to check that the required initial state exists in terms of the mean values and that deviations from this mean lie below a defined threshold level.

In the design of flight experiments it is also important to make provision for repeated testing at each chosen test condition. Results from repeated tests must be examined carefully for differences. Ideally this should be done on board the aircraft or by telemetry so that further testing can be carried out if significant variations are detected.

Investigation of linearity is of great importance and at each test point inputs should be applied for different amplitudes and for different directions. The degree of nonlinearity can then be assessed qualitatively and also in a quantitative fashion in terms, for example, of the amplitude distribution function.

The frequency content of test signals is of great importance for system identification work and it is necessary to ensure that the frequency content of the test input signal used in a given application is appropriate for the modelling objectives in that particular case. Spectral analysis of the test input applied to the vehicle, coupled with simi-lar analysis of the measured response variables, can provide valuable physical insight. For each test condition it is appropriate to carry out tests with different input signals selected to cover different parts of the frequency range. Comparisons can then be made of these data sets with a view to establishing any potential prob-lem areas for the subsequent identification process. For example, the extent of excitation of each of the states at a given part of the frequency range can be of considerable import-ance. Prior knowledge of the states which are excited in a satisfactory fashion can be very helpful in guiding the user of identification software and in interpreting results.

If test input signals are to be applied by the pilot via the normal controls practical limitations of accuracy and repeatability are encountered both in terms of amplitude and timing. The difficulties of applying tests

signals manually restrict the range of input types which can be considered. On the other hand it may be essential in some applications, such as handling qualities studies, for the pilot to apply the test inputs.

Robustness of test inputs is an important but often neglected aspect of the input design process. As already discussed, only an approximate model of the vehicle is available prior to testing and the inputs used should be as insensitive as possible to errors in the model.

A second important point is that inputs should not contain a dc component since this will tend to change the operating condition of the aircraft away from the initial trim state; unless this is specifically required (*eg* classical speed - stability tests (Padfield (1985)).

Tables 1 to 5 summarise robustness conditions and tests for each aspect of the identification process. Special recommendations are included within these tables and for the experimental design aspect (Table 1) the recommendations emphasise the importance of a preliminary flight test. Results from the application of an appropriate broad-band calibration input, such as a frequency sweep, should be of value in the experimental design and should provide useful information to guide the initial choice of a model structure.

2.2 Kinematic (measurement) consistency

The fact that flight data is frequently degraded by measurement and process noise and sensor calibration inaccuracies introduces a need for consistency checks on the data prior to the application of identification techniques to estimate aircraft parameters. Methods commonly used for the investigation of data consistency involve:-

(a) simple comparisons between redundant sensors

(b) comparisons between kinematically redundant sensors (*eg* comparisons of integrated body rotational accelerations with body angular rates)

and

(c) state estimation techniques such as the Kalman Filter/Smoother.

Important questions of robustness arise in connection with all of these methods of consistency checking. In methods (a) and (b) biases and scale factors may be estimated using least squares or maximum likelihood techniques, but instrument modelling errors or the presence of large amounts of measurement noise can cause problems. State estimation methods may be used to reduce the uncertainty level associated with a given signal but these techniques require prior knowledge of measurement and process noise statistics which may not be readily available.

One approach to the investigation of kinematic consistency which may have some advantages, in terms of robustness, over other methods involves the use of a Bayesian estimator (Black (1989), Turner (1991)). For such an estimator confidence figures have to be provided for the initial values of the unknown parameters. Some physical insight can thus be incorporated within the estimation process and this may provide benefits in terms of the robustness of estimates of bias and scale factor parameters.

3 Identification Techniques

The robustness of a given identification technique cannot, in general, be separated from questions of experimental design, choice of model structure, and accuracy of the resulting estimates. However, in the context of the classification of robustness issues given above, the robustness, or otherwise, of a given identification technique is taken to mean the reliability of the method in terms of convergence of the optimisation procedure, susceptibility to measurement and process noise, and accuracy of initial parameter estimates.

Klein, in his AGARD Lecture Series No.104 paper (Klein, (1979)), has provided a useful summary of the identification techniques generally applied to aircraft parameter estimation. The paper gives the theoretical properties of a number of different estimators. These properties provide useful pointers with regard to questions of robustness.

For example, in its most general form, the maximum-likelihood method provides a means of obtaining parameters for a linearised aircraft model from flight data involving both measurement noise and process noise. On the other hand other, less general, forms of output error method are based upon an assumption that only measured outputs are corrupted by noise and that the aircraft experiences no gusts or other

unmodelled disturbances. In the presence of process noise, such as atmospheric disturbances, results from output-error methods can be significantly degraded, leading to poor estimates which show large variances or high correlations. The variance of estimates obtained using equation error methods is affected not only by process noise but also by the noise level associated with all the measurements and the estimates themselves can be significantly biased using this approach even if the measurement noise and process noise components have zero mean value.

Comparisons of the robustness of different techniques can only be carried out if they involve tests in which each method is assessed using the same sets of flight data. The robustness of a given technique can, of course, be influenced considerably by the software implementations and every effort must be made to ensure that identification techniques are not being degraded by poor software design.

Other factors to be considered in making comparisons of this kind include the form of model under consideration (*eg* state space or transfer function) and the particular flight conditions included in the chosen data sets upon which the comparisons are based.

The ease of use of a method and the form of interface provided in a particular computer implementation are matters which are, in principle, quite separate from questions of robustness. However, the diagnostic tools incorporated within a particular software implementation can be of considerable importance. Robustness problems may well remain undetected unless the user is confronted with relevant evidence concerning confidence intervals, goodness of fit and cost function values. This implies a need for a well designed, flexible, user interface with extensive provision for graphical output.

The special recommendation presented in Table 2 for this aspect of the identification process relates to the need for identification tools to incorporate a full and well-engineered user interface which provides information concerning factors such as the goodness of fit, confidence intervals of estimates, the sensitivity to changes of model structure and the sensitivity to changes in test condition. Good graphics facilities are an essential part of this user interface.

4 Model Structure

Questions of robustness in terms of the estimation of model structure are, for linear six-degree-of-freedom rotorcraft identification, traditionally linked to problems associated with equation-error identification methods and to techniques for the determination of model order in transfer function models. However, the use of pseudo-control inputs (*eg* Black and Murray-Smith, (1989)) or the method of successive residuals (DuVal *et al*, (1983)) as a means of reducing the complexity of the parameter estimation problem also involves decisions which relate implicitly to the model structure, and may have a bearing on the accuracy of the estimates of the associated parameters.

In broader terms the model structure estimation process implies an activity in which the model may be expanded in a number of different dimensions. The number of degrees of freedom is the most obvious measure of complexity of a model structure but this aspect cannot be separated from questions of bandwidth, amplitude and helicopter components. It is vital to recognise that in the development of a model structure we can expect to see dramatic changes in effective parameters as the model is expanded. For example, the parameters of a low-frequency reduced-order model may change significantly as additional degrees-of-freedom are introduced or the bandwidth is increased. Such changes demonstrate very clearly the weakness of reduced-order models when used outside their proper range of application.

One important indicator of problems associated with model structure is provided by the residuals which are obtained following the parameter estimation stage of the identification. Correlated residuals can often be an indicator of a possible problem associated with the model structure. The form of the residuals, when interpreted with with physical understanding, may provide clues concerning the precise nature of this problem and the steps to be taken to correct the model structure. Practical difficulties can arise, however, because of the fact that large residuals may also result from the presence of correlated measurement noise in the measured flight data, or from the fact that a particular response variable is of very small amplitude, or from nonlinearities.

The step-wise regression procedures available within the Optimal Subset Regression (OSR) program (Padfield *et al* (1987)) allow the estimation of a first approximation to the parameter estimates in a class of model structures.

This form of equation-error estimation provides one very convenient way of exploring the ability of different linear and nonlinear model structures to fit flight measurements. The step-wise regression procedure applies the least squares fit in a sequence of steps, each time adding or deleting an additional independent variable to the regression equation until a best fit is achieved. At each stage the variable chosen for entry to the regression is the one having the highest partial correlation with the residual. In this process the multiple correlation coefficient, R , is a direct measure of the accuracy of fit while the total F-ratio provides a measure of the confidence ascribed to the fit. The partial F-ratios for individual parameters provide individual confidence measures. Both R and the F-ratios are tracked during the regression process in order to determine the maximum total and partial F-ratios. The regression is terminated when either R reaches a predefined value or the individual F-ratios of remaining parameters fall below a specified critical value. An example, described by Padfield *et al* (1987), has illustrated the value of this process for the case of a pedal doublet response in which it was found necessary to restrict the estimated model structure to simple lateral and directional motions. The relationship between the stability of the Dutch roll and the flight path angle was being investigated and, although it was found initially that the predictive capabilities of the simulation model were poor, a reduced-order upgraded model based on flight data provided greater insight concerning the mechanisms of stability loss with climb angle.

The incorporation of pure time delays within the model structure can lead to improved, and more robust estimates of derivatives within the six-degrees-of-freedom form of description in cases where these derivatives are susceptible to rotor transient effects which are not included in the assumed model structure.

In addition to bandwidth and amplitude a third important model dimension relates to the vehicle's physical components *eg* main rotor, tail rotor etc. Without the use of special load cells, however, knowledge of individual component contributions to force and moment derivatives is very difficult to extract. However, in some situations certain components dominate and in others the relationship between the components' contributions to different parts of the model structure are known and can be used to support the analysis (*eg* N ot = constant × Y ot).

It is recommended in Table 3 that increased emphasis should be given to establishing a valid model structure prior to the parameter estimation stage of the identification process. In order to do this more reliable techniques are needed for the estimation of model structure.

5 Parameter Estimates

One indicator of the robustness of parameter estimates is the value of the associated variance. It should be noted, however, that comparison of variance values obtained using different model structures is not valid.

As mentioned under the heading of model structure, checks of residuals can provide additional insight concerning questions of accuracy. If the identification process is completely accurate, both in terms of model structure and parameter estimates, the residuals will take the form of white noise. The whiteness of residuals is conventionally tested by determining the autocorrelation function of the residual sequence.

An additional measure of the robustness of parameter estimates may be provided by plots of the parameter value versus the length of the record used for the identification. The plots for each parameter should of course converge to a constant value as the record length increases. An example for the case of the Puma helicopter may be found in a recent paper by Black and Murray-Smith (1989) which includes a graph showing the dependence of estimates and the associated variances on record length for a particular flight experiment.

The sensitivity of parameter estimates to the frequency range of the data used in the estimation process can also be revealing and can provide a measure of the robustness of parameter estimates. High sensitivity to the inclusion of additional frequencies in the range used for identification is a good indicator of problems in the experimental design or model structure determination stages. Essentially the requirement, in terms of the frequency-domain, is to establish the range of frequencies over which parameter estimates are essentially constant. This process should then lead to an identified model which is valid for that frequency range.

The robustness of parameter estimates is closely associated with questions of experimental design and the spectral behaviour of the system. Plaetschke and Schulz (1979) have discussed the general problem of identifiability

of derivatives and have proposed the use of frequency-domain techniques for identifiability investigations. Kaletka (1979) has also proposed a method for isolation of significant parameters involving measures based upon time-domain quantities. Both of these approaches provide powerful tools to isolate significant terms and identifiable parameters within the model equations. Clearly, as is emphasised in Table 4, estimated parameters should show low sensitivity to record length in both the time domain and frequency domain.

6 Overall Robustness of the Model

Checks of the overall accuracy of the model resulting from the identification process can be obtained by carrying out tests on the model using data sets which were not used in the identification process. The selection of such data sets to be used for model checking can present problems in that they must be broadly similar to the sets used for the identification in terms of their spectral properties and amplitude and energy distributions. If the differences between the model responses and the corresponding measured variables are all sufficiently small the identified model can then be accepted as a candidate model for the chosen flight condition. It will not, however, be a unique representation and it is possible that other models could give similar results.

An additional check can, of course, be provided by carrying out repeated runs at the same nominal test condition using the same experimental design. An assessment of the changes of structure and parameter estimates under these circumstances can be very revealing, especially when the extent of the model distortion is related to the error bounds of the estimated model parameters. The situation is unsatisfactory if the variations of parameters derived from tests carried out under nominally the same conditions are greater than the estimated error bounds. One of the recommendations shown in Table 5 is that design criteria should be established for verification inputs.

Responses obtained using other test inputs are bound to give differences in the amplitude, frequency and distribution of energy between state variables and are thus likely to give different parameter estimates. The differences may however be understandable in terms of physical reasoning and potentially useful information can sometimes be obtained by making comparisons of results from a number of test signals.

It is also very useful, when comparing parameter estimates with theoretical predictions, to examine the trend of the estimated parameters with some fundamental rotorcraft quantity defining the flight condition. Such quantities include speed, rate of climb or descent and turn rate. As pointed out by Iliff (1979) this simple technique can provide much valuable insight and is readily applied to aircraft where manoeuvres are small perturbations about a point in a much larger envelope.

7 Conclusions and Recommendations

The robustness conditions and associated tests proposed in the previous sections are summarised in Tables 1 to 5. For each robustness condition it is possible to define one or more tests which may be of value. In some cases the proposals which have been made are very tentative and it is unlikely that any examples exist where all these robustness tests have been applied in a systematic fashion. Many cases do exist, however, in which some of the robustness tests shown in the tables have been applied and where valuable insight has been obtained from their use.

This analysis of robustness issues also highlights some of the reasons for the reluctance shown by industry in the past to adopt system identification methods for routine application.

Special recommendations are also presented in the tables for each aspect of the identification process. These provide a summary of the more detailed recommendations contained in each of the earlier sections of this chapter. It is believed that the presentation of robustness issues and corresponding tests in this way, together with these recommendations, can help to define a set of tools necessary for the successful application of system identification techniques for rotorcraft.

Acknowledgments

The author wishes to acknowledge the important contributions made by other members of the AGARD Flight Mechanics Panel Working Group WG-18 in the course of discussions of robustness issues at their meetings. The author wishes to record his particular thanks to Dr. G.D. Padfield for his assistance and for the many valuable suggestions made by him during the preparation of this paper.

References

Black, Colin G:
A Users' Guide to the Bayesian Nonlinear System Identification Program: KINEMOD.
University of Glasgow, Department of Aerospace Engineering, Internal Report, February 1989.

Black, C.G. and Murray-Smith, D.J.:
A Frequency-Domain System Identification Approach to Helicopter Flight Mechanics Model Validation.
Vertica, Vol.13, pp 343-368, 1989.

DuVal, R.W., Wang, J.C. and Demiroz, M.Y.:
A Practical Approach to Rotorcraft Systems Identification.
39th AHS National Forum, St. Louis, May 1983.

Iliff, K.W.:
Aircraft Identification Experience.
AGARD-LS-104, Paper 6, 1979.

Kaletka, J.:
Rotorcraft Identification Experience.
AGARD-LS-104, Paper 7, 1979.

Klein, V.:
Identification Evaluation Methods.
AGARD-LS-104, Paper 2, 1979.

Leith, D. and Murray-Smith, D.J.:
Experience with Multi-Step Test Inputs for Helicopter Parameter Identification. Vertica, Vol.13, No.3, pp. 403-412, 1989.

Murray-Smith, D.J. and Padfield, G.D.:
AGARD-LS-178, Paper No.2, 1991.

Padfield, G.D.:
Flight Testing for Performance and Flying Qualities.
AGARD-LS-139, 1985.

Padfield, G.D., Thorne, R., Murray-Smith, D., Black, C. and Caldwell, A.E.:
U.K. Research into System Identification for Helicopter Flight Mechanics.
Vertica, Vol.11, pp 665-684, 1987.

Plaetschke, E and Schulz, G.:
Practical Input Signal Design.
AGARD-LSP-104, Paper 3, 1979.

Turner, G.P.:
Consistency Analysis of Helicopter Flight Test Data.
RAE Technical Memorandum (to be published) 1991

Tables

Robustness Conditions	Robustness Tests	Special Recommendations
Precision and repeatability of initial conditions	Analysis of mean and standard deviation of all channels prior to control input	The experimental design process should incorporate a preliminary flight test to categorise the dynamic system, including sensors, actuators, control system and airframe. Results from this test should guide the design of optimal test inputs for system identification and should influence the choice of model structure
Repeatability of selected test inputs	Repetition of flight tests and analysis of differences between responses	
Linearity	Repetition of flight tests using different amplitudes and directions of test signals Examination of amplitude distribution functions	
Low correlation between control inputs and between states	Correlation analysis of records	
Frequency content of test input in relation to modelling requirement	Spectral analysis of records	

Table 1 Robustness Aspect of the Experimental Design

Robustness Conditions	Robustness Tests	Special Recommendations
Susceptibility of method to measurement noise	Examination of theoretical properties of the method Results obtained from application of method to simulated response data with added noise	Identification tools must incorporate a full and well engineered user interface exploiting maximum use of simple graphics. The tools should provide information on goodness of fit, confidence intervals, sensitivity to changes in test condition and model structure, etc
Susceptibility of method to process noise	Examination of theoretical properties of the method Results obtained from application of method to simulated response data	

Table 2 Robustness Aspect of the Identification Technique

Robustness Conditions	Robustness Tests	Special Recommendations
Suitability of initial choice of model structure	Application of R^2 and F-ratio tests in stepwise regression procedure	More emphasis must be given to establishing a valid model structure before proceeding to the parameter estimation stage. Reliable tools for the assessment of model structure are required
Suitability of model transfer function order	Examination of residuals in frequency domain	
Presence of significant unmodelled dynamics	Examination of residuals Examination of effects of introducing pure time delay	

Table 3 Robustness Aspect of the Identified Model Structure

Robustness Conditions	Robustness Tests	Special Recommendations
Range of parameter estimates found from different tests	Examination of variance values provided by the chosen estimation method. Examination of residuals to establish whether they show white noise properties (e g by autocorrelation analysis).	Estimated parameters should show low sensitivity to record length in both the frequency domain and time domain
Dependence of estimates on record length	Repeat estimation process for a variety of different record lengths	
Dependence of estimates on frequency range used for estimation	Repeat estimation process using frequency domain approach for a number of different frequency ranges	

Table 4 Robustness Aspect of the Estimated Parameters

Robustness Conditions	Robustness Tests	Special Recommendations
Overall adequacy of estimated model structure and parameters	Examination of residuals	Design criteria are needed for verification inputs to establish model properties in terms of distortion of: 1) Model responses when subjected to verification input 2) Model parameters for verification inputs
Model distortion effects when used with verification inputs	Analysis of flight test data for verification inputs	

Table 5 Robustness Aspect of the Resulting Mathematical Model

Assessment of Rotorcraft System Identification as Applied to the AH-64

D. Banerjee and J.W. Harding
McDonnell Douglas Helicopter Company
Mesa, Arizona

1. Abstract

Flight test data from the U.S. Army/McDonnell Douglas AH-64 Apache attack helicopter was provided to the AGARD FMP Working Group 18 (WG-18) on Rotorcraft System Identification. Results from the application of system identification techniques on the data by several members are compared. The data are processed by the WG members to assure consistency and remove identified measurement biases. Various time-domain identification procedures ranging from linear regression to maximum likelihood are used to identify coupled six degree-of-freedom rigid body models. Stability and control derivative estimates and model eigenvalues are compared. Diagonal terms in the models are consistently identified while coupling derivative estimates vary widely. Eigenvalues associated with the slower modes (phugoid and spiral) are not consistently identified due to the limited 12 second record length of the available data. Roll convergence and Dutch roll modes are consistent between the models. All the models do a good job of predicting primary axis response, however, improved correlation is achieved by eliminating insensitive stability and control derivatives from the parameter sets.

WG-18 members contributing to the AH-64 identification include: McDonnell Douglas Helicopter Company (MDHC), National Aeronautical Establishment (NAE), Deutsche Forschungsanstalt für Luft- und Raumfahrt (DLR), Nationaal Lucht- en Ruimtevaarlaboratorium (NLR), and the U.S. Army Aeroflightdynamics Directorate (AFDD).

2. Notation

a_x	Longitudinal acceleration, m/s^2
a_y	Lateral acceleration, m/s^2
a_z	Normal acceleration, m/s^2
I_x	x-axis body moment of inertia
I_y	y-axis body moment of inertia
I_z	z-axis body moment of inertia
I_{xz}	Body product of inertia
L	x-axis aerodynamic moment
m	Mass
M	y-axis aerodynamic moment
N	z-axis aerodynamic moment
p	Body roll rate, rad/s
q	Body pitch rate, rad/s
r	Body yaw rate, rad/s
u	x-axis velocity, m/s
v	y-axis velocity, m/s
V	Total velocity, m/s
w	z-axis velocity, m/s
X	x-axis aerodynamic force
Y	y-axis aerodynamic force
Z	z-axis aerodynamic force
α	Angle of attack
β	Sideslip angle
δ_x	Longitudinal cyclic control, %
δ_y	Lateral cyclic control, %
δ_p	Pedal control, %
δ_o	Collective control, %
θ	Pitch attitude, rad
τ_x	Longitudinal control time delay, sec
τ_y	Lateral control time delay, sec
τ_p	Pedal control time delay, sec
τ_o	Collective control time delay, sec
ϕ	Roll attitude, rad
ψ	Yaw attitude, rad

3. Introduction

System identification can best be described as the determination of system characteristics from measured data. In flight dynamics, system identification can be used as a means of correlating theory and experiment and is often applied to handling qualities analysis, model validation, and flight control law development. Practical use of these techniques in the rotorcraft industry is hampered by the complex dynamics and severe flight test measurement requirement associated with helicopters. In recent years as these problems are overcome, development of system identification techniques for rotorcraft flight dynamic analysis

has increased. The ultimate goal of such developments for industry is to decrease design costs by reducing the necessary flight testing and re-design for aircraft not performing as designed.

AGARD WG-18 on Rotorcraft System Identification was established in 1987 to evaluate the strengths and weaknesses of different identification approaches and to develop guidelines for the application of identification techniques to rotorcraft design and development. The AH-64 data base was selected as one of three common data bases for investigating different identification methods. Several members worked with the data to identify AH-64 dynamic characteristics. Results from the contributing members are presented in this paper.

4. Flight Testing and Data Evaluation

AH-64 flight test data was provided to WG-18 from an existing data base. The AH-64 aircraft was flown in 1984 in a series of tests for the purpose of transfer function evaluation. These tests were designed to obtain aircraft responses to doublet, pulse, and frequency sweep type inputs in each control axis (longitudinal, lateral, directional, and collective). Table 1 lists the AH-64 maneuvers from the 1984 transfer function tests used by the Working Group. Files 1 through 11 contain doublet and pulse runs suitable for time domain identification. Maneuvers were performed open-loop at a flight condition of 130 knots. Two half-inch doublets starting in opposite directions are included for each control axis. Pulses for both forward and aft longitudinal control and right lateral control are also included.

Control inputs for the 130 knot frequency sweep maneuvers in files 12 through 21 were produced by a specially designed Gold Oscillator Box (GOB). The GOB commands sinusoidal frequency sweeps in two ranges from .1 to 3 Hz and from .3 to 13 Hz in one minute sweeps. A typical two minute run consists of a sweep up to the high frequency and then back down to the starting frequency. A modified Stability Augmentation System (SAS) was used to stabilize the off axes during the sweeps. The primary axes remain open-loop and are stabilized by the pilot.

Flight test measurements for the AH-64, schematic diagram shown in figure 1, were recorded on board the aircraft and telemetered to the ground station for backup recording/filtering and on-line monitoring. Table 2 lists the measurements provided for the AH-64 records. The filter cutoff frequencies listed are the -3dB bandwidth frequencies.

A strap down sensor package near the center of gravity provides body angular rates, angular accelerations, and linear accelerations. Body angular accelerations $(\dot{p}, \dot{q}, \dot{r})$ are measured independently from the angular rates (p, q, r). Euler angles (ϕ, θ, ψ) and Euler rates $(\dot{\phi}, \dot{\theta}, \dot{\psi})$ are provided by the Heading Attitude Reference System (HARS). Euler rates are computed signals within HARS based on the Euler angles. Control positions were taken at the actuators and not the pilot stick or pedals thus eliminating uncertainty in control linkage and actuator dynamics.

Data requirements for system identification are much more stringent than for more common handling qualities analysis or model validation. Issues such as record length, response amplitude, off-axis inputs, measurement accuracy and wind conditions have strong effects on system identification results. For this reason, WG members spent considerable time evaluating the AH-64 data base. Consistency between the measurements was established but several undesirable data characteristics exist. For time-domain identification (files 1-11), the following concerns were recognised:

- Short record length (12 seconds): Parameters associated with long period aircraft modes such as the phugoid, which has a period of about 20 seconds for the AH-64, cannot be adequately identified from short duration records.
- Large amplitude response: Linear models of rotorcraft are appropriate for predicting small amplitude response only. The change in body attitudes were as large as 20 to 30 degrees for both longitudinal and lateral doublets.
- Noisy acceleration measurements: Accelerations had low signal-to-noise ratios due to 4/rev vibrations.
- Quantization errors in Euler angles: Quantization errors were introduced due to the large ranges used when recording Euler angle measurements.

The frequency sweeps (files 12-21) contained some of the same problems above but was not acceptable for frequency-domain identification due to the limited SCAS activity. Sweeps were flown open-loop in the primary axis and closed-loop in the off axes resulting in a high level of correlation among the control inputs, which precludes identification of off axis responses. In addition there was inadequate low frequency content which precludes the identification of the low frequency (speed) derivatives.

The problems above demonstrate the difficulty in using existing data bases for parameter identification. Dedicated flight testing is necessary which takes into account the specific data requirements associated with these techniques. This inhibits industry application of such techniques since dedicated handling qualities testing for system identification is expensive and considered low priority compared to other required testing such as structural loads tests. To date, most data

bases suitable for this work come from research or government sponsored activities.

Data consistency checks were performed by each of the WG members to establish the quality of the recorded measurements. A brief description of the techniques used by each member is provided.

MDHC used several methods beginning with simple comparisons between redundant sensors. The limited data set reduces the availability of most redundant sensors except accelerations. Multiple acceleration measurements were available for the AH-64. Accelerations from the c.g. and the pilot seat (which were transferred to the c.g.) were compared and found to be consistent for several maneuvers. The only differences were small biases in the a_x and a_y signals. Since it could not be determined (at that stage in the consistency checks) which signal contained the bias, no action was taken.

Several comparisons between kinematically redundant sensors were carried out by MDHC (Harding and Bass [1]). The body angular accelerations $(\dot{p}, \dot{q}, \dot{r})$ were integrated and compared to body angular rates (p, q, r). Scale factors and biases identified using least squares are shown in figure 2. In addition, the compatibility between measured body rates (p, q, r) and the attitudes and Euler rates from the Heading Attitude Reference System (HARS) was checked using kinematic relations. Finally, the Euler angles were reconstructed from integrated Euler rates to eliminate quantization errors.

The final phase in data consistency checks was the use of an Extended Kalman Filter/Smoother. The algorithm, as presented by Du Val et al. [2], is derived by posing an optimization problem to find the time histories of the vehicle states that are consistent with both a prescribed dynamic model and available measurements. This method assures data consistency, reduces the effects of measurement noise on the state estimates, and can provide estimates of unmeasured states.

MDHC applied the Extended Kalman Filter/ Smoother to files 1-8. The data was initially sampled at 25 Hz. Measurements used in the reconstruction include: ϕ, θ, ψ, p, q, r, u, v, w, a_x, a_y, and a_z. Processing included a zero phase shift, lowpass filter with a cutoff frequency of 3 Hz after the Kalman filter.

Results from the Kalman filter state estimation for the doublet maneuvers indicated that the angular measurements ϕ, θ, ψ, p, q, and r were generally very good. A bias of about .01 rad/s was identified in the pitch rate signal. Also, the longitudinal acceleration signal had a bias of roughly 2.1 m/s^2. This bias was apparently caused by the accelerometers being calibrated with the helicopter on the ground at a 5 degree nose-up attitude.

NAE performed Consistency checks on files 1-8. The data was initially lowpass filtered with a Butterworth fourth-order zero phase shift filter with a cutoff frequency of 4 Hz. Spectral analysis had revealed considerable excitation at 19 Hz (blade passage frequency). After lowpass filtering, the data was sampled at 20 Hz, excluding the first and last 50 points.

Biases in the data were estimated with a least squares method. The measurements used were: $\dot{\phi}$, $\dot{\theta}$, $\dot{\psi}$, u, v, w, a_x, a_y, a_z, p, q, r, ϕ, θ, and ψ. The least squares procedure is outlined below:

- Integrate Euler rates with measured Euler angle initial conditions and use least squares to determine the 6 biases for the measured attitudes and rates.
- The corrected Euler angles and rates are used in the angular kinematic equations to determine biases in the body angular rates.
- The corrected body angular rates and attitudes enter the translational kinematic equations for determination of biases in the velocities and translational accelerations.

Statistics for the bias estimates indicated the a_x, p, and q biases had small variances with respect to their mean values. These biases were estimated as 2.21 m/s^2, .0025 rad/s, and .011 rad/s respectively.

DLR completed consistency checks on each of the doublet input maneuvers in files 1-8 and also on the concatenation of all the maneuvers. A nonlinear maximum likelihood program was used to estimate scale factors for u, v, w, ϕ, θ, ψ and biases for a_x, a_y, a_z, p, q, and r. The scale factor effects were not large enough to warrant correcting the data, so the data was only altered by removing biases. Biases for a_x, p, and q were identified as 2.26 m/s^2, .0025 rad/s, and .011 rad/s respectively which is comparable with values identified by other members.

NLR initially tried to perform compatibility checks using a linear output error program. However, the bias estimates from the linear program varied considerably between maneuver files. NLR believes the poor results were due to the large pitch and roll excursions, which cannot be adequately represented by the linear kinematics formulation.

NLR therefore adopted an output error program which uses the nonlinear kinematic equations to estimate measurement biases. This technique was applied separately to each maneuver file to estimate the biases in the acceleration measurements and in the body angular rate measurements. The bias estimates obtained from the nonlinear output error program proved to be relatively constant.

The bias estimate for a_x was consistently large with

a mean value of 2.15 m/s^2 indicating the longitudinal accelerometer calibration error. NLR also noted that the a_x time history was very noisy, making it difficult to judge whether the signal was valid. Other biases include a bias on p of .0032 rad/s and a bias on q of .011 rad/s. Data preprocessing consisted of sampling the data at 20 Hz with no filtering.

The AFDD performed consistency checks on all the files. The data was initially lowpass filtered with a four-pole, zero phase shift digital filter supplying a 6dB attenuation at 3 Hz. Analysis was performed at the full sample rate of 100 Hz for the first 11 files, while files 12–21 were decimated to 20 Hz for analysis.

The AFDD used the state estimation program SMACK (Bach [3]) to estimate biases and scale factors. Measurements used in the estimation were ϕ, θ, ψ, p, q, r, V, α, β, a_x, a_y, and a_z. Euler angles and body angular rates were used as measurements in an initial check of angular consistency and were also estimated in this check. Errors on Euler angles were not estimated because of the high reliability of the HARS system from which Euler angle and rate measurements were obtained.

All of the measurements were used in a final 6 DOF check. Biases and scale factors estimated in the angular check were used along with their program-estimated covariances as start-up values in the 6 DOF check. Measurements were also estimated as were angular accelerations in this final check. Biases were assumed to be on a_x and a_y rather than ϕ and θ because of high confidence in HARS data.

Statistics for files 1–11 show biases on a_x, p, and q to have small variances with respect to their mean values, justifying their retention in the error model. These biases were identified as 2.02 m/s^2, .0021 rad/s, and .011 rad/s respectively. The statistics indicated that all error parameters identified for the sweep maneuvers including biases on a_x, a_y, a_z, p, q and r, with the exception of the bias on p for files 20–21, were significant.

5. Model Structure

The model which has been used by WG members investigating the AH-64 is a coupled 6 DOF rigid body model with time delays in the controls. Equations 1–6 are the 6 DOF nonlinear rigid body equations of motion, and equation 7 is the Euler angle relationship between the body-fixed axis system and the vehicle-carried axis system. The rotational equations 4–6 have been simplified by assuming that the aircraft is symmetric about the x-z body axes (vertical plane of symmetry). Representing the changes about the trim condition in the aerodynamic specific forces and moments as linear functions of the aircraft states, the equations of motion reduce to equation 8.

The first and second terms on the right side of this equation are the perturbation accelerations due to aerodynamic forces and moments. The third term, sometimes called the aerodynamic biases, represents the steady state aerodynamic specific forces and moments acting on the aircraft plus the initial aircraft accelerations. The fourth term contains the gravity effects, and the fifth term is the centrifugal specific forces which arise because the body axes represent a moving reference frame.

$$
\begin{aligned}
X &= m(\dot{u} + g\sin\theta + qw - rv) && (1)\\
Y &= m(\dot{v} - g\cos\theta\sin\phi + ru - pw) && (2)\\
Z &= m(\dot{w} - g\cos\theta\cos\phi + pv - qu) && (3)\\
L &= I_x\dot{p} - I_{xz}(\dot{r} + pq) - (I_y - I_z)qr && (4)\\
M &= I_y\dot{q} - I_{xz}(r^2 + p^2) - (I_z - I_x)rp && (5)\\
N &= I_z\dot{r} - I_{xz}(\dot{p} - qr) - (I_x - I_y)pq && (6)
\end{aligned}
$$

$$
\begin{bmatrix} \dot{\phi} \\ \dot{\theta} \\ \dot{\psi} \end{bmatrix} = \begin{bmatrix} 1 & \sin\phi\tan\theta & \cos\phi\tan\theta \\ 0 & \cos\phi & -\sin\phi \\ 0 & \sin\phi\sec\theta & \cos\phi\sec\theta \end{bmatrix} \begin{bmatrix} p \\ q \\ r \end{bmatrix} \quad (7)
$$

$$
\begin{bmatrix} \dot{u} \\ \dot{v} \\ \dot{w} \\ \dot{p} \\ \dot{q} \\ \dot{r} \end{bmatrix} = \begin{bmatrix} X_u & X_v & X_w & X_p & X_q & X_r \\ Y_u & Y_v & Y_w & Y_p & Y_q & Y_r \\ Z_u & Z_v & Z_w & Z_p & Z_q & Z_r \\ L_u & L_v & L_w & L_p & L_q & L_r \\ M_u & M_v & M_w & M_p & M_q & M_r \\ N_u & N_v & N_w & N_p & N_q & N_r \end{bmatrix} \begin{bmatrix} u \\ v \\ w \\ p \\ q \\ r \end{bmatrix} +
$$

$$
\begin{bmatrix} X_{\delta o} & X_{\delta x} & X_{\delta y} & X_{\delta p} \\ Y_{\delta o} & Y_{\delta x} & Y_{\delta y} & Y_{\delta p} \\ Z_{\delta o} & Z_{\delta x} & Z_{\delta y} & Z_{\delta p} \\ L_{\delta o} & L_{\delta x} & L_{\delta y} & L_{\delta p} \\ M_{\delta o} & M_{\delta x} & M_{\delta y} & M_{\delta p} \\ N_{\delta o} & N_{\delta x} & N_{\delta y} & N_{\delta p} \end{bmatrix} \begin{bmatrix} \delta_o(t - \tau_o) \\ \delta_x(t - \tau_x) \\ \delta_y(t - \tau_y) \\ \delta_p(t - \tau_p) \end{bmatrix} +
$$

$$
\begin{bmatrix} a_{xo} \\ a_{yo} \\ a_{zo} \\ \dot{p}_o \\ \dot{q}_o \\ \dot{r}_o \end{bmatrix} + \begin{bmatrix} -g\sin\theta \\ g\cos\theta\sin\phi \\ g\cos\theta\cos\phi \\ 0 \\ 0 \\ 0 \end{bmatrix} + \begin{bmatrix} rv - qw \\ pw - ru \\ qu - pv \\ 0 \\ 0 \\ 0 \end{bmatrix} \quad (8)
$$

Equation 8 is the basic model structure used in the identification procedure by all members working with the time domain AH-64 data. During the parameter estimation process, the nonlinear gravity and centrifugal terms can be calculated directly from the flight data, or calculated from the simulated response data. The stability and control derivatives, aerodynamic biases and measurement biases are estimated.

Estimating the aerodynamic biases would not be necessary if the aircraft initiated each maneuver from an unaccelerated flight condition and the trim conditions of the aircraft were exactly known. In this case, the aerodynamic biases would be simply the steady state aerodynamic specific forces given by equation 9. In practice, however, the aircraft is not in steady flight at the beginning of the maneuver and the trim conditions are not exactly known. Therefore, the estimation of the aerodynamic biases is important in obtaining good results.

$$\begin{bmatrix} a_{xo} \\ a_{yo} \\ a_{zo} \\ \dot{p}_o \\ \dot{q}_o \\ \dot{r}_o \end{bmatrix} = \begin{bmatrix} gsin\theta_0 \\ -gcos\theta_0 sin\phi_0 \\ -gcos\theta_0 cos\phi_0 \\ 0 \\ 0 \\ 0 \end{bmatrix} \tag{9}$$

Additionally, a bias term can be added to the measurement equation and a bias identified for each measurement. Although estimation of both aerodynamic and measurement biases is a standard practice, care must be taken to ensure that the aerodynamic and measurement biases are independent or identifiability problems will result.

A further simplification in the model involves linearising the gravity and centrifugal force terms along with the Euler angle kinematics to yield a complete eight state linear model. This model formulation was not used during the parameter estimation step because the linearized approximations to the gravity, centrifugal force terms, and Euler angle equations will introduce errors in the aerodynamic derivative estimates.

Identification Method

Several different parameter estimation procedures were applied to the AH-64 data. Most of the members used time domain techniques ranging from linear regression to Maximum Likelihood (ML). The AFDD used a frequency domain approach. Because of problems with the frequency sweep data, AFDD was only able to estimate a few control derivatives and time delays. This section describes the estimation techniques applied to the AH-64 data by different WG members.

MDHC used a time domain output error method to estimate a model from files 1, 3, 5, and 7. The output error program iteratively adjusts the model parameter values to minimize the sum of squared weighted errors between measured and simulated responses. Minimization is based on an IMSL finite difference Levenberg-Marquardt algorithm (ZXSSQ) which solves a nonlinear least squares problem. The output error program can accommodate multiple maneuver time histories during a single run. Usually four maneuvers (one for each control axis) are used simultaneously so that all derivatives can be estimated during a single run. In addition to estimating the aerodynamic derivatives, MDHC estimated the initial state derivatives (aerodynamic biases). The outputs from the simulation which were compared with the measurements to form the error (cost function) were u, v, w, a_x, a_y, a_z, p, q, and r.

Because MDHC was unable to identify consistent control time delays from files 1–11, no time delays were used during the identification. However, the discrete-time simulation in the output error program introduces a delay in the simulated outputs of one-half the sample interval or .020 seconds.

The cost function J minimized by the output error program is given by equation 10, where y is the measured response, $\hat{y}$ is the simulated response, W is a diagonal weighting matrix, and the subscript i represents the time index.

$$J = \sum_{i=1}^{N} [y_i - \hat{y}_i]^T \, W^{-1} \, [y_i - \hat{y}_i] \tag{10}$$

The weighting matrix was used simply as a homogeneity factor to account for the different magnitudes of the different measurements. To make all measurements influence the cost function roughly equally, the diagonal elements of W were set equal to the root-mean-square of the perturbation values of the measurement sequences over all maneuver files used for identification (equation 11).

$$W = diag\left[\frac{1}{N}\sum_{i=1}^{N} [y_i - y_0] \, [y_i - y_0]^T\right] \tag{11}$$

where y_0 is the mean value.

NAE's model was estimated using the concatenated data files 1, 3, 5, and 7. Starting with the reconstructed data, NAE first applied stepwise regression to find values for the parameters in the aerodynamic model, as well as estimates of the parameter variances. The regression values of the parameters were then used as starting values for the maximum likelihood algorithm MMLE-3 (Maine and Iliff [4,5]). The cost function and weighting matrix were similar to those in equations 10 and 11. The full set of parameters was identified with a time delay of .100 seconds applied to all the controls.

The measurements compared with the ML output to form the error were: u, v, w, p, q, r, a_x, a_y, and a_z. In addition to the aerodynamic derivatives, aerodynamic biases were estimated for each state equation of each maneuver file. Measurement biases were also estimated for each measurement equation of each maneuver file.

Three models were identified by DLR: one from files 1, 3, 5, and 7 (DLR-1), one from files 2, 4, 6, and 8 (DLR-2), and one from all eight files (DLR-3). A nonlinear ML program was used to estimate derivative values. The measurement vector included: a_x, a_y, a_z, p, q, r, ϕ, θ, $u, v, w, \dot{p}, \dot{q}$, and $\dot{r}$. The parameter covariance matrix provided by the ML program was used to eliminate insignificant model parameters, giving a reduced model order. During the identification procedure, the nonlinear kinematic and gravity terms were calculated from the model response data, and not from the actual measured flight data.

DLR usually estimates equivalent control time delays using the cross-correlation between input and response signals. For the AH-64 data, time delays were not calculated but were assumed to be .100 seconds on all controls which are the average value as identified in the frequency domain by AFDD.

NLR identified two models from two separate groups of data. Each group of data consisted of four doublet maneuvers representing inputs in each control axis. The first group included files 1, 3, 5, and 8 (NLR-1) and the second group files 2, 4, 6, and 7 (NLR-2). The following measurements were used during the identification: ϕ, θ, ψ, p, q, r, V,α, β, a_x, a_y, a_z, δ_o, δ_x, δ_y, δ_p. No filtering was performed on the flight data, and the data was sampled at 20 Hz.

NLR used a two step method. As a first step, all state variables are reconstructed as described in the data evaluation section. In the second step, the reconstructed variables and the measured control variables are used in a stepwise linear regression procedure to estimate parameter values.

Time delays of .100 seconds were applied to the four controls during the identification and verification process to account for time lags in the actual response. These delays were assumed as representative delays, and were not actually calculated from the data.

Because of the limitations of the AH-64 frequency-domain database, AFDD was only able to identify the high frequency control derivatives and time delays for the longitudinal and collective controls. The longitudinal cyclic parameters were obtained from multivariable frequency response matching of the 3 DOF longitudinal dynamics: q/δ_x, a_x/δ_x, w/δ_x, a_z/δ_x, and u/δ_x. The time delay associated with the longitudinal cyclic was estimated as .110 seconds.

The collective stick parameters were obtained from single-input/single-output transfer function model fitting of the collective frequency responses: q/δ_o, r/δ_o, and a_z/δ_o. Collective stick time delay, which was taken as an average from the q, r, and a_z responses, was .089 seconds. The average of all time delays is approximately .100 seconds which is the value used by NAE, DLR, and NLR.

6. Identification Results

Stability and control derivative estimates and the variance of these estimates (when available) are listed in Tables 3 and 4. Statistical analysis of the identified derivatives for each row of Tables 3 and 4 are given to show the identifiability of a particular derivative. Since it is not practical to discuss each derivative, a brief comparison of the primary derivatives associated with helicopter dynamics has been made.

Diagonal terms (X_u, Y_v, Z_w, L_p, M_q, and N_r) in the 6 DOF models were consistently identified by the members as evident by the low variances with respect to the mean values. Contrary to expectations, drag damping (X_u) is well identified despite the lack of significant speed data due to the short record length. The effects of time delays used in the identification process are evident in the pitch and roll damping terms L_p and M_q. Time domain identification results for the BO-105 obtained by the DLR (Kaletka [6]) show, for example, that the identified value of Lp is reduced by 25% when the time delays associated with the rotor and actuators are omitted from the model structure. This reduction in the value of damping derivatives occurs so that the 6 DOF model can match the extra phase lag associated with the higher-order dynamics. MDHC did not include the .100 sec time delay used by the other members; thus values for L_p and M_q are subsequently smaller than those obtained by NAE and DLR which did include the time delay.

The yaw damping derivative, N_r, is the least identifiable of the diagonal terms. Values from the DLR-1 and DLR-2 models using different records for identification vary from -.6071 to -.2457 unlike the other diagonal terms which are consistent between the two models. The verification time histories, discussed later, show good correlation for yaw response to directional inputs for all of the identified models. However, the yaw response to pitch inputs is poor on all the models leading to the possibility that airmass states associated with interactional aerodynamics are needed to uniquely model the yaw equation.

Dihedral effect (L_v) and directional stability (N_v) show good agreement between the various models. Coupling derivatives L_q and M_p are not easily identified since aircraft coupling is not strong. Less significant stability derivatives vary widely as might be expected. Time delays were identified by AFDD during frequency-response identification with the longitudinal and collective sweep data. Results are given in Table 3.

Control derivatives were identified and are shown in Table 4. Derivatives representing control power such as $M_{\delta x}$, $L_{\delta y}$, $N_{\delta p}$, and $Z_{\delta o}$ show reasonable agreement.

Eigenvalues for the identified models are presented in Tables 5 through 8. For comparison, eigenvalues de-

termined for the phugoid and Dutch roll modes from flight test are given in Table 9. These estimates were arrived at through visual inspection of flight data designed to excite the oscillatory modes.

The phugoid eigenvalues of the identified models are not consistent and do not agree well with the phugoid mode estimated from flight test data in Table 9. The speed derivatives Z_u and M_u directly effect the phugoid motion and are shown in Table 3 to vary greatly between the models. The 12 second record length limits the identification of these speed related derivatives and thus the phugoid mode which has a period of roughly 20 seconds. The limited data also effects the identifiability of the spiral mode which is a slow, lightly damped mode.

The roll convergence roots are close between the models as a result of the fairly consistent roll damping derivative L_p. The Dutch roll eigenvalues for most of the identified models agree with each other and with the values from Table 9 indicating that this motion is easily identified from the data. The important lateral stability derivatives associated with Dutch roll Y_v, L_v, N_v, and N_r are relatively consistent between the models.

Responses from the MDHC, NAE, and DLR-1 models identified from files 1, 3, 5, and 7 (controls shown in figure 3) are compared to the flight data used to generate the models. Angular rates are shown in figures 4–6. Each member used slightly different methods to calculate the model responses shown. MDHC linearised the nonlinear gravity and centrifugal force terms about the 130 knot flight condition and combined them with the identified stability and control derivatives to form an eight state linear model. This model was driven with the measured control inputs to generate the model response. To account for initial aircraft accelerations and control offsets, the aerodynamic biases (static force and moment offsets) which were estimated during the parameter identification step were used. The NAE model was driven with the measured control inputs, while the nonlinear gravity and centrifugal force terms were calculated based on reconstructed flight data representing a pseudo-control. Aerodynamic biases and measurement biases which were estimated during the parameter identification were used to account for untrimmed initial states. The DLR model was driven with the measured control inputs, and the nonlinear gravity and centrifugal force terms were calculated from the model response. Again, identified aerodynamic and measurement biases were used.

The identified models are considered acceptable in characterizing the helicopter response. The NAE model appears to show the best match with flight data however the close match may be a result of the response generation approach. The NAE identification procedure includes driving the model with the measured Euler angles and using reconstructed flight data to calculate the nonlinear gravity and centrifugal force terms (pseudo-controls). DLR used a similar ML identification procedure as NAE with the exception that the nonlinear gravity and centrifugal force terms were calculated from the model response instead of the reconstructed flight data. With this technique, the velocities and Euler angles are not exact, however comparisons of body angular rates between the NAE and DLR models and flight data are similar.

The MDHC model does not match the flight data as well as the other two models shown. Much of the discrepancies are attributed to use of linearized gravity and centrifugal force terms. Although the gravity and centrifugal force terms were calculated from reconstructed flight data during the identification they were linearised about the 130 knot flight condition and driven by the model response to create the simulated responses shown.

7. Model Verification

Model verification is performed by comparing identified model response to flight test data not used to generate the model. Figure 7 shows the control inputs for files 2, 4, 6, and 8. For these maneuvers, the angular rate responses of the MDHC, NAE, and DLR-1 models are compared in figures 8 through 10. The NLR-1 model response is compared to files 2, 4, 6, and 7 as shown in figure 11.

Again, MDHC used a different technique for generating the model response. The nonlinear gravity and centrifugal force terms were linearized about the 130 knot flight condition and combined with the identified stability and control derivatives to form an eight state linear model. The other three models were driven with the measured control inputs, while the nonlinear gravity and centrifugal force terms were calculated based on model outputs. On the whole, all of the models do a good job of predicting primary axis response. Careful analysis of the verification plots reveals certain characteristics which can be associated with the various identification procedures.

Both NAE and DLR used ML programs to identify the models, however the results show that the DLR model matches the flight data better. The differences between the two approaches include: 1) handling of nonlinear gravity and centrifugal force terms during identification; 2) the reduced order of the DLR model; and 3) the use of Euler angles and body angular accelerations by DLR in the measurement equations. NAE used pseudo-controls during identification while DLR used the model response to compute the nonlinear gravity and centrifugal force terms. MDHC also used the pseudo-control approach with output-error identification and achieved results similar to NAE.

In comparing the pitch rate responses, the DLR and NLR models show better correlation than MDHC and NAE. The distinguishing feature of the DLR and NLR models is the use of a reduced model structure. Other common factors include a .10 second time delay on controls and the use of ϕ and θ in the measurement equations. The use of time delays on the controls does not appear significant in the verification in this case since MDHC did not use time delays and achieved very similar results as NAE which applied a .10 second delay on all controls. It should be noted that NLR used a stepwise linear regression procedure to estimate parameter values while DLR used a ML method. The reduced model order is likely the reason for the improved longitudinal response prediction.

With identification algorithms ranging from stepwise linear regression to ML each member achieved a certain degree of success with time-domain identification. It is clear that the distinguishing factor between the methods lies in the details of problem set up and data processing rather than the algorithm. An important step in the identification was the estimation of aerodynamic biases to account for residual accelerations at the beginning of each maneuver. Although each member included the aerodynamic biases of equation 8 in their parameter sets, attempts to identify models in which the aerodynamic biases were calculated from equation 9 resulted in less accurate models.

Another important consideration is the treatment of nonlinear gravity and centrifugal force terms. These terms should not be linearized in the identification process to avoid introducing errors in the aerodynamic derivative estimates. They can be linearized to simplify model simulation during verification at the expense of accuracy for large amplitude maneuvers. The final consideration is reducing the parameter set through model structure determination techniques. DLR and NLR eliminated insensitive derivatives from the parameter sets and achieved improved results over MDHC and NAE which identified all of the aerodynamic derivatives from equation 8.

8. Conclusions

The models identified by WG members using several different techniques all predict the aircraft response with reasonable accuracy. Critical to the success of system identification are flight test data quality and content. Data must be evaluated for consistency to assure correct response identification. Data content is important as demonstrated by the problems in identifying the phugoid mode. Long period modes can not be identified accurately without low frequency data (long record lengths). Considering the different aspects of the overall identification processes used by the members, it is difficult to assess the impact of any one procedure on the final results. The unique features of the DLR and NLR models which showed better results, especially in longitudinal response, were the use of attitude measurements in the error equations and reduced parameter sets. In the end, identification of helicopter models from flight test data can be achieved using a variety of the techniques with acceptable accuracy.

Acknowledgements

This paper contains results provided by several WG members whose contributions are greatly appreciated. The authors would also like to thank Mr. Charles Gardner for his significant contribution to the WG effort.

References

[1] Harding, J.W. and Bass, S.M.: Validation of a Flight Simulation Model of the AH-64 Apache Attack Helicopter Against Flight Test Data. 46th Annual Forum of the American Helicopter Society, Washington, D.C., 1990.

[2] Du Val, R.W.; Bruhis, O.; Harrison, J.M.; and Harding, J.W.: Flight Simulation Model Validation Procedure, A Systematic Approach. Vertica, Vol. 13, No. 3, 1989.

[3] Bach, R.E. Jr.: State Estimation Applications in Aircraft Flight Data Analysis (A User's Manual for SMACK). NASA Ames Research Center, May 1988.

[4] Maine, R.E. and Iliff, K.W.: Users' Manual for MMLE3, A General Fortran Program for Maximum Likelihood Parameter Estimation. NASA TP1563, 1980.

[5] Maine, R.E. and Iliff, K.W.: Programmers' Manual for MMLE3, A General Fortran Program for Maximum Likelihood Parameter Estimation. NASA TP1690, 1981.

[6] Kaletka, J.; von Grunhagen, W.; Tischler, M.B.; and Fletcher, J.W.: Time and Frequency-Domain Identification and Verification of BO-105 Dynamic Models. 15th European Rotorcraft Forum, Amsterdam, The Netherlands, 1989.

Table 1: AH-64 Maneuvers at 130 Knots

File No.	Test/TS	Maneuver Title	G.W. (kg)	Time (sec)
1	883/03	Doublet Fwd-Aft (Long)	6692	12.0
2	883/04	Doublet Aft-Fwd (Long)	6692	12.0
3	883/05	Doublet Left-Right (Lat)	6692	12.0
4	883/06	Doublet Right-Left (Lat)	6692	12.0
5	883/07	Doublet Left-Right (Dir)	6692	12.0
6	883/08	Doublet Right-Left (Dir)	6692	12.0
7	883/09	Doublet Up-Down (Coll)	6692	12.0
8	883/10	Doublet Down-Up (Coll)	6692	12.0
9	883/11	Pulse Fwd (Long)	6692	12.0
10	883/12	Pulse Aft (Long)	6692	12.0
11	883/14	Pulse Right (Lat)	6692	12.0
12	884/03	Long. Freq. Sweep .1 to 3 Hz	6692	158.0
13	884/05	Long. Freq. Sweep .1 to 3 Hz	6692	138.0
14	884/06	Long. Freq. Sweep .1 to 3 Hz	6692	114.0
15	888/06	Lat. Freq. Sweep .1 to 3 Hz	6590	127.0
16	888/07	Lat. Freq. Sweep .1 to 3 Hz	6590	138.0
17	888/09	Lat. Freq. Sweep .3 to 13 Hz	6590	138.0
18	889/04	Dir. Freq. Sweep .1 to 3 Hz	6590	118.0
19	889/10	Dir. Freq. Sweep .1 to 3 Hz	6590	141.0
20	890/04	Coll. Freq. Sweep .1 to 3 Hz	6590	140.0
21	890/06	Coll. Freq. Sweep .3 to 13 Hz	6590	131.0

Table 2: List of Measurements for the AH-64

Meas. No.	Description	Units (sense)	Filter Cutoff Freq. (Hz)
2183	Boom Total Airspeed, V *	knots (+ fwd)	0 to 6
5295	Pilot Seat Lateral Accel, a_{yp}	G's (+ rt)	0 to 50
5342	Pilot Seat Vertical Accel, a_{zp}	G's (+ up)	0 to 50
5661	Pilot Seat Long Accel, a_{xp}	G's (+ fwd)	0 to 50
6001	Roll Rate, p †	deg/sec (+ rt down)	0 to 6
6002	Pitch Rate, q †	deg/sec (+ nose up)	0 to 6
6003	Yaw Rate, r †	deg/sec (+ nose rt)	0 to 6
6004	Pitch Angular Accel, $\dot{q}$ †	deg/sec^2(+ nose up)	0 to 6
6005	Roll Angular Accel, $\dot{p}$ †	deg/sec^2(+ rt down)	0 to 6
6006	Yaw Angular Accel, $\dot{r}$ †	deg/sec^2(+ nose rt)	0 to 6
6007	CG Vertical Accel, a_z †	G's (+ up)	0 to 6
6008	CG Lateral Accel, a_y †	G's (+ rt)	0 to 6
6009	CG Longitudinal Accel, a_x †	G's (+ fwd)	0 to 6
6010	Euler Roll Rate, $\dot{\phi}$ ‡	deg/sec (+ rt down)	0 to 50
6011	Euler Pitch Rate, $\dot{\theta}$ ‡	deg/sec (+ nose up)	0 to 50
6012	Euler Yaw Rate, $\dot{\psi}$ ‡	deg/sec (+ nose rt)	0 to 50
6046	Vertical Velocity, w ‡	ft/sec (+ up)	0 to 5
9019	Angle of Attack, α *	deg (+ nose up)	0 to 6
9020	Sideslip Angle, β *	deg (+ nose left)	0 to 6
9021	Roll Attitude, ϕ ‡	deg (+ rt down)	0 to 6
9022	Pitch Attitude, θ ‡	deg (+ nose up)	0 to 6
9023	Yaw Attitude, ψ ‡	deg (+ nose rt)	0 to 6
9031	Coll. Actuator Position, δ_o	percent (+ up)	0 to 50
9032	Pitch Actuator Position, δ_x	percent (+ stk aft)	0 to 50
9033	Roll Actuator Position, δ_y	percent (+ stk rt)	0 to 50
9034	Yaw Actuator Position, δ_p	percent (+ rt)	0 to 50
9217	X Doppler Velocity, u	ft/sec (+ fwd)	0 to 6
9218	Y Doppler Velocity, v	ft/sec (+ rt)	0 to 6

* Boom System: Sta -10.0, BL -25.0, WL 127.0 (in)
† C.G. Sensor Package: Sta 194.0, BL 3.1, WL 142.5 (in)
‡ Heading Attitude Reference System (HARS): Sta 333.4, BL 12.1, WL 104.9 (in)

Table 3: AH-64 Stability Derivative Estimates

Derivative	MDHC	NAE (CRB)	DLR1 (SD)	DLR2 (SD)	DLR3 (SD)	NLR1 (SD)	NLR2 (SD)	mean SD
X_u	-.0036	-.02499 (.00074)	-.02235 (.00113)	-.02929 (.00056)	-.02726 (.00044)	-.0291 (.0041)	-.0335 (.0065)	-.0243 .0098
X_v	-.011	.01727 (.00134)						.0031 .0200
X_w	.034	.01188 (.00089)	.01528 (.00087)	.02231 (.00100)	.02004 (.00060)	-.0252 (.0022)	-.0337 (.0027)	.0064 .0255
X_p	-.524	.3322 (.0388)						-.0959 .6054
X_q	-.804	.03447 (.05973)						-.3848 .5929
X_r	-.332	-.2861 (.0304)						-.3091 .0325
Y_u	-.018	-.01717 (.00110)						-.0176 .0006
Y_v	-.099	-.1136 (.00212)	-.1414 (.00422)	-.1220 (.00262)	-.1249 (.00222)	-.0884 (.0141)	-.1086 (.0098)	-.1140 .0175
Y_w	.039	.02411 (.00163)						.0316 .0105
Y_p	-.254	-.5478 (.06522)	-1.011 (.1068)	-.1952 (.06880)	-.4693 (.05728)			-.4955 .3231
Y_q	-2.70	-2.005 (.1086)						-2.353 .4914
Y_r	.575	1.050 (.05253)	-.010 (.0928)	-.490 (.07262)	-.410 (.05645)	.2675 (.6190)	.3211 (.4036)	.1862 .5436
Z_u	.021	-.01598 (.00618)	.06344 (.00686)	.02609 (.00254)	.02662 (.00250)	.0650 (.0179)	-.2315 (.0332)	-.0065 .1030
Z_v	.060	.01747 (.0100)						.0387 .0301
Z_w	-.416	-.4143 (.00806)	-.5471 (.00566)	-.5060 (00563)	-.5282 (.00411)	-.6406 (.0101)	-.3964 (.0133)	-.4927 .0890
Z_p	.394	-1.192 (.3002)						-.3990 1.1215
Z_q	-15.2	-11.84 (.5276)	-7.01 (.3977)	-4.12 (.2957)	-5.60 (.2512)			-8.754 4.6243
Z_r	1.83	1.259 (.2590)						1.5445 .4038
L_u	-.029	-.03236 (.00129)	-.01997 (.00099)	-.00298 (.00023)	-.00960 (.00025)	-.0161 (.0026)	-.0124 (.0045)	-.0175 .0105
L_v	-.098	-.1046 (.00212)	-.1225 (.00274)	-.1186 (.00129)	-.1062 (.00125)	-.0874 (.0045)	-.0731 (.0030)	-.1015 .0172
L_w	.034	.04027 (.00172)	.01409 (.00167)	.01810 (.00112)	.02973 (.00102)	-.0004 (.0039)	.0088 (.0026)	.0207 .0146

Table 3 (cont.): AH-64 Stability Derivative Estimates

Derivative	MDHC	NAE (CRB)	DLR1 (SD)	DLR2 (SD)	DLR3 (SD)	NLR1 (SD)	NLR2 (SD)	AFDD (CRB)	mean SD
L_p	-2.78	-3.189 (.06496)	-3.637 (.07916)	-3.243 (.03962)	-3.216 (.04130)	-2.073 (.1330)	-1.956 (.1108)		-2.871 .6361
L_q	-.21	-.3659 (.1103)	.7190 (.1103)	.03991 (.06682)	-.5073 (.06556)	.6600 (.2378)	.1225 (.1894)		.0655 .4786
L_r	.537	.1554 (.05535)	-.01303 (.04700)	-1.285 (.03477)	-.5977 (.03034)	.4232 (.1226)	.3253 (.0859)		-.0650 .6553
M_u	.010	.007582 (.00031)	.00273 (.00018)	-.00017 (.00005)	.000839 (.00005)	-.0016 (.0015)	-.0011 (.0026)		.0026 .0045
M_v	.017	.01774 (.00065)	.02557 (.00044)	.01708 (.00018)	.01855 (.00019)	.0133 (.0018)	.0120 (.0014)		.0173 .0044
M_w	.005	.006841 (.00048)	.01301 (.00028)	.01069 (.00021)	.01199 (.00018)	.0129 (.0022)	.0035 (.0013)		.0091 .0040
M_p	.088	.07947 (.01913)	.1144 (.01397)	-.05389 (.00536)	-.03866 (.00667)	-.1536 (.0595)	-.0436 (.0560)		-.0011 .0975
M_q	-.574	-.7565 (.03178)	-.7741 (.01938)	-.7231 (.01214)	-.7392 (.01169)	-.6479 (.1317)	-.3043 (.1116)		-.6456 .1659
M_r	-.092	-.02444 (.01477)							-.0582 .0478
N_u	-.004	-.00395 (.00061)							-.0040 .00004
N_v	.028	.0274 (.00121)	.03936 (.00048)	.04298 (.00025)	.04371 (.00023)	.0371 (.0026)	.0328 (.0016)		.0359 .0067
N_w	-.0003	-.00176 (.00079)				.0075 (.0013)	-.0004 (.0009)		.0013 .0042
N_p	-.122	-.1351 (.0365)	-.05615 (.01391)	-.07313 (.00825)	-.0804 (.00772)	.0226 (.0793)	-.0998 (.0540)		-.0777 .0521
N_q	.701	.7879 (.05107)	.6321 (.01111)	-.02522 (.00974)	.3158 (.00813)	.0923 (.0839)	.2834 (.0614)		.3982 .3139
N_r	-.642	-.7232 (.0274)	-.6071 (.00761)	-.2457 (.00712)	-.4145 (.00544)	-.3292 (.0693)	-.3175 (.0438)		-.0175 .1866
$\tau_{q/\delta x}$								0.110 (.0132)	
$\tau_{w/\delta x}$								0.105 (.0137)	
$\tau_{a_s/\delta x}$								0.117 (.0140)	
$\tau_{q/\delta o}$								0.132	
$\tau_{r/\delta o}$								0.104	
$\tau_{a_s/\delta o}$								0.031	

Table 4: AH-64 Control Derivative Estimates

Derivative	MDHC	NAE (CRB)	DLR1 (SD)	DLR2 (SD)	DLR3 (SD)	NLR1 (SD)	NLR2 (SD)	AFDD (CRB)	mean SD
$X_{\delta o}$	.006	-.00550 (.00068)							.0003 .0081
$X_{\delta x}$	-.025	-.03905 (.00102)	-.03540 (.00115)	-.03509 (.00137)	-.03561 (.00087)	-.0443 (.0040)	-.0798 (.0051)	-.0317 (.0019)	-.0407 .0167
$X_{\delta y}$	.005	-.0202 (.00163)							-.0076 .0178
$X_{\delta p}$	-.008	.01011 (.00081)							.0011 .0128
$Y_{\delta o}$	.049	.02572 (.00120)							.0374 .0165
$Y_{\delta x}$	.046	.03691 (.00174)							.0415 .0064
$Y_{\delta y}$	.015	.02877 (.00262)	.03485 (.00354)	.01495 (.00285)	.02427 (.00222)	.0108 (.0130)	.0011 (.0109)		.0185 .0115
$Y_{\delta p}$	-.031	-.02912 (.00122)	-.000405 (.00191)	-.00307 (.00155)	-.00392 (.00126)	.0132 (.0123)	-.0098 (.0098)		-.0092 .0159
$Z_{\delta o}$	-.153	-.1711 (.00133)	-.2643 (.00500)	-.2267 (.00533)	-.2585 (.00405)	-.2594 (.0230)	-.2705 (.0238)	-.314	-.2397 .0537
$Z_{\delta x}$	.056	.05093 (.00865)	-.1407 (.00592)	-.06232 (.00607)	-.1044 (.00454)	-.2067 (.0180)	.0512 (.0253)	-.234 (.00936)	-.0737 .1177
$Z_{\delta y}$	.041	.09615 (.01217)							.0686 .0390
$Z_{\delta p}$	-.018	-.05368 (.00582)							-.0058 .0252
$L_{\delta o}$	.021	.03025 (.00133)	.01401 (.00131)	-.00584 (.00100)	.01851 (.00086)	-.0062 (.0037)	.0138 (.0030)		.0122 .0136
$L_{\delta x}$	.010	.01524 (.00179)	-.02950 (.00191)	-.04714 (.00145)	-.02092 (.00112)	-.0069 (.0044)	-.0170 (.0039)		-.0137 .0219
$L_{\delta y}$	.124	.1408 (.00266)	.1401 (.00270)	.1349 (.00137)	.1386 (.00153)	.0973 (.0054)	.0925 (.0046)		.1240 .0207
$L_{\delta p}$	-.045	-.04902 (.00120)	-.0208 (.00100)	-.02164 (.00056)	-.02220 (.00061)	-.0434 (.0028)	-.0290 (.0023)		-.0330 .0124
$M_{\delta o}$	.006	.007765 (.00034)	.01122 (.00020)	.01265 (.00018)	.01178 (.00016)	.0125 (.0022)	.0085 (.0017)	.0169	.0109 .0034
$M_{\delta x}$	.017	.01952 (.00052)	.02753 (.00033)	.02879 (.00026)	.02722 (.00020)	.0254 (.0023)	.0227 (.0019)	.0317 (.00095)	.0250 .0049
$M_{\delta y}$	-.009	-.00976 (.00082)	-.00808 (.00046)	.000030 (.00022)	-.00235 (.00026)	-.0008 (.0025)	-.0026 (.0023)		-.0047 .0041
$M_{\delta p}$	.002	.002526 (.00041)							.0023 .0004
$N_{\delta o}$	.004	.000353 (.00059)	.00288 (.00020)	.00907 (.00022)	.00641 (.00017)			.017	.0066 .0059
$N_{\delta x}$	-.015	-.01946 (.00088)	-.01495 (.00026)	-.00136 (.00023)	-.00876 (.00018)				-.0119 .0070
$N_{\delta y}$	.010	.01122 (.00155)	.00786 (.00055)	.00264 (.00034)	.00182 (.00033)	.0013 (.0032)	.0029 (.0022)		.0054 .0042
$N_{\delta p}$	.028	.03150 (.00073)	.02932 (.00022)	.02489 (.00015)	.02912 (.00015)	.0265 (.0016)	.0231 (.0011)		.0275 .0029

Table 5: MDHC Eigenvalues for the AH-64

Eigenvalue	Frequency (rad/s)	Damping	Mode
-.020			Spiral
.143 $\pm i$ .286	.32	-.45	Phugoid
-.321			Pitch Mode 1
-1.25			Pitch Mode 2
-2.98			Roll
-.118 $\pm i$ 1.53	1.53	.077	Dutch roll

Table 6: DLR Eigenvalues for the AH-64

DLR-1			
Eigenvalue	Frequency (rad/s)	Damping	Mode
-.0099			Spiral
.141 $\pm i$.151	.206	-.68	Phugoid
-.220			Pitch Mode 1
-1.633			Pitch Mode 2
-3.810			Roll
-.1695 $\pm i$1.726	1.735	.0977	Dutch Roll

DLR-2			
Eigenvalue	Frequency (rad/s)	Damping	Mode
-.0544			Spiral
.0632			Phugoid
.200			Phugoid
-.110			Pitch Mode 1
-1.423			Pitch Mode 2
-3.390			Roll
-.0771 $\pm i$ 1.777	1.778	.0433	Dutch Roll

DLR-3			
Eigenvalue	Frequency (rad/s)	Damping	Mode
-.0279			Spiral
.135 $\pm i$ .089	.162	-.835	Phugoid
-.162			Pitch Mode 1
-1.542			Pitch Mode 2
-3.358			Roll
-.115 $\pm i$ 1.793	1.797	.0641	Dutch Roll

Table 7: NAE Eigenvalues for the AH-64

Eigenvalue	Frequency (rad/s)	Damping	Mode
-.0036			Spiral
.101 $\pm i$ .2382	.259	-.39	Phugoid
-.3357			Pitch Mode 1
-1.4662			Pitch Mode 2
-3.4044			Roll
-.1069 $\pm i$ 1.460	1.464	.073	Dutch roll

Table 8: NLR Eigenvalues for the AH-64

NLR-1			
Eigenvalue	Frequency (rad/s)	Damping	Mode
-.1669			Spiral
.0028 $\pm i$ .1201	.120	-.023	Phugoid
.2177			Pitch Mode 1
-1.538			Pitch Mode 2
-2.108			Roll
-.1099 $\pm i$ 1.586	1.590	.0691	Dutch Roll

NLR 2			
Eigenvalue	Frequency (rad/s)	Damping	Mode
-.0526			Spiral
-.0987 $\pm i$ .2035	.226	.4363	Phugoid
.3009			Pitch Mode 1
-.8923			Pitch Mode 2
-2.139			Roll
-.0679 $\pm i$ 1.610	1.611	.0421	Dutch Roll

Table 9: Estimated Eigenvalues from AH-64 Flight Data

Eigenvalue	Frequency (rad/s)	Damping	Mode
.087 $\pm i$ .29	.30	-.29	Phugoid
-.083 $\pm i$ 1.64	1.65	.05	Dutch roll

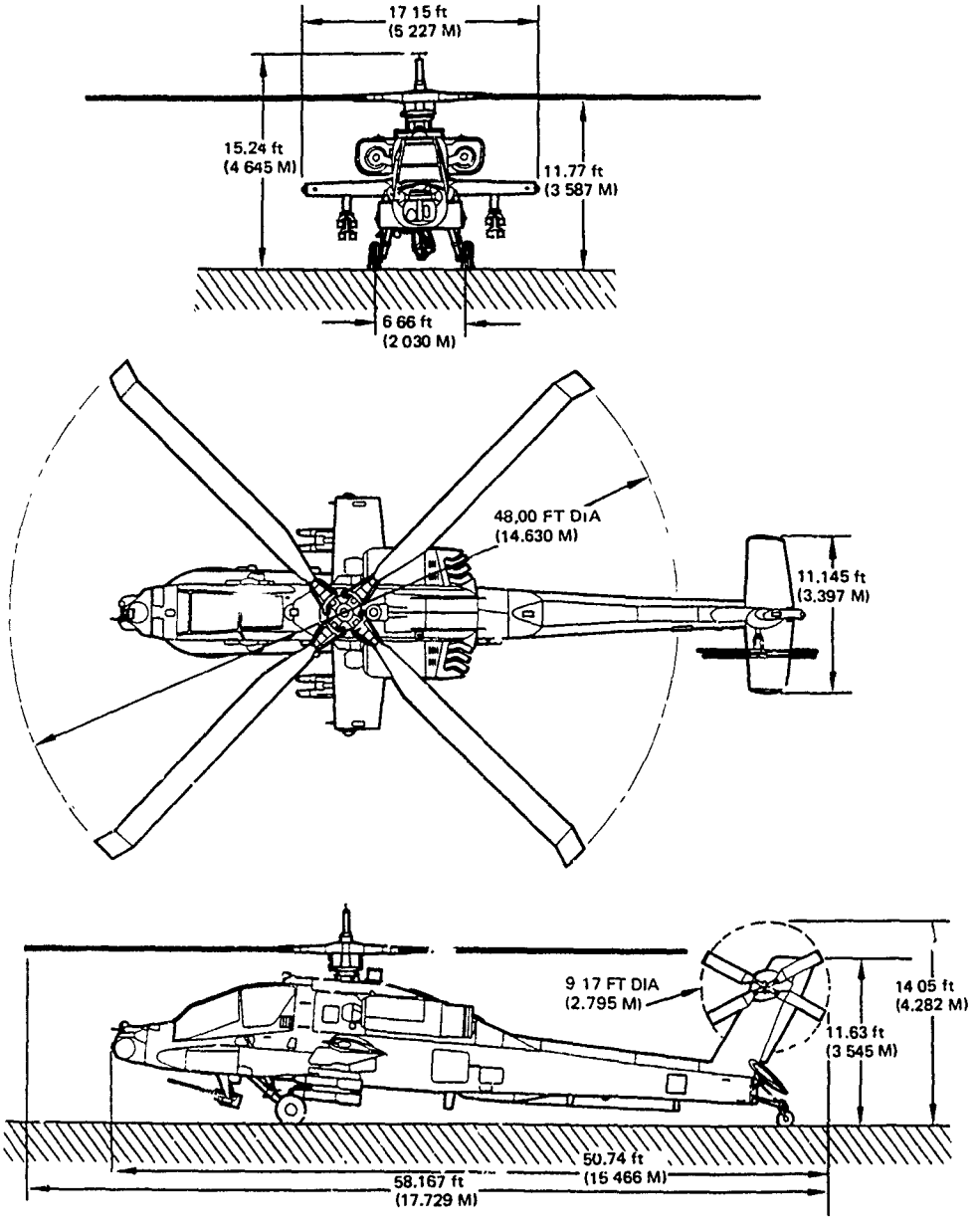

Figure 1: Three-view Drawing of AH-64

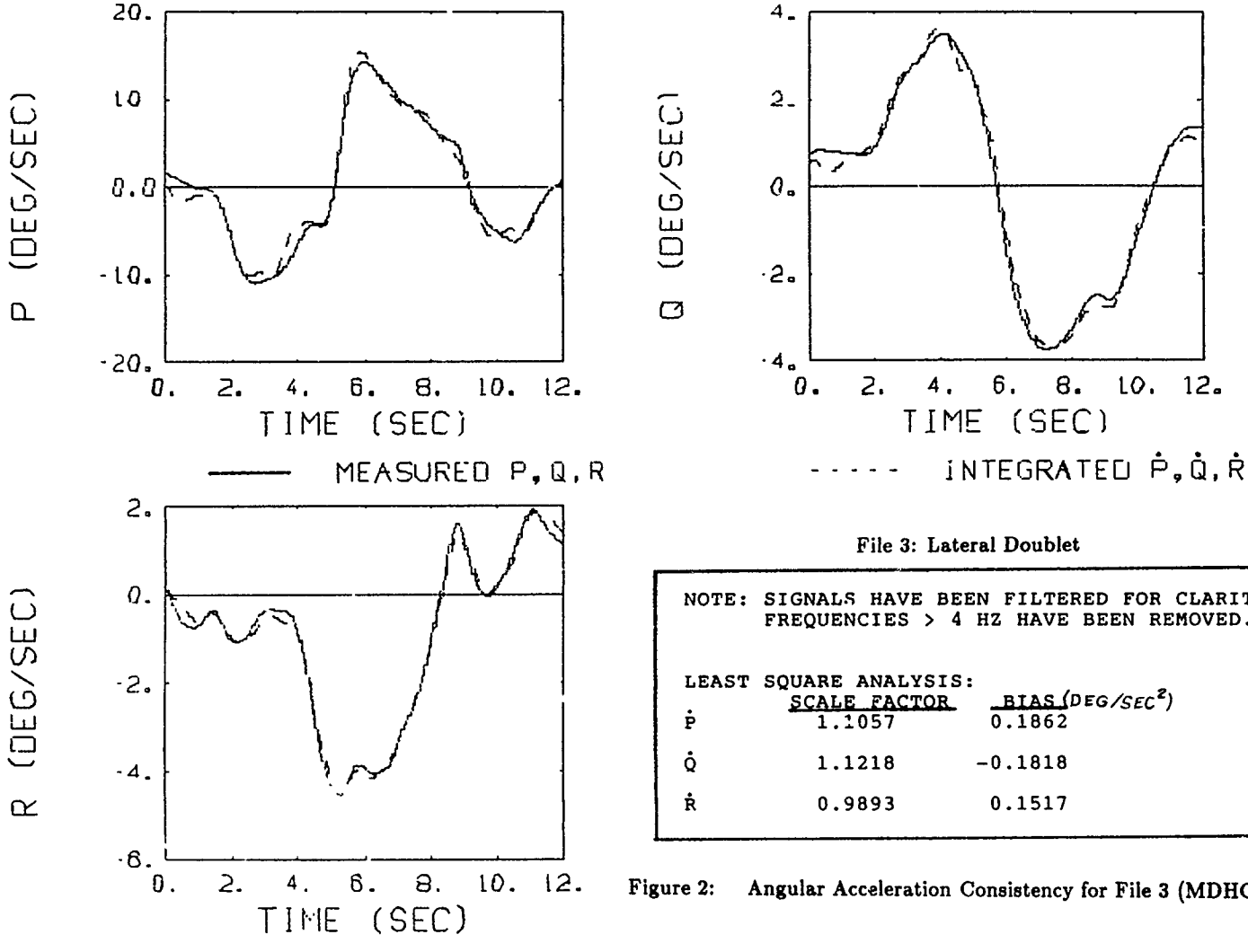

File 3: Lateral Doublet

NOTE: SIGNALS HAVE BEEN FILTERED FOR CLARITY.
FREQUENCIES > 4 HZ HAVE BEEN REMOVED.

LEAST SQUARE ANALYSIS:

	SCALE FACTOR	BIAS (DEG/SEC^2)
$\dot{P}$	1.1057	0.1862
$\dot{Q}$	1.1218	-0.1818
$\dot{R}$	0.9893	0.1517

Figure 2: Angular Acceleration Consistency for File 3 (MDHC)

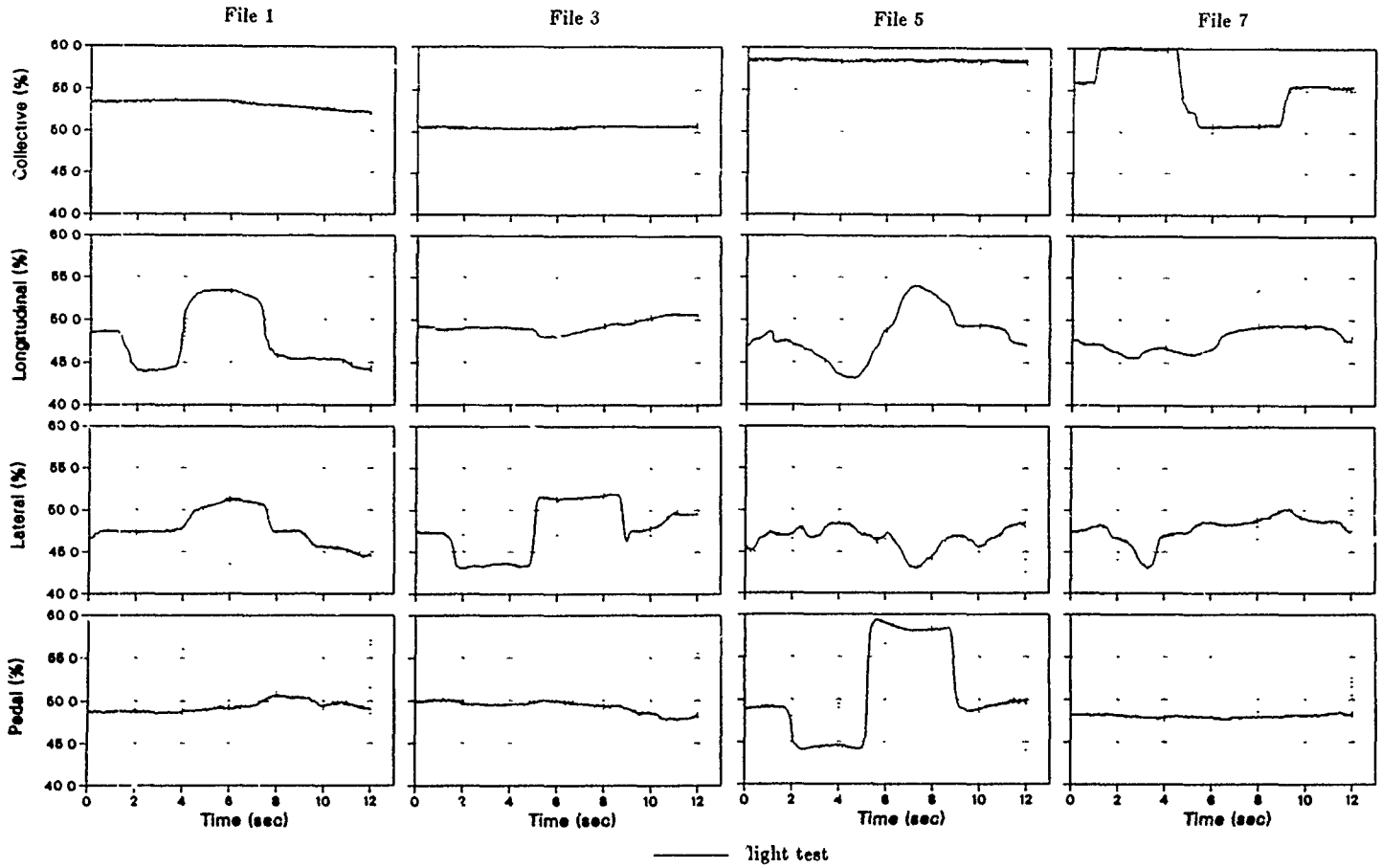

Figure 3: Control Input Time Histories for Identification Files

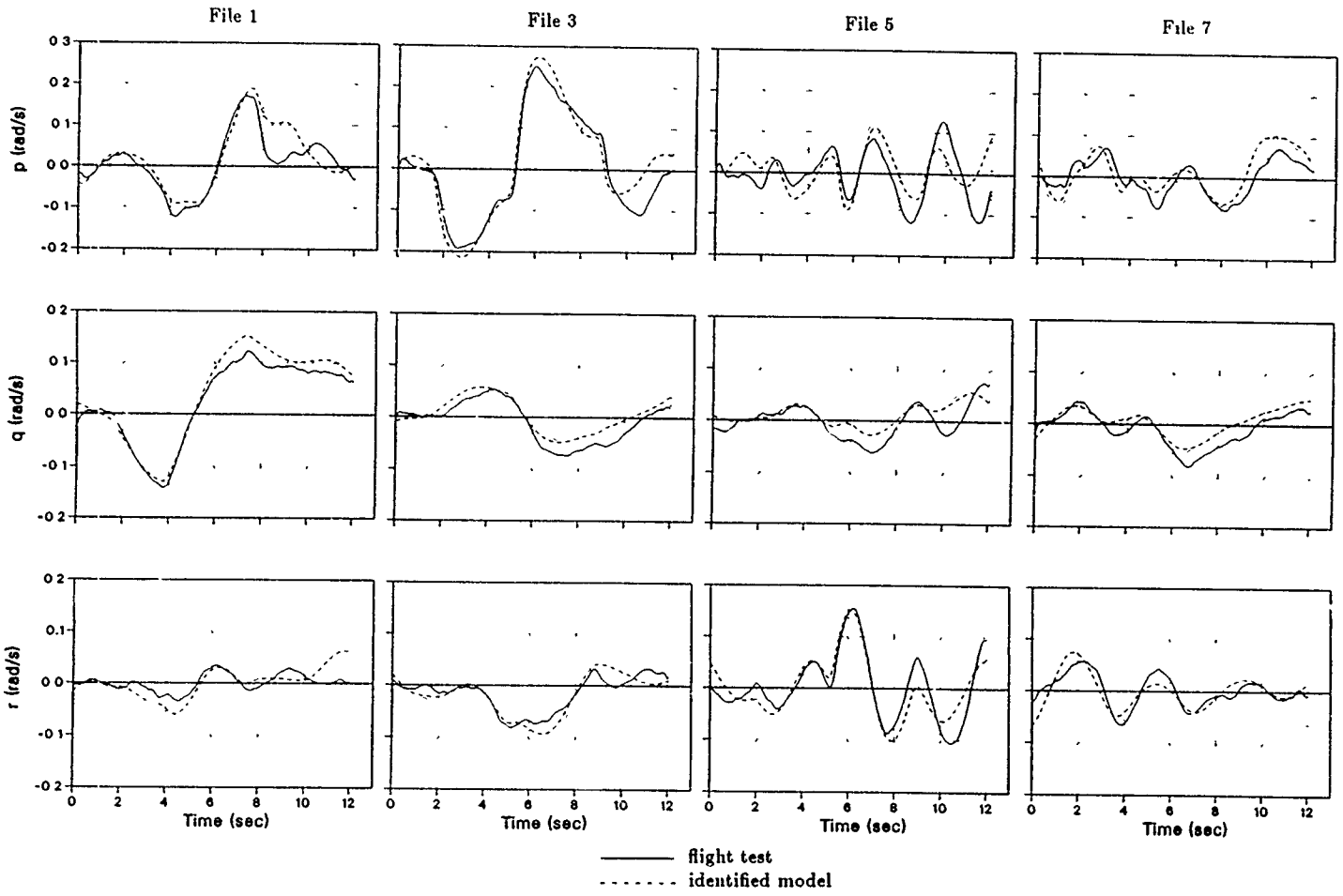

Figure 4: Identification Result: Comparison of Measured Data and the MDHC Identified Model

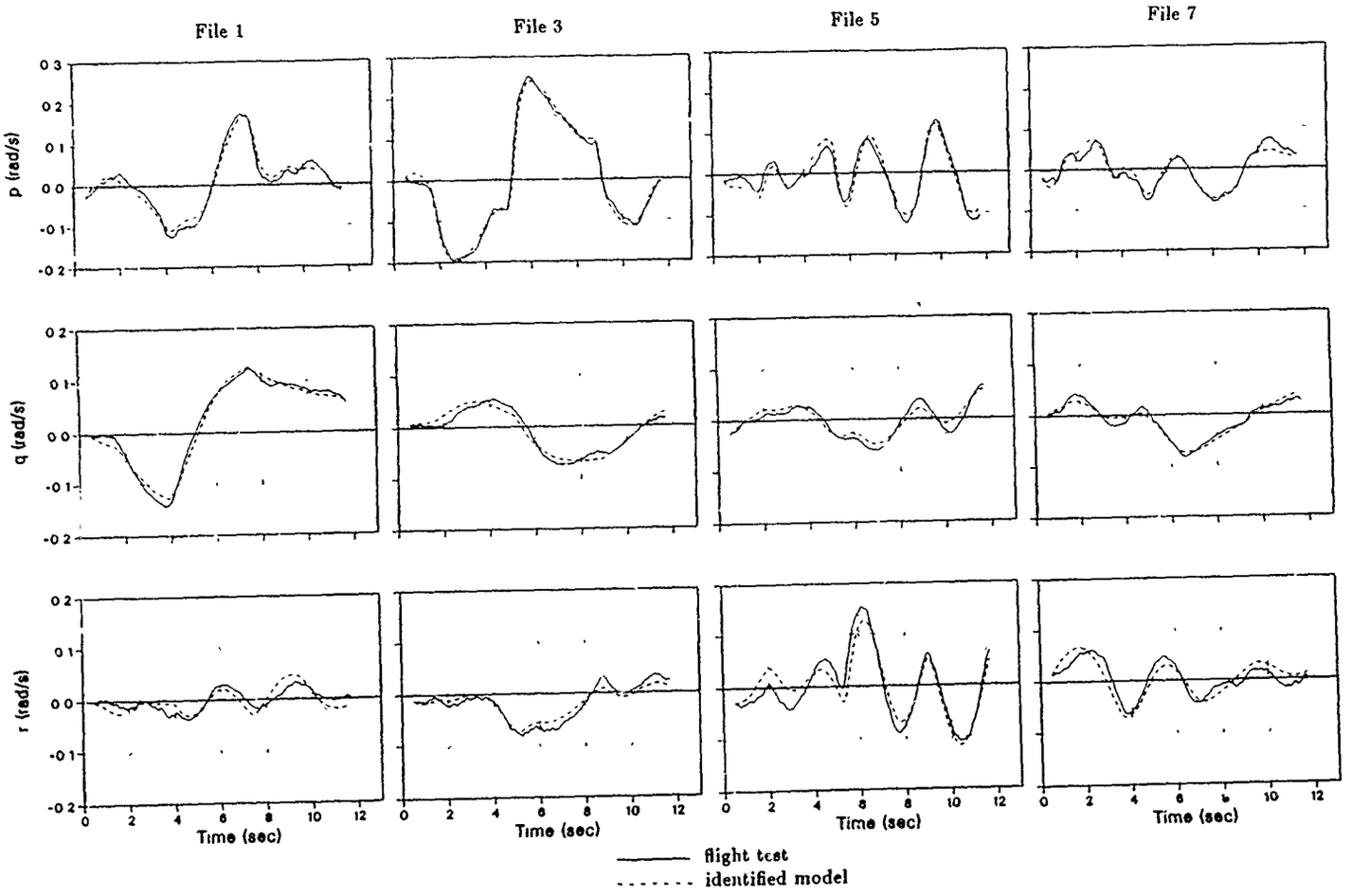

Figure 5: Identification Result: Comparison of Measured Data and the NAE Identified Model

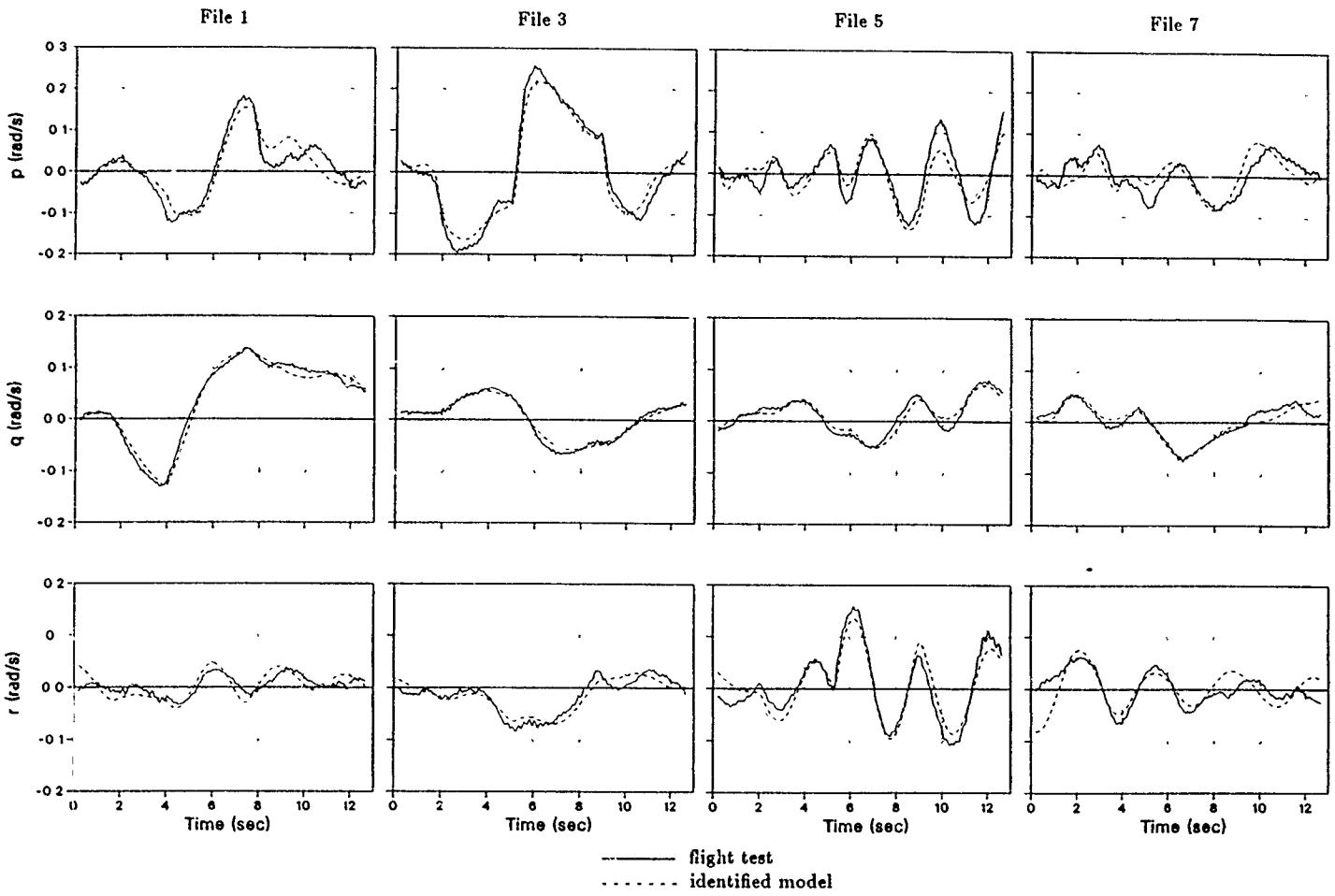

Figure 6: Identification Result: Comparison of Measured Data and the DLR-1 Identified Model

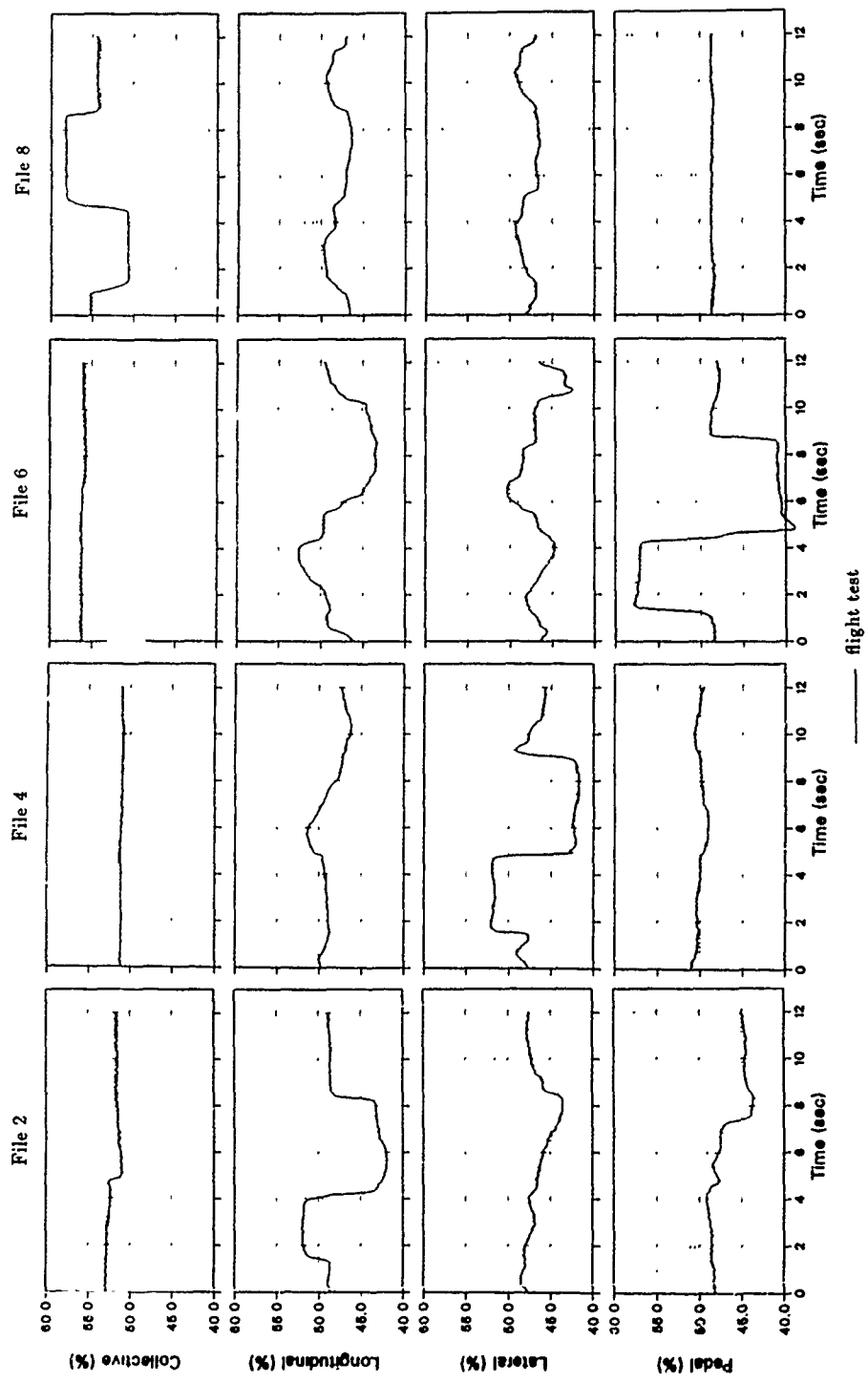

Figure 7: Control Input Time Histories for Verification Files

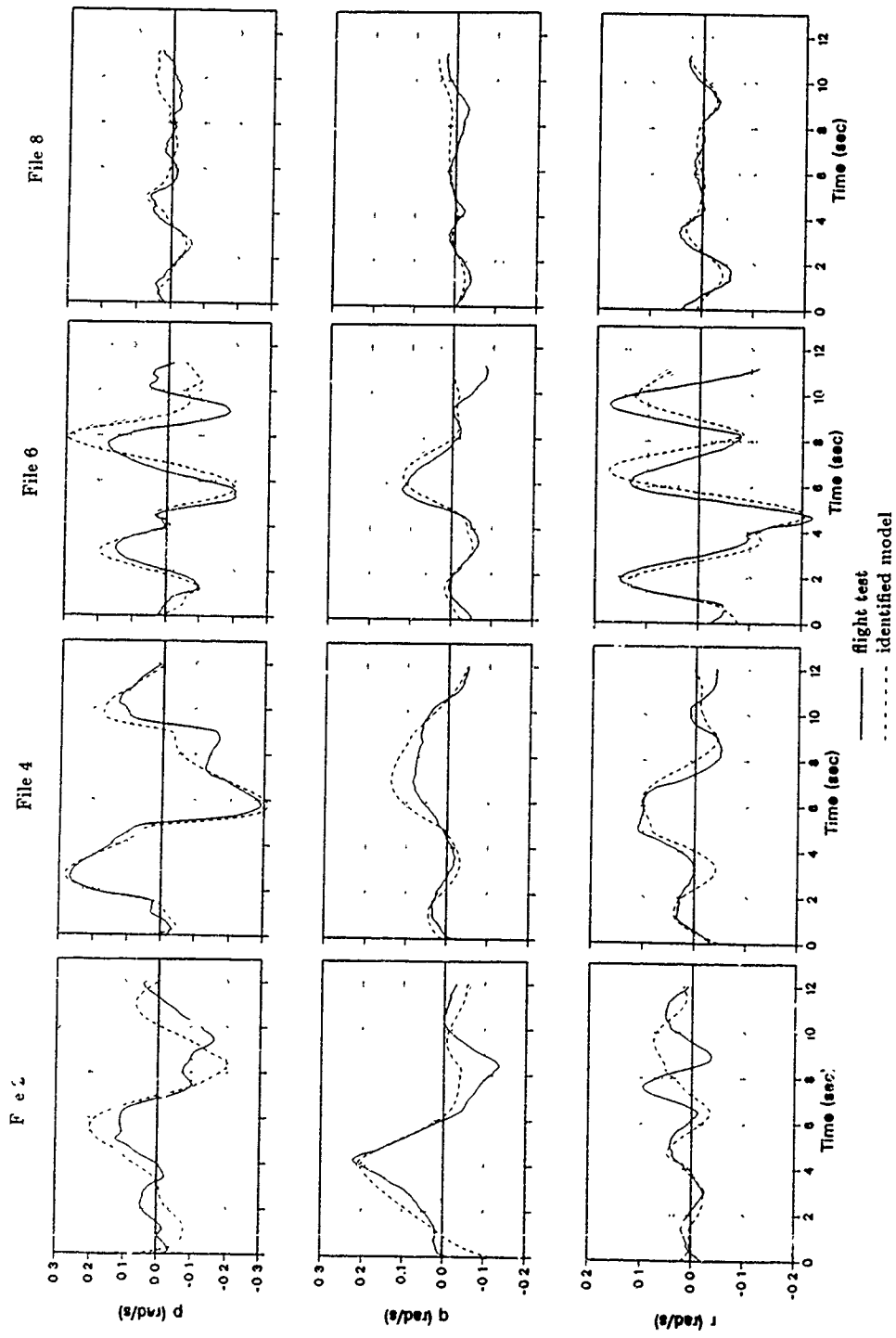

Figure 8: Verification Result: Comparison of Measured Data and the MDHC Identified Model

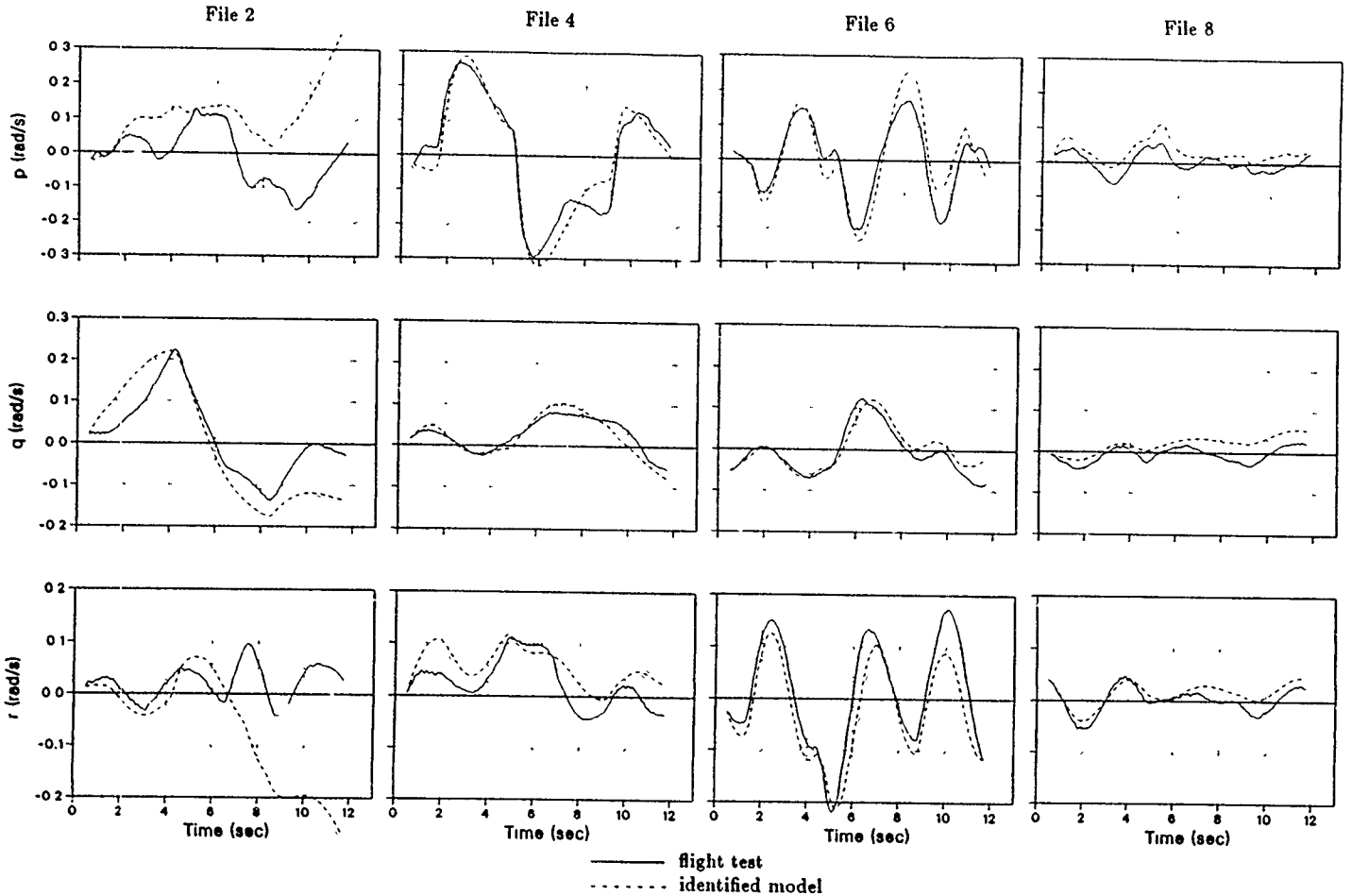

Figure 9: Verification Result. Comparison of Measured Data and the NAE Identified Model

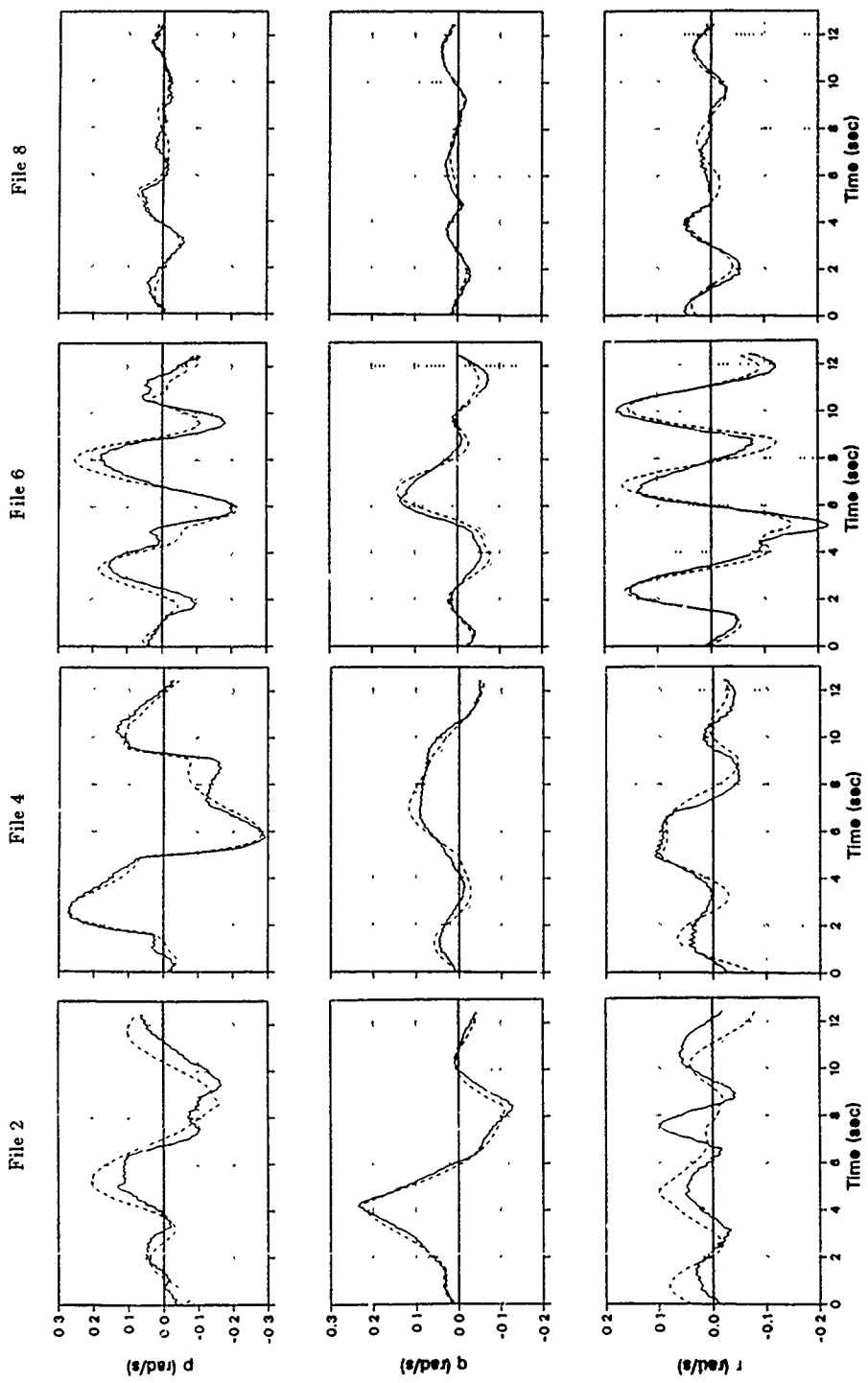

Figure 10: Verification Result: Comparison of Measured Data and the DLR-1 Identified Model

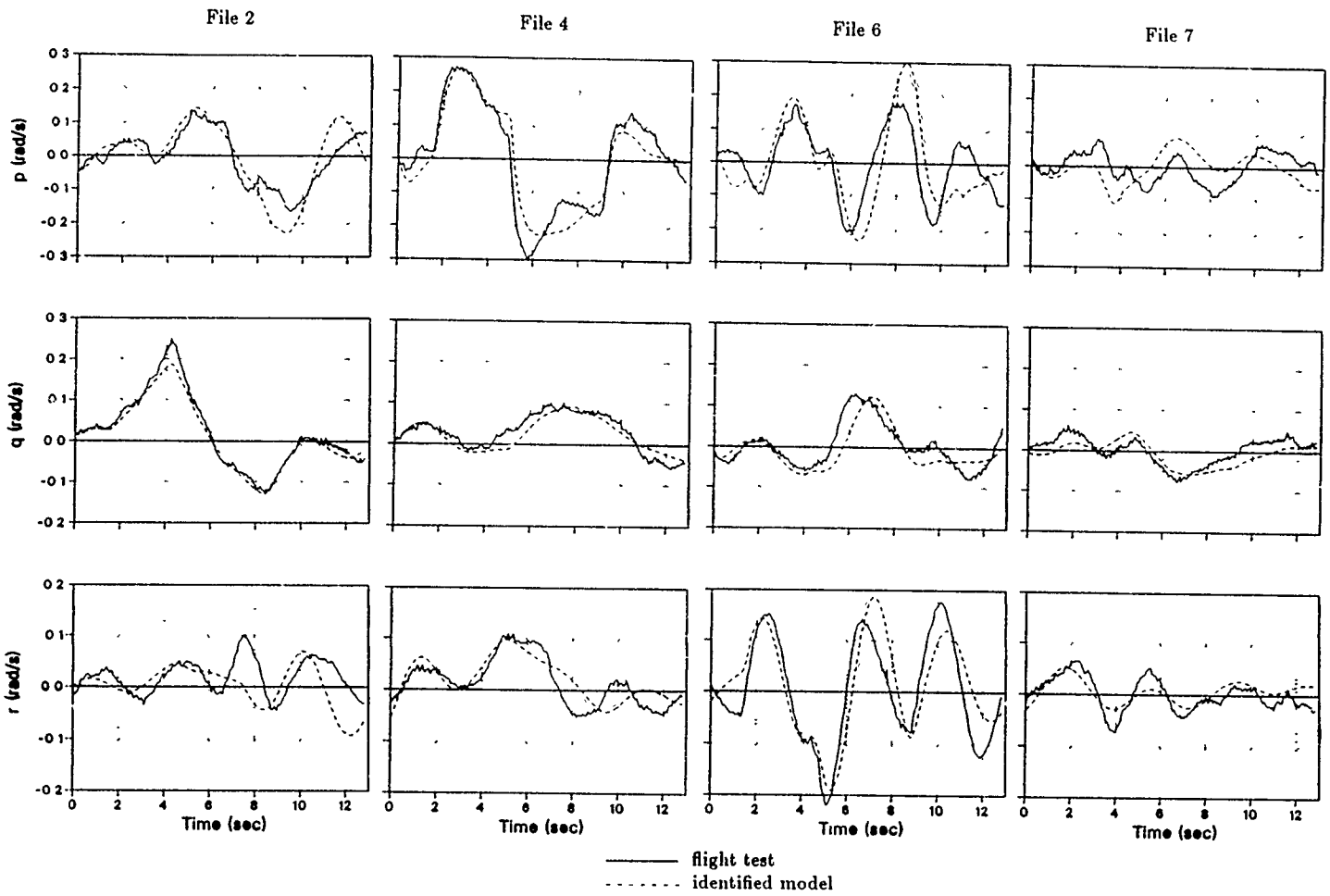

Figure 11: Verification Result: Comparison of Measured Data and the NLR-1 Identified Model

BO 105 IDENTIFICATION RESULTS

by

Jürgen Kaletka
Deutsche Forschungsanstalt für Luft- und Raumfahrt e V (DLR)
Institut für Flugmechanik
DW-3300 Braunschweig, Flughafen, Germany

1. Summary

BO 105 flight test data generated particularly for system identification purposes were provided to the AGARD Working Group WG 18 on *Rotorcraft System Identification* This Lecture first summarises the accomplishments of the Working Group for the data consistency analyses, and the identification and verification results for 6 degrees of freedom models. The individually applied approaches are described and representative results are presented It is shown that the flight test data were appropriate for use of system identification. The discussion of the identification and verification results demonstrates that there are significant differences depending upon the applied identification technique. The Lecture finally addresses the identification of higher order models and presents some results obtained for an extended model with rotor degrees of freedom.

2. Introduction

A flight test program was conducted on a DLR BO 105 helicopter to obtain data especially designed for system identification purposes. Trim configuration was steady state horizonal flight at 80 knots at a density altitude of about 3000 feet. Selected data runs were provided to the AGARD Working Group WG 18 on *Rotorcraft System Identification* to be used as one common data base (together with data bases of the AH-64 from MDHC and SA330 (PUMA) from RAE) for

1. data consistency analysis,
2. identification of 6 degrees of freedom models, and
3. verification of the identified models.

The accomplishments and results of the Working Group have been documented as an AGARD Advisory Report [1]. This Lecture concentrates on the results obtained from the evaluation of the BO 105 flight test data. It is mainly based on the results generated by the Working Group. In addition, the identification of higher order models is addressed.

After a brief description of the BO 105 helicopter, it is concentrated on the flight tests and the results of data consistency analyses. Identification approaches applied by the individual WG Members are characterised and the obtained identification results are presented in the format of tables and representative time history and frequency response plots Verification results for the identified models are shown. Both, identification and verification results are discussed in detail. Finally, it is concentrated on the identification of an extended model including rotor degrees of freedom and results obtained for a 16th order model are presented

3. Description of BO 105

The BO 105 is designed as a multiple purpose light helicopter. Typical use of the highly manoeuvreable twin engine vehicle are transport, offshore, police, and military missions. An important design feature is the hingeless rotor system with four fiber-reinforced composite rotorblades. There are no additional lead/lag dampers The semi-rigid teetering tail rotor is on the left side of the helicopter, working as a pusher.

Pilot control inputs are augmented by two parallel hydraulic servo systems. There is no specific mixing unit, so that control inputs are only mixed at the swash plate. The BO 105 is equipped with two Allison 250 C20 engines located above the cargo compartment

DLR operates two different BO 105 helicopters. The first one is the standard serial type (BO 105-S123) shown in Figure 1 Its instrumentation is designed to meet the requirements of two DLR institutes, the Institut for Flight Mechanics and the Institut for Flight Guidance and Control, both located in Braunschweig This helicopter was used to generate the system-identification flight-test data provided to the Working Group. The second DLR helicopter (BO 105-S3) has been modified for the use as an in-flight simulator. For this ATTHeS helicopter (Advanced Technology Testing Helicopter System) a model-following control system was developed at DLR. Here, highly accurate BO 105 mathematical models were required and the research work conducted at DLR has shown that system identification is the best suited tool to generate such models [2].

To give an impression on the helicopter size and basic characteristics, a three view drawing of the BO 105 is given in Figure 2 and some more details are provided in Table 1.

4. Flight Testing and Data Evaluation

The identification of dynamic systems is always based on the evaluation of the relationship between the measurements of the control inputs and the resulting system response. Therefore, accurate measurements are an indispensable prerequisite for a reliable identification. Usually results are obtained from one flight test run However, when the time duration of the test is too short or when the system is rather complex, the information content of a single run can be insufficient. This is often the case for the identification of helicopters as a high number of unknowns must be determined and the data run length is limited due to helicopter instabilities. To still provide more information for the identification algorithm it is possible to simultaneously evaluate different test runs and generate one common model. This method, known as *multiple* or *concatenated run* evaluation has become a common approach in rotorcraft identification. However, it can only be applied when the concatenated runs have practically the same initial flight test conditions and helicopter and instrumentation status. Therefore, the DLR BO 105 flight test data provided to the Working Group were generated within one flight test program. The tests were especially designed for system identification purposes with particular input signals and carefully controlled initial conditions and conduct of the tests.

The flight test data evaluation with respect to the generation of appropriate data and the analysis of the data quality can be separated into three major steps:

1 on-line data control during the flight tests,

2 first off-line data quality assessment immediately after each flight,

3 detailed data consistency analysis after the end of the flight test program.

The first two steps were done by DLR before the data were released to the Working Group Then, the more thorough analysis was performed by the Working Group. In this section, the approaches and obtained results are presented.

4.1 On-line data control

During the flight tests the measured signals were sent by telemetry to a ground station. They were plotted in the form of quick-look plots and, in addition, selected variables were shown on a monitor The objectives of the quick-look evaluation were

1 to control the conduct of the flight tests and give recommendations to the pilot,

Main emphasis was placed on the atmospheric conditions, the proper input signal and the aircraft response The tests were flown in calm air to avoid gust disturbances. Here, pilot comments proved to be very helpful. Based on outside temperature measurements on board of the helicopter, the required pressure altitude was iteratively determined to make sure that all tests were flown at the same air density level.

The input signals were generated by the pilot. Within one test run only one control was used to excite the on-axis response and to avoid correlation with other controls After an accurate trim configuration was reached, the on-line data evaluation concentrated on the shape of the input signal and possible control coupling Then, it was checked if the resulting helicopter response met two main criteria:

- As the models to be identified are based on small perturbation assumptions, the response amplitudes should not be too large As a certain guideline: the pitch and roll angles should not exceed 25 to 30 degrees.
- The total time length of the test should at least be about 25 seconds to provide sufficient information about the phugoid mode

2. to detect data errors,

The on-line quick-look helped in detecting major and obvious data errors like sensor malfunctions, signal saturations, larger sensor drifts, data drop outs, noise disturbances, etc.. But it has to be considered that only some selected data channels can be observed on-line and therefore, a more detailed data analysis after the flight is necessary.

3 to decide if the test is acceptable

Based on the quick-look evaluation and pilot comments it was decided after each test if the test was acceptable. When it had to be repeated, recommendations were given to the pilot, such as improvement of trim, adjustment of control input amplitudes, input signal generation, etc

4.2 First off-line data quality assessment

Experience in working with measured data has shown that significant errors in the data can occur although great efforts were made to generate accurate data Unfortunately, errors are often only detected during the evaluation phase, when all flight tests are completed and the instrumentation system has probably already been modified for other tests. Then, flight tests cannot be repeated and often it is difficult or impossible to find the physical error source and to correct the data To reduce this risk it is necessary to carefully check the data quality immediately after each test. Therefore, plots of all measured data from the BO 105 data tape were produced for a detailed visual inspection. Emphasis was placed on both data suitability for identification and the detection of errors:

- physically meaningful data,

  With some knowledge of the helicopter response due to a control input most of the measurements can easily be checked for
  - correct sign,
  - realistic magnitude,
  - noise level.

- signal saturation and resolution,

  In preliminary tests the expected maximum helicopter response for the specific tests was determined. Based on these measurements, sensors were selected with an appropriate measuring range. The digitization range was fitted to the expected response range. Both actions help to improve the data accuracy and resolution However, they also increase the risk of data saturation due to a higher amplitude response or higher noise level as expected

- data drop outs,

  For the BO 105 flight tests, unfiltered data were recorded. Therefore, data drop outs are seen as large spikes in time history plots and can easily be detected. If only a few drop outs occur it is relatively easy to correct the data by removing the erroneous samples and replace them by interpolated data. However, some inaccuracy must be accepted, which is particularly true in data parts with higher dynamics. The major 'danger' of data drop outs occurs when data are filtered. Then the errors are no longer obvious and can cause significant inaccuracies in the data

- data recording errors,

- any other data irregularities.

In addition to the visual data check, a first data compatibility analysis was conducted. Using a fast Least Squares technique, the consistency of the rotational measurements (rates and angular measurements) and the translational measurements (linear accelerations and speed components) was investigated. Scale factors, offsets and drifts can be determined. This techniques is applied routinely in DLR flight tests and proved to be a very efficient approach

Before the BO 105 flight test data were provided to the Working Group, first data quality checks and compatibility analyses were performed by DLR to ensure that the data did not contain significant deficiencies.

4.3 BO 105 Data Base provided to the Working Group

From all flight tests, 52 runs were selected by DLR and provided to the Working Group Members. They are listed in Table 2 Flight test data obtained from three different input signals were provided:

1. a modified multi-step 3211 input signal with a total time length of 7 seconds,
2. a frequency sweep from about 0 08 Hz up to the highest frequency the pilot could generate. Time length of the sweep was about 50 seconds followed by the retrim to the initial steady state condition (important for frequency domain evaluation).
3. a doublet with a total time length of 2 second.

Flight data with the input signal starting in opposite direction were generated for the 3211 and doublets For redundancy reasons, one or two repeats of each test were provided (see Table 2). Within a run, only one control was used to excite the on-axis response. For the flights with 3211 and doublet inputs the controls were held constant after the end of the input for at least 20 seconds. Because of the long time duration of the frequency sweeps, these tests required stabilization by the pilot to keep the aircraft response within the limits of small perturbation assumptions for linear mathematical models. To help the pilot generate the inputs, a CRT was used that showed both the desired input and the actual control movement (Figure 3). For the sweeps, the CRT showed the lowest frequency as a 'starting' help. Then, the pilot progressively increased the frequency on his own.

The measured variables provided to the Working Group are given in Table 3 and Table 4. As a representative example from the data base, Figure 4 gives the roll and pitch rate responses due to the three input signals in the same scales. It shows that the input amplitudes were adjusted to generate similar helicopter on-axis response magnitudes. It also demonstrates the highly coupled BO 105 characteristic: the (coupled) roll rate response due to a longitudinal stick input is as high as the primary pitch rate response. More time histories of the measurements will be given in section 5, when identification results are discussed.

4.4 Detailed data consistency analysis in the Working Group

Based on the initial data check results from the 52 data files, DLR suggested a minimum data set of four runs with 3211 input signals to be used for the identification and another set of 4 data runs with doublet control inputs to be applied for the verification of the identified models. Each of these data groups included one run for each control. This proposal was made to reduce the amount of work for each Member and to make results comparable. For the A'DD frequency domain technique the sweep inputs were used for identification.

All Members used the same principle approach to check the data quality. It is based on the comparison of redundant measurement: rates and angular measurements are physically related by the equations

$$\dot{\Phi} = p + \sin\Phi \tan\Theta\, q + \cos\Phi \tan\Theta\, r$$

$$\dot{\Theta} = \cos\Phi\, q - \sin\Phi\, r$$

$$\dot{\Psi} = \frac{\sin\Phi}{\cos\Theta}\, q + \frac{\sin\Phi}{\cos\Theta}\, r$$

The relationship between linear accelerations and speed components is given by·

$$\dot{u} = a_x - g\sin\Theta - w\, q + v\, r$$

$$\dot{v} = a_y + g\sin\Phi\cos\Theta - u\, r + w\, q$$

$$\dot{w} = a_z + g\cos\Phi\cos\Theta - v\, p + u\, q$$

In these nonlinear equations, linear accelerations and rates are taken from measured data and used as 'control' inputs. The integration then yields calculated angles and speed components that can be compared to the measured ones. When differences are seen, a more detailed analysis is needed to isolate the error sources. In general it is tried to estimate scale factors or zero offsets (biases) for the measured data. Depending on the applied method, the estimation procedure is different in its power and complexity. When the technique does not allow the integration of nonlinear systems, all variables on the right hand side are taken from measurements. Then, all terms are known and the equation system can easily be integrated. When nonlinear systems can be handled, there is more flexibility with respect to the use of the attitude angles and speed components: each of these variables can either be treated as a known measured control or as a state variable obtained from the actual integration. This possibility is very useful to isolate erroneous data channels. However, independent from the applied method, some general statements can be made from the BO 105 data evaluation:

1. Due to parameter correlations it is not possible to estimate **all** scale factors **and** biases for **all** measurements. Based on the assumption that rate gyros and linear accelerometers are the more reliable sensors, the usual approach therefore is to estimate:
   - scale factors for attitude angles and speed components,
   - and/or biases for rates and linear accelerations.
2. The error estimation for the angular motion equations causes no major problems.
3. The determination of errors for the translational motion equations is more difficult because of some unique problems:

   The equations are coupled with the rotational equations by the gravity terms. As they have a significant effect, errors in the attitude data also highly influence the comparison of the speed data.

   The linear acceleration measurements have a high noise level due to vibrations Helicopters, and in particular rigid rotor helicopters like the BO 105, generate only small accelerations in the longitudinal and lateral body-fixed axes as the acceleration components due to a speed change are practically compensated by the gravity components. The fact that, on the one side, sensors must have a high measuring range due to the noise level whereas, on the other side, the signal to noise ratio is small (about 0.1 for the BO 105) reduces the high measurement and resolution quality of the linear acceleration data. This is particularly the case for the longitudinal and lateral accelerations.

   Measurement of aircraft speed components is still a major problem and the obtained accuracies are significantly lower than those of the or linear accelerations or angular data. This is also true for the helicopter air data system, which is installed on the BO 105. For the considered flight condition of about 80 knots it cannot improve the data quality in comparison to other data sources like noseboom mounted vanes and pressure sensors

In the Working Group, AFDD, CERT, DLR, NAE, and NLR performed data consistency checks for the BO 105 data. In the following, the individual approaches are characterized.

AFDD

Extensive work on data consistency for all provided BO 105 data runs was done by AFDD. First results, presented in [3], were obtained from the separate evaluation of each individual run. A more detailed study, including concatenated evaluations, is given by [4]. The Kalman Filter Smoother program SMACK (**S**moothing for **A**ir**C**raft **K**inematics) developed at the Ames Research Center was employed. The algorithm is based on a variational solution of a six degrees of freedom linear state and non-linear measurement model and employs a forward smoother and zero-phase-shift backward information filter. The solution is iterative, providing improved state and measurement estimates until a minimum squared-error is achieved. Linearization is about a smoothed trajectory and convergence is quadratic [5]

Consistency checks were performed in two steps:

1. a preliminary three degrees of freedom check including only the Euler angle and body angular rate measurements,
2. a final six degrees of freedom check including the angular variable measurements and the air-data and linear specific force measurements.

This approach allowed initial estimation of the angular-variable error parameters to be performed unbiased by the noisier air-data and specific-force measurements. The values estimated in the angular

solution and their variances were then used as start-up values in the final overall solution. This two-step procedure resulted in a final solution with smaller parameter Cramer-Rao bounds and quicker convergence than a one-step coupled solution. The obtained results are included in Table 5 and Table 6.

CERT

CERT has used an output error minimization technique to estimate scale factors, biases and initial conditions. From the obtained results it was concluded, that the measurement errors were not so significant to justify use of reconstructed data.

DLR

The airdata measurement problem has already been addressed. In the flight tests the measured lateral speed was about 4 m/sec and the vertical speed about -5 m/sec. It was felt that these values were not realistic and contained offsets. Therefore, for each run, the initial vertical trim speed was calculated from steady state horizontal flight using forward speed and pitch angle (this approach was also used by NAE). The lateral speed could not be determined from other measurements. As the pilots were asked to minimize the sideslip during trim, the initial lateral speed was assumed to be zero.

For the state estimation, DLR used the Maximum Likelihood program that is also applied for system identification. The nonlinear kinematic equations were integrated, where the measured rates and linear accelerations were treated as 'inputs' and all other variables were used as states. Calculated attitude angles, heading, and speed components were obtained. Comparing the derived time histories with the measured data two groups of unknowns were estimated:

- scale factors for the speed components, attitude angles and heading,
- biases (offsets) for the rates and linear accelerations.

Both, single and concatenated files were evaluated. The final results, obtained from all files as well as from the suggested files are given in Table 5 and Table 6.

NAE

Consistency checks were performed on all data files. The data was initially lowpass filtered with a Butterworth fourth-order zero phase shift filter with a cutoff frequency of 4 Hz. After lowpass filtering, the data was sampled at 20 Hz, excluding the first and last 50 points.

Biases in the data were estimated with a Least Squares method. The measurements used were: speed components, linear accelerations, rates, attitude angles and heading. The Least Squares procedure is outlined below.

1. Integrate Euler rates with measured Euler angle initial conditions and use Least Squares to determine the 6 biases for the measured attitudes and rates.
2. The corrected Euler angles and rates are used in the angular kinematic equations to determine biases in the body angular rates.
3. The corrected body angular rates and attitudes enter the translational kinematic equations for determination of biases in the velocities and translational accelerations.

Angular data were found to be of good quality and they were then used without any changes for the identification. Speed data, however, were felt to be not acceptable and therefore, for all three speed components, reconstructed data were generated.

NLR

The BO 105 data were originally provided with a sampling rate of 100 Hz. This sampling rate was reduced to 25 Hz. No filter was used for the data reduction. Then NLR applied an output error technique, which uses the nonlinear kinematic equations to estimate measurement biases. Various data runs were evaluated. The obtained results for the biases were comparable with the biases obtained from the combination of the four data runs that were suggested for identification. Visual inspection of the reconstructed time histories with the measured ones confirmed that the quality of the measured data is satisfactory and no significant errors were detected The measured linear accelerations and rates were corrected by the identified biases and the reconstructed speed components were generated for the use in the identification.

The estimated bias terms for the linear accelerations and rates obtained from the data consistency checks of the four combined runs are given in Table 6.

4.5 Discussion of results

In the following, results obtained from the data consistency analysis are illustrated by representative plots and the estimated scale factors and biases are summarized in the form of tables.

In Figure 5 and Figure 6 measurements from two flight tests are shown. Modified 3211 input signals were used for the longitudinal stick (in the first run) and for the pedal (in the second run). Figure 5 compares the measured speed components, attitude angles and heading to reconstructed data. All scale factors were assumed to be one. It is clearly seen that angular variables are in good agreement, whereas the speed components show larger differences In particular, in the lateral speed data two deficiencies are obvious:

1. In the first run there are two sections with 'data drop outs' where the sensor was affected by the

rotor downwash when the helicopter is in climb and
2. a scale factor error, which is best seen during the time of the pedal input.

The longitudinal and vertical speed data show some smaller differences. In a second data consistency evaluation, scale factors were estimated. The factors for the angular data stayed at about one. For the speed components, however, scale factors of about 0.9 for the both the longitudinal and vertical speed, and 0.7 for the lateral speed were identified. (Definition: Measurement = Scale factor * Reconstructed Data). Figure 6 compares the obtained reconstructed data with scale factor corrections and the measurements

Table 5 and Table 6 summarize the results obtained from the data consistency analysis conducted be AFDD, DLR, and NLR. Two different cases must be distinguished·

1 Whe all data runs were considered, each run was evaluated separately Then, the mean values and the so called 'practical' standard deviations were calculated from all individual results.
2. When only the suggested four data runs were considered, they were concatenated so that one single result was obtained. Then, the standard deviation given in the table corresponds to the Cramer-Rao lower bound.

Scale factors and their standard deviations are given in Table 5. For the angular measurements they are close to one and indicated a high data consistency between the measurements of the rates and angles. The scale factors for the forward and vertical speed data are about 0.9 and may be acceptable. But for the lateral speed component there are larger deviations from one and a higher standard deviation. This result is in agreement with the visual inspection of Figure 5 and Figure 6.

Table 6 gives the identified biases for the linear accelerations and rates. The small values confirm the reliability of the measurements.

When deficiencies in measured data are detected, the analyst has to decide how to use this information. In the case of the BO 105 speed measurements, the choice could be made to either use the measured or the reconstructed data. On the one hand, the measured data can still provide useful speed information although they may not be fully compatible with the other measured signals (e.g. linear accelerations). On the other hand, compatible reconstructed data can be generated. However, they are derived from the linear accelerometer and vertical gyro signals and therefore transfer errors from these instruments into the calculated speed data.

Both approaches have their advantages and disadvantage. Consequently, different decisions were also made by the Working Group Members. CERT, DLR, and University of Glasgow used the measured data, whereas AFDD, NAE, and NLR replaced the measurements by reconstructed speed data.

5. Identification of 6 degrees of freedom Models

Based on the results from the data consistency analysis of all data files provided to the Working Group, DLR selected eight flight tests for a more detailed evaluation. Working Group Members then concentrated on this smaller common data base to make the obtained identification results better comparable The eight files were divided into two different data sets with four files each:

1. one run with a longitudinal stick control input,
2. one run with a lateral stick control input,
3. one run with a pedal control input,
4. one run with a collective control input.

For the first data set, flight tests with 3211 control inputs were selected to be used for the identification. The second data set with doublet control inputs was suggested for the verification of the obtained identified models. For the 'identification data runs' it was proposed to use the first 27 seconds of each data run.

Identification results obtained from the suggested data runs with 3211 inputs were provided by CERT, DLR, NAE/University of Toronto, Glasgow University, and NLR. AFDD provided results obtained the flight tests with frequency sweep control inputs. In this section, the identification approaches are characterized. Then, the identification results are summarized in the format of tables of derivatives and eigenvalues. Representative time histories and frequency responses are presented for the comparison of measured data and the response of the identified models.

5.1 Identification approaches

All Working Group Members used a coupled six degrees of freedom rigid body model as derived in the Lecture on *Identification Techniques* [6] for the identification. Main differences in the model structures were the treatment of the nonlinear kinematic and gravity terms, the number of derivatives to be identified, and the determination of equivalent time delays. In the following, these topics are discussed in more detail:

- Treatment of the nonlinear kinematic and gravity terms,

  Including nonlinear terms in the state equations requires that the actual model states are used in the nonlinear terms, like the *state variable* Θ in the gravity term $g \cdot \sin\Theta$. Consequently, an identification method is needed that can handle nonlinear state equations in both the estimation of the unknown parameters and the calculation

of the model responses. Such a 'nonlinear method' was only applied by DLR. As most computer codes for system identification are written for linear systems, nonlinear terms have also to be linearized or, as a compromise, so called 'forcing functions' are used. Here, the variables in the nonlinear expressions are taken from the measured data, e g. the *measured* Θ in $g \cdot \sin \Theta$. Then the nonlinear terms can be calculated and are treated like known control inputs (pseudo controls) in the integration of the state equations. This 'forcing function' approach was applied by NAE. All other Working Group Members used fully linearized models.

- Number of derivatives to be identified,

  The definition of an appropriate model structure still is one of the basic and essential problems in system identification. It is present standard in rotorcraft identification to work with linear coupled six degrees of freedom rigid body models. They have proved to be suitable for various applications. The more difficult problem is to decide which parameters in the state equations can be identified or can be neglected or set to a fixed value. The determination of too many unknowns can lead to severe convergence problems in the identification and to high correlations between the individual parameters, causing inaccuracies and large variances in the estimates. When, on the other side, the number of unknowns is reduced and significant parameters are neglected, the model can no longer adequately describe the helicopter dynamics. There is not yet an unique solution to this model structure problem and consequently, the models used for the BO 105 identification in the Working Group ranged from models with almost all parameters included to highly reduced models From totally 60 possible derivatives, NAE identified 58 parameters, whereas in the model of the Glasgow University the number of unknowns was reduced to 30 parameters. In such reduced models, the derivatives that are neglected and not identified are usually set equal to zero or alternatively, are fixed at values obtained from simulation or wind tunnel results. In the Working Group, neglected derivatives were assumed to be zero.

- Determination of equivalent time delays.

  Six degrees of freedom rigid body models show an immediate on-axis (linear and rotational) acceleration response due to control inputs. The helicopter response however is delayed mainly due to the dynamics of the rotor and the hydraulic actuators. To approximate their effects, equivalent time delays for the controls are usually used. This approach has proved to be suitable and can be considered as a reasonable compromise to extending the model order by additional degrees of freedom.

For the evaluation of the BO 105 data base, significantly different identification techniques were applied. Time- and frequency-domain approaches as well as Least Squares and Maximum Likelihood identification criteria were used. In the following, the individual identification approaches are characterized.

5.1.1 Time-domain identification techniques

Most of the WG Members applied time-domain techniques:

CERT

CERT applied a Maximum Likelihood output error technique for the identification of linear models. The proposed four BO 105 data files were concatenated and evaluated without further modifications. The measurement vector (variables to be fitted by the model response) included 11 variables: linear accelerations, speed components, rates, attitude and roll angles. The structure of the linear model was reduced to 35 derivatives to be identified.

DLR

As a first step, equivalent time delays between the control inputs and the on-axis acceleration responses were determined by a cross-correlation technique. The measured control time histories were then shifted by these time delays. For the identification, a Maximum Likelihood method was used that allows the estimation of nonlinear models. Therefore, the kinematic and gravity terms in the state equations were kept nonlinear and calculated from the model response data. The other terms were linear. Based on first identification results, the significant and identifiable derivatives were determined by evaluating the inverse of the information matrix which gives the standard deviations (Cramer-Rao lower bounds) and the correlation between individual parameters. In the final model structure, 38 derivatives were identified.

For the identification, the measured data were used without modifications except for the lateral and vertical speed. For the horizontal flight trim condition, the lateral speed was about 4 m/sec and the vertical speed about -6 m/sec. These values were felt to be unrealistic and therefore, the lateral speed measurements were corrected to a zero value in trim. The 'true' steady state for the vertical speed was reconstructed from forward speed and attitude angle measurements. Such corrections in the initial conditions are necessary for nonlinear models as they use total amplitude values, whereas for linear systems, the steady state is usually subtracted from the measurements so that the data represent only the deviations from trim.

The measurement vector included 14 variables: linear accelerations, speed components, rates, attitude and roll angles, and rotational accelerations. A concatenated run evaluation was used, however for each individual run the initial conditions were fixed at the mean value of the first data points, and offsets in the

controls and most of the measurement variables were identified in form of bias terms.

NAE

Based on the results from the data consistency evaluation, the measured speed data were felt to be inadequate to be used in the identification. Therefore, NAE concentrated on the reconstruction of more reliable speed variables. First, the initial trim conditions for the lateral and vertical speed were determined from forward speed, roll and pitch angles. Then the time histories obtained from the consistency analysis were used in the measurement vector and for the calculation of the forcing functions. A Maximum Likelihood identification method for linear systems was applied. However, the gravity and kinematic terms in the state equations were kept nonlinear. They were calculated using the measured angles and rates as well as the reconstructed speed components and considered as additionally generated time histories and treated like control variables in the control vector ('pseudo controls').

Equivalent time delay values, suggested by DLR, were used to time-shift the measured control variables before the identification was started. The measurement vector included 9 variables: linear accelerations, reconstructed speed components, and rates. A concatenated run evaluation was applied to identify an almost full set of 58 derivatives, where only N_v and $X_{\delta ped}$ were neglected. Offsets in the controls and measurements were taken into account by estimating bias terms for each individual manoeuvre. Theses biases were used for the force and moment state equations as well as for the speed and linear acceleration measurement equations.

NLR

NLR was the only Working Group Member who applied an equation error method or regression analysis. In this technique, each state equation is treated separately and independently. All state and control variables in the considered equation are taken from the measured data and the unknown parameters are determined by fitting the linear and rotational accelerations by a Least Squares criterion. As in principal all terms in the state equations are treated as pseudo controls, it is essential to work with highly accurate data. Therefore, NLR first concentrated on a data reliability analysis although the 'standard' quite complex NLR approach for flight path reconstruction could not fully be applied as some additionally required measurements were not available.

In the identification step, equivalent time delays for the controls were used and then concatenated manoeuvres were evaluated to identify a model with 36 unknown parameters.

5.1.2 Frequency-domain identification techniques

Identification techniques working in the frequency domain were applied by AFDD and the University of Glasgow.

AFDD

As the data consistency analysis revealed a low quality of the airspeed measurements, AFDD decided to use reconstructed speed data for the identification. A key step in the AFDD frequency-domain identification approach is the extraction of high-quality frequency responses between each input/output pair. AFDD experience has shown that flight test data obtained from frequency sweep control inputs are better suited for this approach than multi-step inputs. Consequently, it was concentrated on the evaluation of the BO 105 flight test data obtained from frequency sweep inputs. These manoeuvres could not be flown using only a single control but some activity in the other controls was required to keep the aircraft response within small perturbation assumptions. Therefore, conditioned frequency responses were determined. Making use of the redundant flight tests, the frequency-sweep manoeuvres were concatenated to increase the reliability of the frequency responses. Then, the unknown model parameters of a linear six degrees of freedom state space model and the equivalent time delays were identified by minimising the weighted Least-Squares error between measured and model frequency responses. The weighting was based on the values of the associated coherences at each frequency point.

A total of 26 frequency responses, with 19 frequencies in each, were matched in the identification process (Table 7). The frequency range of fit was selected individually for each response corresponding to its range of good partial coherence. However, the upper frequency was limited to a maximum of 13 rad/s since a 6 degrees of freedom model is not capable of matching lead/lag and body/rotor flapping dynamics. Without this restriction, physically meaningless derivatives can be obtained. A detailed model structure analysis was conducted based on parameter insensitivities, Cramer-Rao bounds, and cost function changes. The final model included 51 identified parameters (47 derivatives and 4 equivalent time delays).

Glasgow University

Glasgow University applied a frequency-domain identification technique, where the time-domain state space model and the measurement equations

$$\dot{\mathbf{x}}(t) = \mathbf{A}\,\mathbf{x}(t) + \mathbf{B}\,\mathbf{u}(t)$$
$$\mathbf{y}(t) = \mathbf{C}\,\mathbf{x}(t) + \mathbf{D}\,\mathbf{u}(t)$$

are transformed to the frequency-domain format

$$j\omega \cdot \mathbf{x}(\omega) = \mathbf{A}\,\mathbf{x}(\omega) + \mathbf{B}\,\mathbf{u}(\omega)$$
$$\mathbf{y}(\omega) = \mathbf{C}\,\mathbf{x}(\omega) + \mathbf{D}\,\mathbf{u}(\omega)$$

where $\mathbf{x}(\omega)$, $\mathbf{u}(\omega)$, and $\mathbf{y}(\omega)$ are the Fourier transformed variables. The control vector $\mathbf{u}(\omega)$ and the matrices **B** and **D** were modified to compensate for non-periodic states [7].

The unknown parameters in the matrices **A**, **B**, **C**, and **D** are then estimated in the frequency domain,

using a Maximum Likelihood criterion. For the identification, the DLR suggested files with modified 3211 control inputs were used as concatenated manoeuvres. The measurement vector included the Fourier transforms of 11 measured variables: linear accelerations, speed components, rates, and attitude and roll angles. 30 derivatives and 4 equivalent time delays were identified. (In frequency-domain approaches it is not necessary to estimate bias terms).

5.2 Identification results

In this section, BO 105 identification results provided by the Working Group Members are presented and discussed in detail. Tables of the derivatives and eigenvalues of the identified models are given and representative plots of time histories and frequency responses are presented for the comparison of measured data and model responses.

Table 8 to Table 11 list the derivative values identified in the Working Group by AFDD, CERT, DLR, Glasgow University, NAE, and NLR. From the tables the detailed model structures can also be seen. In addition to the stability and control derivatives the associated standard deviations are given. These are the values provided by the identification techniques (Cramer-Rao lower bounds) They represent the theoretically lowest achievable standard deviation. It is well known that for practical use these values are usually too small. Therefore it is often recommended to multiply them by a factor of 5 to 10 to make the standard deviations physically more realistic. Depending on the identification approach, the standard deviations were defined slightly differently. Therefore this information is not intended for comparisons between the results from different Members but more as a help to relate the significance of parameters within one set of results to each other.

There are quite large differences between the identification results. Even for significant parameters, like the diagonal terms of the state matrix, which are related to system damping, some major differences are seen. X_u is between -0.05/s and -0.06/s for time-domain results, but -0.03/s to -0.04/s for the frequency-domain methods. Larger Y_v values in the AFDD and NAE results reflect the lateral speed measurement problem. These two Working Group Members used reconstructed data instead of the measurements. In the data consistency analysis, a scale factor of about 0.7 was determined between the reconstructed and measured lateral speed. Consequently, this factor is also seen in the identified Y_v. The heave damping Z_w shows reasonable agreement.

The identification of the pitch and roll damping L_p and M_q is a major problem for the BO 105. The obtained values highly depend on

- the equivalent time delays,
- the bandwidth of the flight test data, and
- the high correlation with the control derivatives.

These dependencies have different influences in the individual estimation techniques, which explains the large variations within the Working Group results. The yaw damping N_r is in reasonable agreement. From the main (on-axis) control derivatives, $Z_{\delta col}$ and $N_{\delta ped}$ agree fairly well. In the roll and pitch moment control derivatives $L_{\delta lat}$ and $M_{\delta lon}$ the larger differences are caused by the high correlation of these terms with L_p and M_q and the associated problems as discussed above. The coupled off-axis derivatives are not discussed in detail. It is seen that there are also some large differences. However, it should be noted that several of these terms also show larger standard deviations indicating less parameter significance.

The equivalent time delays used for the controls are listed in Table 12. These time delays approximate the effects of rotor and hydraulic dynamics. How important it is to include accurate equivalent time delays in six degrees of freedom models is demonstrated by Figure 7. For two major derivatives, the roll damping L_p and the roll control derivative due to lateral stick $L_{\delta lat}$, the figure shows the high sensitivity of the identification results to time delays It is obvious that special care must be taken to accurately determine equivalent time delay values. In the Working Group DLR extracted time delays by a cross-correlation of the acceleration responses from the measurements and the model response. The obtained values were also used by NLR and NAE The frequency-domain method used by AFDD and University of Glasgow allow the direct estimation of equivalent time delays together with the unknown derivatives.

The eigenvalues of the identified models are given in Table 13. A comparison shows that the phugoid and dutch roll modes are in good agreement with slightly higher damping in the AFDD model. The values for the lower frequency aperiodic pitch mode agree satisfactorily, and all Working Group Members identified the spiral mode to be close to the origin. Major differences, however, are seen in the roll and higher frequency pitch modes. They reflect the different values of the roll and pitch damping derivatives.

The comparison of the derivative and eigenvalue results shows that the values obtained by AFDD, DLR, and NAE (and probably University of Glasgow) are relatively close to each other.

As representative example Figure 8 through Figure 12 show a full set of time-history plots for the comparison of flight test measurements and the response of the DLR identified model for all four data runs used for the identification. It demonstrates that a good agreement was obtained for all variables. From the time histories provided by CERT, University of Glasgow, and NAE the pitch and roll rate responses for the flight tests with longitudinal or lateral stick control inputs are presented in Figure 13 and Figure 14. Some representative results obtained from the AFDD frequency-domain method are given in the format of frequency response fits in Figure 15 and Figure 16.

6. Verification of the Identified Models

The verification of the identified models is a key step in the identification process that assesses the predictive quality of the extracted model. Flight data not used in the identification are selected to ensure that the model is not tuned to specific data records or input forms. In the Working Group, identification results were generated from flight tests with multistep 3211 or frequency-sweep control inputs. Therefore, doublet inputs for each control were used for model verification and comparison.

All Members applied a very similar approach to calculate the responses of the identified models: All model coefficients were fixed and only biases were estimated to account for control and measurement offsets. In all cases, the model was only driven with the measured control variables and no pseudo controls were used. As DLR and NAE worked with a nonlinear model in the identification, the same model was also used for the verification (nonlinear terms were calculated from model states).

Corresponding to the presentation of time-history fits in the previous section on identification results, Figure 17 through Figure 21 compare the time history response predictions of the DLR identified model for all observation variables and for all four doublet control inputs. From the verification results provided by AFDD, CERT, Glasgow University, NAE, and NLR the pitch and roll rate responses due to longitudinal and lateral stick inputs are given in Figure 22 through Figure 24 (for completeness, the DLR result is repeated in the same format). From the complete set of results in Figure 17 through Figure 21 it is seen that the predictive capability of the identified model is very good in both the on- and off-axis response, especially considering the dynamically-unstable and highly-coupled nature of the BO 105. The differences seen in the speed data, and here in particular in the lateral speed, are due to measurement problems. Although there are also some smaller differences in the other variables, the overall agreement is very satisfactory

A first comparison of the verification plots in Figure 22 through Figure 24 demonstrates that basically all model responses match the measured data fairly well. The lower frequency modes (phugoid and pitch) are in good agreement for all models. A closer comparison reveals some larger differences for the time history segments where the doublet control inputs were given. Some models are more damped or the coupling between the pitch and roll motion is less accurate. The fact, however, that none of the models can fully reach the maximum peak amplitudes of the rates demonstrates that six degrees of freedom models cannot describe this higher frequency range completely. It is obvious that a further improvement of the model prediction can only be reached when the model order is extended by additional degrees of freedom, like rotor or inflow dynamics.

7. Discussion of Results

In the list of derivatives (Table 8 to Table 11) and eigenvalues (Table 13) it was seen that the identified values varied significantly. A decision for the more suitable model can only be made on the basis of a comparison between the model responses and the flight test data for both the identification and the verification plots. Therefore, a more detailed evaluation was conducted It also included all frequency-response and time-history fits, which, for space reasons, cannot all be given within this Lecture. It was concluded that the models obtained by AFDD, DLR, NAE, and, with some more deviations, the model from the University of Glasgow showed the more satisfactory overall agreement with the measurements.

The importance of accurate equivalent time delays has already been addressed. The identified values provided by AFDD and DLR (Table 12) are in good agreement, except for the value for the collective control, where larger differences are seen. The DLR time-domain approach for extracting time delays is based on evaluating the cross-correlation of the on-axis (linear or angular) accelerations. The frequency-domain method searches for a time delay in conjunction with the other model parameters that will produce the best match of all of the responses. The use of a single time delay for each input imposes the assumption that all input/output response pairs have the same high-frequency zeros, and thus the same high-frequency phase shift. This corresponds to modelling the rotor response as an actuator. When this assumption is valid, the two methods should produce essentially the same time delays, as they do for the lateral, longitudinal, and pedal inputs. However, this assumption is not acceptable for the collective inputs. Further frequency-domain analyses indicated an effective time delay of about 93 ms for linear responses (u, w, a_z) to collective, but a much larger effective time delay of about 255 ms for angular responses (p, q). The time-domain method reflects the vertical acceleration delay, while the frequency-domain result reflects an average delay. In conclusion, it can be stated that for the collective control a single time delay value is only a poor compromise in characterizing all of the responses. However, a better approach either requires the use of different time delays for each control and each response axis or a higher-order dynamic model is needed.

As a further help for the evaluations of the results, three additional sets of identified derivatives were considered. They were not produced within the Working Group but they were obtained from the same BO 105 data base. These models were extracted by DLR (frequency-domain technique, similar to the University of Glasgow approach; [7]), by Stanford University, USA (a newly developed identification algorithm based on smoothing; [8]), and by Tech-

nische Hochschule Darmstadt, Germany (equation error technique; [9]). Both, the DLR frequency-domain results and the results from Stanford University are in good agreement with the AFDD, DLR, and NAE identified derivatives and eigenvalues and confirm the reliability of the models. All these results have in common, that they were obtained by quite complex identification methods although the individual approaches are very different. Another link between AFDD, DLR, and NAE is their high involvement in rotorcraft system identification since a long time. It is well known and accepted that system identification still is a relatively difficult task and that a successful application requires the analyst's skill and experience. The previously gained experience in these organisations has also certainly been helpful for the BO 105 identification.

The results from the Technische Hochschule Darmstadt are in a very good agreement with the NLR identified values. Both approaches are based on less complicated equation error techniques. In comparison with the more complex iterative methods such techniques are computationally very efficient with respect to computing time and storage requirements. From the obtained results it can be stated that equation error methods are appropriate for the rotorcraft identification when models of lower accuracy can be accepted. Such models are certainly useful for various applications, which may not justify the significantly higher efforts and costs for the extraction of more accurate models by more sophisticated methods.

To give an impression of what system identification can do in comparison to a computational simulation, the measured 3211 control inputs for the longitudinal and lateral stick were used in the DLR simulation program SIMH [10]. The obtained rate responses are compared to the measured time histories in Figure 25. In the figure, the same data section is given for the comparison of the identified (DLR) model response and the measurements.

8. Identification of Extended Models

The Working Group concentrated on the identification of 6 degrees of freedom rigid body models. Such models are useful for various applications. For applications like high-bandwidth control system design, however, they are often no longer appropriate and models with rotor degrees of freedom may be required. The need for such models was discussed in the Working Group and is addressed in the application oriented Lectures on *Flying Qualities Evaluations* [11] and *Flight Control System Optimisation* [12]. It was however beyond the scope of the Group to work on a more detailed study about the identification of higher order models. Therefore, in the following, some representative results from the identification of an extended model are shown that were obtained from a DLR Maximum Likelihood technique working in the frequency domain [13]. A more detailed presentation of the results is given in [14]

6 degrees of freedom models are based on the assumption that the rotor dynamics are at much higher frequencies than the body modes. The steady state rotor influence is absorbed into the rigid body derivatives and the higher frequency dynamics are neglected Such models assume an instantaneous tilt of the rotor tip path plane in response to a control input, and consequently predict an immediate helicopter angular acceleration: the model response leads the real helicopter response Only when rotor dynamics are additionally approximated by equivalent time delays for the controls a more realistic model response is obtained This approach was also used in the Working Group. Figure 26 shows the data segment when the lateral control input was given. The comparison of the model responses demonstrates the improvement obtained from the use of equivalent time delays. The oscillation which is mainly seen at the end of the time history plot is caused by the rotor lead/lag motion that cannot be described by 6 degrees of freedom models.

Models with a more accurate representation of the higher frequency characteristics were needed for the development of the DLR BO 105 in-flight simulator ATTHeS (Advanced Technology Testing Helicopter System). The design of the feedforward controller in the model following control system (MFCS) is based on the inverted BO 105 model Inversion of the equivalent time delays however physically means time 'lead': future values of the state variables are needed which is impossible for an on-line real time process like in-flight simulation. The identified equivalent time delays for the 6 degrees of freedom BO 105 model ranged from 40 milliseconds for the pedal up to about 100 milliseconds for the longitudinal stick and collective. Neglecting these delays leads to drastic errors in the MFCS [2]. Clearly, the rigid body models must be extended by an explicit representation of the rotor dynamics effects. Therefore, a first extended model was defined using pitch and roll accelerations as state variables [2]. This approach gives a good and valid approximation of the rotor influence, in particular in the roll motion. The identified 8 degrees of freedom model was used successfully for the controller design and has helped to improve the in-flight simulation performance significantly [15], [16]. This experience also demonstrated that there is a strong need for models with a more reliable description of the initial response characteristic than the conventional 6 degrees of freedom models can provide. A logical consequence is the identification of models with rotor degrees of freedom. It implies, however, that measurements of the blade motions are required.

8.1 Rotor data

The original DLR BO 105 data base included measurements of the flapping motion for each blade and

the rotor azimuth. (As the Working Group concentrated on 6 degrees of freedom models, these data were not provided to the Group) The measurements and data processing are described in the Lecture on *Instrumentation and Data Processing* [17]. For the use in system identification the measured data were transformed to the nonrotating axis system to describe the tip-path plane motion in terms of coning, longitudinal and lateral flapping.

8.2 Identification result

The basic approach for extending the conventional 6 degrees of freedom rigid body model formulation by rotor degrees of freedom is illustrated in Figure 27. The state vector of the rigid body motion is extended by tip path plane variables. Then, the model structure includes two sets of equations representing the fuselage and the rotor characteristics. The submatrices characterise the rigid body and rotor behavior and the associated couplings. In comparison to the conventional model this structure is closer to reality and can provide a more detailed insight into the helicopter dynamics. However, an increase in model size also implies an increase of unknown parameters and makes the identification more difficult. Problems related to convergence of the method, correlation of the parameters, insufficient information content, etc become more evident. A detailed model structure analysis is necessary to reduce the number of unknowns so far as physically meaningful. Derivatives in the 6 degrees of freedom model that mainly include rotor effects can be eliminated from the fuselage equations as the rotor is now explicitly modeled. The development of an adequate model structure, however, is still a major research task. A first approach to extend the rigid body models by rotor states was presented in [18]. Here, in a so called 'hybrid formulation', highly reduced rotor equations for the regressive flapping mode and an approximation for the lead/lag effects were used. As intended, this formulation predicted an accurate high frequency response of the tip path plane. However, significant errors in the lower frequency range of the rotor response must be accepted.

The DLR approach tried to identify all parameters needed in the rotor equations to represent the total coning and flapping rotor response. Two different model structures were investigated [14]. The best results were obtained from a model where in addition to the rigid body motion, the rotor was represented by linear differential equations for

- coning (a_0) as 2nd order system,
- longitudinal flapping (a_1) as 2nd order system,
- lateral flapping (b_1) as 2nd order system, and
- an approximation of the lead/lag motion as 2nd order transfer function.

The model has 9 degrees of freedom and is of 16th order (including the lead/lag approximation). The measurement equations included the rigid body variables

- linear accelerations and speed components,
- rates and attitude angles,

and the rotor variables,

- coning, longitudinal and lateral flapping, and
- differentiated coning, longitudinal and lateral flapping.

Control variables were the four helicopter controls: longitudinal and lateral stick, collective, and pedal. No use was made of pseudo control inputs, where measured states are treated as controls. In comparison to the 6 degrees of freedom model structure some major changes were made, in particular:

1. As the rotor degrees of freedom are explicitly modeled, no equivalent time delays are needed to approximate rotor dynamics. This is very important for the design of the feedforward controller in the model following control system.
2. The roll and pitch damping derivatives L_p and M_q were neglected in the fuselage equations.
3. Longitudinal and lateral stick and collective control derivatives were eliminated from the fuselage equations and only used in the rotor equations.
4. The fuselage equations were extended by rotor state derivatives to represent the fuselage/rotor coupling.

Making use of the rotor symmetry, some parameters in the rotor equations were constrained to the same identified value (e.g. rotor flapping damping). Known rotor terms that depend upon inertia parameters were fixed. (The structure of the identified models can be seen in Table 14).

Figure 28 presents the obtained identification result for the roll rate, roll acceleration, and lateral flapping responses. The comparison to Figure 26, where the same data segment was shown, illustrates the improved agreement with the measured data. This is also true for the representation of the lead/lag motion.

The complete set of rotor response time histories due to the three main rotor controls is given in Figure 29 for three runs with longitudinal and lateral stick and collective inputs. The fit with the measured data is excellent for the total data length. Some smaller deviations in the coupled responses (mainly in coning) are acceptable.

To visualize the stepwise improvements of the various models, Figure 30 shows the roll rate due to lateral stick frequency responses for the flight test measurements and three different models: two 6 degrees of freedom models (without and with equivalent time delays), and the model with rotor degrees of freedom As expected, the lower frequency range is accurately described by all models. Main differences however are seen for frequencies higher than about 1 Hz. Here, the improvement obtained from the extended model

is obvious. Both amplitude and phase are in good agreement with the measurements up to frequencies of about 3 Hz, which is practically the limit of the information content that can be obtained from pilot flown input signals. (The peak in the amplitude at about 2.3 Hz is caused by the lead/lag motion).

The identified extended model is given Table 14 and Table 15. The obtained eigenvalues are presented in Table 16 together with the eigenvalues from the DLR 6 degrees of freedom model (see also Table 13) A comparison shows that the eigenvalues associated with the rigid body motion stay practically the same (phugoid, dutch roll, spiral and pitch) Higher frequency modes that are neglected or approximated in 6 degrees of freedom models are now included in the extended model: Regressive and advancing flap, roll/flap coupling, and coning. The identified values are physically realistic and characteristic for the BO 105 dynamics. Of course, the high frequency eigenvalues for advancing flapping can be questioned as the data cannot provide useful information for frequencies of about 100 rad/second.

9. Conclusions

BO 105 flight test data specifically generated for system identification purposes were provided to the Working Group. Flight test trim condition was horizontal flight at 80 knots forward speed.

Results obtained from data consistency analysis, identification, and verification were provided by AFDD, CERT, DLR, University of Glasgow, NAE, and NLR The identification approaches included frequency- and time-domain techniques with identification criteria ranging from Least-Squares equation error to Maximum Likelihood output error. Data consistency results proved that the measurement quality was appropriate for system identification. Typical for all aircraft and particularly for helicopters, some inconsistencies were seen in the speed data. Therefore, some Members decided to work with reconstructed speed data instead of the measurements.

Six degrees of freedom derivative models were identified. The comparison of the obtained identification results showed quite large differences in both the identified derivatives and the eigenvalues. This is also true for significant derivatives like the diagonal terms in the state matrix associated to system damping. A more detailed evaluation of all identification and verification results showed that the more complex identification methods, like Maximum Likelihood and Frequency-Response Matching Techniques, gave similar results and provided a good time history agreement with the measurements. Still remaining deficiencies were seen for the higher frequency dynamics. Here, it is evident, that six degrees of freedom models are well suited for the lower- and mid-frequency range where rotor dynamics can be approximated by equivalent time delays. For the higher frequency range, however, the helicopter models must be extended by rotor degrees of freedom

For applications that need a suitable overall system characterization but do not require higher accuracies, less complex but computationally more efficient identification methods, like equation error techniques, are applicable and useful.

First identification results of a model with rotor degrees of freedom were presented. The identified 16th order model (with a second order flapping and coning representation and a second order lead/lag motion approximation) showed excellent agreement between measurements and model response in a wide frequency range. In comparison to 6 degrees of freedom models, a significant improvement of the model accuracy for higher frequencies was obtained. The extraction of higher order helicopter models including rotor degrees of freedom is feasible when appropriate flight test data are available. The obtained results are certainly promising and motivate to continue the identification of extended rotorcraft models for applications that require more accurate models. Future work should concentrate on a more refined model structure and on flight test inputs that can still increase the data information content for the high frequency rotor data.

In conclusion, it can be stated that the BO 105 identification results demonstrate that system identification is a potential tool for extracting reliable helicopter models from flight test data. Depending on the applied evaluation techniques, different accuracy levels for the results are reached. Therefore, it is advisable to establish a close contact between the analyst and the user of the results before system identification is conducted. Then, a reasonable compromise can be defined between the user's application oriented model accuracy needs and the efforts and costs of the identification analysis.

10. Bibliography

[1] Anon.
Rotorcraft System Identification
AGARD Advisory Report AR 280, 1991

[2] Kaletka, J.; von Grunhagen, W.
Identification of Mathematical Models for the Design of a Model Following Control System
45th Annual Forum of the American Helicopter Society, May 1989

[3] Kaletka, J.; Tischler, M.B ; von Grunhagen, W.; Fletcher, J.W.
Time- and Frequency Identification and Verification of BO 105 Dynamic Models
15th European Rotorcraft Forum, September 1989

[4] Fletcher, J.W.
Obtaining Consistent Models of Helicopter Flight-data Measurement Errors Using Kinematic-compatibility and State-reconstruction methods
46th Annual Forum of the American Helicopter Society, May 1990

[5] Bach, R. E. Jr.,
State Estimation Applications on Aircraft Flight-data Analysis (a User's Manual for SMACK),
NASA Ames Research Center, May, 1984

[6] de Leeuw, J H.
Identification Techniques
AGARD LS 178, Paper 5, 1991

[7] Fu, K.-H.; Marchand, M.,
Helicopter System Identification in the Frequency Domain
9th European Rotorcraft Forum, September 1983

[8] Idan, M.
An Identification Algorithm Based on Smoothing
Dissertation, Department of Aeronautics and Astronautics, Stanford University, USA, 1990

[9] Gerlach, R.
Parameterschätzung eines zeitkontinuierlichen Hubschraubermodells
Studienarbeit Nr.I/1632, Institut für Regelungstechnik, TH Darmstadt, Germany, 1991, (in German)

[10] von Grunhagen, W,.
Modellierung und Simulation von Hubschraubern
DLR Institute Report IB 111 88/06, 1988 (in German)

[11] Tischler, M.B.
Application Areas of System Identification. Flying Qualities Evaluation
AGARD LS 178, Paper 13, 1991

[12] Tischler, M.B.,
Application Areas of System Identification Flight Control System Optimisation
AGARD LS 178, Paper 14, 1991

[13] Marchand, M.; Fu, K.H.
Frequency-Domain Parameter Estimation of Aeronautical Systems without and with Time Delay
7th IFAC Symposium, 1985

[14] Fu, K.H.; Kaletka, J.
Frequency-Domain Identification of BO 105 Derivative Models with Rotor Degrees of Freedom
16th European Rotorcraft Forum, 1990 (also: 47th Annual Forum of the American Helicopter Society, 1991)

[15] Bouwer, G.; Pausder, H.-J.; von Grunhagen, W.
Experiences with High Authority Helicopter Fligh Control
16th European Rotorcraft Forum, 1990

[16] Pausder, H.-J.; Bouwer, G.; von Grünhagen, W.
ATTHeS In-Flight Simulation for Flying Qualities Research
International Symposium on In-Flight Simulation for the 90's, DLR Braunschweig, 1991

[17] Kaletka, J.
Instrumentation and Data Processing
AGARD LS 178, Paper 3, 1991

[18] Tischler, M.B.; Gauflman, M.G.
Frequency-Response Method for Rotorcraft System Identification with Application to the BO 105 Helicopter
46th Annual Forum of the American Helicopter Society, 1990

Tables

Overall dimensions		**Main rotor**		**Tail rotor**	
Overall Length	11 84 m	Diameter	9.824 m	Diameter	1.9 m
Fuselage Length	8.45 m	Blades	4	Blades	2
Overall Height	3 03 m	Chord	0.27 m	Chord	0 179 m
		Profile	NACA 23012	Profile	NACA 0012
		Blade Area	5.31 m^2	Solidity	0.12
Mass and moments of inertia		Solidity (Thrust)	0.07	Twist	0 0°
Mass	2200 kg	Tip Sweep	0°	**Horizontal stabilizer**	
I_x	1433 kg m^2	Twist	−6 2°	Span	2.0 m
I_y	4973 kg m^2	Shaft Angle	−3.0°	Chord	0.4 m
I_z	4099 kg m^2			Area	0.8 m^2
I_{zx}	660 kg m^2			Profile	NACA 0010/0020
				Incidence	0°

Table 1. List of physical characteristics of the BO 105

Control Input				Number of runs	Recording time per run in s	Flight Conditions	
Control	Type	Initial displacement	Duration t_i or Frequency content f_i			Airspeed	Altitude
Longitudinal	Doublet	Aft	$t_i \approx 2$s	2	29 ... 32	80 kn	$H_p \approx 3000$ ft
Longitudinal	Doublet	Forward	$t_i \approx 2$s	2	26 ... 28	80 kn	$H_p \approx 3000$ ft
Lateral	Doublet	Right	$t_i \approx 2$s	2	20 ... 26	80 kn	$H_p \approx 3000$ ft
Lateral	Doublet	Left	$t_i \approx 2$s	2	19 ... 26	80 kn	$H_p \approx 3000$ ft
Pedal	Doublet	Right	$t_i \approx 2$s	2	15 ... 27	80 kn	$H_p \approx 3000$ ft
Pedal	Doublet	Left	$t_i \approx 2$s	2	17 ... 18	80 kn	$H_p \approx 3000$ ft
Collective	Doublet	Up	$t_i \approx 2$s	2	19 ... 32	80 kn	$H_p \approx 3000$ ft
Collective	Doublet	Down	$t_i \approx 2$s	2	20 ... 32	80 kn	$H_p \approx 3000$ ft
Longitudinal	Modified 3211	Aft	$t_i \approx 7$s	3	12 ... 24	80 kn	$H_p \approx 3000$ ft
Longitudinal	Modified 3211	Forward	$t_i \approx 7$s	3	25 ... 32	80 kn	$H_p \approx 3000$ ft
Lateral	Modified 3211	Right	$t_i \approx 7$s	3	27 ... 37	80 kn	$H_p \approx 3000$ ft
Lateral	Modified 3211	Left	$t_i \approx 7$s	3	19 ... 31	80 kn	$H_p \approx 3000$ ft
Pedal	Modified 3211	Right	$t_i \approx 7$s	3	25 ... 28	80 kn	$H_p \approx 3000$ ft
Pedal	Modified 3211	Left	$t_i \approx 7$s	3	26 .. 34	80 kn	$H_p \approx 3000$ ft
Collective	Modified 3211	Up	$t_i \approx 7$s	3	24 ... 29	80 kn	$H_p \approx 3000$ ft
Collective	Modified 3211	Down	$t_i \approx 7$s	3	23 ... 36	80 kn	$H_p \approx 3000$ ft
Longitudinal	Frequency sweep	---	$0.08\text{Hz} \le f_i \le 8\text{Hz}$	3	68	80 kn	$H_p \approx 3000$ ft
Lateral	Frequency sweep	---	$0.08\text{Hz} \le f_i \le 7\text{Hz}$	3	68	80 kn	$H_p \approx 3000$ ft
Pedal	Frequency sweep	---	$0.08\text{Hz} \le f_i \le 5.5\text{Hz}$	3	68	80 kn	$H_p \approx 3000$ ft
Collective	Frequency sweep	---	$0.08\text{Hz} \le f_i \le 7\text{Hz}$	3	68	80 kn	$H_p \approx 3000$ ft

Aircraft mass: ≈2200 kg.

Aircraft inertias (manufacturer's estimates) based on 2200 kg and referred to body axes with origin in CG appropriate to tests flown:

$I_x \approx 1700\ \text{kg m}^2$, $I_y \approx 4200\ \text{kg m}^2$, $I_z \approx 4200\ \text{kg m}^2$, $I_{zx} \approx 0\ \text{kg m}^2$

The altitude given is the density altitude. H_p. The actually flown pressure altitude was 4400 ft (at -5°C) $\le H_p \le$ 5200 ft (at -13°C).

Table 2. List of BO 105 data runs provided to the Working Group

Variables		Source	Original Sampling Rate (in Hz)
Group	Quantity		
Control displacements	Forward/Aft Cyclic	Potentiometer	50
	Lateral Cyclic	Potentiometer	50
	Pedal	Potentiometer	50
	Collective	Potentiometer	50

Table 3. Measured BO 105 control variables

Variables		Source	Original Sampling Rate (in Hz)
Group	Quantity		
Air data	Longitudinal airspeed	HADS	50
	Lateral airspeed	HADS	50
	Normal airspeed	HADS	50
Linear accelerations	Longitudinal acceleration	Accelerometer at CG	300
	Lateral acceleration	Accelerometer at CG	300
	Normal acceleration	Accelerometer at CG	300
Attitude angles (Euler angles)	Roll angle	Vertical gyro	50
	Pitch angle	Vertical gyro	50
	Yaw angle	Directional gyro	50
Angular rates	Roll rate	Rate gyro	100
	Pitch rate	Rate gyro	100
	Yaw rate	Rate gyro	100
Rotor	RPM	Tachometer	50

Table 4. Measured BO 105 response variables
Data provided at a uniform sampling rate of 100 Hz.

Scale factor for		AFDD *		DLR *		DLR **		NLR ***	
Symbol	Unit	Value	σ	Value	σ	Value	σ	Value	σ
u	1	0 9556	0.0272	0 9956	0.0104	0.9244	0.0027†	---	---
v	1	0.7043	0.0524	0.6723	0.0955	0.6932	0.0082†	---	---
w	1	0 8751	0 0378	0.9521	0.0913	0.9283	0.0039†	---	---
Φ	1	1 0199	0 0126	1.0144	0.0177	1.0168	0.0005†	---	---
Θ	1	1.0290	0.0352	1.0364	0.0281	1.0351	0 0004†	---	---
Ψ	1	---	---	1.0202	0 1371	1 0392	0 0016†	---	---

* From all files
** From 4 concatenated files proposed for identification
*** From 4 files proposed for identification
† Cramer Rao lower bound

σ = Standard deviation

Table 5. BO 105 data consistency analysis: Mean values of identified scale factors

Bias for		AFDD *		DLR *		DLR **		NLR ***	
Symbol	Unit	Value	σ	Value	σ	Value	σ	Value	σ
a_x	m/s^2	---	---	0 0571	0.1130	0 0194	0.0027†	0 0243	0.0028†
a_y	m/s^2	---	---	0 0443	0.1096	0.0157	0 0047†	0 0016	0.0029†
a_z	m/s^2	---	---	0.0007	0 0456	0 0463	0 0023†	0 0145	0 0023†
p	rad/s	-0 0015	0 0002	-0.0015	0.0005	-0 0013	0.0002†	-0.0015	0.0001†
q	rad/s	-0 0017	0 0002	-0.0016	0 0005	-0.0014	0 0001†	-0 0019	0.0001†
r	rad/s	---	---	-0.0005	0.0019	-0 0002	0 0004†	-0.0011	0 0001†

* From all files
** From 4 concatenated files proposed for identification
*** From 4 files proposed for identification
† Cramer Rao lower bound

σ = Standard deviation

Table 6. BO 105 data consistency analysis: Mean values of identified biases

Compo-nents	Motivator deflections			
	δ_{ton}	δ_{lat}	δ_{ped}	δ_{col}
u	*	*	*	*
v		*	*	
w	*	*		*
p	*	*	*	*
q	*	*	*	*
r	*	*	*	
a_x	*			
a_y	*	*	*	
a_z	*			*

State vector:

$[u\ v\ w\ p\ q\ r\ \Phi\ \Theta]^T$

Mesurement vector·

$[u\ v\ w\ p\ q\ r\ a_x\ a_y\ a_z]^T$

Number of frequencies: 19

Weight: 7 570 deg-error/dB-error

* indicates an input/output frequency response included in the identification cost function

Table 7. Set-up for AFDD frequency-domain identification

Derivative		AFDD		CERT		DLR		Glasgow Uni		NAE		NLR	
Symbol	Unit	Value	σ	Value	σ	Value	σ	Value	σ	Value	σ	Value	σ
X_u	1/s	-0.0385	0 0036	-0 058	0 0014	-0 059	0 0006	-0 032	0 0044	-0 050	0 0094	-0 050	0 0008
X_v	1/s	0 *	---	0 *	---	0 *	---	0 *	---	0 0043	0 0021	0 *	---
X_w	1/s	-0.061	0 0094	0 025	0 0027	0 036	0 0013	-0 0422	0 0064	-0 017	0 002	0 015	0 0014
X_p	m/(rad s)	0 756	0.120	0 *	---	0 *	---	0 *	---	0 479	0 058	0 *	---
X_q	m/(rad s)	2 548	0.273	0 *	---	0 *	---	0 *	---	1 206	0 072	0 *	---
X_r	m/(rad s)	0 *	---	0 *	---	0 *	---	0 *	---	0 232	0 019	0 *	---
Y_u	1/s	0 *	---	0 *	---	0 *	---	0 *	---	-0.061	0 0021	0 *	---
Y_v	1/s	-0 221	0.011	-0.177	0.003	-0.170	0.003	-0 131	0.055	-0.279	0 005	-0 064	0 003
Y_w	1/s	-0.083	0.007	0 *	---	0 *	---	0 *	---	-0.0307	0 0051	0 *	---
Y_p	m/(rad s)	-2.030	0 251	0 *	---	0 *	---	0 *	---	-2.993	0.138	0 *	---
Y_q	m/(rad s)	4.823	0.263	0 *	---	0 *	---	0 *	---	3 021	0.164	0 *	---
Y_r	m/(rad s)	0.950	0.139	0 *	---	1.332	0 045	0 *	---	0 807	0 041	1.191	0.241
Z_u	1/s	0 2457	0 018	0 222	0.006	0 014	0 0034	-0 0883	0 0087	0.1016	0 0063	0 0204	0 0033
Z_v	1/s	0 *	---	0 *	---	0 *	---	0 *	---	-0.135	0 012	0 *	---
Z_w	1/s	-1.187	0 0555	-1 171	0 012	-0.998	0 0072	-0 791	0 0178	-1.106	0 013	-0 875	0 0058
Z_p	m/(rad s)	2 622	0.359	0 *	---	0 *	---	0 *	---	0 385	0.29	0 *	---
Z_q	m/(rad s)	7 011	1 133	0 *	---	5 012	0 28	0 *	---	7 011	1 711	0 *	---
Z_r	m/(rad s)	0 *	---	0 *	---	0 *	---	0 *	---	0 27	0 096	0 *	---

* Eliminated from model structure
σ = Standard deviation

Table 8. BO 105 identification results: List of specific force derivatives with respect to flight variables

Derivative		AFDD		CERT		DLR		Glasgow Uni		NAE		NLR	
Symbol	Unit	Value	σ	Value	σ	Value	σ	Value	σ	Value	σ	Value	σ
L_u	rad/(s m)	-0 061	0 0077	-0 014	0 0008	-0.081	0 0016	-0 027	0 0036	-0 099	0 0032	-0 012	0 0019
L_v	rad/(s m)	-0.207	0 021	-0.092	0 0019	-0.271	0 004	-0 096	0 0090	-0 270	0.0071	-0 038	0 0028
L_w	rad/(s m)	0.168	0 014	0 038	0 0028	0.116	0 0035	0.130	0 0095	0 116	0.007	0 028	0.0048
L_p	1/s	-8.779	0.641	-2.693	0 056	-8.501	0 110	-4 470	0 392	-7 048	0.201	-1 995	0 114
L_q	1/s	3 182	0 624	1.558	0 090	3.037	0 125	0 *	—	4 454	0 222	0 558	0 171
L_r	1/s	0 991	0 187	1.321	0 029	0 410	0 036	1.318	0 14	0.434	0 055	1 221	0.057
M_u	rad/(s m)	0 *	—	0 0115	0 0002	0 029	0 0004	0 0203	0 0005	0.0078	0.001	0 0144	0 001
M_v	rad/(s m)	0 050	0 0034	0 025	0 0006	0 048	0 0012	0 *	—	0 0248	0 0024	0 0039	0 0015
M_w	rad/(s m)	0 096	0 0064	0 356	0.0006	0 053	0 0011	0 0491	0 0011	0 0696	0 0022	0 0186	0 0026
M_p	1/s	-0 998	0.066	-0.491	0 0152	-0 419	0 038	-1 367	0 032	-1 414	0 066	-0.878	0 062
M_q	1/s	-4.493	0.235	-2 26	0 025	-3.496	0 047	-2.217	0 009	-2.992	0 074	-1 441	0 093
M_r	1/s	-0 438	0 052	0 *	—	-0.117	0 013	0 *	—	-0 584	0 019	0 *	—
N_v	rad/(s m)	0 082	0 0049	0 102	0 0009	0.117	0 0012	0 0784	0 0045	0 112	0 0017	0 051	0 0016
N_w	rad/(s m)	-0 119	0 009	0 0025	0 001	0 034	0 006	0 0281	0 008	-0.0634	0 003	0 0195	0 002
N_p	1/s	-0.466	0 15	-1 116	0 025	-1 057	0 025	-1.302	0 017	-0 692	0.061	-1 958	0 06
N_q	1/s	5.432	0 292	0.491	0 029	0 809	0 016	0.959	0 231	3 294	0 107	1 227	0 071
N_r	1/s	-1 070	0.061	-1.116	0.0126	-0.858	0 0068	-0.756	0 0640	-1.017	0.0234	-0 699	0.0347

* Eliminated from model structure
σ = Standard deviation

Table 9. BO 105 identification results: List of specific moment derivatives with respect to flight variables

Derivative		AFDD		CERT		DLR		Glasgow Uni		NAE		NLR	
Symbol	Unit	Value	σ	Value	σ	Value	σ	Value	σ	Value	σ	Value	σ
$X_{\delta col}$	m/(s^2 %)	-0 046	0 004	0 *	—	0 *	—	0 *	—	-0 0222	0.001	0 *	—
$X_{\delta lon}$	m/(s^2 %)	-0 072	0 0045	-0 048	0 0029	-0 028	0 0015	-0 048	0 0016	-0.050	0 0014	-0.027	0 0019
$X_{\delta lat}$	m/(s^2 %)	0 *	—	0 *	—	0 *	—	0 *	—	-0.00176	0 001	0 *	—
$Y_{\delta col}$	m/(s^2 %)	-0.032	0 0031	0 *	—	0 *	—	0 *	—	-0.0152	0 0023	0 *	—
$Y_{\delta lon}$	m/(s^2 %)	0 *	—	0 *	—	0 *	—	0 *	—	-0 0253	0 0032	0 *	—
$Y_{\delta lat}$	m/(s^2 %)	0.066	0 0051	-0 001	0.0015	0 003	0 0013	0 0764	0 0094	0 0705	0 0024	-0 0006	0 0024
$Y_{\delta ped}$	m/(s^2 %)	0 015	0.0039	-0 009	0.0018	-0 011	0.0017	-0.071	0.0425	-0 0274	0 0013	-0.014	0.0032
$Z_{\delta col}$	m/(s^2 %)	-0.388	0 020	-0 273	0 003	-0 349	0 002	-0.259	0 021	-0.337	0 005	-0 242	0 003
$Z_{\delta lon}$	m/(s^2 %)	-0.103	0 0288	-0.0078	0 0041	-0.303	0 008	-0.140	0.0492	-0.175	0 0073	-0.075	0 008
$Z_{\delta lat}$	m/(s^2 %)	0 *	—	0 *	—	0 *	—	0 *	—	0.029	0 0052	0 *	—
$Z_{\delta ped}$	m/(s^2 %)	0 *	—	0 *	—	0 *	—	0 *	—	-0.0059	0 003	0 *	—

* Eliminated from model structure
σ = Standard deviation

Table 10. BO 105 identification results: List of specific force derivatives with respect to control variables

Derivative		AFDD		CERT		DLR		Glasgow Uni		NAE		NLR	
Symbol	Unit	Value	σ	Value	σ	Value	σ	Value	σ	Value	σ	Value	σ
$L_{\delta col}$	rad/(s^2 %)	0 058	0.005	0 0044	0 0012	0 032	0 0011	0 *	---	0.0142	0 003	0 022	0 007
$L_{\delta lon}$	rad/(s^2 %)	0 073	0 0064	-0 0028	0 0016	0 024	0 0025	0 *	---	-0 005	0 0044	0 0301	0 0045
*$L_{\delta lat}$	rad/(s^2 %)	0 179	0 0139	0 0551	0 0009	0 185	0 0023	0 0764	0.0094	0 1361	0 0036	0 0534	0 0024
$L_{\delta ped}$	rad/(s^2 %)	-0 027	0 0045	-0 018	0 0009	-0 028	0 001	-0 0209	0 0046	-0 0172	0 0017	-0 0096	0 0021
$M_{\delta col}$	rad/(s^2 %)	0 073	0 0034	0 034	0 0004	0 057	0 0006	0 039	0 0012	0.048	0 0010	0 032	0 0016
$M_{\delta lon}$	rad/(s^2 %)	0 098	0 0043	0 050	0 0016	0 093	0 001	0 0565	0 0020	0 0787	0 0015	0.054	0 0025
$M_{\delta lat}$	rad/(s^2 %)	0 *	—	-0.0003	0 0003	-0 009	0 0008	0 *	—	0 0106	0 0013	0 005	0 0013
$M_{\delta ped}$	rad/(s^2 %)	0 013	0 0017	0 *	—	0 *	—	0 *	—	0 005	0 0006	0 *	—
$N_{\delta col}$	rad/(s^2 %)	-0 051	0 0041	0 *	—	0 *	—	0 *	—	-0 036	0 0016	0 *	—
$N_{\delta lon}$	rad/(s^2 %)	-0 075	0 005	0 *	—	0 *	—	0 *	—	-0 051	0 002	0 *	—
$N_{\delta lat}$	rad/(s^2 %)	0 033	0 0023	0.0147	0 0004	0 026	0 0005	0 *	---	0 047	0 001	0 045	0 0014
$N_{\delta ped}$	rad/(s^2 %)	0 057	0 0023	0 043	0 0005	0 049	0 0003	0 443	0 0020	0 484	0 0008	0 044	0 0014

* Eliminated from model structure
σ = Standard deviation

Table 11. BO 105 identification results: List of specific moment derivatives with respect to control variables

Delay		AFDD		CERT		DLR		Glasgow Uni		NAE		NLR	
Symbol	Unit	Value	σ	Value	σ	Value	σ	Value	σ	Value	σ	Value	σ
$\tau_{\delta col}$	s	0.168	0.0056	0.0	—	0.040	—	0.102	—	0.040 *	—	0.040 *	—
$\tau_{\delta lon}$	s	0.113	0.0059	0.0	—	0.100	—	0.044	—	0.100 *	—	0.100 *	—
$\tau_{\delta lat}$	s	0.062	0.0056	0.0	—	0.060	—	0.074	—	0.060 *	—	0.060 *	—
$\tau_{\delta ped}$	s	0.044	0.0065	0.0	—	0.040	—	0.0	—	0.040 *	—	0.040 *	—

* From DLR value
σ = Standard deviation

Table 12. BO 105 identification results: Equivalent control time delays

Mode of motion	AFDD	CERT	DLR	Glasgow Uni	NAE	NLR
Phugoid oscillation	[-0.36, 0.30]	[-0.17, 0.32]	[-0.15, 0.33]	[-0.10, 0.35]	[-0.14, 0.33]	[-0.07, 0.33]
Dutch roll oscillation	[+0.22, 2.60]	[+0.13, 2.51]	[+0.14, 2.50]	[+0.16, 2.27]	[+0.13, 2.58]	[+0.17, 2.17]
Roll mode	(8.32)	[+0.99, 2.89] †	(8.49)	(5.12)	(8.47)	(2.38)
Aperiodic pitch mode 1	(6.04)	---	(4.36)	(1.98)	(4.38)	(1.37)
Aperiodic pitch mode 2	(0.49)	(0.66)	(0.60)	(0.64)	(0.63)	(0.71)
Spiral mode	(0.03)	(-0.05)	(0.02)	(-0.007)	(0.03)	(0.04)

† In this case the aperiodic roll mode and the fast pitch mode combine into an oscillatory mode.

Shorthand notation:

s Laplace variable (in 1/s)

$[\zeta, \omega_0]$ represents $(s^2 + 2\zeta\omega_0 s + \omega_0^2)$
with ζ = damping ratio and ω_0 = undamped natural frequency (in rad/s)

$(1/T)$ represents $(s + 1/T)$
with T = time constant (in s)

Table 13. BO 105 identification results: Time constants, damping ratios, and undamped natural frequencies

MODEL STRUCTURE

$$\begin{bmatrix} \dot{x}_{Body} \\ \dot{x}_{Rotor} \end{bmatrix} = \begin{bmatrix} A_{body} & A_{body/rotor} \\ A_{rotor/body} & A_{rotor} \end{bmatrix} \cdot \begin{bmatrix} x_{body} \\ x_{rotor} \end{bmatrix} + \begin{bmatrix} B_{body} \\ B_{rotor} \end{bmatrix} \cdot \delta$$

$$x_{body}^T = [u\ v\ w\ p\ q\ r\ \Phi\ \Theta]$$

$$x_{rotor}^T = [\dot{a}_0\ \dot{a}_1\ \dot{b}_1\ a_0\ a_1\ b_1]$$

$$\delta^T = [\delta_{lon}\ \delta_{lat}\ \delta_{col}\ \delta_{ped}]$$

RIGID BODY MATRIX A_{body}

u	v	w	p	q	r	Φ	Θ
-3.5199D-02	0.0000D+00	1.2113D-02	0.0000D+00	1.2985D+00	5.6685D-01	0.0000D+00	-9.8070D+00
0.0000D+00	-1.0273D-01	0.0000D+00	-1.3823D+00	0.0000D+00	-4.2216D+01	9.8070D+00	0.0000D+00
-6.7246D-03	0.0000D+00	-2.1751D-01	-5.6685D-01	4.3824D+01	0.0000D+00	0.0000D+00	0.0000D+00
-5.9302D-03	-1.0800D-01	-6.8254D-02	0.0000D+00	5.2872D-01	5.2934D-01	0.0000D+00	0.0000D+00
-8.0978D-03	2.8149D-02	-1.9644D-02	-9.0648D-02	9.0000D+00	-4.3021D-01	0.0000D+00	0.0000D+00
-3.9232D-03	1.2763D-01	1.4094D-02	2.9732D-01	2.7619D-01	-8.9522D-01	0.0000D+00	0.0000D+00
0.0000D+00	0.0000D+00	0.0000D+00	1.0000D+00	0.0000D+00	0.0000D+00	0.0000D+00	0.0000D+00
0.0000D+00	0.0000D+00	0.0000D+00	0.0000D+00	1.0000D+00	0.0000D+00	0.0000D+00	0.0000D+00

ROTOR MATRIX A_{rotor}

a_0	$\dot{a}_1$	$\dot{b}_1$	a_0	a_1	b_1
-5.1589D+01	-3.9223D+01	0.0000D+00	-2.0000D+03	-1.4827D+02	0.0000D+00
6.8644D+01	-2.5135D+01	-8.8000D+01	-7.9017D+02	-3.8591D+02	-2.4254D+03
-1.3270D+01	8.8000D+01	-2.5135D+01	1.0142D+03	8.4981D+02	-3.8591D+02
1.0000D+00	0.0000D+00	0.0000D+00	0.0000D+00	0.0000D+00	0.0000D+00
0.0000D+00	1.0000D+00	0.0000D+00	0.0000D+00	0.0000D+00	0.0000D+00
0.0000D+00	0.0000D+00	1.0000D+00	0.0000D+00	0.0000D+00	0.0000D+00

Table 14. Identified model with rotor degrees of freedom: Rigid body and rotor state matrices

RIGID BODY / ROTOR COUPLING MATRIX $A_{body/rotor}$

$\dot{a}_0$	$\dot{a}_1$	$\dot{b}_1$	a_0	a_1	b_1
0.0000D+00	0.0000D+00	0.0000D+00	1.2032D+01	2.6589D+01	0.0000D+00
0.0000D+00	0.0000D+00	3.9631D+00	-2.5150D+01	0.0000D+00	-3.7133D+01
0.0000D+00	0.0000D+00	0.0000D+00	-1.8903D+02	3.0492D+01	0.0000D+00
0.0000D+00	0.0000D+00	1.6822D+00	-8.4862D+00	-6.7502D+00	-1.7832D+02
0.0000D+00	-2.3466D-01	0.0000D+00	-1.3165D+01	-4.0856D+01	0.0000D+00
0.0000D+00	0.0000D+00	0.0000D+00	-2.5549D+00	6.0879D+00	-3.7673D+01
0.0000D+00	0.0000D+00	0.0000D+00	0.0000D+00	0.0000D+00	0.0000D+00
0.0000D+00	0.0000D+00	0.0000D+00	0.0000D+00	0.0000D+00	0.0000D+00

ROTOR / RIGID BODY COUPLING MATRIX $A_{rotor/body}$

u	v	w	p	q	r	Φ	Θ
-3.1842D-01	0.0000D+00	5.8469D+00	-1.0336D+01	4.7646D+01	0.0000D+00	0.0000D+00	0.0000D+00
1.4813D-01	7.3639D-01	-7.7879D-01	8.8000D+01	0.0000D+00	0.0000D+00	0.0000D+00	0.0000D+00
7.3639D-01	1.4813D-01	-8.4343D-01	0.0000D+00	-8.8000D+01	0.0000D+00	0.0000D+00	0.0000D+00
0.0000D+00	0.0000D+00	0.0000D+00	0.0000D+00	0.0000D+00	0.0000D+00	0.0000D+00	0.0000D+00
0.0000D+00	0.0000D+00	0.0000D+00	0.0000D+00	0.0000D+00	0.0000D+00	0.0000D+00	0.0000D+00
0.0000D+00	0.0000D+00	0.0000D+00	0.0000D+00	0.0000D+00	0.0000D+00	0.0000D+00	0.0000D+00

LEAD / LAG APPROXIMATION

$$\delta_{lat} = \frac{s^2 + 1.398\,s + 242.07}{s^2 + 0.516\,s + 218.42} \cdot \delta_{lat\ measured}$$

CONTROL MATRIX B

δ_{lon}	δ_{lat}	δ_{col}	δ_{ped}
0.0000D+00	0.0000D+00	0.0000D+00	0.0000D+00
0.0000D+00	0.0000D+00	0.0000D+00	0.0000D+00
0.0000D+00	0.0000D+00	0.0000D+00	0.0000D+00
0.0000D+00	0.0000D+00	0.0000D+00	-1.5244D-02
0.0000D+00	0.0000D+00	0.0000D+00	0.0000D+00
0.0000D+00	0.0000D+00	0.0000D+00	4.5713D-02
0.0000D+00	0.0000D+00	0.0000D+00	0.0000D+00
0.0000D+00	0.0000D+00	0.0000D+00	0.0000D+00
0.0000D+00	0.0000D+00	2.2778D+00	0.0000D+00
-8.0258D-01	-1.7470D+00	0.0000D+00	0.0000D+00
1.7716D+00	-2.2695D-01	0.0000D+00	0.0000D+00
0.0000D+00	0.0000D+00	0.0000D+00	0.0000D+00
0.0000D+00	0.0000D+00	0.0000D+00	0.0000D+00
0.0000D+00	0.0000D+00	0.0000D+00	0.0000D+00

Table 15. Identified model with rotor degrees of freedom: Coupling matrices, lead/lag approximation, and control matrix

Motion	6 DOF, 8th order	9 DOF, 16th order
	8th order rigid body	8th order rigid body, 2nd order coning 2nd order long/lat flapping 2nd order lead/lag approx.
Phugoid	[−0.15, 0.33]	[−0.22, 0.33]
Dutch Roll	[+0.14, 2.50]	[+0.14, 2.55]
Spiral	(0.02)	(0.03)
Pitch-1	(0.60)	(0.43)
Roll	(8.49)	-
Roll/flap	-	[0.74, 14.7]
Regressing flap	-	[0.84, 6.37]
Pitch-2	(4 13)	-
Advancing flap	-	[0.14, 106]
Coning	-	[0 57, 34 63]
Lead/lag approx.	-	[0.017, 14.78]

Shorthand notation:

$[\zeta, \omega_0]$ implies $s^2 + 2\zeta\omega_0 s + \omega_0^2$

ζ = damping, ω_0 = undamped natural frequency (rad/sec)

(1/T) implies $(s + 1/T)$, (rad/sec)

Table 16. Comparison of BO 105 eigenvalues for different model structures

Figures

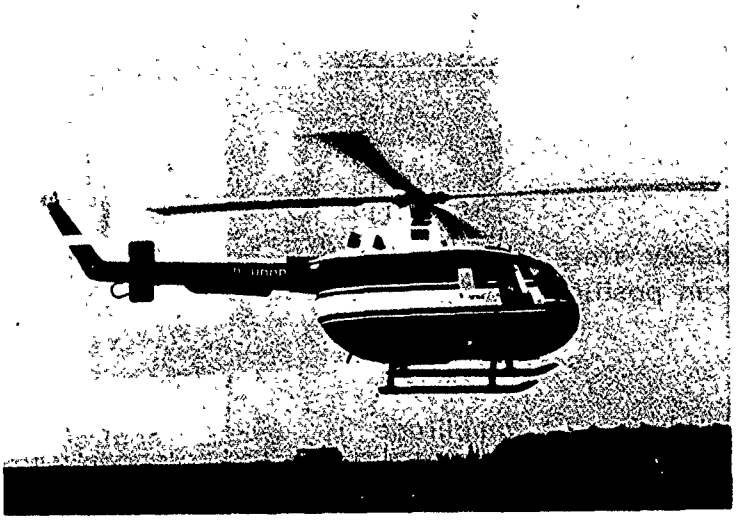

Figure 1. DLR research helicopter BO 105

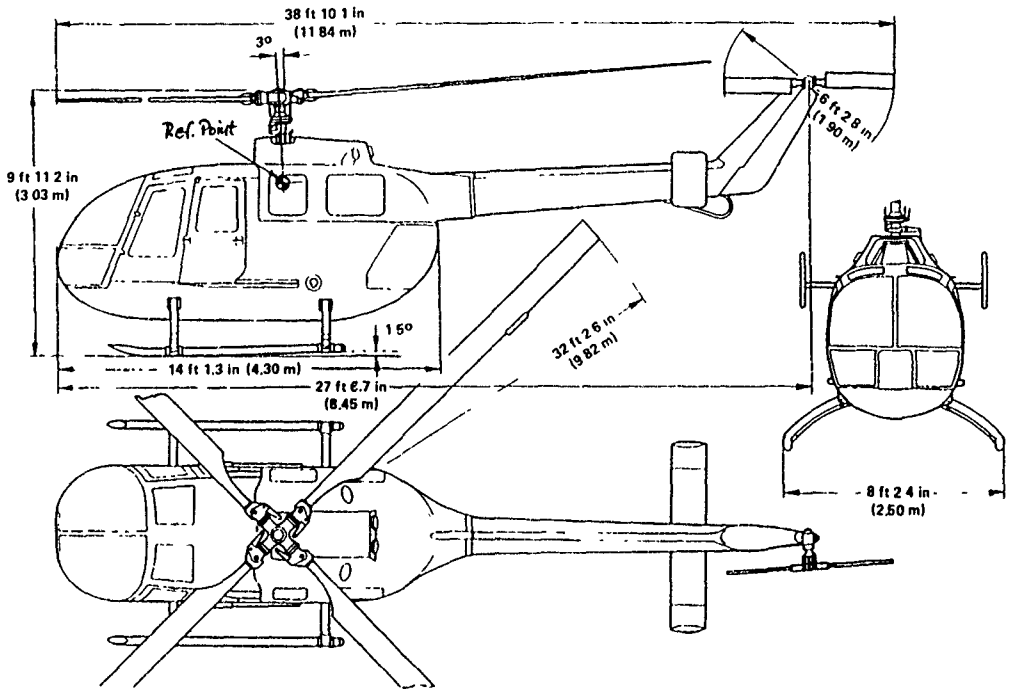

Figure 2. Three view drawing of BO 105

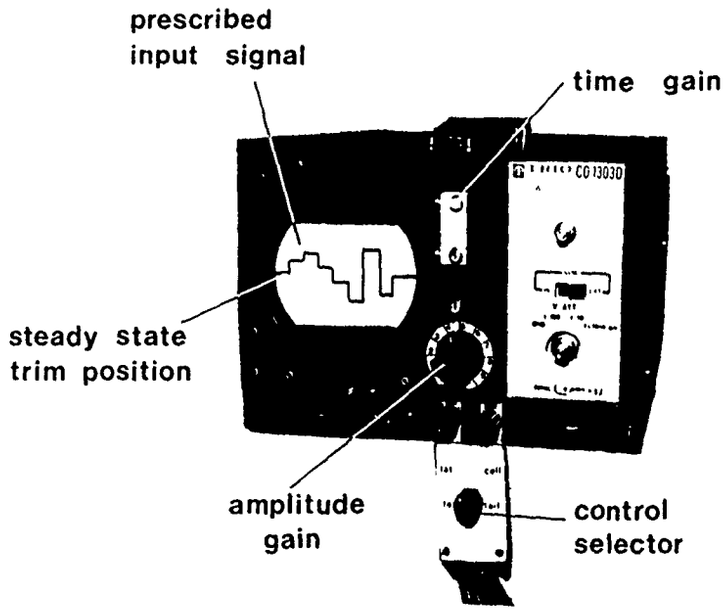

Figure 3. Pilot's display for input signal generation (BO 105)

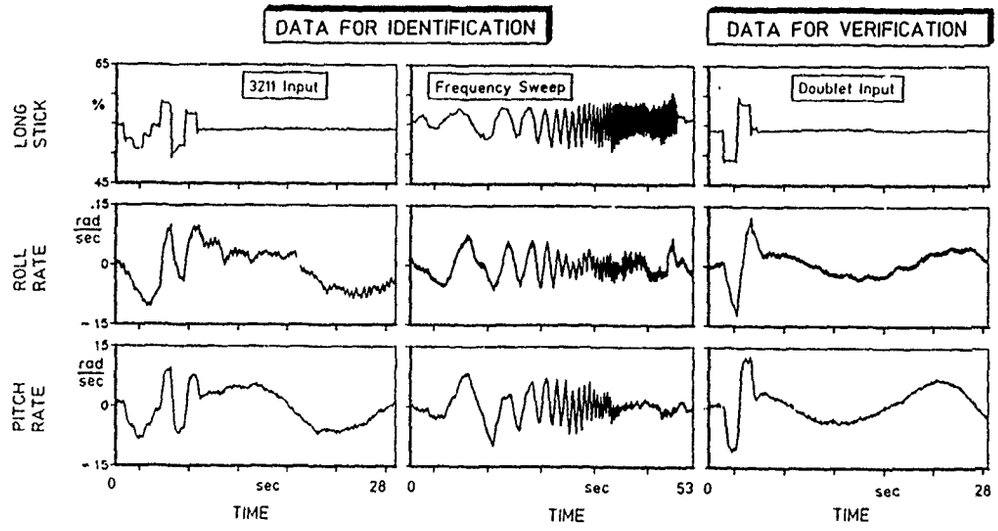

Figure 4. Representative BO 105 flight test data: control input types and rate responses

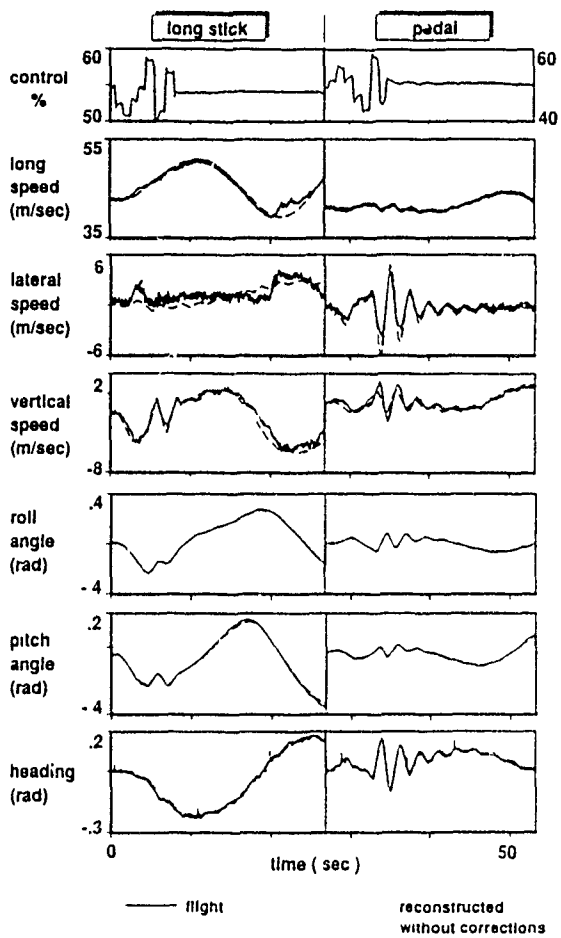

Figure 5. Comparison of measured and reconstructed BO 105 data without scale factor corrections

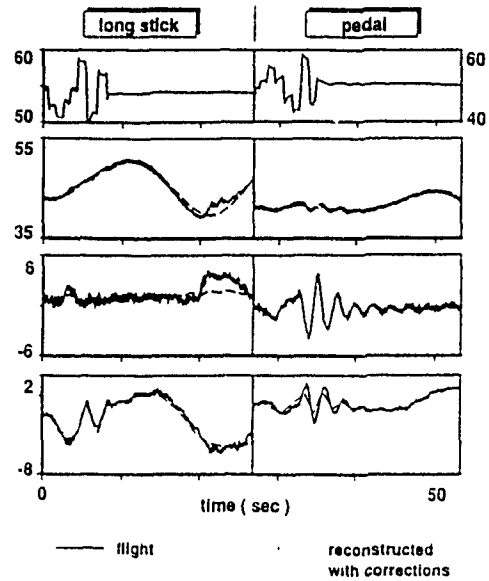

Figure 6. Comparison of measured and reconstructed BO 105 speed data with scale factor corrections

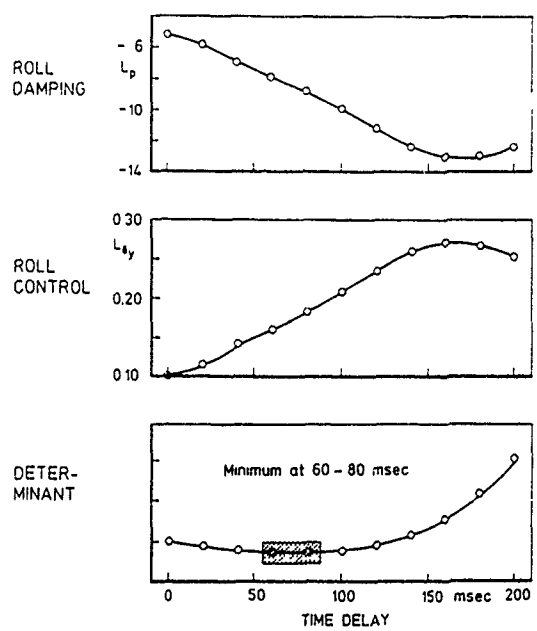

Figure 7. Influence of equivalent time delays on BO 105 identification results

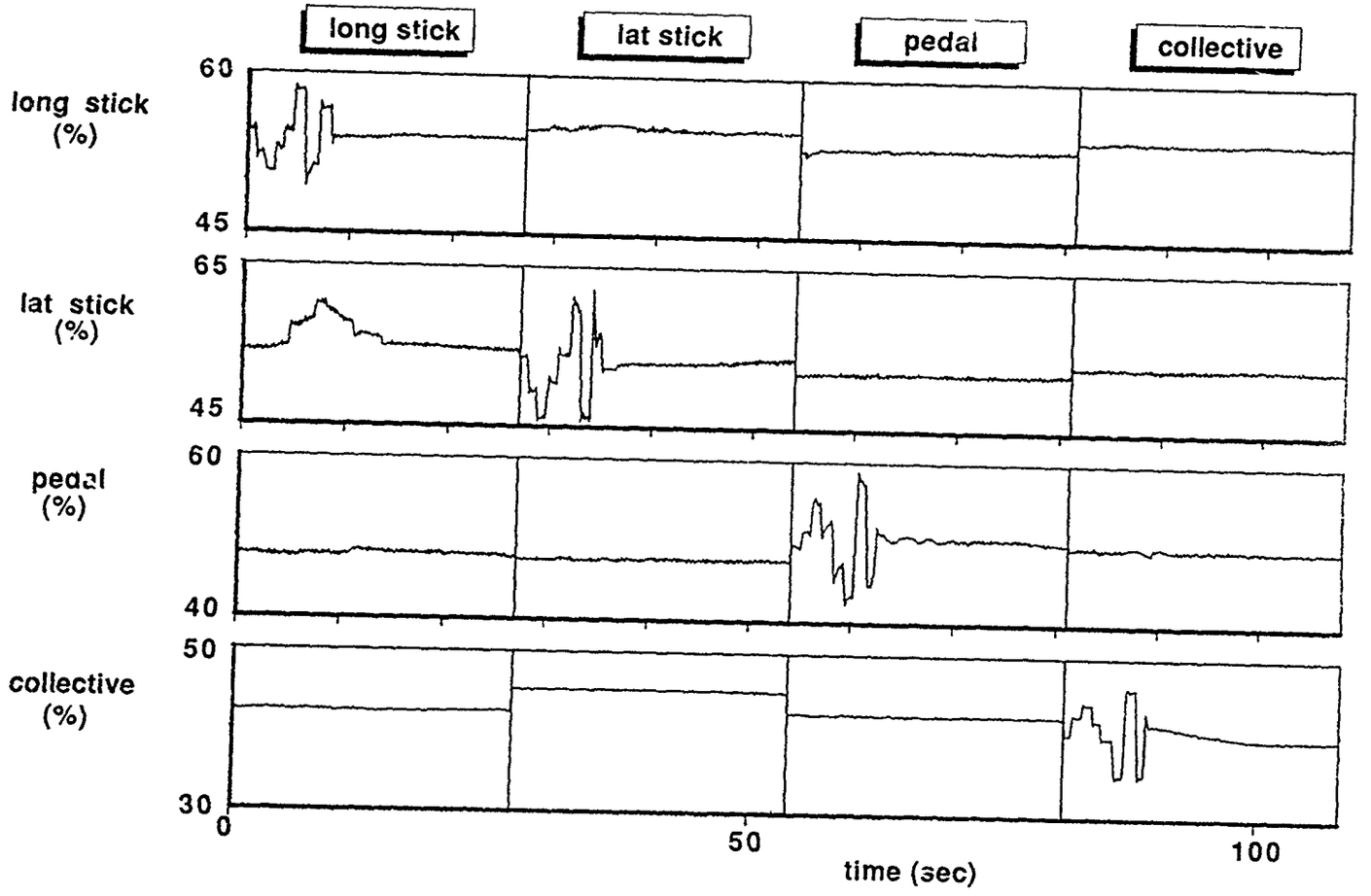

Figure 8. **Input signals of the BO 105 flight test data used for identification**

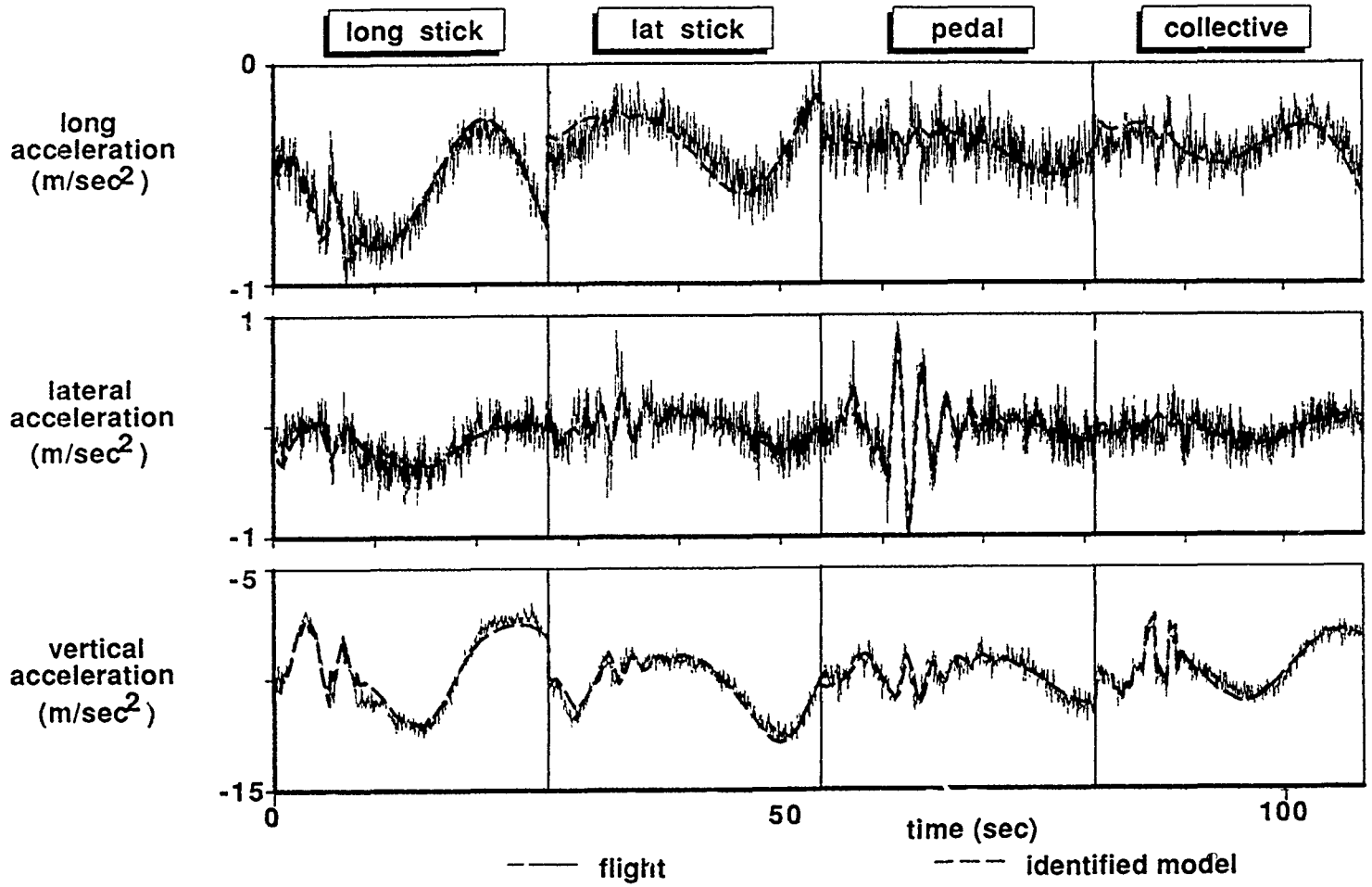

Figure 9. Comparison of BO 105 flight data and response of the identified model for linear accelerations (DLR result)

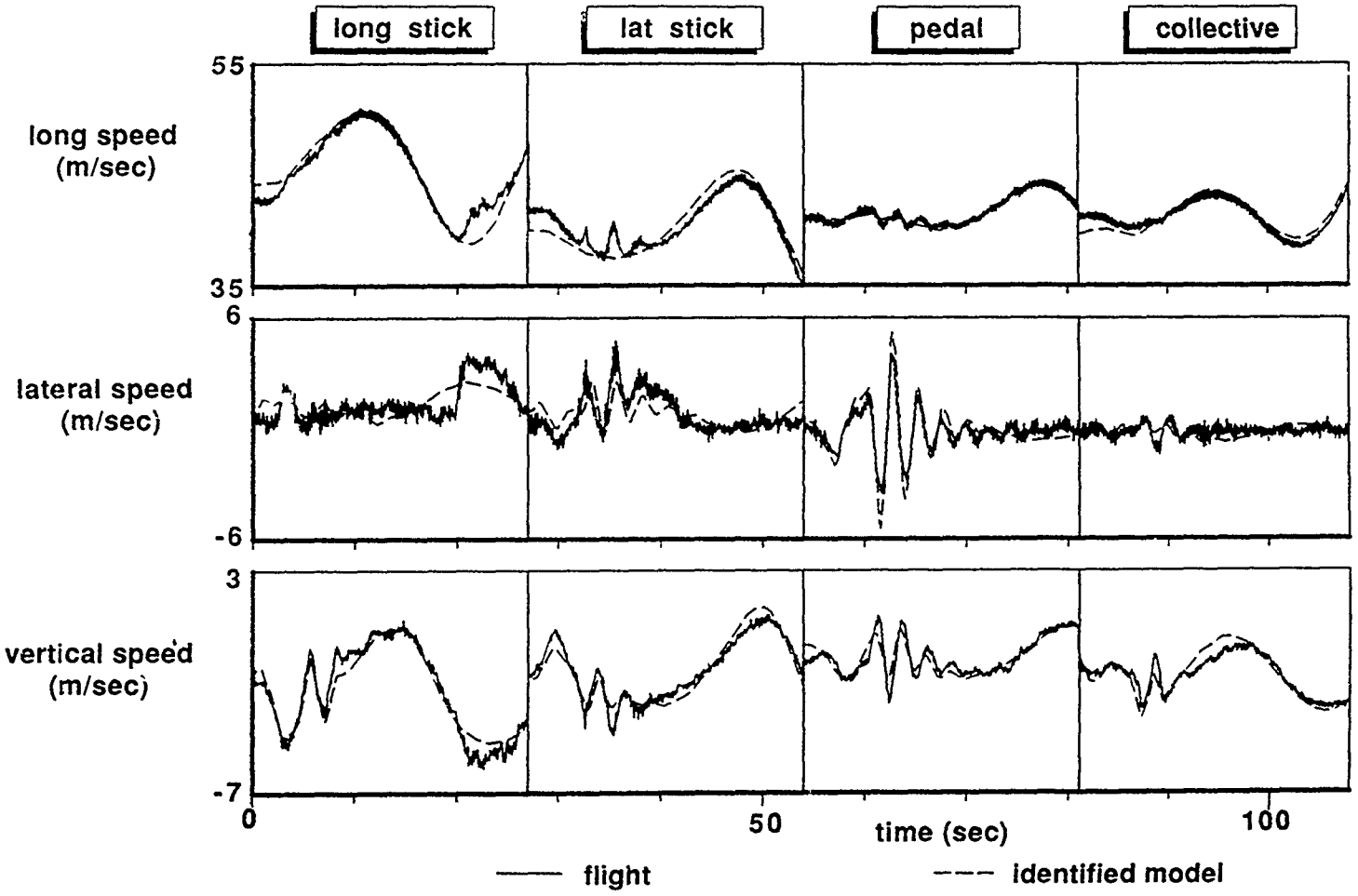

Figure 10. Comparison of BO 105 flight data and response of the identified model for linear speeds (DLR result)

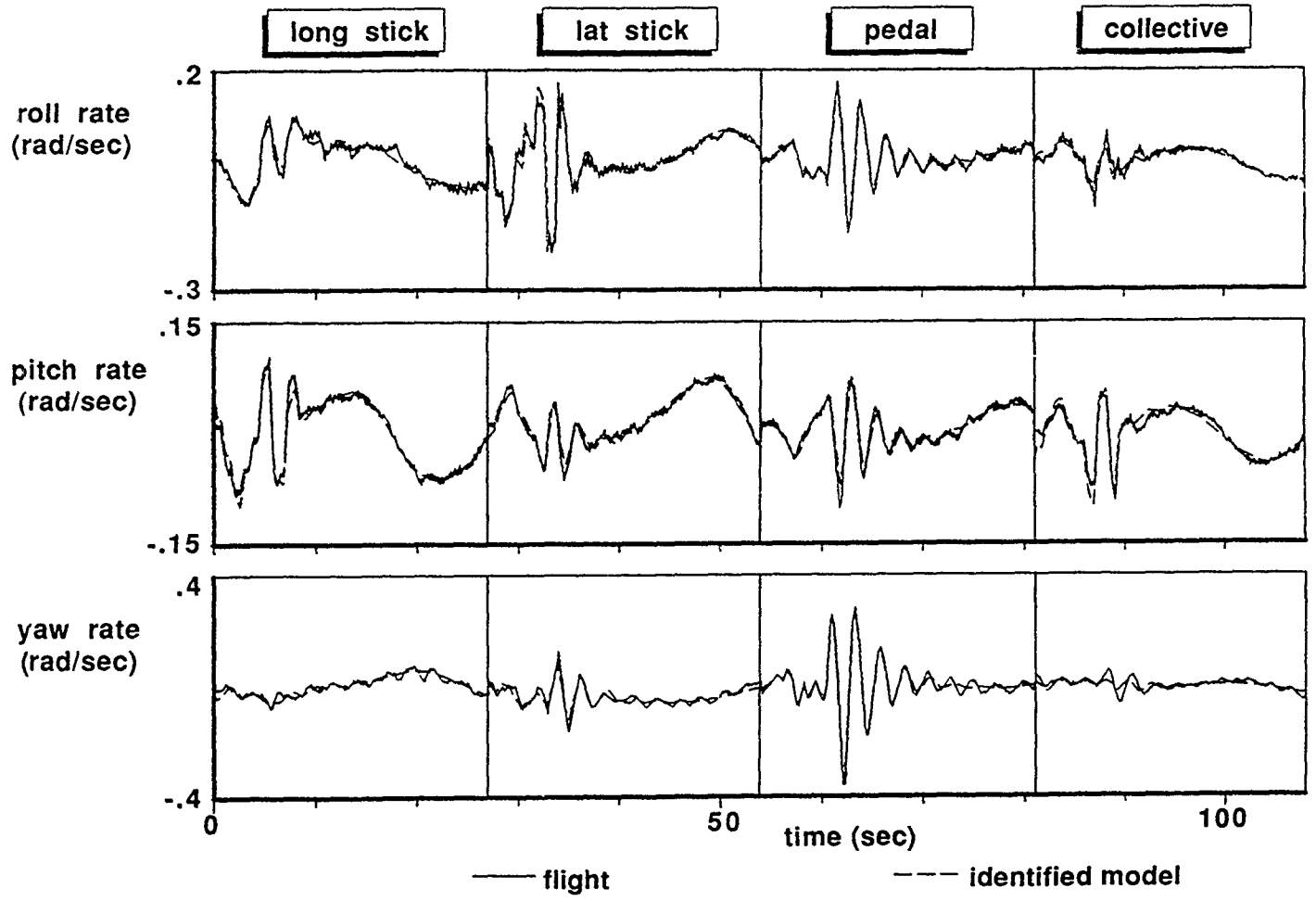

Figure 11. Comparison of BO 105 flight data and response of the identified model for angular rates (DLR result)

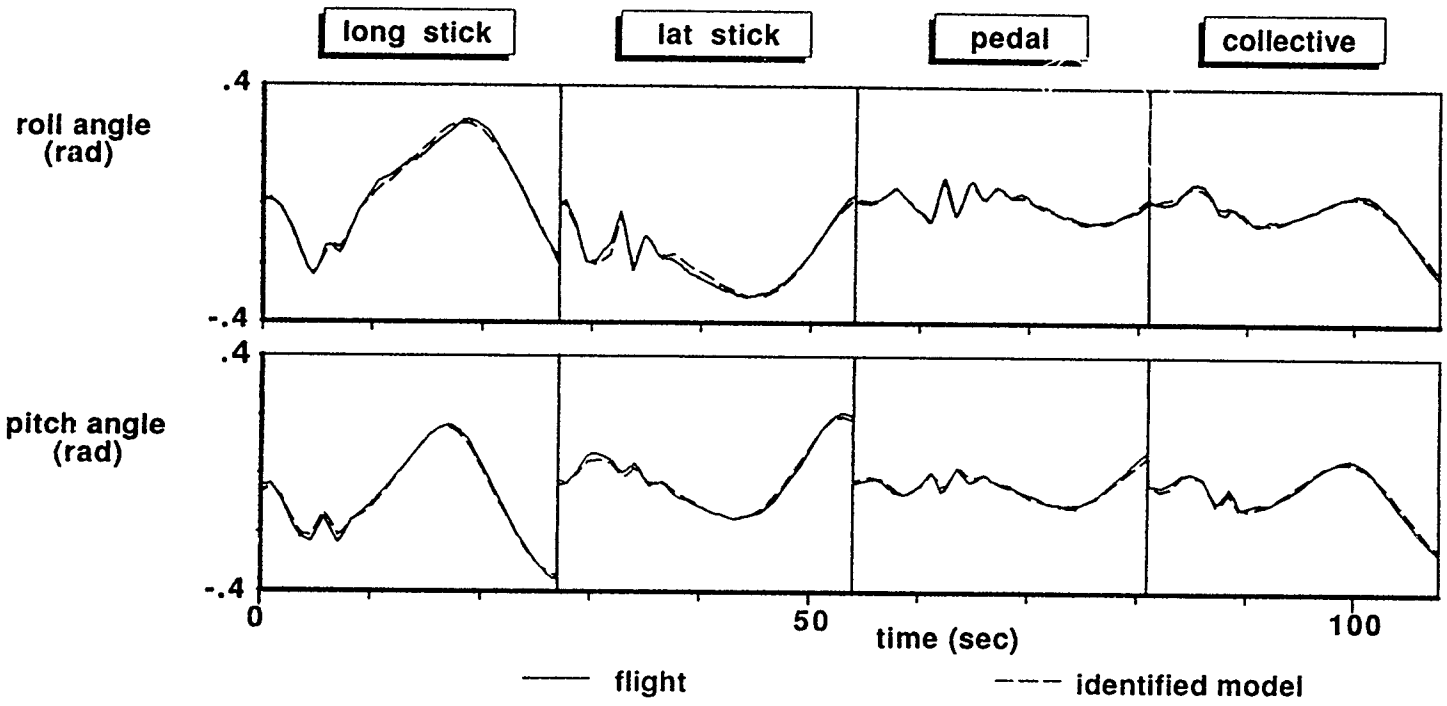

Figure 12. Comparison of BO 105 flight data and response of the identified model for Euler angles (DLR result)

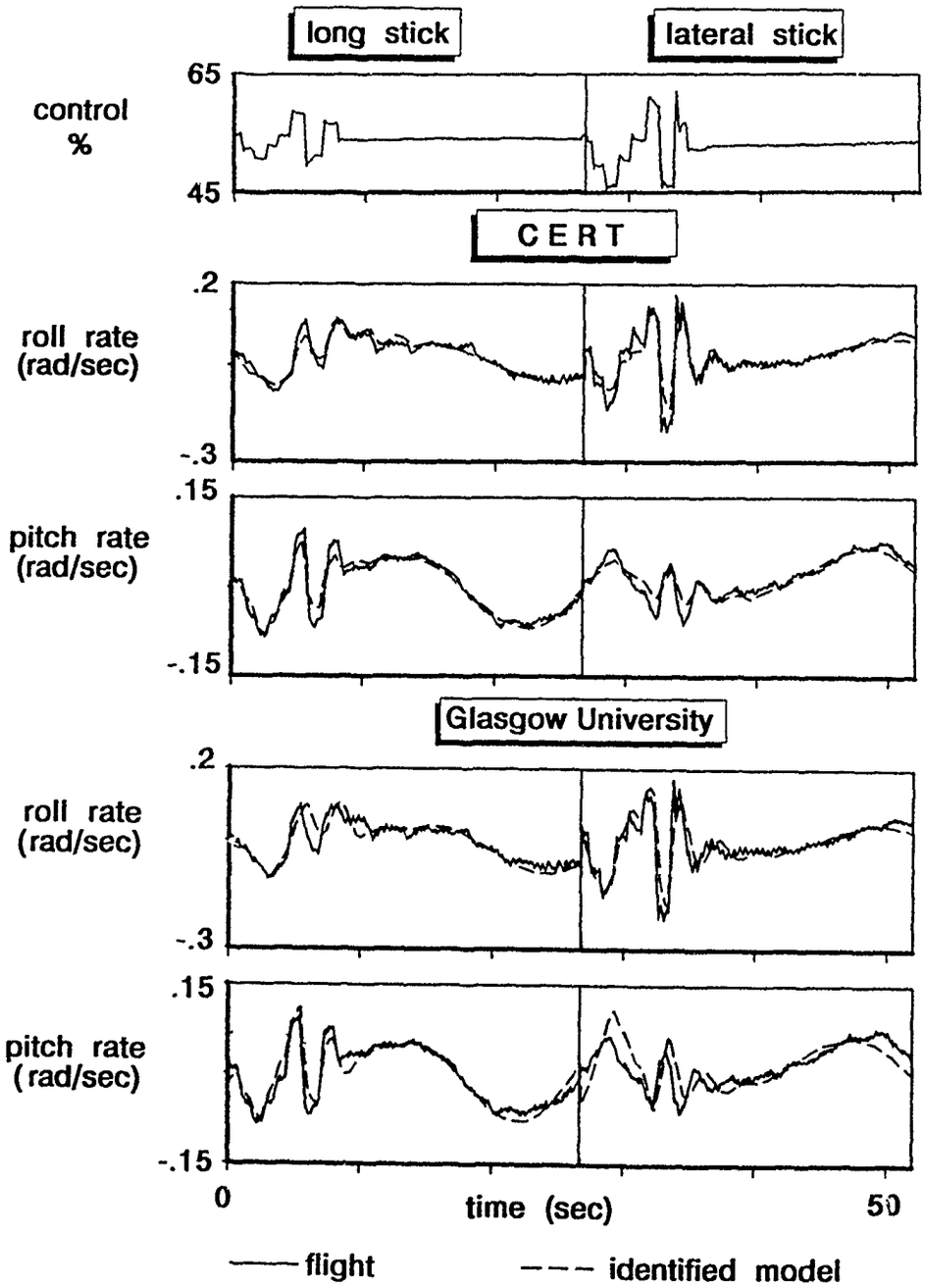

Figure 13. Comparison of measured rates and the response of identified BO 105 models (CERT and Glasgow University results)

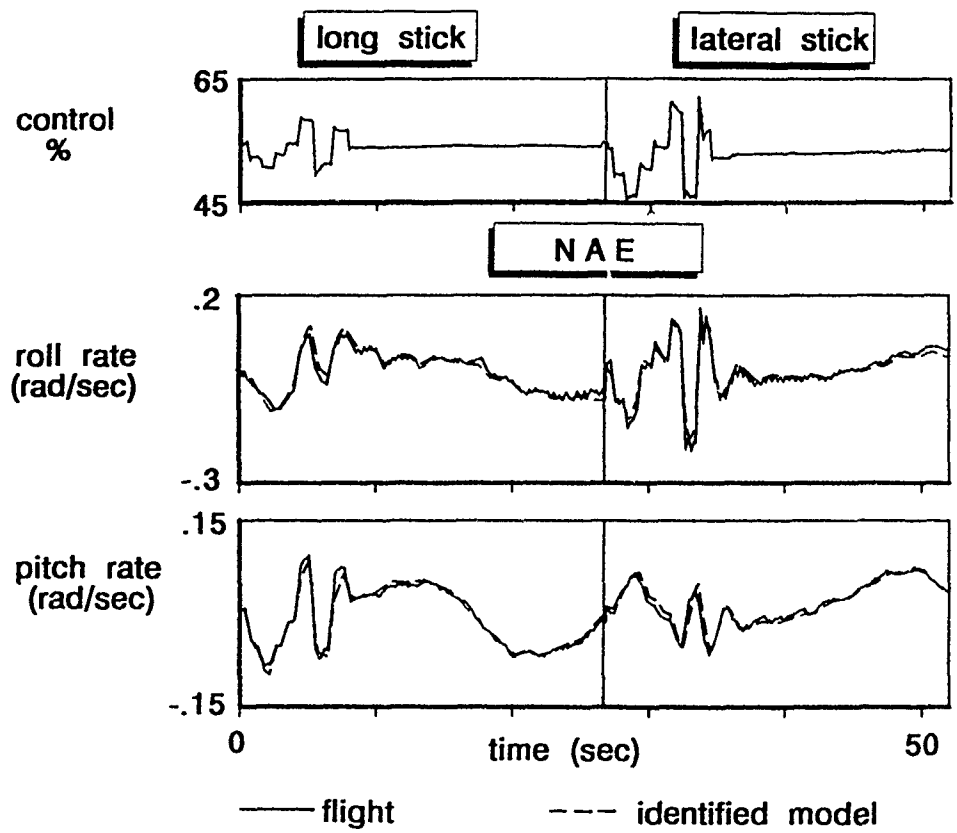

Figure 14. Comparison of measured rates and the response of the identified BO 105 models (NAE results)

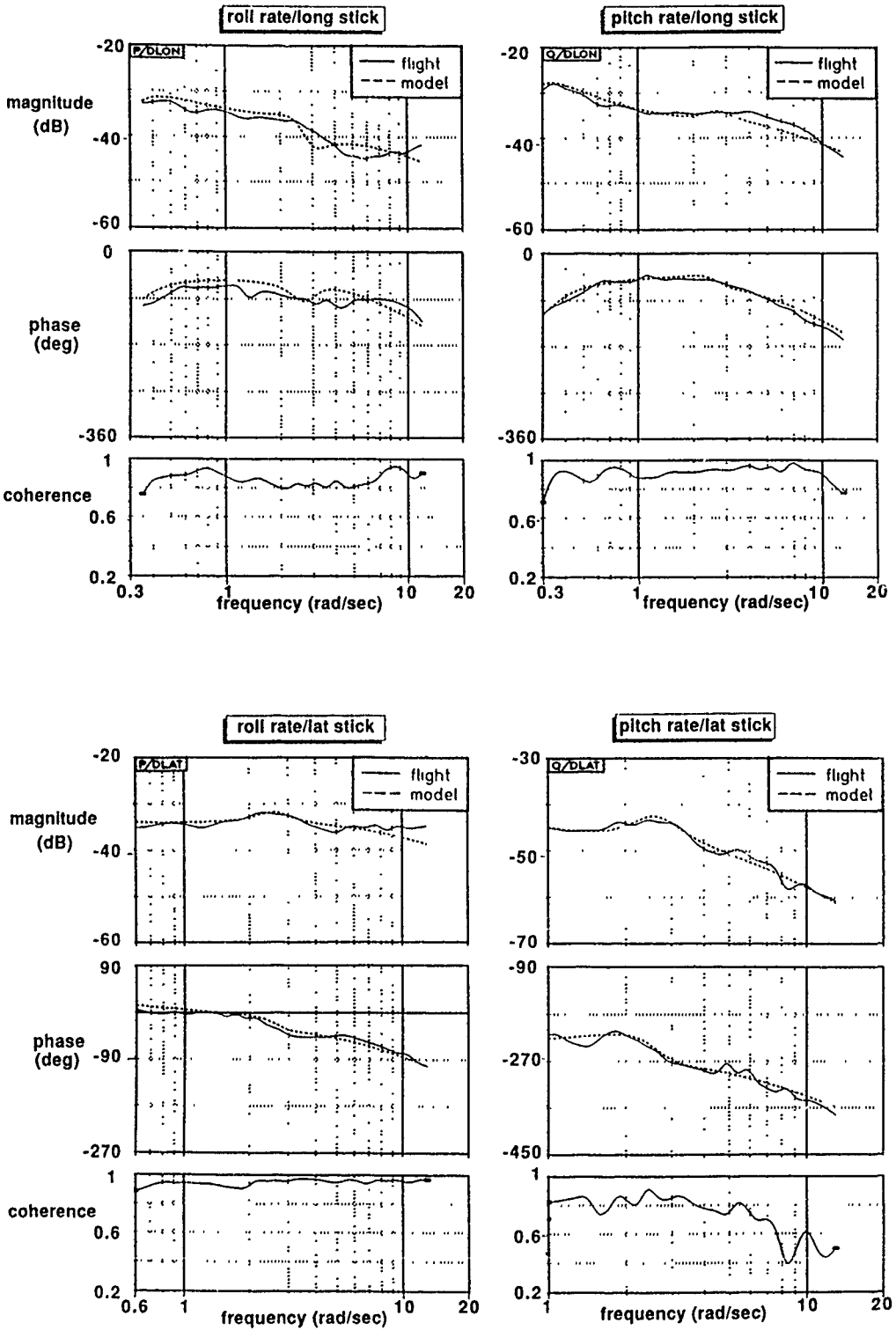

Figure 15. Comparison of BO 105 flight data and identified model frequency responses (roll and pitch rate, representative AFDD results)

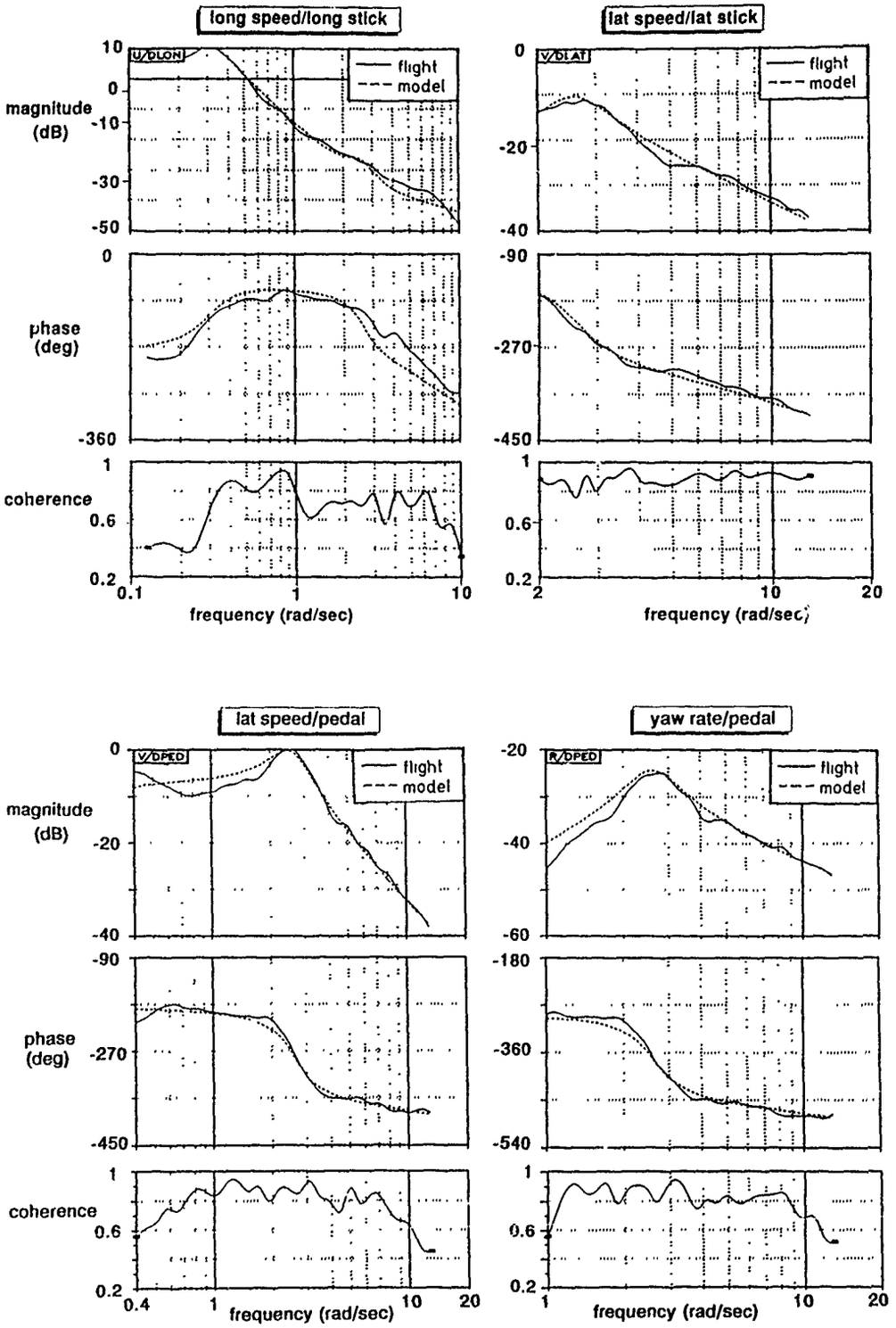

Figure 16. Comparison of BO 105 flight data and identified model frequency responses (linear speeds and yaw rate, representative AFDD results)

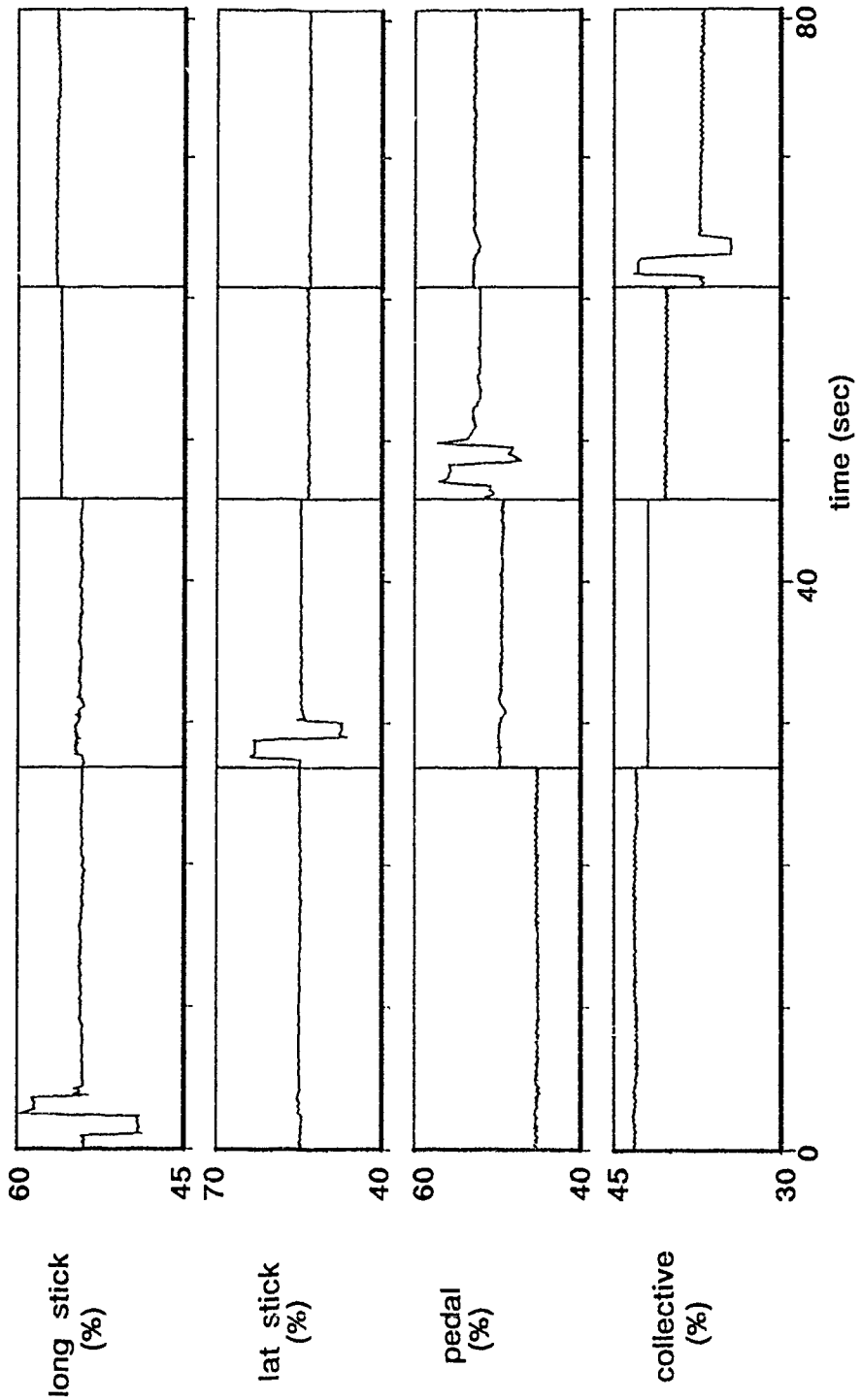

Figure 17. Input signals of the BO 105 flight test data used for verification

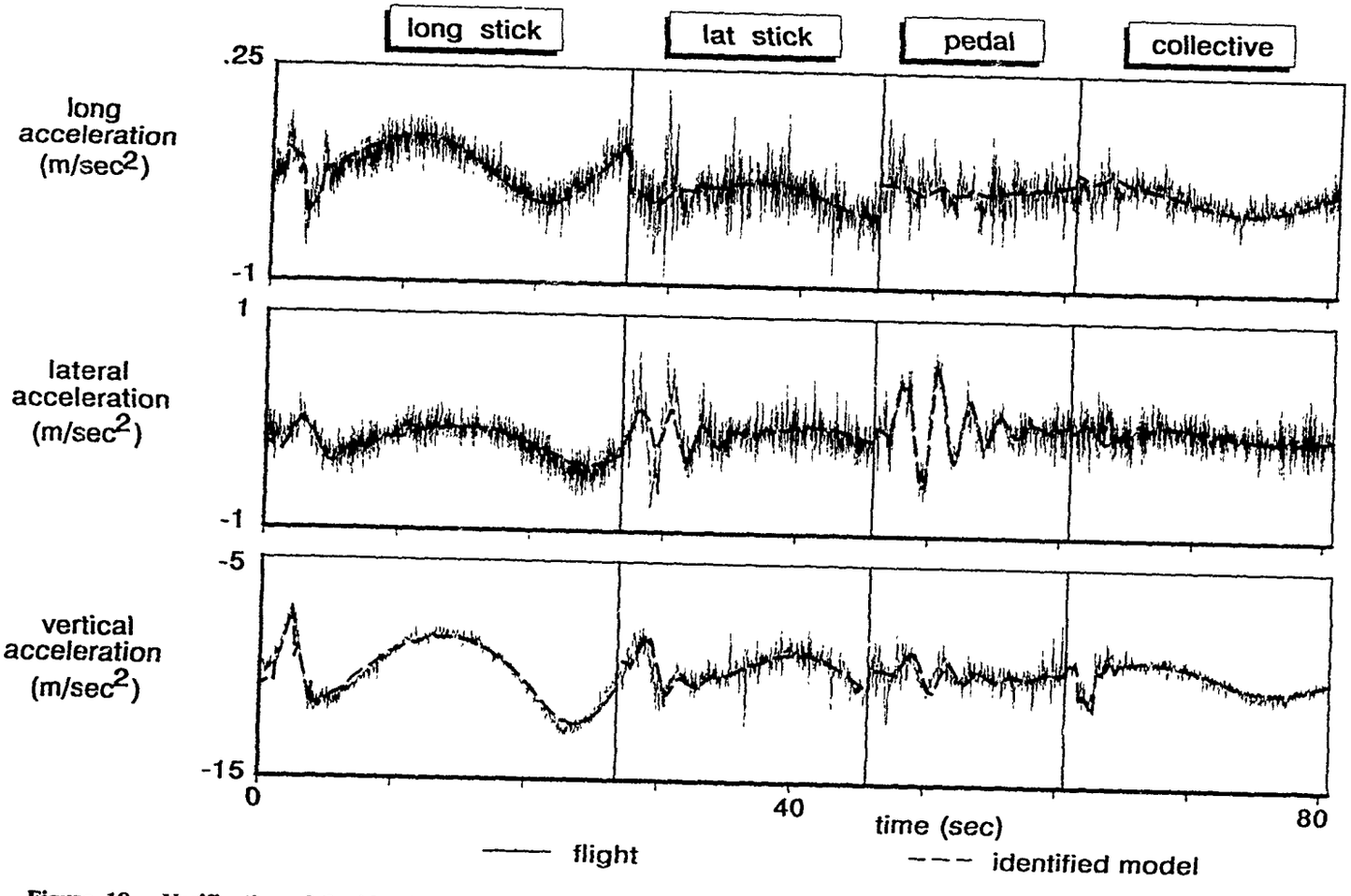

Figure 18. Verification of the identified model (linear accelerations, DLR result)

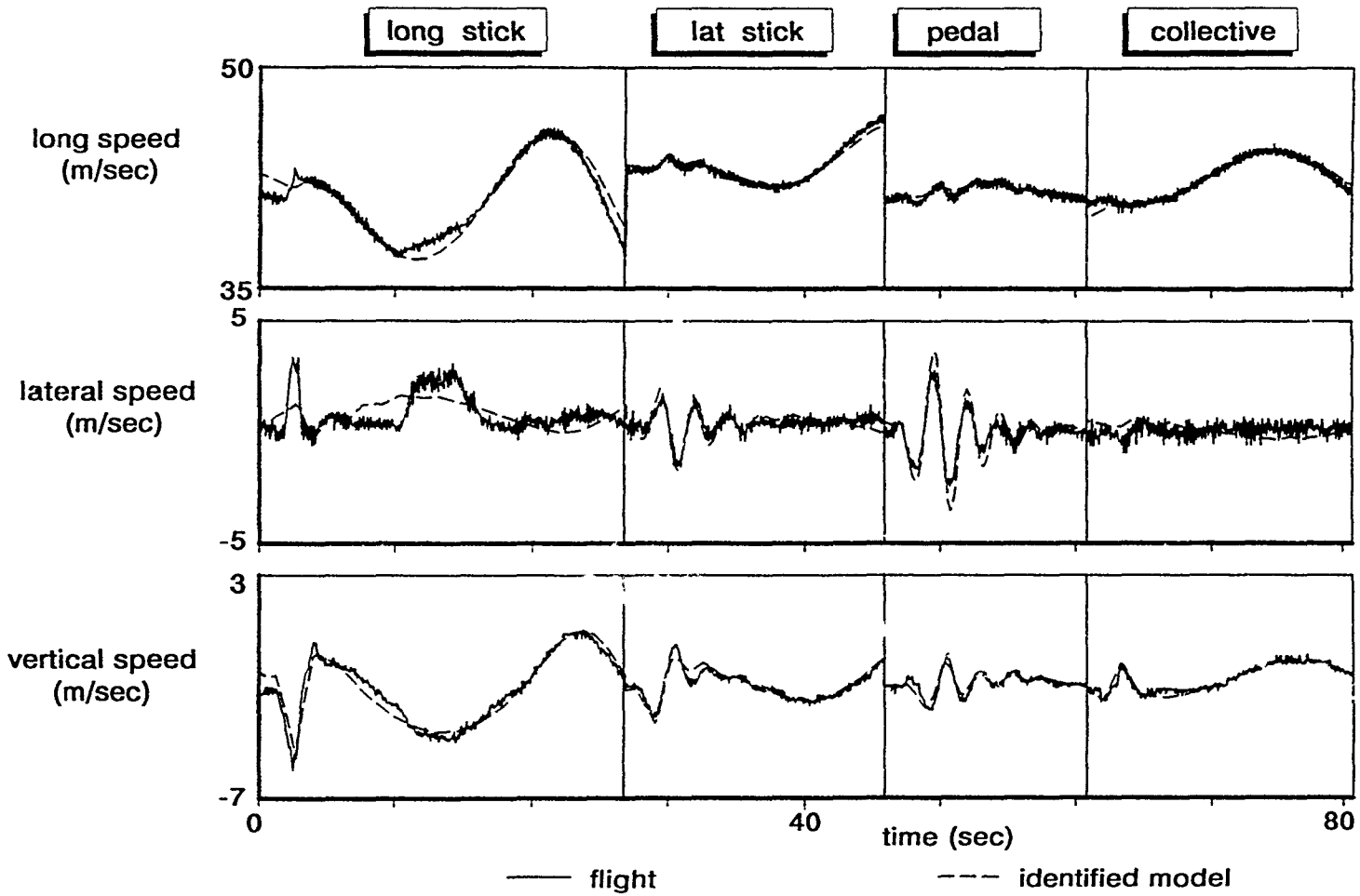

Figure 19. Verification of the identified model (linear speeds, DLR result)

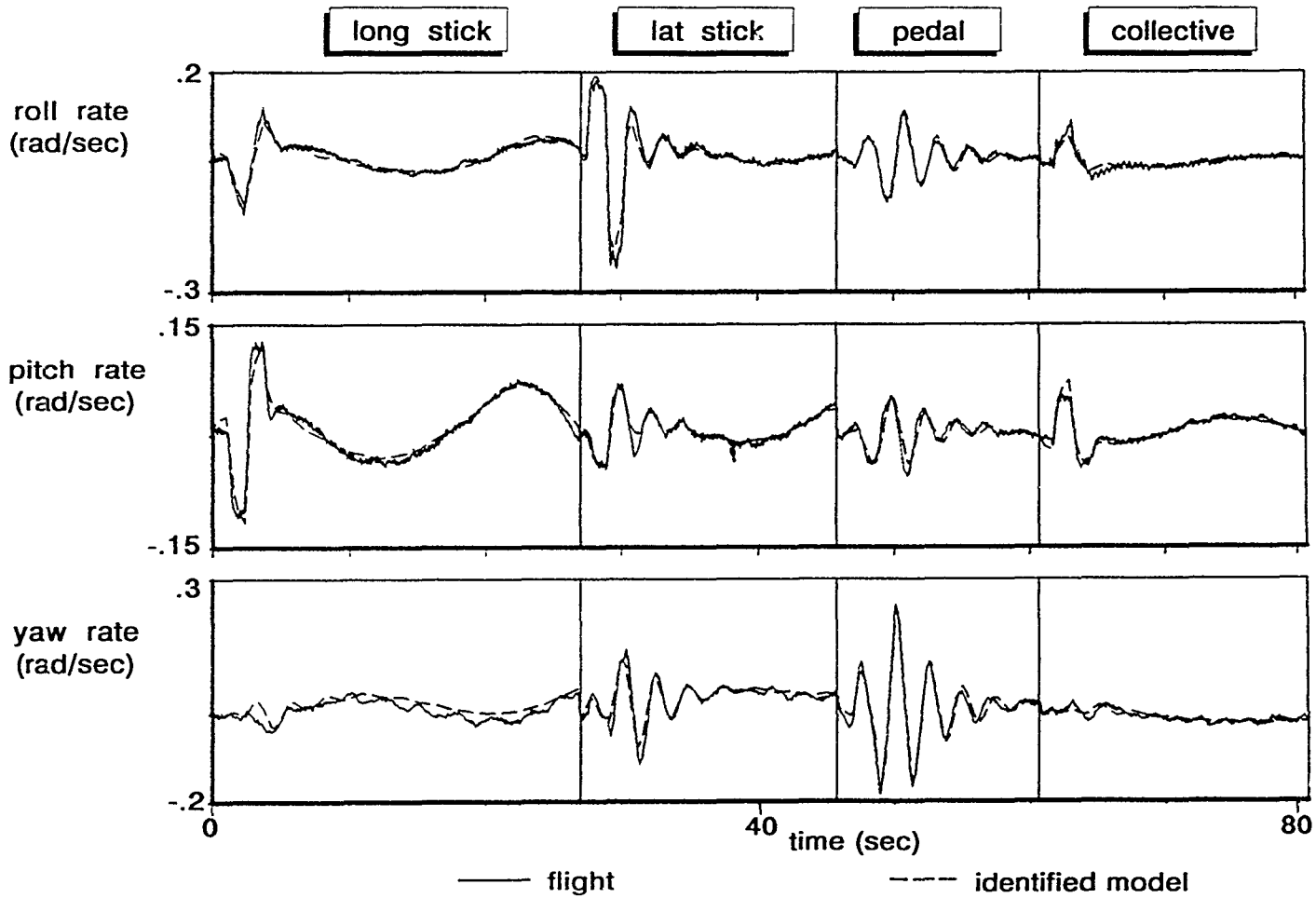

Figure 20. Verification of the identified model (angular rates, DLR result)

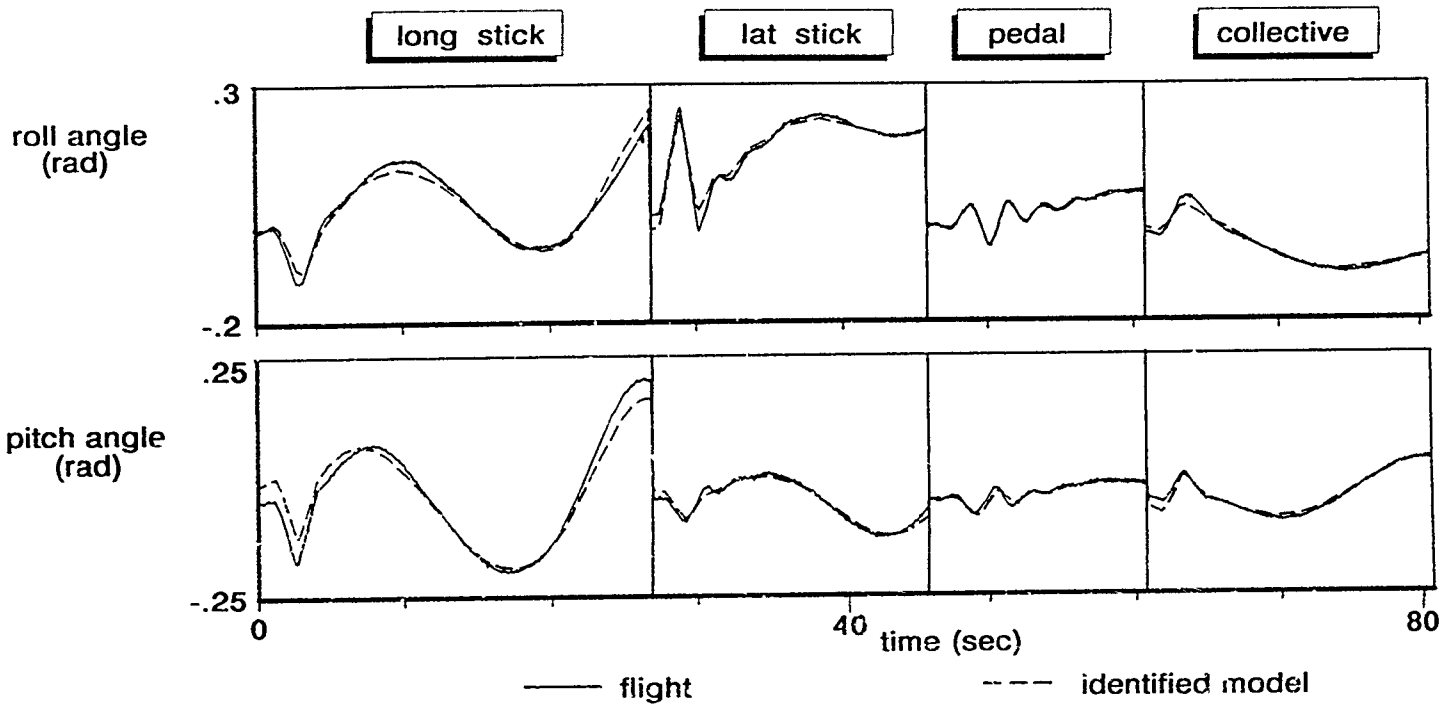

Figure 21. Verification of the identified model (Euler angles, DLR result)

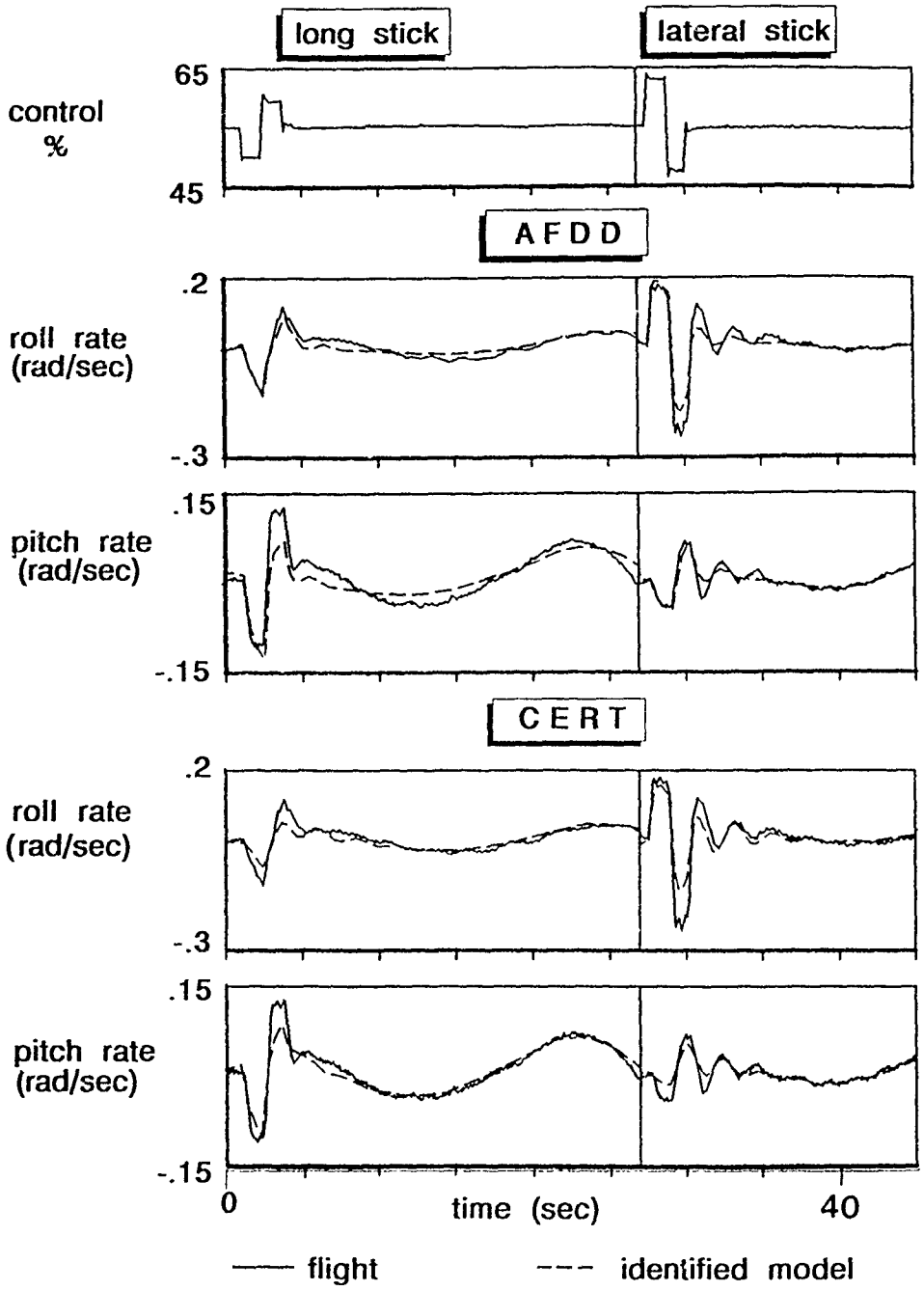

Figure 22. Verifica ion of the identified BO 105 models (AFDD and CERT results)

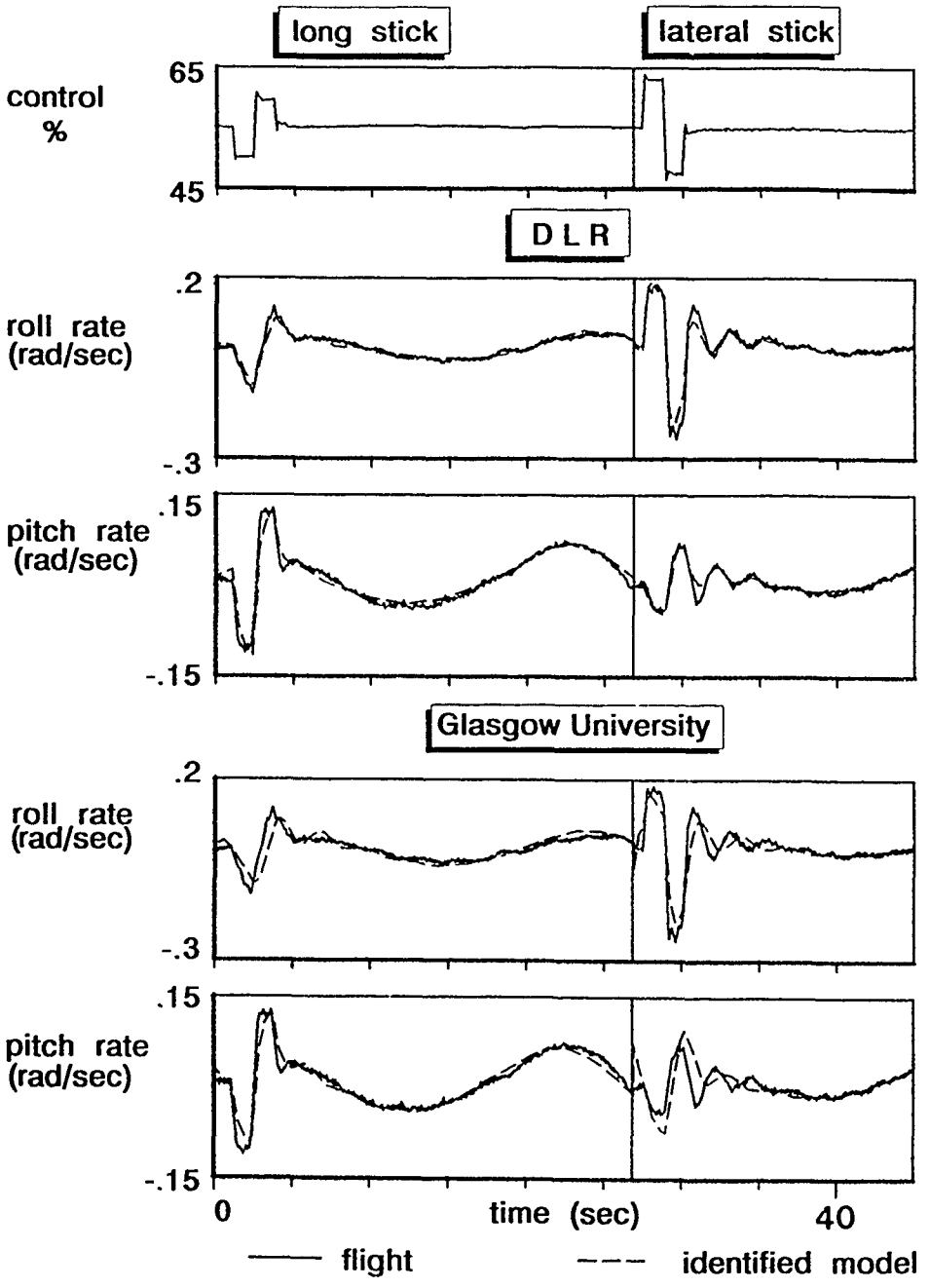

Figure 23. Verification of the identified BO 105 models (DLR and Glasgow University results)

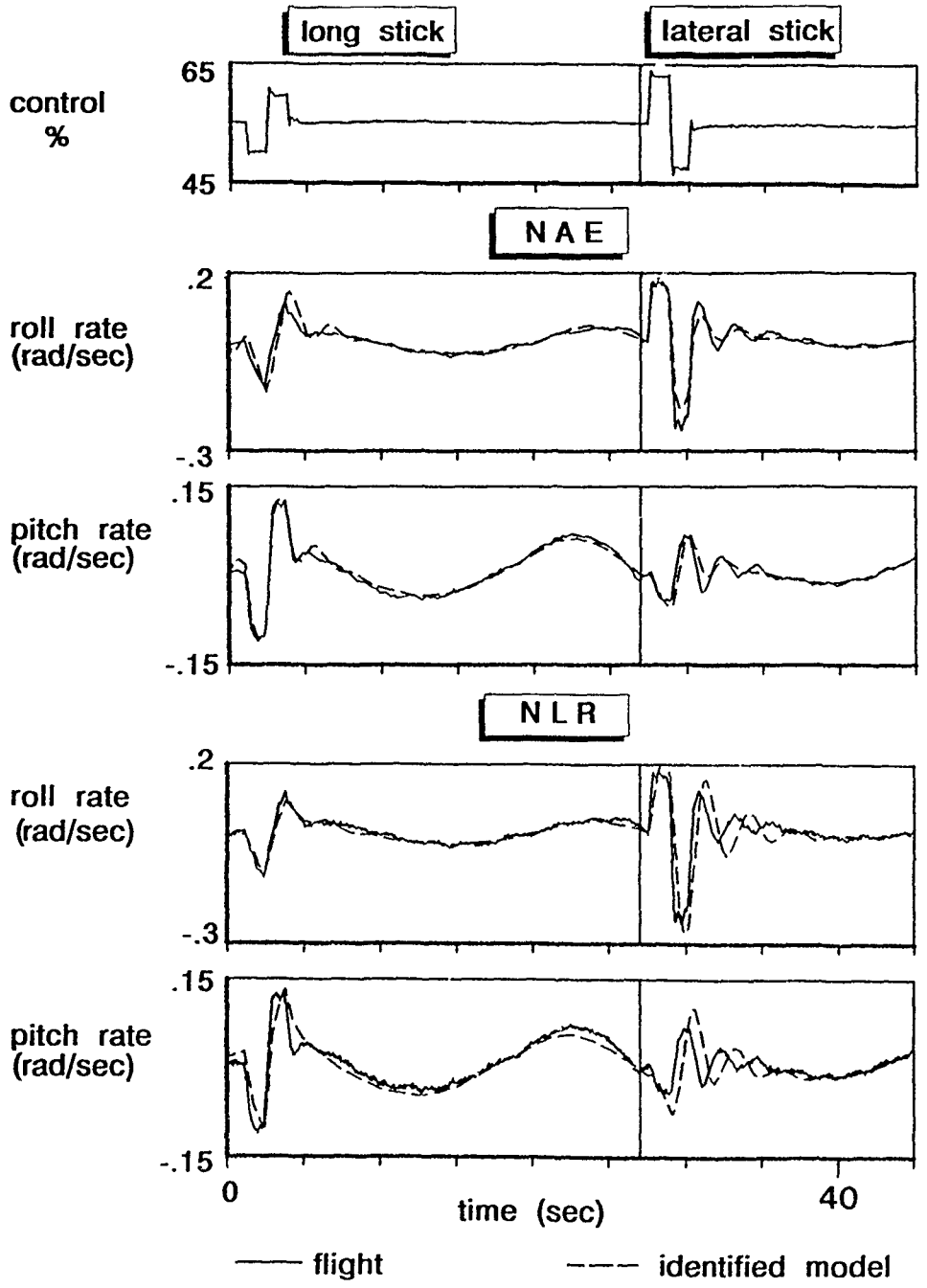

Figure 24. Verification of the identified BO 105 models (NAE and NLR results)

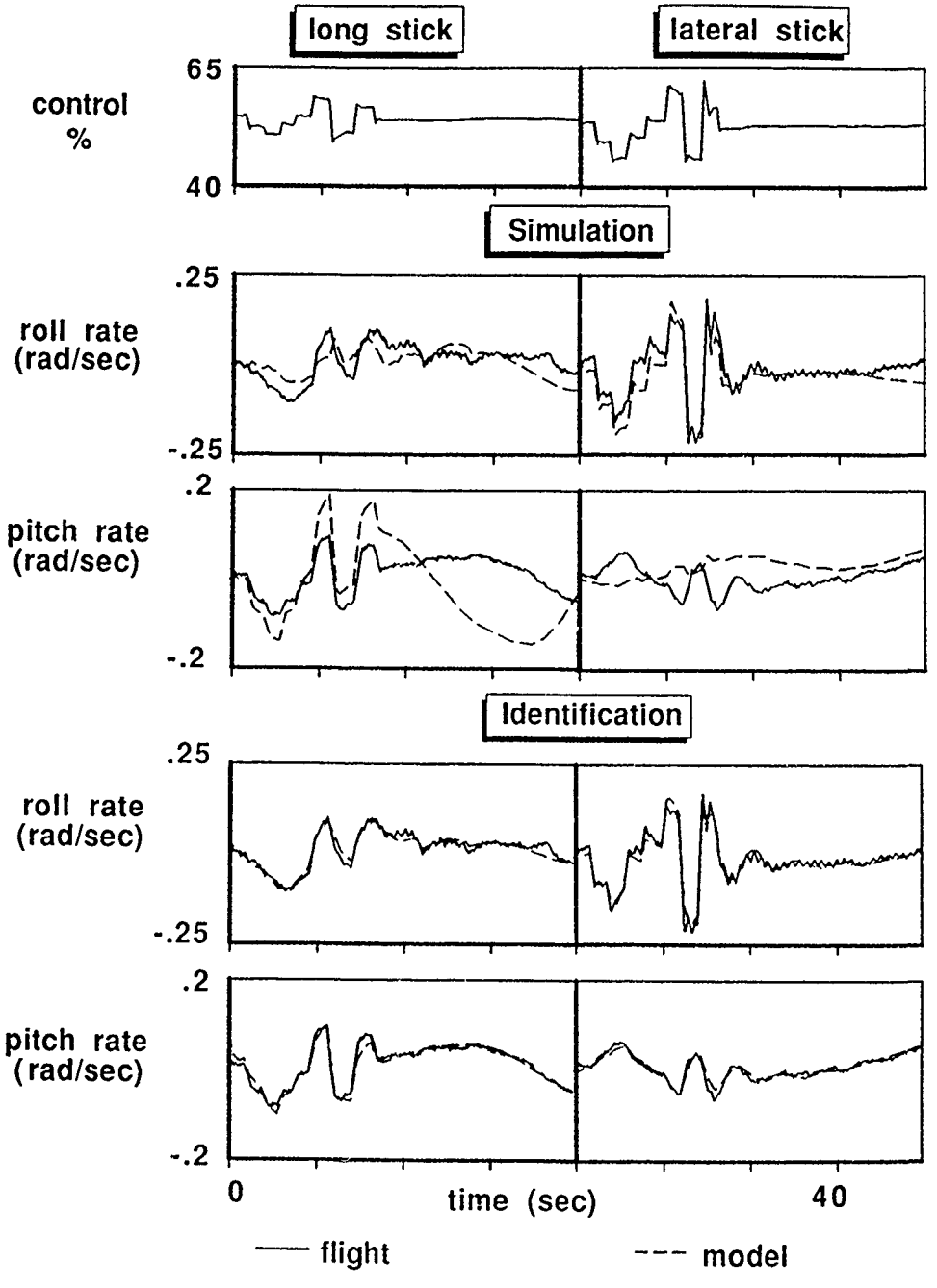

Figure 25. Comparison of BO 105 flight data and results from a computational nonlinear simulation (DLR, CMH)

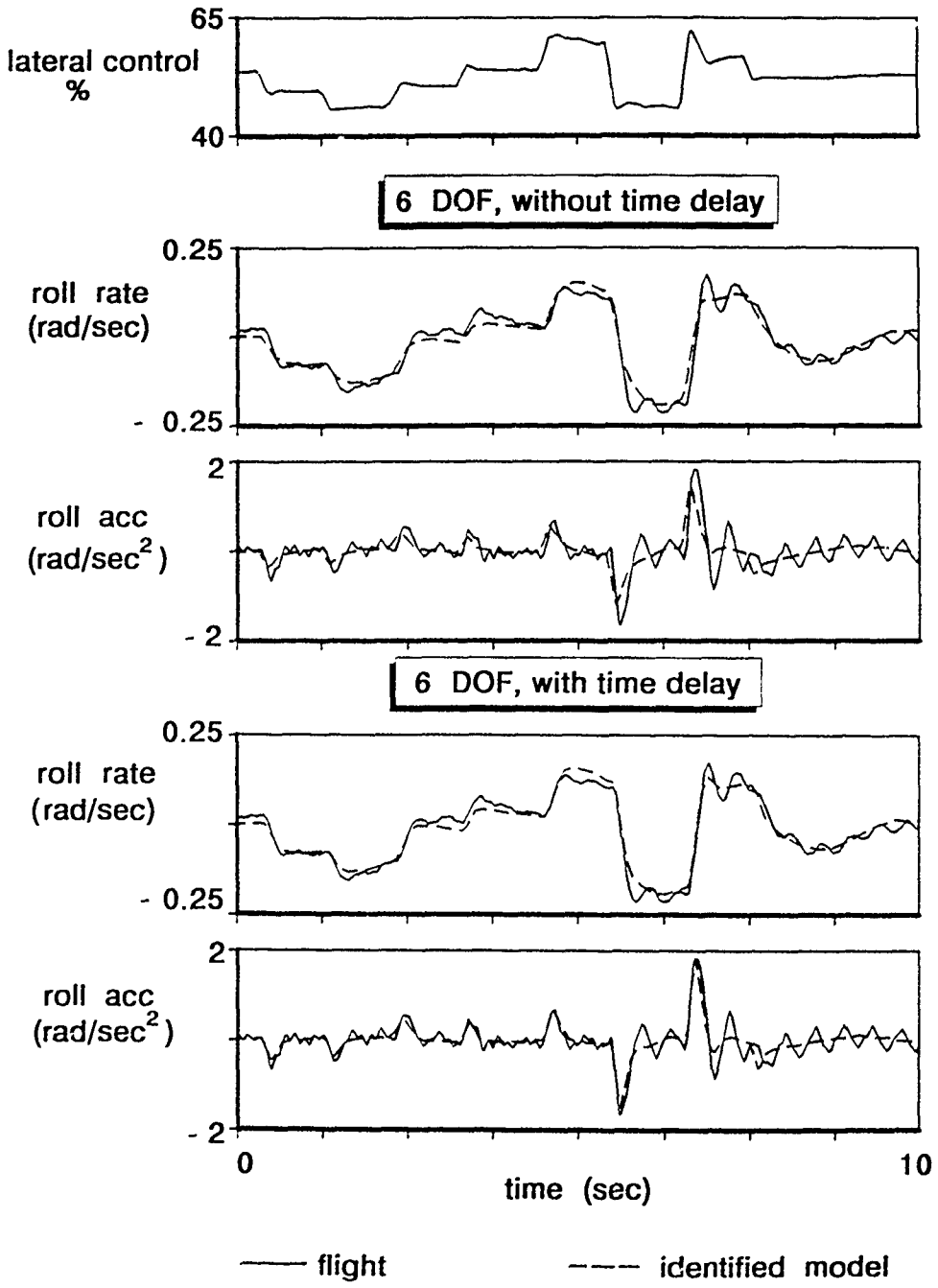

Figure 26. Comparison of identification results for 6 degrees of freedom models without and with equivalent time delays

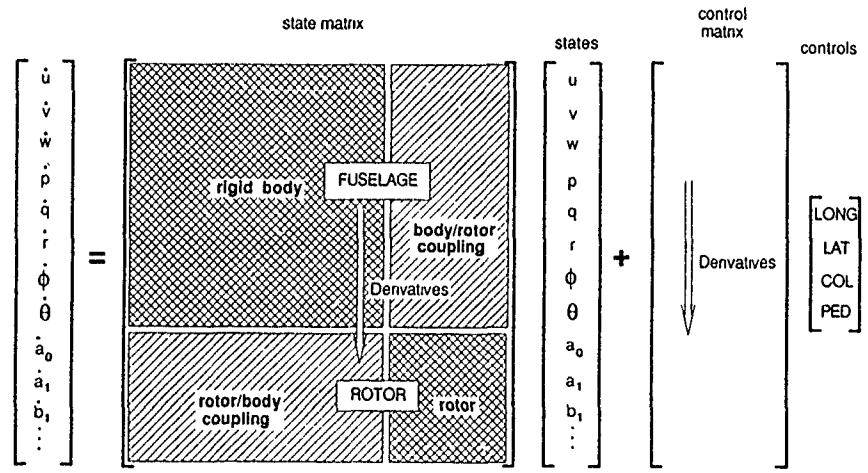

Figure 27. Principal approach to extend 6 degrees of freedom models by rotor degrees of freedom

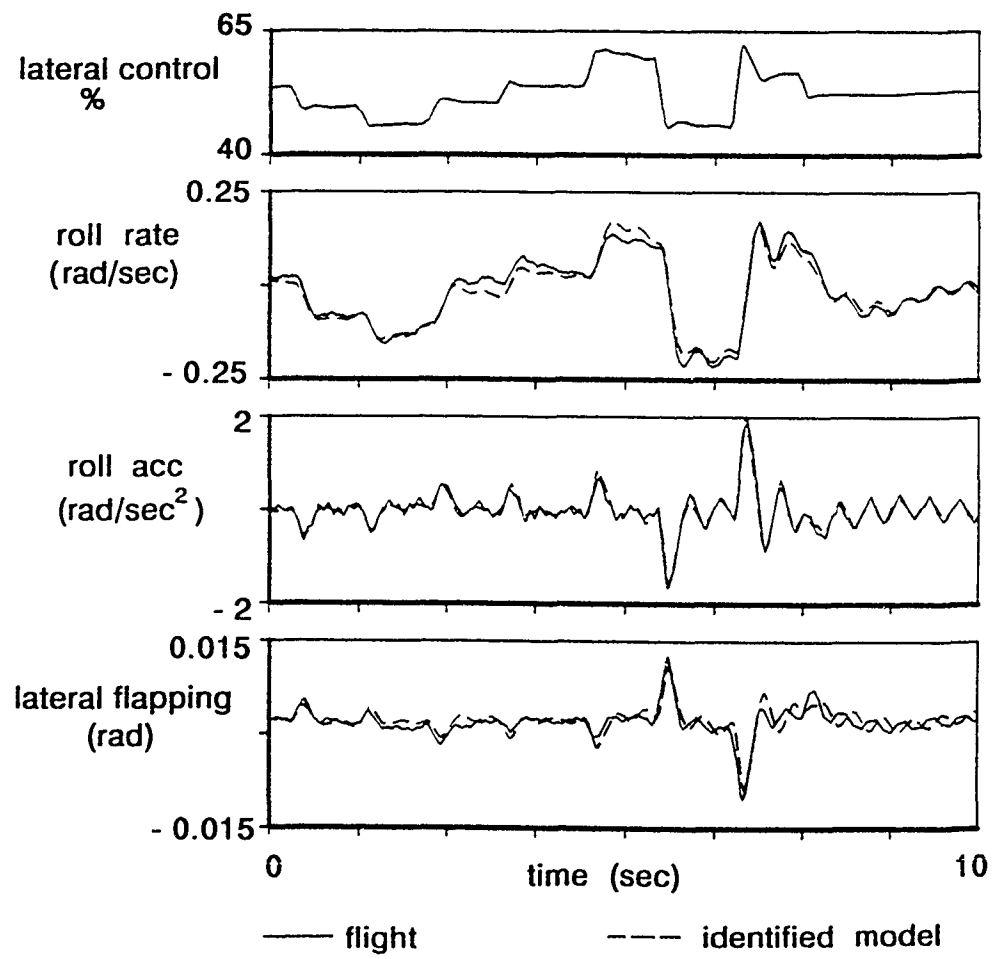

Figure 28. BO 105 identification results for a 16th order model with rotor degrees of freedom

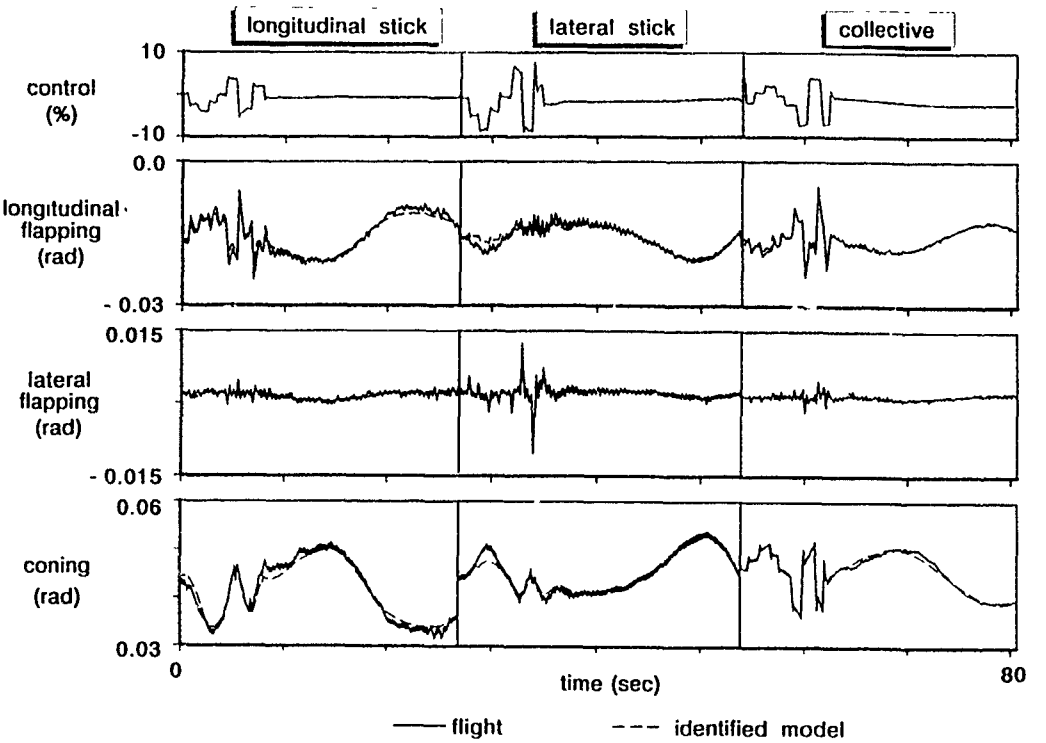

Figure 29. BO 105 identification results for a 16th order model with rotor degrees of freedom

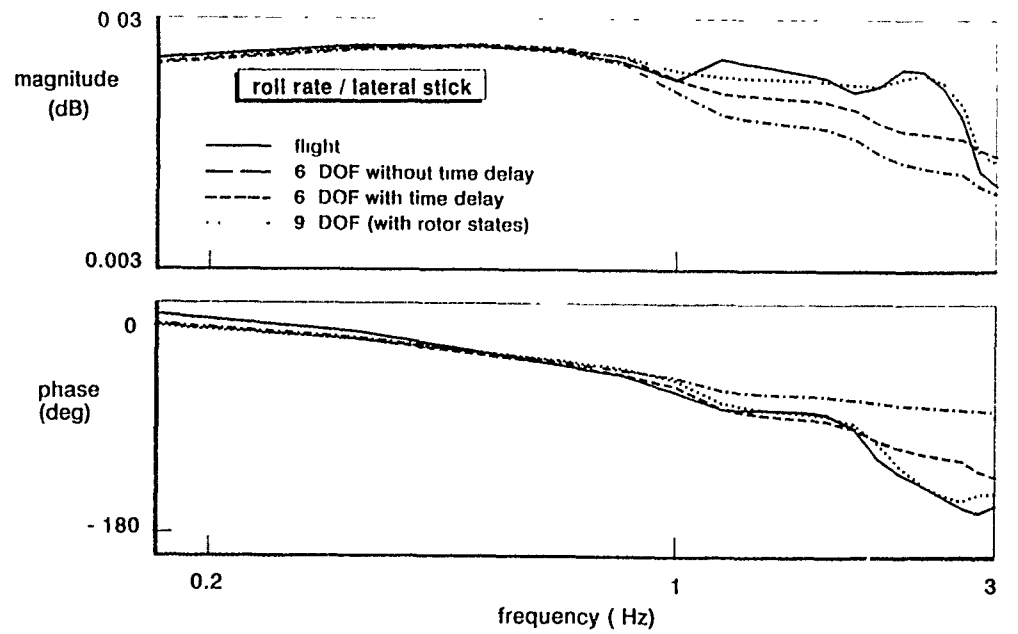

Figure 30. Comparison of the roll rate/lateral stick transfer function for different identified BO 105 models

SA 330 PUMA IDENTIFICATION RESULTS

by

Gareth D. Padfield
Defence Research Agency
Aerospace Division
RAE Bedford, UK

Summary

The SA 330 Puma test data provided by the RAE were analysed with a variety of different identification techniques by six of the participating organisations in AGARD Flight Mechanics Panel Working Group 18. This Paper presents the results of this work. A detailed study of the data kinematic consistency conducted by the RAE is included, highlighting some of the difficulties that can be encountered, even with high quality measurements, and ways of overcoming them. The results of the six degree of freedom identification are discussed in terms of the conventional rigid body modes of motion.

1 Introduction

The Royal Aerospace Establishment provided flight test data from the Research Puma to AGARD WG-18 in December 1987. This Paper describes the aircraft and the associated test database. The results of data consistency analysis, parameter identification and verification analysis are presented. A detailed kinematic consistency study conducted by RAE is included, followed by derivative identification conducted by six of the AGARD participating organisations. The discussion of results is approached from a modal perspective; each of the six degree of freedom modes and their approximations is examined in turn, the major contributing derivatives highlighted and the comparisons between methods discussed. Based on this analysis, some conclusions are drawn that reflect on the confidence in and maturity of system identification methods in helicopter flight mechanics.

2 Helicopter and Instrumentation

The SA 330 Puma is a twin engine, medium support helicopter in the six tonnes category, in service with a number of armed forces including the Royal Air Force to support battlefield operations.

The RAE Research Puma XW 241 (Fig 1) is one of the early development aircraft acquired by RAE in 1974 and extensively instrumented for flight dynamics and rotor aerodynamics research. With its original analogue data acquisition system, the Puma provided direct support during the 1970s to the development of new rotor aerofoils through the measurement of surface pressures on modified blade profiles. In the early 1980s a digital PCM system was installed in the aircraft and a research programme to support simulation model validation and handling qualities was initiated. Over the period between 1981-1988, more than 150 hours of flight testing were carried out to gather basic flight mechanics data throughout the flight envelope of the aircraft. A three-view drawing of the aircraft in its experimental configuration is shown in Fig 2. The aircraft has a four-metal-bladed articulated main rotor (modified NACA 0012 section, 3.8% flapping hinge offset). Basic physical characteristics of the aircraft are provided in Table 1.

Full details of the manoeuvres flown and measurements recorded on the Puma and provided to WG-18 are included in AGARD (1991). Table 2 summarises the data provided; the set eventually selected for primary analysis comprised 3211 inputs on all controls from an 80 kn trim condition. All control inputs were applied by the pilot through the cockpit controls, using a controls fixture to guide the inputs. Manoeuvre times are typically 20-30 s and the recovery was initiated at the test pilot's discretion or when the manoeuvre amplitude had either grown too large or subsided to very small amplitude. Control input amplitudes are typically less than 5% of full range. Response excursions are typically within the range ±10 (kn, deg, deg/s, etc).

The measurements recommended for use by WG-18 are listed in Tables 3 and 4 and were provided to the working group in unprocessed Imperial engineering units. No predistribution corrections were made to reference accelerations or nose-boom vane measurements to the centre of mass. It should be noted that all

kinematic measurements are positive in the usual 'left hand' reference frame sense, except the normal acceleration which is positive up. Many of the measurements were sampled at 128 and 256 Hz but a reduced rate of 64/s was provided to the working group. All channels were passed through anti-aliasing filters at 72 Hz before digitising; in addition, the agility pack data were further filtered by a 2-pole Butterworth at 10.6 Hz. The measurements were recorded in digital PCM (12 bit numbers, 4096 counts) form on magnetic tape on the aircraft. No de-skewing techniques were adopted, resulting in a maximum data skew of about 16 ms.

3 Flight Test Data Evaluation

3.1 General considerations

As noted in the previous section, the Puma datasets provided to WG-18 members had received very limited preprocessing, amounting to decimation down to 64 samples/s and conversion to Imperial engineering units For completeness, the relevant measurements are reproduced in Figs 3 to 6. The response range plotted is 25 s; in some cases the response continues beyond this, in others, recovery is initiated within this range. Prior to model structure and parameter identification it is important to establish the consistency of the kinematic measurements used and, for some identification methods, to determine the properties of any process or measurement noise present in the data. In addition, referencing the measurements to the centre of mass to accord with the reference frame of the dynamic equations, is required. The state estimation procedures applied form part of the system identification methodology and different organisations approached this task in different ways. The following section addresses the RAE approach but some general observations on the raw data in Figs 3 to 6 are worth making at this stage:

(i) Longitudinal cyclic manoeuvres (Fig 3)

The initial response perturbations are all within the 'linear range'; however, during the free response phase, excursions in pitch and roll attitude rise above 0.3 and 0.4 rads respectively. The angular rates and incidence angles remain small however. Roll and yaw excursions during the forward cyclic manoeuvre are of the same order as the pitch excursions and considerably larger than for the aft cyclic manoeuvre. The signal to noise ratios on the x and y accelerations are very low and of the order unity, with a significant component of noise at higher frequency (actually 4/rev) than the frequency of the test manoeuvre. The normal acceleration channel is positive in the unconventional sense as noted but the incidence vane also appears to have an inverted scale factor, the excursions being clearly in the opposite sense to the pitch attitude. While the 'short period' pitch mode appears to be adequately excited, barely one period of the 'phugoid' is contained in the manoeuvre. The initial conditions for incidence and pitch appear inconsistent with steady level flight.

(ii) Lateral cyclic manoeuvres (Fig 4)

Throughout both manoeuvres, response perturbations appear to be within the 'linear range'. The Dutch roll mode is dominant in the free response with roll/yaw/pitch ratio of the order 1/1/0.5. The velocity measurement is supplied in uncalibrated form for the left cyclic manoeuvre (flown on a different occasion to the right cyclic manoeuvre).

(iii) Collective manoeuvres (Fig 5)

All response perturbations lie within the linear range for both manoeuvres; in particular, velocity excursions are very small (5 kn). Recovery action in the roll axis occurs within the 25 s manoeuvre range.

(iv) Pedal manoeuvres (Fig 6)

The dominant mode of response is the lateral/directional Dutch roll with moderate excursions in sideslip (0.2 rads), lateral acceleration (0.1 g) and roll/yaw rate (0.25 rad/s). The phugoid mode appears to have been more strongly excited in the right manoeuvre resulting in greater speed and pitch angle excursions.

From these initial and tentative observations it is clear that some data inconsistencies and noise-related features are present that state estimation can potentially shed light on.

3.2 RAE Bedford kinematic consistency analysis

In previous applications RAE have used an extended Kalman filter (Padfield *et al*, 1987) to derive consistent state estimates for the Puma flight test data. Attempts to estimate noise statistics and calibration correction parameters simultaneously have not succeeded however. For the present activity it was felt that

establishing estimates for the scale factor and bias corrections was important and hence a technique based on output-error estimation was developed (Turner, 1991). The state equations can be written in the usual way for attitudes and velocities.

Attitudes

$$\dot{\phi} = p^* + q^*\sin\phi\tan\theta + r^*\cos\phi\tan\theta \quad . \quad (1)$$

$$\dot{\theta} = q^*\cos\phi - r^*\sin\phi \quad . \quad (2)$$

$$\dot{\psi} = q^*\sin\phi\sec\theta + r^*\cos\phi\sec\theta \quad . \quad (3)$$

Where $p^* = (1 + \lambda_p)p_m - b_p$, etc,
λ_p and b_p are the scale factor and bias corrections respectively and p_m the measurement of roll rate.

Velocities

$$\dot{u} = - q^*w + r^*v + a_x^* - g\sin\theta \quad . \quad (4)$$

$$\dot{v} = - r^*u + p^*w + a_y^* + g\cos\theta\sin\phi \quad . \quad (5)$$

$$\dot{w} = - p^*v + q^*u + a_z^* + g\cos\theta\cos\phi \quad . \quad (6)$$

Where $a_x^* = (1 + \lambda_{ax})a_{xm} - b_{ax}$ etc, and
λ_{ax} and b_{ax} are the scale factor and bias corrections respectively to the measurement $a_{x\,m}$ referred to the centre of mass.

The estimation procedure is configured to run in two sequential passes with the converged results of the attitude pass fixed for the velocity pass. The corresponding measurement equations can be written in the form:

Attitudes

$$\phi_m = (1 + \lambda_\phi)\phi + b_\phi + n_\phi \quad . \quad (7)$$

$$\theta_m = (1 + \lambda_\theta)\theta + b_\theta + n_\theta \quad . \quad (8)$$

$$\psi_m = (1 + \lambda_\psi)\psi + b_\psi + n_\psi \quad . \quad (9)$$

Where the measurement noise vector $[n_\phi, n_\theta, n_\psi]$ is assumed to have a Gaussian distribution with zero mean. The model output is obtained from:

$$\phi_o = (1 + \lambda_\phi)\phi + b_\phi \quad . \quad (10)$$

$$\theta_o = (1 + \lambda_\theta)\theta + b_\theta \quad . \quad (11)$$

$$\psi_o = (1 + \lambda_\psi)\psi + b_\psi \quad . \quad (12)$$

Once again, λ and b represent scale factor and bias corrections respectively.

Velocities

$$V_m = (1 + \lambda_V)(u^{*2} + v^{*2} + w^{*2})^{1/2} + b_V + n_V \quad . \quad (13)$$

$$\beta_m = (1 + \lambda_\beta)\tan^{-1}(v^*/u^*) + b_\beta + n_\beta \quad . \quad (14)$$

$$\alpha_m = (1 + \lambda_\alpha)\tan^{-1}(w^*/u^*) + b_\alpha + n_\alpha \quad . \quad (15)$$

The measurement noise vector $[n_V, n_\beta, n_\alpha]$ is assumed to have a Gaussian distribution with zero mean. The model output follows as for the attitude pass. The velocities u^* , v^* , w^* refer to the velocity components of the boom tip where the vanes and pitot tube are located. Hence, for example, if the point has coordinates x_b, y_b, z_b relative to the centre of mass, we can write:

$$u^* = u + q^*z_b - r^*y_b \ ,$$

$$v^* = v + r^*x_b - p^*z_b \ , \text{ etc} \quad . \quad (16)$$

The vectors of parameters to be estimated in the two-pass-process are:

$$\gamma_a = [\phi(o), \theta(o), \psi(o), b_p, b_q, b_r, \lambda_p, \lambda_q, \lambda_r, b_\phi, b_\theta, b_\psi, \lambda_\phi, \lambda_\theta, \lambda_\psi]^T \quad ..... \quad (17)$$

and

$$\gamma_v = [u(o), v(o), w(o), b_{ax}, b_{ay}, b_{az}, \lambda_{ax}, \lambda_{ay}, \lambda_{az}, b_V, b_\beta, b_\alpha, \lambda_V, \lambda_\beta \lambda_\alpha]^T . \quad ..... \quad (18)$$

Where, $\phi(o)$, $u(o)$, etc, are the state initial values.

The cost function to be minimised in the output-error scheme can be written (Turner (1991)):

$$J = \frac{1}{2}\sum_t z^T S^{-1} z + \frac{N}{2}\log_e|S| + \frac{1}{2}\sum_p \Delta\gamma^T S_\gamma^{-1}\Delta\gamma \quad . \quad (19)$$

The residual vector z represents the difference between the measured and predicted model output vectors:

$$z = z_m - z_o \qquad (20)$$

the residual vector $\Delta\gamma$ represents the difference between the current model parameter estimates and the initial guesses for these parameters:

$$\Delta\gamma = \gamma - \gamma_0 . \qquad (21)$$

S is the measurement (noise) error-covariance matrix and S_γ is an input weighting matrix indicating confidence in the initial guesses provided for the parameter estimates.

The summations in equation (19) are carried out over all N time points (t) and parameters (p) respectively. The Bayesian component (third term in equation (19)) is included to allow some parameters to be held fairly constant during the iterations, for cases where these are known with high confidence *a priori* or over-parameterisation could cause solutions to converge to an obviously incorrect answer. This approach is discussed further by Maine and Iliff (1985). The need for this facility will be demonstrated in the following analysis.

The cost function J is minimised using a Gauss-Newton method, incorporating first and second order partial derivatives with respect to the vector γ.

The steady-state error covariance matrix S is estimated using the definition:

$$S_{est}^{k+1} = \text{Diag}\left[\frac{1}{N}\sum_t (z_m - z_0^k)(z_m - z_0^k)^T\right] , \qquad \ldots\ldots (22)$$

ie the expected value of the off-diagonal terms is zero. z_0^k is the estimated model output obtained by using the model parameter estimates given at the kth iteration.

The formulation given above assumes that process noise is absent and hence that the model equations (1) to (6) are correct. This is not the case in general but the uncertainties of most concern are associated with differences between inertial and local aerodynamic velocities in the velocity pass and vertical gyro anomalies in the attitude pass. These sources of error are often distinctly non-Gaussian and attempts to account for such noise using the usual Kalman filter approach for estimating S will themselves be faulted.

To give some indication of the quality of the unprocessed measurements, Fig 7 shows a comparison of measurements and model output without any calibration corrections. The case examined is the forward cyclic 3211. Some notable observations are:

(a) the reverse scale factor on the incidence vane,

(b) evidence of bias errors manifested in the roll angle and sideslip,

(c) process noise on the velocity measurement.

The output-error optimisation can first be run with the parameter constraint weighting set to very low values (unity) to disable this part of the cost function effectively. The optimised time history comparisons are shown in Fig 8 and corresponding calibration correction estimates in Table 5. The time histories show excellent agreement after 30 iterations. Some observations are:

(i) the roll and pitch time histories have been scaled to about 50% of their original values,

(ii) the initial yaw angle has been shifted by about 30 deg,

(iii) the incidence measurement has been corrected but a negative initial value remains (cf positive pitch angle),

(iv) the process has been incapable of fitting the process noise on the speed measurement.

An examination of the calibration parameters in Table 5 provides evidence for some of these observations. The scaled attitudes are entirely a result of over- parameterisation with the rate and attitude gyro scale factors strongly correlated, *ie*:

$$(1 + \lambda_p) = \frac{1}{1 + \lambda_\phi}$$

$$(1 + \lambda_q) = \frac{1}{1 + \lambda_\theta} . \qquad (23)$$

The scale factor and bias on the yaw channel and the initial value $\psi(o)$ appear also to be correlated, such that,

$$\lambda_\psi \psi(0) \sim b_\psi . \qquad (24)$$

A quite distinct problem arises in the velocity pass, and is manifested in the magnitude of the accelerometer scale factor corrections $\lambda_{ax}, \lambda_{ay}$. These estimates are considered to be physically implausible even though the standard deviations are very small. The expected accuracy of these quality inertial sensors is high and the small amplitude of the excursions in all but the pedal manoeuvres suggests that the effects should actually be very small in equations (4) and (5). In fact, these equations show that for small manoeuvres, du/dt and dv/dt are linearly related to θ and ϕ respectively and that the gravitational terms dominate. The acceleration a_x will however be strongly correlated with du/dt and θ and the optimisation will try to use this signal to minimise errors. Fig 9 shows the individual components of the du/dt and dv/dt variations confirming qualitatively the above points. This is the source of the anomaly and for both the velocity and attitude pass, recourse to parameter constraints has to be sought to achieve realistic solutions.

The selection of the weighting elements of the matrix **S** is not obvious and in general may need to be different for each run. For the present study a ratio of 1 to 10^6 was chosen between corresponding free and fixed parameters. On the basis of the previous arguments, the 'fixed' parameters were selected as:

$$\lambda_p, \lambda_q, \lambda_r, \lambda_{ax}, \lambda_{ay}, \lambda_{az}, b_\psi, \psi(o) .$$

The results for the longitudinal cyclic run are given in Fig 10 along with the optimized calibration corrections in Tables 6 to 8. For the attitude pass the time history comparisons indicate that an excellent fit has been achieved for all runs. The attitude scale factor corrections are small with low standard deviations, except for the pitch attitude in the left cyclic run where a 13% change has been identified. The bias estimates are also in general small, typically of the order 1 deg. Exceptions are the roll biases for the collective runs which are of the order 3 deg. The initial values have been corrected accordingly as shown in Table 8. The results of the attitude pass lead to increased confidence in the measurements but there is sufficient scatter in the results from run to run to cause concern about the accuracy of any particular value.

Turning to the velocity pass results, a more interesting set of comparisons can be observed. In general, a good optimisation has been achieved for each run with one or two exceptions. The integrated velocity data typically exposes the need for bias corrections on the accelerometers and highlights the presence of process noise on the velocity channel. The aft cyclic run has converged with a high scale factor correction estimated for the sideslip velocity. Scale factor corrections are to be expected on the air data measurements on account of static calibration inaccuracies and also the bias effects of process noise present due to local flowfield effects. In general these are less than 10% and the estimates have fairly low standard deviations (<10% of parameter value). The aft cyclic run is a strong exception and attempts to stiffen other parameters to resolve the anomaly have not produced consistent results.

The kinematic consistency analysis described above was conducted by RAE after most of the identification work had been completed by participating organisations. This study has provided insight into some of the pitfalls of state estimation. Estimated calibration correction factors vary from run to run in an unexpected manner although in absolute terms most of the values are small. It is not possible to recommend a definitive set of corrections for these supposedly deterministic errors and therefore, in most cases, filtered measurements are, it could be argued, appropriate for use directly in the model structure and parameter identification stages.

4 Identification Methods

Methods and results for the DLR and Glasgow identification are included in this section. Corresponding data from the other WG-18 organisations will be reported in Padfield (1991).

4.1 DLR

Files for the 80 kn flight condition with 3211 test inputs, which were concatenated for identification purposes, were longitudinal cyclic (aft), lateral cyclic (right), pedal (left) and collective (up) control responses. Files used for verification purposes were longitudinal cyclic (forward), lateral cyclic (left), pedal (right) and collective (down) control responses.. In the model structure and parameter estimation stage of the identification process the chosen state vector was:

$$x = (u, v, w, p, q, r, \phi, \theta)^T \quad (25)$$

and the measurement vector was:

$$y = (a_x, a_y, a_z, p, q, r, \phi, \theta, u, v, w)^T . \quad (26)$$

Estimation was carried out using the DLR non-linear maximum likelihood program (see, *e g* Jategaonkar and Plaetschke, (1983)). All state variables were used and no use was made of pseudo-controls. No elements of the system and control input matrices were fixed and all kine-matic and gravity terms were included. Pure time delays were included for control inputs, except for the pedal input.

4.2 University of Glasgow/RAE

Files principally used for parameter identification involved the 80 kn flight condition with 3211 inputs. Measurements used were speed, incidence, flank angle, pitch rate, pitch angle, roll rate, roll angle, yaw rate, longitudinal acceleration, lateral acceleration, normal acceleration, collective, longitudinal cyclic, lateral cyclic and pedal. The portion of each record used was not the same in all cases. The responses to the collective-down input were truncated after approximately 14 s and were thus significantly shorter than all other records which involved between 20 s and 25 s of data. The sampling frequency used was 32 Hz. No filtering was carried out on the flight data.

Model structure and parameter estimation were carried out using a three-stage approach involving frequency-domain equation-error and output-error techniques (Black and Murray-Smith, (1989); Black (1989)). Work was carried out using both single records and combinations of records. The analysis of combinations of records has involved the application of a technique, developed at the University of Glasgow, for multiple-run identification (Black and Leith, (1990)). This approach retains the individuality of separate runs and avoids some of the known problems of concatenation. It involves the introduction of an additional summation loop in front of the individual cost functions associated with each separate data set. This gives a combined cost function,

$$J_{total} = \sum_{i=1}^{N} J_i \quad (27)$$

for N data sets. Expressions have been derived which show that, under certain conditions (*e g* the cost surface is a close approximation to a quadratic in the vicinity of the minimum), the multiple-run estimates and corresponding standard deviations may be obtained *a priori* using the individual results from the runs forming the basis of the multiple-run identification.

The individual cost functions for the frequency-domain output-error stage of the identification process were based upon a maximum likelihood form of criterion involving summation over a specified frequency range. Pseudo control inputs were used in this approach. In this application the range considered was 0.049 Hz to 0.492 Hz. The error-covariance matrix estimate was updated at each iteration on the basis of predicted model outputs. Convergence is required in both the model parameter values and in diagonal elements of the error-covariance matrix. Minimisation involved a quasi-Newton method together with an optimal linear-search algorithm. Some parameters were fixed in the identification process but no other constraints were included.

A time-domain output-error identification stage was used, following the frequency-domain output-error identification, in order to estimate zero offsets and initial states.

Verification was carried out using data sets which were not used in identification.

5 Identification and Verification Results

The principal results of the studies are as follows:

(i) Tables 9 through 13 contain the stability and control derivatives and equivalent time delays estimated by Glasgow, DLR, ONERA (with and without time delays), NAE and NLR. All 36 stability and 24 control derivatives are included although in many cases (particularly Glasgow, DLR and NLR analyses), some are deleted *a priori*, on the assumption of the small contribution to an adequate model structure.

(ii) Table 14 contains the eigenvalues corresponding to the assembled state matrices (with known gravitational and kinematic terms). Included are the US Army results derived from transfer function fitting of the roll rate, yaw rate and sideslip response to lateral cyclic and pedal.

(iii) Tables 15 to 18 contain results from the modal analysis described in more detail in the next section.

(iv) Figs 11 and 12 illustrate the Glasgow time history fits for translational and angular velocities corresponding to the identification and verification runs respectively. The concatenated runs for the identification are, from left to right, longitudinal cyclic (aft), lateral cyclic (right), pedal (left) and collective (up). Inputs for the verification runs correspond to the opposite directions.

(v) Figs 13 and 14 illustrate similar results from the DLR.

(vi) Fig 15 shows Helistab results for varying static stability derivatives (discussed in relation to longitudinal dynamics below).

The derivatives in Table 9 to 13 are accompanied by their standard deviations in parenthesis. Values of the latter below 5% of the associated parameters are deemed to be estimated with very high confidence. Nearly all the major derivatives (dampings, primary control, roll/yaw sideslip) fall into this category. Many of the cross coupling derivatives fall outside this category. The most disturbing feature is the variation of derivative estimates across the methods. Comparing results from Glasgow, DLR and ONERA (with time delay), there is some consistency (<20%) across derivatives like L_v, Z_{col}, Z_w and N_{ped}, while other, equally important, effects are estimated with variations of 50% and higher, *eg* L_p, M_q, L_{lat}, M_{lon}. In some cases, very small but important derivatives are estimated with striking consistency, *eg* Y_v, and others much less so, *eg* M_w, X_u. The total damping, computed either from the sum of matrix diagonal elements or eigenvalue real parts, varies from greater than 5 (Glasgow, DLR) to less than 3 (NAE, NLR). These anomalies are a source of concern and insufficient effort has been focused on resolving them to date. In most cases the same or very similar time histories were used in the identification, but the different cost functions, minimisation algorithms and parameter constraints used will all lead to particular solutions and exacerbate the non-uniqueness of system identification process. The variation of results across the methods cannot be fully accounted for without recourse to more detailed examination. The issue is raised, however, as to which, if any, of the approaches is the better. This is also difficult to resolve; the DLR and Glasgow multi-run results are classic examples. Roll and pitch damping are estimated to be greater than 2 and 1 respectively; the *Helistab* simulation predictions are -1.68 and -0.71 respectively and are considered to be reasonable theoretical estimates of these effects. Is the simple *Helistab* theory really 50% in error, or are the flight derived estimates in some sense biased? Such a question must have a validated answer before system identification methods can be used entirely with confidence. In the next section, the results summarised above will be examined in more detail with respect to the dynamic modes of motion to support an improved understanding of the variations discussed.

6 Discussion of Results

From the compendium of results contained in Tables 9 to 13 and Figs 3 to 6, we can extract subsets that reflect the fundamental properties of the dynamic modes under suitable conditions. In the mid-speed range, articulated-rotor helicopters typically exhibit conventional flight modes, *eg* short period, roll subsidence, etc; while couplings can be moderate, *eg* roll/pitch, they manifest themselves as forced motions and tend not to have a strong effect on modal frequencies and dampings. Most of the dynamic excursions in the test manoeuvres can be considered to be within the normal linear range, at least as far as the aerodynamic loads are concerned. The estimated stability and control derivatives should therefore be reasonably close to their physical counterparts; assembling the approximating factors from these can provide insight into the corresponding fit errors and the overall confidence levels in the results.

(i) Longitudinal short period mode

The approximate characteristic equation for this mode is very well documented in textbooks and has received detailed scrutiny by Padfield (1981).

$$\lambda^2 - (Z_w + M_q)\lambda + Z_w M_q - M_w(Z_q + V) = 0 . \quad \text{..... (28)}$$

This approximation assumes that speed is constant during the pitch manoeuvre. Table 15 shows a comparison of the approximate results with the eigenvalue data from Table 14; included are the RAE *Helistab* simulation results. In most cases the agreement is within 20%, some better than 5%. Where the

comparisons are good, attention can be focused on the simple components of the approximation. A comparison of results across the methods reveals stronger variations in damping and frequency. Why this should be so is difficult to explain without access to the details of the estimation algorithms and procedures. In order that these comparisons can be related to the short period time responses, the control effectiveness ratios need to be compared as shown in Table 15. Both cyclic and collective control sensitivities/damping ratios are included and these show a similar level of variation between methods. Another key parameter featuring in equation (28) is the static stability derivative M_w, which serves to couple pitch and heave and turn what would otherwise be a pair of subsidences into an oscillation. The variation across the results is again strong and reflects the variations in short period frequency ω_{sp}. The standard deviations for the parameter estimates discussed are typically quite small, indicating good confidence in the values.

The key time histories for pitch short period behaviour are pitch rate and incidence for the identification run in response to longitudinal cyclic control. Both the DLR and Glasgow analyses used air data measurements. An obvious question to address is how such distinct derivatives and associated modal characteristics can result in such similar time responses. A comparison of the Glasgow and DLR results illustrates the point adequately; using the Glasgow results as a reference, the DLR results indicate,

(a) 25% difference in damping,

(b) 40% difference in frequency,

(c) 300% difference in static stability M_w.

The fits for the verification runs shown in Figs 12 and 14 are poorer, particularly the Glasgow incidence comparison.

Overall the results are inconclusive regarding the relative merits of one technique over another, with regard to estimating short period characteristics.

(ii) Longitudinal phugoid

With only 25 s of response, the information content on the low frequency phugoid mode is low. In general however, the match of the u velocity component is quite good and reveals a complete cyclic of the phugoid mode. The approximate formulae for damping and frequency set out in Padfield (1981) is based on the assumption that the phugoid is characterised by weakly damped vertical and horizontal motions. The damping is composed of a large number of small effects including the drag derivative X_u. It is shown by Padfield (1981) that this approximation is unlikely to be valid at 80 kn and, of course, with barely one oscillation cycle of data, such weak damping would not be easy to estimate. The frequency on the other hand is dominated by a particular combination of derivatives:

$$\omega_p^{*2} \cong -g \cos\theta_0 \frac{Z_w M_u}{(M_q Z_w - M_w(Z_q + V))} . \quad (29)$$

Table 16 shows a comparison of ω_p derived from equation (29) with the corresponding eigenvalues of the full system taken from Table 14. It is clear that the estimation methods agree very well on these parameters and that the approximation in equation (29) gives good agreement, with variations generally less than 10%. It should be noticed that this correlation results from combining individual effects (*ie* ω_{sp}, M_u) that typically vary by more than 100%. This result suggests that some correlation exists between the identified parameters, *eg* the ratio of M_u to ω_{sp} is roughly a constant. Both the static stability derivatives M_u and M_w are small, poorly identified (based on the scatter between different methods), but at the same time play a key role in the form of the response history. Fig 15 shows *Helistab* results for the Puma at 80 kn in response to a clinical 3211 input on longitudinal cyclic. The short term response is strongly sensitive to M_w and the longer term to M_u. The range of derivative values depicted cover those values estimated by the different organisations. These results confirm the classical importance of these derivatives to vehicle behaviour.

The results for the two longitudinal modes described above suggest some conflict in the estimation of physically meaningful characteristics for both modes simultaneously.

(iii) Roll subsidence

The role damping L_p is the key derivative here and Table 10 indicates an estimation range between -0.7 (NAE) and -2.5 (DLR). The standard deviations are very small for all

estimates. It is interesting to note that the two examples cited above correspond to cases with effective time delays of zero and 125 ms respectively. It is known (Padfield, 1987) that the roll damping can sometimes be grossly underestimated if no account is taken of the effective delay introduced by the actuation and rotor system. This could well have played a part here. The roll mode eigenvalues given in Table 14 correlate well with the damping in most cases. Table 17 compares the rate sensitivity ratio for the various cases revealing a spread from 0.015 to 0.03 (rad/s %). Such a wide variation is not reflected in the short term roll response to lateral cyclic shown in identified responses, *eg* Glasgow traces. As will the longitudinal modes however, the quality of lateral mode estimation cannot be fully discussed in isolation.

(iv) Dutch roll

The approximating polynomial for the Dutch roll mode is more difficult to derive and will depend on the extent of coupling between roll, yaw and sideslip. The most general single mode formulation has been derived by Padfield (1991) and assumes that sideslip and sideways velocity can be regarded as weakly coupled.

The quadratic then takes the form:

$$\lambda^2 + 2\zeta\omega_r)\lambda + \omega_r^2 = 0 , \qquad (30)$$

where

$$(2\zeta\omega_r)^* = \frac{-\left[N_r + Y_v + \sigma\left\{\frac{L_r}{V} - \frac{L_v}{L_p}\right\}\right]}{\left(1 + \frac{\sigma L_r}{L_p V}\right)} , \qquad \ldots\ldots (31)$$

$$\omega_r^{*2} = \frac{(VN_v + \sigma L_v)}{\left(1 + \frac{\sigma L_r}{L_p V}\right)} , \qquad (32)$$

$$\sigma = \frac{(g - N_p V)}{L_p} . \qquad (33)$$

A comparison of Dutch roll damping and frequency for the different methods is provided in Table 18. The frequency is generally predicted very well by the approximation, being dominated by the directional stability N_v . In most cases about 75% of the damping is predicted by the approximation; the variation between methods is, however, quite large. Time history matches are good, particularly for yaw, but also roll and pitch. The quality of comparison in the verification runs is less good with even small mismatches in frequency and damping clearly visible in some cases (*eg* Glasgow results). Equations (31) and (32) highlight the role of the yaw/roll coupling derivatives (L_r , N_p) in the Dutch roll dynamics. In general, these parameters are expected to be physically less dominant and smaller than their primary counterparts (L_p , N_r). The results shown in Table 10 suggest the contrary in some cases (*eg* NAE - L_r/L_p , DLR, NLR - N_p/N_r). To an extent these apparent distortions can be explained by the effects of inertial coupling between roll and yaw, but by no means entirely. The potential for parameter correlation in the Dutch roll analysis is believed to be very high, especially with such low damping and the almost anti-phase relationship between roll and yaw. More discussion on the Dutch roll results are contained in one of the application case studies in this lecture series (see Padfield (1991)).

(v) Spiral mode

The usual approximation for the slow spiral mode takes the form (Padfield and DuVal, 1982):

$$\lambda_s \equiv \frac{g}{V}\frac{(L_v N_r - N_v L_r)}{(L_p N_v - N_p L_v + \frac{g}{V}L_v)} . \qquad (34)$$

A cursory examination of the time histories indicates that there is little evidence of any spiral mode excitation at all in the dynamic response. A comparison of approximate and full model results for just the Glasgow and DLR data reveals the poor correlation particularly for the former, which is typical of results from all the different methods.

Glasgow

$$\lambda_s^* = -0.022$$

$$\lambda_s = -0.005$$

DLR

$$\lambda_s^* = -0.0673$$

$$\lambda_s = -0.048 .$$

Like the phugoid damping, the spiral mode is difficult to identify, being a residue of two quite strong effects (*cf* numerator in equation (34)) and is probably better identified in part by conventional 'turns-on-one-control' manoeuvres (Padfield, 1985).

(vi) Cross coupling

The prediction and estimation of cross coupling effects on helicopters has presented serious hurdles and has been reported in much of the published identification work. An underlying concern has been that if the coupling effects are poorly estimated or distorted then this will reflect on the primary responses too, and in many cases this has led to the neglecting of coupling effects or their relegation to pseudo controls. Regarding the current Puma analysis the following observations can be made:

(a) Lateral velocity, roll and yaw response for the longitudinal cyclic inputs are poorly predicted in both identification and verification runs. The flight data indicates that the Dutch roll mode has been strongly excited while this mode is practically absent for the reconstructed responses. Most of the related derivatives, *eg* L_q, L_w, N_q, N_w are estimated with low confidence and often have unrealistic values (*eg* L_q). The analyses do not normally provide data on the sensitivity of the overall cost function to individual time history fits . This kind of information could prove very useful in understanding some of the anomalies, *eg* the roll response to longitudinal cyclic is as pronounced as the pitch response and yet, in most cases, the optimisation appears to have ruled out roll as a contribution to the minimising process.

(b) In contrast, the pitch and heave responses during the lateral cyclic and pedal manoeuvres appear to be reasonably well modelled. This is particularly true for the DLR identification and verification results. Both the contributing derivatives M_p and M_v are estimated with high confidence although the former is of opposite sign to that predicted from purely aerodynamic considerations (*Helistab* value = -0.22). The relatively high value of M_v is surprising and almost certainly a major contribution to the pitch response in the Dutch roll.

(c) In general the collective responses provide the poorest comparisons. The Dutch roll mode is clearly excited yet few of the methods appear to capture the corresponding roll and yaw motions. The pitch/collective coupling is generally well represented, suggesting compatibility between the estimated character of the short period mode in response to cyclic and collective inputs.

(vii) Control derivatives

The control effectiveness is one of the few derivatives with a direct physical interpretation; following an application of control an aerodynamic force is generated that induces measurable fuselage translational and rotational accelerations. Control derivatives are by far the most important parameters for control law design and having accurate estimates across the required frequency range is vital for maximising robustness. The Puma estimates are contained in Tables 11 and 12. Some notable features are:

(a) Primary cyclic derivatives are estimated with low standard deviations but vary across the methods by more than 50% relative to the Glasgow reference value.

(b) Cross cyclic control derivatives are estimated with low confidence, sometimes not at all, and sometimes with different signs.

(c) With the exception of the DLR value the pitching moment from collective is estimated with strong consistency.

(d) The collective sensitivity Z_{col} is estimated with confidence but again varies between methods; the heave sensitivity Z_{col}/Z_w appears to be reasonably constant across the methods however.

(e) The yaw control derivative N_{ped} varies by about 25% of the Glasgow reference value; the corresponding sideforce derivatives are generally estimated with low confidence however and do not relate kinematically with N_{ped}.

(f) The X and Y control derivatives are generally small and poorly estimated.

(viii) General

An important factor to recognise in system identification is that the values of the estimated parameters within a given model structure are

instrinsically linked to one another. This is particularly acute within the individual modes of motion as demonstrated in the above discussion, *eg* if the value of M_q was varied in equation (29) then other parameters, say M_u, would need to change to give the same value of ω_p^*. Hence, any individual parameter distortions or errors propagate throughout the model structure. Cross-coupling derivatives can have a most insidious affect in the context, corrupting the values of more important primary stability and control derivatives. This linkage or correlation has been demonstrated on several occasions above and appears to be common to all of the different approaches taken. The phenomenon is, of course, intrinsic to the basic multi-run, full-state model structure analysis, whether output-error or equation-error. Classically it can be described as over-parameterisation and can only be overcome by constraining the model structure or improving the information content in the test data. The latter is primarily dependent on the control input shaping; the 3211 runs used for the SA 330 analysis were composed of a 7 s forced response following by 18 s of free response. The spectrum of the control input and hence the force response is relatively broad up to about 3 rad/s. The free response, constituting over 70% of the manoeuvre, is made up entirely of the natural modes with relative magnitudes dependent on the 'initial conditions' at the termination of the control input. In practice, the weakly damped Dutch roll and phugoid dominate the response. The information content will therefore be quite different from data obtained from persistent excitation, *e g* frequency sweep. No analysis of the sensitivity of parameter estimates to information content was carried out on the SA 330 data by WG-18. There appears to be potential for improved understanding of the results through such analysis; additional interactive tools could help here, allowing the fit weightings to be varied across different measurements and data time/frequency slices.

With regard to model structure constraints, again only limited work was achieved by WG-18 amounting to the fixing of particular derivatives to zero, the treatment of cross coupling as pseudo controls (Padfield, 1991) and the single mode transfer function analysis by the US Army (Padfield, 1991). Further analysis is required before general conclusions can be drawn but, once again, there is potential for improved understanding through creative model structure constraints allied to the information content analysis discussed above.

7 Conclusions

Six of the participating organisations in AGARD WG-18 conducted system identification on the SA 330 Puma flight test data provided by the Royal Acrospace Establishment, UK. This Paper has reviewed the test data itself and the various identification methods applied by the different organisations. A six degree of freedom model structure was assumed for all the work. Results have been presented including estimates of stability and control derivatives and comparison of test and reconstructed time histories for the collection of multi-step control input manoeuvres. Special consideration has been given to the RAE data consistency analysis and also a physical interpretation of the derivatives through approximations to the dynamic modes of motion. From the results presented the following observations and conclusions can be drawn.

(i) Calibration factor corrections derived from a systematic output-error analysis has highlighted a variability from run to run that cannot be fully explained from the analysis. A constrained optimisation was required to achieve a realistic solution in most cases. The correction factors are generally small and readily account for integrated inertial errors that otherwise grow during the manoeuvres.

(ii) Many of the primary derivatives are estimated with a strong confidence by the various methods. However, the variation between results from different methods is a cause for concern. Typically, very good time history fits are achieved by two methods with widely differing (>50%) derivative estimates.

(iii) Cross coupling derivatives are generally estimated with low confidence; on occasions the values are still significant which must, in turn, cast doubt on the distorted values of the associated primary derivatives.

(iv) An analysis of the modal behaviour through approximate formulae has proved useful in highlighting the importance or otherwise of particular combinations of derivatives. Some correlation between modal estimates has been observed, *eg* phugoid period and short period damping, Dutch roll and roll subsidence, *ie* an M_q value appropriate to the phugoid may not be best for the pitch mode. The results are somewhat inconclusive, however, and further information content and model structure analysis is required to support an improved understanding of the results.

(v) Potentially useful analysis tools to support the identification have been identified, *eg* sensitivity of the cost function to the fits of individual time histories, or portions of response.

Acknowledgments

The author would like to express his gratitude for the support provided by colleagues on AGARD WG-18 in the derivation of results presented in this Paper; particular thanks to David Murray-Smith and his team at Glasgow University. Thanks also to Graham Turner at RAE Bedford for results of the data consistency analysis in section 3.2.

References

AGARD
Rotorcraft System Identification
AGARD Advisory Report No. 280, 1991

Black, C.G.
A Users' Guide to the System Identification Programmes OUTMOD and OFBIT
University of Glasgow, Department of Aerospace Engineering Report, 1989

Black, C.G.; Murray-Smith,D.J.
A Frequency Domain System Identification Approach to Helicopter Flight Mechanics Model Validation
Vertica, Vol.13, No.3, 1989

Black, C.G.; Leith, D.J.
On the Combination of Data-Sets for Helicopter System Identification
University of Glasgow, Department of Aerospace Engineering Report No 9016, 1990

Jategaonkar, R.; Plaetschke, E.
Maximum Likelihood Parameter Estimation from Flight Test Data for General Nonlinear Systems
DFVLR-FB-83-14, 1983

Maine, R.; Iliff, K.W.
Identification of Dynamic Systems: Theory and Formulation
NASA Reference Publication 1138, 1985

Padfield, G.D.
On the Use of Approximate Models in Helicopter Flight Mechanics
Vertica, Vol. 5, No.3, 1981

Padfield, G.D.; DuVal, R.W.
Applications of System Identification Methods to the Prediction of Helicopter Stability, Control and Handling Characteristics
NASA CP-2219, 1982

Padfield, G.D.
Flight Testing for Performance and Flying Qualities
AGARD Lecture Series LS-139 'Helicopter Aeromechanics', 1985

Padfield, G.D. *et al.*
UK Research into System Identification for Helicopter Flight Mechanics
Vertica, Vol.11, No.4, 1987

Padfield, G.D.; DuVal, R.W.
Application Areas for Rotorcraft System Identification: Simulation Model Validation
Paper No.12, AGARD LS-178, 1991

Padfield, G.D.
Results of AGARD WG-18 System Identification analysis applied to test data from the RAE research Puma helicopter
RAE Technical Report (in preparation), 1991

Turner, G.P.
Consistency Analysis of Helicopter Flight Test Data
RAE Technical Memorandum (in preparation), 1991

Mass and moments of inertia	
Mass	5805 kg
Manufacturer's estimates based on $m = 5800$kg	
I_x	9638 kg m^2
I_y	33240 kg m^2
I_z	25889 kg m^2
I_{zx}	2226 kg m^2
Main rotor	
Diameter	15 09 m
Blades	4
Chord	0 54 m
Airfoil	NACA 0012
Blade Area (from hub)	16 2 m^2
Blade Area (from cutout)	12 33 m^2
Solidity (Thrust)	0.0917
Twist	8°
Shaft Angle	5°
Nominal rotorspeed	27 rad/s
Tail rotor	
Diameter	3.042 m
Blades	5
Chord	0.18 m
Airfoil	NACA 0012
Solidity	0.19
Twist	0°
Main/tail rotor gearing	4 82
δ_3 angle	−45°
Horizontal stabilator	
Span	2 11 m
Area	1 4 m^2
Incidence	− 1°
Vertical tail	
Span	1 14 m
Area	1.34 m^2
Incidence	− 1 5°

Table 1 Physical characteristics of the RAE Research SA-330

Control Input						Flight Conditions		
Control	Type	Initial displacement	Duration t_i or Frequency content f_i	File name	Number of runs	Recording time per run in s	Mass	Airspeed	Altitude
Longitudinal	3211	Aft	$t_i \approx 7$s	3211A 080	1	30	5805 kg	80 kn	$H_p \approx 3800$ ft
Longitudinal	3211	Forward	$t_i \approx 7$s	3211F 080	1	30	5819 kg	80 kn	$H_p \approx 3800$ ft
Longitudinal	3211	Aft	$t_i \approx 7$s	F568FAC.AFT	1	30	5805 kg	80 kn	$H_p \approx 3800$ ft
Longitudinal	3211	Forward	$t_i \approx 7$s	F568FAC.FWD	1	30	5819 kg	80 kn	$H_p \approx 3800$ ft
Longitudinal	3211	Aft	$t_i \approx 7$s	3211A 100	1	25	5760 kg	100 kn	$H_p \approx 2000$ ft
Longitudinal	3211	Forward	$t_i \approx 7$s	3211F 100	1	40	5778 kg	100 kn	$H_p \approx 2000$ ft
Lateral	3211	Right	$t_i \approx 7$s	F568LAT.RGT	1	30	5846 kg	80 kn	$H_p \approx 3800$ ft
Lateral	3211	Left	$t_i \approx 7$s	F550LAT.LFT	1	40	5705 kg	80 kn	$H_p \approx 1850$ ft
Pedal	3211	Right	$t_i \approx 7$s	F576PED RGT	1	30	5791 kg	80 kn	$H_p \approx 3150$ ft
Pedal	3211	Left	$t_i \approx 7$s	F576PED LFT	1	30	5764 kg	80 kn	$H_p \approx 3200$ ft
Collective	3211	Up	$t_i \approx 7$s	F568COL.UPC	1	30	5760 kg	80 kn	$H_p \approx 4150$ ft
Collective	3211	Down	$t_i \approx 7$s	F568COL.DWN		20	5751 kg	80 kn	$H_p \approx 4100$ ft
Longitudinal	2121	Aft	$t_i \approx 6$s	3211A 060	1	30	5823 kg	60 kn	$H_p \approx 1800$ ft
Longitudinal	2121	Forward	$t_i \approx 6$s	3211F 060	1	30	5782 kg	60 kn	$H_p \approx 1900$ ft
Longitudinal	Frequency sweep	—	0 05Hz $\leq f_i \leq$ 5Hz	SWEEP 060	1	80	5737 kg	60 kn	$H_p \approx 3000$ ft
Longitudinal	Frequency sweep	—	0 05Hz $\leq f_i \leq$ 5Hz	SWEEP 080	1	80	5737 kg	80 kn	$H_p \approx 3000$ ft
Longitudinal	Frequency sweep	—	0 05Hz $\leq f_i \leq$ 5Hz	SWEEP.100	1	80	5737 kg	100 kn	$H_p \approx 3000$ ft

Inertias

Aircraft inertias (manufacturer's estimates) based on aircraft mass of $m \approx 5800$ kg and referred to body axes with origin in center of mass appropriate to tests flown

$I_x \approx$ 9640 kg m^2, $I_y \approx$ 33240 kg m^2, $I_z \approx$ 25890 kg m^2, $I_{zx} \approx$ 2230 kg m^2

Table 2 SA-330 manoeuvres flown

Variables		Source	Original Sampling Rate (in Hz)
Group	Quantity		
Control displacements	Forward/aft cyclic	Potentiometer	128
	Lateral Cyclic	Potentiometer	128
	Pedal	Potentiometer	128
	Collective	Potentiometer	128

Table 3 SA-330 Control Variables
Data provided at a uniform sampling rate of 64 Hz.

Variables		Source	Original Sampling Rate (in Hz)
Group	Quantity		
Air data	Angle of attack	Noseboom vane	128
	Angle of sideslip	Noseboom vane	128
	Airspeed	Pitot	128
	Climb rate	Static pressure	128
Linear accelerations	Longitudinal acceleration	Agility package	256
	Lateral acceleration	Agility package	256
	Normal acceleration	Agility package	256
Attitude angles (Euler angles)	Roll angle	Vertical gyro and agility package	128
	Pitch angle	Vertical gyro and agility package	128
	Yaw angle	Directional gyro	128
Angular rates	Roll rate	Rate gyro and agility package	256
	Pitch rate	Rate gyro and agility package	256
	Yaw rate	Rate gyro and agility package	256
Rotor	RPM	Tachometer	256

Table 4 SA 330 Response Variables
Data provided at a uniform sampling rate of 64 Hz.

	Attitude Pass		Velocity Pass	
Initial Conditions	$\phi(0)$	−0.031 (0.0029)	u(0)	44.507 (0.1276)
	$\theta(0)$	0.015 (0.0013)	v(0)	2.033 (0.1052)
	$\psi(0)$	−5.867 (0.2057)	w(0)	0.912 (0.1484)
Biases	p	0.000 (0.0001)	a_x	0.203 (0.0195)
	q	0.000 (0.0000)	a_y	0.336 (0.0055)
	r	−0.007 (0.0003)	a_z	−0.583 (0.0334)
	ϕ	0.060 (0.0040)	V	−0.370 (0.2324)
	θ	0.000 (0.0023)	β	−0.041 (0.0021)
	ψ	−0.795 (0.1584)	α	−0.048 (0.0034)
Scale Factors	p	−0.440 (0.0202)	a_x	1.596 (0.1282)
	q	−0.472 (0.0183)	a_y	1.233 (0.0573)
	r	−0.004 (0.0102)	a_z	0.061 (0.0034)
	ϕ	0.814 (0.0711)	V	−0.071 (0.0056)
	θ	0.842 (0.0690)	β	−0.098 (0.0053)
	ψ	−0.238 (0.0060)	α	−2.007 (0.0063)

Table 5 Initial condition, bias, and calibration factor estimates with free optimisation

	p^*	q^*	r^*	a_x^*	a_y^*	a_z^*	ϕ	θ	ψ	V	β	α
FAC FWD	0.000 (0.0003)	0.000 (0.0003)	0.000 (0.0003)	0.000 (0.0003)	0.000 (0.0003)	0.000 (0.0003)	-0.010 (0.0029)	0.008 (0.0008)	0.000 (0.0005)	-0.102 (0.0050)	-0.134 (0.0055)	-1.944 (0.0100)
FAC AFT	0.000 (0.0003)	0.000 (0.0003)	0.000 (0.0003)	0.000 (0.0003)	0.000 (0.0003)	0.000 (0.0003)	-0.008 (0.0021)	-0.058 (0.0009)	0.004 (0.0031)	-0.059 (0.0048)	-0.672 (0.0115)	-2.018 (0.0117)
LAT LFT	0.000 (0.0003)	0.000 (0.0003)	0.000 (0.0003)	0.000 (0.0003)	0.000 (0.0003)	0.000 (0.0003)	0.032 (0.0065)	-0.133 (0.0028)	0.010 (0.0018)	-0.017 (0.0077)	-0.122 (0.0138)	0.000* (0.0003)
LAT RGT	0.000 (0.0003)	0.000 (0.0003)	0.000 (0.0003)	0.000 (0.0003)	0.000 (0.0003)	0.000 (0.0003)	0.002 (0.0013)	-0.015 (0.0042)	0.003 (0.0004)	-0.027 (0.0063)	-0.085 (0.0065)	-1.999 (0.0253)
COL UPC	0.000 (0.0003)	0.000 (0.0003)	0.000 (0.0003)	0.000 (0.0003)	0.000 (0.0003)	0.000 (0.0003)	-0.024 (0.0048)	-0.071 (0.0023)	-0.004 (0.0002)	-0.124 (0.0050)	-0.023 (0.0053)	-1.666 (0.0120)
COL DMN	0.000 (0.0003)	0.000 (0.0003)	0.000 (0.0003)	0.000 (0.0003)	0.000 (0.0003)	0.000 (0.0003)	-0.025 (0.0015)	-0.093 (0.0051)	-0.002 (0.0002)	-0.083 (0.0061)	-0.032 (0.0054)	-1.857 (0.0157)
PED LFT	0.000 (0.0003)	0.000 (0.0003)	0.000 (0.0003)	0.000 (0.0003)	0.000 (0.0003)	0.000 (0.0003)	-0.009 (0.0015)	-0.006 (0.0015)	0.000 (0.0002)	-0.086 (0.0070)	-0.049 (0.0038)	-1.947 (0.0165)
PED RGT	0.000 (0.0003)	0.000 (0.0003)	0.000 (0.0003)	0.000 (0.0003)	0.000 (0.0003)	0.000 (0.0003)	-0.025 (0.0016)	-0.021 (0.0016)	0.002 (0.0006)	-0.062 (0.0053)	-0.022 (0.0031)	-2.021 (0.0077)

Table 6 SA-330 data consistency analysis with constrained optimisation: Scale factors

	p	q	r	a_x	a_y	a_z	ϕ	θ	ψ^*	V	β	α
FAC FWD	-0.001 (0.0001)	-0.001 (0.0001)	0.004 (0.0002)	-0.118 (0.0072)	0.669 (0.0055)	0.056 (0.0052)	-0.013 (0.0017)	-0.008 (0.0026)	0.000 (0.0003)	0.489 (0.2232)	-0.071 (0.0020)	-0.011 (0.0027)
FAC AFT	-0.001 (0.0000)	0.000 (0.0000)	-0.001 (0.0001)	0.258 (0.0043)	0.079 (0.0070)	0.194 (0.0039)	0.022 (0.0013)	0.021 (0.0013)	0.000 (0.0003)	4.237 (0.1904)	0.001 (0.0012)	-0.070 (0.0032)
LAT LFT	-0.002 (0.0003)	-0.005 (0.0000)	0.000 (0.0001)	-0.101 (0.0067)	0.085 (0.0077)	0.146 (0.0036)	-0.019 (0.0029)	-0.009 (0.0064)	0.000 (0.0003)	0.896 (0.2478)	-0.036 (0.0040)	0.050 (0.0044)
LAT RGT	-0.001 (0.0000)	-0.001 (0.0000)	-0.002 (0.0000)	0.054 (0.0016)	0.098 (0.0009)	0.056 (0.0029)	-0.001 (0.0003)	0.006 (0.0013)	0.000 (0.0003)	-0.706 (0.2443)	0.013 (0.0027)	-0.072 (0.0028)
COL UPC	-0.001 (0.0001)	-0.001 (0.0000)	0.002 (0.0001)	0.087 (0.0037)	-0.494 (0.0014)	0.046 (0.0044)	0.064 (0.0020)	0.011 (0.0026)	0.000 (0.0003)	0.148 (0.2349)	-0.037 (0.0029)	-0.089 (0.0019)
COL DMN	-0.001 (0.0000)	0.002 (0.0000)	0.001 (0.0000)	-0.013 (0.0055)	-0.115 (0.0023)	0.060 (0.0031)	0.064 (0.0034)	0.004 (0.0021)	0.000 (0.0003)	0.357 (0.2485)	-0.016 (0.0023)	-0.065 (0.0014)
PED LFT	-0.002 (0.0000)	0.002 (0.0000)	-0.003 (0.0000)	-0.055 (0.0055)	0.130 (0.0027)	0.004 (0.0033)	0.016 * (0.0013)	0.003 (0.0019)	0.000 (0.0003)	0.376 (0.2531)	0.008 (0.0046)	-0.039 (0.0031)
PED RGT	-0.002 (0.0000)	0.006 (0.0000)	-0.003 (0.0000)	0.349 (0.0058)	0.042 (0.0014)	0.052 (0.0031)	0.017 (0.0018)	0.030 (0.0019)	0.000 (0.0003)	1.078 (0.2189)	0.000 (0.0017)	-0.087 (0.0015)

() = Standard Deviation
* = parameter constrained in algorithm

Table 7 SA-330 data consistency analysis with constrained optimisation: Biases

	$\phi(0)$	$\theta(0)$	$\psi(0)^*$	u(0)	v(0)	w(0)
F568FAC.FWD	0.015 (0.0019)	0.036 (0.0026)	-5.259 (0.0003)	44.178 (0.1337)	3.682 (0.1113)	2.929 (0.1241)
F568FAC.AFT	-0.024 (0.0014)	0.000 (0.00 3)	-0.466 (0.0003)	39.538 (0.1063)	-0.490 (0.1528)	0.239 (0.1163)
F550LAT.LFT	0.023 (0.0030)	0.030 (0.0074)	-0.815 (0.0003)	40.049 (0.2070)	0.886 (0.1828)	-0.951 (0.1749)
F568LAT.RGT	-0.007* (0.0003)	0.035 (0.0014)	-2.218 (0.0003)	41.431 (0.1094)	-0.997 (0.1199)	-0.270 (0.1136)
F568COL.UPC	-0.046 (0.0022)	0.010 (0.0028)	-5.065 (0.0003)	45.100 (0.1036)	2.080 (0.1353)	-1.689 (0.1217)
F568COL.DMN	-0.043 (0.0035)	0.023 (0.0023)	-5.444 (0.0003)	41.890 (0.1124)	0.600 (0.1036)	0.366 (0.0755)
F576PED.LFT	0.001 (0.0013)	0.038 (0.0019)	-5.039 (0.0003)	42.810 (0.1912)	-0.793 (0.2073)	3.172 (0.1331)
F576PED.RGT	-0.021 (0.0018)	-0.004 (0.0020)	-1.281 (0.0003)	42.303 (0.1057)	-0.273 (0.0672)	0.877 (0.0602)

Table 8 SA-330 data consistency analysis with constrained optimisation: Initial conditions

Derivative		DLR		CERT 1		CERT 2		Glasgow Uni		NAE		NLR	
Symbol	Unit	Value	σ	Value	σ	Value	σ	Value	σ	Value	σ	Value	σ
X_u	1/s	-0 039	0 0003	-0 027	0.0018	-0 026	0.0018	-0 029	0 0079	-0.031	0 0013	-0 025	0 0007
X_v	1/s	0 *	—	-0 024	0 0031	0 *	—	0 *	—	-0 007	0 0023	0 *	—
X_w	1/s	0 069	0 0011	0 078	0 0053	0 07	0 0026	0 043	0 0164	0 042	0 0036	0 037	0 0017
X_p	m/(rad s)	0 *	--	-0 344	0 0942	-0 063	0 0536	0 *	—	0 269	0.0866	0 *	—
X_q	m/(rad s)	-2.199	0.035	0 171	0 2008	0 *	—	0 *	—	0 502	0 1398	0 *	—
X_r	m/(rad s)	0 *	—	-0.669 0 0853	-	0.436	0 0533	0 *	—	-0 220	0 0815	0 193	0 0598
Y_u	1/s *	0 *	—	0 008	0 0023	0 018	0 0024	0 *	—	0.004	0 0014	0 *	—
Y_v	1/s	-0 135	0 0019	-0.135 0 0037	-	0.126	0 0032	-	0 135	0.0263	-	0 105	0 0023
Y_w	1/s	0 *	—	-0.038	0 0059	-0.096	0.0061	0 *	—	-0.031	0 0036	0 *	—
Y_p	m/(rad s)	1.439	0.0596	0 793	0 1124	0 530	0.1064	0.696	0.0103	0.297	0.0870	0 *	—
Y_q	m/(rad s)	0 *	—	0 034	0 2052	0 *	—	0 *	—	1 582	0.1393	0 *	—
Y_r	m/(rad s)	1.27	0.0459	0 280	0.1032	0.380	0 0898	0 *	—	1.358	0 0818	0 193	0 0598
Z_u	1/s	0 008	0 0029	-0 030	0 0057	0 059	0.0064	-0 0434	0.0134	-0 020	0 0029	-0 070	0 0021
Z_v	1/s	0 *	--	0 029	0 0062	0.016	0 0054	0 *	—	-0 024	0 0040	0 *	—
Z_w	1/s	-1.025	0 0098	-0 836	0 0142	-1.041	0 0160	-1.191	0 0119	-0.641	0 0056	-0 689	0 0050
Z_p	m/(rad s)	0 *	—	2 323	0 1823	0.855	0 1676	0 *	—	0 523	0.1441	0 *	—
Z_q	m/(rad s)	0 *	—	-7 07	0 3072	-7 14	0.3041	0 *	—	-7.677	0 2076	0 *	—
Z_r	m/(rad s)	0 *	—	3 542	0 1708	1.407	0 1476	0 *	—	-0 630	0 1355	0 *	—

* Eliminated from model structure
σ = Standard deviation

Table 9 SA-330 Identification Results: List of of specific force derivatives with respect to flight variables

Derivative Symbol	Derivative Unit	DLR Value	DLR σ	CERT 1 Value	CERT 1 σ	CERT 2 Value	CERT 2 σ	Glasgow Uni Value	Glasgow Uni σ	NAE Value	NAE σ	NLR Value	NLR σ
L_u	rad/(s m)	0.019	0 0006	0.012	0.0006	0 038	0 0007	0 010	0.0019	0.003	0.0002	0 006	0 0006
L_v	rad/(s m)	-0.066	0.0012	-0.055	0.0009	-0 067	0 0009	-0.064	0 0014	-0 032	0.0003	-0 044	0 0012
L_w	rad/(s m)	-0.090	0 0021	-0.035	0 0017	-0.067	0.0017	-0.027	0.0060	-0 019	0 0006	-0.020	0 0014
L_p	1/s	-2 527	0 0534	-1.195	0.0275	-1 694	0 0242	-2.012	0 0695	-0.725	0.0166	-1 090	0 0437
L_q	1/s	2.225	0 0772	-0.309	0 0633	-1.942	0.0394	0.420	0.0762	0.450	0.0288	0.283	0 0579
L_r	1/s	-0 259	0 0343	0.345	0.0234	-0.601	0 0204	0 554	0 0787	0.888	0 0156	0 540	0 0376
M_u	rad/(s m)	0.110	0.0001	0.007	0.0001	0.010	0.0002	0 013	0.0002	0.003	0 0001	0.008	0.0003
M_v	rad/(s m)	-0.170	0 0002	-0 012	0.0002	-0.013	0.0002	-0.021	0.0015	-0.006	0.0002	-0 014	0 0006
M_w	rad/(s m)	-0.004	0.0004	-0.010	0.0004	-0.018	0.0004	-0.012	0.0015	-0.006	0 0003	-0.014	0 008
M_p	1/s	0 194	0 0090	0.110	0 0052	0 059	0.0044	-0.035	0.0237	0.173	0.0085	0.020	0 0186
M_q	1/s	-1.108	0.0171	-0 663	0.0190	-0.735	0 0164	-1.356	0.0085	-0.280	0.0142	-0 542	0.0330
M_r	1/s	0 *	—	-0.039	0.0062	-0.151	0.0051	0 *	—	0.383	0 0082	0 *	—
N_u	rad/(s m)	0 *	—	0.002	0 0003	-0.002	0.0004	0 *	—	0.006	0.0002	0 *	—
N_v	rad/(s m)	0.027	0.0002	0 034	0.0004	0.035	0 0004	0.029	0.0006	0.008	0.0003	0 039	0 0010
N_w	rad/(s m)	0 *	—	0.013	0 0008	0.045	0 0010	0 010	0.0014	0.019	0 0003	0 010	0 0014
N_p	1/s	-0 395	0.0092	-0 031	0.0102	0 194	0.0129	-0.321	0 0106	-0.301	0.0159	0 295	0 0397
N_q	1/s	0 056	0.0075	-0 441	0 0215	-0.951	0.0283	0 *	—	-1 343	0 0257	-0.526	0.0510
N_r	1/s	-0.362	0.0065	-0.475	0.01	-0 341	0 0121	-0.388	0 0348	-0.736	0 0154	-0 288	0 0295

* Eliminated from model structure
σ = Standard deviation

Table 10 SA-330 Identification Results: List of specific moment derivatives with respect to flight variables

Derivative		DLR		CERT 1		CERT 2		Glasgow U..I		NAE		NLR	
Symbol	Unit	Value	σ	Value	σ	Value	σ	Value	σ	Value	σ	Value	σ
$X_{\delta col}$	$m/(s^2 \%)$	0 *	—	0.016	0 0019	0 0127	0 0017	0.064	0.0054	0.030	0 0054	0.013	0 0012
$X_{\delta lon}$	$m/(s^2 \%)$	0.052	0.0006	0.031	0.0027	0 026	0 0021	0.092	0.0173	0 096	0 0069	0 006	0 0014
$X_{\delta lat}$	$m/(s^2 \%)$	0 *	—	0 *	—	0 *	—	0 *	—	-0.007	0 0023	0 *	—
$X_{\delta ped}$	$m/(s^2 \%)$	0 *	—	0 *	—	0 *	—	0 *	—	-0 035	0 0073	0 *	—
$Y_{\delta col}$	$m/(s^2 \%)$	0 *	—	-0 028 0.002	-	0.002	0 0020	0 *	—	-0 031	0 0053	0 *	—
$Y_{\delta lon}$	$m/(s^2 \%)$	0 *	—	-0 001 0.0028	-	0.005	0.0024	0 *	—	-0 002	0.0068	0 *	—
$Y_{\delta lat}$	$m/(s^2 \%)$	0.018	0.0015	0.016	0.0024	0 030	0 0024	0.018	0 0033	-0.031	0 0059	0 012	0.0020
$Y_{\delta ped}$	$m/(s^2 \%)$	-0 002	0.0017	0.006	0.0029	0 020	0.0029	-0.044	0 0274	0.157	0.0071	0.044	0.0027
$Z_{\delta col}$	$m/(s^2 \%)$	-0 223	0 0038	-0 139	0.0027	-0 202	0 0029	-0.236	0.0204	-0 031	0.0072	-0.165	0 0037
$Z_{\delta lon}$	$m/(s^2 \%)$	0 0147	0 005	0 062	0 0034	0 103	0 0037	0.383	0.0748	C.204	0 0082	0 0106	0 0042
$Z_{\delta lat}$	$m/(s^2 \%)$	0 *	—	0 *	—	0 *	—	0 *	—	-0 031	0 0064	0 *	—
$Z_{\delta ped}$	$m/(s^2 \%)$	0 *	—	0 *	—	0 *	—	0 *	—	0 157	0.0099	0 *	—

* Eliminated from model structure
σ = Standard deviation

Table 11 SA-330 Identification Results: List of specific force derivatives with respect to control variables

Derivative		DLR		CERT 1		CERT 2		Glasgow Uni		NAE		NLR	
Symbol	Unit	Value	σ	Value	σ	Value	σ	Value	σ	Value	σ	Value	σ
$L_{\delta col}$	rad/(s^2 %)	-0 022	0 0009	0 007	0 0005	-0 012	0 0005	0 *	—	-0 012	0 0013	-0.015	0 0008
$L_{\delta lon}$	rad/(s^2 %)	0 0147	0 005	0 062	0 0034	0.103	0 0037	0 383	0 0748	0 204	0 0082	0 0106	0 0042
$L_{\delta lat}$	rad/(s^2 %)	-0 051	0 0012	-0 025	0 0006	-0 035	0 0006	-0 031	0.0017	-0 022	0 0003	-0 029	0 0009
$L_{\delta ped}$	rad/(s^2 %)	0 011	0 0007	0 014	0 0005	0.001	0 00005	0 020	0 004	0 019	0 0003	0 018	0 0011
$M_{\delta col}$	rad/(s^2 %)	0 010	0 0001	0 006	0 0001	0.005	0 0001	0 005	0 0004	0 005	0 0001	0 005	0 0005
$M_{\delta lon}$	rad/(s^2 %)	-0 031	0 0002	-0 020	0 0003	-0.021	0.0003	-0 036	0 0008	-0 016	0 0002	-0 026	0 0006
$M_{\delta lat}$	rad/(s^2 %)	0 00	0 0002	0 *	—	0 *	—	0 *	—	0.001	0.0002	0.00	0 0005
$M_{\delta ped}$	rad/(s^2 %)	0 *	—	0 *	—	0 *	—	0 *	—	0 004	0.0002	0 *	—
$N_{\delta col}$	rad/(s^2 %)	0 *	—	0 001	0 0002	0.006	0 0002	0 *	—	0 007	0.0002	0.006	0 0008
$N_{\delta lon}$	rad/(s^2 %)	-0 001	0 0002	-0 009	0 0004	-0 017	0 0005	0 *	—	-0 014	0 0003	-0 007	0 0010
$N_{\delta lat}$	rad/(s^2 %)	-0 008	0 0002	0 00	0 0002	0 002	0 0002	-0 007	0 0004	-0.001	0 0002	0 00	0 0009
$N_{\delta ped}$	rad/(s^2 %)	-0 022	0 0001	0 *	—	-0 031	0 0003	-0 025	0 0008	-0.028	0 0003	-0 032	0 0011

* Eliminated from model structure
σ = Standard deviation

Table 12 SA-330 Identification Results: List of specific moment derivatives with respect to control variables

Delay		DLR		CERT 1		CERT 2		Glasgow Uni		NAE		NLR	
Symbol	Unit	Value	σ	Value	σ	Value	σ	Value	σ	Value	σ	Value	σ
$\tau_{\delta col}$	s	0 094	—	0 *	—	0.170	—	0.0095	—	0 *	—	0 125	—
$\tau_{\delta lon}$	s	0 125	—	0 *	—	0 125	—	0.0806	—	0 *	—	0 125	—
$\tau_{\delta lat}$	s	0 125	—	0 *	—	0 125	—	0 0099	—	0 *	—	0.125	—
$\tau_{\delta ped}$	s	0 *	—	0 *	—	0 *	—	0 *	—	0 *	—	0.125	—

* Eliminated from model structure
σ = Standard deviation

Table 13 SA-330 Identification Results: Equivalent control time delays

Mode of motion	AFDD	DLR	CERT		Glasgow Uni	NAE	NLR
			Without control time delays	With control time delays			
Phugoid oscillation		[-0 014, 0 261]	[-0 040, 0 270]	[-0 025, 0 266]	[0 001, 0 270]	[-0 111, 0 280]	[-0 003, 0.042]
Dutch roll oscillation	[0 250, 1 263]	[0 075, 1 375]	[0 119, 1 350]	[0.119, 1 360]	[0 147, 1 350]	[0 111, 1 304]	
Short period oscillation		[0 939, 1 [illegible]6]	[0 865, 0.964]	[0.934, 1 200]	[0 934, 1 399]	[0 960, 0 566]	[0 741, 0 143]
Roll mode	(0.930)	(3 021)	(1.37)	(1 39)	(2 066)	(1.09)	(1 18)
Spiral mode	(0.023)	(0 048)	(-0.005)	(0 020)	(0 005)	(0 114)	(-0.062)

Shorthand notation:

s Laplace variable (in 1/s)

$[\zeta, \omega_0]$ represents $(s^2 + 2\zeta\omega_0 s + \omega_0^2)$
with ζ = damping ratio and ω_0 = undamped natural frequency (in rad/s)

$(1/T)$ represents $(s + 1/T)$
with T = time constant (in s)

Table 14 SA-330 Identification Results: Time constants, damping ratios and undamped natural frequencies

	Glasgow	DLR	CERT1	CERT2	NAE	NLR	Helistab
$Z_w + M_q$	-2.55	-2.133	-1.5	-1.78	-1.086	-1.34	-1.496
$-2\zeta_{sp}\omega_{sp}$	-2.64	-2.115	-1.67	-2.24	-0.921	-1.23	-1.742
$M_q Z_w^+$	2.107	1.268	0.884	1.356	0.18	0.947	1.38
ω_{sp}^2	1.96	1.053	0.94	1.85	0.32	0.816	1.629
$M_{\delta lon}/M_q$	0.0265	0.028	0.03	0.029	0.057	0.048	0.0435
$Z_{\delta col}/Z_w$	0.198	0.218	0.166	0.194	0.048	0.24	0.266
M_w	-0.012 (0.0015)	-0.004 (0.0004)	-0.01 (0.0004)	-0.018 (0.0004)	-0.002 (0.0001)	-0.014 (0.008)	-0.02

Table 15 SA-330 characteristics of short period mode

	GLASGOW	DLR	CERT1	CERT2	NAE	NLR	HELISTAB
ω_p	0.27	0.261	0.269	0.266	0.278	0.264	0.221
ω_p^*	0.268	0.282	0.255	0.274	0.211	0.24	0.195
X_u	-0.029	-0.039	-0.027	-0.026	-0.031	-0.025	-0.024
M_u	0.013	0.01	0.007	0.01	0.003	0.008	0.0074

Table 16 SA-330 comparison of phugoid characteristics
ω_p-approximation equation (6.3.30)

	GLASGOW	DLR	CERT1	CERT2	NAE	NLR	HELISTAB
$\frac{L_{\delta lat}}{L_p}$	0.0154	0.02	0.024	0.021	0.03	0.027	0.025

Table 17 SA-330 comparison of roll rate sensitivity

	Glasgow	DLR	CERT1	CERT2	NAE	NLR	Helistab
$(2\zeta_r\omega_r)^*$	0.291	0 167	0.261	0.408	0.565	0.477	0.39
$2\zeta_r\omega_r$	0.4	0.208	0.321	0.324	0.39	0.302	0.326
ω_r^*	1.34	1.36	1.43	1.23	0.865	1.24	1.19
ω_r	1.4	1.375	1.35	1.36	1.3	1.31	1.06

Table 18 SA-330 characteristics of Dutch roll mode

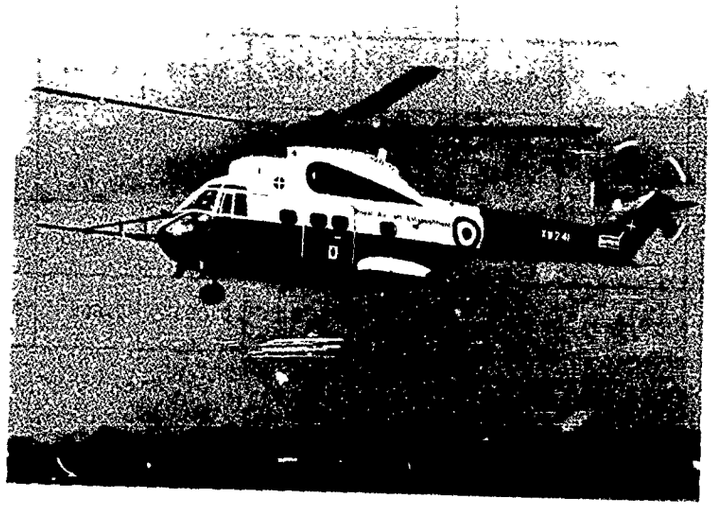

Fig 1 RAE research SA330 Puma

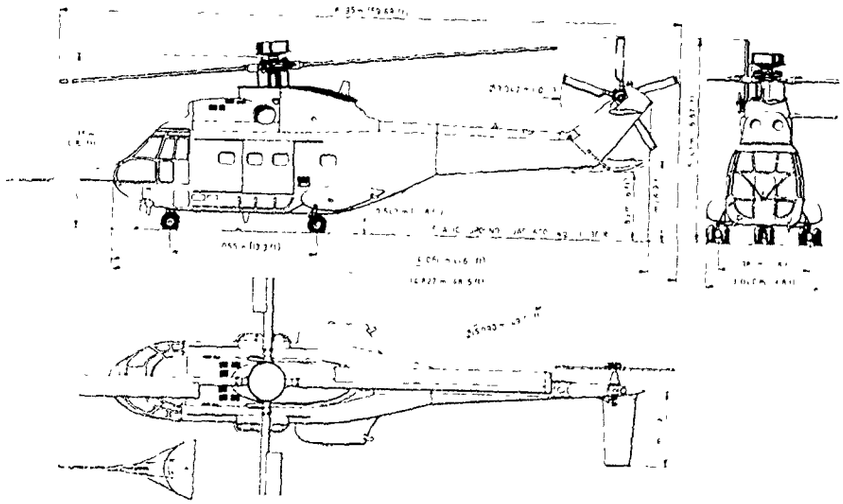

Fig 2 3-view drawing of RAE research SA330 Puma

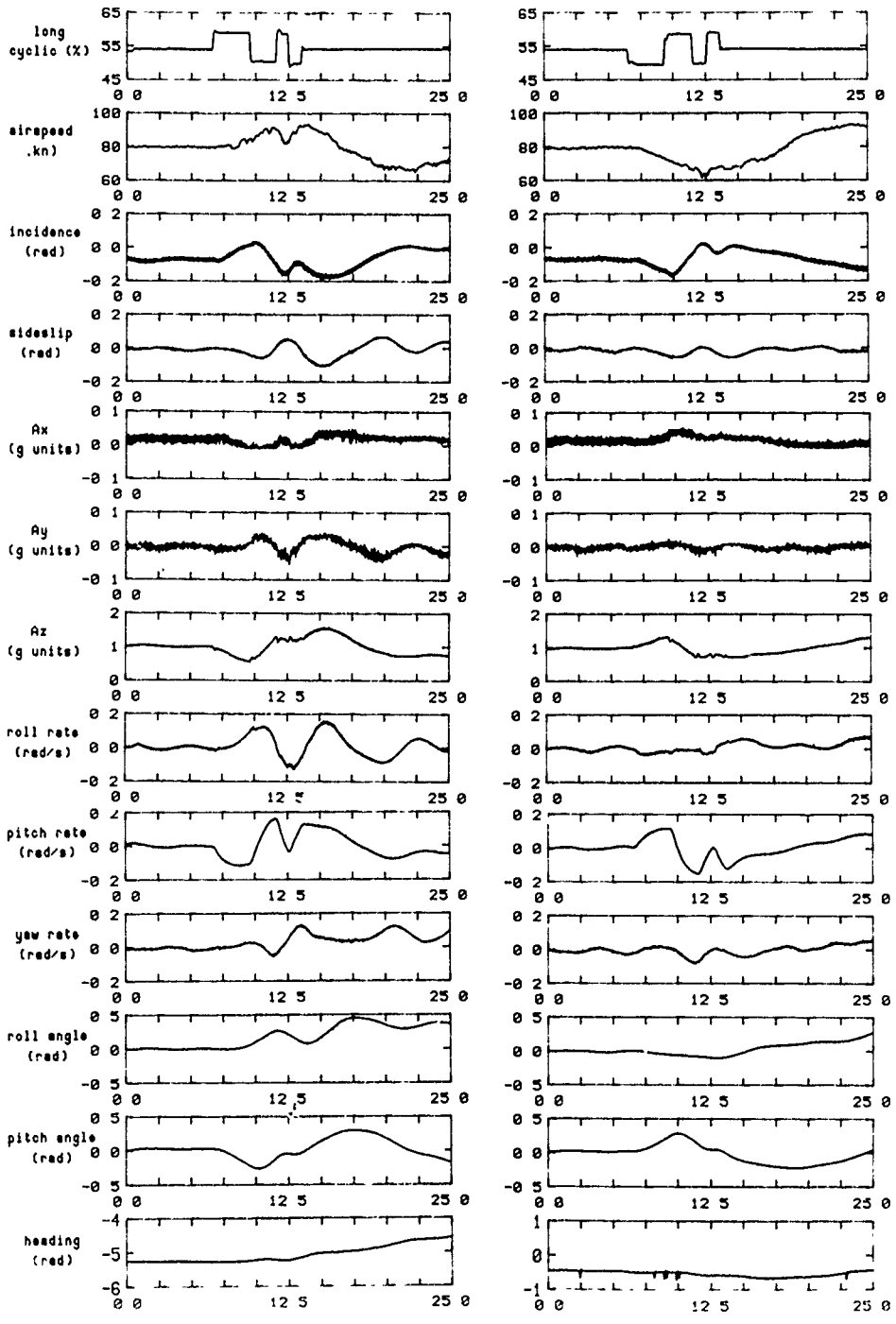

Fig 3 SA330 Puma database - response to 3211 longitudinal cyclic inputs (F568FAC.FWD & F568FAC.AFT)

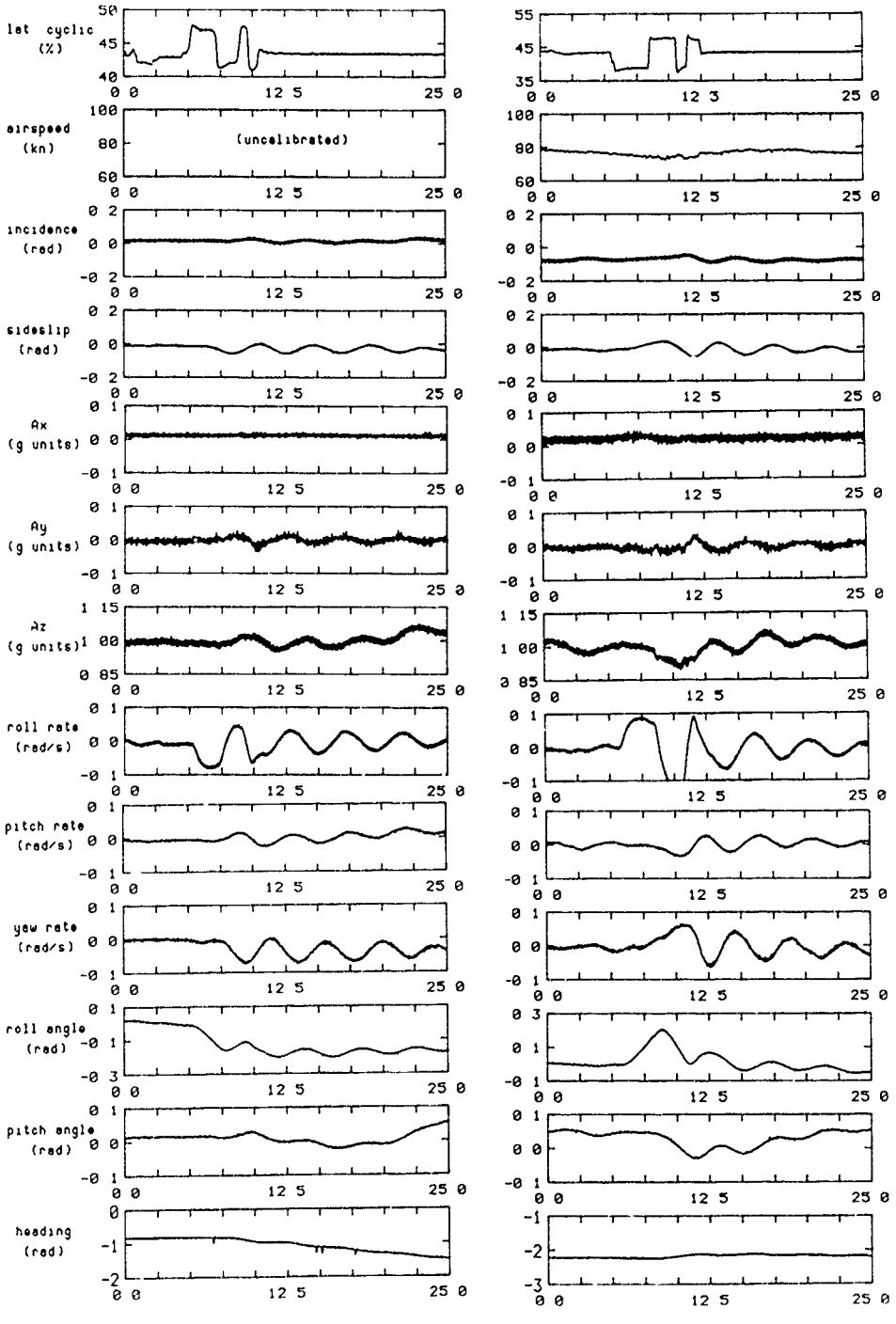

Fig 4 SA330 Puma database - response to 3211 lateral cyclic inputs (F550LAT.LFT & F568LAT.RGT)

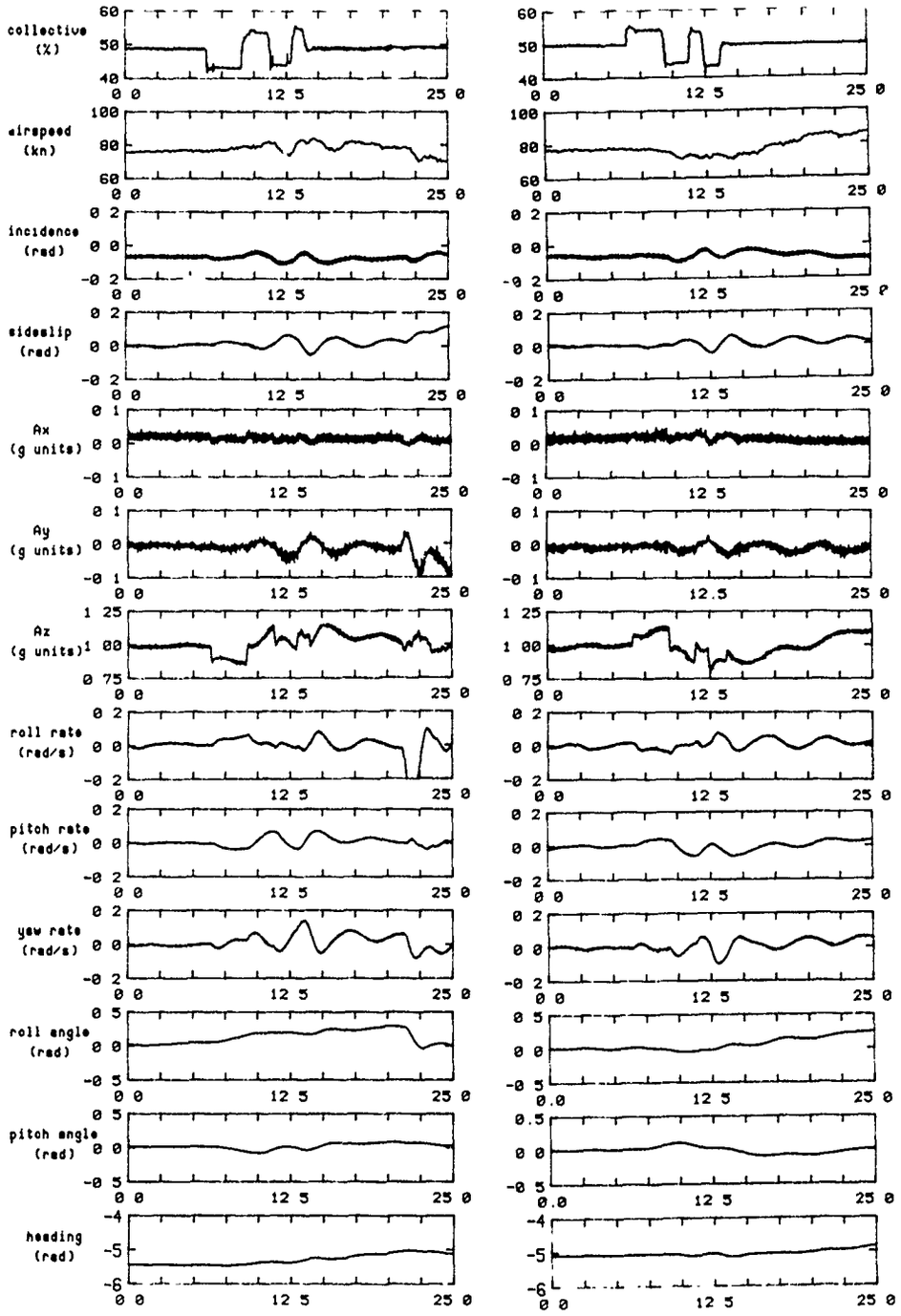

Fig 5 SA330 Puma database - response to 3211 collective inputs (F568COL.UPC & F568COL.DWN)

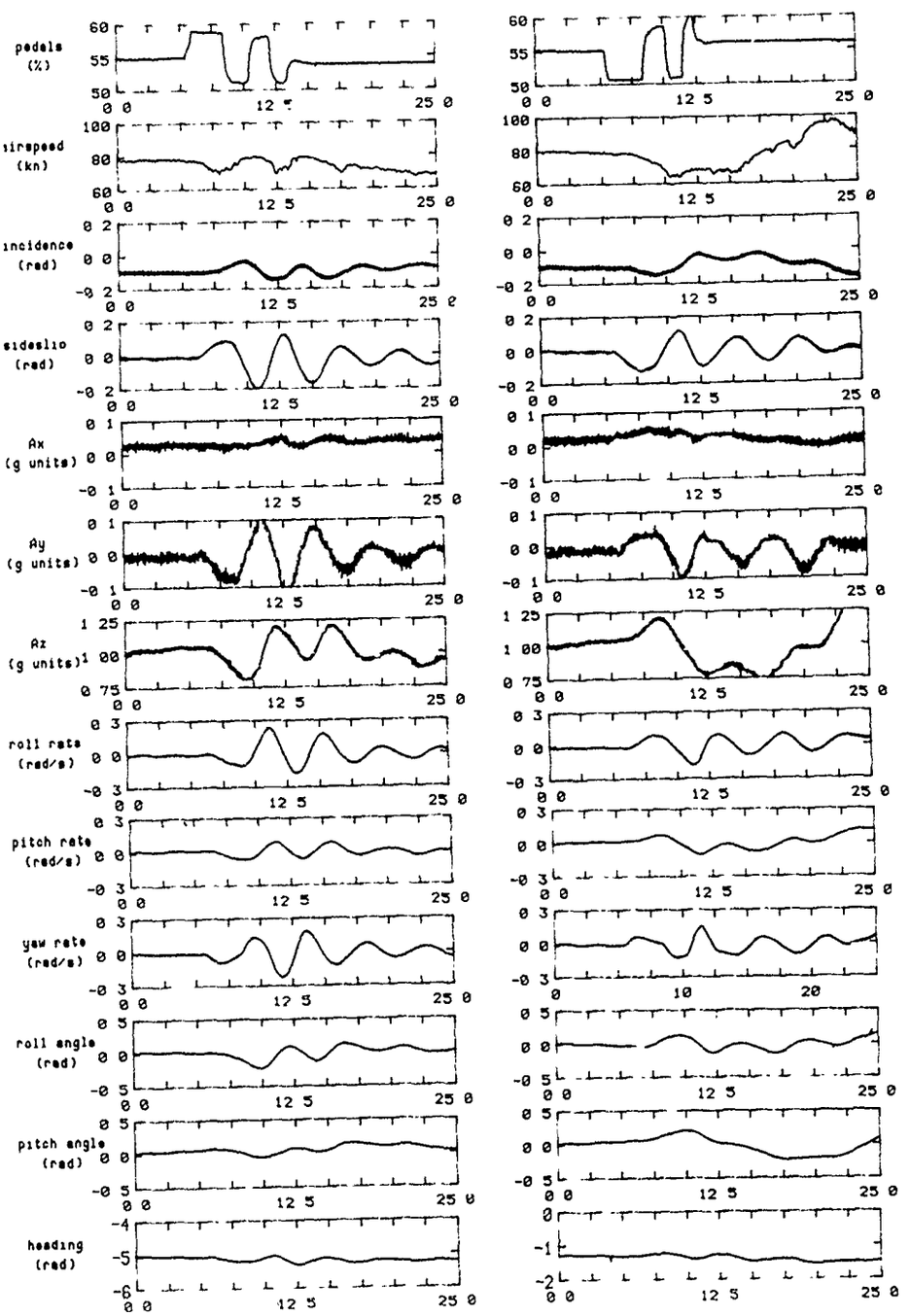

Fig 6 SA330 Puma database - response to 3211 pedal inputs (F576PED.LFT & F576PED.RGT)

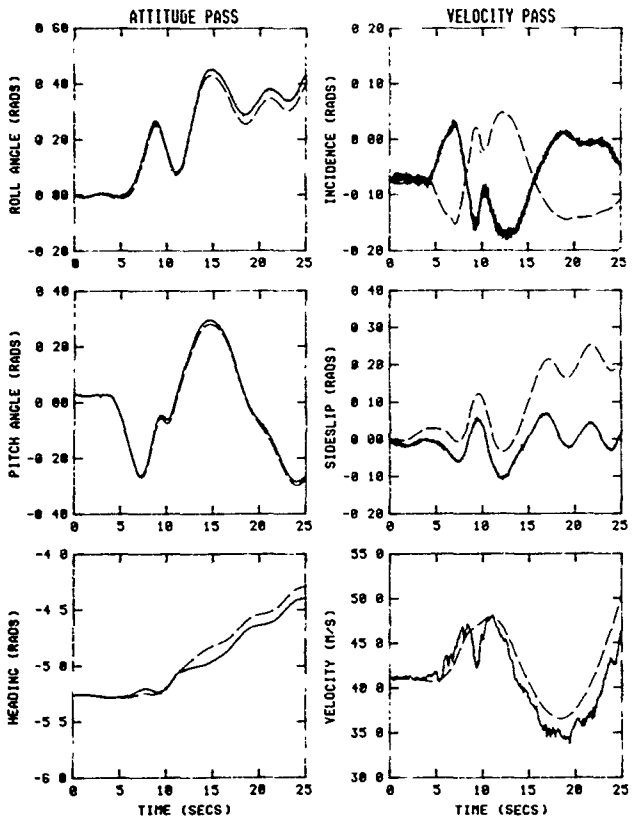

Fig 7 Comparison of measured attitudes and air data with reconstructed inertial measurements - Puma F568FAC.FWD

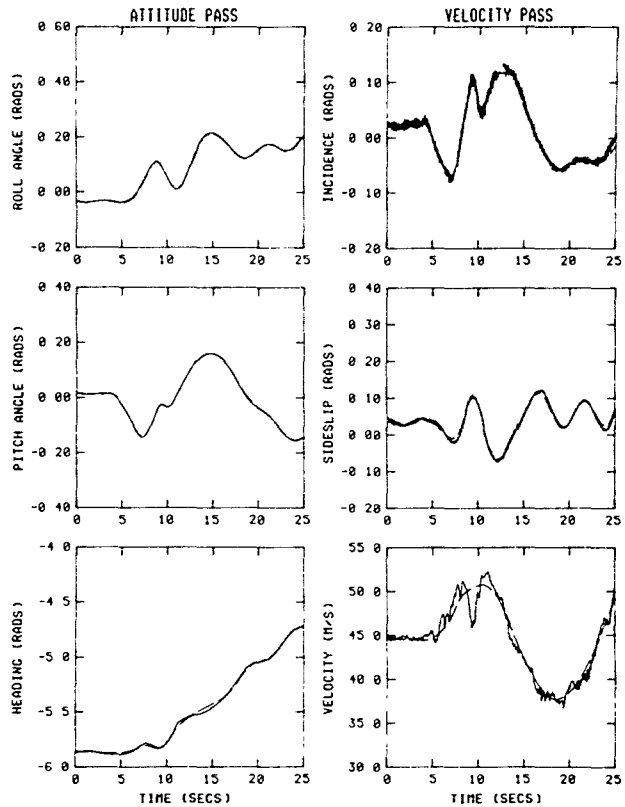

Fig 8 Comparison of measured attitudes and air data with free optimisation of reconstructed inertial measurements - Puma F568FAC.FWD

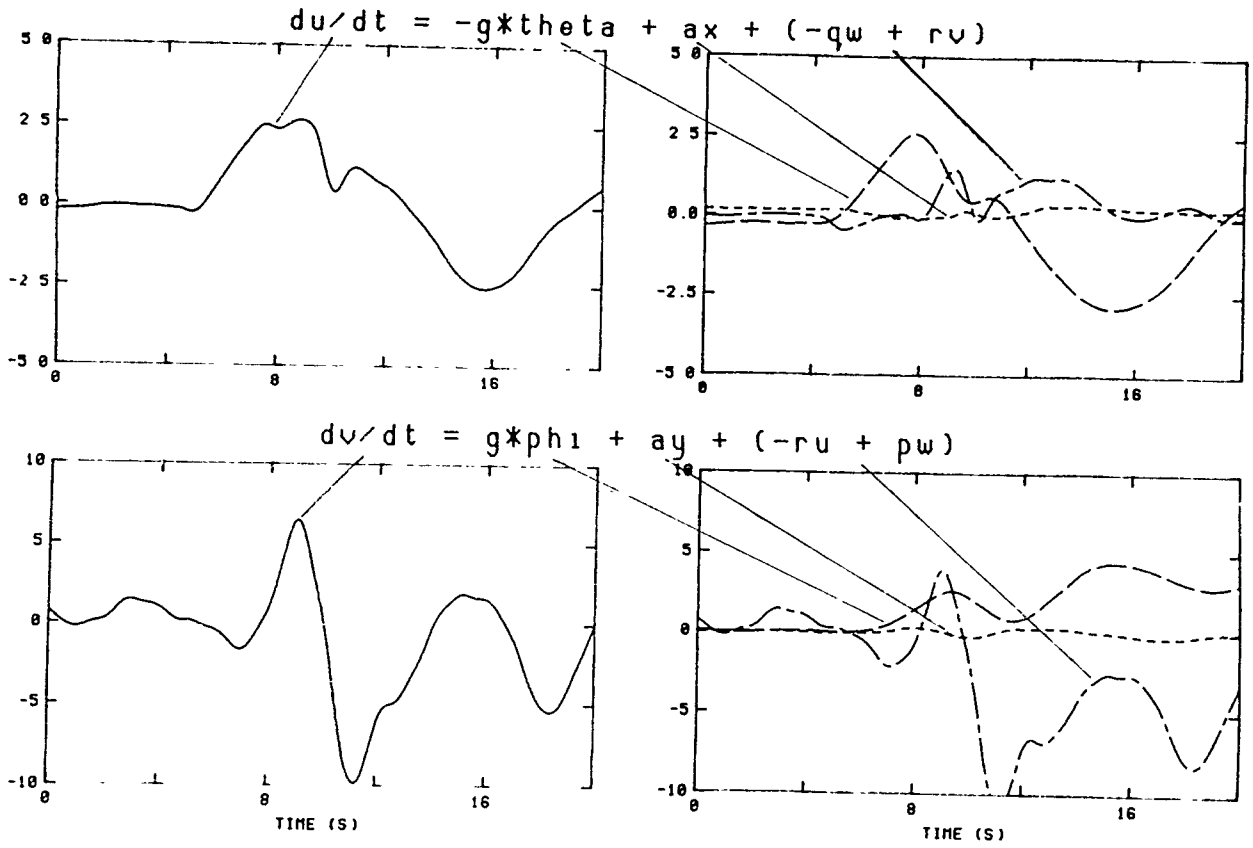

Fig 9 **Components of velocity derivatives - F568FAC.FWD**

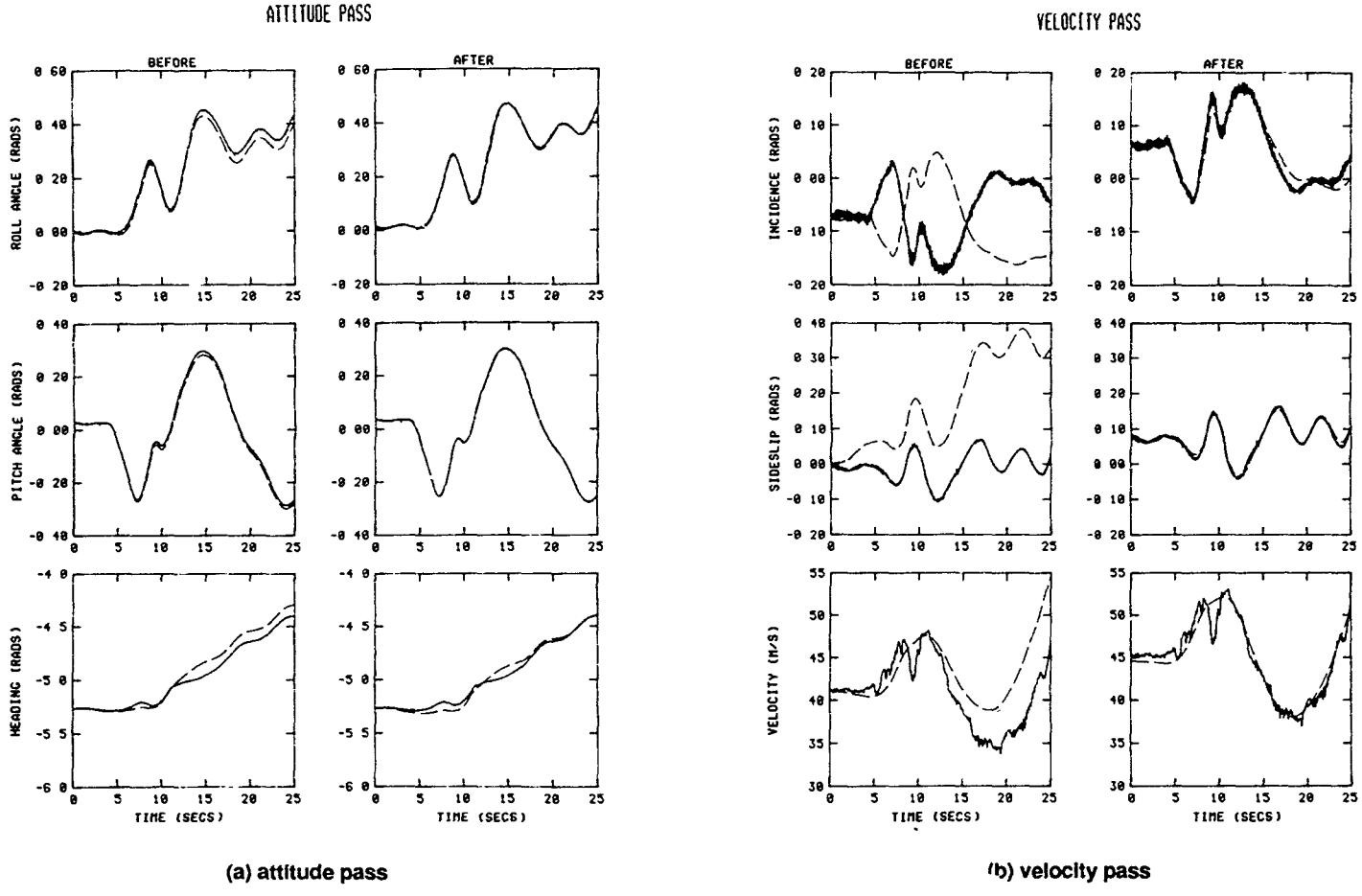

(a) attitude pass

(b) velocity pass

Fig 10 Comparison of measured attitudes and air data with constrained optimisation of reconstructed inertial measurements - Puma F568FAC.FWD

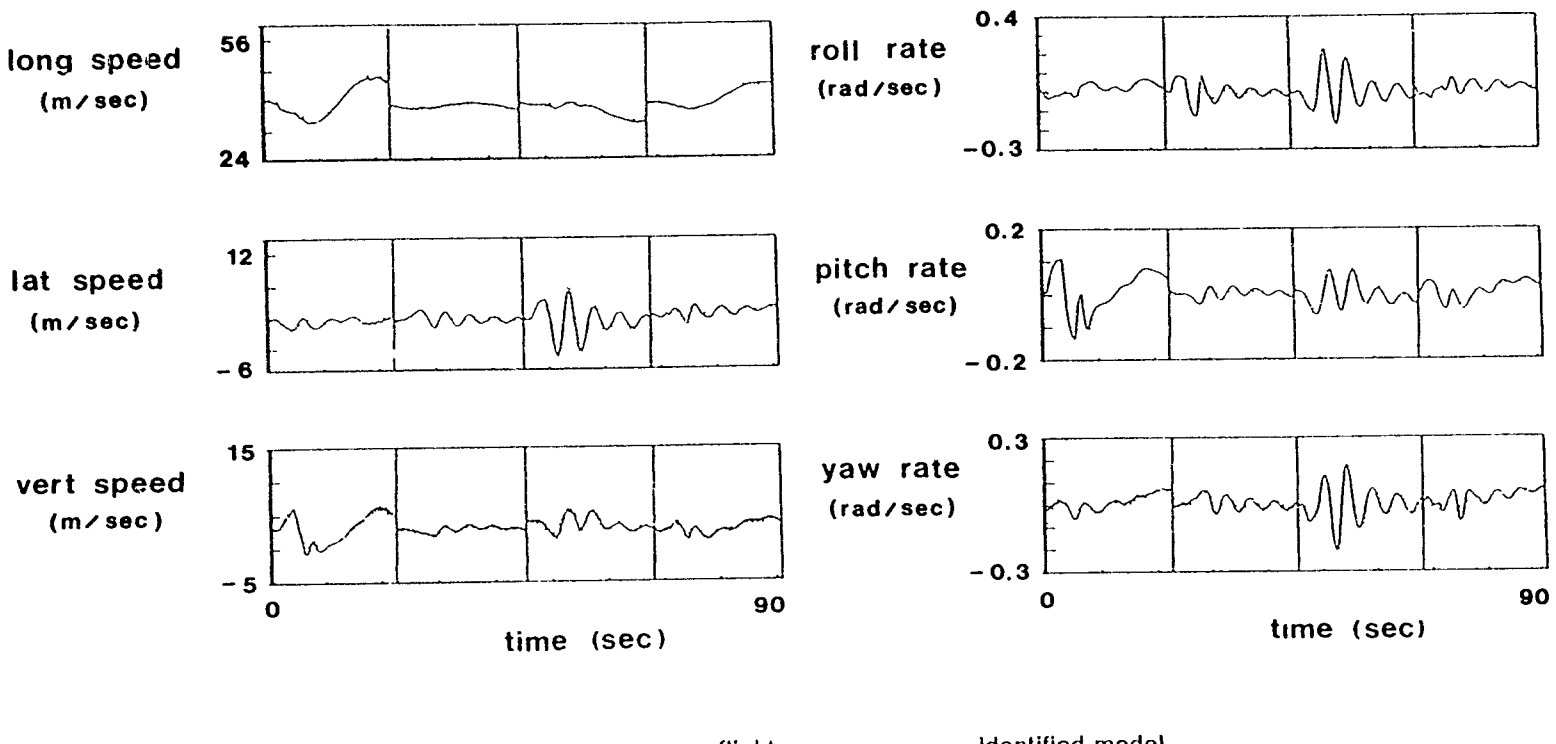

Fig 11 Comparison of flight and estimated time histories - Glasgow (identification)

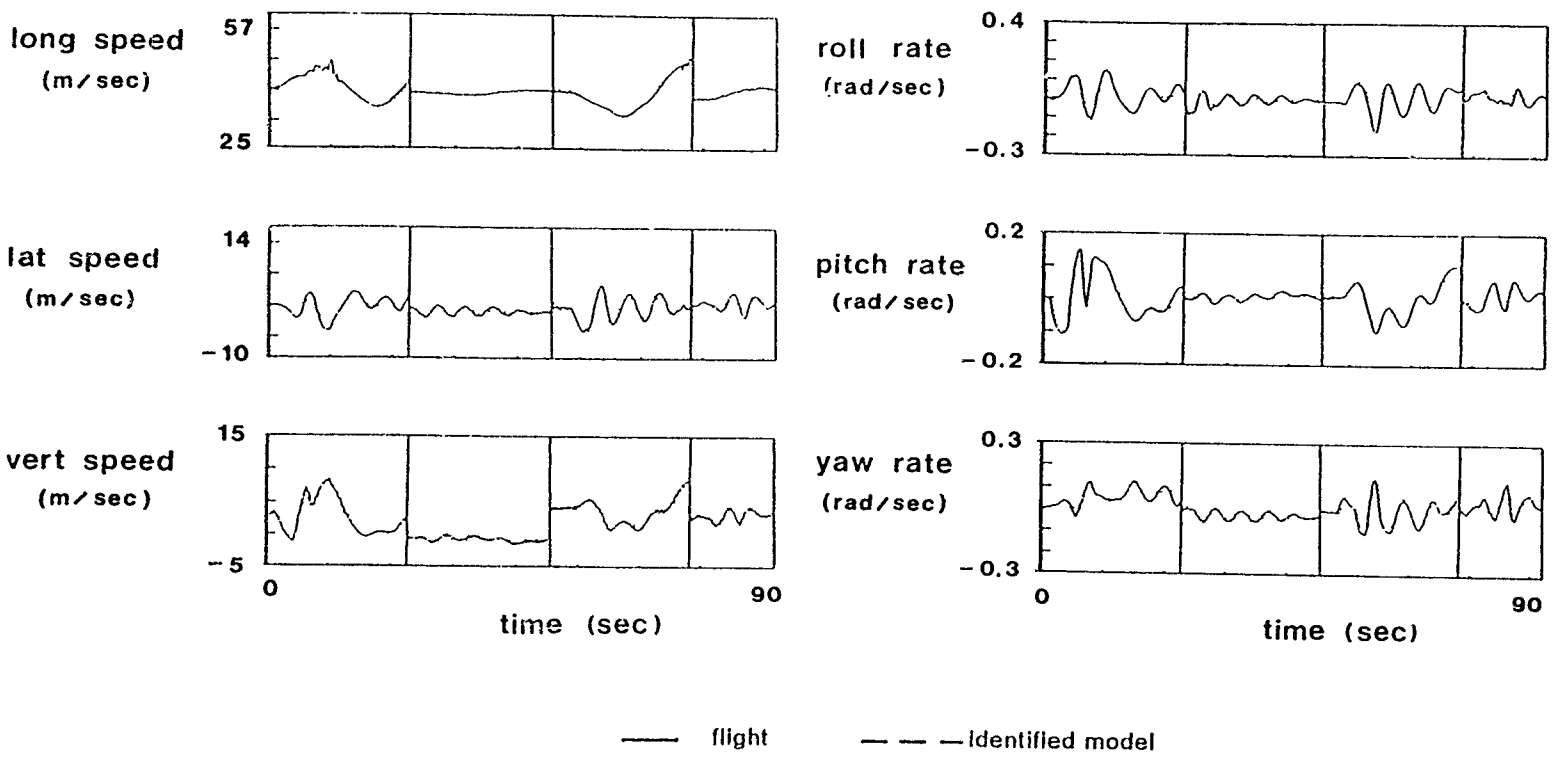

Fig 12 Comparison of flight and estimated time histories - Glasgow (verification)

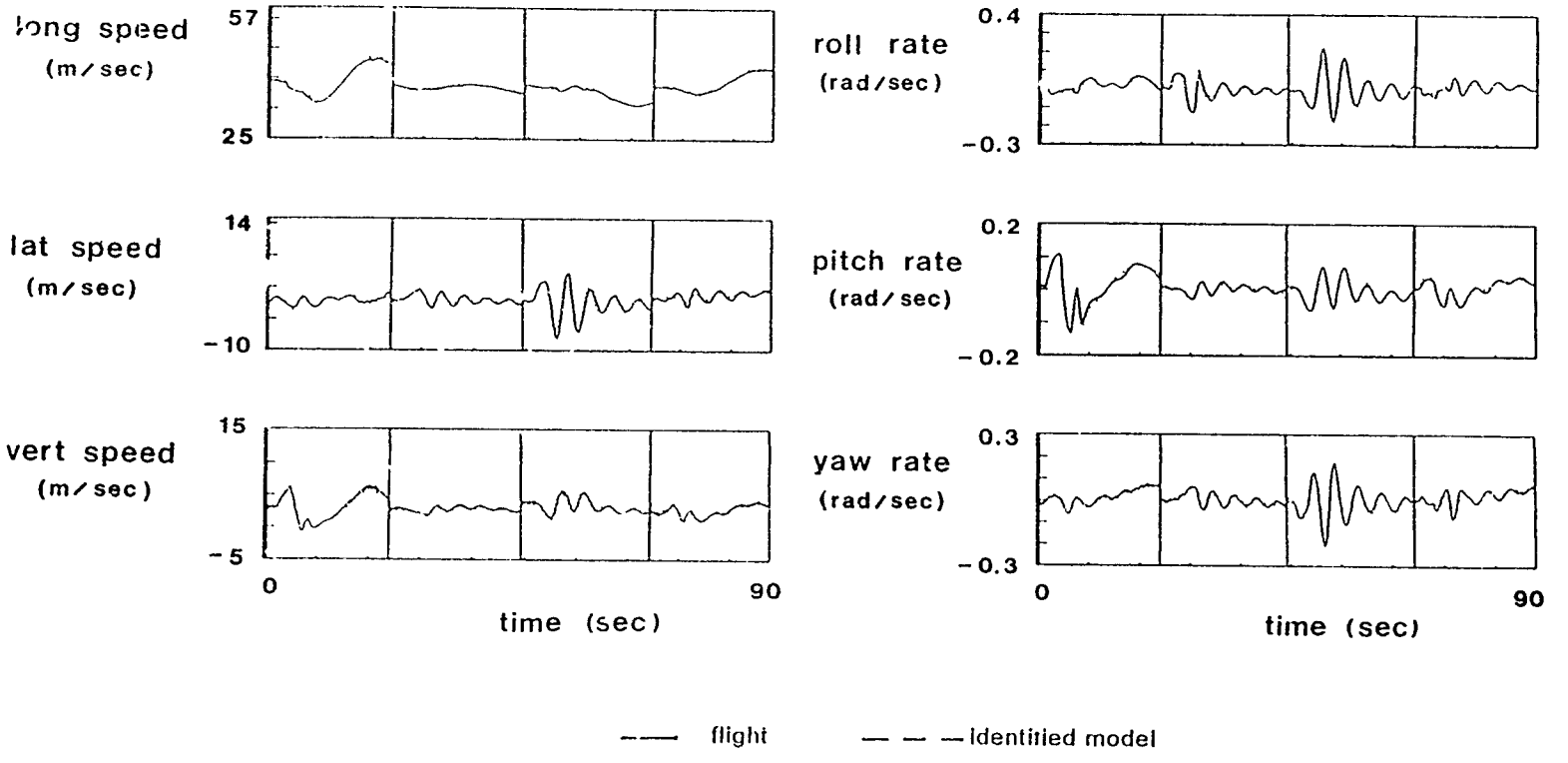

Fig 13 Comparison of flight and estimated time histories - DLR (identification)

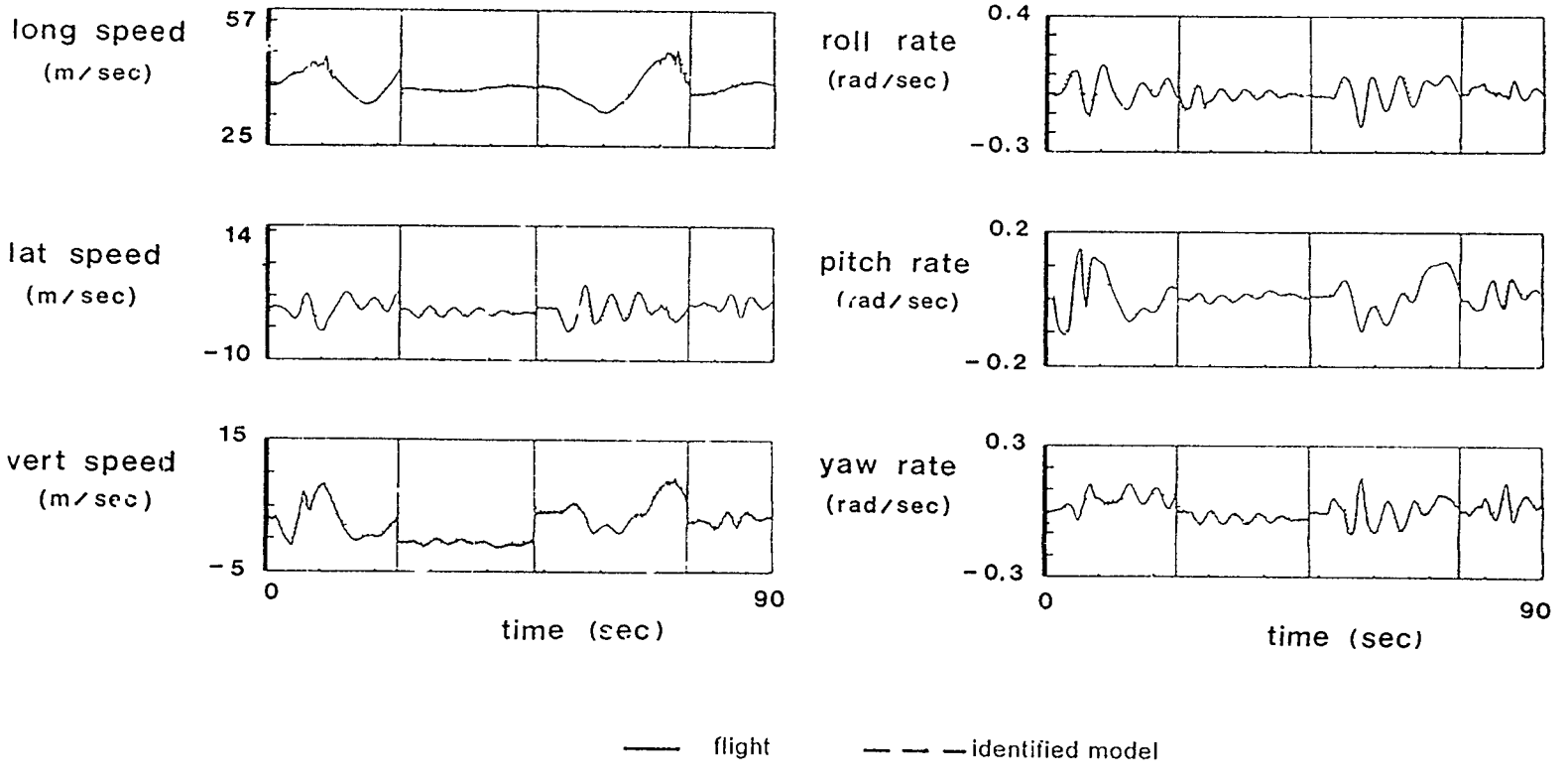

Fig 14 Comparison of flight and estimated time histories - DLR (verification)

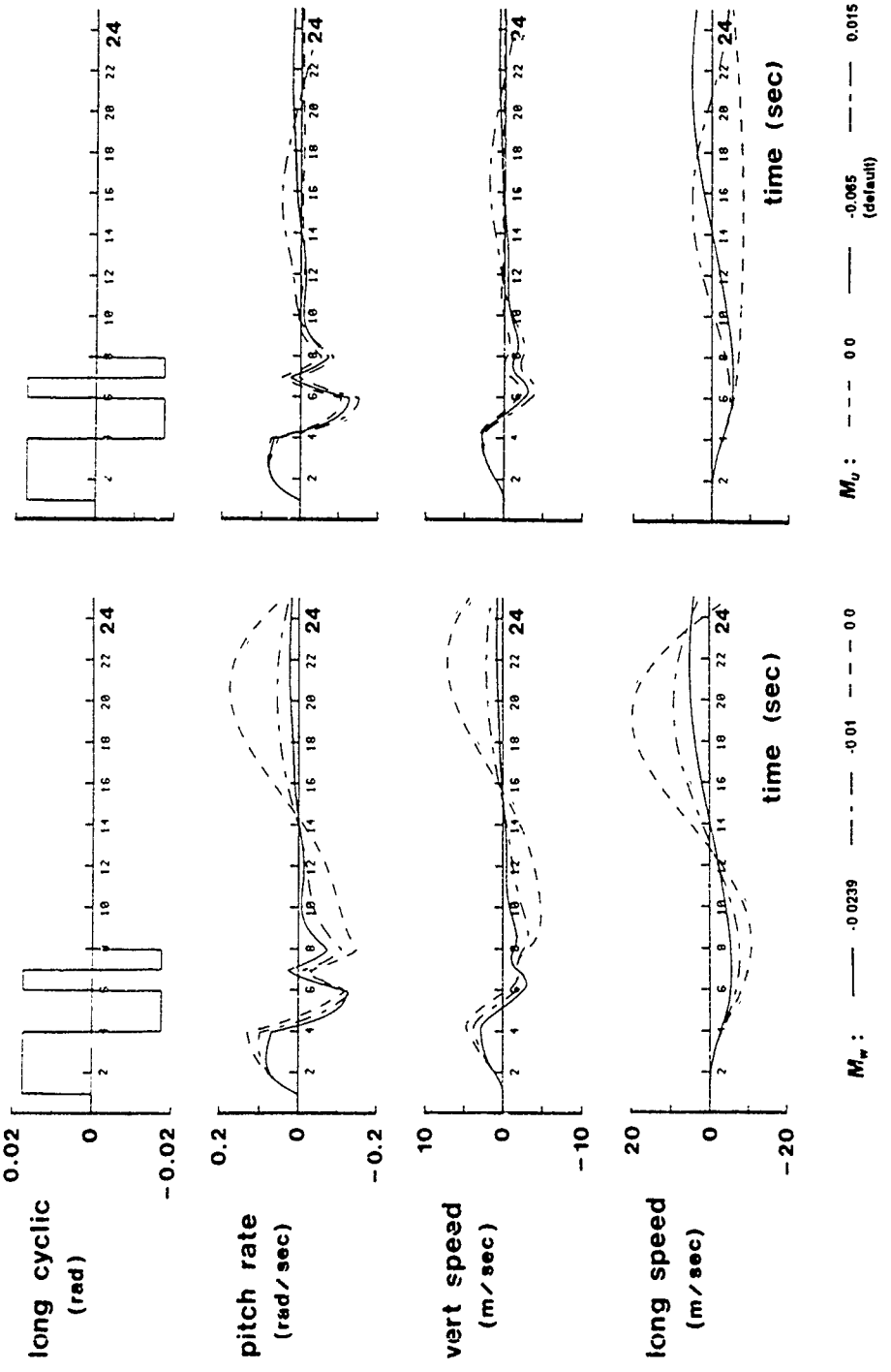

Fig 15 Hellstab cyclic reponses for M_w and M_u - Puma 80 kn

Industry View on Rotorcraft System Identification

D. Banerjee and J.W. Harding
McDonnell Douglas Helicopter Company
Mesa, Arizona

1. Abstract

An industry perspective on rotorcraft system identification is presented based on responses from eight major rotorcraft manufacturers to a questionnaire sent out by the AGARD FMP Working Group 18 on Rotorcraft System Identification. Several manufacturers are implementing system identification techniques for model validation and flight control law development. Concerns over costly data requirements and nonstandardised procedures are echoed. An example of the application of system identification for design support at McDonnell Douglas Helicopter Company (MDHC) is discussed.

The contributing rotorcraft manufacturers include: MDHC, Aerospatiale, Agusta, Bell Helicopter Textron Inc. (BHTI), Boeing Helicopters, Messerschmidt-Bölkow- Blohm (MBB), Sikorsky, and Westland.

2. Introduction

System identification can best be described as the determination of system characteristics from measured data. In flight dynamics, system identification can be used as a means of correlating theory and experiment and is often applied to handling qualities analysis, model validation, and flight control law development. Practical use of these techniques in the rotorcraft industry is hampered by the complex dynamics and severe flight test measurement requirement associated with helicopters. In recent years as these problems are overcome, development of system identification techniques for rotorcraft flight dynamic analysis has increased. The ultimate goal of such developments for industry is to decrease design costs by reducing the necessary flight testing and re-design for aircraft not performing as designed.

One objective of the Working Group was to develop guidelines for the application of identification techniques for design and development. To be effective in achieving this objective, it was important to get information on the industry's experience with and perception of the methodology as applied to solve rotorcraft development problems. The WG sent questionnaires to the eight major rotorcraft manufacturers requesting information on the use of system identification methods and the responses are summarized in this paper.

3. Industry Response

MDHC is working with both time- and frequency-domain identification. For time-domain identification, both Output Error (OE) and Maximum Likelihood (ML) techniques are used. OE identification has been applied to flight simulation model validation (Du Val, et al. [1]) and WG-18 activities. In a separate effort, ML was used to identify a reduced order stability derivative model to support flight control law development. This work is described later in this paper. A frequency response method based on the CIFER software package (Tischler, 1990 [2]) is currently being applied to AH-64 flight test data. MDHC is moving aggressively to implement system identification techniques in linear handling qualities and non-linear flight simulation models and also in other applications where modeling parameters are not adequately quantified.

Aerospatiale has conducted a joint activity with ONERA. Aerospatiale was responsible for the flight testing and has concluded that requirements for high quality measurements, careful testing, and test time durations preclude short flight test development. ONERA was responsible for the development and validation of time-domain identification tools. Identified linear models were not found to be as useful for validating and improving simulation models as expected.

Agusta uses a least-squares identification technique to minimize the error between flight test and simulated time histories (computed by the nonlinear ARMCOP program). Models are defined in ARMCOP by a set of parameters which include geometric and aerodynamic characteristics of the main and tail rotors, fuselage, vertical fin, and horizontal stabilizer. A subset of these parameters is selected to be identified and their values are subjected to constraints. A set of 'effective parameters' is found for each flight condition. This technique has been applied to both A109 and SA-330 (WG-18) flight test data.

BHTI uses force determination methods for structural dynamics analysis, however, no formal system identification methods are used in the handling qualities group. BHTI states that the system identification field

has not reached the same level of maturity as force determination as evidenced by the lack of validated software. Development and validation of the techniques for use by the helicopter industry is encouraged.

Boeing's most recent experience with system identification occurred on the ADOCS program where frequency response analysis techniques (Tischler, 1987 [3]) were used to document the closed loop command/response characteristics of the aircraft. Close correlation of both gain and phase characteristics between analytical predictions and flight test results have provided a higher level of confidence in predictive capability. Time-domain methods including Maximum Likelihood Estimation (MLE) and Orthogonalized Projection Estimation (OPE) algorithms have been applied to analytical and flight test response data for the purpose of identifying open-loop aircraft characteristics in terms of stability and control derivatives. The MLE methods appear to be more robust than the OPE techniques. A limitation of system identification methods is the requirement for a substantial amount of data and a large number of sensors specific to handling qualities work which often are at a lower priority than loads and stress related parameters.

MBB, in a joint research program with DLR, identified a model from BO105 flight data taken at 70 knots (Rix [4]). In addition, an extended flight envelope was identified (Kloster [5]). Difficulties in the flight data included vibration effects, drifts in speed measurements, and poor accuracy in horisontal linear accelerations. Comparisons between identified derivative models and theoretical results from non-linear simulation and quasi-static models were made. Time history agreement was good while derivative comparisons were sometimes poor. MBB expressed the need for a standardized identification procedure which gives comparable results.

Sikorsky invested significant effort in helicopter parameter identification in the early 70's but became disenchanted when it became obvious that the derived parameters, while able to reproduce time histories accurately, were physically meaningless. More recently, frequency-domain methods have been used to validate the GEN HEL model against flight test data from the CH-53E helicopter taken during the Technical Evaluation Program (TEP). Frequency-domain methods are now used routinely with simulation and in handling qualities work to show compliance with some parts of the new specification. *At this time, based on our experience, no parameter identification code is available that is robust and mature enough for industry use.*

Westland has no specific experience that has been thought of as system identification. The perception of the methodology is that it reproduces a particular phenomenon under a particular set of circumstances without necessarily advancing the understanding of the phenomenon. *Any success is related to engineering experience, flair, judgement, and understanding of the physical factors involved and which underlie the proposed model structure rather than any sophisticated system identification methodology.*

4. Recent Application of System Identification

One of the enhancing characteristics of MDHC's new MD520N NOTAR™ equipped aircraft is the degree to which yaw response is decoupled from collective control changes. This inherent decoupling reduces pilot workload when compared to other single rotor helicopters. As is often the case, however, a new design brings both advantages and disadvantages. The MD520N is statically unstable in yaw in one rather narrow region of its flight regime, i.e., in partial power descents in the mid speed range (around 60 knots). At that flight condition, the vertical fins do not produce sufficient yaw moment to overcome the adverse moment created by the fuselage. The divergence is slow enough that a pilot can stabilize it without significant difficulty. However, the increased workload was considered objectionable, and a solution was deemed necessary.

Several modifications to arrive at an aerodynamic solution were tested, but none was completely satisfactory. While an aerodynamic solution would certainly have been preferred, it was finally decided to try an active feedback control approach. The MD520N yaw control system consisted of a variable pitch tail boom pressurisation fan, circulation control slots, thruster control ports, and two variable incidence vertical fins, all mechanically linked and controlled by the pilot with pedals. Several actuation approaches were considered, with the final choice being to dedicate one vertical fin, with limited authority, to the active yaw control system, and retaining the remainder of the mechanical control system intact. The advantages of this approach are:

- Simple mechanical redesign and installation
- Minimal impact on hover and low speed sideward and rearward flight characteristics
- Requires relatively small actuation forces
- Feedback control system failures can not possibly affect the mechanical control system and are easily overridden by the pilot.

With a design approach decided, it only remained to determine the required feedback measurements and associated gains and time constants. To support the analysis and design, a model of the aircraft dynamics was needed. No simulation of the vehicle had been developed, but a great deal of flight test data was available. A 3 DOF linear model of the lateral/directional

axes was assumed adequate for the required analysis. The model structure, along with flight test recordings of input stimuli and output responses, was input to a ML system identification program to determine the coefficients of the linear model.

The model states were roll rate, yaw rate, sideslip angle, and roll attitude. The inputs were lateral cyclic and pedal control. The model outputs were the model states plus lateral acceleration. A 30 second flight test segment was used for the identification procedure. This segment covered the problem flight condition at 60 knots in a partial power descent (approximately 800 ft/min) where the pilot controlled sideslip for the first 7 seconds, then allowed the yaw divergence for approximately 4 seconds, then re-established control over sideslip (approximately 10 seconds), and finally continued sideslip control for the remainder of the segment. The measurements were uniformly sampled at 100 Hz.

The ML system identification algorithm uses a Kalman filter formulation of the system model where the state transition matrix and the input and output matrices are defined as functions of the parameters to be estimated. The identification procedure is iterative and, therefore, must be given an initial estimate of the parameters. The procedure adjusts the parameters at each iteration with the goal of minimizing the sum of the square of the Kalman filter innovation sequence over the entire time history. At any point, the model output time history may be compared to the flight test data to judge the degree of match.

The figure shows the model output time histories superimposed on the flight test data along with the lateral and directional control inputs. The yaw rate and sideslip fit is quite good. Roll attitude matches very well considering the poor resolution in the flight test data. Roll rate and lateral acceleration do not match as well due to possible longitudinal coupling and the breakdown of the linear assumption for large sideslip angles.

A yaw controller that uses sideslip as a measurement would be ideal for providing the required static stability. Unfortunately, sideslip sensors have many practical limitations, particularly in helicopter applications. Therefore, a controller was designed using yaw rate and lateral acceleration measurements. A wash-out on yaw rate was included to reduce the adverse yaw effect in turns. A lag on lateral acceleration was included for noise rejection. The identified 3 DOF linear model, the yaw controller structure, and a pilot model for roll stabilization were combined to simulate the problem. Classical frequency domain and root locus techniques were used to determine the gains and time constants for the yaw controller. Simulations were run with sensor noise and biases and an aircraft vibration model to check performance under more realistic conditions. The controller, along with a gain and time constant change mechanism, was installed in the flight test vehicle. Several flights were conducted to validate the controller performance and gain margins and to fine tune the controller parameters for the problem flight condition as well as the entire flight envelope. During flight test, the yaw rate gain was reduced to half of the design gain to reduce control activity and provide a smoother ride at high speed.

5. Conclusions

From an industry standpoint, requirements for dedicated flight testing to produce a high quality data base are a limiting factor to the application of these techniques. Although several major manufacturers are implementing system identification in various forms, concerns still exist over the robustness of these methods to provide accurate stability and control derivatives. The need for a standardized methodology is recognized.

Acknowledgements

The authors would like to thank those companies which responded to the questionnaire and Mr. Don Caldwell for providing the details of his work on the MD520N yaw stabilization.

References

[1] Du Val, R.W.; Bruhis, O.; Harrison, J.M.; and Harding, J.W.: Flight Simulation Model Validation Procedure, A Systematic Approach. Vertica, Vol. 13, No. 3, 1989.

[2] Tischler, M.B. and Cauffman, M.G.: Frequency-Response Method for Rotorcraft System Identification with Applications to the BO-105 Helicopter. 46th Annual Forum of the American Helicopter Society, Washington, D.C., 1990.

[3] Tischler, M.B.: Frequency-Response Identification of XV-15 Tiltrotor Aircraft Dynamics. NASA TM-89428, ARMY TM-87-A-2, 1987.

[4] Rix, O.; Huber, H.; and Kaletka, J.: Parameter Identification of a Hingeless Rotor Helicopter. 33rd Annual Forum of the American Helicopter Society, Washington, D.C., 1977.

[5] Kloster, M.; Kaletka, J.; and Schäufele, H.: Parameter Identification of a Hingeless Rotor Helicopter in Flight Conditions with Increased Instability. 6th European Rotorcraft and Powered Lift Aircraft Forum, Paper No. 58, Bristol 1980.

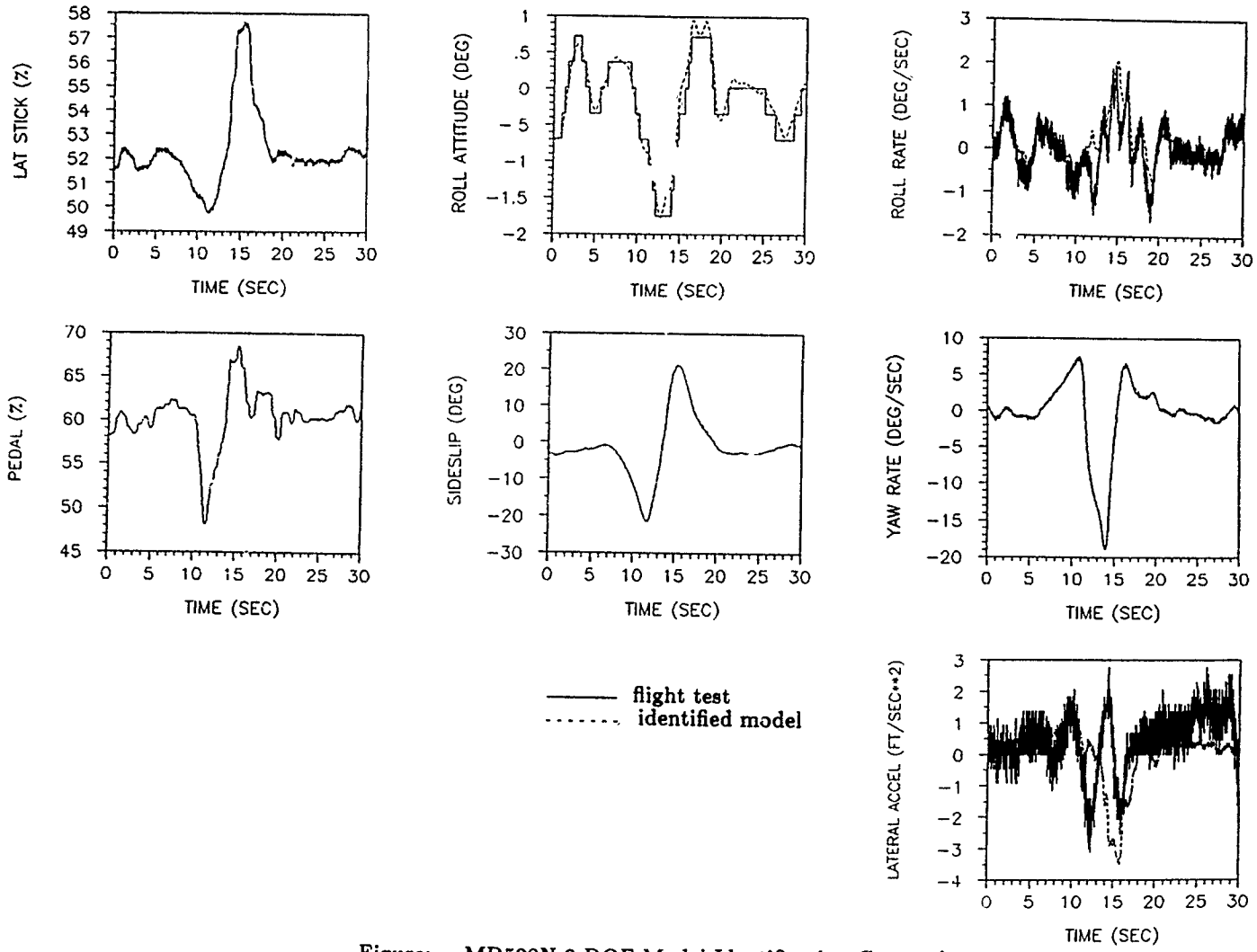

Figure: MD520N 3 DOF Model Identification Comparison

APPLICATION AREAS FOR ROTORCRAFT SYSTEM IDENTIFICATION SIMULATION MODEL VALIDATION

by

Gareth D. Padfield
Defence Research Agency
Aerospace Division
RAE Bedford, UK

and

Ronald W. DuVal
Advanced Rotorcraft Technology Inc
Mountain View, Ca, US

Summary

The role of system identification in the validation of rotorcraft simulation models is examined in terms of the overall 'functional' fidelity and individual component 'physical' fidelity. Validation acceptance criteria are discussed in terms of modelling range and accuracy for the three fundamental flight mechanics problems - trim, stability and response. Model development and upgrading are described as a natural part of validation, and the role that system identification can play in highlighting model deficiencies is discussed. An example from the six-degree-of-freedom analysis conducted by AGARD WG-18 is presented to illustrate functional validation and the merits of model distortion analysis in identifying deficiencies. Results from a more detailed analysis of the SA 330 blade flapping dynamics are presented to illustrate physical validation.

1 Introduction

The potential of simulation as a flight dynamics and performance support tool is considerable both in research and project applications, from design through development and certification. Some uses are listed below:

(a) Developing control laws for handling qualities and disturbance rejection.

(b) Checking compliance with flying qualities requirements for both clinical mission-task-elements and general flying tasks.

(c) Checking adequacy of control and stability at the edges of the flight envelope.

(d) Establishing control strategy following engine failure during various flight phases *e g* take-off.

(e) Developing functional integration of flight control with navigation, fire control, engine control systems etc.

(f) Developing display formats for operations in reduced usable-cue-environments.

In addition, the current and future potential value of simulation in pilot training is very high both in reducing flight hours required and improving safety. Examples include procedural operations, tactical operations and emergency situations.

Confidence in the results of simulation in these applications can be directly related to the fidelity or validity of the simulation, encompassing the full range of cues to which the pilot is exposed. At a fundamental level all cues are generated by the mathematical model at the heart of a simulation and, while it is not sufficient, it is certainly necessary that a model must be a valid representation of the 'real world' to be fit for useful work.

In a general sense, model validation refers to establishing the range and accuracy of a theoretical model for predicting the behaviour of an aircraft in response to pilot commands and external disturbances (*eg* gusts). The activity can more appropriately be described as calibration, highlighting the need for a scientific approach to the design of supporting experiments, in addition to the specialist efforts required for interpretation and analysis. The modelling range can be conveniently defined in terms of frequency and amplitude which, structurally, reflects the modal content and degree of nonlinearity. Within this range, we can draw a distinction between functional and physical validation, the former concerned with overall model response fidelity, the latter with the accuracy of the underlying modelling assumptions. Many of the rotorcraft modelling assumptions, (*eg* for inflow distribution, blade dynamics, interference effects etc) will have a limited range of fairly precise validity, and a broader range of marginal validity. In combination, the functional validity is difficult to quantify and depends upon the application. But validation involves much more than calibration and checking modelling assumptions; improvements are implicit in the process of validation, and any method that defines the limits of application of a model should also be able to identify the modelling features needing further development or the areas where assumptions are breaking down.

The role of system identification in the validation activity is illustrated in Fig 1. Parameters in an identified model structure, derived from test data, are compared with the same physical parameters in a theoretical model. The quality of the comparison will determine the verification effort required using different data sets and whether a model upgrade or further experiments need to be conducted. The product of this incremental and iterative exercise is a simulation model, fit for use over the range of conditions covered by the validation. In practice, use is likely to be extended beyond this range, towards conditions uncharted in the real-flight environment, often for safety reasons. The importance of validation for this special application is paramount.

For the purposes of discussion the validation process can be organised into the following steps.

(1) Establish acceptance criteria.

(2) Conduct flight tests and collect data.

(3) Conduct simulation tests and compare results.

(4) Analyse discrepancies and modify model to satisfy acceptance criteria.

In this paper, we distinguish between the functional and physical fidelity and validation of a simulation model. As noted above, the former relates to the overall goodness of fit of aircraft response to controls and disturbances, the latter to the accuracy of model component behaviour and modelling assumptions. The topics are connected through the requirement to establish sensitivities of fidelity to the modelling assumptions. In the following sections, each step in the validation process is discussed from the standpoint of both functional and physical validation. The topic of acceptance criteria for simulation models is covered in section 2; the flight testing and data requirements are not treated in this paper, but are dealt with adequately in other papers in this Lecture Series and in the report of AGARD WG-18 (AGARD, 1991). Sections 3 and 4 discuss the role of system identification in the simulation validation activity and the methodologies for conducting comparisons and analysing discrepancies; section 5 presents examples from both functional and physical validation activities drawn from the RAE Research SA 330 Puma (Fig 2) flight test database.

2 Validation Acceptance Criteria

2.1 Functional fidelity

2.1.1 *Objective*

When the intended use of a simulation model is for real time piloted investigations, then the principal objective of validation is calibrating the fidelity of the model outputs that provide the

piloting motion and visual cue sources, displacement, velocity and acceleration in the six spacial degrees of freedom. In addition, the control positions relate directly to the modelling accuracy. A framework for discussing and analysing model fidelity can be developed in terms of the range over which the model is valid and the accuracy criteria and level within this range.

2.1.2 *Scope*

When discussing model range and accuracy it is important to define exactly what the model is intended to predict. In flight dynamics the three important problem areas are trim, stability and response. In mathematical terms, these can be expressed as different solution forms of the general nonlinear evolutionary equations of motion (ignoring hereditary effects),

$$\frac{d\mathbf{x}}{dt} = \mathbf{f}(\mathbf{x},\mathbf{u},t) \quad , \tag{1}$$

where $\mathbf{x}(t)$ is the state vector comprising, in general, fuselage, air mass and rotor states; $\mathbf{f}(\mathbf{x},\mathbf{u},t)$ is a general forcing function comprising contributions from inertial, gravitational and aerodynamic sources and an explicit dependence on time to allow for prescribed disturbances and non-stationary effects ; $\mathbf{u}(t)$ is the control vector.

The trim solution is given by,

$$\mathbf{f}(\mathbf{x}_e,\mathbf{u}_e) = 0 \quad , \tag{2}$$

where the subscript e refers to the equilibrium or trim values.

The stability solution is given by,

$$\det\left[\lambda \mathbf{I} - \left(\frac{\partial \mathbf{f}}{\partial \mathbf{x}}\right)_{\mathbf{x}_e}\right] = 0 \quad , \tag{3}$$

where the values of λ correspond to the exponents of the small perturbation exponential transients *ie* the eigenvalues of the linearisation of $\mathbf{f}(\mathbf{x},\mathbf{u},t)$ about the trim point $\mathbf{x}_e$.

The response solution is given by,

$$\mathbf{x}(t) = \mathbf{x}(0) + \int_0^t \mathbf{f}(\mathbf{x},\mathbf{u},t)dt \quad . \tag{4}$$

Model accuracy is therefore related to the controls $\mathbf{u}$ required to hold a state $\mathbf{x}$, the location of the system eigenvalues λ and associated vectors and the time response $\mathbf{x}(t)$ to control inputs and disturbances expressed in the time or frequency domain. All three need to be quantified to give a comprehensive measure of model accuracy. Just how accurate the model has to be, relative to test data, depends upon the application. For example, the examination of trends during research and feasibility studies is not nearly as critical as predicting handling and control problems in a test programme to expand the flight envelope. On the other hand, if the flying qualities requirements are a primary design driver in a particular area, then predicting the correct behaviour at the earliest possible stage of a project is very desirable.

2.1.3 *Range*

Before discussing the application of system identification to these three problems, some definition of the range of validity is required. The natural dimensions of model range are frequency and amplitude and they embrace all three flight dynamics problems.

(a) Trim states are defined by the envelope of velocity (airspeed, V), flight path angle (γ), sideslip angle (β) and turn rate (ω), achievable within the limits of the control ranges, power and aerodynamic or structural limits. With four controls available, only four vehicle states can be defined or controlled independently and the selection given above, although arbitrary, is a natural piloting choice of primary variables. In this case, the secondary trim variables are the body attitudes, (ϕ,θ,ψ), rates (p,q,r), velocities (u,v,w), torque, rotor speed and corresponding rotor flap and lag angles.

(b) The range over which the rotorcraft stability is to be assessed can be defined by a bounded region in the complex plane, which includes all coupled rotor/fuselage modes that impact on the flight dynamics problem under investigation. In addition to the usual linear behaviour about trim states, the stability analysis should also encompass any limit cycle behaviour through equivalent linearisation or a describing function approach.

(c) The response problem presents the greatest challenge, with respect to the validation range, encompassing, as it does, small and large amplitude transient, open loop dynamics and forced, closed loop manoeuvres. The US flying qualities requirements, ADS-33C (AVSCOM, 1989), presents response criteria in different forms depending on the response amplitude. In general, small amplitude response is governed by the bandwidth criteria, moderate amplitude by the quickness or attack parameter and large amplitudes by the control power. Three features of ADS-33C are worth highlighting, however.

(i) They represent minimum acceptable criteria, and therefore do not necessarily require a vehicle or simulation to be exercised across its full dynamic range to satisfy handling requirements.

(ii) They represent necessary, but not sufficient, criteria. For example, the format is single input/single output, while in practice, a simulation has to be good for situations where the pilot uses a combination of controls to manoeuvre from one trim state to another.

(iii) ADS-33C is presented in a format based on a collection of one or two parameter criteria, and the method of extracting the parameters from test data is clearly defined. In particular, with one or two exceptions, the parameters are not derived from an assumed model structure so much as direct pointwise extraction from graphical data.

While the new flying qualities format has its shortcomings, these are generally acknowledged and exist because of the inadequate database of test results available from which to construct the criteria. As a definition of response range it is certainly incomplete but is a useful starting point; more work is needed to develop and expand the format to provide a comprehensive set able to exercise the vehicle dynamics fully.

2.1.4 *Accuracy*

While there can be no absolute criteria for the validity of a simulation model, there is a clear requirement for quantifying accuracy criteria.

(a) Predicted trim states should match flight estimates to within X% of full trim range for controls, attitudes and power requirements. The value of X may be as small as O(1) for hover power predictions, <5 for control margins at the flight envelope limits and O(10) for fuselage attitudes across the speed range.

(b) Predicted stability should match flight estimates to within Y% of the modulus of the corresponding eigenvalue. Individual criteria for each of the system modes are likely to be more useful when a wide modulus separation is present.

(c) Predicted response, in the extended format of ADS-33C, derived from time and frequency responses to controls and disturbances, should match flight estimates to within Z % of full response range. This criterion does not include the standard time history comparison test, on

the grounds that long term departures of flight and simulation responses, following initial, short-duration, control or disturbance inputs, do not generally imply poor validation; the smallest difference in initial conditions or modelling errors will always integrate to large values given enough time, and accurate piecewise comparisons of time histories after 20 or 30 seconds, for example, would be an unreasonable validation test. A potentially useful criterion format here would take account of this characteristic by weighting the time response error function $\mathbf{e}(t)$ with the matrix function $W(t)$ appropriately in the cost function J.

$$J = \int \mathbf{e}\, W(t)\, \mathbf{e}^T dt \quad . \tag{5}$$

For particular applications the criterion could take different forms. Tischler (1990), for example, presents criteria for the engineering validation of a nonlinear simulation model to be used for piloted investigations of helicopter accidents. For short term responses *'the peak value and 50% rise-time of the simulation and flight values shall match to within 20% of the flight values.'* For long term responses *'the stability trends shall be consistent with the flight data.'* For off-axes response, *'the trend of the response shall have the correct sign following the on-axes input during the time period up to 100% rise-time.'*

To be acceptable, a set of simulation validation criteria must be substantiated by pilot subjective opinion, supported by analysis quantifying the level of similarity between pilot control strategy in flight and simulation. This is still a very immature topic, requiring fundamental research to establish rules and how they relate to the different application areas.

2.2 Physical fidelity

Functional fidelity and validation are associated with the modelled behaviour of an aircraft's six degrees of kinematic freedom. For handling qualities investigations and piloted simulation experiments, these are the key variables of interest. However, as noted above, goodness of fit of overall time or frequency responses provides little insight into specific modelling deficiencies or required improvements. Only the very experienced engineer can be expected to be able to diagnose the source of problems from such data. If a model is required to support engineering development or studies into more generic design trade-offs, then a different approach is needed. We have described physical fidelity and validation as the attribute and activity addressing the underlying modelling assumptions. More than anything else, physical validation is concerned with quantifying the range and accuracy of the collection of these assumptions. Fig 3 attempts to encapsulate this idea; the functional relationship between the overall system input $\mathbf{y}$ and output $\mathbf{x}$ is represented by the operator $\mathbf{F}$. Internal dynamic elements have their own operators; physical validation is concerned with these more primitive modelling elements. An immediate requirement, beyond the scope of functional validation, is for significantly more detailed measurements of behaviour internal to the model. Examples are,

(a) If the rotor induced inflow model structure and parameter values are to be validated, then measurements of the azimuthal and radial load and incidence distribution may be required.

(b) If the elastic blade deformation approximations are to be validated, then measurements of blade strain/bending moments may be required.

(c) If the blade element aerodynamic formulations are to be validated, then detailed loadings need to be measured.

(d) If the rotor-wake/fuselage/empennage interactional aerodynamic model is to be validated then measurements of the flowfield and surface pressures may be required.

(e) If the tail rotor thrust/torque modelling is to be validated, the measurements of these and the rotor states may be required.

Similar requirements fall on all of the individually modelled elements. The complete task is very difficult and expensive to accomplish in flight and most component model validation has been conducted at model scale in wind tunnels.

The *scope* of physical validation and fidelity is therefore considerably greater than for functional fidelity as discussed above. The ***range*** of interest covers all the operating conditions that component elements will be exposed to in the applications of interest, *eg* a stall model for section aerodynamics will be required to expose handling effects in limiting conditions; a main rotor wake/tail-rotor interactional model will be required to establish tail rotor control limits for hovers in side winds. ***Accuracy*** requirements will vary according to the application, as for functional validation. In fact, the two levels of validation are related strongly in this respect; the sensitivity of the functional fidelity to the accuracy of modelling assumptions, hence the details of physical validation, is of central interest in the development of an engineering simulation. System identification plays a role common to both.

3 System Identification in Functional and Physical Validation

System identification is, in a general sense, a sophisticated form of curve fitting and has application to all three problem areas - trim, stability and dynamic response. Practically all the published work on rotorcraft system identification has been concerned with linearised models and, except for some notable exceptions (Padfield, editor, 1988), with the functional validation of conventional six-degree-of-freedom model structures. The evolutionary equations for small perturbation about a trim condition take the form,

$$\frac{dx}{dt} - Ax = Bu + g(t) \quad , \tag{6}$$

where $x(t) = [u,w,q,\theta,v,p,\phi,r]$, $u(t) = [\theta_0, \theta_{1s}, \theta_{1c}, \theta_{tr}]$.

A and B are the state and control matrices of stability and control derivatives respectively and $g(t)$ is a general vector forcing function.

u, v, w and p, q, r are the aircraft translational and rotational velocities about the body axes; ϕ and θ are Euler roll and pitch angles and $\theta_0, \theta_{1s}, \theta_{1c}, \theta_{tr}$ are the main rotor and tail rotor controls.

While the trim and response problems are inherently nonlinear, some useful results can be derived using the linearised form given by (6).

3.1 Trim

For the trim problem, system identification can be applied to the steady-state algebraic form of (6). Let A_a be the matrix of unknown aerodynamic derivatives and A_{ig} be the matrix of inertial and gravitational derivatives, then the steady state form of (6) can be written as,

$$[A_a \; B] \begin{bmatrix} x \\ u \end{bmatrix} = - A_{ig} \, x \quad . \tag{7}$$

In principle, a wide enough range (over small amplitudes) of new trim conditions, close to the original, can be established to enable estimates of derivatives or, in most cases, ratios of derivatives to be derived from the test data. Examples from classical stability and control testing include the speed stability derivative M_u , the rolling and yawing moments with sideslip (L_v, N_v) and pitch manoeuvre margin in steady turns.

Simulation model validation requires that the simulation trim or initial conditions match those of the reference flight test data and that the simulated configuration is representative of the vehicle that generated the reference data (CG position, weight, control modes, atmospheric conditions, etc.).

Such static comparisons are usually performed by trimming the simulation to the desired flight condition and comparing the simulated trim variables with those obtained from the flight test data. This is often complicated by the difficulty in establishing trim results accurately from flight test data where the aircraft can be in a constant state of perturbation from gusts and sporadic control inputs. Identified discrepancies in trim results are difficult to relate to physical phenomena since there is no dynamic excitation to help isolate the source of the discrepancies. A trial and error approach is often required in which alternate modelling assumptions are used to determine their impact on the comparison. An example of such an approach is given in Fig 4. These plots show comparisons of trim values for the collective control position and aircraft pitch attitude as a function of airspeed for the UH-60 Black Hawk helicopter. Flight test data is compared with two types of simulation model. One is based on a blade element rotor model with rigid articulated blades and the other on a blade element rotor model with elastic articulated blades. The effect of the blade elasticity on high speed trim characteristics is evident from this figure. While the elastic model data presented was generated using a physically based modal representation of blade elasticity, a functional approach using empirical modifications to the effective collective feathering as a function of airspeed has also been demonstrated to provide a good fit to the test data. In both cases, however, the starting assumption was that the trim problem was related to blade elasticity so a certain amount of engineering intuition was required.

3.2 Stability

The stability problem centres around deriving good estimates of the A matrix elements or a set of equivalent parameters. This application area has received by far the most attention and many of the ground rules and pitfalls are fairly well understood. Two aspects can dominate the likelihood of success:

(a) Test inputs and aircraft motion excursions should be as small as possible for the linearity assumptions to hold good and yet large enough that the noise content is small relative to the response signal. The requirements conflict and, in practice, both will be compromised.

(b) Test inputs need to excite the aircraft modes, the stability of which are under investigation. This requires *a priori* knowledge of the modal distribution and usually some iteration to optimise the input shape. Doublets, multi-steps (*eg* 3211) and frequency sweeps are all in common use.

Test input design is therefore a most critical issue in deriving robust parameter estimates and hence stability information. Frequency domain identification has gained favour in recent years because of the ease with which different model structures can be explored over different frequency ranges. Data derived from frequency sweep inputs are particularly suitable to transfer function modelling, whereby the modal character, and hence model structure, is matched by polynomial fitting, providing direct estimates of both system open-loop poles (eigenvalues) and closed-loop zeros.

3.3 Response

In order to decouple the problems of static trim and dynamic response validation, dynamic results are often compared as perturbations about a trim condition. This is a risky approach since the nonlinearities in the simulation can cause significant coupling of the trimmed flight condition into the dynamic response. Trim problems are relatively easy to correct on a functional basis ice control variables can be biased to achieve the required trim. The biases are often justified by citing uncertainty in the control rigging or in the available test data for control positions. This is also a risky practice since it treats the symptoms rather than the illness and can further impact the validation of the dynamic response. Ideally, static and dynamic comparisons should complement each other in isolating the physical cause of simulation discrepancies.

To some extent, the response problem receives partial treatment when identifying the stability characteristics. The model matching and identification is achieved on time or frequency response histories and such comparisons are often put forward as evidence that the model validation has been successful or otherwise. In reality this test or demonstration, while potentially being convincing on one level, is never enough to ensure true validation and in many cases can be very misleading. Derivatives estimated from an identification that produces an excellent response fit can often bear little resemblance to the values of their theoretical counterparts, leaving the engineer perplexed as to what needs more validation, the theory or the system identification method. With good quality test data and careful application of a comprehensive identification analysis however, robust values of derivatives can be estimated that can be used to glean insight into the force and moment character at small amplitude and hence support the validation of the full nonlinear model.

A recommendation made in an earlier section was the use of the ADS-33C flying qualities criteria as a format for demonstrating simulation validation. This is particularly appropriate when the simulation is being applied to establishing compliance with the requirements. A complete and substantiated flying qualities criteria should contain a specification for every effect that can impact the pilot's impression of the aircraft's ability to perform a flying task. An equivalence between simulation and flight in this sense, should then imply validation of response characteristics as far as pilot subjective opinion is concerned. No existing criteria fully complies with the CACTUS rules (complete, appropriate, correct, testable, unambiguous, substantiated) however (Padfield, 1988), and as ADS-33C currently stands, compliance will not guarantee validation.

The principal role of system identification in supporting this comparison is through equivalent system model matching. The only criterion in ADS-33C that requires the formal use of system identification is the height response to collective, where a least squares fit of a delayed first-order model to the response to a step input is made, to establish key handling parameters. This criteria is discussed in more detail in another paper in this Lecture Series and in the final report of AGARD WG-18 (Tischler, 1991). Other criteria where parameters can be alternatively derived from identified models include pitch, roll and yaw bandwidth, lateral/directional oscillation characteristics and torque response to collective. The use of equivalent systems or reduced order models for deriving such criteria is particularly appealing; considerable insight can be gained, from parameterised models, into the effects of design parameters on an aircraft's ability to meet design criteria.

The validity of a nonlinear simulation model and its theoretical foundations, in terms of its accuracy over a given range of steady state and dynamic conditions, can only be partially judged, as noted above, through comparison with small perturbation linearised approximations. The use of system identification in the validation of full nonlinear model structures has received limited attention in the aerospace community. The research of Klein and Batterson (1983) is a notable exception, where the authors estimate parameters associated with higher order polynominal terms (spline functions) by using different amplitude ranges in the responses. A good *a priori* knowledge and understanding of the likely behaviour, and hence mathematical formulation, is essential for the success of this approach. Another approach to identifying nonlinear models is to work directly with the nonlinear model structure and the set of fundamental parameters, *eg* aerodynamics, structural, inertial and geometric. The parameters can be 'tuned' to minimise the error between measured and predicted responses. The approach appears attractive but the limited experience to date has exposed identifiability problems. The large number of 'adjustable' parameters precludes their simultaneous estimation and determining which parts of the simulation should be modified is a difficult task which relies mainly on engineering judgement. Therefore, the effectiveness of the parameter estimation approach depends on accurately isolating these problem areas, as parameter estimates will be affected by errors elsewhere in the simulation.

An intuitive approach to performing dynamic comparison is to drive the simulation controls with the control time history obtained from the flight test reference data and compare the dynamic response with that of the reference data. This can be referred to as closed loop simulation since the simulated six-degree-of-freedom airframe motion is obtained from integrating the accelerations produced by the applied loads that result from the prescribed control. The task of identifying the problem areas in the model is hampered by the fact that the method relies on comparing response data. This is a major drawback of functional validation. It is difficult to infer, from typical

measured responses, the specific shortcomings in the simulation. Parameters are often embedded in approximations to component forces and moments, while the aircraft response is related to these forces and moments through coupled, nonlinear differential equations. Other disadvantages in this approach are the considerable CPU times required and potential convergence problems. To correct problems associated with matching simulated responses, alternate techniques of inverse simulation have been proposed (Thomson and Bradley (1988), DuVal *et al* (1989)). This is the term given to the method whereby selected state variables are constrained to be equivalent for the test and model results and the simulation model partially inverted to determine the unconstrained motion. The constrained degrees of freedom can be considered as 'open loop' in the computer simulation. Both closed and open loop techniques require that the test data be properly conditioned to assure consistency with both redundant sensors and kinematic relationships. Kalman Filter/Smoother techniques can provide a systematic basis for this conditioning.

Closed loop simulation

A schematic representation of this methodology is shown in Fig 5. The simulation is first initialized to the starting test conditions and test vehicle configuration. The simulation is then driven with the recorded history of flight test controls and the simulation's dynamic response is compared to that of the flight vehicle. This is the most commonly used comparison approach. Its advantages are that it is simple to implement and requires minimal sensor data. Its disadvantage is that the cumulative error build up due to the closed loop integration of simulation loads causes the simulated vehicle to diverge from the flight test trajectory and consequently limits the validity of the comparison. This approach is suitable for supporting functional validation but the coupling between dynamic subsystems cannot be isolated in this method, so it is limited in its application to physical validation.

Open loop simulation

A schematic representation of open loop simulation comparisons is shown in Fig 6. In the example shown, the procedure is to disable the integration of the airframe rigid body motion in the simulation and drive the simulation with controls and rigid body motion data obtained from the flight test as if it were in a wind tunnel. The resulting simulation loads can then be compared with flight test data to provide a systematic approach for isolating and correcting discrepancies (DuVal *et al*, 1989). Since the simulated flight vehicle follows the actual flight test trajectory, the comparison can be performed without concern for a cumulative error build up. This approach requires more extensive data collection than is generally available from flight tests. Load cells and/or accelerometers must be placed at the boundaries of vehicle subsystems to facilitate isolation of the mathematical model and direct comparison of subsystem loads. The implementation of the simulation run is more difficult since the capability to suspend the integration of selected degrees of freedom is required and the ability to input the airframe motion as well as the controls from the flight test data is also necessary.

4 Analysing Discrepancies and Upgrading the Model

Once the comparisons have been performed and discrepancies have been identified, it is necessary to analyse these discrepancies to determine their source and to postulate potential model upgrades. The upgrades must then be implemented and their effectiveness evaluated. This is often an iterative process since the adequacy of a proposed upgrade cannot be determined without implementing and testing it with the simulation. System Identification methodology plays a critical role in this stage of the validation process. There are two potential sources of error in the model; the model structure and the model parameter values. They are strongly related and must be jointly addressed.

(a) incorrect parameter set - this would include those parameters directly related to, and measurable as, physical attributes, *eg* inertias, geometry, and those derived from approximation theory as effective parameters, *eg* effective hinge offset/spring strength, aerodynamic force coefficients,

(b) incorrect model structure - this would include both model degrees of freedom and nonlinear formulations.

As pointed out above, the two ways are connected; an effective parameter is often an approximation to a more complex effect, *eg* quasi-steady form of another degree of freedom or local linearisation of a nonlinear function. There will always be a limit to the range over which the approximation is valid and, ultimately, a breakdown in the value of an effective parameter is indicative of a model structure deficiency. It is important to understand which of the above is the cause in a particular situation. In general, deficiencies in the second category are more difficult and time consuming to cure, although once achieved, the upgraded model will offer more opportunity to expand the application range. Unless evidence is strongly to the contrary, however, deficiencies in the first category should be exhausted before recourse to structural upgrades.

Two key points are worth highlighting at this stage. Firstly, the experimental test database, from both model and full scale, needs be carefully assembled to support the validation activity. In the limit it is desirable to measure every variable that plays a part in the simulation, (*eg* individual component force and moment contributions), but in reality this is rarely achieved. It must be recognised that a limited measurement database will limit the upgrading potential. Secondly, an underlying principal, that brings a systematic methodology to the validation activity, is that every modelling approximation or assumption employed needs to be checked, across the range of application, through correlation with test data. This is the essence of physical validation.

4.1 Model structure determination

The modelling assumptions used in developing a simulation may be inappropriate under certain conditions. While empirical parameters can always be added to the simulation to fit the test data, the resulting model may not exhibit correct behaviour between available test points. The only way to have confidence in a simulation outside the specific test points available for validation is to use physically based models that are tuned with physically meaningful parameters. The first indication that a model is not structurally correct often comes when parameter identification is attempted and the resulting parameter values are found to be physically meaningless. At this point a more systematic approach to evaluating the model must be taken. The starting point is usually to examine the discrepancies in the acceptance criteria and attempt to relate these discrepancies to specific vehicle states and physical phenomena. Statistical correlation of the comparison errors with measured states and controls may provide an initial insight into the nature of the problem. For example, correlation of the error with rotor speed or lead-lag angle may indicate that a more sophisticated representation of the coupled engine/drive train/rotor model is required. Regression is an essential tool in such an investigation. Stepwise or subset regressions can be particularly useful by finding the state or control most correlated with the comparison error, fitting it to the error through regression, and then repeating the procedure with the residual error and the remaining states and controls. Another valuable tool for model structure determination is the frequency response. By examining the magnitude and phase of comparison errors versus frequency, the bandwidth in which these errors predominate can be determined and this can then be related to the known bandwidth of relevant physical phenomena to determine the missing pieces. An example is to examine the error in simulated and measured flapping response to cyclic input. Excessive error levels in the frequency range associated with, say, dynamic inflow would suggest that this effect is not properly modelled or that its coupling with the flapping is incorrect. This example will be returned later in section 5.2.

A modification to the structure of a model subset may take one of two forms; an increase in the number of states utilized in the subset model or the addition of nonlinearities to the model. It is often difficult to distinguish between these two causes. Regression is an important tool for performing such an analysis. Correlation of the modelling error with derivatives of the model states can indicate that a higher order dynamic model is required. Strong correlation with the states of other subsystems indicate the need to model cross coupling. If regression is unable to fit the error with some linear combination of system states, then nonlinear functions of the states may be required. These functions can also be tested with regression, so long as the regression is linear in the coefficients to be identified.

4.2 Parameter identification

The process of model structure determination and parameter identification is usually an iterative one, since unreasonable parameters will result from an incorrect model structure and may therefore lead to a reformulation of the model structure. Regression is an effective tool in the initial stages since it supports both model structure determination and parameter identification, but once the structure is reasonably well determined, a more robust identification is required for the parameters. Equation Error methods, such as regression, may be biased in the presence of measurement noise. Output Error methods are generally more suitable for experimental data where measurement noise is a concern. Output Error identification also provides more effective identification of the stability matrix than regression since it takes into account the time correlation of a dynamic system while regression essentially looks at a snapshot of the correlation at each point in time independently of other time points. Maximum Likelihood Identification is the most general form in that it is unbiased in the presence of both process and measurement noise; however, stability and convergence problems, particularly for nonlinear systems, tend to make it less practicable than the Output Error approach. It is interesting to note that both Equation Error and Output Error methods are special cases of Maximum Likelihood. Equation Error results from a low measurement noise assumption in Maximum Likelihood and Output Error results from a low process noise assumption.

In the functional validation example which follows this section, six-degree-of-freedom stability and control derivatives are referred to extensively. Two points are worth making at this stage:

(i) Derivatives estimated by a system identification method are effective parameters; for very small amplitude they are equivalent to the first order terms in a Taylor expansion of the applied forces and moments about the trim condition. Aircraft motion excursions in typical test data are generally of more moderate amplitude, however, and any nonlinearities will be embodied in the resultant derivative. It is important therefore, when comparing derivatives from flight and theory, to check for variations with motion amplitude from both sources.

(ii) Derivatives, predicted from a theoretical model, are themselves functions of a large number of, more fundamental, configuration and model parameters, *eg* rotor radius, lift curve slope, moments of inertia etc. Fig 7 illustrates how, for the RAE simulation model *Helistab*, two of the pitching moment derivatives vary with three model parameters - the effective rotor flap stiffness, rotor flap inertia and centre of gravity location. There can be many more fundamental parameters than derivatives, depending on the model complexity. Model deficiencies in the first category above, *ie* incorrect parameters, can sometimes be identified through an exploration of the required fundamental parameter distortions required to match derivatives. This parameter distortion or 'fudge factor' technique is often used in simulation validation to accommodate pilot subjective opinion. The technique is prone to considerable misuse, with a genuine source of modelling error being compensated for by distortions in an unrelated parameter. Careful applications can bear fruit, however, particularly with respect to corrections in effective parameters. Optimising the distortions to match derivatives is inherently nonlinear and multi-objective; system identification is the natural tool for such problems.

All airframe manufacturers and research laboratories have experience of simulation model validation based on comparison with test, with the attendant development and upgrading activities. Houston (1989) and Ballin *et al* (1990) present typical results from contemporary studies conducted at UK and US Government research laboratories. Houston's work focusses on vertical axis dynamics of an SA-330 at hover, illustrating how coning and air mass dynamics are required model elements in the prediction of body motion up to about 20 rad/s. Errors in this model structure are computed as distortions in the model parameters providing some insight into the validity of assumptions associated with local momentum theory and the use of rigid blades. Measurements of blade flapping motion were essential in providing confidence in these transfer function results. Ballin sets out to upgrade the US Army's *Genhel* UH-60 simulation model based on open-loop frequency and time domain flight test results. Ballin's work is an excellent example of investigative upgrading, based on non-parametric frequency response models. The *Genhel* software incorporates a blade-element rotor model with flap, lag and air mass dynamics and runs in real-time with a 6.67 ms frame on an AD-100 computer. The comparative technique proved effective in evaluating various modelling

improvements, *eg* new dynamic inflow model, lag damper characteristics, and establishing a model which is *'fully adequate for real-time handling qualities'* up to 10 rad/s.

5 Examples

5.1 Functional validation (six-degree-of-freedom)

5.1.1 *General*

The framework for simulation model validation and the application areas of system identification have been set out in earlier sections. Establishing criteria for model range and accuracy and highlighting the required model developments were the two specific areas addressed. The AGARD WG-18 test databases are insufficient to cover the full range of issues included in the trim, stability and response problems. All three aircraft databases are, however, typical of those used to support simulation model validation and a number of useful examples can be derived from them, one of which will be detailed here. The primary simulation model used in this case study is the RAE Helistab model (Padfield, 1981,1988). This model is intrinsically nonlinear and can be trimmed in a general condition of sideslipping, turning, descending flight. Coning and first harmonic flap and rotorspeed/engine governor degrees of freedom complement the fuselage states. Current developments include three degree-of-freedom rotor lag and inflow dynamics. Rotor aerodynamics are derived from linear blade element/momentum theory and the rigid blade/centre hinge-spring analogue is used to model both hingeless and small-offset articulated rotors. Fuselage and tail surface aerodynamics are nonlinear functions of incidence, sideslip and rotor downwash. The quasi-steady, six degree-of-freedom version is used for the comparisons discussed here. Fig. 8 shows a comparison of test and theory for the three translational and three rotational velocities for two Puma test runs - pedal and lateral cyclic inputs. Fundamental questions that can be asked of the system identification approach are:

(a) Can a comparison of flight-estimated and theoretically-predicted aerodynamic derivatives shed light on the model strengths and weaknesses?

(b) Can the stability characteristics of the the aircraft dynamic modes be correctly estimated?

These two questions and their answers are closely related. Often, approximations for mode frequency and damping can be derived from simplifying assumptions and expressed in terms of a limited number of parameters. Comparisons of the equivalent modal parameters from flight and theory and their constituent parts can be effective at highlighting areas of overall simulation model deficiency. Later in this section this approach will be explored for the Dutch roll motion, but before this, a number of relevant observations can be made from an examination of the comparisons in Fig 8.

(a) Pedal response (Fig 8a)

(i) speed changes are greater in flight (5 m/s);

(ii) initial yaw, roll and sideslip responses are distinctly greater in the simulation;

(iii) the Dutch roll mode appears more damped and of lower frequency in the simulation.

(iv) the pitch and heave responses appear considerably smaller in the simulation.

(b) Lateral cyclic response (Fig 8b)

(i) roll response appears sharper and less damped in the simulation;

(ii) the Dutch roll response in roll and yaw is greater in flight;

(iii) the pitch and heave responses are smaller in the simulation;

(iv) speed changes are small during the manoeuvre (5 m/s)

Some of these observations will be reviewed in the light of the system identification analysis later in this section.

The complete set of *Helistab* stability and control derivatives and corresponding eigenvalues are contained in Table 1 for the 80 kn flight condition. Data are also included on aircraft configuration and the magnitude of the perturbations used to generate the derivatives numerically.

5.1.2 *Lateral - directional Dutch roll motion*

The dominant motion throughout the responses shown in Fig 8a&b is the weakly damped Dutch roll mode. The lateral-directional dynamics of the Puma at the 80 kn flight condition appear to be classical with a roll subsidence and spiral motion completing the modal set. It is of interest to explore whether the mismatch in the Dutch roll response between flight and simulation illustrated can be explained through the estimated derivatives. Table 2 compares the primary lateral/directional derivatives from flight and simulation, the former taken from the DLR and University of Glasgow analyses using time and frequency domain system identification techniques respectively. Numbers in parenthesis are the standard deviations of the parameter estimates; as a rough rule of thumb, values below 10-15% of the parameter itself are considered to imply a high confidence level. The Dutch roll eigenvalues are also included in the Table and show that the fourth-order lateral sub-system provides a reasonably good approximation in all three cases. This is a significant result in itself, indicating that although the pitch and heave motions are appreciable, they do not have a first order effect on frequency and damping at this flight condition. Lower order approximations to the Dutch roll mode can be derived for a range of different cases, the simplest being when the motion is pure yaw. This is clearly inappropriate in the present case with the roll/yaw ratio approximately unity (see Fig 8a). A more general and useful approximation can be derived by isolating the spiral dynamics with the sideways-velocity degree of freedom,

$$v_0 = v + V\beta \ . \tag{8}$$

The lateral equations can then be written in the alternate form (Padfield and DuVal, 1982)

$$\frac{d}{dt}\begin{bmatrix} \dot{v}_0 \\ v \\ \dot{v} \\ p \end{bmatrix} - \begin{bmatrix} 0 & 0 & Y_v & g \\ 0 & 0 & 1 & 0 \\ -N_r & -VN_v & N_r + Y_v & g - N_p V \\ L_r/V & L_v & -L_r/V & L_p \end{bmatrix} \begin{bmatrix} \dot{v}_0 \\ v \\ \dot{v} \\ p \end{bmatrix} = 0 \ . \tag{9}$$

The partitioning shown divides the dynamics into the three modes of increasing modulus - spiral, Dutch roll and roll subsidence. If the conditions for 'weak coupling' between the partitioned degrees of freedom are met (Milne, 1965), then the approximation to the Dutch roll eigenvalue can be written,

$$\lambda^2 + 2\zeta\omega_n\lambda + \omega_n^2 = 0 \ . \tag{10}$$

where

$$2\zeta\omega_n = \frac{-\left[N_r + Y_v + \sigma\left\{\frac{L_r}{V} - \frac{L_v}{L_p}\right\}\right]}{\left(1 + \frac{\sigma L_r}{L_p V}\right)}, \tag{11}$$

$$\omega_n^2 = \frac{(VN_v + \sigma L_v)}{\left(1 + \frac{\sigma L_r}{L_p V}\right)}, \tag{12}$$

$$\sigma = \frac{(g - N_p V)}{L_p}. \tag{13}$$

This approximation shows how the Dutch roll damping is affected by the derivatives L_v, N_p and L_r, in addition to the yaw damping N_r. Likewise, the frequency is modified by L_v in addition to the primary stiffness N_v. The approximate eigenvalues for all three cases are shown in Table 2 ($\lambda^{(3)}$) along with the coefficients of equation (9). In general there is excellent agreement with the Dutch roll eigenvalues for each case. The *Helistab* damping prediction is double the flight estimate, confirming the observation made in section 5.5.1, and the frequency is 20% lower in the simulation. Comparing the make-up of the Dutch roll characteristics from (9), the following points can be made:

(a) *Helistab* over-estimates the basic yaw damping (estimated from flight) by 60%.

(b) *Helistab* underestimates the principal roll derivatives by 20%.

(c) Flight estimate of N_p is more than double the *Helistab* value.

(d) Flight estimate of N_v is 20% higher than the *Helistab* value.

(e) L_r from flight is negative, from theory positive; the flight values are estimated with low confidence.

(f) Yaw control derivative N_{tr} from flight is nearly half the *Helistab* value.

On the basis of these observations, assuming that the flight derivatives estimated with high confidence are 'correct', a set of corresponding hypotheses can be made concerning the simulation model validation.

(a) The yaw damping and control sensitivity are dominated by the tail rotor; the simple tail rotor model (with fin blockage) adopted in *Helistab* needs refinement.

(b) The uniform increase in primary roll derivatives (L_v, L_p, L_{1c}) suggests an incorrect roll moment of inertia or rotor Lock number, the latter possibly reflecting the effects of unmodelled dynamic inflow.

(c) The derivative N_p has a strong destabilising effect on the Dutch roll mode, accounting for about 65% of the damping decrement (*ie* the additional term). The larger flight value could be explained by an incorrect product of inertia I_{xz} in the simulation. More subtle aerodynamic effects are difficult to accommodate within the simple rotor model structure in *Helistab*.

(d) The directional stability is clearly underpredicted by *Helistab*; this is unlikely to be a tail rotor effect in view of (a) above. In fact, the evidence suggests that N_v due to the tail rotor should actually be less than predicted. The fuselage and empennage contributions to N_v in *Helistab* are derived from wind tunnel data and an obvious conclusion is that these do not relate directly to the flight situation.

(e) The positive L_r from *Helistab* comes entirely from the tail rotor, is stabilising, but is not significant in the Dutch roll damping. The negative and higher DLR flight estimate is not insignificant, but is perplexing as no well understood mechanism gives rise to such an effect. The relatively high value of the standard deviation for this derivative suggests a low confidence factor.

(f) In addition to the above effects, the absence of a rotor wake/tail rotor/empennage interaction model in the simulation must have a significant impact on the results, particularly the yawing derivatives.

Such hypotheses form the starting point for a second phase of the validation exercise; some appear plausible and consistent but others are more dubious. The sensitivity of key derivatives and the Dutch roll eigenvalue to some of the physical parameters discussed above is summarised in Table 3. The DLR flight estimates and baseline *Helistab* results are compared with five cases as follows.

(a) Twenty per cent change in the roll inertia I_{xx} increases the roll derivatives, decreasing the modal damping and increasing the frequency slightly.

(b) Increasing the perturbation size on the sideslip velocity v to 5 m/s from the default value of 1.5 m/s, increases the weathercock stability to within 3% of the flight estimate. The strongly nonlinear fuselage and empennage aerodynamic forces and moments with sideslip account for this effect. The value of 5 m/s could be argued to give a more appropriate equivalent linearisation, consistent with the magnitude of the sideslip excursions in the response to pedal input. However, this effect serves to increase the damping to double the flight estimate.

(c) A 50% increase in the product of inertia I_{xz} leads to a corresponding 50% increase in N_p, but only a marginal decrease in stability.

(d) Reducing the efficiency of the tail rotor by a 40% reduction in the blade lift-curve slope reduces the magnitude of the yaw derivatives by a similar amount. While the damping and control sensitivity approach the flight estimates, the weathercock stability also decreases, departing even further from the flight estimate. The modal characteristics are now considerably different from the flight values.

(e) Reducing the linear coefficient in the fuselage yawing moment function with sideslip (parameter FN1) increases the directional stability without affecting the yaw damping. Both modal frequency and damping increase.

(f) The results obtained from combining the above five effects are shown in the final column in Table 3 and compared with the baseline *Helistab* results in Fig 9. The results are shown as a ratio with the DLR flight estimates. While most of the derivatives are within 15% of the flight estimates, the yaw control sensitivity and mode damping, although considerably improved relative to the baseline values, are still high relative to the flight values.

Tuning of model parameters to improve functional fidelity is acceptable within constraints consistent with the uncertainties in the parameters. Some of the distortions used above are large and somewhat arbitrary; they will need to be compared with values obtained from dissimilar manoeuvres for verification or otherwise. As demonstrated above, obtaining improvements across a range of derivative predictions and response characteristics will generally require distortions in several parameters simultaneously. All will need checking against other conditions, *e g* damping/control sensitivity from step inputs, dihedral and weathercock stability from sideslip tests, before a high confidence is achieved. In any case, more detailed component measurements (*e g* main/tail rotor thrust/moment) and model structural changes may be required before a simulation deficiency is fully understood and rectified. It should be remembered that derivatives encapsulate

any nonlinear effects when derived from experimental data and tests at varying amplitudes will be required to establish the presence and importance of such effects. Nevertheless, as a starting point, the flight estimates have enabled considerably more validation evidence to be gathered systematically, compared with any speculation derived from the observations in section 5.1.2. There remains the question, of course, as to the validity of the flight estimated derivatives. The time history comparisons of the DLR lateral sub-system and flight data are presented in Fig 10; the fit is not as good as the fully coupled six degree-of-freedom response shown in Fig 11, (taken from Padfield (1991)). The coupling effects clearly contribute to the response, even though the damping and frequency are not affected significantly; the simplified approximation cannot shed any new light on the nature of the lateral to longitudinal coupling in the Dutch roll.

The Glasgow derivatives, shown in Table 2, show reasonable consistency with the DLR results with two notable exceptions - L_r and L_{1c}. The large positive value of L_r accounts for the greater stability of the Dutch roll mode according to the Glasgow estimates ($t_{1/2} \sim 4$ s , compared with 8 s for DLR). The lower roll control sensitivity and damping from the Glasgow analysis correlate with the lower estimate for effective time delay shown in Table 2 (Black, 1987), highlighting the fact that these are strictly equivalent parameters; the effects of higher order dynamics have been ignored as such but encompassed within the effective time delay. The *'true'* value of some of the stability and control derivatives cannot therefore be estimated. The Dutch roll approximations do show, however, that useful insight into modelling accuracy can be gained from an analysis of the derivative contributions to the component terms..

Table 4 shows a comparison of Dutch roll eigenvalues for the BO-105 (DLR Model 3 (Kaletka, 1991)) and AH-64 Apache derived from the DLR flight estimated derivatives, with the corresponding approximations derived from (9) alongside the SA-330 Puma results. The comparisons are very good, apart from the BO-105 frequency estimate, adding support to the value of the approximation across different aircraft types. As a concluding note to this section, Fig 12 illustrates the current Dutch roll handling qualities criteria from ADS-33C. The criteria are expressed in terms of handling qualities level boundaries for damping and frequency for different mission task elements (MTE). The data points correspond to flight estimates and theoretical predictions for all three aircraft; the Puma theoretical result is derived from the *Helistab* case discussed, the BO-105 point from the DLR blade-element model *Simh* and the AH-64 result from the MDHC *Flyrt* nonlinear rotor-map model. It is interesting to note that for all three aircraft, theory predicts about twice the damping measured in flight. This suggests that the fidelity of the main rotor modelling has little impact on this parameter; main rotor wake/tail-rotor interaction is a more likely common modelling deficiency. Moreover, on the criteria diagram the data points lie on either side of the Level 1/2 or Level 2/3 boundaries, depending on the aircraft role (*ie* MTE). Considering the aircraft types under consideration, the Level 2/3 boundary is probably more appropriate. A conclusion that can be drawn is that none of the simulation models (which are state-of-the-art for disc, blade element and rotor-map models respectively) are capable of predicting Dutch roll damping adequately for compliance demonstration. This is considered to be a reflection on simulation modelling in general and the detailed analysis of the Puma data has provided some insight into how, for this aircraft, *Helistab* is deficient.

5.2 Physical validation (Puma inflow)

5.2.1 *Overview and objective*

The process of physical validation requires close coupling between modelling and testing. First a suitable subset of the dynamic and aero ynamic physical phenomena must be isolated and a mathematical model of this subset must be derived from first principles. The subset must be chosen to facilitate identification of parameters for the selected subset. Just as in functional validation, too many parameters can result in identified values that are physically meaningless due to over parameterisation and, depending on the degrees of freedom included in the subset, the parameters of the model may not be observable from available test data. The interaction of the selected subset with other modelling subsets must be determined to establish the input and output data requirements of the subset. The dynamic relationship between this input and output data must then be derived based on the physics of the modelled subset. Test data requirements are then established to support validation of the specified model subset. At a minimum, these requirements

should include the interface data for the subset in order to isolate it from the rest of the system model. Recording of certain internal degrees of freedom of the model subset may also be required to ensure observability of the parameters to be identified.

The example presented below is taken from DuVal (1989b), where the objective is to validate a physically based model of coupled rotor flapping/first harmonic inflow dynamics derived for a forward flight manoeuvre using the RAE Puma test data.

5.2.2 *Approach*

The following steps were carried out to accomplish the objectives of this study.

(i) *Establish structure of baseline math model.* After reviewing the literature, a baseline model was chosen to reflect generally accepted technology. The rotor dynamics model was based on the work of Chen (1980) with modifications made to account for the French rotation of the Puma Helicopter and the inclusion of first harmonic inflow components. The inflow dynamics model was based on the work of Goanker and Peters (1984), together with a Glauert model of the quasistatic, velocity dependent first harmonic inflow. The notation used conforms to Chen to facilitate comparison.

(ii) *Perform consistency tests on flight test data.* Since the test data was to be used to validate the math model, it was essential that the data be consistent. A series of comparisons of redundant sensors and sensors that can be compared through known kinematic relationships was used to eliminate sensor biases and isolate faulty measurements.

(iii) *Establish consistency of model structure with flight test data.* Having established the consistency of the flight test data, the validity of the baseline model structure was tested by examining the equation error resulting from applying the test data to the baseline model for a nominal set of model parameter values. The baseline model structure was then extended as required to assure consistency.

(iv) *Identify parameters of model from flight test data.* An output error parameter identification method was used to identify selected parameters of the validated model structure. The technique was first tested using simulated data generated from the baseline model. It was then applied to the lateral manoeuvre at 100 knots and a set of ten parameters were identified. These parameters were then used with the model to predict the response for the longitudinal manoeuvre and the results were compared with flight test data to verify the parameters.

5.2.3 *Cyclic flapping/first harmonic inflow model*

It was decided to use an isolated model of coupled rotor/inflow dynamics rather than a fully coupled rotor/fuselage dynamics model. This approach of dealing with isolated subsets of the total system allows for a systematic validation of each subsystem independently and reduces the complexity of each model to a manageable level. In order to isolate the mathematical model of a subsystem, the variables involved in cross coupling with other subsystems are treated as measured inputs or pseudo-controls acting on the isolated subsystem.

The cyclic flapping model is a two degree of freedom model with second order dynamics modified to include first harmonic inflow components. The dynamics of the longitudinal and lateral disc flapping states (a_{1s} and b_{1s}) are driven by the longitudinal and lateral cyclic pitch controls (B_1 and A_1), first harmonic dynamic inflow (p_i and q_i) and a quasistatic first harmonic inflow based on advance ratios (μ_x and μ_y). The cyclic inflow dynamics are also driven by the roll and pitch rates (p and q) and nonlinear functions (u_a and u_b) of coning angle and coning angle rate (a_0 and $\dot{a}_0$), uniform inflow (λ_c), collective pitch (θ_0), and advance ratio (μ). The baseline model has the form:

$$\begin{bmatrix} \ddot{a}_{1s} \\ \ddot{b}_{1s} \end{bmatrix} + F_1 \begin{bmatrix} \dot{a}_{1s} \\ \dot{b}_{1s} \end{bmatrix} + F_2 \begin{bmatrix} a_{1s} \\ b_{1s} \end{bmatrix} = G_1 \begin{bmatrix} A_1 \\ B_1 \end{bmatrix} + G_2 \begin{bmatrix} p_i \\ q_i \end{bmatrix} + G_3 \begin{bmatrix} p \\ q \end{bmatrix} + \begin{bmatrix} u_a \\ u_b \end{bmatrix} \tag{14}$$

where

$$u_a = \frac{1}{2}\gamma\Omega^2 a_0 \mu_x B_{32} + \gamma\Omega^2 \theta_0 \mu_y B_{32} + \frac{1}{2}\gamma\Omega^2 \lambda_c \mu_y B_{21} + \frac{1}{2}\gamma\Omega^2 \dot{a}_0 \mu_y B_{32}$$

$$u_b = \frac{1}{2}\gamma\Omega^2 a_0 \mu_y B_{32} - \gamma\Omega^2 \theta_0 \mu_x B_{32} - \frac{1}{2}\gamma\Omega^2 \lambda_c \mu_x B_{21} - \frac{1}{2}\gamma\Omega^2 \dot{a}_0 \mu_x B_{32} \qquad (15)$$

and

$$F_1 = \begin{bmatrix} \frac{1}{2}\gamma\Omega(B_{43} - B_{32}\varepsilon_1) & 2\Omega \\ -2\Omega & \frac{1}{2}\gamma\Omega(B_{43} - B_{32}\varepsilon_1) \end{bmatrix}$$

$$F_2 = \begin{bmatrix} \varepsilon_\beta\Omega^2 - \frac{1}{4}\gamma\Omega^2\mu_x\mu_y B_{21} & \frac{1}{2}\gamma\Omega^2(B_{43} - B_{32}\varepsilon_1 + \frac{1}{4}(\mu_x^2 - \mu_y^2) B_{21}) \\ -\frac{1}{2}\gamma\Omega^2(B_{43} - B_{32}\varepsilon_1 - \frac{1}{4}(\mu_x^2 - \mu_y^2) B_{21}) & \varepsilon_\beta\Omega^2 - \frac{1}{4}\gamma\Omega^2\mu_x\mu_y B_{21} \end{bmatrix}$$

$$G_1 = \begin{bmatrix} \frac{1}{2}\gamma\Omega^2(B_{43} + \frac{1}{4}(\mu_x^2 - \mu_y^2) B_{21}) & \frac{1}{4}\gamma\Omega^2\mu_x\mu_y B_{21} \\ \frac{1}{4}\gamma\Omega^2\mu_x\mu_y B_{21} & \frac{1}{2}\gamma\Omega^2(B_{43} - \frac{1}{4}(\mu_x^2 - \mu_y^2) B_{21}) \end{bmatrix} \qquad (16)$$

$$G_2 = \begin{bmatrix} 0 & \frac{1}{2}\gamma\Omega B_{43} \\ \frac{1}{2}\gamma\Omega B_{43} & 0 \end{bmatrix}$$

$$G_2 = \begin{bmatrix} 2\Omega(1+\varepsilon_\beta) & -\frac{1}{2}\gamma\Omega B_{43} \\ \frac{1}{2}\gamma\Omega B_{43} & 2\Omega(1+\varepsilon_\beta) \end{bmatrix}.$$

The uncertain parameters are the Lock Number (γ), and the Tip Loss Factor, (B), where

$$B_{43} \approx \frac{B^4}{4} - \frac{B^3}{3}e, \qquad B_{32} \approx \frac{B^3}{3} - \frac{B^2}{2}e, \qquad B_{21} \approx \frac{B^2}{2} - Be$$

and e is defined as the nondimensional hinge offset.

The inflow is represented as a two-degree-of-freedom model with first order dynamics and is given by:

$$\begin{bmatrix} \dot{p}_i \\ \dot{q}_i \end{bmatrix} + F_3 \begin{bmatrix} p_i \\ q_i \end{bmatrix} = G_4 \left(\begin{bmatrix} p \\ q \end{bmatrix} - \begin{bmatrix} 0 & \Omega \\ \Omega & 0 \end{bmatrix} \begin{bmatrix} A_1 - b_{1s} \\ B_1 + a_{1s} \end{bmatrix} + \begin{bmatrix} \dot{a}_{1s} \\ \dot{b}_{1s} \end{bmatrix} \right), \qquad (17)$$

where

$$F_3 = \begin{bmatrix} \frac{1}{\tau} & 0 \\ 0 & \frac{1}{\tau} \end{bmatrix}, \qquad G_4 = \begin{bmatrix} k & 0 \\ 0 & k \end{bmatrix}. \tag{18}$$

The uncertain parameters are the inflow time constant τ, and the gain on the forcing function (k).

The equations are linearised about the trimmed condition to simplify further the relationship. This results in the elimination of the nonlinear forcing functions (u_a and u_b) since there is little variation in these variables. Equations (14) through (18) otherwise remain the same except that the states are now interpreted as perturbations from the trim condition.

5.2.4 *Validation and modification of model*

Validation of the test data is described in DuVal *et al* (1989b) and will not be covered here; the validity of the baseline model structure is next evaluated. It is essential to validate the model structure prior to identifying parameters. As discussed above and throughout this paper, if the model structure is incorrect, parameters may still be identified that track the data accurately, but they can be physically meaningless. The inflow equation is first integrated, using nominal parameter values and the measured time histories of forcing functions. The resulting inflow time history is then used in the flapping equation with nominal parameters and measured values of the other states and controls and the correlation between the homogeneous equation and each forcing function is evaluated. The homogeneous equation was found to be most correlated with controls and body rates as expected, so the coefficients of the controls and body rates that minimize the error between the homogeneous equation and the corresponding forcing functions were identified by regression. The resulting forcing functions are compared with the homogeneous equations in Fig 13. The poor comparison indicates that the model structure is incomplete. The remaining error appeared to be correlated with both the velocity time histories and a bias in the flapping azimuth reference. A mathematical representation of the error in cyclic flapping and feathering due to biases in the blade azimuth references is given in Fig 14. In order to be completely general, separate biases were assumed for the blade azimuths associated with both flapping and feathering measurements. The velocity dependence is most likely related to the quasistatic (Glauert) component of first harmonic inflow so a matrix of coefficients relating these velocities to the homogeneous equation was also added to the model structure. Regression was then used to determine preliminary values for the velocity coefficients and the azimuth biases. The resulting forcing functions are compared with the homogeneous equations in Fig 15. This fit has improved significantly over that of Fig 13 and this indicates that the model structure is reasonably close since the resulting parameters identified by the regression are close to the nominal values and are therefore physically meaningful.

Having determined the modifications to the model structure required to assure consistency with the test data for physically reasonable values of the model parameters, the final step in the system identification process is to identify values for selected parameters. Ten parameters were selected based on the results of the model structure determination process and an understanding of which parameters had well defined values and which were uncertain. The parameters to be identified were the Lock number γ, the tip loss factor (B), the inflow time constant τ, the inflow gain (k) (related to the deficiency function), biases on the zero azimuth reference for both the flapping and feathering measurements (ψ_1 and ψ_2), and a matrix of four coefficients relating longitudinal and lateral velocity perturbations to the two first harmonic inflow components (k_1, k_2, k_3, k_4). The estimates of the system states $(\hat{a}_{1s}, \hat{b}_{1s}, \hat{p}_i, \hat{q}_i)$ for specified values of the parameter set (θ_0) are then given by the following equations:

$$\begin{bmatrix}\ddot{\hat{a}}_{1s}\\ \ddot{\hat{b}}_{1s}\end{bmatrix}+F_1(\theta_p)\begin{bmatrix}\dot{\hat{a}}_{1s}\\ \dot{\hat{b}}_{1s}\end{bmatrix}+F_2(\theta_p)\begin{bmatrix}\hat{a}_{1s}\\ \hat{b}_{1s}\end{bmatrix}=G_1(\theta_p)\,T^T(\psi_2)\begin{bmatrix}A_{1m}\\ B_{1m}\end{bmatrix}+G_3(\theta_p)\begin{bmatrix}p\\ q\end{bmatrix}$$

$$+G_2(\theta_p)\left(\begin{bmatrix}p_1\\ q_1\end{bmatrix}+\begin{bmatrix}k_1 & k_2\\ k_3 & k_4\end{bmatrix}\begin{bmatrix}\mu_x\\ \mu_y\end{bmatrix}\right) \qquad (19)$$

$$\begin{bmatrix}\dot{\hat{p}}_1\\ \dot{\hat{q}}_1\end{bmatrix}+F_3(\theta_p)\begin{bmatrix}\hat{p}_1\\ \hat{q}_1\end{bmatrix}=G_4(\theta_p)\left\{\begin{bmatrix}p\\ q\end{bmatrix}-\begin{bmatrix}0 & \Omega\\ \Omega & 0\end{bmatrix}\left(T^T(\psi_2)\begin{bmatrix}A_{1m}\\ B_{1m}\end{bmatrix}-\begin{bmatrix}\hat{b}_{1s}\\ \hat{a}_{1s}\end{bmatrix}\right)+\begin{bmatrix}\hat{a}_{1s}\\ \hat{b}_{1s}\end{bmatrix}\right\},$$

where

$$\theta_p=[\gamma, B, \tau, k]^T .$$

As shown in Fig 14, the cyclic flapping measurements (a_{1S}, b_{1S}) are related to the actual flapping states through the coordinate transformation,

$$\begin{bmatrix}a_{1_{2m}}\\ b_{1_{sm}}\end{bmatrix}=\begin{bmatrix}\cos\psi_1 & \sin\psi_1\\ -\sin\psi_1 & \cos\psi_1\end{bmatrix}\begin{bmatrix}a_{1s}\\ b_{1s}\end{bmatrix}=T(\psi_1)\begin{bmatrix}a_{1s}\\ b_{1s}\end{bmatrix} \qquad (20)$$

where ψ_1 represents the bias on the zero azimuth reference point associated with the flapping measurement.

5.2.5 *Results of Modification*

As discussed in 4.2, there are three basic methods for parameter identification; the Equation Error method, the Output Error method and the Maximum Likelihood method.

The simplest is the Equation Error method. This approach finds the parameters, θ_0, of the system that minimize some error function, g, based on the model, given the measurements, z, and inputs, u_C:

$$g(z,\theta_0,u_C) = 0 . \qquad (21)$$

It is simple to implement if the equations are linear in the parameters, and can also be used for the model structure determination. The Equation Error method requires measurements of all states and controls, and gives biased parameter estimates in the presence of significant measurement noise.

The Output Error method generates system states, x, by integration of the system dynamic equations for a given set of parameter values, θ_0, and a given input history, u_C:

$$\dot{x} = f(x, u_C, \theta_0) . \qquad (22)$$

In this approach, the parameters are iteratively adjusted by a second order gradient technique to minimize an error function, g, in the outputs, z, the system states, x, the controls, u_C, and the parameters, θ_0:

$$g(x, u_C, z, \theta_0) = 0 . \qquad (23)$$

This method would give biased estimates if the model structure has significant error. It does not require that all states be measured, however, since it produces state histories from the dynamic model.

The third method for parameter identification is Maximum Likelihood. In this case the state and output equations are combined in an Extended Kalman Filter. The states estimates are then obtained from the equation

$$\dot{\hat{x}} = f(\hat{x}, u_c, \hat{\theta}_p) + K[g(\hat{x}, u_c, z, \hat{\theta}_p)] \quad . \tag{24}$$

and the parameters are again iteratively adjusted by a second order gradient method to minimize the error function, $g(\hat{x}, u_c, z, \hat{\theta}_0)$. Maximum Likelihood also does not require all states to be measured. It is the most general identification method since it gives unbiased estimates in the presence of both process and measurement noise. However, the Kalman gains reduce the sensitivity of measurement errors to parameter changes and result in slower convergence.

While the Equation Error method is the simplest, it could not be used in this application because there were two unmeasured states (the first harmonic inflow components). Of the remaining candidates, the Output Error method is the simplest, but its application requires that there is no significant process noise. The model structure validation work had demonstrated that the data could be reasonably well matched with the selected model, indicating a low level of process noise, so the Output Error method was selected.

The Output Error method was applied to identify the parameters of the model given by equation (19) using flight test data from the longitudinal doublet manoeuvre at 100 knots. The initial values of the parameters and the converged values obtained from the identification are shown in Table 5 along with the uncertainty in the estimate, as determined by the Output Error method. The Tip Loss Factor (B) and the Lock Number (γ) are relatively close to the initially assumed values and have an uncertainty of less than one percent. The identified inflow time constant is, however, nearly twice the initially assumed value of 0.5 seconds and the gain on the inflow forcing function is more than five times lower than the initially assumed value.

The azimuth biases for the feathering and flapping measurements are seen to be nearly equal at around 20°. It was later determined that a 10° bias would be present due to collective lead-lag and an additional 10° could result from time skew in the data collection, so the identified values appear reasonable.

The coefficients relating longitudinal and lateral velocity perturbations to first harmonic inflow components are difficult to interpret physically so the validity of their identified values is difficult to assess. These terms, however, have the most significant effect on being able to match the measured flapping data with the model. Physically, the first harmonic inflow dependence on velocity should be related to the classical Glauert first harmonic inflow distribution and to fuselage interference effects on the flow field.

A comparison of the estimated cyclic flapping response and the measured response, corrected for the identified azimuth bias, is shown in Fig 16. The comparisons are seen to be reasonably good. The corresponding first harmonic inflow components are shown in Fig 17. They have been separated into dynamic inflow components, as generated by the dynamic inflow model, and the velocity dependent or Glauert components, as generated by the application of the identified velocity coefficients to the measured velocity perturbation. The results are normalized by the tip speed. The Glauert component due to velocity perturbations in the manoeuvre appears to be as significant as the dynamic inflow component generated from momentum theory.

As a final check on the validity of the identified model structure and parameter values, they are applied to measured input data from the lateral doublet manoeuvre and the resulting flapping estimates are compared with the measured data. The results, as shown in Fig.18, indicate the same level of accuracy as obtained in the longitudinal manoeuvre. The flapping has been scaled the same in both the longitudinal and lateral manoeuvre plots to allow direct comparison of error levels. The longitudinal manoeuvre was selected for use in the identification since there was significantly more excitation in both axes.

5 Conclusions

This paper has provided a treatment of rotorcraft simulation model validation from functional and physical standpoints. Acceptance criteria for validation have been discussed and presented and the role of system identification in achieving these covered. Examples from the RAE Puma test database have been presented that illustrate six-degree-of-freedom functional fidelity and a more detailed physical validation of blade flapping dynamics.

A number of conclusions can be drawn from the discussions presented:

(1) Validation as an activity can be considered in two stages; firstly, establishing the range and accuracy of the simulation model and, secondly, establishing the modelling deficiencies and required upgrades. This paper has proposed a framework for the application of system identification in these two stages.

(2) Accuracy and range can be defined in terms of three flight mechanics problem areas - trim, stability and response. Range can conveniently be defined in terms of the frequency and amplitude of the intended operation. Accuracy requirements depend critically on the intended application.

(3) System identification can play a role in all three problem areas.

(4) Functional fidelity provides a measure of the overall accuracy of the aircraft's response to controls and disturbances; physical validation is concerned more with the accuracy of the underlying modelling assumptions.

(5) The use of system identification in model upgrading has to be complemented with a good understanding of the underlying physical assumptions and mathematical approximations.

(6) The example chosen to highlight the value of system identification in functional validation has been the Dutch roll motion of the SA 330 Puma. A simple approximation for Dutch roll damping and frequency has highlighted the possible origins of modelling deficiencies. Current simulation models are poor at predicting cross coupling effects. Of perhaps greater significance is the over-estimation of Dutch roll damping by current simulation models leading to a more favourable compliance with ADS-33C, *ie* Level 2 rather than Level 3 handling qualities.

(7) Physical validation has been illustrated with an example of coupled blade flapping/inflow dynamics. A suitable model structure incorporating first harmonic and velocity dependent, quasistatic inflow was established using equation error techniques; model parameters were then estimated using an output error method.

Acknowledgments

The authors would like to thank members of AGARD WG-18 for assistance in the preparation of this paper, particularly Professor Daniel Schrage and his colleagues at Georgia Tech. Grateful thanks also to Andy McCallum and Jane Smith at RAE for help with producing the flight/*Helistab* comparisons. The BO-105 *Simh* value of Dutch roll damping was produced by Wolfgang Von Grunhagen of the DLR Braunschweig and the *Flyrt* value for the AH-64 by Jeff Harding of MDHC.

References

AGARD:
AGARD Advisory Report No.280 (1991)

AVSCOM:
Aeronautical Design Standard - ADS33C ; Handling qualities requirements for military rotorcraft., US AVSCOM, St Louis (1989)

Ballin, M.B.; Dalang-Seretan, Marie-Alix:
Validation of the dynamic response of a blade-element UH-60 simulation model in hovering flight.
Proceedings of the 46th AHS Forum, Washington DC, May 1990

Black, C.G.:
Consideration of trends in stability and control derivatives from helicopter system identification.
Proceedings of the 13th European Rotorcraft Forum (Paper 7.8), Arles, France (1987)

Chen, Robert T.N:
Effects of Primary Rotor Parameters on Flapping Dynamics,
NASA TP 1431, January 1980

DuVal, R.W., *et al,*:
Flight simulation model validation procedure; a systematic approach.
Vertica Vol.13 No.3, pp 311-326 (1989a)

DuVal, R.W.:
Identification of a coupled flapping/inflow model for the Puma helicopter from flight test data.
Vertica, Vol.13, No.3, (1989b)

Gaonkar, Gopal H. and Peters, David A.:
A Review of Dynamic Inflow and Its Effect on Experimental Correlations.
Proceedings of the Second Decennial Specialists' Meeting on Rotorcraft Dynamics, NASA Ames Research Center, November 1984.

Houston, S.S.:
Identification of a coupled body/coning/inflow model of Puma vertical response in the hover.
Vertica Vol.13 No.3 (1988)

Kaletka,.J.:
Case Study No.11: BO105
Chapter 6.2, AGARD Advisory Report No.280 (1991)

Klein, V.; Batterson, J.G.:
Determination of aeroplane model structure from flight data using splines and stepwise regression.
NASA TP 2126 (1983)

Milne, R.D.:
The analysis of weakly coupled dynamical systems.
International Journal of Control, Vol.2 No.2 (1965)

Padfield, G.D.:
A theoretical model of helicopter flight mechanics for application to piloted simulation.
RAE Technical Report 81048 (1981)

Padfield, G.D.; DuVal, R.W.:
Applications of system identification methods of the prediction of helicopter stability control and handling characteristics;
'Helicopter Handling Qualities'. NASA CP 2219 (1982)

Padfield, G.D.:
Theoretical modelling for helicopter flight dynamics: development ana validation.
Proceedings of ICAS 88, Jerusalem (1988a)
RAE Technical Memorandum FM 25 (1989)

Padfield, G.D.:
Helicopter handling qualities and control: is the helicopter community prepared for change?
Conference overview paper, R.Ae.Soc. International Conference 'Helicopter Handling Qualities and Control', London (1988b)

Vertica Special Edition, Vol.13, No.3 (1989)

Padfield, G.D.:
Case Study 111: SA 330 Puma
Chapter 6.3, AGARD Advisory Report No.280 (1991)

Tischler, M.B.:
Non-real time math model update and engineering validation.
US Army AFDD note (unpublished) (1990)

Tischler, M.B.,
System identification methods for handling-qualities studies,
Chapter 8.2, AGARD Advisory Report No.280 (1991)

Thomson, D.G.; Bradley, R.:
Validation of helicopter mathematical models by comparison of data from Nap-of-the-Earth flight tests and inverse simulation.
Proceedings of the 13th ERF, Milan (1988)

Stability Derivatives						
	u	w	q	v	p	r
X	-0.02413	0.0022	0.7411	0.0073	0.3303	0.00
Z	-0.0482	-0.7302	41.077	0.0255	0.5669	0.00
M	0.0074	-0.0199	-0.7661	-0.0049	-0.2211	0.00
Y	-0.0044	-0.0203	0.3207	-0.1248	-0.751	-40.897
L	-0.0058	-0.0525	0.7583	-0.0549	-1.6771	0.142
N	0.0098	0.0326	-0.1643	0.0216	-0.1741	-0.5697

Control Derivatives				
	θ_0	θ_{1s}	θ_{1c}	θ_{tr}
X	-2.0546	-9.546	0.4862	0.00
Z	-96.795	-27.7184	0.00	0.00
M	1.5626	6.4123	-0.3238	0.00
Y	-2.4806	-0.2069	9.6746	4.1414
L	-6.4913	-0.6815	22.8395	2.059
N	-5.9196	1.4955	2.5202	-8.22

mode	eigenvalue	perturbation amp for derivative computation.
roll subsidence	-1.6833	u, v, w - 1.5 m/s
pitch short period	-0.8710 ± 0.9332i	p, q, r - 0.05 rad
Dutch roll	-0.1630 ± 1.0171i	ϕ, θ - 0.05 rad
phugoid	-0.0104 ± 0.2214i	controls - 0.005 rad
spiral	-0.1199	

SA 330 Puma Flight and Configuration Data
V = 80kn, ρ = 1.0978 kg/m^3, mass = 5805kg, I_{xx} = 9638kgm^2
I_{yy} = 33240kgm^2, I_{zz} = 25889kgm^2, I_{xz} = 2222kgm^2, x_{cg} = 37.5mm

Table 1

***Helistab* Data**

Derivative	Flt est - DLR	Flt est - Glasgow	*Helistab*
Y_v	-0.135(0.0019)	-0.135(0.0263)	-0.125
L_v	-0.066(0.0012)	-0.064(0.00149)	-0.055
N_v	0.027(0.0002)	0.029(0.00069)	0.0216
L_p	-2.527(0.0534)	-2.012(0.0695)	-1.677
N_p	-0.395(0.0092)	-0.3216(0.0106)	-0.174
L_r	-0.259(0.0343)	0.554(0.0787)	0.142
N_r	-0.362(0.0065)	-0.3887(0.0348)	-0.57
L_{lat}	-0.051(0.0012)	-0.0317(0.0017)	-0.043
N_{lat}	-0.008(0.0002)	-0.00738(0.00047)	-0.0047
L_{ped}	0.011(0.0007)	0.0209(0.004)	0.0109
N_{ped}	-0.022(0.0001)	-0.0254(0.00086)	-0.0436
τ_{lat}	0.125	0.01(0.015)	0.0
τ_{ped}	0.0	0.0	0.0
$\lambda(1)$	-0.104 ± 1.37i	-0.200 ± 1.35i	-0.163 ± 1.017i
$\lambda(2)$	-0.089 ± 1.27i	-0.154 ± 1.329i	-0.166 ± 1.08i
$2\zeta\omega_n$	0.1674	0.291	0.390
ω_n^2	1.842	1.791	1.417
$\lambda(3)$	-0.081 ± 1.34i	-0.157 ± 1.39i	-0.199 ± 1.199i

$\lambda(1)$ - Dutch roll (fully coupled)
$\lambda(2)$ - Dutch roll (lateral subset)
$\lambda(3)$ - Dutch roll (2nd order roll/yaw/sideslip) approx.

Table 2

Comparison of SA 330 Puma lateral/directional characteristics

Derivative	Flt Est	Helistab	Ixx*0.8	v = 5 m/s	Ixz*1.5	atr*0.6	FN1*0.5	combine
L_v	-0.066	-0.055	-0.069	-0.055	-0.053	-0.05	-0.0506	-0.0543
N_v	0.027	0.0216	0.02	0.028	0.0195	0.001	0.0404	0.0232
L_p	-2.527	-1.68	-2.108	-1.68	-1.724	-1.669	-1.677	-2.18
N_p	-0.395	-0.174	-0.211	-0.174	-0.252	-0.207	-0.174	-0.344
L_r	-0.259	0.142	0.178	0.142	0.0.075	0.0953	0.142	0.064
N_r	-0.362	-0.57	-0.567	-0.57	-0.572	-0.383	-0.57	-0.383
L_{lat}	-0.051	-0.043	-0.0522	-0.043	-0.043	-0.042	0.0416	-0.054
N_{lat}	-0.008	-0.0047	-0.0055	-0.0047	-0.0065	-0.0046	-0.0046	-0.008
L_{ped}	0.011	0.011	0.014	0.011	0.0058	0.0074	0.011	0.005
N_{ped}	-0.022	-0.0436	-0.0432	-0.0436	-0.0437	-0.0292	-0.0435	-0.0292
Re(λ)	-0.104	-0.163	-0.157	-0.205	-0.151	0.053	-0.252	-0.128
Im(λ)	1.37	1.017	1.046	1.14	1.03	0.675	1.344	1.160

Table 3

**Lateral/Directional derivatives/Dutch roll eigenvalues;
Comparison with distorted parameters**

Case\Aircraft	SA - 330	BO - 105	AH - 64
Flight - 6 dof	-0.104 ± 1.37i	-0.35 ± 2.5i	-0.170 ± 1.726i
Flight - 3 dof	-0.081 ± 1.34i	-0.33 ± 3.21i	-0.171 ± 1.843i
Theory - 3 dof	-0.163 ± 1.017i	-0.65 ± 2.61i	-0.407 ± 1.857i

Table 4

Dutch roll mode eigenvalues; comparison of flight estimates (DLR) with theory (SA - 330, RAE *Helistab*; BO - 105, DLR *Simh*; AH - 64, MDHC *Flyrt*)

Parameter	Initial	Final	% std. error
B	0.9	0.98	0.2
γ	9.5	9.1	0.9
$-1/\tau$	-2.0	-1.1	7.0
k	2.0	0.34	6.5
Ψ_1	0.0	18.8 deg	3.3
Ψ_2	0.0	21.2 deg	3.1
k_1	0.0	0.042	17.0
k_2	0.0	0.37	2.1
k_3	0.0	-0.23	4.3
k_4	0.0	0.28	2.7

Table 5

Identified Parameters for Puma Inflow Example

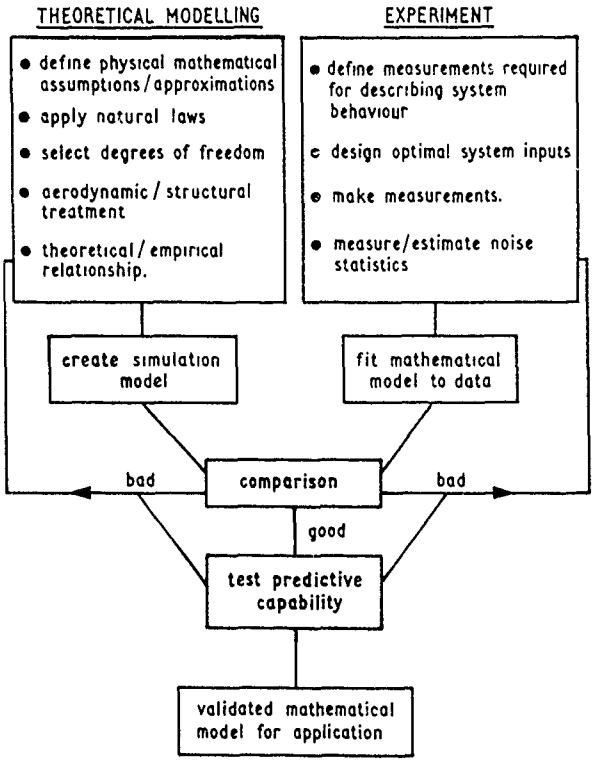

Fig.1 The Role of System Identification

Fig.2 The RAE Research SA330 Puma

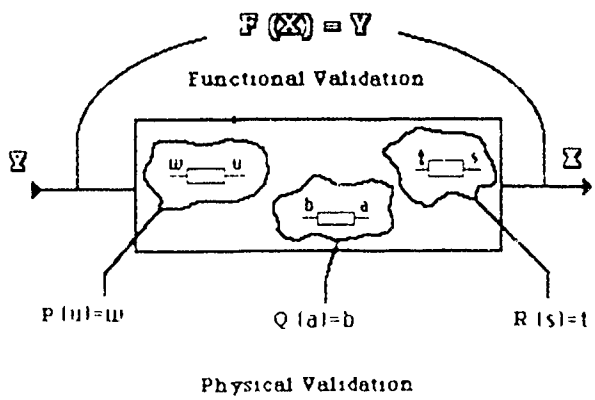

Fig.3 Functional and Physical Validation

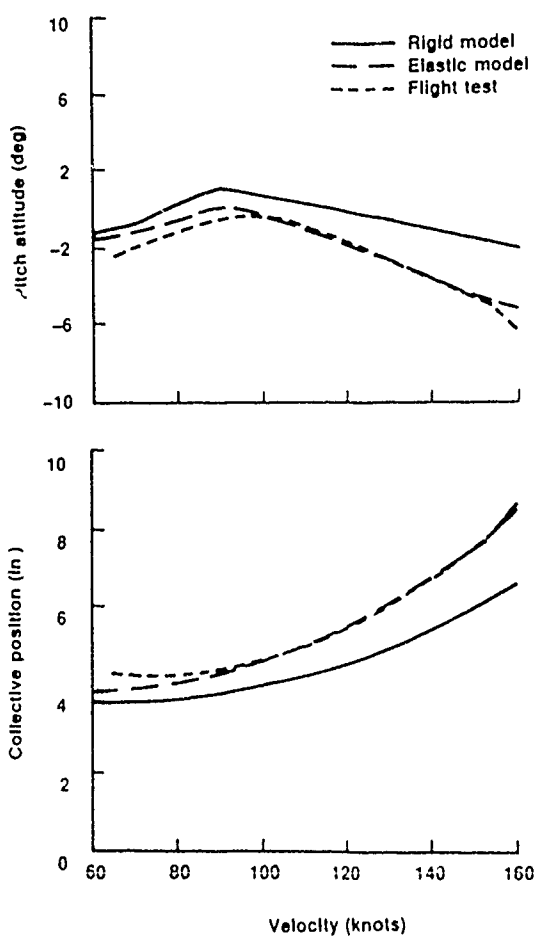

Fig.4 Trim Comparison of Rigid and Elastic Blade Element Simulations with Flight Test Data

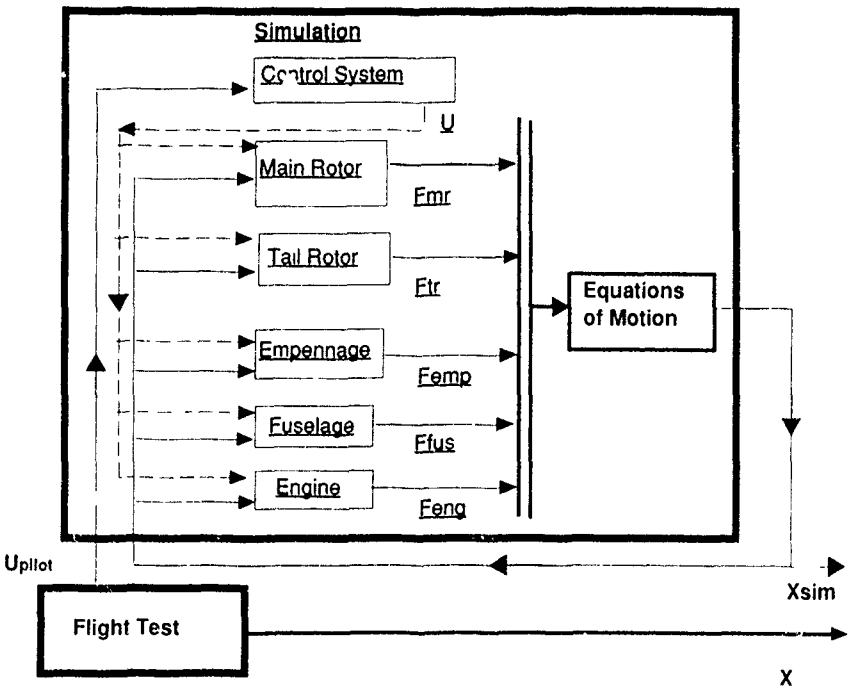

Fig.5 Closed Loop Simulation Methodology Validation

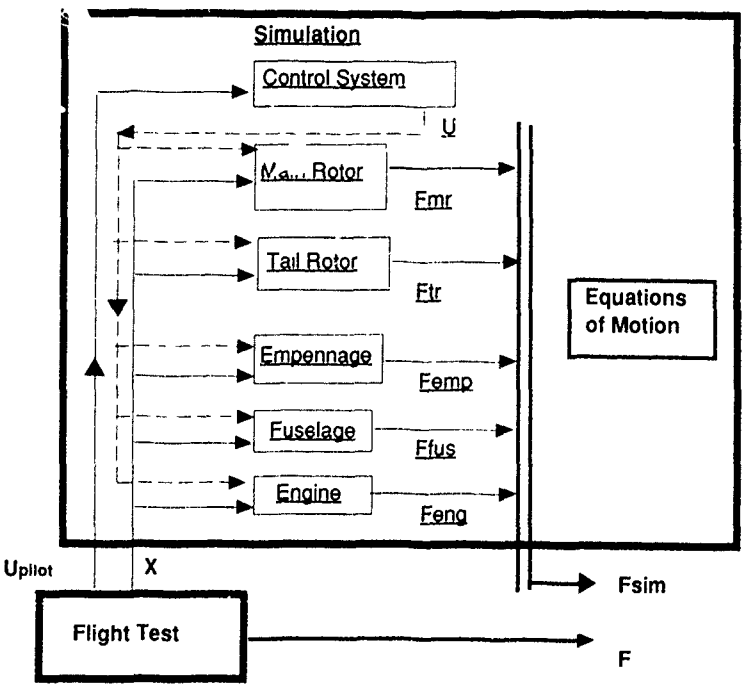

Fig.6 Open Loop Simulation Methodology Validation

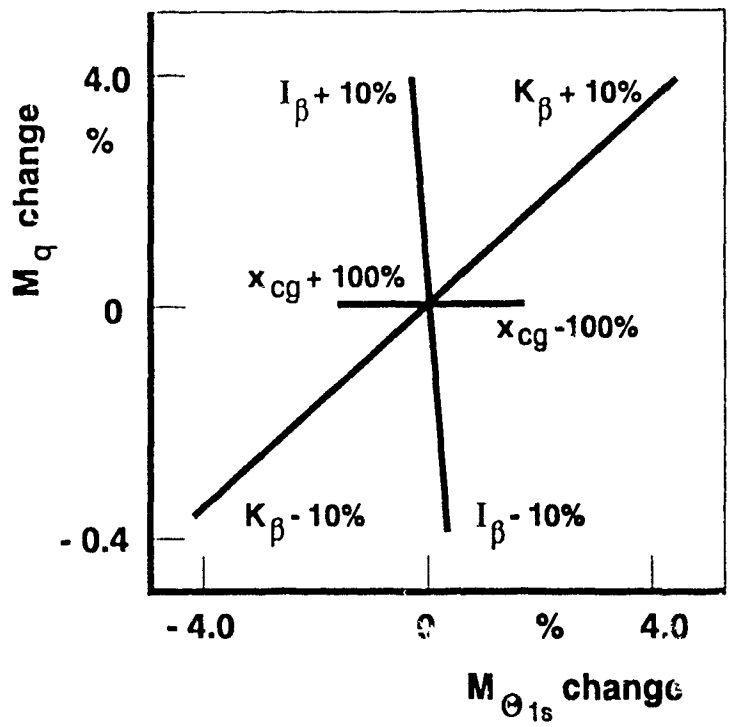

Fig.7 Hellstab Derivative Changes

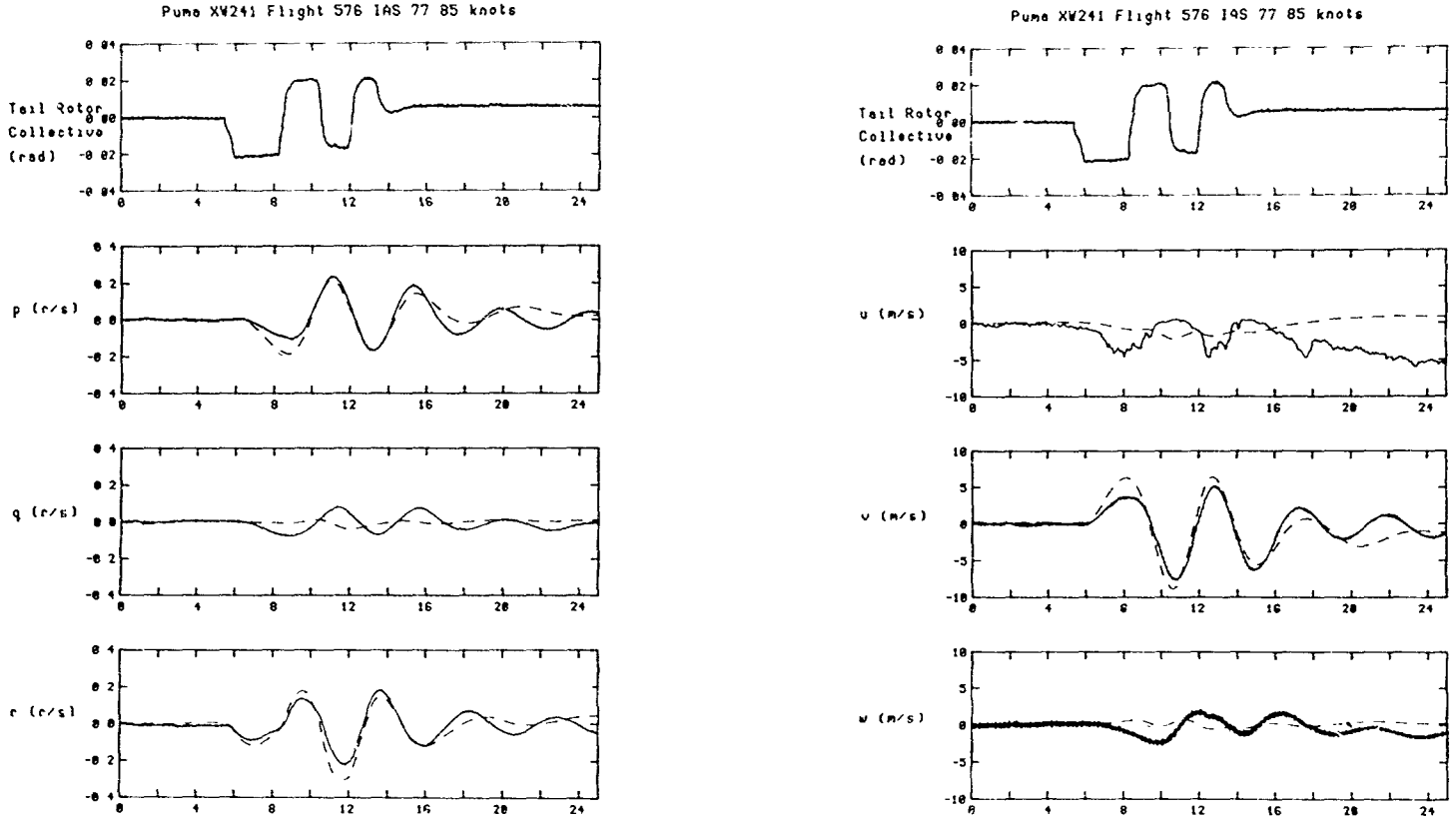

(a) Pedal Input

Fig.8 Comparison of Flight and Helistab Responses

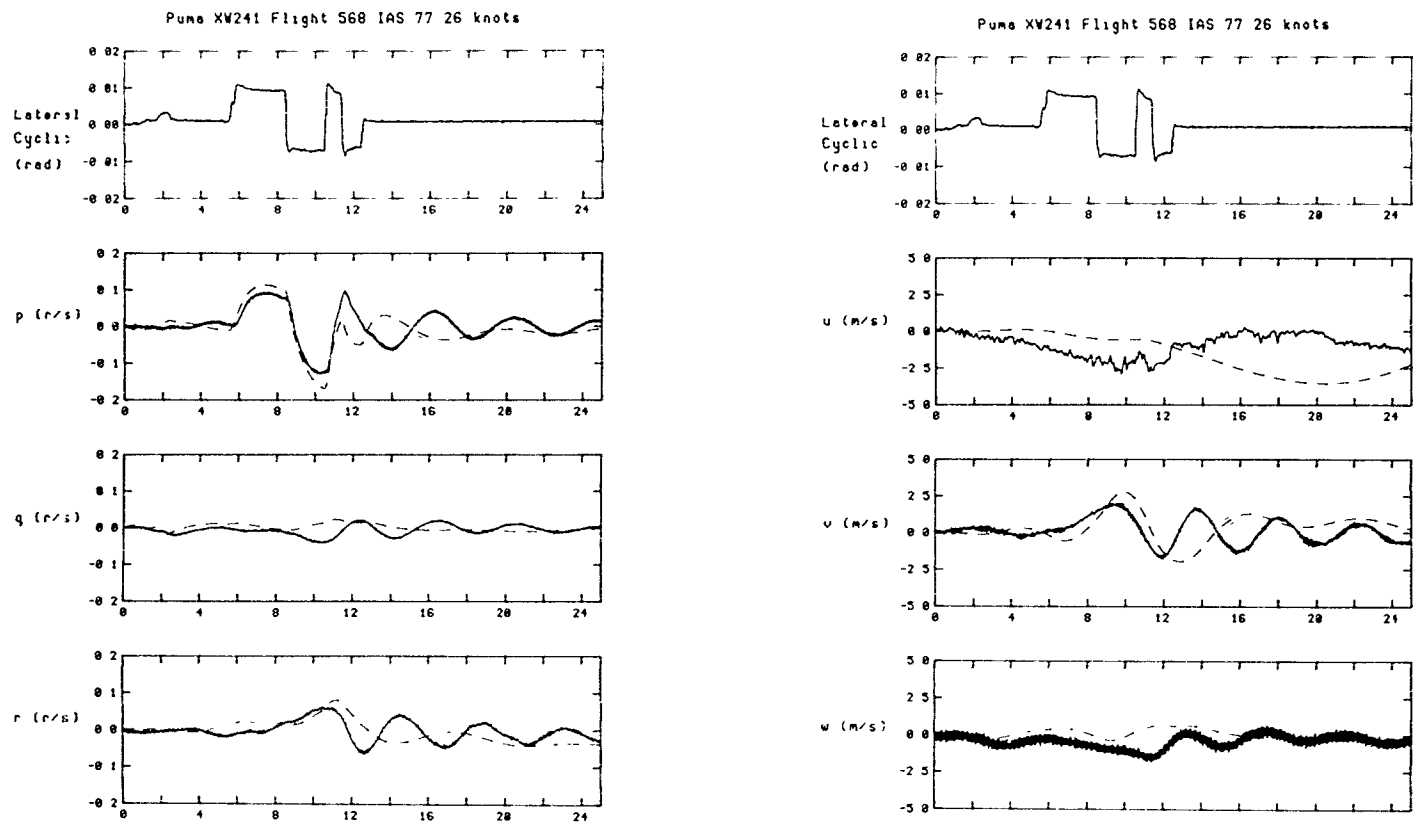

b) Lateral Cyclic Input

Fig.8 Comparison of Flight and Helistab Responses (conc)

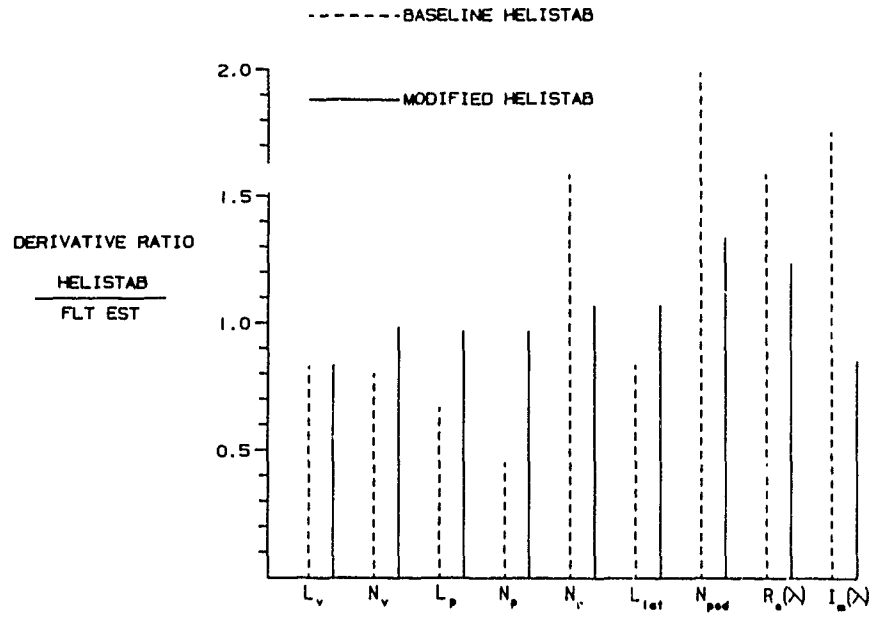

Fig.9 Comparison of normalised (with DLR flight estimate) Helistab Derivatives before and after Model Distortions

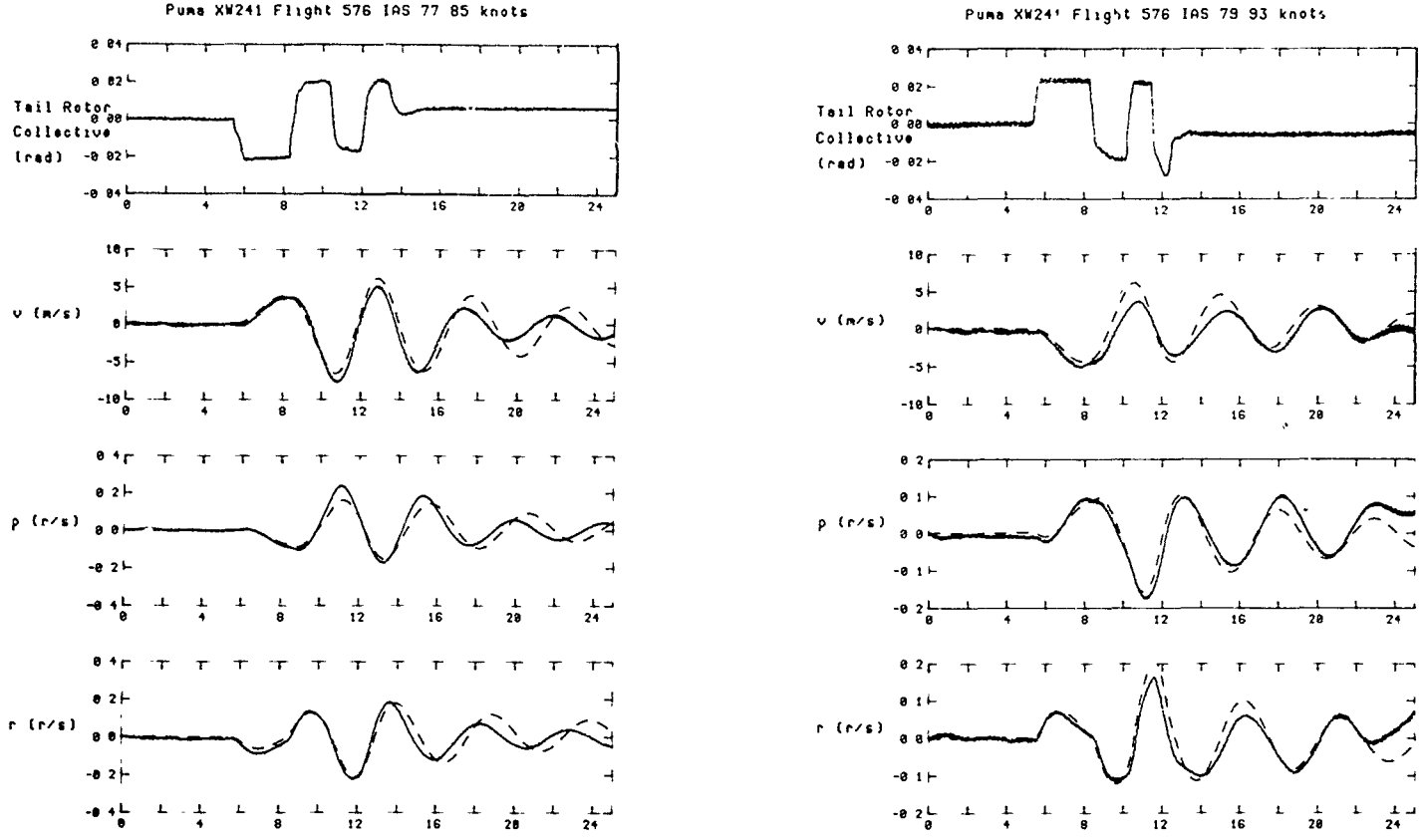

Fig.10 Comparison of Flight and Reconstructed (DLR estimates) Responses to Pedal Inputs (3dof)

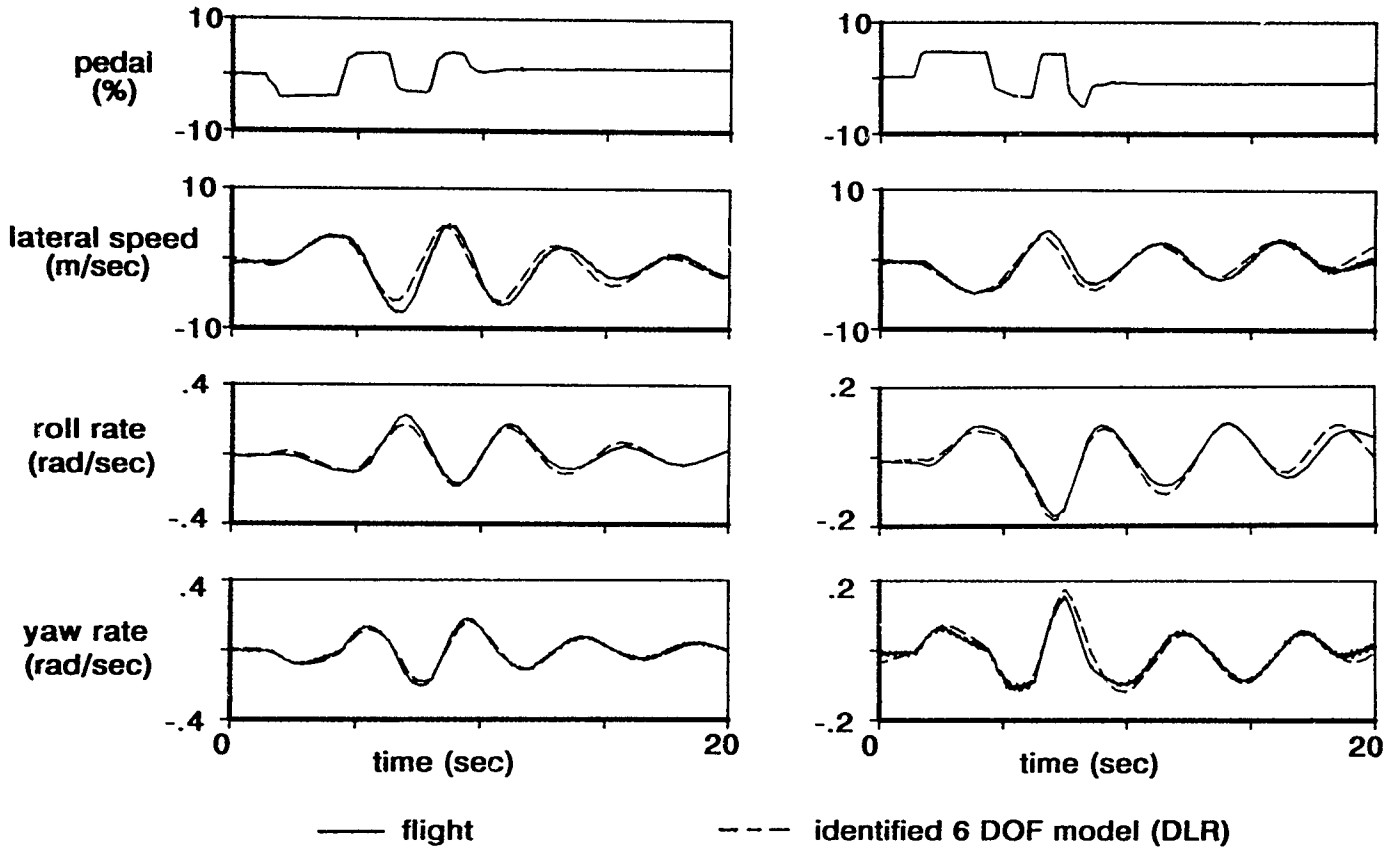

Fig.11 Comparison of Flight and Reconstructed (DLR estimates) Responses to Pedal Inputs (6dof)

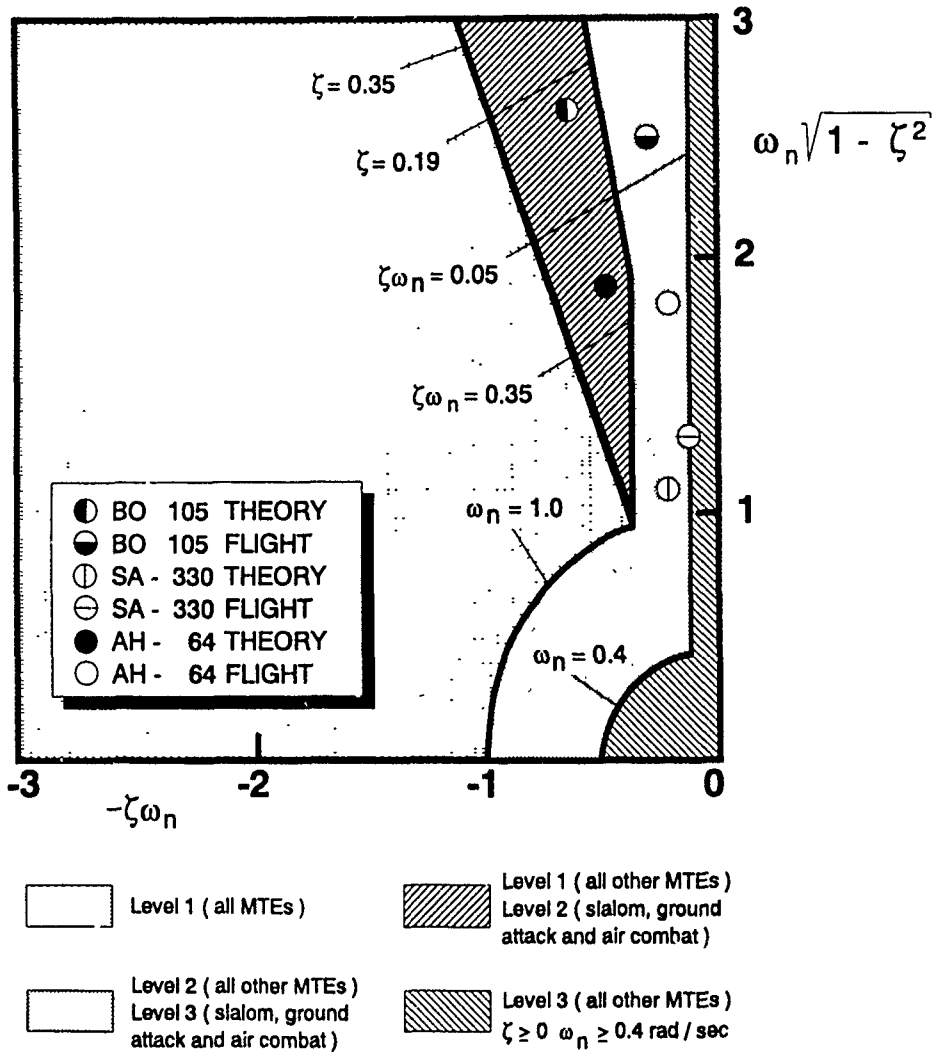

Fig.12 Comparison of Flight Estimates and Theoretical Predictions for Dutch Roll Stability with ADS33C Criteria

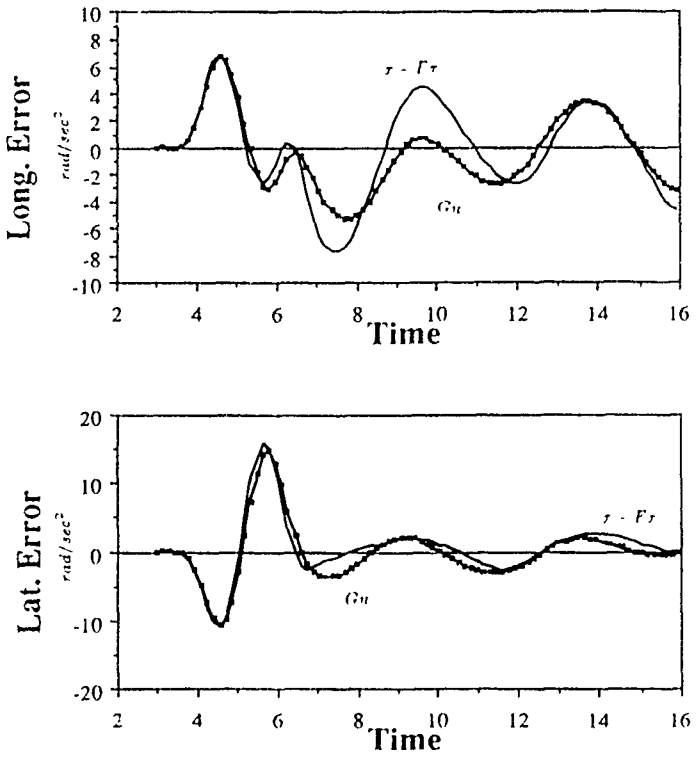

Fig.13 Regression Against Controls and Body Rates

$$\begin{bmatrix} a_{1sm} \\ b_{1sm} \end{bmatrix} = \begin{bmatrix} \cos\ \psi_1 & \sin\ \psi_1 \\ -\sin\ \psi_1 & \cos\ \psi_1 \end{bmatrix} \begin{bmatrix} a_{1s} \\ b_{1s} \end{bmatrix}$$

$$= T(\psi_1) \begin{bmatrix} a_{1s} \\ b_{1s} \end{bmatrix}$$

$$\begin{bmatrix} A_{1m} \\ B_{1m} \end{bmatrix} = \begin{bmatrix} \cos\ \psi_2 & \sin\ \psi_2 \\ -\sin\ \psi_2 & \cos\ \psi_2 \end{bmatrix} \begin{bmatrix} A_1 \\ B_1 \end{bmatrix}$$

$$= T(\psi_2) \begin{bmatrix} A_1 \\ B_1 \end{bmatrix}$$

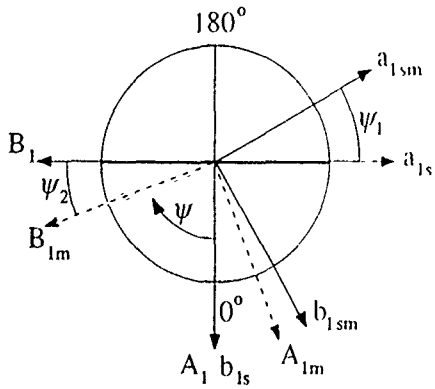

$$\beta = a_0 - a_1 \cos\psi - b_1 \sin\psi$$

$$\theta = A_0 - A_1 \cos\psi - B_1 \sin\psi$$

Fig 14 Measurement Errors

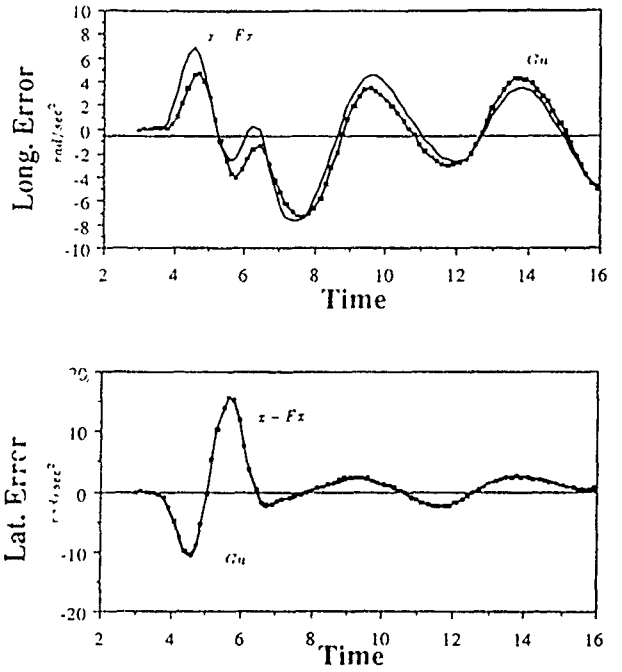

Fig.15 Regression Against Controls, Body Rates, Velocity and Phase Angle

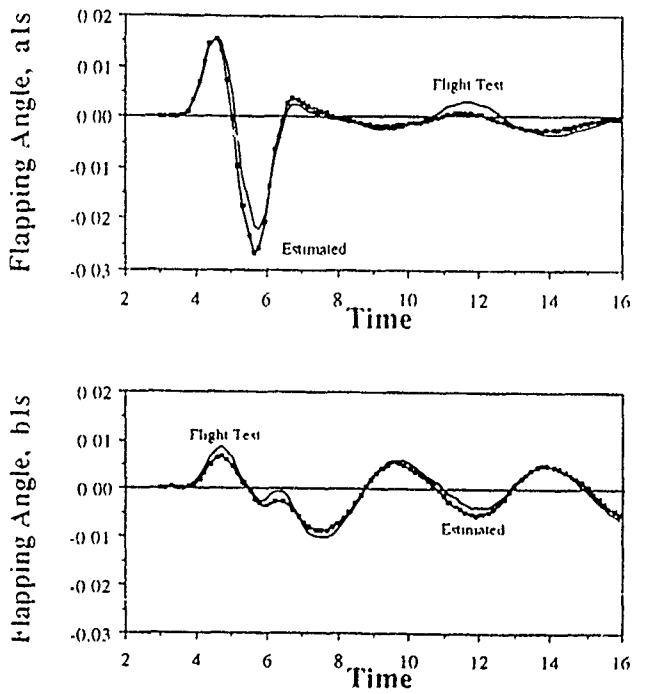

Fig.16 Results of Output Error Identification for Longitudinal Test Manoeuvre

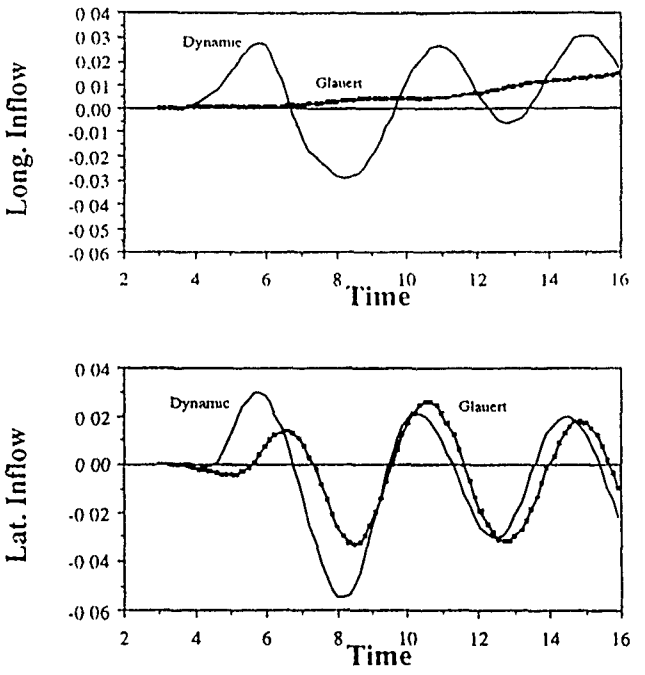

Fig.17 Inflow Effects on Flapping

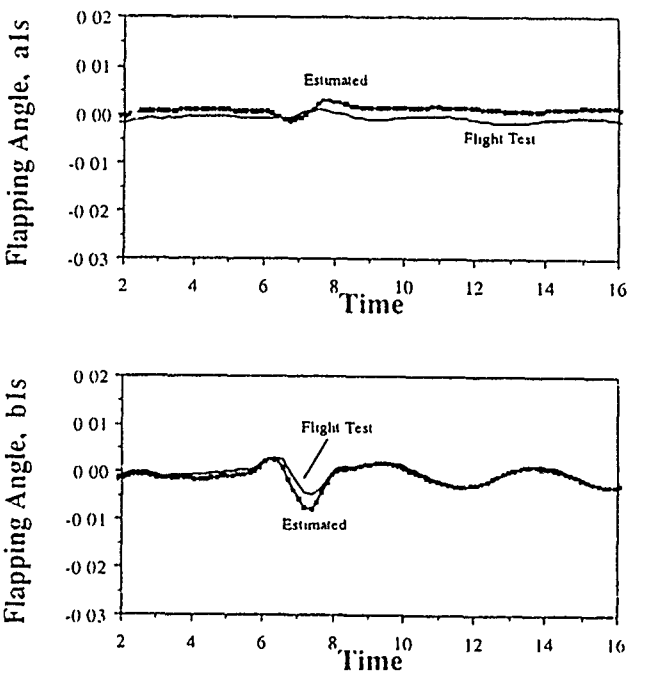

Fig.18 Results of Output Error Identification for Lateral Test Manoeuvre

SYSTEM IDENTIFICATION METHODS FOR HANDLING-QUALITIES EVALUATION

by
Mark B. Tischler
Aeroflightdynamics Directorate
U.S. Army Aviation Research & Technology Activity
Ames Research Center, Moffett Field, CA 94035-1099

SUMMARY

System identification methods for rotorcraft handling-qualities studies are discussed in this paper. A key factor that has been responsible for the broad and successful application of system identification techniques in the handling-qualities community is probably the relatively simplicity of the models which are desired for pilot-in-the-loop analyses as compared to the full 6-DOF models required for most other applications. Generally, these analyses consider only the on-axis, single-input/single-output response of the pilot/vehicle system. The extracted vehicle model may be nonparametric, such a frequency-response, or a low-order parametric model, such as a transfer function, or a simplified decoupled state-space representation. Both time- and frequency-domain methods have been widely used for these applications and are discussed in this paper. The requirements for flight testing, data analyses, and modeling for handling-qualities applications of system identification are contrasted with the requirements for extracting multi-input/multi-output state-space models for flight mechanics purposes. Typical handling-qualities analysis results are illustrated using the WG18 databases for the BO-105 and AH-64 helicopters.

1. INTRODUCTION

System identification techniques have seen wide application in the fixed-wing and rotary-wing handling-qualities communities for characterizing the dynamics of air vehicles and piloted simulations. The extracted models are commonly used in closed-loop analyses of the pilot/vehicle system (Fig. 1) to expose potential handling-qualities deficiencies and to check vehicle compliance design specifications (Refs. 1 and 2). A key factor that has been responsible for the broad and successful application of system identification techniques in the handling-qualities community is probably the relative simplicity of the models which are desired for pilot-in-the-loop analyses as compared to the full six or more degrees-of-freedom models required for most other applications. Generally, these analyses consider only the on-axis, single-input/single-output response of the pilot/vehicle system. The extracted vehicle model may be non-parametric, such as frequency-response, or a low-order parametric model, such as a transfer function, or a simplified decoupled state-space representation. Both time-domain and frequency-domain methods have been widely used for these applications.

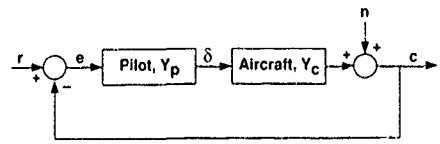

Fig. 1 Pilot/vehicle system block diagram.

This paper discusses system identification methods for rotorcraft handling-qualities studies. The requirements for flight testing, data analyses, and modeling for handling-qualities applications of system identification are contrasted with the requirements for extracting multi-input/multi-output state-space models for flight mechanics purposes. Typical handling-qualities analysis results are illustrated using the WG18 databases for the BO 105 and AH-64 helicopters.

2. BASIC HANDLING-QUALITIES CONCEPTS

Pilot/vehicle interaction in closed-loop control tasks is commonly analyzed by first modeling the pilot as a low-order compensator, and then analyzing the pilot/vehicle feedback system as a servomechanism (Fig. 1). This section uses *classical control theory* to analyze the pilot/vehicle servomechanism and to illustrate basic handling-qualities concepts, although state-space based optimal methods are also available in the literature and have been used successfully (Ref. 2).

In attitude tracking tasks, the pilot attempts to null the error e between the commanded aircraft attitude r and the actual aircraft attitude c through suitable motion of the aircraft stick, δ (Fig. 1). The rate of pilot stick inputs $d\delta/dt$ is characterized by the cross-over frequency ω_c, a fundamental handling-qualities parameter, defined as the frequency at which the compensated open-loop magnitude response of c/e is 0 dB. Higher cross-over frequencies allow tighter closed-loop tracking, but imply higher stick deflection rates, and thus higher workload. The cross-over frequency is selected by the pilot to achieve the task performance requirements in the presence of noise or disturbances. A large body of test data (Ref. 2) indicates that the cross-over frequency for attitude tracking tasks is typically in the range of $1 \text{ rad/s} \le \omega_c \le 3 \text{ rad/s}$.

Classical servomechanism theory can be used to show that good closed-loop characteristics (e.g., stability margins and command tracking) require that the overall compensated open-loop response c/e displays an average K/s characteristic (–20 dB/decade magnitude slope) in the cross-over frequency region. While the pilot ($Y_p = \delta/e$) can compensate for poor rotorcraft characteristics ($Y_c = c/\delta$) to achieve the desired overall cross-over characteristics ($c/e = Y_pY_c$), this leads to increased pilot workload and resulting poor handling-qualities ratings. The minimum workload is achieved when the pilot can act as a pure gain regulator through a neuromuscular delay (Ref. 2):

$$Y_p = K_p \exp(-\tau s) \qquad (1)$$

where typical values of time delay are $0.2\ s < \tau < 0.4\ s$.

Simplified pilot/vehicle analyses (Ref. 2) assume that the pilot acts as a pure gain regulator (ignoring τ), and selects the maximum cross-over frequency ω_c that can be achieved while maintaining acceptable stability margins (e.g., phase margin = 45°, gain margin = 6 dB). This maximum achievable pure-gain pilot cross-over frequency is termed the "bandwidth frequency" (ω_{bw}) in the handling-qualities community, and can be determined by inspection of the attitude response of the helicopter alone (Y_c) as obtained from system identification (Fig. 2). The bandwidth frequency can also be considered as the inverse closed-loop time constant ($1/T_c$), since:

$$\frac{c}{r} \approx \frac{\omega_c}{s + \omega_c} \qquad (2)$$

thus,

$$\frac{1}{T_c} = \omega_c = \omega_{bw}$$

High bandwidth responses, and thus associated short rise times, are desirable for aggressive closed-loop piloting tasks, such as air-to-air tracking and air refueling. Lower bandwidth responses (and associated longer rise times) are acceptable for less aggressive tasks such as up-and-away cruise flight and maneuvering.

Task requirements for increased piloting aggressiveness lead to the need for **higher** cross-over frequencies

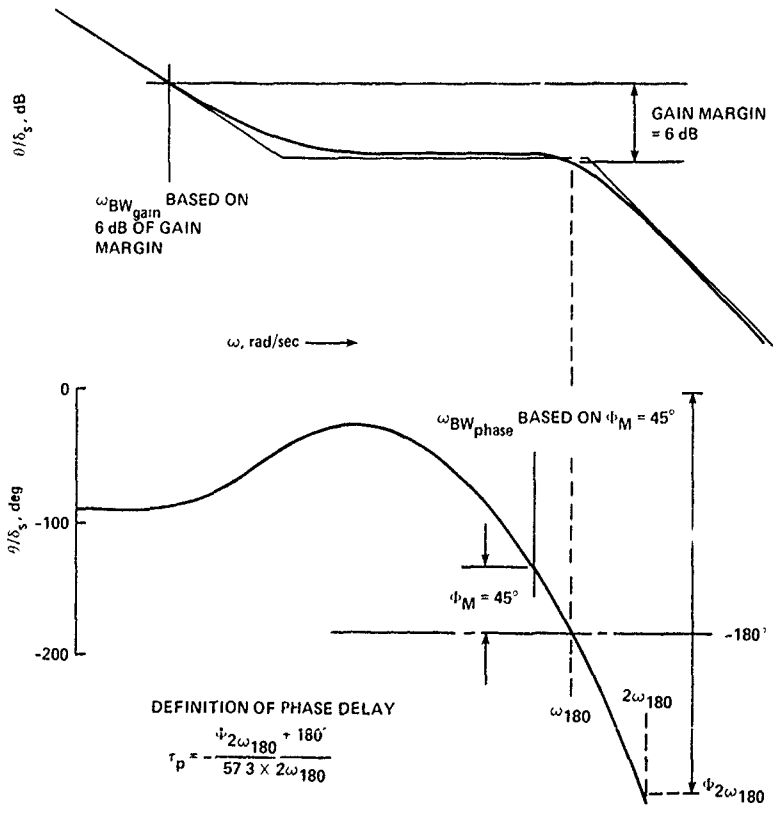

Fig. 2 Determination of bandwidth and phase delay criteria values.

than can be achieved by the simple pure gain piloting technique of Eq. (1). The increased phase lag (i.e., deteriorating phase margin) associated with higher cross-over frequencies must be offset by pilot-supplied lead, i.e., control anticipation. These requirements for pilot lead cause an increase in pilot workload and a degradation in perceived handling qualities. A measure of the rate of deterioration in the aircraft phase margin and, therefore, the requirement for pilot-supplied lead is obtained from a handling-qualities metric referred to as phase delay τ_p:

$$\tau_p = -\frac{\Phi_{2\omega 180} + 180^\circ}{57.3 \times 2\omega_{180}} \qquad (3)$$

High values of phase delay indicate that when the pilot attempts to rapidly increase the cross-over frequency, there will be large demands for pilot lead. This, in turn, leads to poor handling-qualities and increased probability of pilot induced oscillations (Ref. 2). Tasks which can be considered as "low gain" require lower cross-over frequencies and are, therefore, not as sensitive to large phase delays. The current *US Handling-Qualities Requirements for Military Rotorcraft* ADS-33C (Ref. 3) specifies desirable levels of bandwidth and phase delay for on-axis attitude responses (e.g., $c/\delta = \phi/\delta_{lat}$ in Fig. 1) appropriate to a variety of piloting tasks. Desirable (Level 1) handling-qualities for the roll response to lateral stick inputs are shown in Fig. 3 for:

(a) high gain (target acquisition and tracking) tasks and

(b) all other piloting tasks.

Compliance with these specifications must be demonstrated for the flight vehicle (and/or simulation) using non-parametric frequency-response identification techniques.

Non-parametric models identified in the frequency-domain are very useful for these handling-qualities analysis because:

1. They are rapidly obtained from flight tests.

2. They contain no inherent assumptions of model structure or order.

3. The handling-qualities metrics (ω_{bw}, τ_p) are determined directly from inspection.

Frequency-response testing and analysis techniques initially developed and demonstrated for helicopters using the XV-15 (Ref. 4) and the Bell 214-ST aircraft (Ref. 5) have become a standard part of the rotorcraft specification compliance testing procedure.

Parametric models are needed in handling-qualities studies which use parametric analysis tools such as root

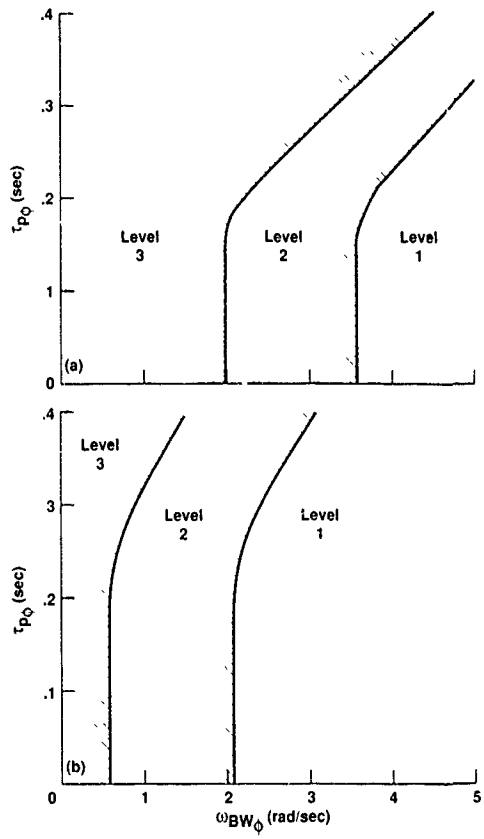

Fig. 3 Requirements for roll response to lateral stick inputs.

locus, and stat-space based methods (Ref. 2). Also, the correlation of subjective handling-qualities ratings with vehicle-based aerodynamic characteristics (e.g., roll damping and roll control sensitivity) is often used in the development of handling-qualities design criteria. Parametric models used for this purpose are generally low-order, decoupled single-input/single-output transfer-function representations of the "effective" aircraft response characteristics important in the pilot cross-over frequency range. For example, in the fixed-wing handling-qualities specification, a second-order model must be identified to allow characterization of the short-period response of aircraft pitch attitude to longitudinal inputs and demonstrate compliance with the design criteria. The ADS-33C specification for rotorcraft gives desirable characteristics of the vertical velocity response to collective inputs in terms of a first-order transfer-function model $\dot{h}/\delta_{col}$. An excellent review and analysis of helicopter handling-qualities using parametric system identification of low-order models is given by Houston and Horton (Ref. 6) based on SA-330 and Lynx flight test and simulation data. Both frequency-domain and time-domain methods are employed in the handling-qualities communities for parametric system identification.

The following sections demonstrate the application of both non-parametric and parametric system identification methods for handling-qualities studies.

3. NON-PARAMETRIC MODEL IDENTIFICATION FOR HANDLING-QUALITIES STUDIES

This section discusses special requirements for identification of non-parametric (frequency-response) models and presents an illustrative example using the BO 105 data base.

Non-parametric models used in the evaluation of handling-qualities based on bandwidth and phase delay metrics must be accurate in the frequency range of the data used in the calculation (e.g., Eq. (3) for τ_p):

$$0.5\omega_{bw} < \omega < 2.5\omega_{180} \qquad (4)$$

As seen in Fig. 3, the range of acceptable bandwidth frequencies in the pitch and roll axis is roughly 1 rad/s – 4 rad/s. Based on Eq. (4), and assuming a simple second-order closed-loop attitude response characteristic, the required range of accurate identification is roughly 0.5 rad/s to 15 rad/s. Clearly the very low frequency behavior of the phugoid (and spiral) dynamics are not as important for handling-quality applications as they are to the requirements for identifying a complete 6 DOF flight mechanics model.

The frequency-sweep input is particularly well suited for achieving accurate non-parametric (frequency-response) identification because it produces an even distribution of spectral content across the desired frequency range. The range of excitation is determined by selecting the period of the lowest frequency input and the cycle rate of the highest frequency input. At least two complete frequency sweeps are concatenated to increase the amount of data used in the spectral analyses and thus reduce the variance in the spectral estimates. Three frequency sweeps are executed consecutively in each of the primary axes to ensure that two good runs are obtained. Instrumentation requirements for identifying handling-qualities models are essentially the same as those required for identifying the more complete flight mechanics. As before, the instrumentation characteristics must be carefully selected to minimize their influence on the aircraft response characteristics being identified. Further, the characteristics of the sensors and filters must be well known so that their effect can be incorporated in the analyses and not cause the extracted response characteristics to be biased by the instrumentation dynamics. Finally, the flight tests must be conducted during periods of minimum ambient wind and turbulence to reduce the random errors in the identification.

Flight-test inputs for flight-mechanics model identification are typically difficult to execute for the hover flight condition. However, the reduced identification frequency-range needed for handling-qualities applications allows much shorter record lengths and higher minimum excitation frequencies, thus reducing difficulty of achieving acceptable excitation even in hover. Furthermore most handling-qualities applications are concerned with the augmented (i.e., stability control augmentation system engaged) vehicle response characteristics, for which the aircraft dynamics are generally more stable and more nearly decoupled than the bare airframe.

Attitude response identification (e.g., ϕ/δ_{lat}) in the mid- and high-frequency range is best achieved using the angular-rate signals (p/δ_{lat}) which have better frequency content compared to the attitude measurement variables. Then, the required response is obtained by applying numerically a 1/s correction

$$\frac{\phi}{\delta_{lat}} = \frac{1}{s}\ \frac{p}{\delta_{lat}}$$

in the frequency domain.

Figure 4 shows an example of the ϕ/δ_{lat} response for the BO 105 obtained from the AGARD WG18 frequency sweep data at 80 kn (events 44, 45, 46). The bandwidth and phase delay metrics are readily obtained from the figure and Eq. (3) to yield:

$$\omega_{bw} = 5.72 \text{ rad/s} \qquad (5)$$

$$\tau_p = 0.062 \text{ s}$$

These values are then spotted on the ADS-33C specifications in Fig. 3. The BO 105 characteristics are seen to be in the desirable range even for the most demanding piloting tasks. This is a reflection of the high effective hinge offset of the BO 105 hingeless rotor, and the lack of additional time delays in this unaugmented aircraft. Much larger effective time delays are usually associated with flight control system augmentation in advanced rotorcraft (Ref. 7).

The presence of the lead-lag dynamics causes a dip in the phase curve near the $2\omega_{180}$ frequency as indicated in Fig. 4. This causes the phase characteristics to be a nonlinear function of frequency and makes the phase delay calculation extremely sensitive to the identified value of $2\omega_{180}$. In such circumstances, the phase delay parameter should be determined by a least-squares fit to the phase data in the piloted cross-over region (ADS-33C) as illustrated in Fig. 5. The results show that for the present case, the least-squares calculation produces essentially the same phase delay value as was obtained directly from the two point approximation in Fig. 4.

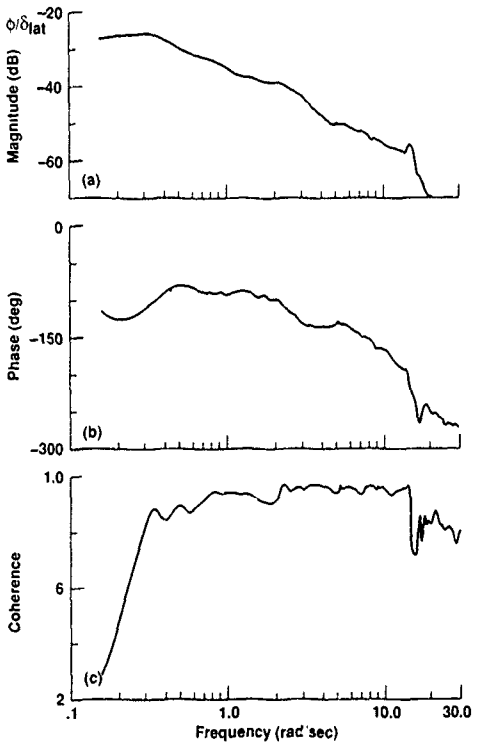

Fig. 4 Roll attitude response to lateral stick (φ/δ_{lat}) identified from BO 105 frequency-sweep data.

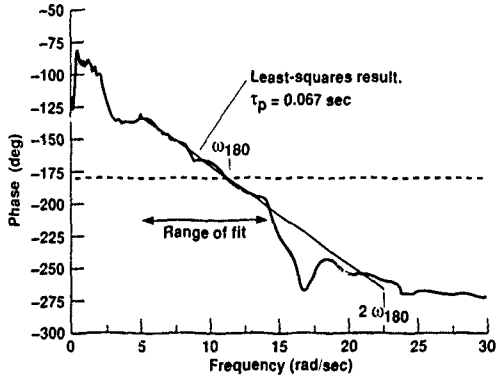

Fig. 5 Determination of phase delay using least squares fitting procedure.

4. PARAMETRIC MODEL IDENTIFICATION FOR HANDLING-QUALITIES ANALYSES

Handling-qualities analyses based on parametric models of the pilot/aircraft system of Fig. 1 must be accurate in the region encompassing the pilot cross-over, ω_c. As a rule of thumb, the frequency range of validity should encompass:

$$0.3\ \omega_c \le \omega \le 3.0\ \omega_c \qquad (6)$$

The pilot's feedback loop suppresses the dynamics at lower frequencies, while the natural roll-off behavior of system response reduces the importance of the high-frequency dynamics. Thus, closed-loop pilot/vehicle characteristics are dominated by the open-loop response c/e in the frequency range of Eq. (6).

Parametric system identification methods for application to handling-qualities must be tailored to be most accurate in the frequency range of Eq. (6), with considerably reduced accuracy being acceptable outside of this frequency range. This suggests that handling-qualities models for attitude task analyses (1 rad/s $\le \omega_c \le$ 3 rad/s) should be accurate in the frequency range of 0.3 rad/s to 9 rad/s. WG18 identification results indicate that a quasi-steady model formulation will be quite acceptable for characterizing helicopter dynamics in this frequency range. Furthermore, as discussed earlier, parametric handling-qualities models are generally assumed to have a very simple decoupled, first- or second-order structure to expose the dominant characteristics of concern to the pilot. This is especially true for analyzing handling-qualities of augmented vehicle dynamics, since augmentation tends to suppress most of the coupled and secondary open-loop vehicle dynamics. Clearly, model structures for handling-qualities analyses applications are significantly simpler than the 6 DOF flight mechanics models identified by WG18. The rudimentary models adopted to represent the pilot (e.g., Eq. (1)) make a more accurate modeling of the rotorcraft dynamics inappropriate.

The simple parametric model structures adopted for handling-qualities analyses allow considerable relaxation of the input design requirements and computational algorithms needed for parametric system identification. The main requirement is to acquire data with record lengths on the order of 2 to 3 time constants of the modes included in the model. For example, a typical heave damping constant ($Z_w = -0.5\ s^{-1}$) implies a time constant of 2 seconds. Thus, desirable record lengths to identify this parameter from flight data would be of the order of 4 to 6 seconds. These record lengths are considerably shorter than necessary to identify the coupled and lower frequency behavior for a full 6 DOF flight mechanics model. Rapid identification algorithms based in both frequency-domain (Refs. 5 and 6) and time domain (Ref. 3) are available for this application. The following two examples based on the WG18 AH-64 data-based illustrate the use of time-domain and frequency-domain system identification methods to extract lower-order parametric handling-qualities models.

4.1 Time-Domain Identification Example

The ADS-33C specification requires the identification of the first-order model of vertical response to collective:

$$\frac{\dot{h}}{\delta_{col}} = \frac{K\ \exp(-\tau s)}{T_{\dot{h}} s + 1} \tag{7}$$

based on a simplified time-domain output-error technique. The required analysis assumes that the input is a pure step. This yields the simple closed-form solution for the vertical rate response:

$$\dot{h}_{est}(t) = K\left[1 - \exp\left(-\frac{t-\tau}{T_{\dot{h}}}\right)\right] \quad \text{for } t > \tau \tag{8}$$

$$\dot{h}_{est}(t) = 0 \qquad \text{for } t \le \tau \tag{9}$$

Although not contained in the current specification, the constraint of Eq. (9) is necessary to yield a casual model response (Ref. 8). In practice, the starting time (t = 0) is assumed to be at the mid-point of the control input, since a finite time will always be required to achieve the full input during flight testing. The parameters of Eq. (7) are to be obtained by a nonlinear optimization search to minimize the squared-error (ε^2) between the model output and flight test data:

$$\varepsilon^2 = (\dot{h}_{est} - \dot{h}_{data})^2 \tag{10}$$

Table 1 presents the ADS-33C specifications of the parameter values for desirable handling-qualities (Level 1).

Table 1 Comparison of equation parameters with specification

Level	$T_{\dot{h}}$ (in seconds)	τ (in seconds)
1	5.0	0.20
2	∞	0.30

The collective step response of the AH-64 for the 130 kn flight condition shown in Fig. 6 was obtained by using the first portion of the doublet record (flight 883, event 10). The input is assumed to begin at t = 1.2 s, which corresponds to the mid-point of the initial collective step. The end-of-record is taken at t = 4.51 s, which corresponds to the point of collective control reversal. Therefore, the total record length used in the identification

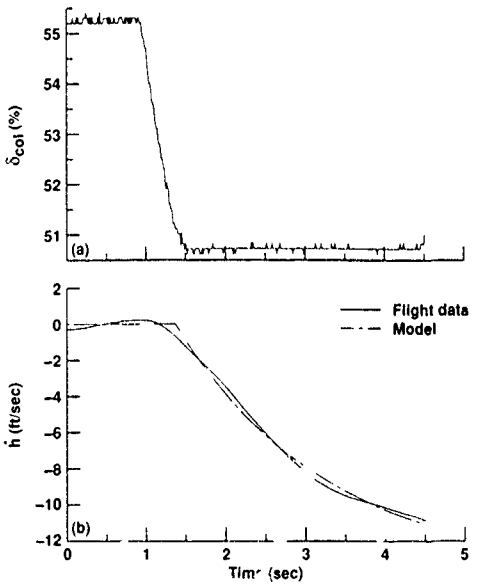

Fig. 6 Flight data and handling-qualities model identification (Eq. (8)) for vertical rate response

procedure is t = 3.31 s. Considering an approximate heave damping value (Z_w = -0.5 s^{-1}) based on the AH-64 results obtained by the DLR, the system time constant is about 2 seconds, thus indicating that the record length is marginally acceptable for the current identification problem.

The transfer-function parameters identified using the data of Fig. 6 are:

$$\begin{aligned} K &= -1.60\ \text{ft}\,s^{-2}/\% = -0.488\ \text{m}\,s^{-2}/\% \\ \tau &= 0.192\ \text{s} \\ T_{\dot{h}} &= 1.86\ \text{s} \end{aligned} \tag{11}$$

The model response as estimated from Eqs. (8), (9), and (11) is shown in Fig. 6. The correlation coefficient r^2 is a measure of the accuracy with which the identified model satisfactorily characterizes the flight test data:

$$r^2 = \frac{\sum_{i=1}^{n} (\dot{h}_{est} - \bar{\dot{h}}_{data})^2}{\sum_{i=1}^{n} (\dot{h}_{data} - \bar{\dot{h}}_{data})^2} \tag{12}$$

where $\bar{\dot{h}}$ denotes the mean value of $\dot{h}$. For the results of Fig. 6 is:

$$r^2 = 1.017 \tag{13}$$

The specification requires a correlation coefficient in the range of 0.97 to 1.03. Therefore, while there are significant deviations between the model predictions and the flight test data, the fit is considered to be satisfactory for handling-qualities applications. Comparison of the Eq. (10) parameters with the specification (Table 1) indicates that the AH-64 achieves desirable (Level 1) handling-qualities characteristics for the vertical response.

When a helicopter is operating with the automatic flight control system disengaged, as in the present case, the parameters of Eq. (10) correspond to the bare airframe stability and control derivatives:

$$Z_{\delta col} = K = -0.488 \text{ m s}^{-2}/\% \qquad Z_w = -\frac{1}{T_h} = -0.54 \text{ s}^{-1} \qquad \tau = \text{rotor delay} = 0.192 \text{ s} \tag{14}$$

The DLR results for these parameters as obtained form the full 6 DOF model identification are repeated below for comparison with Eq. (14).

$$Z_{\delta col} = -0.264 \text{ m s}^{-2}/\% \qquad Z_w = -0.547 \text{ s}^{-1} \qquad \tau = 0.117 \text{ s} \tag{15}$$

The rather crude identification technique of Eq. (8) yields an accurate identification of heave damping (Z_w). The normal sensitivity ($Z_{\delta col}$) and time delay (τ) are somewhat overestimated, and may be correlated—trading off one against the other in the simple identification scheme. The Level 1 specification is achieved even for the overestimated time delay of Eq. (14), although the pilot opinion of the model of Eq. (15) would probably more accurately reflect the true aircraft behavior.

4.2 Frequency-Domain Identification Example

Frequency-domain methods provide a reliable approach for extracting physically meaningful low-order handling-qualities models because:

1. model structure can be selected based on a visual inspection of the non-parametric frequency-response identification results, and

2. the frequency range of fit can be restricted to the model's range of applicability (Ref. 9).

This approach is illustrated using the WG18 frequency sweep data for the AH-14.

The frequency response of pitch rate due to longitudinal actuator inputs was obtained (from flight 883 events 3 and 5) using the frequency-response identification techniques described above and is presented in Fig. 7. Good coherence is achieved in the frequency range from 0.6 rad/s (corresponding to the starting frequency of the automated sweep) to 10 rad/s. The coherence function of nearly unity indicates excellent identification accuracy and response linearity in this range. Visual inspection of the frequency response of Fig. 7 indicates a fundamental first-order characteristic. Attempts to fit the pitch rate response with a second-order model, or a simultaneous fit of the pitch rate and normal acceleration responses with the short period model proposed by RAE (Ref. 6) resulted in overparameterization. The second-order pitch rate transfer function reduced to a first-order form, thus indicating a very weak coupling between pitch rate and vertical responses. This finding is further supported by the very small identified values of the Mw coupling derivative determined by the DLR ($M_w = 0.013$) and the NAE and MDHC ($M_w = 0.00513$). The following decoupled pitch rate response was obtained from a 20-point match over the frequency range of from 0.6 rad/s to 10 rad/s:

$$\frac{q}{\delta_{lon}} = \frac{M_{\delta lon} \exp(-\tau_{lon} s)}{s - M_q}$$

$$M_{\delta lon} = 0.0274 \text{ s}^{-2}/\% \qquad M_q = -0.7754 \text{ s}^{-1} \qquad \tau_{lon} = 0.0993 \text{ s} \tag{16}$$

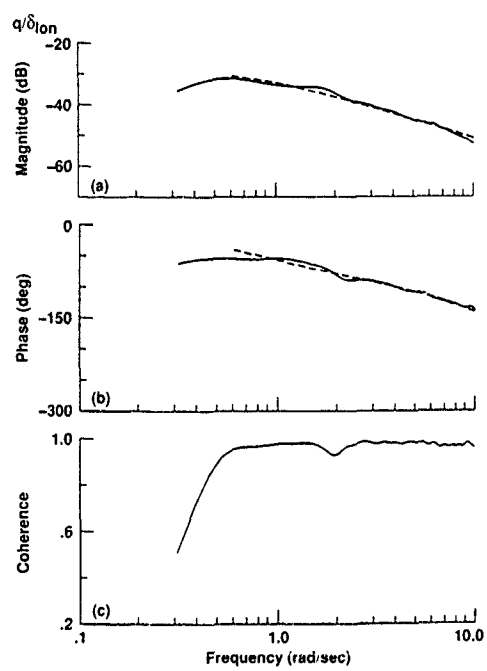

Fig. 7 Pitch attitude response to longitudinal cyclic (q/B1s) identified from AH-64 frequency-sweep data.

The frequency response comparison between the low-order transfer function model (Eq. (16)) and flight test data is excellent over the frequency range of the fit as shown in Fig. 7. For comparison with the above simple model results, the parameters obtained by the DLR for the full 6 DOF model are repeated below:

$$M_{\delta lon} = 0.02757 \ s^{-2}/\% \qquad M_q = -0.7741 \ s^{-1} \qquad \tau_{lon} = 0.100 \ s \tag{17}$$

The agreement between the first-order, 1 DOF, handling-qualities model and the full 6 DOF results is remarkable (compare Eqs. (16) and (17)), substantiating the use of the simplified model in the limited frequency range of applicability.

The utility of the simplified transfer function model was checked using time domain verification for a doublet input. As seen in Fig. 8, the predicted and measured responses of pitch rate and pitch attitude are nearly identical for the 8 seconds record length shown in the figure. This 8 seconds record corresponds to about 6 time constants of the identified pitch rate mode. Clearly, the transient pitch rate response characteristics of the AH-64 that are of interest to handling-qualities are satisfactorily captured by this very simple first-order transfer-function model.

As seen in Fig. 7, the poor coherence at low frequency is not satisfactory for allowing an extraction of the bandwidth and phase delay parameters from the identified frequency-response. However, these parameters can be obtained by extrapolating the transfer function model response into the needed frequency range:

$$\omega_{bw} = 0.678 \ rad/s \qquad \tau_p = 0.074 \ s \tag{18}$$

Comparison of these values with the ADS-33C specifications (Fig. 3) indicates Level 2 handling-qualities for the unaugmented AH-64 in the nonaggressive piloting tasks. Level 2 handling-qualities for a failed (or disengaged) AFCS condition is generally considered acceptable.

5. CONCLUSIONS

Key considerations in the application of system identification techniques to handling-qualities studies that were highlighted in this section are:

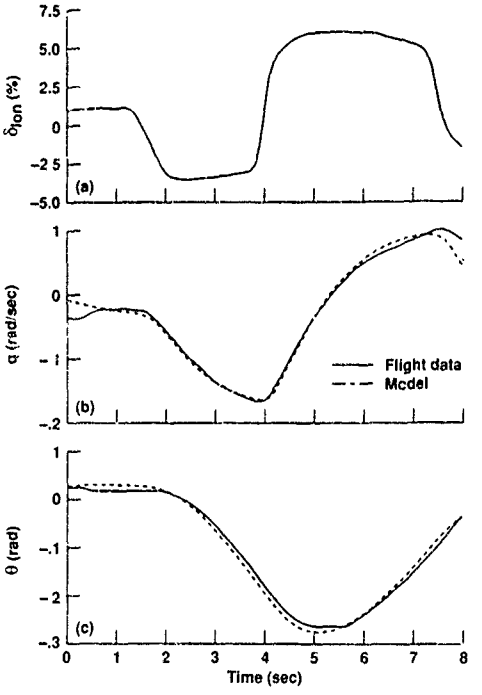

Fig. 8 Time-domain verification of first-order pitch model (Eq. (16)) of the AH-64.

1. Requirements on flight testing, models structure, and identification algorithms are substantially eased because of

   a. the rather restricted frequency range of applicability needed for analyzing pilot-in-the-loop handling-qualities; and

   b. the desire for simple handling-qualities models which capture the inherent dynamic characteristics using a few number of parameters.

2. Non-parametric models are very useful for handling-qualities and are easily obtained in the frequency domain from frequency-sweep flight test data.

3. Simple parametric models are useful for characterizing the dominant vehicle characteristics in the frequency range of interest to handling-qualities and for establishing handling-qualities design guidelines.

4. Examples of frequency and time domain identification techniques applied to the BO 105 and AH-64 databases illustrate that rather simple modeling and identification methods can reliably be used to support rotorcraft handling-qualities studies.

REFERENCES

1. Wilhelm, K. and Nieuwpoort, T. "Handling Qualities Evaluation Techniques," To be published in: AGARD AR-279, 1991.

2. Anon. "Advances in Flying Qualities," AGARD Lecture Series LS-157, 1988.

3. Anon. "Handling Qualities Requirements for Military Rotorcraft," AGARD Lecture Series LS-157, 1988.

4. Tischler, M. B., Leung, J. G. M., and Dugan, D. C. "Frequency-Domain Identification of XV-15 Tilt-Rotor Aircraft Dynamics in Hovering Flight," AIAA/AHS 2nd Flight Testing Conference, Las Vegas, 1983.

5. Tischler, M. B., Fletcher, J. W., Diekmann, V. L., Williams, R. A., Cason, R. W. "Demonstration of Frequency-Sweep Testing Technique using a Bell 214-ST Helicopter," NASA TM-89422, 1987.

6. Houston, S. S. and Horton, R. I. "The Identification of Reduced Order Models of Helicopter Behaviour for Handling Qualities Studies," 13th European Rotorcraft Forum, Arles, France, 1987.

7. Tischler, M. B. "Digital Control of Highly Augmented Combat Rotorcraft," NASA TM-88346, 1987.

8. Howitt, J. "Comments on the Proposed MIL-H-8501 Update Criterion on Height Rate Response Characteristics," RAE Working Paper WP FM 041, 1990.

9. Chen, R. T. N. and Tischler, M. B "The Role of Modeling and Flight Testing in Rotorcraft Parameter Identification," Vertica, Vol. 11, No. 4, 1987.

SYSTEM IDENTIFICATION REQUIREMENTS FOR HIGH-BANDWIDTH ROTORCRAFT FLIGHT CONTROL SYSTEM DESIGN

by
Mark B. Tischler
Aeroflightdynamics Directorate
U.S. Army Aviation Research & Technology Activity
Ames Research Center, Moffett Field, CA 94035-1099

SUMMARY

The application of system identification methods to high-bandwidth rotorcraft flight control system design is examined. Flight test and modeling requirements are illustrated using flight test data from a BO-105 hingeless rotor helicopter. The proposed approach involves the identification of nonparametric frequency-response models, followed by parametric (transfer function and state space) model identification. Results for the BO-105 show the need for including coupled body/rotor flapping and lead-lag dynamics in the identification model structure to allow the accurate prediction of control system bandwidth limitations. Lower-order models are useful for estimating nominal control system performance only when the flight data used for the identification are bandlimited to be consistent with the frequency range of applicability of the model. The flight test results presented in this paper are consistent with theoretical studies by previous researchers.

SYMBOLS

GM	gain margin (of open-loop response), dB
K_ϕ	roll angle feedback gain, %/rad
Kp	roll rate feedback gain, %/rad/sec
Lp	roll damping derivative, 1/sec
p	roll rate = $\dot{\phi}$ (linear model), rad/sec
$\gamma^2_{\delta_a p}$	coherence from lateral control inputs to roll rate outputs
δ_a	lateral control input, %
ς	damping ratio
τ	time delay, sec
τ_p	phase delay (of closed-loop response), sec
$\Phi_{2\omega_{180}}$	phase angle (deg) of closed-loop system when the frequency = $2 \times \omega_{180}$
ϕ	roll angle, rad
ϕ_c	roll angle command input to command model, rad
ϕ_e	roll angle error signal = $\phi_m - \phi$, rad
ϕ_m	roll angle command input to stability loop, rad
ω	frequency, rad/sec
ω_{BW}	bandwidth frequency (of closed-loop response), rad/sec. For attitude command systems, the bandwidth is defined as frequency at which the phase angle is –135°
ω_c	design crossover-frequency (of open-loop response) to give 45° phase margin, rad/sec
ω_u	frequency at which instability occurs due to increasing feedback gain, rad/sec (frequency value at which the root locus branch crosses the imaginary axis)
ω_{180}	frequency where the phase angle of closed-loop system = –180°, rad/sec
ω_2	upper frequency of transfer function fitting range, rad/sec

1. INTRODUCTION

System identification procedures provide an excellent tool for improving mathematical models used for rotorcraft flight control system design. Dedicated flight tests of a prototype helicopter can be conducted to update the flight mechanics to update the flight mechanics models and optimize control system gains early in the development process. Such an approach has already been taken by Kaletka and von Grunhagen (Ref. 1) in the development of a fly-by-wire BO-105, and by Bosworth and West (Ref. 2) in the development of the X-29A.

The identification of models for use in flight control system design involves requirements that are considerably different from those encountered in other applications such as piloted simulation and wind tunnel model

validation. Models identified for use in simulation and wind tunnel validation must be generally accurate over a wide spectrum of frequencies from trim (zero frequency) and phugoid (low frequency) to the dominant transient responses of the longitudinal short-period and roll-subsidence modes (mid/high frequency). Therefore, in terms of stability and control derivatives, the low-frequency parameters such as the speed derivatives may be just as important to a pilot's perception of simulation fidelity as an accurate value of roll damping.

Practical flight control system design requires models that are:

1. highly accurate in the crossover frequency range—to exploit the maximum achievable performance from the helicopter; and,

2. robust in the crossover range with respect to flight condition, and input form and size—to ensure that closed-loop stability/performance is maintained. The control system design can be made sufficiently robust to compensate for poor model robustness, but at the expense of performance.

These requirements are especially difficult for advanced high-bandwidth control systems where the crossover range occurs at frequencies near the limit of current identification capabilities.

This paper examines in detail these requirements for system identification application to high-bandwidth flight control design. Much of this paper discusses the need in control system design for higher-order models that include rotor dynamics. It is interesting to note that the inclusion of rotor flapping dynamics in an optimal control system design methodology was investigated by Hall and Bryson (Ref. 3) many years ago.

The roll response of the BO-105 helicopter (Fig. 1) at a trim condition of 40 m/s is used throughout to illustrate the main points of the analysis. The high-bandwidth/highly-coupled rotor system of the BO-105 presents the control system designer with a "most difficult case" scenario. Flight data presented in this paper were collected by the DLR Institute for Flight Mechanics as part of the AGARD WG18 on Rotorcraft System Identification.

Fig. 1 BO-105 case study helicopter.

2. SIMPLE MODEL-FOLLOWING CONTROL SYSTEM

Figure 2 shows a simple design of the roll channel for control system based on an explicit model-following concept. An attitude-command/attitude-hold configuration is shown, with only roll angle feedback for the present. The error signal is formed from the difference between the actual roll angle response and that of the desired command model.

The control law design problem for this simple system involves the selection of the stabilization loop gain K, and an appropriate command model. Design requirements based on the U.S. military handling qualities specification (Ref. 4) are for an overall closed-loop roll attitude bandwidth ϕ / ϕ_c (based on 45° phase margin) in the range of ω_{BW} = 2-4 rad/sec. The desired stabilization loop bandwidth of ϕ / ϕ_m is selected as twice this range $(\omega_{BW})_{STAB}$ = 4-8 rad/sec to achieve good model-following and gust rejection (Ref. 5). This implies a stabilization loop crossover frequency (of ϕ / ϕ_c) in the same range, with associated satisfactory phase and gain margins. The following section addresses the identification and modeling aspects for achieving these desired stabilization loop characteristics ϕ / ϕ_m. Command model selection (ϕ_m / ϕ_c) is not addressed herein, because it is not an identification issue.

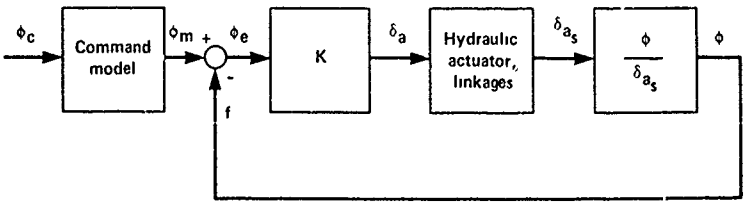

Fig. 2 Simple explicit model following control system.

3. IDENTIFICATION MODELS FOR CONTROL SYSTEM DESIGN

Identification models for use in control system design can be categorized as non-parametric (e.g., frequency-response) or parametric (e.g., transfer-functions and state-space models). Both types of models are discussed in this section.

3.1. Nonparametric Frequency-Response Model

Nonparametric identification models are highly useful as starting points for control system design because they contain no inherent assumptions on model order or structure. The frequency response is complete and accurate (within the frequency-range of good coherence), and provides the fundamental open-loop characteristics needed for both classical and modern frequency-domain based design methods. The identified frequency-response is a describing function model of locally-linearized nonlinear behavior. The severity of this assumption can be checked by comparing extracted describing functions for different input amplitudes.

A robust control system design requires a model that is accurate over a frequency range that spans the intended crossover region. However, the helicopter's dynamics and thus the achievable crossover frequency are unknown at this stage. Thus a nonparametric model that is accurate over a broad frequency range is desirable. Pilot generated frequency-sweeps are especially well suited for this purpose (Refs. 6 and 7). Piloted frequency-sweeps of the BO-105 were conducted over a range of frequencies from 0.1 Hz - 5 Hz (0.63-31.4 rad/sec) to excite all the dynamic modes of concern (Fig. 3).

The identified open-loop (ϕ/δ_a) frequency response of the BO-105 body/rotor/actuator system for the 40 m/s flight condition shown in Figure 4 was obtained using the spectral analysis techniques of Ref. 8. The spectral analysis was optimized for accuracy in the frequency-range of 1-30 rad/sec, which covers all modes of concern near the crossover range. The associated coherence (Fig. 4c) indicates accurate identification in this frequency range. The Bode plot of Fig. 4 shows that with roll attitude feedback only, a maximum crossover frequency (ϕ/ϕ_e) of $\omega_c = 5.72$ rad/sec can be achieved for phase and gain margins of 45° and 6 dB, respectively. These

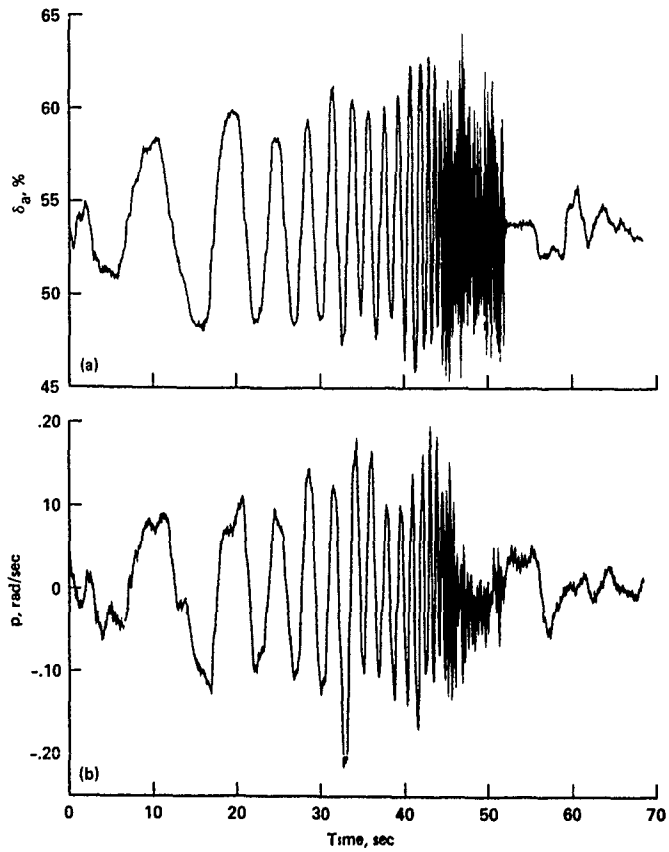

Fig. 3 Flight data of roll axis frequency-sweep. a) Pilot lateral stick input, δ_a; b) roll rate, p.

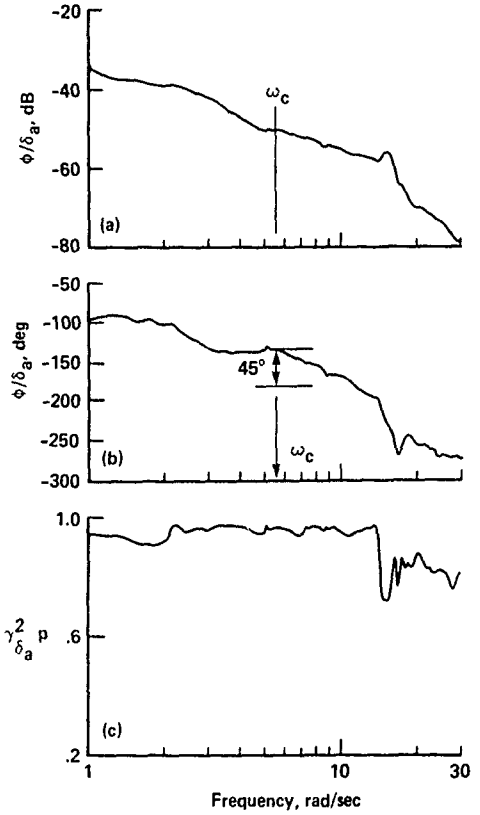

Fig. 4 Frequency-response identification.

characteristics meet the design specs for this simple system. However, roll rate feedback will be necessary to offset additional lags in a practical design implementation (Ref. 5).

3.2. Parametric Model

A parametric model of the roll response is useful to facilitate detailed control design studies. The fundamental considerations in deriving such a parametric model are:

1. desired frequency-range of validity
2. model order
3. estimate of model accuracy
4. model robustness

3.2.1. Frequency-range of validity

The frequency-range of model validity should extend substantially on either side of the crossover frequency. As a rule of thumb, dynamics modes with frequencies of 0.3-3.0 times the crossover frequency will contribute substantially to the closed-loop response. In the present case, this indicates that the parametric model should be valid in the frequency range of 2-18 rad/sec, which includes all of the classical attitude response modes (short period, dutch roll, and roll subsidence) and the regressing rotor modes (flapping and lead-lag), and dynamic inflow (for lower speed conditions). Accurate characterization outside of this frequency range is not important to control system design for the design bandwidth selected here. Closed-loop control suppresses all low frequency open-loop response, so that accurate knowledge of the speed derivatives (phugoid and spiral dynamics) is of little importance.

3.2.2. Model order

The model order must be high enough to capture the important dynamic characteristics in the frequency-range of model validity. In the frequency-domain, this means a sufficient number of states to achieve a "good fit" of the nonparametric response of Fig. 4 is needed in the desired frequency range. However, if the model order is excessive, model parameters will exhibit large variability to small changes in flight condition, input form, and input size which will compromise robustness (Ref. 9).

3.2.3. Estimate of model accuracy

Flight control design requires an estimate of the accuracy of the aerodynamic parameters. Modern MIMO methods that feedback all outputs to all controls require a consistent level of accuracy in the characterization of all of the on- and off-axis responses. Metrics such as the Cramer-Rao lower bound, multi-run scatter, and frequency-response errors are useful for assessing model accuracy.

3.2.4. Model robustness

Models must be robust with respect to flight condition, input form, and input size. Model structure determination methods are useful in reducing parameter insensitivity and correlation, which in turn improves model robustness. Also model verification with alternative input forms, and magnitudes are useful in this regard.

4. A HIGH-ORDER MODEL FOR ROLL RESPONSE

A 7th-order model is selected as the "baseline model" that captures the key dynamics in the frequency-range of concern (2-18 rad/sec):

1. coupled roll/rotor flapping dynamics (2nd order)

2. lead-lag/air resonance (2nd order)
3. dutch roll dynamics (2nd order)
4. roll angle integration (1st order)
5. actuator dynamics (equivalent time delay)

Dynamic inflow modes are not explicitly included in the above list, because of their small influence at this forward flight speed (40 m/s). (Implicit effects of inflow on the rotor modes are captured in matching the frequency-response data.) The roll angle response to lateral stick transfer-function for the baseline model is then 4th-order numerator and 7th-order denominator. The model parameters shown in Table 1a were obtained from a frequency response fit of Fig. 4 from 1-30 r/s using 50 pts. The frequency-response comparison with the data is seen in Fig. 5 to characterize the dynamics accurately in the range of concern, thus indicating that model is of sufficiently high order. The mismatch near the lead-lag mode (13 rad/sec) reflects the reduced accuracy (lower coherence) of the flight data in this frequency range (Fig. 4). The 45° phase margin crossover frequency for the baseline model is taken from Fig. 5 as $\omega_c = 5.32$ r/s which is within 7% of the data, and the baseline gain margin and the frequency for closed-loop instability (ω_u) matches the data (Table 1b).

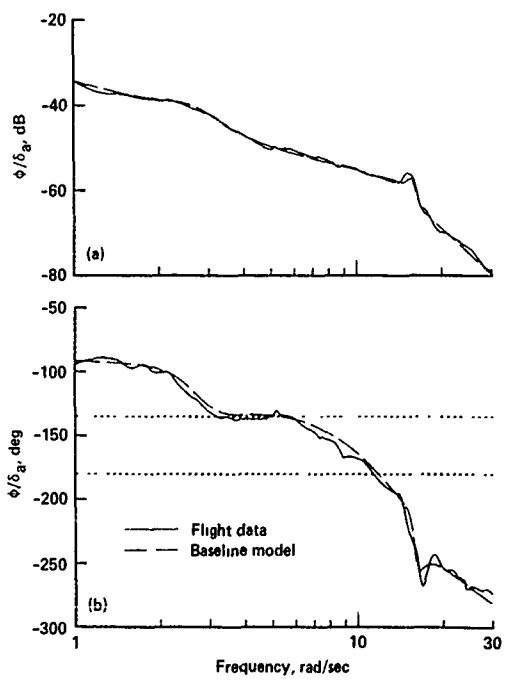

Fig. 5 Comparison of baseline model (7^{th} order) and flight data.

The transfer function model indicates a highly coupled body-roll/rotor-flapping mode ($\zeta = 0.51$, $\omega = 13.7$ r/s) as is expected for the hingeless rotor system (high effective hinge offset) of the BO-105. Helicopters with low effective hinge offset rotors (or equivalently low flapping stiffness), such as some articulated systems, will generally exhibit two essentially decoupled first order modes; (1) body angular damping (L_p,M_q), (2) 1st order rotor regressing. The decoupled rotor mode is often modelled by an effective time delay. The degree of body/rotor coupling is determined by the flapping stiffness as illustrated in Fig. 6 from Heffley (Ref. 10). The lead-lag mode is very lightly damped ($\zeta = 0.0421$) due only to structural damping of the hingeless rotor and the low aerodynamic damping. The total modal damping $\sigma = -\zeta\omega = 0.666$ rad/sec agrees very well with previously published experimental data (Ref. 11). Significant roll/yaw coupling is apparent from the separation of the

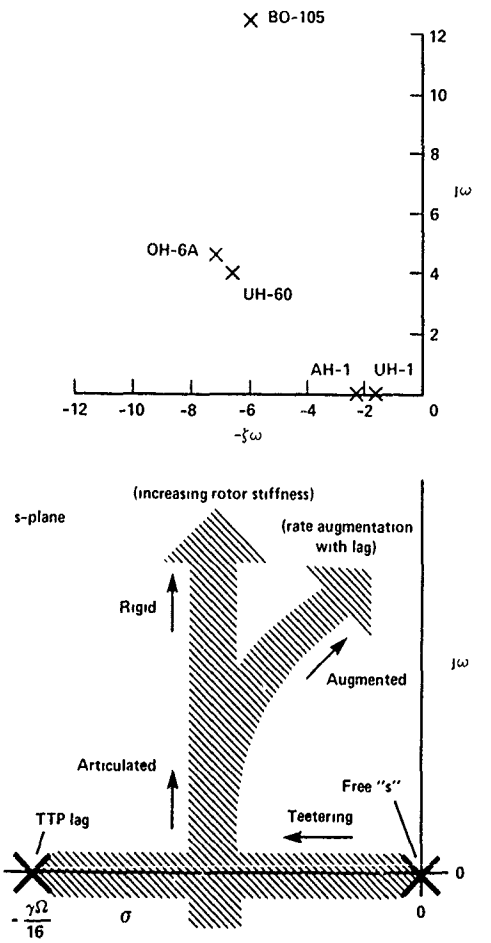

Fig. 6 Short-term eigenvalue locations as a function of flapping stiffness.

complex pole/zero combination of the dutch roll mode. Finally, the equivalent time delay corresponds well to known control system hydraulics and linkage lags.

Figure 7 shows the root locus for variation in the roll angle gain K_ϕ (of Fig. 2). The pole at the origin moves to the crossover range, and the dutch roll mode is driven into the neighboring zero in a stable manner. The lead-lag mode is also driven toward the neighboring complex zero, and is slightly stabilized $(\zeta = 0.0440)$ for the nominal crossover frequency $(\omega_c = 5.32)$. The attitude feedback gain (K) is limited by the destabilization of the rotor/flapping mode. Added time delay to account for unmodelled dynamics does not change these results significantly.

The closed-loop frequency response of ϕ / ϕ_m (from Fig. 2) shown in Fig. 8 for K = 322.9%/rad indicates that good model-following will be achieved out to the desired stabilization-loop bandwidth frequency (4-6 r/s). The closed-loop data curve also shown in the figure was

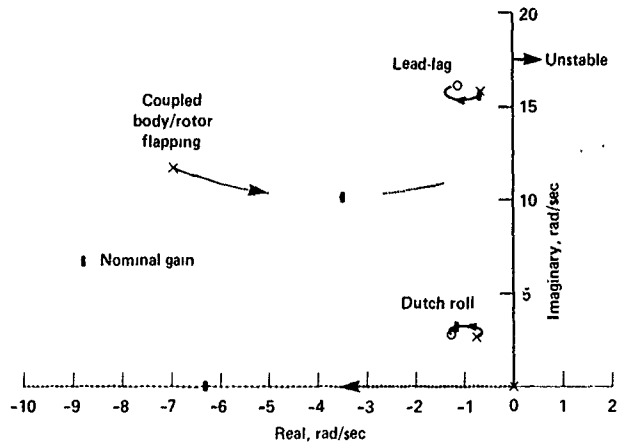

Fig. 7 Stabilization loop root locus, varying roll attitude feedback gain, K_ϕ.

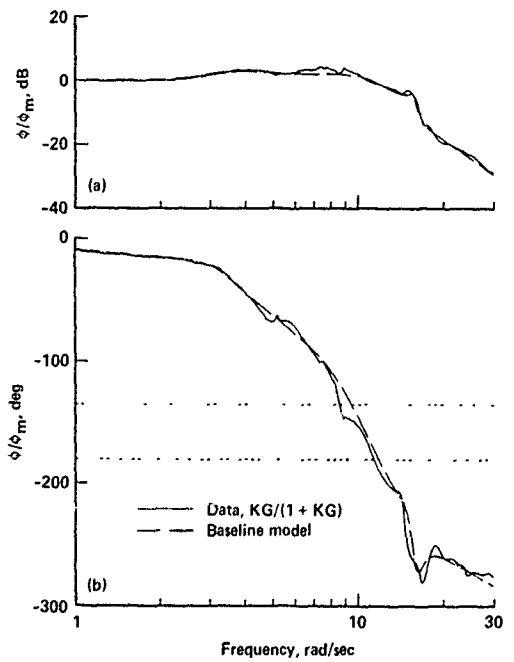

Fig. 8 Comparison of closed loop response, ϕ / ϕ_m of baseline model vs. data.

generated by calculating KG/[1 + KG] for each frequency, using the open-loop data curve of Fig. 4. The good agreement between the closed-loop baseline model response and the (calculated) data over the broad frequency range (1-30 r/s) further demonstrates the validity of the 7th-order model for predicting high-bandwidth flight control system performance.

Two important quantitative metrics of closed-loop performance (ϕ/ϕ_m) are bandwidth (ω_{BW}) and phase delay (τ_p). Closed-loop bandwidth ω_{BW} is defined in the handling-qualities community (Ref. 4) as the frequency at which phase margin of the closed-loop response, ϕ/ϕ_m in this case, is 45°. (This definition applies for attitude command systems as in the present study.) The phase delay is a measure of the phase rolloff near the bandwidth frequency and reflects the total effective time delay of the high frequency dynamic elements (rotor and actuator in this simple case). The phase delay, τ_p is defined as (Ref. 4):

$$\tau_p = -\frac{\Phi_{2\omega_{180}} + 180°}{57.3 \times 2\omega_{180}}$$

where,

ω_{180} = frequency where the phase of ϕ/ϕ_m = −180°

$\Phi_{2\omega_{180}}$ = phase angle at a frequency of $2 \times \omega_{180}$

The bandwidth and phase delay metrics are well predicted by the higher-order model as shown in Table 1b.

An additional feedback of roll-rate will be required in the control system to offset lags and time delays associated with practical design implementation. Figure 9 shows a root locus for variation of roll-rate feedback gain K_p. For no additional time delay, rotor/flapping mode stability remains the limitation on rate feedback gain, although the lead-lag mode damping is clearly reduced for moderate gain levels. When 50 msec of additional time delay is included to account for filters and computational delay in a practical digital control system implementation (Ref. 5), the lead-lag mode becomes rapidly destabilized and sets the limit on rate feedback. (A lag and a pure delay have the same effect on destabilizing the lead-lag mode for this case.) This result illustrates the need for accurate knowledge of the lead-lag dynamics in high-bandwidth control system design. Analytical studies by Diftler (Ref. 12), Miller and White (Ref. 13), and Curtiss (Ref. 14) have made the same conclusions. A flight test investigation by Chen and Hindson (Ref. 15) using a variable-stability CH47 helicopter demonstrated the importance of rotor dynamics and control system lags in determining feedback gain bandwidth limits.

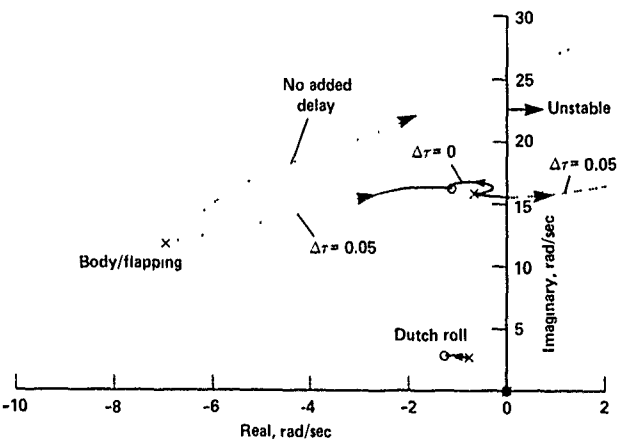

Fig. 9 Stabilization-loop root locus, varying roll-rate gain, K_p.

5. LOWER-ORDER MODELS FOR BROAD-BAND ROLL RESPONSE

Two levels of approximation that are commonly made in formulating models for identification are considered in this section; (1) omit lead-lag dynamics (5^{th} order); (2) quasi-steady rotor dynamics (4^{th} order).

A 5th-order roll-attitude response model was obtained by refitting the frequency response data without the lead-lag mode (Table 1). The transfer function result is consistent with 7th-order model, with only slight variations in the remaining parameters. This indicates that the lead-lag/air-resonance mode can be modelled as a one way-coupled (parasitic mode), similar in nature to an aircraft structural mode. Thus, the lead-lag transfer functions (quadratic dipoles) could be appended onto a 8 dof identification model (flapping dynamics only). This approach has been successfully applied in the state-model identification of BO-105 dynamics (Ref. 16).

The frequency-response matches of the 5th-order model matches the high-order model very well (Fig. 10), except of course for the omission of the lead-lag mode. The fitting error shown in Table 1a, indicates only a slight degradation relative to the 7th-order model. The roll-angle gain is again limited by destabilization of the coupled roll/flapping mode. Of course, roll-rate limitations due to lead-lag instability will not be detected by this model. Comparison of the closed-loop response (ϕ/ϕ_m) of the 5th-order and 7th-order model (Fig. 11) shows that the reduced-order model is very accurate except for the lead-lag mode omission. The quantitative metrics match the baseline model results (Table 1b).

Table 1a Roll response models, ϕ/δ_a

Mode	Fitting range	Transfer function	Fit cost
Baseline model 7th order	1-30 r/s	$\frac{2.62[0.413, 3.07][0.0696, 16.2]e^{-0.0225s}}{(0)[0.277, 2.75][0.0421, 15.8][0.509, 13.7]}$ †	12.1
Coupled body/rotor 5th order	1-30 r/s	$\frac{2.47[0.490, 3.11]e^{-0.0218s}}{(0)[0.319, 2.71][0.413, 13.5]}$	26.8
Broad-band quasi-steady 4th order	1-30 r/s	$\frac{0.200[0.283, 2.04]e^{-0.0743s}}{(0)[0.214, 2.13](9.87)}$	102.3
13 r/s band-limited quasi-steady 2nd order	1-13 r/s	$\frac{0.300e^{-0.0838s}}{(0)(14.6)}$	44.2

†Shorthand notation: $[\zeta, \omega]$ implies $s^2 + 2\zeta\omega s + \omega^2$, ζ = damping ratio, ω = undamped natural frequency (rad/sec); and (1/T) implies s + (1/T), rad/sec.

Table 1b Comparison of performance estimates

Model	Open-loop metrics ϕ/ϕ_c		Closed-loop metrics (ϕ/ϕ_m)		
	ω_c (rad/sec)	GM (dB)	ω_u (rad/sec)	ω_{BW} (rad/sec)	τ_p (sec)
Data	5.72	6.39	11.4	8.58	0.0658
Baseline model	5.32	6.51	11.8	9.46	0.0659
Coupled body/rotor	5.33	5.70	11.5	9.62	0.0682
Broad-band quasi-steady	4.28	10.2	10.2	6.98	0.0545
13 r/s band-limited	5.26	7.96	11.1	8.33	0.0600

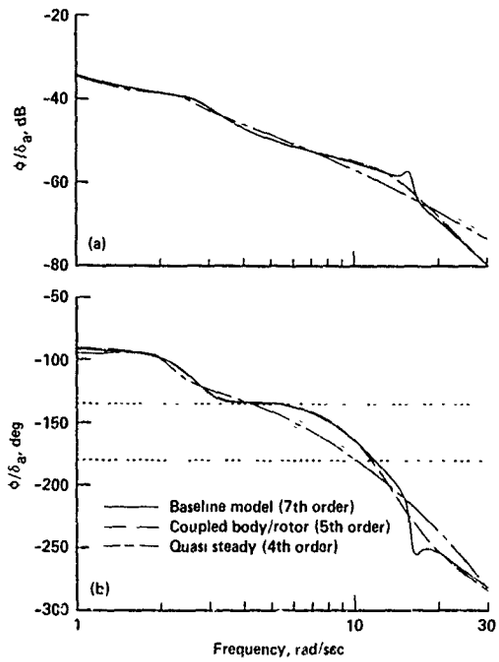

Fig. 10 Lower-order broad band models.

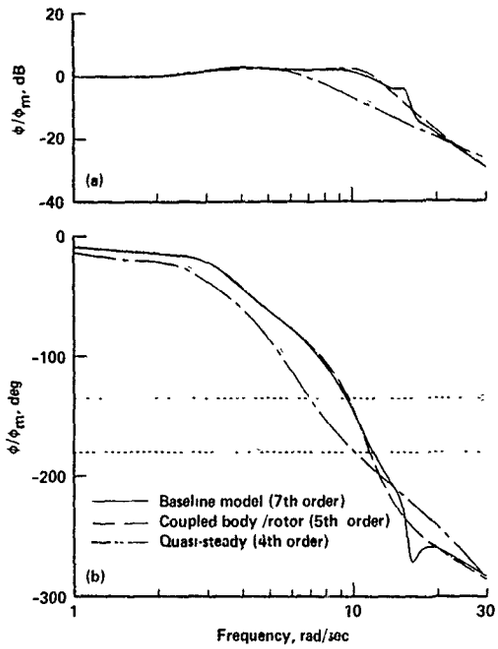

Fig. 11 Closed loop responses of lower-order broad-band models.

A 4th-order model is obtained by adopting a quasi-steady assumption for the roll dynamics and treating the rotor as an equivalent time delay. The resulting transfer function model fit is given in Table 1. The time delay of 0.0743 sec now accounts for 0.023 sec from the hydraulics/actuator system and 0.051 sec from the effective rotor delay. The quasi-steady roll damping mode is estimated at $L_p = -9.87$ r/s. The dutch roll pole/zero quadratic has been de-tuned for this single axis fit. (This could be improved by considering a simultaneous match of β/δ_f, which will enforce the correct dutch roll location (Ref. 8).) The frequency-response of this model is seen in Fig. 10 to be a poor approximation, especially at higher-frequency, as expected by the adoption of a crude rotor flapping approximation. This is further emphasized by the three-fold increase in the fitting cost relative to the 5th-order model (Table 1). The 45° phase margin cross-over frequency is under-predicted by 20% relative to the baseline model, while the gain margin is overpredicted by 57% (Table 1b).

The root locus versus attitude gain for this model (Fig. 12) indicates that the gain limitation is due to the destabilization of a coupled 2nd-order pure rigid body mode. Thus, the quasi-steady fails to capture key dynamics of the coupled roll/flapping mode. Finally, the closed-loop bandwidth is underestimated by 26% as indicated in Fig. 11 and Table 1b. Overall, the use of the 4th order model to match the full frequency range (1-30 r/s) is seen to be inappropriate.

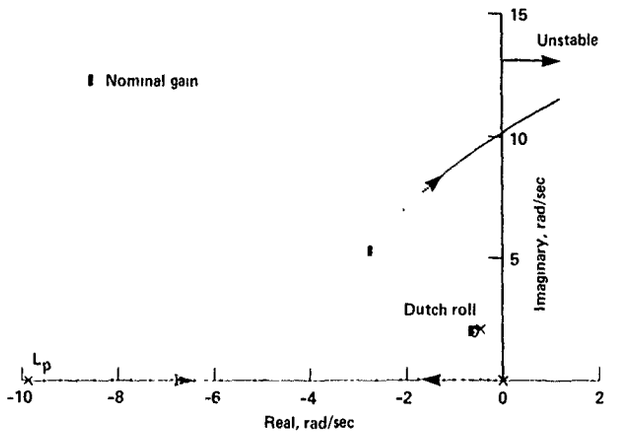

Fig. 12 Stabilization-loop root locus for 5th order (quasi-steady) model varying attitude gain, K_ϕ.

6. QUASI-STEADY MODELS FOR LOW-FREQUENCY ROLL RESPONSE

The utility of the quasi-steady approximation in characterizing the lower-frequency dynamics was investigated. For this study, the dutch roll dynamics were omitted. Figure 13 shows the variation in L_p and the fitting cost for changes in the upper fitting frequency, ω_2, from 8-30 r/s. The roll damping rises from $L_p = -9.3$ for $\omega_2 = 8$ r/s, to $L_p = 20.4$ for $\omega_2 = 15$ r/s; however, the cost function remains fairly constant in this range. For ω_2 beyond 14 r/s, the cost function rises dramatically, indicating a poor characterization of the dynamic response. Note that for the $\omega_2 = 30$ r/s, the roll damping drops to $L_p = -9.6$, which closely corresponds to the 4th-order model of Table 1a. The extreme sensitivity in the model parameters and cost function for values of ω_2 greater than 14 r/s shows that this frequency is the limit of the validity of the quasi-steady assumption. For ω_2 below 14 r/s the cost function remains fairly constant at CF = 45, which roughly corresponds with the 5th order fitting error, the higher-order model being more accurate as expected. The variability in L_p seen even for $\omega_2 = 7$-13 r/s will be limited by the simultaneous fit of multiple responses in the full model identification (Ref. 16). The ϕ/δ_a frequency-response for the $\omega_2 = 13$ r/s case is shown in Fig. 14 to have comparable accuracy as the baseline model in the range of 1-13 r/s (except for the omission of the dutch roll mode). The estimated crossover frequency is nearly identical to the high-order baseline model. Also, the closed-loop performance metrics are much closer to the baseline model than was the 4th-order model (Table 1b). The 1st order model for $\omega_2 = 30$ r/s, also shown in Fig. 14, is seen to poorly characterize the response at both low and high frequency. The frequency range of the fit is clearly inappropriate for the quasi-steady model structure. A similar analysis conducted on the pitch response indicates a useful bandwidth for the quasi-steady assumption of 13 r/s. Thus, the overall useful bandwidth of the quasi-steady model structure is 13 r/s.

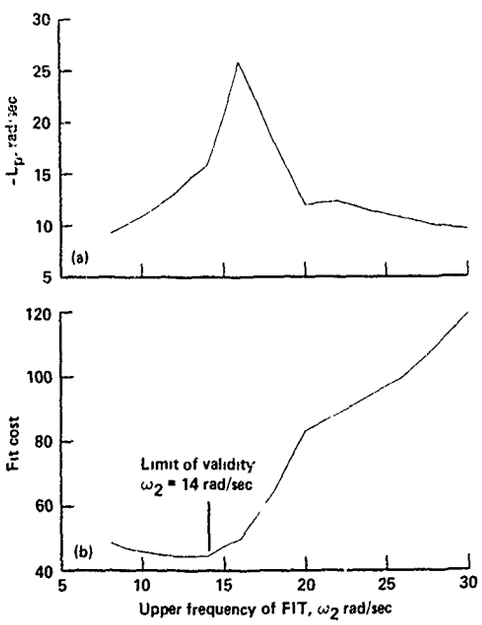

Fig. 13 Effect of upper frequency limit ω_2 on quasi-steady identification; lower limit of fit is fixed, $\omega_1 = 1.0$ r/s.

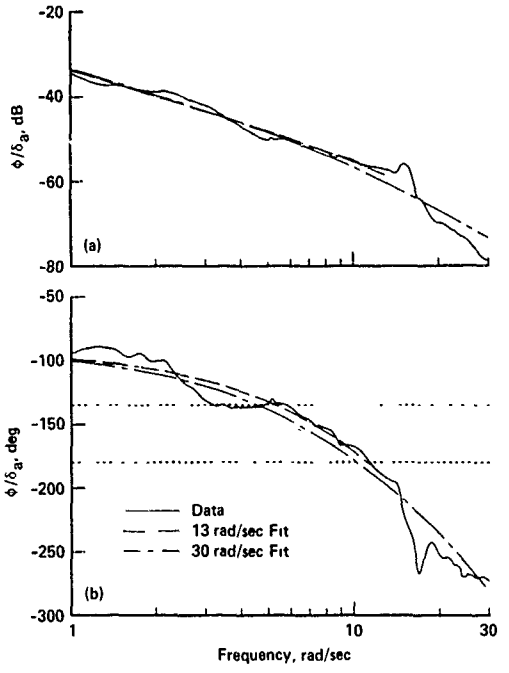

Fig. 14 Bandlimited and broad-band quasi-steady models.

This analysis indicates that improved utility of the quasi-steady models can be achieved if the data are band-limited to below the rotor flapping frequency (13 r/s in this case) before the identification is completed. This band-limitation is easily accomplished in frequency-domain identification methods, since the fitting range is an explicit function of frequency (Refs. 16 and 17). In time-domain methods, the data should be filtered to eliminate the high-frequency dynamics (Ref. 6). Although the coupled rotor/flapping instability can still not be replicated with such band-limited quasi-steady models, the nominal control system performance may be adequately estimated.

7. CONCLUSIONS

(1) An accurate model for helicopter control system studies requires coupled body/rotor flapping and lead-lag dynamics. The lead-lag response may be treated as a one-way coupled parasitic mode for the case study evaluated herein.

(2) For a single-rotor hingeless helicopter, the coupled body/rotor-flapping mode limits the gain on attitude feedback, while the lead-lag mode limits the gain on attitude-rate feedback.

(3) Quasi-steady models that approximate the rotor response by an equivalent delay are useful for estimating nominal control system performance if the data used in the identification is bandlimited to frequencies below the coupled body/rotor response.

REFERENCES

1. Kaletka, J. and von Grunhagen, W. "Identification of Mathematical Derivative Models for the Design of a Model Following Control System," 45th Annual National Forum of the American Helicopter Society, Boston, MA, May 22-24, 1989.

2. Bosworth, J. T. and West, J. C. "Real-Time Open-Loop Frequency Response Analysis of Flight Test Data," AIAA Paper 86-9738, 3rd AIAA Flight Testing Conference, Las Vegas, 1986.

3. Hall, W. E., Jr. and Bryson, A. E., Jr. "Inclusion of Rotor Dynamics in Controller Design," AIAA J. Aircraft, Vol. 10, 1973, pp. 200-206.

4. Hoh, R. H., Mitchell, D. G., Aponso, B. L., Key, D. L., and Blanken, C. L. "Proposed Specification for Handling Qualities of Military Rotorcraft. Vol. 1-Requirements," USAAVSCOM Tech Report 87-A-4. May 1988.

5. Tischler, M. B. "Digital Control of Highly Augmented Combat Rotorcraft," NASA TM-88346, May 1987.

6. Chen, R. T. N. and Tischler, M. B. "The Role of Modeling and Flight Testing in Rotorcraft Parameter Identification," System Identification Session, 42nd Annual National Forum of the American Helicopter Society, Washington, DC, June 1986.

7. Tischler, M. B., Fletcher, J. W., Diekmann, V. L., Williams, R. A., and Cason, R. W. "Demonstration of Frequency-Sweep Testing Technique using a Bell 214-ST Helicopter," NASA TM-89422, April 1987.

8. Tischler, M. B. "Frequency-Response Identification of XV-15 Tilt-Rotor Aircraft Dynamics," NASA TM-89428, May 1987.

9. Taylor, L. W., Jr. "Application of a New Criterion for Modeling Systems," AGARD CP-172, November 1974.

10. Heffley, R. K., Bourne, S. M., Curtiss, H. C., Jr., and Hess, R. A. "Study of Helicopter Roll Control Effectiveness Criteria," NASA CR-177404, April 1986.

11. Warmbrodt, W. and Peterson, R. L. "Hover Test of a Full-Scale Hingeless Rotor," NASA TM-85990, August 1984.

12. Diftler, M. A. "UH-60A Helicopter Stability Augmentation Study," paper no. 74, 14th European Rotorcraft Forum, Milano, Italy, September 20-23, 1988.

13. Miller, D. G. and White, F. A. "Treatment of the Impact of Rotor-Fuselage Coupling on Helicopter Handling Qualities," 43rd Annual Forum of the American Helicopter Society, May 1987.

14. Curtiss, H. C., Jr. "Stability and Control Modeling," paper no. 41, 12th European Rotorcraft Forum, Garmisch-Partenkirchen, Federal Republic of Germany, September 1986.

15. Chen, R. T. N. and Hindson, W. S. "Influence of Higher-Order Dynamics on Helicopter Flight Control System Bandwidth," AIAA J. Guidance, Vol. 9, 1986, pp. 190-197.

16. Tischler, M. B. and Cauffman, M. G. "Frequency-Response Method for Rotorcraft System Identification with Applications to the BO-105 Helicopter," Dynamics I-Session, 46th Forum, American Helicopter Society, Washington, DC, May 21-23, 1990.

17. Tischler, M. B. "Advancements in Frequency-Domain Methods for Rotorcraft System Identification," 2nd International Conference on Basic Rotorcraft Research, College Park, Maryland, Feb. 1988.

Bibliography

This bibliography was prepared by the German Federal Armed Forces Defence and Information Centre (DokFizBw), Bonn, Germany in association with the Lecture Series Director (Dr. P. Hamel) and one of the authors (Mr. J. Kaletka), both of the DLR Institute for Flight Mechanics.

Quest Accession Number 91A17282
91A17282 NASA IAA Conference Paper Issue 05
Helicopter parameter identification using a trained multi-perceptron neural network
(AA)LAM, QUANG M , (AB)PELOSI, LOUIS P (AC)CLAPP, RICHARD H , (AD)KAM, MOSHE
(AC)(Symetica Corp , Command and Control Div Warminster, PA), (AD)(Drexel University, Philadelphia, PA)
IN AHS, Annual Forum, 46th, Washington, DC, May 21-23, 1990 Proceedings Volume 2 (A91-17201 05-01) Alexandria, VA, American Helicopter Society, 1990 p 1017-1033 900000 p 17 refs 24 In EN (English) p 653

A trained multi-perceptron is used to perform helicopter parameter identification A learning algorithm based on error back-propagation is adopted in order to copy an input-output mapping into the network , which then realizes a parameter identification algorithm The resulting architecture is used to reconstruct the stability and control derivatives of a UH-60A helicopter model, using simulated data at hover mode The simulated data is generated with various system noise intensities to mimic realistic true helicopter data The studied neural network identifier is found to be useful to the estimation task for the following reasons (1) it does not require a priori information, (2) it is relatively insensitive to system uncertainties (e g , levels, model structures), (3) it demonstrates high relaxation on input designs and output samples, and (4) it has self-learning ability to adjust the parameter estimate motion to compensate for incorrect model structure selection and to assure the fidelity of the identified model in comparison with the 'true' system responses
Author

Category code 08 (aircraft stability/control)
Controlled terms *AIRCRAFT MODELS /*NEURAL NETS /*PARAMETER IDENTIFICATION /*SELF ORGANIZING SYSTEMS /*UH-60A HELICOPTER / AIRCRAFT STABILITY / ALGORITHMS / COMPUTERIZED SIMULATION / NOISE INTENSITY / STABILITY DERIVATIVES /

Quest Accession Number 90A45156
90A45156# NASA IAA Conference Paper Issue 20
Parameter identification of linear systems based on smoothing
(AA)BRYSON, A. E , (AB)DAN, M
(AA)(Stanford University, CA)
Stanford Univ , CA (90380476)
AIAA PAPER 90-2800 IN AIAA Atmospheric Flight Mechanics Conference, Portland, OR, Aug 20-22, 1990, Technical Papers (A90-45134 20-03) Washington, DC, American Institute of Aeronautics and Astronautics 1990 p 238-248 Research supported by NASA and Advanced Rotorcraft Technology, Inc 900000 p 11 refs 22 In EN (English) p 3155

A parameter identification algorithm for linear systems is presented It is based on smoothing test data with different sets of system model parameters The smoothing pass through the data provides all the information needed to compute the gradients of the smoothing performance measure with respect to the parameters The parameters are updated using a quasi-Newton procedure, until convergence is achieved The advantage of this algorithm over standard maximum likelihood identification algorithms is the computational savings in calculating the gradient This approach is extended to identify one set of parameters from several test runs The performance of this algorithm is demonstrated in identifying the parameters of a linear model describing the rigid body dynamics of the DLR BO-105 research helicopter from flight test data The identification results are presented and compared to recently published models using maximum likelihood and frequency-domain algorithms The models presented are in good agreement with each other
Author

Category code 08 (aircraft stability/control)
Controlled terms *AIRCRAFT MANEUVERS /*AIRCRAFT MODELS /*DATA SMOOTHING /*LINEAR SYSTEMS /*MAXIMUM LIKELIHOOD ESTIMATES /*PARAMETER IDENTIFICATION / FLIGHT ENVELOPES / GOODNESS OF FIT / MATHEMATICAL MODELS / NEWTON METHODS /

Quest Accession Number 91A17207
91A17207 NASA IAA Conference Paper Issue 05
Frequency-response method for rotorcraft system identification with applications to the BO-105 helicopter
(AA)TISCHLER MARK B (AB)CAUFFMAN, MAVIS G,
(AA)(U S Army, Aeroflightdynamics Directorate, Moffett Field CA), (AB)(Sterling Federal Systems, Inc , Palo Alto, CA)
IN AHS, Annual Forum, 46th, Washington, DC May 21-23, 1990, Proceedings Volume 1 (A91-17201 05-01) Alexandria, VA, American Helicopter Society, 1990, p 99-137 900000 p 39 refs 26 In EN (English) p 647

The present comprehensive frequency-response method for rotorcraft system identification extracts a complete set of nonparametric input/output frequency responses which characterizes coupled helicopter dynamics, while conducting a search for a state-space model matching the frequency-response data set By subsequently combining the results of multiinput frequency-response analyses obtained from a range of spectral windows into a single optimized response, the manual optimization of windows is obviated A nine-degree-of-freedom hybrid model which encompasses coupled body/rotor flapping and lead-lag dynamics, and is accurate to 30 rad/sec, is applied to flight control design, it is found that the maximum roll rate gain is limited by the destabilization of the lead-lag dynamics
O C

Category code 05 (aircraft design, testing, performance)
Controlled terms *BO-105 HELICOPTER /*FLAPS (CONTROL SURFACES) /*FREQUENCY RESPONSE / HELICOPTER CONTROL /*ROTOR BODY INTERACTIONS /*ROTORCRAFT AIRCRAFT / AERODYNAMIC CHARACTERISTICS / DEGREES OF FREEDOM / FLIGHT CONTROL / SPECTRAL METHODS / SYSTEM IDENTIFICATION /

Quest Accession Number 90A33057
90A33057# NASA IAA Journal Article Issue 13
Comparison of test signals for aircraft frequency domain identification
(AA)YOUNG, PETER, (AB)PATTON, RONALD J
(AB)(York, University, England)
(AIAA Atmospheric Flight Mechanics Conference, Minneapolis, MN, Aug 15-17, 1988, Technical Papers, p 161-169) Journal of Guidance, Control, and Dynamics (ISSN 0731-5090), vol 13, May-June 1990, p 430-438 Research supported by SERC and Royal Aircraft Establishment Previously cited in issue 21, p 3487, Accession no A88-50593 900600 p 9 refs 20 In EN (English) p 1962

Category code 05 (aircraft design, testing, performance)
Controlled terms *AIRCRAFT CONTROL /*CONTROL SYSTEMS DESIGN /* DYNAMIC CONTROL /*HELICOPTER CONTROL /*REMOTELY PILOTED VEHICLES / CURVE FITTING / FEEDBACK CONTROL / FREQUENCY SCANNING / HELICOPTER PERFORMANCE / LEAST SQUARES METHOD / STRUCTURAL ANALYSIS / SYSTEM IDENTIFICATION / TRANSFER FUNCTIONS /

Quest Accession Number 90A45333
90A45333*# NASA IAA Journal Article Issue 20
System identification requirements for high-bandwidth rotorcraft flight control system design
(AA)TISCHLER, MARK B
(AA)(NASA, Ames Research Center, U S Army, Aeroflightdynamics Directorate, Moffett Field, CA)
National Aeronautics and Space Administration Ames Research Center, Moffett Field, CA (NC473657)
Journal of Guidance, Control, and Dynamics (ISSN 0731-5090), vol 13, Sept -Oct 1990, p 835-841 901000 p 7 refs 17 In EN (English) p 3157

The application of system identification methods to high-bandwidth rotorcraft flight control system design is examined Flight test and modeling requirements are illustrated using flight test data from a BO-105 hingeless rotor helicopter. The proposed approach involves the identification of nonparametric frequency-response models followed by parametric (transfer funtion and state space) model identification Results for the BO-105 show the need for including coupled body/rotor flapping and lead-lag dynamics in the identification model structure to allow the accurate prediction of control system bandwidth limitations Lower-order models are useful for estimating nominal control system performance only when the flight data used for the identification are band-limited to be consistent with the frequency range of applicability of the model. The flight test results presented in this paper are consistent with theoretical studies by previous researchers
Author

Category code 08 (aircraft stability/control)
Controlled terms *CONTROL SYSTEMS DESIGN /*FLIGHT CONTROL /* HELICOPTER CONTROL /*SYSTEM IDENTIFICATION / FLIGHT TESTS / FREQUENCY RESPONSE / ROLLING MOMENTS /

Quest Accession Number 90N18389
90N18389# NASA STAR Conference Paper Issue 11
Time and frequency-domain identification and verification of BO-105 dynamic models
(AA)KALETKA, JUERGEN, (AB)GRUENHAGEN, WOLFGANG V , (AC)TISCHLER, MARK B , (AD)FLETCHER, JAY W
(AB)(Deutsche Forschungs- und Versuchsanstalt fuer Luft- und Raumfahrt, Brunswick, Germany, F R)
Army Aviation Research and Development Command, Moffett Field, CA (AZ143936) Aeroflight Dynamics Directorate
AD-A216828 890915 p 26 Presented at the 15th European Rotorcraft Forum, Amsterdam, Netherlands, 12-15 Sep 1989 In EN (English) Avail NTIS HC A03/MF A01 p 1456

Mathematical models for the dynamics of the DLR BO 105 helicopter are extracted from flight test data using two different approaches frequency-domain and time-domain identification Both approaches are reviewed Results from an extensive data consistency analysis are given Identifications for 6 degrees of freedom (DOF) rigid body models are presented and compared in detail The extracted models compare favorably and their prediction capability is demonstrated in verification results Approaches to extend the 6 DOF models are addressed and first results are presented System identification is broadly defined as the deduction of system characteristics from measured data It provides the only possibility to extract both non-parametric (e g , frequency responses) and parametric (e g , state space matrices) aircraft models from flight test data and therefore gives a reliable characterization of the dynamics of the actually existing aircraft Main applications of system identification are seen in areas where higher accuracies of the mathematical models are required Simulation validation, control system design (in particular model-following control system design for in-flight simulation), and handling qualities
GRA

Category code 05 (aircraft design, testing, performance)
Controlled terms *DATA PROCESSING /*DYNAMIC MODELS /*FLIGHT SIMULATION /*FLIGHT TESTS /*HELICOPTERS /*RIGID STRUCTURES / AIRCRAFT MODELS / CONSISTENCY / DEGREES OF FREEDOM / PREDICTION ANALYSIS TECHNIQUES / QUALITY /

Quest Accession Number 90A19723
90A19723# NASA IAA Preprint Issue 06
UH-60 flight data replay and refly system state estimator analysis
(AA)MORTON, MARK S
AIAA PAPER 90-0181 AIAA, Aerospace Sciences Meeting, 28th, Reno, NV, Jan 8-11, 1990 12 p 900100 p 12 refs 9 In EN (English) p 767

Research currently underway at the University of Alabama Flight Dynamics Lab (UAFDL) investigates concepts for implementation of a ground-based UH-60 Flight Data Replay and Refly System (UH-60 FDRRS) A variation of a Linearized Extended Kalman filter is implemented which utilizes a mathematical model of the UH-60 to accurately re-create a UH-60 helicopter flight based on flight measurements Presented in this paper is a the development of the UH-60 mathematical model, an experimental verification of the Kalman filter implementation, and an experimental evaluation of filter sensitivity to initial condition errors, measurement sample rate reductions, and

model parameter variations. Results indicate that vehicle dynamics are represented with sufficient fidelity by the UH-60 mathematical model for both filter design and piloted simulation, providing a replay and a refly capability. Experimental analysis of the Kalman filter indicates that the current filter exhibits a robust tracking ability for low measurement sample rates, demonstrates relatively fast, stable convergence in the presence of initial condition errors, yet manifests a notable performance degradation due to weight variations.
Author

Category code 08 (aircraft stability/control)
Controlled terms *FLIGHT SAFETY /*FLIGHT SIMULATION /*KALMAN FILTERS /*PILOT TRAINING /*STATE ESTIMATION /*UH-60A HELICOPTER / ARMED FORCES (UNITED STATES) / FLIGHT RECORDERS / HELICOPTER CONTROL /

Quest Accession Number . 90A12775
90A12775 NASA IAA Journal Article Issue 02
Experience with multi-step test inputs for helicopter parameter identification
(AA)LEITH, D ., (AB)MURRAY-SMITH, D J
(AB)(Glasgow, University, Scotland)
Vertica (ISSN 0360-5450), vol. 13, no 3, 1989, p 403-412 890000
p 10 refs 10 In EN (English) p 154

A test input design method developed to provide test signals with good properties for helicopter parameter identification is described. The features that should be present in the autospectrum of a desirable test signal are presented. Data on 1221 and double-doublet inputs are analyzed.
K K

Category code 08 (aircraft stability/control)
Controlled terms. *EXPERIMENT DESIGN /*HELICOPTER PERFORMANCE /* PARAMETER IDENTIFICATION / FLIGHT MECHANICS / MAXIMUM LIKELIHOOD ESTIMATES / OPTIMAL CONTROL / ROBUSTNESS (MATHEMATICS) / SPECTRAL METHODS / SYSTEM IDENTIFICATION / SYSTEMS SIMULATION /

Quest Accession Number 90A12774
90A12774 NASA IAA Journal Article Issue 02
Time domain parameter identification techniques applied to the UH-60A Black Hawk Helicopter
(AA)TEARE, D A ., (AB)FITZSIMONS, P M ., (AC)TONGUE, B H ., (AD)SCHRAGE, D P
(AD)(Georgia Institute of Technology, Atlanta)
Vertica (ISSN 0360-5450), vol. 13, no 3, 1989, p 393-401 890000
p 9 refs 7 In EN (English) p 259

The modeling and system identification of rotorcraft is described. The least squares and maximum likelihood methods are applied to flight test data from the UH-60A Black Hawk Helicopter. The trimmed flight conditions studied are forward flight at 100 knots and hover. Consideration is given to the derivation of helicopter equations of motion and the linearization of the equations of motion.
K K

Category code 63 (cybernetics)
Controlled terms *AERODYNAMIC CHARACTERISTICS /*LEAST SQUARES METHOD /*MAXIMUM LIKELIHOOD ESTIMATES /*PARAMETER IDENTIFICATION /* UH-60A HELICOPTER / EQUATIONS OF MOTION / HELICOPTER PERFORMANCE / MATHEMATICAL MODELS / SYSTEM IDENTIFICATION /

Quest Accession Number 90A12773
90A12773 NASA IAA Journal Article Issue 02
The application of linear maximum likelihood estimation of aerodynamic derivatives for the Bell-205 and Bell-206
(AA)DE LEEUW, J H ., (AB)HUI, K
(AA)(Toronto, University, Downsview, Canada), (AB)(National Aeronautical Establishment, Flight Research Laboratory, Ottawa, Canada)
Vertica (ISSN 0360-5450), vol 13, no 3, 1989, p 369-392 890000
p 24 refs 26 In EN (English) p.145

The application of parameter estimation techniques to helicopters to determine the stability and control derivatives is described. The model adopted for the helicopter is a linear fully coupled six-degree-of-freedom rigid body system. The estimation of the parameter values in this model (the stability and control derivatives) is carried out on the basis of flight tests in which the helicopter is excited by suitable control inputs.
K K

Category code 05 (aircraft design, testing, performance)
Controlled terms *AERODYNAMIC STABILITY /*AIRCRAFT CONTROL /*BELL AIRCRAFT /*HELICOPTER PERFORMANCE /*MAXIMUM LIKELIHOOD ESTIMATES /* STABILITY DERIVATIVES / CONTROL SYSTEMS DESIGN / FLIGHT CONTROL / FLIGHT SIMULATION / FLIGHT TESTS / PARAMETER IDENTIFICATION / SYSTEM IDENTIFICATION /

Quest Accession Number 90A12772
90A12772 NASA IAA Journal Article Issue 02
A frequency-domain system identification approach to helicopter flight mechanics model validation
(AA)BLACK, C G (AB)MURRAY-SMITH, D .I
(AB)(Glasgow, University, Scotland)
Vertica (ISSN 0360-5450), vol 13, no 3, 1989, p 343-368 Research supported by the Ministry of Defence Procurement Executive 890000
p 26 refs 23 In EN (English) p 154

The development of methods for the validation of complex nonlinear models of helicopter dynamics using measured flight data is discussed. The transformation to the frequency domain is addressed as well as equation-error methods in the frequency domain. Advantages of the methodology include the use of a restricted frequency range for the estimation of parameters of the rigid-body model and the incorporation of time delays into the model.
K K

Category code 08 (aircraft stability/control)
Controlled terms *AIRCRAFT MODELS /*FLIGHT MECHANICS /*HELICOPTER PERFORMANCE /*ROTOR AERODYNAMICS /*SYSTEM IDENTIFICATION / DEGREES OF FREEDOM / FREQUENCY RESPONSE / MATHEMATICAL MODELS / PARAMETER IDENTIFICATION / PITCHING MOMENTS /

Quest Accession Number 90A12770
90A12770 NASA IAA Journal Article Issue 02
Flight simulation model validation procedure, a systematic approach
(AA)DU VAL, R W ; (AB)BRUHIS, O ., (AC)HARRISON, J M ., (AD)HARDING, J W
(AB)(Advanced Rotorcraft Technology, Inc ., Mountain View, CA), (AD)(McDonnell Douglas Helicopter Co ., Mesa, AZ)
Vertica (ISSN 0360-5450), vol 13, no 3, 1989, p 311-326. 890000
p 16 refs 6 In EN (English) p 144

A flight simulation model validation procedure is applied to the FLYRT model of the U S Army/McDonnell Douglas AH-64 Apache attack helicopter. The procedure uses an Extended Kalman Filter/Smoother Algorithm to estimate the 'true' states and aerodynamic loads from flight test data. FLYRT is then driven by these estimated states and controls to produce comparison aerodynamic loads. Discrepancies are further isolated by comparing measured flapping to simulated flapping data. System identification techniques are applied to improve the flapping representation. The measured flapping exhibits a significant torsional flexibility effect and velocity dependence due to first harmonic inflow is also observed. The flapping model is upgraded to include these effects and the upgraded model is shown to produce good flapping correlation at low speed.
Author

Category code 05 (aircraft design, testing, performance)
Controlled terms *AEROELASTICITY /*AH-64 HELICOPTER /*AIRCRAFT MODELS /*FLIGHT SIMULATION /*ROTOR AERODYNAMICS /*SYSTEM IDENTIFICATION / AERODYNAMIC LOADS / FLUTTER ANALYSIS / HELICOPTER DESIGN / MATHEMATICAL MODELS / STATE ESTIMATION /

Quest Accession Number 90A12771
90A12771* NASA IAA Journal Article Issue 02
Advancements in frequency-domain methods for rotorcraft system identification
(AA)TISCHLER, MARK B
(AA)(NASA, Ames Research Center, U S Army, Aeroflightdynamics Directorate, Moffett Field, CA)
National Aeronautics and Space Administration Ames Research Center, Moffett Field, CA (NC473657)
Vertica (ISSN 0360-5450), vol 13, no 3, 1989, p 327-342 890000
p 16 refs 19 In EN (English) p 154

A new method for frequency-domain identification of rotorcraft dynamics is presented. Nonparametric frequency-response identification and parametric transfer-function modeling methods are extended to allow the extraction of state-space (stability and control derivative) representations. An interactive computer program DERIVID is described for the iterative solution of the multi-input/multi-output frequency-response matching approach used in the identification. Theoretical accuracy methods are used to determine the appropriate model structure and degree-of-confidence in the identified parameters. The method is applied to XV-15 tilt-rotor aircraft data in hover. Bare-airframe stability and control derivatives for the lateral/directional dynamics are shown to compare favorably with models previously obtained using time-domain identification methods and the XV-15 simulation program.
Author

Category code 08 (aircraft stability/control)
Controlled terms *AERODYNAMIC STABILITY /*FREQUENCY RESPONSE /* ROTOR AERODYNAMICS /*SYSTEM IDENTIFICATION /*XV-15 AIRCRAFT / COMPUTERIZED SIMULATION / FLIGHT SIMULATION / ITERATIVE SOLUTION / MATHEMATICAL MODELS / PARAMETER IDENTIFICATION / TRANSFER FUNCTIONS /

Quest Accession Number . 90A12769
90A12769* NASA IAA Journal Article Issue 02
Identification of rotor flapping equation of motion from flight measurements with the RSRA compound helicopter
(AA)WANG, JI C ., (AB)TALBOT, PETER D
(AA)(San Jose State University, CA), (AB)(NASA, Ames Research Center, Moffett Field, CA)
San Jose State Univ ., CA (S8413977)
NCC2-267 Vertica (ISSN 0360-5450), vol 13, no 3, 1989, p. 295-309 890000 p 15 refs 23 In EN (English) p 154

The application of an integrated rotorcraft identification method to the linear modeling of rotor system dynamics is studied. Two approaches used to describe the rotor flapping parameters in the rotor state dynamic equations and the period coefficients of the blade flapping equation of motion are presented. In the first approach, the parameters are identified in the nonrotating reference frame, in the second, the blade equivalent damping and spring periodic coefficients as well as other periodic coefficients are identified in the rotating reference frame.
K K

Category code 08 (aircraft stability/control)
Controlled terms *AIRFOIL OSCILLATIONS /*HELICOPTER PERFORMANCE /* PARAMETER IDENTIFICATION /*ROTOR AERODYNAMICS /*SYSTEM IDENTIFICATION / FLIGHT TESTS / MATHEMATICAL MODELS / RESEARCH AIRCRAFT / ROTARY WINGS / SYSTEMS INTEGRATION /

Quest Accession Number 90A12768
90A12768 NASA IAA Journal Article Issue 02
System identification strategies for helicopter rotor models incorporating induced flow
(AA)BRADLEY R., (AB)BLACK, C G ., (AC)MURRAY-SMITH, D J.
(AC)(Glasgow, University, Scotland)

Vertica (ISSN 0360-5450), vol 13, no 3, 1989, p 281-293 Research supported by the Ministry of Defence of England 890000 p 13 refs 7 In EN (English) p 144

A technique based primarily on frequency-domain output-error methods is presented for the identification of rotor models Strategies involving different forms of model structure using induced-flow models based on either momentum or vortex theory are presented The importance of induced-flow effects for the flight data sets used is studied
K K

Category code 05 (aircraft design, testing, performance)
Controlled terms *AIRCRAFT MODELS /*HELICOPTER CONTROL /*HELICOPTER PERFORMANCE /*ROTOR AERODYNAMICS /*SYSTEM IDENTIFICATION / CONTROL SYSTEMS DESIGN / MATHEMATICAL MODELS / MOMENTUM THEORY / ROTARY WINGS / STATE ESTIMATION /

Quest Accession Number 90A12767
90A12767* NASA IAA Journal Article Issue 02
Identification of a coupled flapping/inflow model for the PUMA helicopter from flight test data
(AA)DU VAL, RONALD, (AB)BRUHIS, OFER, (AC)GREEN, JOHN
(AC)(Advanced Rotorcraft Technology, Inc , Mountain View, CA)
Advanced Rotorcraft Technology, Inc , Mountain View, CA (A0237073)
Vertica (ISSN 0360-5450), vol. 13, no 3, 1989, p 267-280 Research supported by NASA 890000 p 14 In EN (English) p 154

A model validation procedure is applied to a coupled flapping/inflow model of a PUMA helicopter blade The structure of the baseline model is first established Model structure and flight test data are checked for consistency Parameters of the model are then identified from the flight test data
Author

Category code 08 (aircraft stability/control)
Controlled terms *AIRCRAFT MODELS /*FLIGHT TESTS /*HELICOPTER PERFORMANCE /*ROTARY WINGS /*ROTOR AERODYNAMICS /*SYSTEM IDENTIFICATION / AIRFOIL OSCILLATIONS / COUPLED MODES / FLIGHT SIMULATION / MATHEMATICAL MODELS / PARAMETER IDENTIFICATION /

Quest Accession Number 90A12766
90A12766 NASA IAA Journal Article Issue 02
Identification of an adequate model for collective response dynamics of a Sea King helicopter in hover
(AA)FEIK, R A , (AB)PERRIN, R H
(AB)(Department of Defence, Aeronautical Research Laboratories, Melbourne, Australia)
Vertica (ISSN 0360-5450), vol 13, no 3, 1989, p 251-265 890000 p 15 refs 16 In EN (English) p 154

A mathematical representation of a vertical acceleration response characteristics of a helicopter in hover has been developed, including blade flapping, inflow, and rotor speed dynamics A Maximum Likelihood parameter estimation technique has been applied to assess the adequacy of the model, and to identify the relevant parameters, using flight data from a Sea King Mk 50 helicopter A number of conclusions related to the validity of the modeling approach have resulted from comparisons between predicted and identified parameters, and further investigation of some aspects are indicated
Author

Category code 08 (aircraft stability/control)
Controlled terms *DYNAMIC RESPONSE /*HELICOPTER PERFORMANCE /*HOVERING /*PARAMETER IDENTIFICATION /*ROTOR AERODYNAMICS /*SH-3 HELICOPTER /*VERTICAL MOTION / AIRCRAFT MODELS / MATHEMATICAL MODELS / MAXIMUM LIKELIHOOD ESTIMATES / ROTOR SPEED / STATE ESTIMATION /

Quest Accession Number 90A12765
90A12765 NASA IAA Journal Article Issue 02
Identification of a coupled body/coning/inflow model of Puma vertical response in the hover
(AA)HOUSTON, S S
(AA)(Royal Aerospace Establishment, Flight Dynamics Div , Bedford, England)
Vertica (ISSN 0360-5450), vol. 13, no 3, 1989, p 229-249 890000 p 21 refs 19 In EN (English) p 153

An attempt is made to better understand helicopter behavior in the hover through the identification of a coupled three-degree-of-freedom model of the Puma aircraft The model can be used to explain why quasi-steady theory fails to predict heave axis damping and control sensitivity The verification of the model using an input dissimilar to that used in the identification process confirms that the Puma exhibits quasi-steady heave damping and control sensitivity significantly lower than that predicted by theory.
K K

Category code 08 (aircraft stability/control)
Controlled terms *AEROELASTICITY /*HELICOPTER PERFORMANCE /*HOVERING /*INTERACTIONAL AERODYNAMICS /*SYSTEM IDENTIFICATION /*UNSTEADY AERODYNAMICS / AIRCRAFT MODELS / COUPLED MODES / DEGREES OF FREEDOM / FLIGHT TESTS / MATHEMATICAL MODELS / VIBRATION DAMPING /

Quest Accession Number 90A12764
90A12764 NASA IAA Journal Article Issue 02
Identification of mathematical derivative models for the design of a model following control system (for fly-by-wire helicopter)
(AA)KALETKA, JUERGEN; (AB)VON GRUENHAGEN, WOLFGANG
(AB)(DLR, Institut fuer Flugmechanik, Brunswick, Federal Republic of Germany)
(AHS, Annual Forum, 45th, Boston, MA, May 1989) Vertica (ISSN 0360-5450), vol 13, no 3, 1989, p. 213-228. 890000 p 16 refs 9 In EN (English) p 153

Accurate mathematical models were required for the design of a model following control system for the DLR BO 105 fly-by-wire helicopter ATTHeS (Advanced Technology Testing Helicopter System) These models were extracted from flight test data by system identification techniques Conventional 6-DOF rigid-body models turned out to be not appropriate, because they cannot accurately represent the initial response characteristics of the helicopter Therefore, an extended model with 8 DOF, including rotor dynamic effects, was derived and identified Both identification and verification results demonstrate the improved short-term response of the extended model and prove its applicability for the control system design Results obtained from in-flight simulation measurements confirm the reliability of the 8-DOF model
Author

Category code 08 (aircraft stability/control)
Controlled terms *CONTROL SYSTEMS DESIGN /*FLIGHT SIMULATORS /*FLY BY WIRE CONTROL /*HELICOPTER CONTROL /*MODEL REFERENCE ADAPTIVE CONTROL /*SYSTEM IDENTIFICATION / AIRCRAFT MODELS / DEGREES OF FREEDOM / FLIGHT SIMULATION / FLIGHT TESTS / MATHEMATICAL MODELS / RELIABILITY ANALYSIS /

Quest Accession Number 89A38554
89A38554* NASA IAA Journal Article Issue 16
Experimental studies in system identification of helicopter rotor dynamics
(AA)MCKILLIP, ROBERT, JR
(AA)(Princeton University, NJ)
Princeton Univ , NJ (P3732113)
NAG2-415 (Associazione Industrie Aerospaziali and Associazione Italiana di Aeronautica e Astronautica, European Rotorcraft Forum, 14th, Milan, Italy, Sept 20-23, 1988) Vertica (ISSN 0360-5450), vol 12, no 4, 1988, p 329-336 880000 p 8 refs 14 In EN (English) p 2435

Recent experiments investigating the system identification of helicopter rotor dynamics are described The identification makes use of a two-pass procedure that estimates the rotor dynamic states prior to estimation of the dynamic equation parameters Estimation of the rotor states is made possible through use of the predictive information contained in blade-mounted accelerometers combined with a specialized processing scheme utilizing these signals Descriptions of the experimental hardware and the system identification technique are given, as well as implementation issues for using the procedure on other similarly instrumented rotor blades Finally, comparisons with other identification techniques using the same data are presented It is demonstrated that the approach is an attractive one for measurement of a helicopter rotor's dynamic behavior
Author

Category code 05 (aircraft design, testing, performance)
Controlled terms *DYNAMIC MODELS /*HELICOPTER DESIGN /*ROTARY WINGS /*ROTOR AERODYNAMICS /*SYSTEM IDENTIFICATION / ELASTIC BODIES / FLOW DISTRIBUTION /

Quest Accession Number 90A12763
90A12763 NASA IAA Journal Article Issue 02
System identification collaboration - The role of AGARD
(AA)HAMEL, PETER
(AA)(DLR, Institut fuer Flugmechanik, Brunswick, Federal Republic of Germany)
Vertica (ISSN 0360-5450), vol 13, no 3, 1989, p 207-212 890000 p 6 In EN (English) p 133

The benefits of rotorcraft system identification are discussed as well as a requirement for multidisciplinary collaboration and the AGARD (Advisory Group for Aerospace Research and Development) working group FMP-WG 18 The objectives of the working group are to evaluate the strength and weakness of the different approaches and to develop guidelines for the application of identification techniques to be used more routinely in design and development Another goal is to define an integrated and coordinated methodology for application of system identification based on the strengths of each method
K K

Category code 01 (aeronautics)
Controlled terms *FLIGHT MECHANICS /*FLIGHT TESTS /*HELICOPTER PERFORMANCE /*SYSTEM IDENTIFICATION / HELICOPTER CONTROL / HELICOPTER DESIGN / WIND TUNNEL TESTS /

Quest Accession Number 90A12471
90A12471 NASA IAA Book/Monograph Issue 02
Inverse problems in controlled system dynamics Nonlinear models (Russian book)
Obratnye zadachi dinamiki upravliaemykh sistem Nelineinye modeli
(AA)KRUT'KO, PETR D
Moscow, Izdatel'stvo Nauka, 1988, 328 p In Russian 880000 p 328 refs 85 In RU (Russian) p 239

Based on the concepts of the inverse problems in control system dynamics, a theory is developrd for the synthesis of motion control algorithms for nonlinear systems The structure of the algorithms and their parameters are determined on the basis of the prescribed motion trajectories for the controlled systems The theory developed here is used for solving a variety of applied problems, including problems concerned with the synthesis of control algorithms for robotic manipulators and aircraft The dynamics of the synthesized systems is investigated, and the results of mathematical modeling are discussed
V L.

Category code 63 (cybernetics)
Controlled terms *AUTOMATIC CONTROL /*CONTROL THEORY /*DYNAMICAL SYSTEMS /*NONLINEAR SYSTEMS /*TRAJECTORY CONTROL / ACCELERATION (PHYSICS) / ALGORITHMS / BODY KINEMATICS / CENTER OF MASS / DEGREES OF FREEDOM / FLIGHT ALTITUDE / HELICOPTERS / MANIPULATORS / MATHEMATICAL MODELS / PARAMETER IDENTIFICATION / REENTRY VEHICLES / ROBOTICS / STATISTICAL ANALYSIS / STRUCTURAL VIBRATION / TRAJECTORY OPTIMIZATION /

Quest Accession Number 89A35261
89A35261 NASA IAA Conference Paper Issue 14
Frequency domain techniques applied to the identification of helicopter dynamics
(AA)YOUNG, P , (AB)PATTON, R J
(AB)(York, University, England)
IN International Conference on Control 88, Oxford, England, Apr 13-15, 1988, Proceedings (A89-35251 14-63). London, Institution of Electrical Engineers, 1988, p 153-158. Research supported by SERC and Royal Aircraft Establishment 880000 p. 6 refs 14 In EN (English) p 2219

The application of frequency domain techniques to the identification of helicopter dynamics using a scale-model helicopter as a test system is described Simulations of the helicopter using linear models of longitudinal and lateral motion are detailed A comparison is made between the performances of two input signals in identifying the transfer functions of the models
K K

Category code 63 (cybernetics)
Controlled terms *CONTROL SYSTEMS DESIGN /*DYNAMIC CONTROL /* HELICOPTER CONTROL /*SYSTEM IDENTIFICATION / FEEDBACK CONTROL / FREQUENCY RESPONSE / PARAMETER IDENTIFICATION / ROTOR AERODYNAMICS / SCALE MODELS / SPECTRAL METHODS /

Quest Accession Number 89N29341
89N29341# NASA STAR Technical Report Issue 24
Identification of an adequate model for collective response dynamics of a Sea King helicopter in hover
(AA)FEIK, R A , (AB)PERRIN, R H
Aeronautical Research Labs., Melbourne (Australia) (AF441057)
AD-A208060, ARL-AERO-TM-399 880700 p 30 In EN (English) Avail NTIS HC A03/MF A01 p 3387

A mathematical representation of vertical acceleration response characteristics of a helicopter in hover is developed, including blade flapping, inflow, and rotor speed dynamics A maximum likelihood parameter estimation technique is applied to assess the adequacy of the model, and to identify the relevant parameters, using flight data from a Sea King Mk 50 helicopter A number of conclusions related to the validity of the modelling approach have resulted from comparisons between predicted and identified parameters, and further investigation of some aspects is indicated
GRA

Category code 05 (aircraft design, testing, performance)
Controlled terms *ACCELERATION (PHYSICS) /*DYNAMIC RESPONSE /* HELICOPTERS /*HOVERING /*MATHEMATICAL MODELS /*PARAMETER IDENTIFICATION /*ROTOR AERODYNAMICS /*SH-3 HELICOPTER /*VERTICAL FLIGHT / DYNAMIC CHARACTERISTICS / FLAPPING / LINEARITY / MAXIMUM LIKELIHOOD ESTIMATES / ROTOR DYNAMICS /

Quest Accession Number 89A23360
89A23360# NASA IAA Preprint Issue 08
Consideration of trends in stability and control derivatives from helicopter system identification
(AA)BLACK, C G
(AA)(Glasgow, University, Scotland)
AAAF, European Rotorcraft Forum, 13th, Arles, France, Sept 8-11, 1987, Paper 27 p Research supported by the Ministry of Defence Procurement Executive 870900 p 27 refs 21 In EN (English) p 1111

Methods for valicating a complex nonlinear model of helicopter dynamics against measured flight data are considered It is shown that a frequency-domain output-error estimation technique is a feasible and practical approach to the successful estimation of a rigid-body model which excludes rotor degrees of freedom Problems arising in the identification of lateral stability derivatives, which are associated with strong correlations between some of the response variables in the 'Dutch-roll' type mode, are solved using rank-deficient versions of the information matrix
K K

Category code 08 (aircraft stability/control)
Controlled terms *AIRCRAFT MODELS /*HELICOPTER PERFORMANCE /*SYSTEM IDENTIFICATION / FLIGHT TESTS / NONLINEAR SYSTEMS / PARAMETER IDENTIFICATION /

Quest Accession Number 89A23322
89A23322# NASA IAA Preprint Issue 08
Validation of a mathematical model of the Sea King Mk50 helicopter using flight trials data
(AA)WILLIAMS, M J , (AB)ARNEY, A. M , (AC)PERRIN, R H , (AD)FEIK, R. A.
(AD)(Department of Defence, Aeronautical Research Laboratories, Melbourne, Australia)
AAAF European Rotorcraft Forum, 13th, Arles, France, Sept 8-11, 1987, Paper 13 p 870900 p 13 refs 8 In EN (English) p 1106

Validation of a mathematical model of a Sea King Mk50 helicopter, by comparing model predictions with flight data, is described Comparisons of both performance and flight dynamic characteristics show that the model provides an adequate representation of flight characteristics over a range of airspeeds Some specific deficiencies which remain are noted and summarized The use of System Identification techniques to investigate model limitations and to develop improved representations of dynamic characteristics is discussed The approach is illustrated by examples from Sea King flight measurements, including an assessment of the effects of inflow, flapping, and engine dynamics on vertical acceleration response to collective inputs at hover
Author

Category code 05 (aircraft design, testing, performance)
Controlled terms *FLIGHT TESTS /*HELICOPTER PERFORMANCE /* MATHEMATICAL MODELS /*MILITARY HELICOPTERS / ACCELERATION (PHYSICS) / DYNAMIC RESPONSE / HELICOPTER CONTROL / SYSTEM IDENTIFICATION /

Quest Accession Number 89A22872
89A22872# NASA IAA Journal Article Issue 07
Flight test and data analysis techniques for helicopter parameter estimation
(AA)SATTLER, D E , (AB)KOBIERSKI, R D
(AA)(Carleton University, Ottawa, Canada)
(CASI, Flight Test Symposium, Ottawa, Canada, Mar 24, 25, 1988) Canadian Aeronautics and Space Journal (ISSN 0008-2821), vol 34, Dec 1988, p 213-223 Research supported by DND 881200 p 11 refs 6 In EN (English) p 931

Intended specifically to provide insight into flight test and data analysis techniques for helicopter parameter estimation, this paper commences with a brief review of aircraft parameter estimation The equations of motion for an aircraft are then presented in a form appropriate for use with helicopter parameter estimation A traditional method for helicopter parameter estimation is presented, whereby control derivatives and associated time delays are obtained from step input data, static stability derivatives are obtained from trim data, and dynamic stability derivatives are obtained from fixed-frequency excitation The attractive features of this method are found to be the simplicity of the concept and a concurrent better understanding of the processes involved Also presented is a second, more advanced method which employs a modified maximum likelihood estimator to explore the methodology of pilot interactively generated manual control during parameter estimation data generation This method is shown to provide significantly improved confidence levels associated with estimation of all stability and control derivatives Experience gained in the use of parameter estimation techniques during this research program indicates that helicopter parameter estimation has now matured to a level suitable for engineering applications
Author

Category code 08 (aircraft stability/control)
Controlled terms *FLIGHT CONTROL /*FLIGHT TESTS /*HELICOPTER CONTROL /*PARAMETER IDENTIFICATION / DATA PROCESSING / DYNAMIC STABILITY / EQUATIONS OF MOTION / MAXIMUM LIKELIHOOD ESTIMATES / STABILITY DERIVATIVES / STATIC STABILITY /

Quest Accession Number 89A18938
89A18938# NASA IAA Preprint Issue 06
Three-dimensional interactive system identification of helicopte. rotor/body dynamics
(AA)MCKILLIP, ROBERT M , JR
(AA)(Princeton University, NJ)
AHS, Annual Forum, 44th, Washington, DC, June 16-18, 1988, Paper 11 p 880600 p 11 refs 12 In EN (English) p 772

System identification results on UH-60 Blackhawk flight test data in hover are described Simple quasi-static models of the helicopter's flight dynamics characteristics were generated using a two-pass estimation approach The method incorporates Kinematic Observer theory for the initial state estimation phase, and a factorized Kalman Filter for the stability derivative extraction The study also employs the novel use of a graphics workstation in order to aid the identification process, through superposition of both flight test data and identified responses in real time This approach allows the identification engineer to visualize and understand significantly larger amounts of data than would be possible through examination of purely numerical data alone, providing an interactive environment for modeling of flight dynamics
Author

Category code 05 (aircraft design, testing, performance)
Controlled terms *FLIGHT CONTROL /*ROTOR AERODYNAMICS /*ROTOR BODY INTERACTIONS /*SYSTEM IDENTIFICATION /*UH-60A HELICOPTER / AERODYNAMIC STABILITY / FLIGHT TESTS / HELICOPTER CONTROL / HOVERING / KALMAN FILTERS /

Quest Accession Number 89A13522
89A13522# NASA IAA Conference Paper Issue 03
Theoretical modelling for helicopter flight dynamics - Development and validation
(AA)PADFIELD, G D
(AA)(Royal Aerospace Establishment, Bedford, England)
IN ICAS, Congress, 16th, Jerusalem, Israel, Aug 28-Sept 2, 1988, Proceedings Volume 1 (A89-13501 03-05) Washington, DC, American Institute of Aeronautics and Astronautics, Inc , 1988, p 165-177 880000 p 13 refs 17 In EN (English) p 264

The complexity of developing a fully validated and accurate mathematical model is discussed, and different modeling levels necessary to predict lateral, directional, longitudinal, and vertical axis dynamics are examined System identification techniques are employed to compare flight rest results with theoretical predictions. The measurement set required to validate aeroelastic models is considered
R R

Category code 05 (aircraft design, testing, performance)
Controlled terms *AIRCRAFT MODELS /*FLIGHT CHARACTERISTICS /*FLIGHT TESTS /*HELICOPTER PERFORMANCE / AEROELASTICITY / FLIGHT SAFETY / FLIGHT SIMULATION / SYSTEM IDENTIFICATION /

Quest Accession Number 88A51770
88A51770* NASA IAA Conference Paper Issue 22
Active control rotor model testing at Princeton's Rotorcraft Dynamics Laboratory
(AA)MCKILLIP, ROBERT M , JR
(AA)(Princeton University, NJ)
Princeton Univ , N. J (P3732113)
NAG2-415 IN International Conference on Rotorcraft Basic Research, 2nd, College Park, MD, Feb. 16-18, 1988, Proceedings (A88-51751 22-01) Alexandria, VA, American Helicopter Society, 1988, 9 p Research supported by the Engineering Foundation. 880000 p 9 refs 19 In EN (English) p 3657

A description of the model helicopter rotor tests currently in progress at Princeton's Rotorcraft Dynamics Laboratory is presented The tests are designed to provide data for rotor dynamic modeling for

use with active control system design The model rotor to be used incoporates the capability for Individual Blade Control (IBC) or Higher Harmonic Control through the use of a standard swashplate on a three bladed hub Sample results from the first series of tests are presented, along with the methodology used for state and parameter identification Finally, pending experiments and possible research directions using this model and test facility are outlined

Category code 09 (research and support facilities (air))
Controlled terms *ACTIVE CONTROL /*AIRCRAFT MODELS /*ROTOR AERODYNAMICS /*ROTORCRAFT AIRCRAFT / PARAMETER IDENTIFICATION / ROTARY WINGS / STATE ESTIMATION / V/STOL AIRCRAFT /

Quest Accession Number 88A51769
88A51769 NASA IAA Conference Paper Issue 22
Some basic issues in helicopter system identification
(AA)FITZSIMONS, P M , (AB)TEARE, D , (AC)PRASAD, J V R , (AD)SCHRAGE, D P , (AE)TONGUE, B H
(AE)(Georgia Institute of Technology, Atlanta)
DAAL02-86-K-0160 IN International Conference on Rotorcraft Basic Research, 2nd, College Park, MD, Feb 16-18, 1988, Proceedings (A88-51751 22-01) Alexandria, VA, American Helicopter Society, 1988, 10 p 880000 p 10 refs 6 In EN (English) p 3645

Significant advancement has been made in the field of aircraft state estimation and parameter identification for fixed wing aircraft over the last two decades. By comparison, the progress for rotary wing aircraft has been relatively slow due to important issues and problems which need to be resolved A highly coupled, high order system which is basically unstable summarizes some of the important issues and problems Other issues, which are more basic, deal with the type of input used to excite the system, length of the signal used, consistency checks, and the handling of errors This paper will address some of the basic issues in helicopter system identification using simulated and flight test data for the UH-60A Black Hawk helicopter
Author

Category code 05 (aircraft design, testing, performance)
Controlled terms *AIRCRAFT STABILITY /*HELICOPTER CONTROL /*SYSTEM IDENTIFICATION /*UH-60A HELICOPTER / LEAST SQUARES METHOD / PARAMETER IDENTIFICATION / ROTOR AERODYNAMICS / STATE ESTIMATION /

Quest Accession Number 88A51768
88A51768* NASA IAA Conference Paper Issue 22
Advancements in frequency-domain methods for rotorcraft system identification
(AA)TISCHLER, MARK B
(AA)(NASA, Ames Research Center, U S Army, Aeroflightdynamics Directorate, Moffett Field, CA)
National Aeronautics and Space Administration Ames Research Center, Moffett Field, Calif (NC473657)
IN International Conference on Rotorcraft Basic Research, 2nd, College Park, MD, Feb 16-18, 1988, Proceedings (A88-51751 22-01) Alexandria, VA, American Helicopter Society, 1988, 18 p 880000 p 18 refs 19 In EN (English) p 3645

A new method for frequency-domain identification of rotorcraft dynamics is presented Nonparametric frequency-response identification and parametric tranfer-function modeling methods are extended to allow the extraction of state-space (stability and control derivative) representations An interactive computer program DERIVID is described for the iterative solution of the multi-input/multi-output frequency-response matching approach used in the identification Theoretical accuracy methods are used to determine the appropriate model structure and degree-of-confidence in the identified parameters The method is applied to XV-15 tilt-rotor aircraft data in hover Bare-airframe stability and control derivatives for the lateral/directional dynamics are shown to compare favorably with models previously obtained using time-domain identification methods and the XV-15 simulation program
Author

Category code 05 (aircraft design, testing, performance)
Controlled terms *AERODYNAMIC STABILITY /*PARAMETER IDENTIFICATION /*ROTORCRAFT AIRCRAFT /*SYSTEM IDENTIFICATION / FLIGHT TESTS / HOVERING / TRANSFER FUNCTIONS / XV-15 AIRCRAFT /

Quest Accession Number 88A51461
88A51461* NASA IAA Conference Paper Issue 22
Determination of rotor derivatives and rotor hub force and moment derivatives from flight measurements with the RSRA compound helicopter
(AA)WANG, JI C , (AB)TALBOT, PETER D
(AA)(San Jose State University, CA), (AB)(NASA, Ames Research Center, Moffett Field, CA)
San Jose State Univ , Calif (SB413977)
NCC2-267 IN Society of Flight Test Engineers, Annual Symposium, 18th, Amsterdam, Netherlands, Sept 28-Oct 2, 1987, Proceedings (A88-51450 22-05) Lancaster, CA, Society of Flight Test Engineers, 1987, p 13-1 to 13-17 870000 p 17 refs 18 In EN (English) p 3643

A case study of the application of an integrated rotorcraft identification method to the linear modeling of rotor system dynamics and rotor hub loads is presented. Applying the method to flight data obtained from the RSRA compound helicopter, the rotor derivatives in the rotor state dynamic equation are identified along with blade equivalent damping and spring periodic coefficients A rigid blade flapping equation of motion can be derived from the identified rotor state equation. It is shown that the concept of rotor hub load derivatives is useful for small maneuvering loads The hub load derivatives can be used to relate the hub dynamic load to rotor/fuselage motion and applied inputs.
C.D

Category code 05 (aircraft design, testing, performance)
Controlled terms *AERODYNAMIC FORCES /*COMPOUND HELICOPTERS /* ROTARY WING AIRCRAFT /*ROTOR SYSTEMS RESEARCH AIRCRAFT /*STABILITY DERIVATIVES / EQUATIONS OF MOTION / FLIGHT TESTS / HUBS / PARAMETER IDENTIFICATION / WIND TUNNEL TESTS /

Quest Accession Number 88A51751
88A51751 NASA IAA Meeting Paper Issue 22
International Conference on Rotorcraft Basic Research, 2nd, University of Maryland, College Park, MD, Feb 16-18, 1988, Proceedings
Conference sponsored by the University of Maryland and AHS Alexandria, VA, American Helicopter Society, 1988, 542 p For individual items see A88-51752 to A88-51785 880000 p 542 In EN (English) Members, $50., nonmembers, $75 p 3628

The papers presented in this volume provide an overview of current theoretical and experimental research related to rotorcraft technology The contributions are grouped under the following headings performance and loads, rotor/body interactional dynamics and wake studies, dynamics, system identification, active controls and flight safety, CFD applications in rotorcraft, and composite analyses Specific topics discussed include rotor-airframe aerodynamic interaction phenomena, minimum weight design of rectangular and tapered helicopter rotor blades with frequency constraints, advancements in frequency-domain methods for rotorcraft system identification, and flow field prediction for helicopter rotors with advanced blade tip shapes using CFD techniques.
V L

Category code 01 (aeronautics)
Controlled terms *CONFERENCES /*HELICOPTER DESIGN /*ROTOR BODY INTERACTIONS /*ROTORCRAFT AIRCRAFT / ACTIVE CONTROL / AERODYNAMIC STABILITY / AIRCRAFT CONSTRUCTION MATERIALS / AIRCRAFT STABILITY / COMPOSITE STRUCTURES / COMPUTATIONAL FLUID DYNAMICS / ENGINE AIRFRAME INTEGRATION / FINITE ELEMENT METHOD / HELICOPTER CONTROL / INTERACTIONAL AERODYNAMICS / ROTOR BLADES / SYSTEM IDENTIFICATION / TECHNOLOGY ASSESSMENT /

Quest Accession Number 88N26524
88N26524# NASA STAR Conference Paper Issue 20
Frequency domain identification of the dynamics of a scaled remotely-piloted helicopter
(AA)YOUNG, P , (AB)PATTON, R J.
York Univ (England) (Y1794104) Dept of Electronics
In DFVLR, System Identification in Vehicle Dynamics p 153-172 (SEE N88-26518 20-31) Sponsored by the United Kingdom Science and Engineering Research Council and the United Kingdom Ministry of Defence 870000 p. 20 In EN (English) Avail NTIS HC A18/MF A01, DFVLR, VB-PL-DO, 90 60 58, 5000 Cologne, Fed Republic of Germany, 109 Deutsche marks p 2786

A linear digital simulation of a radio-controlled model helicopter was performed to evaluate the validity of applying frequency domain identification to structural estimation of a complex nonlinear system The control and telemetry systems, the sensors and the associated signal conditioning developed for the radio-controlled helicopter facility are described Sine-wave frequency sweeps were applied to each input in turn to excite all the dominant modes of the system, and the time series data were analyzed to obtain the system transfer functions The closed-loop transfer functions are found by least-squares curve fitting, and the poles and zeros are determined for each case Comparing these modes with the corresponding elements in the transfer function matrix obtained from the Levernier algorithm gives results which demonstrate the usefulness of the frequency domain approach in identification
ESA

Category code 08 (aircraft stability/control)
Controlled terms *DYNAMIC RESPONSE /*HELICOPTER CONTROL /*RADIO CONTROL /*SCALE MODELS /*SYSTEM IDENTIFICATION / DIGITAL SIMULATION / NONLINEAR SYSTEMS / TIME SERIES ANALYSIS / TRANSFER FUNCTIONS /

Quest Accession Number 87A48959
87A48959 NASA IAA Preprint Issue 21
UK research into system identification for helicopter flight mechanics
(AA)PADFIELD, G D., (AB)THORNE, R , (AC)MURRAY-SMITH, D , (AD)BLACK, C , (AE)CALDWELL, A E
(AB)(Royal Aircraft Establishment, Bedford, England), (AE)(Glasgow, University, Scotland)
European Rotorcraft Forum, 11th, London, England, Sept 10-13, 1985, Paper 29 p 850900 p 29 refs 38 In EN (English) p 3473

The integration of input design, state estimation, model structure estimation, and parameter identification into a methodology and its application to helicopter flight dynamics are examined The three levels for modeling of rotorcraft flight behavior and related loadings are discussed The integrated methodology developed for helicopter system identification and its implementation in the parameter estimation package are described The methodology was validated using data from simulation models, and an example of flight data analysis using the integrated methodology is presented
I F

Category code 66 (systems analysis)
Controlled terms *CONTROL SYSTEMS DESIGN /*FLIGHT MECHANICS /* HELICOPTER DESIGN /*RESEARCH AND DEVELOPMENT /*SYSTEM IDENTIFICATION / AERODYNAMIC STABILITY / FLIGHT PATHS / PARAMETER IDENTIFICATION / SYSTEMS INTEGRATION / UNITED KINGDOM /

Quest Accession Number 87A43457
87A43457# NASA IAA Preprint Issue 19
Experience with frequency-domain methods in helicopter system identification
(AA)BLACK, C G , (AB)MURRAY-SMITH, D J , (AC)PADFIELD, G D
(AB)(Glasgow, University, Scotland), (AC)(Royal Aircraft Establishment, Bedford, England)
MOD-2048/028/XR/STR DGLR, European Rotorcraft Forum, 12th, Garmisch-Partenkirchen, West Germany, Sept 22-25, 1986, Paper 27 p 860900 p 27 refs 26 In EN (English) p 2951

Most applications of system identification techniques to helicopters have involved time-domain methods using reduced-order mathematical models representing six-degree-of-freedom rigid-body motion. Frequency-domain techniques provide an interesting alternative

approach in which data which lies outside the frequency range of interest may be disregarded This not only provides a basis for establishing reduced order models which are valid over a defined range of frequencies but also results in a significant data reduction in comparison with time-domain methods This paper presents a systematic approach to frequency-domain identification using both equation-error and output-er or techniques Results are presented from flight data from the Puma helicopter to illustrate the application of the frequency-domain approach to the estimation of parameters of the pitching moment and normal force equations These results are assessed both on a statistical basis and through comparisons with theoretical values
Author

Category code 08 (aircraft stability/control)
Controlled terms *FREQUENCY RESPONSE /*HELICOPTERS /*PARAMETER IDENTIFICATION /*SYSTEM IDENTIFICATION / LEAST SQUARES METHOD / PITCHING MOMENTS / SOFTWARE TOOLS / TRANSFER FUNCTIONS /

Quest Accession Number 87A34854
87A34854 NASA IAA Journal Article Issue 14
Helicopter aeromechanics research at DFVLR - Recent results and outlook
(AA)HAMEL, P , (AB)GMELIN, B , (AC)KALEKTA, J., (AD)PAUSDER, H -J , (AE)LANGER, H -J.
(AE)(DFVLR, Braunschweig, West Germany)
Vertica (ISSN 0360-5450), vol 11, no 1-2, 1987, p 93-108 870000 p 16 refs 26 In EN (English) p 2107

Under the general objectives (1) to adapt the helicopter flying qualities to the pilots' capabilities, (2) to increase the mission effectiveness, and (3) to reduce technical and economical risks of helicopter producers and operators in view of the integration of advanced technologies and increasing automation, DFVLR Institute for Flight Mechanics is conducting research activities in the field of helicopter aeromechanics In keeping with these objectives the activities are concentrated on three major areas (1) wind tunnel simulation using large Mach-scaled rotor and helicopter models in the German-Dutch Wind Tunnel (DNW), (2) development of mathematical helicopter models from flight test data by system identification procedures, (3) handling qualities investigations using in-flight simulation The paper covers the relevant methodologies and facilities at DFVLR as well as various recent results of the research activities
Author

Category code 05 (aircraft design, testing, performance)
Controlled terms *FLIGHT CHARACTERISTICS /*HELICOPTERS /*RESEARCH AND DEVELOPMENT /*WIND TUNNEL TESTS / AIRCRAFT MANEUVERS / CONTROLLABILITY / INTERNATIONAL COOPERATION / MATHEMATICAL MODELS / TEST FACILITIES / WIND TUNNEL APPARATUS /

Quest Accession Number 87A19287
87A19287* NASA IAA Conference Paper Issue 06
The role of modeling and flight testing in rotorcraft parameter identification
(AA)CHEN, R T N , (AB)TISCHLER, M B
(AA)(NASA, Ames Research Center, Moffett Field, CA), (AB)(NASA, Ames Research Center, U S Army, Aeroflightdynamics Directorate, Moffett Field, CA)
National Aeronautics and Space Administration Ames Research Center, Moffett Field, Calif (NC4736S7)
IN American Helicopter Society, Annual Forum, 42nd, Washington, DC, June 2-4, 1986, Proceedings Volume 2 (A87-19201 06-01) Alexandria, VA, American Helicopter Society, 1986, 38 p 860000 p. 38 refs 42 In EN (English) p 726

The importance of recognizing that each lower-order model used for rotorcraft parameter identification has a limited range of applicability is illustrated in some detail Examples are given to illustrate the use of conditioning the test input signals and the potential of using multi-axis test inputs to enhance the parameter identifiability The paper discusses the benefits and limitations of using frequency sweeps as flight-test input signals for identification of frequency response for rotorcraft and for the subsequent fitting of parametric transfer-function models This paper demonstrates the major role played by analytical modeling and the understanding of the physics involved in the rotorcraft flight dynamics, particularly understanding the limit of lower-order models, in achieving successful rotorcraft parameter identification
Author

Category code 05 (aircraft design, testing, performance)
Controlled terms *AIRCRAFT MODELS /*FLIGHT TESTS /*PARAMETER IDENTIFICATION /*ROTORCRAFT AIRCRAFT /*TRANSFER FUNCTIONS / DEGREES OF FREEDOM / HOVERING / RIGID STRUCTURES /

Quest Accession Number 87A19239
87A19239 NASA IAA Conference Paper Issue 06
Integrated system identification methodology for helicopter flight dynamics
(AA)PADFIELD, G. D
(AA)(Royal Aircraft Establishment, Flight Research Div , Bedford, England)
IN American Helicopter Society, Annual Forum, 42nd, Washington, DC, June 2-4, 1986, Proceedings Volume 1 (A87-19201 06-01), Alexandria, VA, American Helicopter Society, 1986, p 441-455 860000 p 15 refs 19 In EN (English) p.728

The need for an integrated helicopter system identification methodology including state, model structure, and parameter estimation to reduce the levels of measurement noise and isolate important degrees of freedom is emphasized The required processes in a systematic methodology are described Stability variations with flight path angle for a Puma helicopter reveal how reduced-order models can occasionally offer an adequate description of vehicle dynamics
K k

Category code 08 (aircraft stability/control)
Controlled terms *FLIGHT MECHANICS /*HELICOPTER CONTROL /*SYSTEM IDENTIFICATION / LATERAL CONTROL / LONGITUDINAL CONTROL / REGRESSION ANALYSIS / ROLL / YAW /

Quest Accession Number 87A19238
87A19238 NASA IAA Conference Paper Issue 06
Non-iterative parameter identification techniques
(AA)FITZSIMONS, P M , (AB)JONNALAGADDA, V R P , (AC)TONGUE, B H , (AD)SCHRAGE, D P
(AD)(Georgia Institute of Technology, Atlanta)
IN American Helicopter Society, Annual Forum, 42nd, Washington, DC, June 2-4, 1986, Proceedings Volume 1 (A87-19201 06-01) Alexandria, VA, American Helicopter Society, 1986, p. 431-439 Research sponsored by the McDonnel Douglas Helicopter Co 860000 p 9 refs 11 In EN (English) p 617

Assuming a linear and time-invariant model structure, descriptions of three different noniterative techniques that can be used to obtain parameter estimates are given The techniques are deterministic (recursive) least squares, the extended Kalman filter, and the statistically linearized filter The methods are used to identify the parameters of a one-state two-parameter system and a four-state twenty-four parameter system (taken from a linearized longitudinal model of an Advanced Light Helicopter in forward flight)
K K

Category code 66 (systems analysis)
Controlled terms *CONTROL SIMULATION /*FLIGHT STABILITY TESTS /* HELICOPTER DESIGN /*PARAMETER IDENTIFICATION / AIRCRAFT MODELS / KALMAN FILTERS / LEAST SQUARES METHOD / LINEAR FILTERS /

Quest Accession Number 87A16193
87A16193 NASA IAA Conference Paper Issue 04
Frequency domain parameter estimation of aeronautical systems without and with time delay
(AA)MARCHAND, M (AB)FU, K -H
(AB)(DFVLR, Institut fuer Flugmechanik, Brunswick, West Germany)
IN Identification and system parameter estimation 1985, Proceedings of the Seventh Symposium, York, England, July 3-7, 1985 Volume 1 (A87-16176 04-63), Oxford and New York, Pergamon Press, 1985, p. 669-674 850000 p 6 refs 12 In EN (English) p 446

The paper considers the application of frequency domain methods to flight test data from rotorcraft and fixed wing aircraft In particular, a modified frequency domain output error method is presented which can be applied to linear systems with time delays In contrast to existing methods, the new approach enables the combination of data from several maneuvers for one evaluation, the use of test records with arbitrary initial state conditions x(t = 0), and the direct identification of time delays (instead of using Pade-approximation) Results are presented from the identication of a six-degrees-of-freedom helicopter model (Bo-105 Research Helicopter of the DFVLR) as well as from the identifiation of an equivalent low order system with time delay (HFB 320-In-Flight-Simulator of the DFVLR)
Author

Category code 08 (aircraft stability/control)
Controlled terms *AIRCRAFT CONTROL /*FLIGHT MECHANICS /*PARAMETER IDENTIFICATION /*TIME LAG / FLIGHT TESTS / LINEAR SYSTEMS / MAXIMUM LIKELIHOOD ESTIMATES / SYSTEM IDENFIFICATION / TEMPORAL DISTRIBUTION /

Quest Accession Number 87N16813
87N16813# NASA STAR Thesis Issue 09
Identification of a dynamic model of a helicopter from flight tests / Ph D Thesis
(AA)MILNE, GARTH W
Stanford Univ , Calif (S0380476) Dept of Aeronautics and Astronautics
861200 p 297 In EN (English) Avail Issuing Activity p 1140

Techniques for identifying continuous models of dynamic systems were applied to the unstable longitudinal hover dynamics of a CH-47B Chinook helicopter The equation error method with carefully filtered 7 18 Hz data produced good pitch transfer function models Frequency response plots for increasing order models were used to determine the model order. The linear inter-sample equivalent produced better continuous models from identified ARMA models than the zero order hold assumption The 300% overshoot in the vertical acceleration step response arising from dynamic inflow and rotor coning was also identified The MIMO Maximum Likelihood identification method with process and measurement noise was then examined High Kalman gain increases the high-frequency weighting, increasing sensitivity to unmodeled dynamics Low-noise sensors and the absence of measurement noise above 3 Hz (following pre-filtering to remove rotor noise) resulted in high Kalman gains and singular measurement noise covariance estimates, requiring use of the Maine-Iliff MMLW3 algorithm formulation. A discrete gradient version of this algorithm was developed for the PC-MATLAB language on IBM-PC type computers, and was used for longitudinal derivative identification The algorithm is attractive for instructional use A User's Manual is included
Author

Category code 05 (aircraft design, testing, performance)
Controlled terms *CH-47 HELICOPTER /*DYNAMIC MODELS /*HOVERING /* MAXIMUM LIKELIHOOD ESTIMATES /*SYSTEM IDENTIFICATION /*TRANSFER FUNCTIONS / ALGORITHMS / COMPUTER PROGRAMS / ERRORS / GYROSCOPES / KINEMATICS / PITCH (INCLINATION) / USER MANUALS (COMPUTER PROGRAMS) /

REPORT DOCUMENTATION PAGE

1. Recipient's Reference	2. Originator's Reference	3. Further Reference	4. Security Classification of Document
	AGARD-LS-178	ISBN 92-835-0640-5	UNCLASSIFIED

5. Originator	Advisory Group for Aerospace Research and Development North Atlantic Treaty Organization 7 rue Ancelle, 92200 Neuilly sur Seine, France
6. Title	ROTORCRAFT SYSTEM IDENTIFICATION
7. Presented on	4th—5th November 1991 Ottobrunn, Germany, 7th—8th November 1991 in Rome, Italy and 13th—14th November 1991 in College Park, Maryland United States.

8. Author(s)/Editor(s)	9. Date
Various	October 1991
10. Author's/Editor's Address	**11. Pages**
Various	258

12. Distribution Statement This document is distributed in accordance with AGARD policies and regulations, which are outlined on the back covers of all AGARD publications.

13. Keywords/Descriptors

Rotary wing aircraft
Flight tests
Aerodynamic stability
Flight control
Proving
Identifying
Mathematical models
AH-64 helicopter
BO-105 helicopter
PUMA helicopter

14. Abstract

For fixed wing aircraft, system identification methods to determine stability and control derivatives from flight test data are used with confidence. The application of the same techniques to rotorcraft is not so far advanced mainly because of the helicopter aeromechanical complexity. Only a few specialists, mostly in research organisations, have concentrated on this field and the application in industry is still sporadic.

The Lecture Series is intended to establish an improved dialogue between government organisations, research institutions, and industry in order to apply these tools more routinely in rotorcraft design, development, and evaluation.

The Lecture Series is supported by an unique flight test data set which was generated and analysed within a recent Working Group in the Flight Mechanics Panel of AGARD (WG18). It is based on the findings of the Working Group including a documentation of the data bases, the applied identification methodologies, the major application areas. Flight test obtained from three different helicopters (AH-64, BO 105, and PUMA) were evaluated. For each of the three helicopters, comparisons of the obtained results are discussed, covering data quality evaluations, identification, and the verification of the obtained models.

The Lecture Series was prepared under the sponsorship of the Flight Mechanics Panel and the Consultant and Exchange Programme of AGARD.

AGARD Lecture Series 178 Advisory Group for Aerospace Reseearch and Development, NATO ROTORCRAFT SYSTEM IDENTIFICATION Published October 1991 258 pages For fixed wing aircraft, system identification methods to determine stability and control derivatives from flight test data are used with confidence. The application of the same techniques to rotorcraft is not so far advanced mainly because of the helicopter aeromechanical complexity Only a few specialists mostly in research organisations, have concentrated on this field and the application in industry is still sporadic PTO	AGARD-LS-178 Rotary wing aircraft Flight tests Aerodynamic stability Flight control Proving Identifying Mathematical models AH-64 — helicopter BO-105 — helicopter PUMA — helicopter	AGARD Lecture Series 178 Advisory Group for Aerospace Reseearch and Development, NATO ROTORCRAFT SYSTEM IDENTIFICATION Published October 1991 258 pages For fixed wing aircraft, system identification methods to determine stability and control derivatives from flight test data are used with confidence The application of the same techniques to rotorcraft is not so far advanced mainly because of the helicopter aeromechanical complexity Only a few specialists, mostly in research organisations, have concentrated on this field and the application in industry is still sporadic P.T.O.	AGARD-LS-178 Rotary wing aircraft Flight tests Aerodynamic stability Flight control Proving Identifying Mathematical models AH-64 — helicopter BO-105 — helicopter PUMA — helicopter
AGARD Lecture Series 178 Advisory Group for Aerospace Reseearch and Development NATO ROTORCRAFT SYSTEM IDENTIFICATION Published October 1991 258 pages For fixed wing aircraft, system identification methods to determine stability and control derivatives from flight test data are used with confidence. The application of the same techniques to rotorcraft is not so far advanced mainly because of the helicopter aeromechanical complexity Only a few specialists, mostly in research organisations, have concentrated on this field and the application in industry is still sporadic PTO	AGARD-LS-178 Rotary wing aircraft Flight tests Aerodynamic stability Flight control Proving Identifying Mathematical models AH-64 — helicopter BO-105 — helicopter PUMA — helicopter	AGARD Lecture Series 178 Advisory Group for Aerospace Reseearch and Development, NATO ROTORCRAFT SYSTEM IDENTIFICATION Published October 1991 258 pages For fixed wing aircraft, system identification methods to determine stability and control derivatives from flight test data are used with confidence The application of the same techniques to rotorcraft is not so far advanced mainly because of the helicopter aeromechanical complexity Only a few specialists, mostly in research organisations, have concentrated on this field and the application in industry is still sporadic P.T.O	AGARD-LS-178 Rotary wing aircraft Flight tests Aerodynamic stability Flight control Proving Identifying Mathematical models AH-64 — helicopter BO-105 — helicopter PUMA — helicopter

The Lecture Series is intended to establish an improved dialogue between government organisations, research institutions, and industry in order to apply these tools more routinely in rotorcraft design, development, and evaluation

The Lecture Series is supported by an unique flight test data set which was generated and analysed within a recent Working Group in the Flight Mechanics Panel of AGARD (WG18) It is based on the findings of the Working Group including a documentation of the data bases, the applied identification methodologies, the major application areas Flight test obtained from three different helicopters (AH-64, BO 105, and PUMA) were evaluated For each of the three helicopters, comparisons of the obtained results are discussed, covering data quality evaluations, identification, and the verification of the obtained models

The Lecture Series was prepared under the sponsorship of the Flight Mechanics Panel and the Consultant and Exchange Programme of AGARD

ISBN 92-835-0640-5

The Lecture Series is intended to establish an improved dialogue between government organisations, research institutions, and industry in order to apply these tools more routinely in rotorcraft design, development, and evaluation

The Lecture Series is supported by an unique flight test data set which was generated and analysed within a recent Working Group in the Flight Mechanics Panel of AGARD (WG18) It is based on the findings of the Working Group including a documentation of the data bases, the applied identification methodologies, the major application areas Flight test obtained from three different helicopters (AH-64, BO 105, and PUMA) were evaluated For each of the three helicopters, comparisons of the obtained results are discussed, covering data quality evaluations, identification, and the verification of the obtained models

The Lecture Series was prepared under the sponsorship of the Flight Mechanics Panel and the Consultant and Exchange Programme of AGARD

ISBN 92-835-0640-5

The Lecture Series is intended to establish an improved dialogue between government organisations, research institutions, and industry in order to apply these tools more routinely in rotorcraft design, development, and evaluation

The Lecture Series is supported by an unique flight test data set which was generated and analysed within a recent Working Group in the Flight Mechanics Panel of AGARD (WG18) It is based on the findings of the Working Group including a documentation of the data bases, the applied identification methodologies, the major application areas Flight test obtained from three different helicopters (AH-64, BO 105, and PUMA) were evaluated For each of the three helicopters, comparisons of the obtained results are discussed, covering data quality evaluations, identification, and the verification of the obtained models.

The Lecture Series was prepared under the sponsorship of the Flight Mechanics Panel and the Consultant and Exchange Programme of AGARD.

ISBN 92-835-0640-5

The Lecture Series is intended to establish an improved dialogue between government organisations, research institutions, and industry in order to apply these tools more routinely in rotorcraft design, development, and evaluation

The Lecture Series is supported by an unique flight test data set which was generated and analysed within a recent Working Group in the Flight Mechanics Panel of AGARD (WG18) It is based on the findings of the Working Group including a documentation of the data bases the applied identification methodologies, the major application areas Flight test obtained from three different helicopters (AH-64, BO 105, and PUMA) were evaluated For each of the three helicopters, comparisons of the obtained results are discussed, covering data quality evaluations, identification, and the verification of the obtained models

The Lecture Series was prepared under the sponsorship of the Flight Mechanics Panel and the Consultant and Exchange Programme of AGARD

ISBN 92-835-0640-5

AGARD

NATO OTAN

7 RUE ANCELLE · 92200 NEUILLY-SUR-SEINE

FRANCE

Téléphone (1)47.38.57.00 · Télex 610 176
Télécopie (1)47.38.57.99

DIFFUSION DES PUBLICATIONS
AGARD NON CLASSIFIEES

L'AGARD ne détient pas de stocks de ses publications, dans un but de distribution générale à l'adresse ci-dessus. La diffusion initiale des publications de l'AGARD est effectuée auprès des pays membres de cette organisation par l'intermédiaire des Centres Nationaux de Distribution suivants. A l'exception des Etats-Unis, ces centres disposent parfois d'exemplaires additionnels; dans les cas contraire, on peut se procurer ces exemplaires sous forme de microfiches ou de microcopies auprès des Agences de Vente dont la liste suite.

CENTRES DE DIFFUSION NATIONAUX

ALLEMAGNE
Fachinformationszentrum,
Karlsruhe
D-7514 Eggenstein-Leopoldshafen 2

BELGIQUE
Coordonnateur AGARD-VSL
Etat-Major de la Force Aérienne
Quartier Reine Elisabeth
Rue d'Evere, 1140 Bruxelles

CANADA
Directeur du Service des Renseignements Scientifiques
Ministère de la Défense Nationale
Ottawa, Ontario K1A 0K2

DANEMARK
Danish Defence Research Board
Ved Idraetsparken 4
2100 Copenhagen Ø

ESPAGNE
INTA (AGARD Publications)
Pintor Rosales 34
28008 Madrid

ETATS-UNIS
National Aeronautics and Space Administration
Langley Research Center
M/S 180
Hampton, Virginia 23665

FRANCE
O.N.E.R.A. (Direction)
29, Avenue de la Division Leclerc
92320, Châtillon sous Bagneux

GRECE
Hellenic Air Force
Air War College
Scientific and Technical Library
Dekelia Air Force Base
Dekelia, Athens TGA 1010

ISLANDE
Director of Aviation
c/o Flugrad
Reykjavik

ITALIE
Aeronautica Militare
Ufficio del Delegato Nazionale all'AGARD
Aeroporto Pratica di Mare
00040 Pomezia (Roma)

LUXEMBOURG
Voir Belgique

NORVEGE
Norwegian Defence Research Establishment
Attn: Biblioteket
P.O. Box 25
N-2007 Kjeller

PAYS-BAS
Netherlands Delegation to AGARD
National Aerospace Laboratory NLR
Kluyverweg 1
2629 HS Delft

PORTUGAL
Portuguese National Coordinator to AGARD
Gabinete de Estudos e Programas
CLAFA
Base de Alfragide
Alfragide
2700 Amadora

ROYAUME UNI
Defence Research Information Centre
Kentigern House
65 Brown Street
Glasgow G2 8EX

TURQUIE
Milli Savunma Başkanlığı (MSB)
ARGE Daire Başkanlığı (ARGE)
Ankara

LE CENTRE NATIONAL DE DISTRIBUTION DES ETATS-UNIS (NASA) NE DETIENT PAS DE STOCKS DES PUBLICATIONS AGARD ET LES DEMANDES D'EXEMPLAIRES DOIVENT ETRE ADRESSEES DIRECTEMENT AU SERVICE NATIONAL TECHNIQUE DE L'INFORMATION (NTIS) DONT L'ADRESSE SUIT.

AGENCES DE VENTE

National Technical Information Service
(NTIS)
5285 Port Royal Road
Springfield, Virginia 22161
Etats-Unis

ESA/Information Retrieval Service
European Space Agency
10, rue Mario Nikis
75015 Paris
France

The British Library
Document Supply Division
Boston Spa, Wetherby
West Yorkshire LS23 7BQ
Royaume Uni

Les demandes de microfiches ou de photocopies de documents AGARD (y compris les demandes faites auprès du NTIS) doivent comporter la dénomination AGARD, ainsi que le numéro de série de l'AGARD (par exemple AGARD-AG-315). Des informations analogues, telles que le titre et la date de publication sont souhaitables. Veuiller noter qu'il y a lieu de spécifier AGARD-R-nnn et AGARD-AR-nnn lors de la commande de rapports AGARD et des rapports consultatifs AGARD respectivement. Des références bibliographiques complètes ainsi que des résumés des publications AGARD figurent dans les journaux suivants:

Scientifique and Technical Aerospace Reports (STAR)
publié par la NASA Scientific and Technical
Information Division
NASA Headquarters (NTT)
Washington D.C. 20546
Etats-Unis

Government Reports Announcements and Index (GRA&I)
publié par le National Technical Information Service
Springfield
Virginia 22161
Etats-Unis

(accessible également en mode interactif dans la base de données bibliographiques en ligne du NTIS, et sur CD-ROM)

Imprimé par Specialised Printing Services Limited
40 Chigwell Lane, Loughton, Essex IG10 3TZ